

Solving all the problems of our universe, one neutrino mass model at a time

Dissertation
zur
Erlangung des Doktorgrades (Dr. rer. nat.)
der
Mathematisch-Naturwissenschaftlichen Fakultät
der
Rheinischen Friedrich-Wilhelms-Universität Bonn

von
Maximilian Berbig
aus
Bad Neuenahr-Ahrweiler

Bonn, 23.06.2023

Angefertigt mit Genehmigung der Mathematisch-Naturwissenschaftlichen Fakultät der Rheinischen
Friedrich-Wilhelms-Universität Bonn

1. Gutachter: Prof. Herbert „Herbi“ Dreiner, Ph.D.
2. Gutachter: Prof. Dr. Manuel Drees

Tag der Promotion: 26.09.2023
Erscheinungsjahr: 2023

I couldn't understand entropy and flunked thermodynamics.

Yoichiro Nambu [1]

Acknowledgments

I would like to thank my supervisor Prof. Herbert “Herbi” Dreiner for giving me the freedom to find an area of theoretical particle physics, that suits my skill-set and where I can make at least some kind of contribution. Thank you for teaching me the importance of communicating science to the public and for encouraging me to expand my horizon by attending conferences and traveling to give talks. I even started adding little historical anecdotes during my presentations; guess where I got that from? I would also like to thank Prof. Manuel Drees for being the second referee of this thesis, in fact for the third time in a row since my Bachelor thesis. I learned a lot from your questions and comments during the theory seminar and especially in the journal club, which helped improve my capacity for critical thinking. Most of all I would like to express my gratitude and respect to Dr. Andreas Trautner, who was an invaluable source of intellectual and inter-personal support ever since the days of the self-interacting neutrinos. Thank you for always taking my drafts and half-cooked ideas seriously and for providing crucial insights into the sociological aspects of this very strange but marvelous job.

Furthermore I would like to thank the rest of the Dreiner group, namely Julian Günther, Dominik Köhler, Saurabh Nangia, Martin Schürmann and Apoorva Shah as well as the numerous past group members for tolerating my idiosyncrasies throughout the years. In this context I would also like to mention Christa Börsch, Lora Schindler, Andreas Wißkirchen and Patricia Zündorf, whose tireless efforts have kept the BCTP running and who are always very helpful and patient e.g. when I get confused by the travel expenses again.

On the more personal side of things I would like to acknowledge Dr. Jonathan Lozano de la Parra, Dr. Simon Holtz and Dr. Yong Xu for their support and many moments of levity throughout the last years. I also want Hendrik and Laura Nachbar to know that their friendship means a lot to me.

Last but definitely not least I want to express my sincere gratefulness to my mother Ursula Berbig, who since my childhood has fostered my abilities, and who instilled the curiosity and perseverance into me that lead me to walk the path of a theoretical physicist.

Summary

The masses and mixing in the neutrino sector can not be explained by the Standard Model (SM) of particle physics and might be a harbinger for new degrees of freedom at energies scales far above or comparable to the electroweak scale. This thesis tries to find correlations between the associated models and the many unresolved issues in modern cosmology: The work covered in the first part tries to address the tension in the determination of the Hubble constant, which differs depending on whether it is extracted from cosmic microwave background data or local measurements using Cepheid variable stars as standard candles. We discuss a particle physics model realizing strong neutrino self-interactions that delay the neutrino free streaming before recombination that also generates a large amount of dark radiation from the equilibration of an entire dark sector. In the following we chapter we try to address the nature of dark matter in the form of a keV-scale neutrino, which is sterile under the SM gauge interactions, but couples to an abelian gauged B-L symmetry. We demonstrate that both the light neutrino and heavier dark matter mass can arise via loop diagrams involving the same scalar sector. Dark matter and dark radiation in the form of right handed neutrinos are produced via out-of-equilibrium gauge mediated scatterings from the SM fermions. The part of this thesis devoted to the “S.M.A.S.H.E.D.” model extends a previous model known as SMASH (Standard Model Axion Seesaw Higgs Inflation), which was able to explain inflation, QCD axion dark matter, neutrino masses and the stability of the electroweak vacuum, to incorporate Dirac neutrinos. We generate a neutrino masses via a tree-level dimension six operator and showcase how the associated fermions lead to novel features in the context of Dirac Leptogenesis. This idea is followed by chapter, where the SM fermion and gauge sector receive a copy in the form of a so called mirror sector. We connect the neutrinos to their mirror counterparts via a bidoublet Higgs field. An exchange symmetry between the two sectors can solve the strong CP problem and we discuss the associated cosmology. Next we focus on the influence of very long lived right handed neutrinos (RHN) in the basic Type I Majorana Seesaw mechanism on the tensor modes predicted by cosmic inflation. We are able to show that the successful generation of the observed baryon asymmetry from Leptogenesis would lead to a damping of the primordial gravitational waves at frequencies above 0.1 Hz. The last chapter of this thesis deals with the entire class of Dirac Seesaw models: All Dirac Seesaws come with a Pseudo-Nambu-Goldstone-boson that we call the Diraxion, which can allow for a simultaneous explanation of the observed baryon asymmetry and the dark matter relic abundance. This scenario can be tested via isocurvature fluctuations, improved dark radiation limits, cosmic neutrino background searches and the dynamics of an associated GeV-scale scalar called the Saxion.

List of publications

This thesis consists of the following publications

- **The Hubble tension and a renormalizable model of gauged neutrino self-interactions,**
Maxilimian Berbig, Dr. Sudip Jana, Dr. Andreas Trautner, PHYS.REV.D 102 (2020) 11, 115008, DOI: 10.1103/PhysRevD.102.115008, arXiv: 2004.13039 [hep-ph]
- **Freeze-In of radiative keV-scale neutrino dark matter from a new $U(1)_{B-L}$,**
Maxilimian Berbig, JHEP 09 (2022) 101, DOI: 10.1007/JHEP09(2022)101, arXiv: 2203.04276 [hep-ph]
- **S.M.A.S.H.E.D.: Standard Model Axion Seesaw Higgs inflation Extended for Dirac neutrinos,**
Maxilimian Berbig, JCAP 11 (2022) 042, DOI: 10.1088/1475-7516/2022/11/042, arXiv: 2207.08142 [hep-ph]
- **Type II Dirac seesaw portal to the mirror sector: Connecting neutrino masses and a solution to the strong CP problem,**
Maxilimian Berbig, PHYS.REV.D 106 (2022) 11, 115018, DOI: 10.1103/PhysRevD.106.115018, arXiv: 2209.14246 [hep-ph]
- **Impact of high-scale Seesaw and Leptogenesis on inflationary tensor perturbations as detectable gravitational waves,**
Maxilimian Berbig, Dr. Anish Ghoshal, JHEP 05 (2023) 172, DOI: 10.1007/JHEP05(2023)172, arXiv: 2301.05672 [hep-ph]

as well as the draft

- **Diraxogenesis,** *Maxilimian Berbig, arXiv: 2307.14121 [hep-ph],*

which was uploaded to a pre-print server after the submission of this thesis.

Contents

1	Structure of this thesis	1
2	Motivation	3
2.1	Neutrino masses	3
2.1.1	Observational information about the neutrino sector	3
2.1.2	Majorana or Dirac?	5
2.2	Cosmology	8
2.2.1	Recombination	8
2.2.2	Dark Matter	12
2.2.3	Primordial Nucleosynthesis	13
2.2.4	Inflation	14
2.2.5	Baryogenesis	17
3	Hubble Tension	19
3.1	Contribution and Context	19
3.2	Appendix: Abstract	21
3.3	Appendix: Introduction	21
3.4	Appendix: Parameter Region	22
3.5	Appendix: The Model	23
3.6	Appendix: Phenomenology	26
3.7	ADDENDUM: Why do we need the singlet?	29
3.8	Appendix: BBN	32
3.9	Appendix: Discussion	33
3.10	Appendix: Note	34
3.11	Appendix: Acknowledgments	34
4	Radiative keV-scale DM	35
4.1	Contribution and Context	35
4.2	Appendix: Abstract	36
4.3	Appendix: Introduction	37
4.4	Appendix: The model	37
4.4.1	The Dirac Scotogenic model	37
4.4.2	Extension for radiative DM mass	41
4.4.3	UV completion	44
4.5	Appendix: Dark Matter	46
4.5.1	Lyman bound for FIMPs	47
4.5.2	Out of equilibrium Higgs decays	47

Contents

4.5.3	Super WIMP contribution	52
4.5.4	Gauge Scattering	52
4.5.5	Dark matter phenomenology	56
4.6	Appendix: Dark Radiation	59
4.6.1	Dark Matter as dark radiation	59
4.6.2	Right handed neutrinos as dark radiation	60
4.7	Appendix: Inflation and candidates for the inflaton	64
4.7.1	The SM like Higgs	66
4.7.2	The B-L breaking singlet	67
4.7.3	The inert doublet or singlet scalars	68
4.8	Appendix: Baryogenesis	70
4.9	Appendix: Summary	73
4.10	Appendix: Acknowledgments	74
5	S.M.A.S.H.E.D.	75
5.1	Contribution and Context	75
5.2	Appendix: Abstract	76
5.3	Appendix: Introduction	77
5.4	Appendix: The model	78
5.4.1	KSVZ-axion	79
5.4.2	Neutrino masses	82
5.4.3	Landau poles for the SM gauge couplings	85
5.4.4	Axion to photon coupling	90
5.4.5	Collection of limits on the axion to photon coupling	91
5.4.6	Axion to fermion coupling	92
5.5	Appendix: Unification	93
5.6	Appendix: Cosmology of S.M.A.S.H.	93
5.6.1	Inflation and reheating	93
5.6.2	Axion dark matter	95
5.6.3	Vacuum stability and Leptogenesis	96
5.7	Appendix: Dirac-Leptogenesis in S.M.A.S.H.E.D.	97
5.7.1	Overview	97
5.7.2	CP violation	98
5.7.3	Enhancement of the asymmetry parameter	101
5.7.4	Sphaleron redistribution coefficient	102
5.7.5	Analytical estimates	105
5.7.6	Boltzmann equations	110
5.7.7	Cross sections and rate densities	113
5.7.8	CP-violating rate densities	114
5.7.9	Numerical results	116
5.7.10	Lightest neutrino mass	122
5.8	Appendix: Dark radiation	122
5.8.1	Contribution of the axion	123
5.8.2	Contribution of the right handed neutrinos	123

5.9	Appendix: Summary	125
5.10	Appendix: Acknowledgements	126
6	Type II Dirac Seesaw	127
6.1	Contribution and Context	127
6.2	Appendix: Abstract	128
6.3	Appendix: Introduction	129
6.4	Appendix: The model	130
6.5	Appendix: Vacuum structure	133
6.6	Appendix: Full Scalar Potential	135
6.6.1	Minimization of the scalar potential: Original Higgs-Parity model	135
6.6.2	Minimization of the scalar potential: Inclusion of the bidoublet .	139
6.6.3	Sufficient conditions for vacuum stability	142
6.7	Appendix: Scalar and Gauge Bosons	142
6.8	Appendix: Strong CP problem	144
6.8.1	Tree level	145
6.8.2	Loop level	145
6.9	Appendix: Low-energy phenomenology	146
6.9.1	Dipole moments and lepton flavor violation	147
6.9.2	Collider bounds	148
6.10	Appendix: Cosmology	148
6.10.1	Reheating	148
6.10.2	Dark Radiation	149
6.10.3	Leptogenesis from decays	149
6.10.4	Inflationary Affleck-Dine Leptogenesis	151
6.10.5	Origin of the dimension five operator for Affleck-Dine Leptogenesis	154
6.11	Appendix: Conclusion	155
6.12	Appendix: Acknowledgments	155
7	Seesaw impact on Gravitational Waves	157
7.1	Contribution and Context	157
7.2	Appendix: Abstract	158
7.3	Appendix: Introduction	159
7.4	Appendix: Decays of a long-lived RHN	162
7.4.1	Type I Seesaw mechanism	162
7.4.2	Conditions for intermediate matter domination	162
7.4.3	Non-thermal Leptogenesis	165
7.4.4	Dark Matter and Dark Radiation Co-genesis	168
7.5	Appendix: Gravitational Waves	172
7.5.1	Distortion of the inflationary tensor mode spectrum	172
7.5.2	Other GW sources	174
7.5.3	Detectors and signal-to-noise ratio	175
7.5.4	Dark radiation bounds from BBN and CMB decoupling	176
7.5.5	Impact of free-streaming particles	176

7.6	Appendix: Results	179
7.6.1	General results	179
7.6.2	Signal-to-noise ratio	183
7.7	Appendix: Conclusions and Discussions	186
7.8	Appendix: Acknowledgements	187
8	Diraxiogenesis	189
8.1	Contribution to the project	189
8.2	Introduction	189
8.3	Models	192
8.3.1	Dirac Weinberg operator	192
8.3.2	The three Dirac Seesaws	193
8.3.3	Saxion	197
8.3.4	Saxion Couplings	198
8.3.5	Diraxion	199
8.3.6	Higher dimensional operator from a second scalar field	201
8.3.7	Diraxion couplings	202
8.4	Two-field dynamics	204
8.4.1	Equations of motion	204
8.4.2	Initial Saxion field value	204
8.4.3	Saxion oscillation	207
8.4.4	Generating the Diraxion rotation	209
8.5	Dirac-Lepto-Axiogenesis	214
8.5.1	Dissipation coefficient from Dirac Weinberg operator	214
8.5.2	Chemical potentials and Boltzmann equation	214
8.5.3	Baryon Asymmetry	216
8.6	Dark Matter	220
8.6.1	Dark Matter decay	220
8.6.2	Standard Misalignment	222
8.6.3	Topological Defect decay	223
8.6.4	Kinetic Misalignment and fragmentation	225
8.6.5	Parametric Resonance from Saxion oscillations	228
8.7	Dark Radiation	229
8.7.1	Freeze-In scattering from Dirac Weinberg operator	230
8.7.2	Out-of-equilibrium Saxion decays	232
8.8	Isocurvature perturbations	233
8.8.1	Dark Matter and Baryon isocurvature	233
8.8.2	Dark Radiation isocurvature	236
8.8.3	One Loop corrections	237
8.9	Thermalization	240
8.9.1	Early Thermalization	240
8.9.2	Early Thermalization from Type III Dirac Seesaw	241
8.9.3	Late Thermalization	242
8.9.4	Thermalized Saxion decays	245

Contents

8.9.5 Maximum Yield	246
8.10 Discussion	246
8.11 Conclusion	250
9 Conclusion	253

1 Structure of this thesis

We begin this manuscript with a brief review of the neutrino sector as well as the present day status of cosmological observations and contemporary ideas about the early universe in chapter 2. The bulk of this thesis is material collected from my publications in chapters 3-7 followed by a chapter with new unpublished material in 8. During the review of my work I realized that there were some sentences in the published papers, that were either too imprecise, not entirely correct or just involved typos. In order to be as transparent as possible I decided to leave the aforementioned passages intact (except for the typos) and added additional commentary in the form of the following visual aid:

■ ADDENDUM: This is an addendum. Addenda are hidden like easter-eggs throughout this thesis. There is no reward for finding them all, but I hope that they help to clarify some aspects of my writing. ■

In chapter 3 section 3.7 that expands upon the material presented in the paper was added. We summarize all of our findings and phenomenological predictions in chapter 9.

2 Motivation

2.1 Neutrino masses

2.1.1 Observational information about the neutrino sector

Since the 1990s we have observed flavor oscillations of solar, atmospheric and reactor neutrinos, which we interpret as a mismatch between the eigenstates of the weak interaction and the neutrinos mass eigenstates. These oscillations constitute direct evidence for the massive nature of neutrinos and the question about the origin of the sub-eV neutrino mass scale is one of the most pressing issues in particle physics today. The probability for such an oscillation between flavor states of neutrinos with an energy E propagating over a distance L in a two neutrino toy-model is proportional to

$$P_{\text{osc.}} \sim \sin \left(\frac{\Delta m_{12}^2 L}{4E} \right)^2, \quad \text{with} \quad \Delta m_{12}^2 \equiv m_1^2 - m_2^2. \quad (2.1)$$

From this basic example one can already see, that oscillation experiments can only determine the difference between squared neutrino masses, but not their overall scale. The current paradigm involves three massive neutrinos and we have observed two of the aforementioned mass splittings: The first one is $\Delta m_{\text{sol}}^2 \simeq 10^{-4} \text{ eV}^2$ from oscillations of neutrinos produced inside the sun and the second one $|\Delta m_{\text{atmo}}^2| \simeq (2 - 3) \cdot 10^{-3} \text{ eV}^2 \gg \Delta m_{\text{sol}}^2$ arises due to neutrinos produced from the decays of pions and muons produced via cosmic ray interactions in the upper atmosphere. Because of a matter effect inside the sun called the Michejew-Smirnow-Wolfenstein effect [2,3] we know the sign of Δm_{sol}^2 , but since atmospheric oscillations proceed in vacuo we have no such information about Δm_{atmo}^2 . This leaves two experimentally allowed choices for the ordering of the mass eigenstates, namely the normal hierarchy (NO) with $m_3 > m_2 \gg m_1$ or the inverted hierarchy (IO) with $m_3 \ll m_1 < m_2$. For both orderings one finds $\Delta m_{21}^2 = \Delta m_{\text{sol}}^2$ and for NO one takes $\Delta m_{\text{atmo}}^2 = \Delta m_{32}^2 > 0$ implying $\Delta m_{31}^2 = \Delta m_{\text{sol}}^2 + \Delta m_{\text{atmo}}^2 > 0$. On the other hand one for IO one starts from $\Delta m_{\text{atmo}}^2 < 0$ from which one can deduce that $\Delta m_{31}^2 = \Delta m_{\text{sol}}^2 - |\Delta m_{\text{atmo}}^2| < 0$ and consequently $\Delta m_{32}^2 = -|\Delta m_{\text{atmo}}^2|$. For the numerical values we refer to global fits to data from oscillation experiments [4] together with Super-Kamiokande [5,6] data about atmospheric neutrinos. Apart from solar neutrino data the long baseline reactor experiment KamLAND [7] was used to determine Δm_{sol}^2 , whereas Δm_{atmo}^2 is measured from the medium baseline reactor experiments Daya-bay [8], Reno [9] and Double-Chooz [10] together with the long baseline accelerator experiments K2K [11], T2K [12], MINOS [13] and NO ν A [14]. By setting the lightest neutrino mass to zero ($m_1 = 0$ for NO and $m_3 = 0$ for IO) one deduces that the mass spectra for NO

2 Motivation

and IO are given by

$$m_2 \simeq \sqrt{\Delta m_{\text{sol.}}^2} \simeq 8.6 \times 10^{-3} \text{ eV}, \quad m_3 \simeq \sqrt{\Delta m_{\text{sol.}}^2 + \Delta m_{\text{atm.}}^2} \simeq 0.05 \text{ eV} \quad (2.2)$$

and

$$m_1 \simeq \sqrt{|\Delta m_{\text{sol.}}^2 + \Delta m_{\text{atm.}}^2|} \simeq 0.0492 \text{ eV}, \quad m_2 \simeq \sqrt{|\Delta m_{\text{atm.}}^2|} \simeq 0.05 \text{ eV}. \quad (2.3)$$

The mixing in the lepton sector is described by the Pontecorvo-Maki-Nagakawa-Sakata matrix. Maki, Nagakawa and Sakata where the first to consider mixing between two massive neutrinos in [15], whereas Pontecorvo suggested oscillations between neutrinos and anti-neutrinos in [16]. The PMNS matrix is given in terms of three rotation angles and three phases (one phase) for Majorana (Dirac) neutrinos. The global fit of reference [4] found

$$\sin(\theta_{12})^2 = 0.304_{-0.012}^{+0.012}, \quad (2.4)$$

$$\sin(\theta_{23})^2 = 0.573_{-0.020}^{+0.016}, \quad (2.5)$$

$$\sin(\theta_{13})^2 = 0.02219_{-0.00063}^{+0.00062}, \quad (2.6)$$

$$\delta_{CP} = 197_{-24}^{+27} \text{ } \circ. \quad (2.7)$$

The angle θ_{12} was measured by solar neutrino experiments and KamLAND [7]. Analyses of MINOS [13] data determined the angle θ_{23} and the last angle θ_{13} was measured at Daya-bay [8], Reno [9] and Double-Chooz [10]. Note that currently there is a tension in the determination of the CP violating angle δ_{CP} [17], depending on whether it is extracted from NO ν A [14] or T2K [12].

Apart from oscillation experiments there exists another laboratory probe for the neutrino mass: The experiment KATRIN conducts a high precision measurement of the momentum of electrons produced in β -decay of tritium. Non-zero neutrino masses would modify the end point of this spectrum, which can be used to set a limit on the neutrino mass scale [18]

$$m_\nu < 0.8 \text{ eV}. \quad (2.8)$$

If neutrinos are Majorana particles there could be neutrinoless double-beta-decay [19], however we do not explore this possibility in our work.

For the longest time cosmology provided the only limit on the neutrino mass scale. Since neutrinos decouple from the weak interaction while relativistic, they would be hot dark matter. Structure formation arguments disfavor hot dark matter, so that neutrinos can only be a subleading fraction of the dark matter relic density. This line of reasoning can be used to set an upper limit on the sum of the neutrino masses from CMB data, baryon acoustic oscillations and gravitational lensing [20]

$$\sum m_\nu < 0.12 \text{ eV}. \quad (2.9)$$

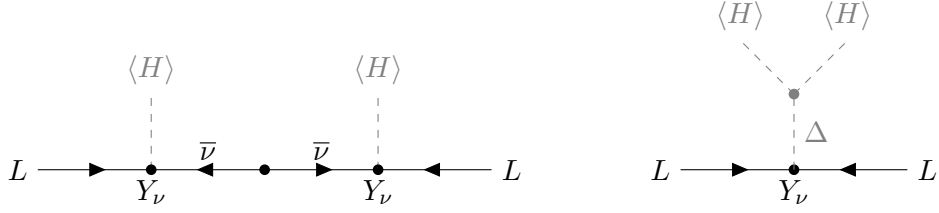


Figure 2.1: Diagrammatic representation of the Type I Seesaw (*left*) and the Type II Seesaw (*right*). The Type III Seesaw has the same Feynman diagram as the Type I Seesaw if one replaces the SM gauge singlets $\bar{\nu}$ with hyperchargeless weak triplets T .

Note that the above bound holds for a degenerate neutrino mass spectrum and for the normal hierarchy (NO) or inverted hierarchy (IO) one finds instead that [21]

$$\text{NO: } \sum m_\nu < 0.15 \text{ eV}, \quad \text{IO: } \sum m_\nu < 0.17 \text{ eV}. \quad (2.10)$$

2.1.2 Majorana or Dirac?

As far as we know all Standard Model fermions with electric charge, such as the electron, have Dirac mass terms from the Higgs vev

$$\mathcal{L} = Y_l L H^\dagger \bar{e} + \text{h.c.}, \quad (2.11)$$

which prompts one to define a four component Dirac spinor

$$E = \begin{pmatrix} e \\ \bar{e}^\dagger \end{pmatrix}, \quad (2.12)$$

constructed from the two component spinors for the left-chiral electron e (embedded in L before electroweak symmetry breaking) and left-chiral positron \bar{e} . In the above we used the two-component-spinor notation from reference [22]. Dirac neutrino masses could arise in the same way if one introduces a right chiral neutrino $\bar{\nu}$, but due to the size of the Higgs vev of 246 GeV, this would require a tiny Yukawa coupling of the order of $10^{-13} - 10^{-14}$. Particle physicists would like to have an argument, for why this number should be so small, which has stimulated the developments of alternative ideas. Most of the community is focused on investigating Majorana neutrino mass models. The rational behind this is, that neutrinos are electrically neutral and if they do not carry any additional conserved quantum number, such as lepton number, there is nothing that forbids them from coupling to themselves and being self-conjugate. There is a unique dimension five operator, called the Weinberg operator [23], constructed only from Standard Model fields that would give rise to such Majorana masses

$$\mathcal{L}_5 = \frac{c_5}{\Lambda_{\text{UV}}} (L e H)(L e H) + \text{h.c.}, \quad (2.13)$$

2 Motivation

with $\epsilon = i\sigma_2$, c_5 a dimensionless Wilson coefficient and Λ_{UV} a cut-off scale. Majorana neutrinos would be described by the following four component spinor

$$N = \begin{pmatrix} \nu \\ \nu^\dagger \end{pmatrix}. \quad (2.14)$$

A tree-level UV completion to this operator was first found in the context of the grand unified theory SO(10) [24, 25] and goes under the name of “Type I Seesaw” [26–30]. This mechanism relies on a new right chiral SM gauge singlet neutrino $\bar{\nu}$ with a Majorana mass M_N :

$$\mathcal{L} = Y_\nu L \epsilon H \bar{\nu} + M_N \bar{\nu} \bar{\nu} + \text{h.c.} \quad (2.15)$$

Integrating $\bar{\nu}$ out as depicted in figure 2.1 generates a (pseudo-Majorana) neutrino mass of

$$m_\nu^{\text{I}} \simeq Y_\nu^2 \frac{v_H^2}{M_N}, \quad (2.16)$$

which is automatically small for $M_N \gg Y_\nu v_H$, hence the name. Later it was realized that there are two other unique UV completions for this operator at tree-level [31]: One can introduce a scalar triplet Δ with $Y = 1$ decomposing as

$$\Delta = \begin{pmatrix} \frac{\Delta^+}{\sqrt{2}} & \Delta^{++} \\ \Delta^0 & -\frac{\Delta^+}{\sqrt{2}} \end{pmatrix}, \quad (2.17)$$

which has the following couplings to leptons and Higgses (here κ is a dimensionful parameter)

$$\mathcal{L} = Y_\nu L \epsilon \Delta L + \kappa H^\dagger \epsilon \Delta H^\dagger + \text{h.c.} \quad (2.18)$$

and is known as the “Type II Seesaw” [32–36]. The active neutrino mass follows from a tiny vev $v_\Delta \simeq \kappa v_H^2 / \mu_\Delta^2$ of the neutral component of Δ , induced via the trilinear coupling to the SM Higgs, to be

$$m_\nu^{\text{II}} \simeq Y_\nu \kappa \frac{v_H^2}{\mu_\eta^2}, \quad (2.19)$$

and this mechanism features two sources of suppression as one can take both $\mu_\Delta \gg v_H$ and $\mu_\Delta \gg \kappa$. Note that the simultaneous presence of both couplings in (2.18) explicitly breaks Lepton number. In particular there will be no Goldstone boson from the CP-odd component of Δ^0 due to the explicit breaking proportional to κ . Another way to see this is the fact that we take $\mu_\Delta^2 > 0$ to induce the vev v_Δ . Since $\mu_\Delta^2 \gg v_\Delta > 0$ the CP-even and odd components of Δ^0 will be nearly mass degenerate up to small splitting proportional to v_Δ . The fermionic messenger could also be a hyperchargeless triplet fermion T decomposing as

$$T = \begin{pmatrix} \frac{T^0}{\sqrt{2}} & T^+ \\ T^- & -\frac{T^0}{\sqrt{2}} \end{pmatrix}, \quad (2.20)$$

which is known as a “Type III Seesaw” [37] and essentially resembles (2.15) without the asymmetric contractions due to ϵ .

Apart from the above mechanisms there also exist extended Seesaws: When one introduces more than one right chiral neutrino this opens up the possibility to construct e.g. a “Double Seesaw” [38], the “Inverse Seesaw” [39] or the “Linear Seesaw” [40]. Iterating the suppression factor is known as building “Nested Seesaws”, where the aforementioned “Double Seesaw” is just one example for the Type I scenario and one can repeat the same idea also for the Type II scheme [41, 42]. Furthermore one can either mix and merge different Seesaws mechanisms [43] or engineer a situation, where different neutrino masses originate from multiple separate Seesaws, which is known as a “Hybrid Seesaw” [44, 45]. In fact all fermion masses of the Standard Model could arise from an “universal Seesaw” [46]. On top of that there exists a tremendous amount of literature on one- and multi-loop neutrino mass models (see e.g. [47] for a review), not to mention that one can combine tree- and loop-level mechanisms in non-trivial ways.

While Majorana neutrinos come with additional signatures such as neutrinoless double-beta-decay [19], there is a priori no reason to discard the possibility of pure Dirac neutrinos. The only arguments against parametrically light Dirac neutrinos are aesthetical in nature and appeal to the idea of minimality: To avoid the direct coupling of $\bar{\nu}$ to H as well as unwanted Majorana masses usually requires additional symmetries and the dimension five equivalent of (2.13) for Dirac neutrinos needs an additional scalar singlet σ

$$\mathcal{L}_5 = \frac{c_5}{\Lambda_{\text{UV}}} (L\epsilon H)\bar{\nu}\sigma + \text{h.c.} \quad (2.21)$$

Furthermore one typically integrates out Dirac fermions to form the aforementioned operator, which involves twice as many Weyl spinors and additional Yukawa couplings to both chiralities. If one drops this purely theoretical prejudice one finds that there exist a class of tree-level Dirac Seesaws [48–53] mimicking their Majorana counterparts. Chapter 8 will introduce them and their associated phenomenology in detail. Chapter 6 deals with a Dirac version of the Type II Seesaw, that similar to its Majorana pendant offers electrically singly and doubly charged scalars unlike previous models, which only featured single charged ones. Chapter 5 showcases that (2.21) is not inevitable and that one can also generate dimension six operators that do not rely on singlet scalars. While most of this thesis deals with Dirac neutrinos masses from tree-level mechanisms, a one loop model known as the “Dirac-Scotogenic model” [54, 55] is extended to generate the dark matter mass in chapter 4.

Light Dirac neutrinos could also come from compositeness of the right chiral neutrino [56] or right chiral neutrinos propagating in extra dimensions [57, 58], so that the Yukawa coupling is automatically small due to the small overlap between the wavefunctions of the different chiralities. While the neutralino sector, made up by the neutral charginos and Higgsinos in minimal ($N = 1$) supersymmetric (SUSY) extensions of the Standard Model can feature Majorana masses depending on the spectrum of soft SUSY breaking

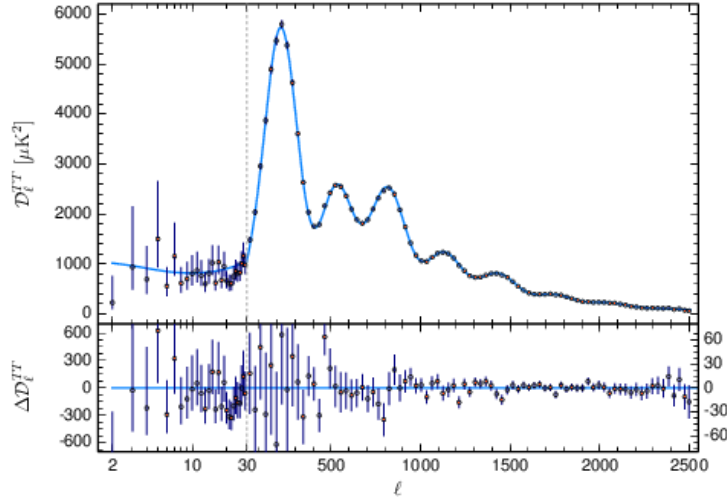


Figure 2.2: Plot of the anisotropic temperature power spectrum as function of the multipole moment ℓ , which corresponds to the angular separation taken from [20].

gaugino masses, there also exist models with Dirac gauginos that come at the precise of requiring $N = 2$ supercharges [59].

2.2 Cosmology

For an introduction to the most relevant concepts and terminology in cosmology I refer the reader to the following excellent textbooks:

- INTRODUCTION TO THE THEORY OF THE EARLY UNIVERSE: HOT BIG BANG THEORY [60] by *Valery A. Rubakov, Dmitry S. Gorbunov*
- INTRODUCTION TO THE THEORY OF THE EARLY UNIVERSE: COSMOLOGICAL PERTURBATIONS AND INFLATIONARY THEORY [61] by *Valery A. Rubakov, Dmitry S. Gorbunov*
- THE EARLY UNIVERSE [62] by *Edward W. Kolb, Michael S. Turner*

2.2.1 Recombination

The universe started out as plasma in which photons had only a short mean free path due to e.g. Compton scattering with the charged particles making up the plasma. As the universe cools down neutral atoms are formed and the photons can now freely propagate without scattering; the universe has become transparent and the decoupled photons remain as the cosmic microwave background (CMB). While naively one would expect this to occur around the temperature of the hydrogen binding energy 13.6 eV, the formation

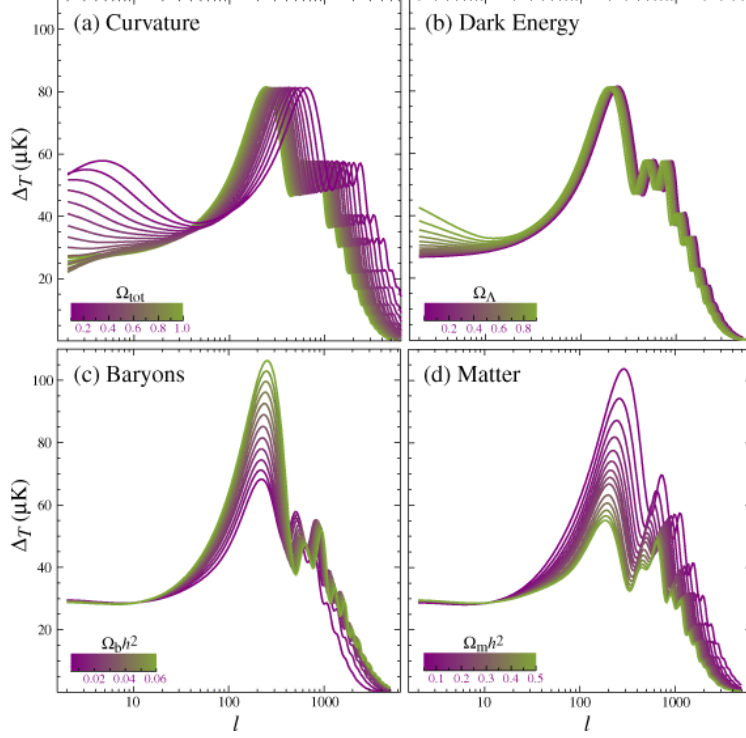


Figure 2.3: Impact of varying the curvature parameter (a), the dark energy density (b), the baryon energy density (c) and the total matter energy density (d) on the acoustic peaks of the CMB temperature power spectrum taken from reference [63].

of neutral atoms actually takes place somewhat later at around 0.3 eV [60]. This can be understood from the fact that abundant photons from the high energy tail of the Boltzmann distribution disintegrate most of the newly formed atoms at temperatures of around 13.6 eV, so one has to wait until lower temperatures to depopulate the high energy tail sufficiently. Thomson scattering, which is the low energy limit of Compton scattering, decouples at $T = 0.26$ eV [60], which is known as the temperature of last scattering. The

2 Motivation

CMB gives rise to an almost perfect black-body spectrum with a temperature of [64]

$$T = (2.725\,48 \pm 0.000\,57) \text{ K}, \quad (2.22)$$

but there are also small spectral distortions in the form of anisotropic temperature fluctuations with relative size $\Delta T/T \simeq \mathcal{O}(10^{-5})$ and fluctuations of the photon polarization. Satellite missions such as COBE [65], WMAP [66] and more recently Planck [20] have measured these anisotropies and allow us to e.g. understand the CMB temperature power spectrum as function of the multipole moment ℓ , which encodes the angular information on the sky. The lowest multipole moments $\ell < 100$ are called the Sachs-Wolfe plateau followed by the acoustic peaks in the range $100 \leq \ell \leq 1000$ and eventually the damping tail at $\ell > 1000$. Studying the acoustic peaks allows us to determine the energy densities of the various components that make up the cosmological concordance model called Λ CDM and we depict the total spectrum in figure 2.2 and the aforementioned peaks in figure 2.3. One conventionally normalizes all energy densities ρ_i for a species i to the critical density $\rho_c = 3H_0^2/(8\pi G_N)$, where $H_0 = h \cdot 100 \text{ km s}^{-1} \text{ Mpc}^{-1}$ with $h \simeq 0.7$ is the expansion rate of the universe today and G_N denotes Newton's constant, by defining $\Omega_i \equiv \rho_i/\rho_c$. If the total energy density of our universe equaled ρ_c , so that $\Omega_{\text{tot}} = 1$, then it would be spatially flat ($\Omega_{\text{curv}} = 0$). One can extract the value of Ω_{tot} from the position of the first acoustic peak, which would move to larger ℓ for smaller Ω_{tot} (see panel (a) in figure 2.3) and the observational limit $\Omega_{\text{curv}} h^2 = 0.001 \pm 0.002$ [20] is compatible with a spatially flat universe. Increasing the dark energy density would shift the entire peak spectrum to lower ℓ , as can be seen from panel (b) in figure 2.3. If one increases the total energy density in baryonic and dark matter one finds from panel (d) in 2.3 that all the peaks shrink, whereas increasing only the baryonic contribution increases e.g. the first and third peaks, while reducing the second one as is evident from panel (c) in 2.3. This is why one can extract the baryonic energy density $\Omega_B h^2 = 0.0224 \pm 0.0001$ [20] from the ratio of the first and second peak. From the third peak one can determine the dark matter relic density to be $\Omega_{\text{DM}} h^2 = 0.120 \pm 0.001$ [20]. The number of relativistic, degrees of freedom is conventionally parameterized as the effective number of neutrino species N_{eff} . The SM prediction for three generations of relativistic neutrinos reads [67--73]

$$N_{\text{eff.}} = 3.0432 \pm 0.0002, \quad (2.23)$$

where effects from the non-instantaneous neutrino decoupling, neutrino oscillations, thermal corrections and next-to-leading order corrections to the QED rates were taken into account. For a detailed summary of all effects consult [73]. Additional relativistic particles with an energy density ρ_{DR} would change this number by [74]

$$\Delta N_{\text{eff.}}(T) = \frac{4}{7} g_{*\rho}(T) \left(\frac{10.75}{g_{*S}(T)} \right)^{\frac{4}{3}} \frac{\rho_{\text{DR}}(T)}{\rho_{\text{SM}}(T)} \quad \text{with} \quad \rho_{\text{SM}}(T) = \frac{\pi^2}{30} g_{*\rho}(T) T^4, \quad (2.24)$$

where $g_{*\rho}(T)$ ($g_{*S}(T)$) is the number of relativistic degrees of freedom in the energy (entropy) density. If there were additional sources of dark radiation, then there would be

more damping of the acoustic CMB peaks at large ℓ [75]. One can fit the number of relativistic degrees of freedom from the CMB data to be [20]

$$N_{\text{eff.}} = 2.99 \pm 0.17. \quad (2.25)$$

One can also combine Planck data with baryon acoustic oscillations, gravitational lensing and direct measurements of the helium abundance [76] (see the next paragraph) to find [20]

$$N_{\text{eff.}} = 2.97^{+0.58}_{-0.54}. \quad (2.26)$$

By using energy density in baryons one can infer their number density $n_B \simeq \Omega_b \rho_c / m_H$, where m_H is the mass of a hydrogen atom, and compare this to the number density of photons today to find [60]

$$\eta_B \equiv \frac{n_B}{n_\gamma} = 6.2 \times 10^{-10}, \quad (2.27)$$

which can be re-expressed as the baryon asymmetry today [60]

$$\Delta_B \equiv \frac{n_B - n_{\bar{B}}}{s} = 0.88 \times 10^{-10}, \quad (2.28)$$

where we used that the entropy density s today satisfies $s \simeq 7 n_\gamma$ and the fact that $n_B - n_{\bar{B}} = \text{const.}$ at temperatures below the electroweak crossover. These quantities are small because baryons are non-relativistic today and hence their number density is Boltzmann suppressed compared to the photons. The real question is why the baryon asymmetry is non-zero, since for a baryon symmetric universe all the baryons and anti-baryons would have annihilated into ration. Explaining the baryon asymmetry of the universe is one of the major unresolved questions in modern cosmology and we will try to find solutions to this conundrum in chapters 5, 6, 7 and 8.

CMB data also constraints isocurvature perturbations: If all species making up the cosmic plasma receive the same fluctuation to their individual energy densities, one speaks of adiabatic or curvature perturbations, since the perturbation of the overall energy momentum tensor is connected to the gravitational curvature via Einstein's field equations. On the other hand if only one species experiences a perturbation, or there is a relative perturbations between different species, one speaks of isocurvature modes. Single field inflation is expected to produce adiabatic perturbations, whereas additional light spectator fields present during inflation can be imprinted with isocurvature perturbations. The Planck mission determined the amplitude of the power spectrum for adiabatic perturbations $\mathcal{P}_\zeta(k_*)$ and they constrain the admixture of adiabatic and dark matter isocurvature perturbations with the amplitude \mathcal{P}_{DM} at the pivot scale $k_* = 0.05 \text{ Mpc}^{-1}$ to be [77]

$$\beta_{\text{iso}} \equiv \frac{\mathcal{P}_{\text{DM}}(k_*)}{\mathcal{P}_{\text{DM}}(k_*) + \mathcal{P}_\zeta(k_*)} < 0.038, \quad (2.29)$$

2 Motivation

which implies

$$\mathcal{P}_{\text{DM}}(k_*) < \frac{\beta_{\text{iso}}}{1 - \beta_{\text{iso}}} \mathcal{P}_\zeta(k_*) \simeq 8.7 \times 10^{-11}. \quad (2.30)$$

One can recast this limit for baryonic isocurvature modes by using the observed [20] values of $h^2 \Omega_B = 0.0224$ as well as $h^2 \Omega_{\text{DM}} = 0.12$ [78]

$$\mathcal{P}_B(k_*) < \left(\frac{\Omega_{\text{DM}}}{\Omega_B} \right)^2 \cdot \frac{\beta_{\text{iso}}}{1 - \beta_{\text{iso}}} \mathcal{P}_\zeta(k_*) \simeq 2.5 \times 10^{-9}. \quad (2.31)$$

Currently (as of the writing of this thesis in June 2023) there persists another cosmological mystery, that has to do with the inference of the Hubble rate today: Local measurements using cosmic distance ladder methods calibrated with Cepheid variable stars find [79]

$$H_0 = (73.2 \pm 1.3) \text{ km s}^{-1} \text{ Mpc}^{-1}, \quad (2.32)$$

which is in conflict with the value fitted from the CMB assuming ΛCDM [20]

$$H_0 = (67.27 \pm 0.60) \text{ km s}^{-1} \text{ Mpc}^{-1}, \quad (2.33)$$

at a statistical significance of 4.1σ [80]. This has prompted many proposals for modifications of ΛCDM to resolve this “Hubble tension”. The authors of reference [75] found that this tension can not be resolved by adding more dark radiation, which as previously explained would change the high- ℓ tail of the temperature power spectrum too much. If neutrinos were not free streaming due to new self-interactions at the time of recombination, their reduced drag on the plasma can compensate for larger amounts of dark radiation, which is known as the self-interacting-neutrino-solution [75]. In chapter 3 we present a concrete, renormalizable and UV-complete particle physics model to generate the required strong self-interactions in the neutrino sector.

2.2.2 Dark Matter

We saw in section 2.2.1 that there is a component of dark matter that is about five times as abundant as the usual baryonic matter that e.g. this thesis consists of. Here we just briefly review the most basic features of this strange non-luminous substance. Dark Matter was first proposed almost one hundred years ago [81] to solve the “missing-mass-problem”, where the observed rotation curves of galaxy clusters require more mass than what can be inferred from their brightness. Our current understanding of the formation of large scale structures also requires dark matter. As the name dark matter implies, this species does not have sizeable or unsuppressed couplings to electromagnetism. The most well studied production mechanism is “Freeze-Out” from a thermal bath. Production via interactions that never equilibrate with the thermal bath is known as “Freeze-In” [82]. There are also non-thermal production modes for e.g. scalar condensates [83--85] or via inflaton decays during reheating (see section 2.2.4). Our work only deals with Freeze-In and non-thermal dark matter. Bosonic dark matter can in principle be arbitrarily light,

which stimulated the development of “ultra-light” dark matter, with Compton wavelengths on galactic scales [86]. However for fermionic dark matter there exist stringent lower limits on the dark matter mass due to phase space arguments following from their Fermi-Dirac statistics. These arguments exclude single species fermionic dark matter below about 100 eV [87]. Dark matter should either be absolutely stable, which could be the consequence of a symmetry argument similar to the proton’s stability in the SM due to B-L conservation, or long-lived enough on cosmological time scales. One needs a life-time above about ten times the age of the universe (which is around 13 billion years old), where the exact number [88] depends on whether dark matter decays to e.g. visible matter or dark radiation [89].

2.2.3 Primordial Nucleosynthesis

Going backwards in time from recombination we arrive at the epoch of primordial or Big Bang Nucleosynthesis (BBN), which constitutes the earliest point in the history of our universe, that we have observational data about. During this epoch the light elements up to ^7Li are formed. Heavier elements are produced from lighter ones in the hot interior of stars in a process known as astration. BBN commences after the decoupling of the neutrinos and neutrons from the weak interactions at temperatures of $\mathcal{O}(1 \text{ MeV})$ or equivalently one second after the Big Bang. It turns out that the formation of heavier elements proceeds via a chain of reactions that first needs to produce deuterium. Deuterium is produced later than naively expected at temperatures of around 80 keV (about three minutes after the Big Bang), again because of photo-dissociation from the high-energy tail of the Boltzmann distribution. In order to test the theoretically predicted abundances of light nuclei observationally, one needs to find regions with low-metallicity (few heavy elements) and a low star formation rate, so that the primordial abundances are unaffected by astration. For all elements except lithium the data is in good agreement with the predictions, which essentially depend only one free parameter: the previously introduced baryon-to-photon-ratio η_B . Thus BBN constitutes a second independent determination of this parameter, leading to a value of [90]

$$\eta_{\text{BBN}} = (6.143 \pm 0.190) \times 10^{-10}, \quad (2.34)$$

which agrees with the result deduced from recombination in (2.27). The theory of BBN however predicts more Lithium than is observed, which is known as the “Lithium problem”. This problem will most likely be explained by an improved understanding of the nuclear physics behind lithium depletion in stars or other astrophysical effects, which of course has not stopped phenomenologists from coming up with exotic beyond the Standard Model solutions to this discrepancy, see e.g. [91] for a recent example. Setting this issue aside we can extract one more important piece of information for the purpose of this thesis from BBN: Additional dark radiation would increase the expansion rate of the universe, leading to an earlier decoupling from weak interactions, so that BBN would start earlier, also implying that less neutrons would have decayed by the time of the onset of nucleosynthesis. Overall this would increase the nuclear abundances and

2 Motivation

one can set a limit on the total number of relativistic degrees of freedom [90]

$$N_{\text{eff.}} = 2.86 \pm 0.15, \quad (2.35)$$

which constraints the abundances of new light particles. The recent Subaru survey of ten extremely metal poor galaxies by the EMPRESS collaboration revealed less helium than predicted by BBN, which together with previous determinations of the deuterium abundance implies [92]

$$N_{\text{eff.}} = 2.37^{+0.19}_{-0.24}. \quad (2.36)$$

Since this number is in tension with the SM prediction in (2.23), this situation was tentatively named the “helium anomaly”.

2.2.4 Inflation

Inflation offers a dynamical mechanism to replace the Big Bang before the beginning of the radiation dominated phase of cosmic expansion. This passage is supposed to be a short summary of the relevant ideas and is by no means intended to offer a complete overview over the subject. The first version [93] of cosmic inflation was developed as way to dilute the abundance of magnetic monopoles expected from the spontaneous symmetry breaking of a Grand Unified Theory [94] by a phase of exponential expansion. The first proposals of inflationary cosmologies, nowadays known under the moniker “old inflation”, relied on our universe being stuck in a metastable false vacuum driving the exponential expansion and ended via quantum tunneling to the true vacuum. This approach had the drawback of not being able to explain how inflation ended in a radiation dominated universe; in modern terminology it was unable to reheat the universe. The previous drawback stimulated the development of “new inflation” [95, 96] which focuses on the evolution of scalar field in a very flat potential satisfying so called slow-roll conditions. Here inflation ends when the field-velocity of the inflaton becomes so large that the slow-roll approximation introduced further along in this paragraph breaks down. While early theories assumed thermal initial conditions for the inflaton (e.g. a pre-existing thermal bath before the inflationary phase), it was shown in [97] that slow roll inflation is an attractor solution for any sufficiently flat potential and works even with chaotic initial conditions. In this picture the inflaton field can either have Planckian or trans-Planckian initial field values (“large field inflation”) or start from a sub-Planckian field value (“small field inflation”). There is also a third family of scenarios known as “hybrid inflation” [98], which is a class of two-field models that essentially combine slow roll inflation with a phase transition, that is responsible for the exit from the inflationary regime.

Inflation has the appealing advantage of being able to explain many of the shortcomings of the hot Big Bang theory: If one extrapolates the current horizon size back to the Planck time, one finds that our visible universe consisted of a very large number of causally disconnected regions. This begs the question why the universe today and especially the CMB are almost homogeneous and isotropic, if all of these patches never were in

causal contact to begin with, which is also known as the “horizon problem”. In the inflationary picture this is solved by the fact that the initial singularity is moved back from the conformal time $\tau = 0$ to $\tau = -\infty$ so that the past light cones of separated CMB photons have had sufficient time to intersect [99]. The next problem is called the “flatness problem” and involves the observed value of the spatial curvature parameter Ω_{curv} defined in section 2.2.1, which essentially has to be put in by hand as an initial condition since the natural expectation for these quantity during the Planck era would give rise to a much larger value of Ω_{curv} than what is observed today [61]. During inflation this problem is solved because the initial energy density of spatial curvature is diluted by the large, nearly exponential expansion of space. The last initial value problem concerns the entropy of the visible universe today: Since the expansion of the universe proceeded adiabatically to a good approximation (except during the electroweak and QCD crossover transitions, where the number of relativistic degrees of freedom changed rapidly), there is no mechanism to generate the observed amount of entropy except putting it in by hand as initial data. This can be solved via inflationary reheating: After the slow-roll phase the inflaton oscillates coherently around the minimum of its potential, implying that its energy density redshifts like non-relativistic matter. If the inflaton has couplings to radiation fields the condensate can then decay to radiation either perturbatively (instantaneous reheating) or via the non-perturbative process of parametric resonance [100] (also known as “preheating”), which takes the enhancement of the production of bosonic final states from stimulated emission into account. Since there is no thermal bath present during the inflaton decay, this process proceeds out of thermal equilibrium and releases entropy.

Let us end this paragraph by focusing on the basic ingredients and predictions of slow roll inflation: Assume the inflaton φ has a potential $V(\varphi) \ll M_{\text{Pl}}^4$ so that its equation of motion in the expanding space-time reads

$$\ddot{\varphi} + 3H\dot{\varphi} + V'(\varphi) = 0, \quad (2.37)$$

where the prime denotes a derivative with respect to φ and a dot stands for a temporal derivative. The Friedmann equation is given by

$$H^2 = \frac{8\pi}{3M_{\text{Pl}}^2} \left(\frac{\dot{\varphi}^2}{2} + V(\varphi) \right), \quad (2.38)$$

and the equation of state in terms of the energy density ρ and the pressure density P is found to be

$$\omega \equiv \frac{P}{\rho} = \frac{\frac{\dot{\varphi}^2}{2} - V(\varphi)}{\frac{\dot{\varphi}^2}{2} + V(\varphi)}. \quad (2.39)$$

The slow-roll approximation consists of neglecting the acceleration $\ddot{\varphi}$ compared to the Hubble friction $3H\dot{\varphi}$, which implies that [61]

$$\eta \equiv \frac{M_{\text{Pl}}^2}{8\pi} \frac{V''(\varphi)}{V(\varphi)} \ll 1. \quad (2.40)$$

2 Motivation

Nearly exponential expansion of space requires the equation of state $\omega \simeq -1$ so that the potential energy dominates over the kinetic energy, which can be cast as [61]

$$\varepsilon \equiv \frac{M_{\text{Pl.}}^2}{16\pi} \left(\frac{V'(\varphi)}{V(\varphi)} \right)^2 \ll 1. \quad (2.41)$$

One can then compute the inflationary Hubble rate from the potential and (2.38). Inflation ends once either of these slow-roll parameters ε or η grows as large as 1. Conventionally the almost exponential expansion of space between an earlier time with field value φ and the end of inflation at φ_E is parameterized by the Number of e -foldings [61]

$$N_e(\varphi) = \text{Log} \left(\frac{a(\varphi_E)}{a(\varphi)} \right) = \frac{2\sqrt{\pi}}{M_{\text{Pl.}}} \int_{\varphi_E}^{\varphi} \frac{d\varphi}{\sqrt{\varepsilon}}. \quad (2.42)$$

Solving the flatness and horizon problems typically requires $N_e \simeq 50 - 60$ [61]. One of the most striking predictions of inflation is that quantum fluctuations imprinted on the inflaton lead to fluctuations of the energy density, which manifest as scalar perturbations, whose power spectrum measured at the pivot scale k_* is close to the scale invariant Harrison Zel'dovich spectrum [101, 102]. These adiabatic fluctuations described by Gaussian statistics are also the seeds for the formation of large scale structure. The power spectrum as a function of the wave-number k is described by a power law with amplitude \mathcal{P}_ζ and spectral tilt n_S , which would be equal to one for a perfectly scale invariant spectrum

$$P_S(k) = \mathcal{P}_\zeta \left(\frac{k}{k_*} \right)^{n_S-1}. \quad (2.43)$$

In terms of the slow-roll parameters one finds [61]

$$\mathcal{P}_\zeta = \frac{8}{3\varepsilon} \frac{V(\varphi)}{M_{\text{Pl.}}^4}, \quad n_S - 1 = 2\eta - 6\varepsilon. \quad (2.44)$$

Measurements of the matter power spectrum from the CMB by e.g. Planck at $k_* = 0.05 \text{ Mpc}^{-1}$ agree well with this idea and constrain [77]

$$\mathcal{P}_\zeta = (3.044 \pm 0.014) \times 10^{-9}, \quad n_S = 0.9649 \pm 0.042. \quad (2.45)$$

Similarly inflation predicts a spectrum of primordial tensor modes also known as gravitational waves with a spectrum of the form

$$P_T(k) = \mathcal{P}_T \left(\frac{k}{k_*} \right)^{n_T}. \quad (2.46)$$

While scalar perturbations have been observed in the CMB, primordial tensor modes would correspond to so called primordial B -modes in the CMB polarization, which are so far unobserved (B -modes from the gravitational lensing of E -modes were observed though, see e.g. [103]) so we only have an upper bound on the amplitude defined as [61]

$$\mathcal{P}_T = \frac{128}{3} \frac{V(\varphi)}{M_{\text{Pl.}}}, \quad (2.47)$$

conventionally expressed in terms of the tensor-to-scalar-ratio r [61]

$$r \equiv \frac{\mathcal{P}_T}{\mathcal{P}_\zeta} = 16\varepsilon. \quad (2.48)$$

The most stringent limit comes from BICEP2/Keck at the scale $k_* = 0.05 \text{ Mpc}^{-1}$ [104]

$$r < 0.036. \quad (2.49)$$

Monomial inflation models φ^p with $p > 1$ are excluded [77] because their potentials are not shallow enough and lead to too large r . The bounds on r and n_s also exclude e.g. natural inflation [105] and hybrid inflation from spontaneous Supersymmetry breaking [106]. On the other hand it was found that e.g. polynomial inflation [107, 108], Starobinsky's R^2 -model [109], extra scalar fields with a coupling $|\varphi|^2 R$ [110] or α -attractors [111] are still allowed. An overview over inflationary model building can be found in [112]. So far we have no observational information on n_T , however in single field inflation one finds the consistency relation [61]

$$n_T = -\frac{r}{8}. \quad (2.50)$$

Chapters 4-8 involve inflation and reheating to some extent, whereas the inflationary tensor modes are the focus of chapter 7.

2.2.5 Baryogenesis

The observed value of the baryon-to-photon ratio extracted from the CMB in equation (2.27) and BBN in (2.34) requires a dynamical explanation, because the quasi-exponential expansion during cosmic inflation would have diluted away any pre-existing baryon excess. Long before cosmologists thought about inflation and before particle physicists had found a microscopic theory realizing such a dynamical mechanism for Baryogenesis, Andrei Sakharov determined the necessary conditions that would be required [113]:

1. Baryon number violation
2. C and CP violation
3. deviation from thermal equilibrium

The first condition just means that in order to generate non-zero baryon number from an initially baryon symmetric state one needs a violation of baryon number. Intuitively the second condition encodes the requirement of having interactions that favor particles over anti-particles (or vice versa). Since C-violation would only lead to asymmetries between different chiralities one also needs violation of CP for asymmetries between the same chiralities. One can also deduce the second Sakharov condition from more formal density matrix arguments [60]. The last condition is rooted in the fact that the number densities in cosmology depend on the phase space distribution functions for particles and anti-particles, which apart from temperature depend on the chemical potential, whose

2 Motivation

sign is different for particles and anti-particles, and the mass of the particle species. CPT-conservation ensures that particles and anti-particles have the same mass, so their distribution functions can only differ if there is a non-zero chemical potential. In thermal equilibrium however one finds that all chemical potentials vanish [62].

Since the electroweak sphaleron process violates $B+L$ by six units [114, 115], one can convert an asymmetry in lepton number (produced in a $B-L$ violating channel) into an asymmetry in baryon number. This scenario, where $B-L$ is broken by the Majorana mass of heavy right chiral neutrinos, is known as Leptogenesis [116] and chapter 7 discusses the basic mechanism. In chapters 5 and 6, we showcase explicit models that can realize Leptogenesis for Dirac neutrinos [117]. The last chapter of this thesis 8 deals with a scenario inspired by “spontaneous Baryogenesis” [118, 119], which dynamically breaks CPT in the early universe plasma.

3 The Hubble tension and a renormalizable model of gauged neutrino self-interactions

3.1 Contribution and Context

The following chapter is based on the publication

Phys.Rev.D 102 (2020) 11, 115008, arXiv: 2004.13039 [hep-ph]

in collaboration with Dr. Andreas Trautner (AT) and Dr. Sudip Jana (SJ), that was based on the Master’s thesis [120] of the author (MB). AT had the initial idea to construct UV-complete renormalizable model that communicates a gauge interaction from the sterile neutrino sector to the active neutrinos via mass mixing between them and introduced MB to the tension in the determination of the Hubble constant. MB suggested using a second “neutrinophilic” Higgs doublet and together we found that the most simple anomaly-free model requires a sterile Dirac neutrino. During the later stages of the project MB proposed to focus on solving the aforementioned tension in the context of gauge bosons with non-negligible masses. MB carried out all calculations and made all the plots, which were cross-checked and improved upon by AT. SJ contributed to the limits from electroweak precision observables, the estimate for gauge-kinetic mixing and charged Higgs boson searches as well as to the proposed explanation for the MiniBooNE anomaly. AT wrote the majority of the manuscript and MB provided suggestions and input on all aspects of the writing.

As motivated in section 2.2.1 there persists a tension between determinations of the Hubble parameter from the cosmic microwave background and local Cepheid measurements. The analysis in reference [75] suggested that this discrepancy can be solved by a modification of Λ CDM involving both more dark radiation and a new source of neutrino self-interactions parameterized by the cross section $\sigma^{4\nu}$

$$N_{\text{eff.}} = 4.02 \pm 0.29, \quad \sigma^{4\nu} = (5 \text{ MeV})^{-2}. \quad (3.1)$$

Additional dark radiation alone would increase the damping of the large ℓ multipoles and increase the phase-shift at low ℓ [75]. In the Standard Model neutrinos are free-streaming at the time of recombination and exert a gravitational pull on the baryonic plasma [121], which has the same net effect as additional dark radiation. By delaying the free-streaming via a large $\sigma^{4\nu}$ we can allow for larger $\Delta N_{\text{eff.}}$ [75]. The aim of this project

3 Hubble Tension

was to construct a UV-complete, renormalizable model that can realize the required self-interactions via a vector mediator from a gauge symmetry. The key ingredient of our approach is that the required novel interaction only becomes fast (on cosmic timescales) between the epochs of primordial nucleosynthesis and the decoupling of the cosmic microwave background. We further elucidate how our model automatically generates a dark radiation abundance of $\Delta N_{\text{eff.}} \simeq 1$ before or during recombination, that is required to implement the aforementioned self-interacting neutrino solution. We begin with a single eV-scale Dirac neutrino, that is sterile under the SM gauge group but charged under a new abelian gauge symmetry. This gauge interaction with its $\mathcal{O}(10 \text{ eV})$ scale Z' is communicated to the SM neutrinos via mass mixing with the additional neutrino. Such a mixing only generates new interactions for the active neutrinos but not their observed mass scale. Thus our setup is compatible with all (or at least most of the) mass mechanisms proposed in the literature. To generate the aforementioned mixing we introduce a second “neutrino-philic” Higgs doublet with a vacuum expectation value (vev) far below the electroweak scale. In order to comply with Z to invisible decays we have to introduce a singlet scalar, that is also charged under our new gauge symmetry. On top of the published material we added a section explaining the mechanism behind the introduction of the singlet scalar. To summarize we

- constructed a model for long-ranged vector self interactions of the active neutrinos via mass-mixing
- generated the required amount of dark radiation needed for the “self-interacting-neutrino-solution”
- discussed the extended scalar sector with a focus on invisible decays to light states and searches for charged Higgses
- found a potential connection between our set-up and short baseline anomalies

Current status of this solution to the Hubble tension

Updated analyses of Planck data [122, 123] revealed that the bimodal fit for the neutrino-self interaction cross section was a result of the choice of dataset and essentially disappears, when one takes also the Planck 2018 polarization data into account. This does not mean that the self-interacting neutrino solution is ruled out, it is just not favored anymore. Polarization data from the Atacama Cosmology Telescope however seems to favor self-interacting neutrinos over pure ΛCDM [124]. A catalog of the most relevant beyond the Standard Model solutions to the Hubble tension can be found in [80]. One scenario still favored by data involves a Majoron with decays and inverse decays to neutrinos [125]. Since our setup involves resonant Z' exchange, which is nothing more than production of Z' from an inverse decay followed by a decay to neutrinos [126], it is actually a kind of hybrid between this Majoron scenario and the self-interacting neutrino solution (which assumes a constant cross section for sub-MeV energies). Thus the proposed model might actually still be viable, however checking this would require a dedicated cosmological analysis beyond the scope of our original work. Coincidentally the resonant exchange of

a scalar mediator was studied earlier this year in [127] and the authors found a similar mass region for the mediator around the eV-scale, which can lower the Hubble tension down to $(2.3 - 2.8)\sigma$ depending on the dataset used.

3.2 Appendix: Abstract

We present a simple extension of the Standard Model that leads to renormalizable long-range vector-mediated neutrino self-interactions. This model can resolve the Hubble tension by delaying the onset of neutrino free-streaming during recombination, without conflicting with other measurements. The extended gauge, scalar and neutrino sectors lead to observable signatures, including invisible Higgs and Z decays, thereby relating the Hubble tension to precision measurements at the LHC and future colliders. The model has a new neutrinoophilic gauge boson with $m_{Z'} \sim \mathcal{O}(10 \text{ eV})$ and charged Higgses at a few 100 GeV. It requires hidden neutrinos with active-hidden mixing angles larger than 5×10^{-4} and masses in the range $1 \div 300 \text{ eV}$, which could also play a role for short baseline neutrino oscillation anomalies.

3.3 Appendix: Introduction

There is convincing evidence that neutrinos played a substantial role during the epoque of big bang nucleosynthesis (BBN) at $T \sim \text{MeV}$, closely monitored by early element abundances. The lowest temperature scale indirectly probed for neutrinos is $T \sim \text{eV}$, where observations of the cosmic microwave background (CMB) fit well to a history of our universe that does not only comply with the cosmological standard model (ΛCDM), but also with the expectation of the Standard Model of particle physics (SM), including exactly three generations of neutrinos.

However, evidence is accumulating *not only* for a discrepancy between local measurements of today's Hubble rate H_0 [128--132] and therelike global determinations based on ΛCDM together with CMB [133], baryonic acoustic oscillations (BAO) and large scale structure (LSS) datasets [134--143], *but also* for an increasing tension in other parameters [144, 145]. Resolving these discrepancies might require a modification of ΛCDM , preferentially, perhaps, shortly before the era of recombination [146, 147]. Many new physics (NP) scenarios have been discussed, see [125, 147--149]. Naturally, any consistent modification of ΛCDM must be in compliance with a consistent modification of the Standard Model of particle physics (SM).

The positive correlation of H_0 and N_{eff} with the amplitude of the matter power spectrum σ_8 , as observed in CMB data [133], prohibits a resolution of the H_0 tension simply by increasing N_{eff} alone (LSS prefers low σ_8). However, a delay in the onset of neutrino free-streaming during recombination could achieve both: breaking the positive correlation of H_0 and σ_8 , while solving the Hubble tension (HT) at the cost of increasing ΔN_{eff} during recombination [75, 150--154]. Taking into account an effective four-neutrino

3 Hubble Tension

interaction $G_{\text{eff}}^{4\nu}(\bar{\nu}\nu)(\bar{\nu}\nu)$ a good, bi-modal fit to CMB data is obtained with [75, 154]

$$G_{\text{eff}}^{4\nu} \equiv \frac{g_{\text{eff}}^2}{m_{Z'}^2} \approx \begin{cases} (5 \text{ MeV})^{-2} & (\text{SI}), \text{ or} \\ (100 \text{ MeV})^{-2} & (\text{WI}) \end{cases} \quad (3.2)$$

The weakly interacting mode (WI) should be interpreted as an upper limit on $G_{\text{eff}}^{4\nu}$ such that cosmological parameters stay close to ΛCDM [150, 151], without resolving above tensions. Therefore, we focus on the strongly interacting mode (SI), which considerably alters cosmology to resolve the tensions in H_0 and σ_8 while being consistent with local astronomical observations [75, 154].

A valid alternative to heavy new physics would be to generate $G_{\text{eff}}^{4\nu}$ by the exchange of a light mediator. However, it is basically excluded to have very light mediators that recouple during recombination [155, 156] and the same is true for light mediators which are thermalized during BBN [90]. Nonetheless, six orders of magnitude in temperature between BBN and CMB are enough to establish a mass scale, say after a phase transition, and subsequently integrate it out to obtain a decoupling behavior of neutrinos during CMB resembling (3.2). In this way, neutrinos *recouple* by the new interactions only after BBN, and fall out of equilibrium during recombination, see Fig. 3.1.

Here we provide arguably the simplest renormalizable and phenomenologically viable extension of the SM that leads to vector mediated four-neutrino interactions of above characteristic. We first outline the parameter space suitable to address the HT, then present our model and discuss its phenomenology.

3.4 Appendix: Parameter Region

The effective four-neutrino interaction strength in our model is

$$G_{\text{eff}}^{4\nu} \equiv \frac{g_{\text{eff}}^2}{m_{Z'}^2} \equiv \frac{g_X^2 \varepsilon_m^4}{m_{Z'}^2}, \quad (3.3)$$

where g_X is the gauge coupling of a new $U(1)_X$ symmetry, $\varepsilon_m \ll 1$ a mixing between active and hidden ($U(1)_X$ charged) neutrinos, and $m_{Z'}$ the mass of the new gauge boson after $U(1)_X$ breaking. Equating the resulting thermally averaged interaction rate with the Hubble rate, $G_{\text{eff}}^{4\nu} T^5 \approx T^2/M_{\text{Pl}}$, confirms $T_{\text{dec.}} \approx 0.5 \text{ eV}$.

On the other hand, for a range of temperatures $T \gg m_{Z'}$, while ε_m is relevant, the new gauge boson will be effectively massless, inducing a long-range four-neutrino interaction with thermally averaged rate $\Gamma \sim g_{\text{eff}}^4 T$. Requiring this interaction not to thermalize neutrinos prior to BBN, but before recombination, demands

$$2 \times 10^{-7} \lesssim g_X \varepsilon_m^2 \lesssim 5 \times 10^{-6}. \quad (3.4)$$

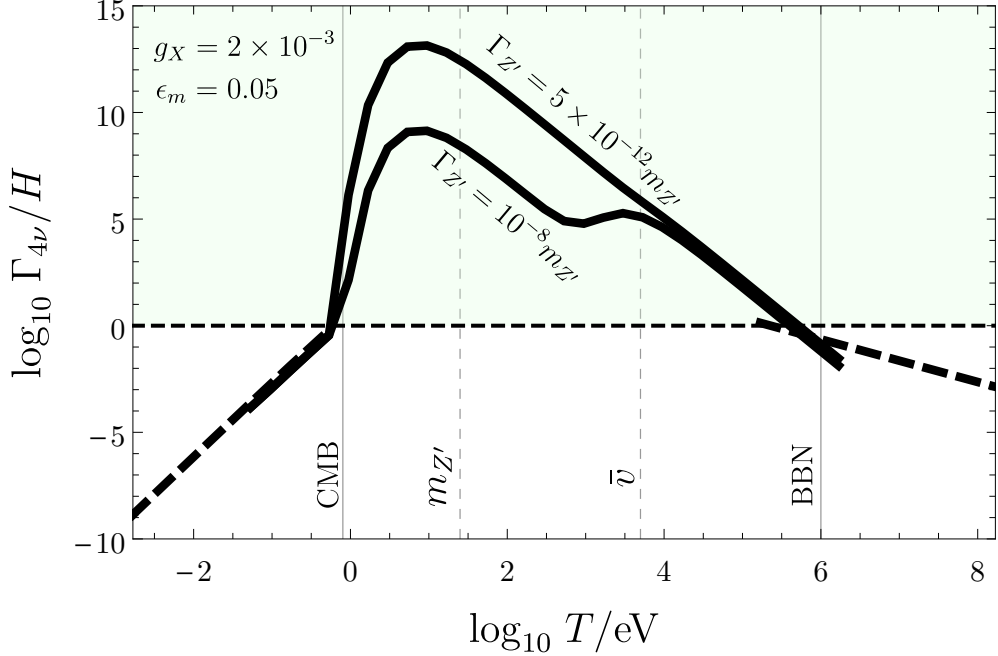


Figure 3.1: Thermally averaged four-neutrino interaction rate relative to the Hubble rate as a function of Temperature for $m_{Z'} = 25$ eV and two different values of the Z' width.

Knowing g_{eff} and $G_{\text{eff}}^{4\nu}$ we can compute

$$1 \lesssim m_{Z'} \lesssim 25 \text{ eV} \quad (\text{SI}). \quad (3.5)$$

Parametrizing $m_{Z'} = g_X \bar{v}$ we can furthermore constrain the effective $U(1)_X$ -breaking vacuum expectation value (VEV)

$$\bar{v} := \frac{m_{Z'}}{g_X} \approx \varepsilon_m^2 \times 5 \text{ MeV} \quad (\text{SI}). \quad (3.6)$$

Fig. 3.1 illustrates this particular re- and decoupling behavior, computed exactly within our model. Eq. (3.6) implies a hierarchy between the relevant scales in the model of

$$\xi := \bar{v}/v_h \approx \varepsilon_m^2 \times 2 \times 10^{-5} \quad (\text{SI}), \quad (3.7)$$

where $v_h = 246$ GeV is the SM Higgs VEV.

3.5 Appendix: The Model

Next to the new $U(1)_X$ gauge symmetry we introduce a pair of SM-neutral chiral fermions $N_{1,2}$ and two new scalars Φ, S with charges shown in Tab. 3.1¹. New interactions for

¹A model similar to ours, albeit in a different parameter region has been investigated in [157--159]. However, baryons are neutral under our $U(1)_X$, implying the absence of large non-standard neutrino-matter

3 Hubble Tension

Field	Φ	N_1	N_2	S	X_μ
Lorentz	S	RH	RH	S	V
$SU(2)_L \times U(1)_Y$	$(\mathbf{2}, -\frac{1}{2})$	$(\mathbf{1}, 0)$	$(\mathbf{1}, 0)$	$(\mathbf{1}, 0)$	$(\mathbf{1}, 0)$
$U(1)_X$	+1	+1	-1	+1	0
$U(1)_L$	0	+1	-1	0	0

Table 3.1: New fields and their charges under Lorentz, SM gauge, new $U(1)_X$ gauge symmetry as well as under global Lepton number (S=Scalar, RH=right-handed Weyl fermion, V=vector).

SM-leptons are

$$\mathcal{L}_{\text{new}} = -y \bar{L} \tilde{\Phi} N_1 - M N_1 N_2 + \text{h.c.}, \quad (3.8)$$

where $\tilde{\Phi} := i\sigma_2 \Phi^*$, y is a Yukawa coupling, and M has mass-dimension one. We treat the one generation case here, but consider three generations of SM leptons and multiple generations of hidden fermions below.

We consider the most general scalar potential consistent with all symmetries,

$$V = V_H + V_\Phi + V_S + V_{H\Phi} + V_{HS} + V_{\Phi S} + V_3, \quad (3.9)$$

with

$$V_\Sigma := \mu_\Sigma^2 \Sigma^\dagger \Sigma + \lambda_\Sigma \left(\Sigma^\dagger \Sigma \right)^2 \quad (\Sigma = H, \Phi, S), \quad (3.10)$$

$$V_{H\Phi} := \lambda_3 \left(H^\dagger H \right) \left(\Phi^\dagger \Phi \right) + \lambda_4 \left(H^\dagger \Phi \right) \left(\Phi^\dagger H \right), \quad (3.11)$$

$$V_{DS} := \lambda_{DS} \left(D^\dagger D \right) \left(S^* S \right) \quad (D = H, \Phi), \quad (3.12)$$

$$V_3 := -\sqrt{2} \mu \left(H^\dagger \Phi \right) S^* + \text{h.c.} \quad (3.13)$$

The scalars are decomposed as $S = \frac{1}{\sqrt{2}} (s + ia_s)$,

$$H = \begin{pmatrix} h^+ \\ \frac{1}{\sqrt{2}} (h + ia_h) \end{pmatrix}, \text{ and } \Phi = \begin{pmatrix} \phi^+ \\ \frac{1}{\sqrt{2}} (\phi + ia_\phi) \end{pmatrix}. \quad (3.14)$$

We choose parameters such that all neutral scalars obtain VEVs $v_\sigma := \langle \sigma \rangle$ for $\sigma = h, \phi, s$, and assume CP conservation in the scalar sector. v_h spontaneously breaks EW-symmetry, v_s breaks $U(1)_X$, and v_ϕ breaks both. Fixing the HT requires $v_h \gg v_s, v_\phi$, cf. (3.7), and

interactions.

we expand all of our expressions to leading order in that hierarchy.

The photon is exactly the same massless combination of EW bosons as in the SM, mixed by the electroweak angle $c_W := m_W/m_Z$ ². By contrast, the very SM-like Z boson contains a minuscule admixture of the new gauge boson X ,

$$Z_\mu = c_X (c_W W_\mu^3 - s_W B_\mu) + s_X X_\mu , \quad (3.15)$$

with an angle³

$$s_X \approx -2 c_W \frac{g_X}{g_2} \left(\frac{v_\phi}{v_h} \right)^2 \ll 1 \quad \text{and} \quad c_X \approx 1 . \quad (3.16)$$

Masses of the neutral gauge bosons up to $\mathcal{O}(\xi^2)$ are

$$m_Z \approx \frac{g_2 v_h}{2 c_W} \quad \text{and} \quad m_{Z'} \approx g_X \bar{v} := g_X \sqrt{v_\phi^2 + v_s^2} . \quad (3.17)$$

The neutrino mass matrix in the gauge basis $(\nu, \bar{N}_1, \bar{N}_2)$ is

$$M_\nu = \begin{pmatrix} 0 & -yv_\phi/\sqrt{2} & 0 \\ -yv_\phi/\sqrt{2} & 0 & M \\ 0 & M & 0 \end{pmatrix} . \quad (3.18)$$

Upon 13--rotating by an angle ε_m ,

$$\tan \varepsilon_m := (yv_\phi)/(\sqrt{2}M) , \quad (3.19)$$

M_ν reveals an *exact* zero eigenvalue, corresponding to approximately massless active neutrinos, and a Dirac neutrino N with $M_N := \sqrt{M^2 + y^2 v_\phi^2}/2$. The massless active neutrinos mix with \bar{N}_2 proportional to s_{ε_m} generating (3.3). Defining $\tan \gamma := v_\phi/v_s$, one can show that

$$M = (y/\sqrt{2}) \varepsilon_m s_\gamma (G_{\text{eff}}^{4\nu})^{-1/2} \ll 5 \text{ MeV} . \quad (3.20)$$

Owing to constraints discussed below the parameter range one should have in mind is $2 \times 10^{-5} \lesssim y \lesssim 6 \times 10^{-3}$, $\varepsilon_m \lesssim 0.05$ and $s_\gamma \lesssim 0.2$. $M_N \approx M$ then turns out to be in the range $1 \div 300$ eV.

Non-zero active neutrino masses are required by neutrino oscillation phenomenology, and also for a successful resolution of the Hubble tension with self-interacting neutrinos [75, 154]. The mass generation for active neutrinos $m_\nu \ll yv_\phi$ can be realized as a small perturbation to the diagonalization of M_ν . In particular, our mechanism is compatible with an effective Majorana mass in $[M_\nu]_{11}$, and, therefore, with any type

²We use abbreviations $\sin \theta_i \equiv s_i$, $\cos \theta_i \equiv c_i$, and $\tan \theta_i \equiv t_i$ for all angles θ_i in this work.

³ s_X can be modified by gauge-kinetic mixing, we comment on this below Eq. (3.28).

3 Hubble Tension

of mass generation mechanism that gives rise to the Weinberg operator [160]. Another minimal possibility in the present model would be to populate $[M_\nu]_{33}$ like in the inverse Seesaw mechanism [161–163]. Also Dirac masses are possible but require additional fermions. This shows that, ultimately, any of the commonly considered neutrino mass generation mechanisms is compatible with our model.

3.6 Appendix: Phenomenology

The scalar sector of the model corresponds to 2HDM+scalar singlet. However, both of the new scalars are charged under the hidden neutrino-specific $U(1)_X$ which considerably alters phenomenology with respect to earlier works [164–169]. Masses of the physical scalars, to leading order in $\xi \equiv \bar{v}/v_h$, are ⁴

$$m_H^2 = 2 \lambda_H v_h^2, \quad m_\Phi^2 = m_A^2 = \frac{2 v_h \mu}{s_{2\gamma}}, \quad (3.21)$$

$$m_{\Phi^\pm}^2 = \frac{v_h \mu}{t_\gamma} - \frac{\lambda_4}{2} v_h^2, \quad (3.22)$$

$$m_{h_S}^2 \approx \xi^2 v_h^2 \left(2\lambda_S - \frac{\lambda_{HS}^2}{2\lambda_H} \right) + \mathcal{O}(\gamma\mu/v_h). \quad (3.23)$$

The neutral scalar mass matrix is diagonalized by three orthogonal rotations $O = R(\theta_{13})R(\theta_{12})R(\theta_{23})$, such that

$$O^T M_{\text{n.s.}}^2 O = \text{diag}(m_{h_S}^2, m_H^2, m_\Phi^2). \quad (3.24)$$

The mixing angles, to leading order in ξ , are given by

$$s_{12} \equiv s_{S\Phi} = s_\gamma, \quad s_{13} \equiv s_{HS} = \xi \frac{p t_\gamma + q}{2 v_h \lambda_H}, \quad (3.25)$$

$$s_{23} \equiv s_{\Phi H} = \xi s_\gamma \frac{\mu (p t_\gamma + q) - 2\lambda_H v_h p}{2 \lambda_H v_h (\lambda_H v_h s_{2\gamma} - \mu)}, \quad (3.26)$$

where we use $\lambda_{34} := \lambda_3 + \lambda_4$ and

$$p := \lambda_{34} v_H s_\gamma - \mu c_\gamma, \quad q := \lambda_{HS} v_H c_\gamma - \mu s_\gamma. \quad (3.27)$$

For the parameter region envisaged to resolve the Hubble tension, there are two new light bosonic fields: next to Z' there is a scalar h_S with mass in the keV range.

To prevent possible reservations about these light states straightaway, let us discuss their coupling to the SM. The only way in which h_S couples to fermions other than neutrinos is via mixing with the SM Higgs. Operators involving h_S linearly can be written as $\mathcal{O}_{h_S} = c_{S\Phi} s_{HS} \times \mathcal{O}_{H \rightarrow h_S}^{\text{SM}}$. Hence, couplings to fermions are suppressed by

⁴We use tadpole conditions to trade $\mu_{H,\Phi,S}$ for other parameters. $m_{\Phi^\pm}^2, m_{h_S}^2 > 0$ imply constraints on the parameter space, see Fig. 3.2.

3.6 Appendix: Phenomenology

their Yukawa couplings and there are no new flavor changing effects. Ref. [170] collects bounds on this scenario. Besides BBN, discussed below, the strongest constraint arises from SN1987A burst duration and requires $(c_{S\Phi}s_{HS})^2 \lesssim 10^{-12}$. Parametrically, $(c_{S\Phi}s_{HS})^2 \sim \xi^2 \sim \varepsilon_m^4 \times 10^{-10}$, avoiding the bound for $\varepsilon_m \lesssim 0.1$.

The dominant coupling of Z' to SM fermions other than neutrinos is by $Z - Z'$ mixing. Given (3.16), Z' couples to the SM neutral current with strength $2g_X(v_\phi/v_h)^2 = 2g_X\xi^2 s_\gamma^2$. For momentum transfer below $m_{Z'}$ this gives rise to new four-fermi (NSI) operators of effective strengths

$$\left(G_{\text{eff}}^{(2\nu)(2f\neq\nu)}/G_F\right) = -2\sqrt{2}\varepsilon_m^2 s_\gamma^2, \quad \text{and} \quad (3.28a)$$

$$\left(G_{\text{eff}}^{(4f\neq\nu)}/G_F\right) = 4\sqrt{2}\xi^2 s_\gamma^4 \approx \varepsilon_m^4 s_\gamma^4 \times 2 \times 10^{-9}. \quad (3.28b)$$

Such feeble effects are currently not constrained by experiment.

We note that the vector mixing of (3.16) can be modified by gauge-kinetic mixing of the U(1) field strengths $\mathcal{L}_\chi = -(s_\chi/2)B^{\mu\nu}X_{\mu\nu}$ [171,172]. This shifts the Z' coupling to the SM neutral current by a negligible amount proportional to $\chi \mathcal{O}(m_{Z'}/m_Z^2)$ [173,174] (given $m_{Z'} \ll m_Z, \chi \ll 1$). More important is the introduction of a coupling of Z' to the electromagnetic current scaling as $c_W c_X \chi$. Experimental constraints on this are collected in [175,176] and our model could, in principle, saturate these limits. Therefore, we stress that $\chi \neq 0$ would neither affect our solution to the HT, nor the H and Z decay rates in Eqs. (3.31) and (3.32) below (to leading order), which are fixed by Goldstone boson equivalence.

We thus focus on effects directly involving neutrinos. For $T \lesssim v_\phi$, neutrino mixing is active. As required by direct-search bounds [177–180] and PMNS unitarity [181] (as extracted from [182]) we assume [157,158]

$$\varepsilon_m^{(e)} \leq 0.050, \quad \varepsilon_m^{(\mu)} \leq 0.021, \quad \varepsilon_m^{(\tau)} \leq 0.075, \quad (3.29)$$

for mixing with e, μ, τ flavors. These are the most conservative bounds in the mass range set by Eq. (3.20), and often larger mixings can be allowed, especially for light masses and non- e flavors. For $M \lesssim 10$ eV oscillation experiments become important, requiring a dedicated analysis, see e.g. [183], nonetheless still allowing (3.29). Since nothing in our resolution of the HT is required to depend on flavor, we adopt $\varepsilon_m \sim 5 \times 10^{-2}$ as a universal benchmark value.

Couplings of neutrinos to Z' at low T are given by $g_X\varepsilon_m^2$ with a strength set by (3.4). This gives rise to the four-fermion operators (3.3,3.28), but also to the possibility of Z' emission off neutrinos. Eq. (3.4) together with $g_X \lesssim 1$ implies a *lower* bound $\varepsilon_m \gtrsim 5 \times 10^{-4}$. This fuels the intuition that this model is testable.

Constraints on neutrinos directly interacting with light mediators are collected in

3 Hubble Tension

[125, 184--191]. The strongest laboratory constraints arise from meson [184, 192--201] and nuclear double-beta decays [202--206]. However, even the most stringent bounds for the least favorable flavor structure cannot exclude $g_{\text{eff}} \lesssim 10^{-5}$ for light $m_{Z'}$. While most experiments constrain light scalar (majoron) emission, the present study emphasizes the need to reanalyze those also for light vectors. The most important constraint is SN1987A neutrino propagation through the cosmic neutrino background (CνB) [207]. The exact bound depends on the neutrino masses and rank of y , but even the most pessimistic assumptions allow $g_{\text{eff}} \lesssim 5 \times 10^{-4}$ for $m_{Z'} < 60$ eV.

The $\bar{\nu}\nu \leftrightarrow \bar{\nu}\nu$ scattering cross section via Z' exchange is approximated by

$$\sigma^{(4\nu)}(s) = \frac{g_X^4 \varepsilon_m^8}{12 \pi} \frac{s}{(m_{Z'}^2 - s)^2 + m_{Z'}^2 \Gamma_{Z'}^2}. \quad (3.30)$$

To generate Fig. 3.1 we include the t -channel and use Maxwell-Boltzmann thermal averaging [208], while noting that a more refined analysis should employ Fermi-Dirac statistics [209, 210]. For $m_{Z'} > 2M_N$, Z' decays to $\bar{N}_1 N_1$, $\bar{N}_2 N_2$, $\bar{\nu} N_2 (\nu \bar{N}_2)$ and $\bar{\nu}\nu$, while for $m_{Z'} \lesssim M_N$ only the last channel is accessible. The respective total widths are $\Gamma_{Z'}/m_{Z'} \approx 10^{-7}$ or 10^{-12} , corresponding to Z' lifetimes from micro- to tens of picoseconds. We show thermally averaged rates (dashed) obtained by dimensional analysis for $T \gg v_\phi$. For $T \ll m_{Z'}$ we reproduce the scaling of the effective operator (3.2). Obviously, before recombination $\Gamma_{4\nu}(T)$ differs from the effective theory. This would not qualitatively change the conclusions of [75, 150--154], which are based on the (non-)free-streaming nature of neutrinos, see also [211]. Nonetheless, this motivates a dedicated cosmological analysis to tell if our specific temperature dependence could be discriminated from the effective model.

Finally, we discuss the coupling of neutrinos to h_S . For massless active neutrinos and conserved lepton number, diagonalization of (3.18) is exact in s_{ε_m} . This prevents a quadratic coupling of neutrinos to h_S . Hence, SM neutrinos couple to h_S only in association with hidden neutrinos, or suppressed by their tiny mass (e.g. $[M_\nu]_{11} \sim m_\nu$ produces such a coupling). In both cases effects are unobservably small, also because of the vastly suppressed coupling of h_S to matter targets.

Also modification of Z decays to neutrinos are unobservably small. Even if N mixes with ν , the invisible Z width is unaltered for $M_N \ll m_Z$ [177]. The vertex $Z\bar{N}\nu$ also leads to N production from neutrino upscattering on matter targets, suppressed by ε_m compared to G_F . N decays invisibly leaving an unaccompanied recoil as signature.

Any consistent model of strong neutrino self-interactions requires a modification of the SM scalar sector. These are amongst the most visible effects of this model. The necessary modifications imply new invisible decays of SM Z and Higgs. To leading order

3.7 ADDENDUM: Why do we need the singlet?

in ξ , rates of the most prominent decays are

$$\Gamma_{H \rightarrow h_S h_S} = \frac{v_h^2}{32 \pi m_H} \left[\lambda_{HS} c_\gamma^2 + \lambda_{34} s_\gamma^2 - \frac{\mu s_{2\gamma}}{v_h} \right]^2, \quad (3.31)$$

$$\Gamma_{H \rightarrow Z' Z'} = \Gamma_{H \rightarrow h_S h_S}, \quad \Gamma_{Z \rightarrow Z' h_S} = \frac{m_Z g_2^2 s_\gamma^4}{192 \pi c_W^2}, \quad (3.32)$$

and to leading order in ξ and γ (the exact expression in γ is known)

$$\Gamma_{H \rightarrow ZZ'} \stackrel{\gamma \ll 1}{=} \frac{g_2^2}{c_W^2} \frac{(m_H^2 - m_Z^2)^3}{m_H^3 m_Z^2} \frac{\xi^2 s_\gamma^4}{16 \pi} \left(1 + \frac{\lambda_{HS}}{4 \lambda_H} \right)^2. \quad (3.33)$$

$\Gamma_{H \rightarrow \text{inv.}} \leq 1.3$ MeV [212--214] and $\Gamma_{Z \rightarrow \text{inv.}}^{\text{new}} \leq 2.0$ MeV [215] constrain the parameters as shown in Fig. 3.2. $\Gamma_{Z \rightarrow Z' h_S}$ requires $\gamma \lesssim 0.4$. $\Gamma_{H \rightarrow \text{inv.}}$, without fine tuning, demands $\lambda_{HS}, \lambda_{34}, (\mu s_{2\gamma}/v_h) \lesssim \mathcal{O}(10^{-2})$. $\Gamma_{H \rightarrow ZZ'}$ then is merely a rare Higgs decay with $\text{BR}(H \rightarrow ZZ') \approx 10^{-8} \varepsilon_m^4 s_\gamma^4$.

The model without S is excluded by $\Gamma_{Z \rightarrow Z' h_S}$, which would be given by (3.32) with $\gamma \rightarrow \pi/4$. The constraints on γ further limit the allowed mass range of M , cf. Eq. (3.20), and we show corresponding values of M in Fig. 3.2.

Charged scalars Φ^\pm couple to ℓ^\pm and N via (3.8). Constraints on y arise from $\ell_1 \rightarrow \ell_2 \gamma$ and measured lepton magnetic moments, both mediated by a loop of Φ^\pm and N . Exact constraints are given in [157]. Here it suffices to note that certainly $y \lesssim \mathcal{O}(1)$ for all flavors, as much tighter constraints are found below.

The coupling of Φ^\pm to quarks is suppressed by $s_\gamma \xi$ and standard LHC searches [216, 217] do not apply. At LEP, Φ^\pm could have been pair-produced via s -channel γ/Z or t -channel N , or singly-produced associated with charged and neutral leptons. Φ^\pm dominantly decays to $N_\alpha \bar{\ell}_\beta$ with BRs set by y . N further decays to neutrinos via Z' . The final state for Φ^\pm hence is $\ell_\beta^\pm + \text{MET}$. LEP limits on Φ^\pm pair-production [218] and a reinterpreted LEP selectron search [219--222] imply a lower bound $m_{\Phi^\pm} > 100$ GeV⁵.

Regarding electroweak precision, there are no new tree-level contributions to $\rho \equiv \alpha T$. We follow [225] for one-loop corrections. T is always enhanced compared to the SM, staying in the allowed interval $T = 0.09 \pm 0.13$ [226] for $|m_{\Phi^\pm} - m_\Phi| \lesssim 120$ GeV.

3.7 Addendum: Why do we need the singlet?

In this section we summarize the idea behind adding the singlet scalar. As explained in [120] if there was no singlet scalar, then the lightest scalar would come from the neutral component of the new doublet Φ and for the extent of this section we will call it

⁵Sometimes $m_{\Phi^\pm} \gtrsim 275$ GeV is quoted based on [223]. However, this requires assumptions on Φ^\pm -BRs see [224, Sec. 4.7] for details.

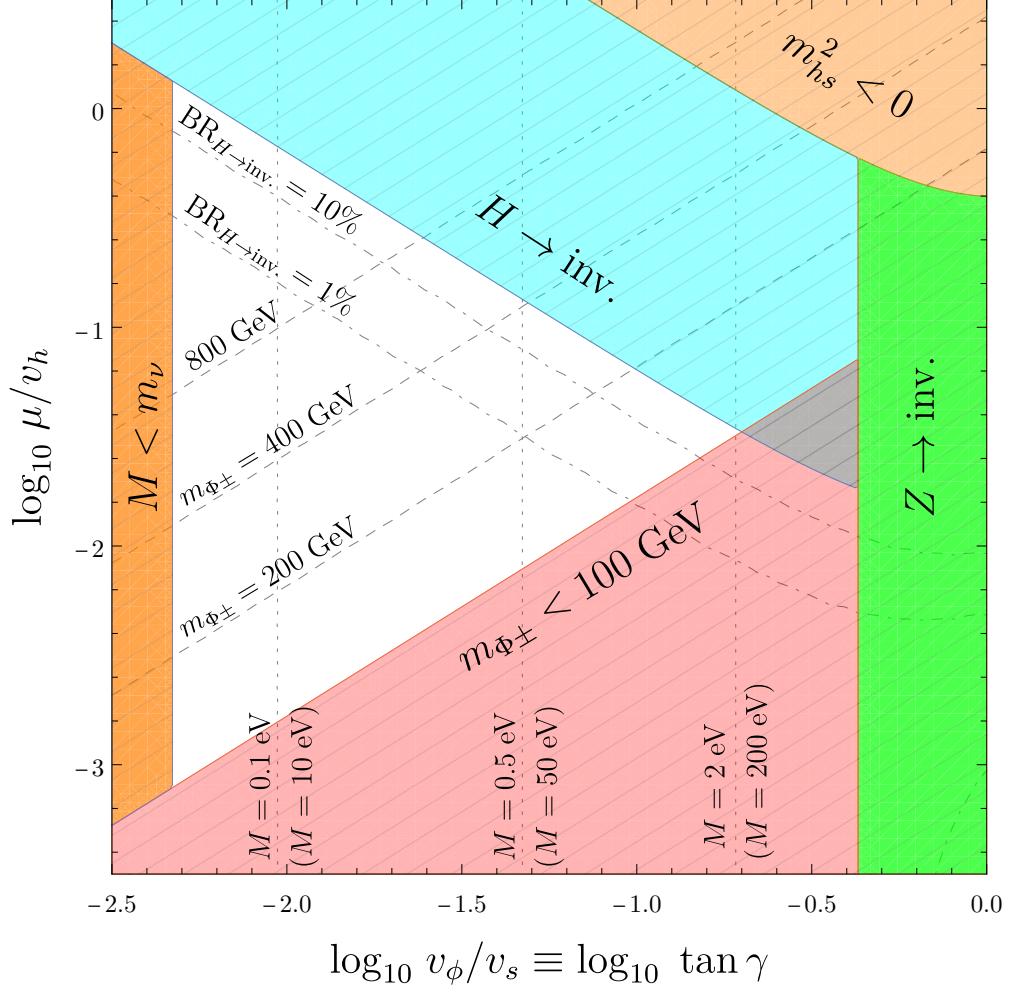


Figure 3.2: Allowed region (blank) in the $\tan \gamma$ -- (μ/v_h) plane. The region is independent of any other free parameters as long as $\lambda_{HS}, \lambda_{34} \ll \mathcal{O}(10^{-2})$ (for definiteness, we have chosen scalar potential parameters as $\lambda_{HS} = 0.001$, $\lambda_3 = 0.002$, $\lambda_4 = 0.003$, $\lambda_\Phi = 0.3$, $\lambda_S = 0.4$, $\lambda_{\Phi S} = 0.5$). The Hubble tension can be resolved in the entire allowed region. We show equilines of the corresponding hidden neutrino mass M for benchmark parameters $\varepsilon_m = 0.05$, $g_X = 2 \times 10^{-3}$, and $y = 6 \times 10^{-5}(6 \times 10^{-3})$. In the orange region $M < m_\nu$ (for $y = 6 \times 10^{-5}$) which is inconsistent with our assumptions.

\tilde{h}_Φ . Since Φ couples to both hypercharge and weak isospin, it is not surprising that there is a new decay mode for the Z -boson and by explicit calculation one finds

$$\Gamma \left(Z \rightarrow Z' \tilde{h}_\Phi \right) \simeq \frac{g_2^2}{192\pi \cos(\theta_W)^2} m_Z \simeq 8 \text{ MeV.} \quad (3.34)$$

3.7 ADDENDUM: Why do we need the singlet?

The total decay width of the Z was measured at LEP and from this one can extract the partial width for decays to electrically uncharged non-hadronic states, a.k.a “invisible” final states [227]

$$\Gamma_{\text{tot}}(Z \rightarrow \text{Invisibles}) = (499.0 \pm 1.5) \text{ MeV}. \quad (3.35)$$

Compared to the theoretical prediction of [215]

$$\Gamma_{\text{SM}}(Z \rightarrow \text{Invisibles}) = (501.3 \pm 0.6) \text{ MeV}. \quad (3.36)$$

this leaves

$$\Gamma_{\text{new}} = \Gamma_{\text{SM}} - \Gamma_{\text{tot}} = (2.3 \pm 1.6) \text{ MeV} \quad (3.37)$$

for contributions from new physics. Consequently the decay in (3.34) would be ruled out by data. The fact that the leading order contribution in (3.34) does not depend on any new coupling like g_X or a small mixing angle can be understood in two ways: The gauge kinetic term of the second doublet $(D_\mu \Phi)^\dagger D^\mu \Phi$ involves an operator of the form $v_\Phi Z_\mu Z'^\mu \tilde{h}_\Phi$ which gives rise to a squared matrix element, which is proportional to $(g_2 g_X v_\Phi / \cos(\theta_W))^2$. Summing over the polarizations of the Z' the gives a factor of $1/m_{Z'}^2$, and by using that $m_{Z'} = g_X v_\Phi$ one finds that the new parameters all divide out, leaving only known electroweak couplings. On the other hand we can employ the Goldstone-boson-equivalence theorem [228] for the production of the longitudinal Z' : For the electroweak sector we work in the unitary gauge ($\xi_2, \xi_Y = \infty$), which decouples all would-be-Nambu-Goldstone bosons responsible for making the electroweak gauge fields massive and for the $U(1)_X$ we work in 't Hooft-Feynman gauge ($\xi_X = 1$), which retains the would-be-Nambu-Goldstone boson \tilde{a}_Φ in the spectrum. The gauge kinetic term of Φ then leads to an operator of the form $Z_\mu (\partial^\mu \tilde{a}_\Phi) \tilde{h}_\Phi$ and the matrix element squared will be essentially given by $(g_2 / \cos(\theta_W))^2 p^2$, where $p^2 = m_Z^2$ comes from the derivative coupling and gets canceled by the $1/m_{Z'}^2$ from the polarization sum for the Z -boson (the factor of m_Z in (3.34) comes from the phase space integral).

In order to make our model phenomenologically viable we introduce a singlet scalar with $U(1)_X$ charge, which is accompanied by a mixing angle γ . Due to the mixing in the scalar sector there are now four decay modes and because mixing is a unitary operation the couplings split up as follows:

- $\Gamma(Z \rightarrow h_S Z') \sim \sin(\gamma)^4$
- $\Gamma(Z \rightarrow h_S A) \sim \sin(\gamma)^2 \cos(\gamma)^2$
- $\Gamma(Z \rightarrow \Phi Z') \sim \sin(\gamma)^2 \cos(\gamma)^2$
- $\Gamma(Z \rightarrow \Phi A) \sim \cos(\gamma)^4$

As it turns out we can make both Φ and A (much) heavier than m_Z , since their mass gets a contribution from the trilinear term $\sqrt{2} \mu (H^\dagger \Phi) S^*$ involving all three scalars.

3 Hubble Tension

This means that only the mode $Z \rightarrow h_S Z'$ is kinematically allowed and we can make the corresponding partial width compatible with data for $\gamma \lesssim 0.4$. Note that this idea of decoupling a light state originating from a doublet scalar by adding a singlet scalar is very similar to the idea behind the DFSZ axion [229, 230]: The original Weinberg-Wilczek axion [231, 232] was embedded in a two Higgs doublet model and later ruled out because it would have lead to a too large branching ratio for Kaon decays due to the process $K^+ \rightarrow \pi^+ a$. The remedy came in the form of “invisible-axion”-models [229, 230] that add a scalar singlet so that the physical axion is a linear combination of the phases of all three scalar fields.

3.8 Appendix: BBN

The bound on $\Delta N_{\text{eff}}^{\text{BBN}}$ during BBN [90] prohibits any of the new light species, Z' , N , or h_S , to be in thermal equilibrium with the SM during BBN. Ultimately, a thermal QFT analysis seems worthwhile to fully explore the early universe cosmology of this model for $T \gg v_\phi$. The coupled Boltzmann equations then should be solved to track abundances precisely, but this is beyond the scope of this letter. Nonetheless, an order of magnitude estimate suffices to clarify that there are parameters for which BBN proceeds as usual.

While m'_Z is fixed by (3.5), M_N is limited by (3.20), and $m_{h_S} \approx \xi v_h \sqrt{2\lambda_S} \approx 7\varepsilon_m^2 \sqrt{\lambda_S}$ MeV. Hence, neither of these states can simply be pushed beyond the MeV scale to avoid BBN constraints. Instead, we discuss the possibility that all of them are sufficiently weakly coupled to the SM such that a thermal abundance is not retained. While all of the new fields thermalize with the SM at EW temperatures, this changes once the heavy scalars freeze out. The abundance of new light states is subsequently diluted by reheating in the SM. We thus focus on temperatures around BBN.

The coupling of Z' to the SM, as well as active-hidden neutrino mixing ε_m , is only effective after the $U(1)_X$ breaking phase transition [233]. This warrants that Z' does not thermalize with the SM between EW and BBN. Regarding h_S , the most relevant processes for thermalization are $e^+e^- \leftrightarrow h_S h_S$, $e^-\gamma \leftrightarrow e^- h_S$, and $\nu\bar{\nu} \leftrightarrow h_S h_S$. None of them reaches thermal equilibrium due to the highly suppressed couplings of h_S . The leading process thermalizing N ’s with the SM is $e^+e^-(\nu\bar{\nu}) \leftrightarrow N\bar{N}$ via t -channel Φ^\pm (Φ, A) exchange, which scales as $\Gamma \sim (y/m_{\Phi^\pm})^4 T^5$. Requiring this to be absent after QCD (EW) epoch demands $y \lesssim 6 \times 10^{-3(5)} (m_{\Phi^\pm}/100 \text{ GeV})$. Together with above bounds on ε_m and $\gamma \lesssim 0.2$ this implies $M \lesssim 300(3) \text{ eV}$. Consistency of our analysis requires $m_\nu \ll y v_\phi \ll M$, implying $y \gg 2 \times 10^{-5} (m_\nu/0.05 \text{ eV})$ and a lower bound on γ , shown in orange in Fig. 3.2 for $m_\nu = 0.05 \text{ eV}$ ⁶. Noteworthy, this limits M_N to values which can resolve short baseline neutrino anomalies: *Either* in the well-known way with eV-scale states, see e.g. [183, 234], which however is already in considerable tension with other experiments [183] and certainly requires specific assumptions on the flavor dependence of

⁶This is the minimal possible value of m_ν for at least one generation, as allowed by neutrino oscillation experiments.

the mixing angle ε_m . Or, by realizing the novel ‘‘decaying sterile neutrino solution’’ for $M_N \sim \mathcal{O}(100) \text{ eV}$ [235, 236], which requires the assumption $\varepsilon_m^e \gg \varepsilon_m^\mu$ [235].

Finally, we note that despite bearing some danger for BBN, the new states can also be a virtue: To resolve the HT with self-interacting neutrinos, N_{eff} must be enhanced to $\Delta N_{\text{eff}}^{\text{CMB}} \approx 1$ during recombination [75, 154], requiring some energy injection in the dark sector after BBN. The thermalization of N, h_S, Z' with n flavors of active neutrinos after BBN produces entropy [237] which is released back to the neutrino background after the new states decay, before recombination. This would heat the neutrinos to $T'_\nu \approx [1 + 30/7n]^{1/12} T_\nu$ resulting in $\Delta N_{\text{eff}}^{\text{CMB}} \approx 1.03, 0.93, 0.74$ for $n = 3, 2, 1$. Regarding the decays of the light states to neutrinos, we note that h_S decays to $\bar{N}_1 \nu$ and $\bar{N}_1 N_2$, but in absence of L -violation not to $\bar{\nu} N_2$, $\bar{N}_{1(2)} N_{1(2)}$ or $\bar{\nu} \nu$ (or all processes barred), with $\Gamma_{h_S} \propto y^2 s_\gamma^2$. τ_{h_S} , therefore, is extremely dependent on the exact parameters ranging from milli- to picoseconds. Two-body decays $N \rightarrow Z' \nu$ contribute, provided $M_N > m_{Z'} + m_\nu$. For $M_N < m_{Z'} + m_\nu$, on the other hand, only three-body decays $N \rightarrow (2\nu) \bar{\nu}$ are possible with lifetime $\tau_N \sim (8\pi)^{-3} M_N^5 G_{\text{eff}}^{4\nu^2} \varepsilon_m^{-2}$. Depending on the exact parameters, a population of N , thus, *could* but doesn’t have to decay before recombination.

3.9 Appendix: Discussion

We have presented a consistent (renormalizable and phenomenologically viable) model that leads to vector-mediated neutrino self-interactions. In a narrow region of parameter space these interactions have the right strength to resolve the tensions between local and global determinations of H_0 and σ_8 ⁷. To consistently implement such interactions in the SM, we had to introduce a second Higgs doublet and a new Dirac fermion, both charged under a new $U(1)_X$ gauge symmetry. Phenomenological consistency required the introduction of the $U(1)_X$ charged SM singlet scalar S .

There are several new states, all with very lepton-specific couplings: h_S with mass of $\mathcal{O}(10 \text{ keV})$, as well as Φ , pseudo-scalar A and the charged scalars Φ^\pm all with masses of $\mathcal{O}(100 \text{ GeV})$. The new, naturally neutrinoophilic fore carrier has a mass of $m_{Z'} \sim \mathcal{O}(10 \text{ eV})$, and the new hidden neutrinos masses in the range $M_N \sim 1 \div 300 \text{ eV}$ and mixing angles $\varepsilon_m > 5 \times 10^{-4}$. The allowed parameter space can be narrowed down by more precise measurements of $H_0 \rightarrow \text{inv.}$ and searches for leptophilic charged Higgses at the HL-LHC and future colliders such as ILC, CLIC, or FCC-he/hh. Other testable signatures include non-standard neutrino matter interactions with maximal strength $G_{\text{eff}}^{(2\nu)(2f \neq \nu)} \sim \mathcal{O}(10^{-4}) G_F$, as well as distortions of short baseline neutrino oscillations.

That our model works without specifying the mechanism of neutrino mass generation may feel like a drawback to some. We think this is a virtue, as it renders this scenario compatible with all standard neutrino mass generation mechanisms.

⁷Our model is viable also in a different parameter space not discussed here: For $m_{Z'} \ll \text{eV}$ and $g_X \ll 10^{-7}$, active neutrinos recouple only after recombination, with crucial impacts on the CνB.

3 Hubble Tension

The least appealing feature of our model, perhaps, is the introduction of several new scales (v_ϕ, v_s, μ, M), and some hierarchies among them. We have nothing to say here about this or any other hierarchy problem but simply accepted this fact for the reason that we are convinced that this is the simplest renormalizable model in which *active* neutrinos pick up gauged self-interactions. Stabilizing these hierarchies against radiative corrections might require smaller scalar quartic cross-couplings than the direct constraints discussed above. Suchlike would not contradict any of our findings.

Finally, our analysis also shows that “model independent” considerations are actually not always valid in concrete models. On the contrary, only complete models allow to directly relate early universe cosmology, like the Hubble tension, to physics testable in laboratories.

3.10 Appendix: Note

During the completion of this work, Ref. [238] appeared on the arXiv which discusses a different UV complete model for self-interacting neutrinos.

3.11 Appendix: Acknowledgments

We would like to thank V. Brdar, L. Graf, and M. E. Krauss for useful conversations as well as O. Fischer, A. Ghoshal, M. Ratz, and S. Vogl for comments on the manuscript. In particular we thank S. Vogl for pointing out the entropy production in the hidden sector re- and de-coupling dynamics. This work benefited from using the computer codes **SARAH** [239], **FeynArts/FormCalc** [240, 241], and **PackageX** [242].

4 Freeze-In of radiative keV-scale neutrino dark matter from a new $U(1)_{B-L}$

4.1 Contribution and Context

The following chapter is based on the single-author publication

JHEP 09 (2022) 101, arXiv: 2203.04276 [hep-ph]

and the author of this thesis was responsible for the conception and implementation of all aspects of the publication.

The starting point of this project was the observation that a dark matter fermion χ could receive its mass from the SM Higgs doublet via a Weinberg operator of the form $\bar{\chi}\chi H^\dagger H$. This observation prompted the question of whether such a DM candidate could also be produced from the very same operator. Phase space arguments [87] require fermionic dark matter (DM) with masses above a scale of about 100 eV in order to be gravitationally bound inside a halo, which is why (single species) fermionic DM must have masses of at least a keV. Structure formation studies [243] refined this limit further and depending on the warmness of DM one typically needs masses above 5-16 keV. We start from the Dirac Scotogenic model [54, 55] that explains the neutrino mass scale via loop diagrams involving heavy vector-like neutrinos and both an inert doublet and singlet scalar. Usually the particles running inside the loop are good thermal WIMP dark matter candidates, but here we use additional SM singlet fermions. These fermions get their masses from loop diagrams involving the doublet and singlet scalars together with new vector-like leptons. The active neutrino masses require super-heavy sterile neutrinos with masses at the 10^{11} GeV scale, whereas the DM particles only need vector-like leptons with masses around the 10 TeV scale, potentially accessible at next generation colliders due to their electroweak gauge interactions. In this theory the particle content is dictated by a new gauged $U(1)_{B-L}$ symmetry. As a consequence of this charge assignment only two of the SM neutrinos and the Dirac dark matter become massive. In order to forbid Majorana masses for any of the new fermions and to ensure the stability of dark matter we impose an additional \mathcal{Z}_5 symmetry by hand. This symmetry forbids any mixing between dark matter and the neutrinos. We assume that all the particles running in the loop are too heavy to be produced in the early universe plasma. It turns out that the production from out-of-equilibrium Higgs decays overproduces keV-scale dark matter (it produces the correct amount of lighter dark matter excluded by structure formation) unless reheating occurs at low temperatures $T_{RH} \lesssim 5$ GeV. Successful Big Bang Nucleosynthesis requires $T_{RH} \gtrsim 4$ MeV [244, 245]. These arguments lead us to consider the joint production of dark

4 Radiative keV-scale DM

matter and right handed neutrino dark radiation from the out-of-equilibrium (also known as “Freeze-In” [82]) gauge scatterings of the SM fermions via the exchange of the B-L gauge boson Z' . If the production from gauge scatterings is supposed to be the dominant mode, we predict that the DM mass has to be below the MeV-scale, since otherwise production from the SM fermions via off-shell Higgs exchange becomes the dominant production channel. In that case the DM could be as heavy as $m_{\text{DM}} \lesssim 2 \text{ GeV}$, as allowed by Higgs to invisible decays, but we choose to focus on the keV-scale instead. The right handed neutrinos would contribute to dark radiation by an amount of $\Delta N_{\text{eff.}} \lesssim 0.012$. Bounds on off-shell Z' from four-lepton-operators at LEP II constrain the B-L breaking vev to be above 6.9 TeV [215] and depending on the combination of m_{DM} and T_{RH} our model can work for a vev at the 100 TeV scale. Our scenario involves two doublet and two singlet scalars. Only one doublet gets a vev and is identified with the SM Higgs. Out of the singlets only one field gets a vev and is identified with the B-L breaking scalar, which has no direct couplings to fermions. The last part of this chapter checks, whether this model can generate the required value of the reheating temperature. We find that the most likely candidate for the inflaton field is the inert singlet scalar and for concreteness we assume a non-minimal coupling to gravity. Reheating and Baryogenesis might involve additional vector-like quarks. This work introduces

- a model for radiative one-loop keV-scale dark matter Dirac masses
- a symmetry argument for why only two of the light neutrinos have masses
- a production channel for both dark matter and dark radiation via Freeze-In from Z' exchange with the SM fermions
- a reason to consider GeV-scale reheating temperatures

4.2 Appendix: Abstract

We extend the Dirac Scotogenic model with the aim of realizing neutrino masses together with the mass of a keV-scale dark matter (DM) candidate via the same one-loop topology. Two of the Standard Model (SM) neutrinos become massive Dirac fermions while the third one remains massless. Our particle content is motivated by an anomaly free $U(1)_{\text{B-L}}$ gauge symmetry with exotic irrational charges and we need to enforce an additional \mathbb{Z}_5 symmetry. The dark matter candidate does not mix with the active neutrinos and does not have any decay modes to SM particles. DM is produced together with dark radiation in the form of right handed neutrinos via out of equilibrium annihilations of the SM fermions mediated by the heavy B-L gauge boson. In order to avoid DM over-production from Higgs decays and to comply with Lyman- α bounds we work in a low temperature reheating scenario with $4 \text{ MeV} \lesssim T_{\text{RH}} \lesssim 5 \text{ GeV}$. Our setup predicts a contribution to $\Delta N_{\text{eff.}}$ that decreases for larger DM masses and is below the sensitivity of upcoming precision measurements such as CMB-S4. A future observation of a signal with

$\Delta N_{\text{eff}} \gtrsim 0.012$ would exclude our scenario. We further sketch how inflation, reheating and Affleck-Dine Baryogenesis can also be potentially realized in this unified framework.

4.3 Appendix: Introduction

In most models of the Scotogenic variety one uses the lightest stable particle from the loop diagram for the neutrino masses as a DM candidate. For the original scotogenic model [246–249] this is either the lightest neutral component of the inert scalar doublet η or the lightest sterile neutrino produced as thermal WIMPS. In the Dirac version of the model [54, 55] the DM can either the lightest neutral component of η or the singlet σ or the lightest vector-like neutrino. Later it was realized that keV scale FIMP DM is also possible in the scotogenic picture [250], but no mechanism was proposed for why this particular sterile neutrino is so much lighter than the other two. Reference [251] analyzed a model based on the DFSZ axion scenario [229, 230], where a one loop diagram with vector-like fermions generates the keV-scale Majorana masses for a DM candidate. The authors of [252–254] showed that it is possible to construct models in which both the active and the sterile neutrino masses are obtained from loop diagrams. Recently a loop based extension of the Seesaw scenario [29, 30, 255] with keV to GeV scale Majorana dark matter was put forth in [256], where two different scalar couplings were responsible for the mass generation and production from out of equilibrium Higgs decays. Unlike previous constructions we focus on Dirac neutrinos. We choose an abelian gauge symmetry as the guiding principle for building our model. After reviewing the Dirac Scotogenic model in section 4.4.1 we introduce our mechanism for generating the DM mass via a dimension five operator that resembles the Weinberg operator [23] in 4.4.2. In 4.5.2 we find that producing such a dark matter from out of equilibrium Higgs decays is not compatible with Lyman- α bounds on the DM mass. Section 4.5.4 demonstrates that the gauge symmetry is crucial for producing the correct amount of DM in the freeze-in scenario. We compute the minuscule amount of dark radiation produced by a similar freeze-in process in section 4.6. The necessary cosmic history can be realized in an inflationary context as explained in section 4.7. We close by illustrating how our set-up can potentially realize Affleck-Dine Baryogenesis [257] in section 4.8.

4.4 Appendix: The model

4.4.1 The Dirac Scotogenic model

Let us begin by reviewing the most salient features of the Scotogenic Model for Dirac neutrinos [54, 55]. The goal is to generate the first diagram in figure 4.1. We follow the treatment of [258], where a U(1) symmetry is imposed on the fermionic sector that gets softly broken by the following trilinear term in the scalar potential

$$V(H, \eta, \sigma) \supset \frac{\kappa}{\sqrt{2}} \left(\eta^\dagger H \sigma + \text{h.c.} \right), \quad (4.1)$$

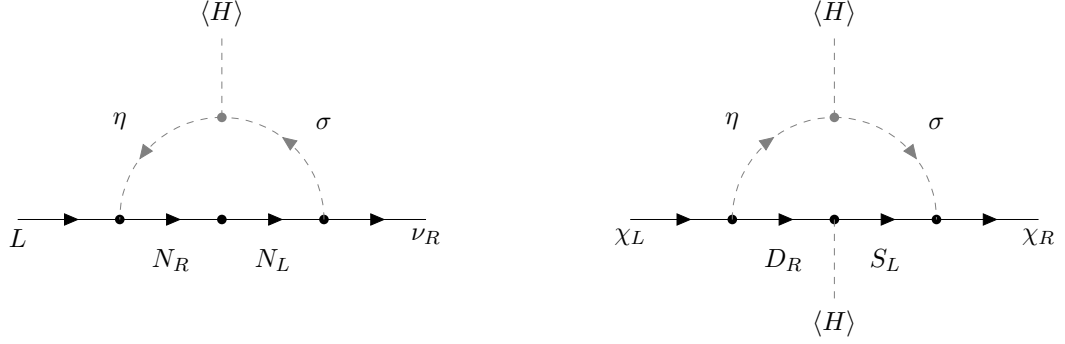


Figure 4.1: Feynman diagrams in the gauge basis responsible for the creation of the neutrino and dark matter (χ) Dirac masses at the one loop level.

where κ is a dimensionful parameter of mass dimension one. Here H is the SM Higgs and η, σ are inert doublet and singlet scalars with charges under the new symmetry. All particles and charges can be found in table 4.1. We start from $U(1)_{B-L}$ and assign conventional B-L charges -1 to L and e_R , whereas the right handed neutrinos ν_R have the charge $Q_1 \neq -1$ so that the tree level mass term $\overline{L}\epsilon H^\dagger \nu_R$ is forbidden by the symmetry. Here $\epsilon = i\sigma_2$ denotes the anti-symmetric tensor in two dimensions.

To generate this operator at loop level requires a soft $U(1)_{B-L}$ breaking by $1 + Q_1$ units. Since we assume that H is uncharged under the new group, this means that the term $\kappa \eta^\dagger H \sigma$ has to have the same total charge $Q_\eta - Q_\sigma = 1 + Q_1$. This soft breaking can be UV completed by considering the vev $\kappa = \lambda_{IV} v_\phi$ of another singlet scalar ϕ with charge $-1 - Q_1$, as will be shown in section 4.4.3. On the fermionic side we introduce two generations of vector-like pairs of SM singlets (N_L, N_R) with B-L charge Q_N

$$\mathcal{L} \supset -Y_{LN} \overline{L}\epsilon \eta^\dagger N_R - Y_{NR} \overline{N_L}\sigma \nu_R - M_N \overline{N_L}N_R + \text{h.c.} \quad (4.2)$$

In order to forbid a Dirac mass with L and ν_R we have to require that $Q_N \neq \pm 1, \pm Q_1$. We also need to forbid the following operators [258]:

- $\overline{N_L^c} N_L$ and $\overline{N_R^c} N_R$ with $2Q_N$
- $\overline{\nu_R^c} \nu_R$ with $2Q_1$
- $\overline{N_L} \nu_R, \overline{N_R} \nu_R$ with $-Q_N + Q_1, Q_N + Q_1$
- $(H^\dagger \eta) (H^\dagger \eta)$ with $2Q_\eta$ together with $\overline{N_R^c} N_R$ would create $\overline{\nu_L^c} \nu_L$ at loop level [246]
- $\sigma \sigma$ with $2Q_\sigma$ together with $\overline{N_L^c} N_L$ would create $\overline{\nu_R^c} \nu_R$ at loop level [256]

All of the above combinations of charges need to be non-zero and not divisible by $|1 + Q_1|$. If they were divisible by the only source of soft breaking, then an integer number of insertions of the trilinear scalar coupling in some loop diagram can generate the unwanted mass term. Once we know Q_1 we can fix all the other charges of the model. We will use

field	SU(2) _L	U(1) _Y	U(1) _{B-L}	\mathcal{Z}_5	generations
L	2	-1/2	-1	-4	3
e_R	1	-1	-1	1	3
H	2	1/2	0	0	1
ν_R	1	0	-2	1	2
N_L	1	0	-3	-3	2
N_R	1	0	-3	2	2
χ_L	1	0	Q_4	0	1
χ_R	1	0	Q_3	0	1
D_L	2	-1/2	$1 + Q_3$	-1	1
D_R	2	-1/2	$1 + Q_3$	4	1
S_L	1	0	$1 + Q_3$	-1	1
S_R	1	0	$1 + Q_3$	4	1
η	2	1/2	-2	-4	1
σ	1	0	-1	1	1
ϕ	1	0	1	0	1

Table 4.1: Charges and representations for all particles participating in the neutrino or dark matter mass generation. The integers n in the fifth column are an abbreviation for ω^n , where $\omega = e^{\frac{2i\pi}{5}}$.

the criterion of anomaly freedom to determine the rest of the particle spectrum and to find Q_1 in the next section. Before we do let us continue with our short review of the Dirac Scotogenic model: The active Dirac neutrino mass arises due to the first diagram in 4.1 and depends on the mass mixing in the scalar sector:

$$\mathcal{L} \supset - m_\sigma^2 |\sigma|^2 - m_\eta^2 |\eta|^2 - \frac{\kappa}{\sqrt{2}} \left(\eta^\dagger H \sigma + \text{h.c.} \right) \quad (4.3)$$

$$- \lambda_\eta \left(\eta^\dagger \eta \right)^2 - \lambda_\sigma |\sigma|^4 \quad (4.4)$$

$$- \lambda_{H\eta} \left(H^\dagger H \right) \left(\eta^\dagger \eta \right) - \lambda_{H\sigma} \left(H^\dagger \eta \right) \left(\eta^\dagger H \right) \quad (4.5)$$

$$- \lambda_{H\sigma} \left(H^\dagger H \right) |\sigma|^2 \quad (4.6)$$

4 Radiative keV-scale DM

After we expand all the fields into their components

$$H = \begin{pmatrix} h^+ \\ \frac{h_R + v_H + i h_I}{\sqrt{2}} \end{pmatrix}, \quad \eta = \begin{pmatrix} \eta^+ \\ \frac{\eta_R^0 + i \eta_I^0}{\sqrt{2}} \end{pmatrix}, \quad \sigma = \frac{\sigma_R^0 + i \sigma_I^0}{\sqrt{2}} \quad (4.7)$$

and in the absence of CP -violation there is no mass mixing between the CP -even (subscript R) and odd bosons (subscript I). We set $m_\eta^2, m_\sigma^2 > 0$ in order to have an inert doublet and singlet. The real and imaginary components only mix among each other. The mass matrix after EWSB reads

$$(\eta_R^0, \sigma_R^0) \cdot \begin{pmatrix} \tilde{m}_\eta^2 & \frac{\kappa v_H}{2} \\ \frac{\kappa v_H}{2} & \tilde{m}_\sigma^2 \end{pmatrix} \cdot \begin{pmatrix} \eta_R^0 \\ \sigma_R^0 \end{pmatrix}, \quad (4.8)$$

and the same holds for the CP -odd fields, where

$$\tilde{m}_\eta^2 \equiv m_\eta^2 + (\lambda_{H\eta 1} + \lambda_{H\eta 2}) v_H^2, \quad \text{and} \quad \tilde{m}_\sigma^2 \equiv m_\sigma^2 + \lambda_{H\sigma} v_H^2. \quad (4.9)$$

We find two mass eigenstates in each case with the masses

$$m_{1,2}^2 = \frac{1}{2} \left(\tilde{m}_\eta^2 + \tilde{m}_\sigma^2 \pm \sqrt{(\tilde{m}_\eta^2 - \tilde{m}_\sigma^2)^2 + \kappa^2 v_H^2} \right) \quad (4.10)$$

and the mass eigenstates read

$$\begin{pmatrix} \eta_R^0 \\ \sigma_R^0 \end{pmatrix} = \begin{pmatrix} \cos(\alpha) & \sin(\alpha) \\ -\sin(\alpha) & \cos(\alpha) \end{pmatrix} \begin{pmatrix} S_1 \\ S_2 \end{pmatrix}, \quad \begin{pmatrix} \eta_I^0 \\ \sigma_I^0 \end{pmatrix} = \begin{pmatrix} \cos(\alpha) & \sin(\alpha) \\ -\sin(\alpha) & \cos(\alpha) \end{pmatrix} \begin{pmatrix} A_1 \\ A_2 \end{pmatrix}. \quad (4.11)$$

The mixing angle is given in terms of the model parameters as

$$\sin(2\alpha) = \frac{\kappa v_H}{2\Delta m_S^2}, \quad \text{with} \quad \Delta m_S^2 \equiv \frac{m_1^2 - m_2^2}{2}. \quad (4.12)$$

Four diagrams contribute to the active neutrino masses: one mediated by each of the scalars $S_{1,2}$ and $A_{1,2}$. Since S_1 and A_1 (S_2 and A_2) are mass degenerate there are only two distinct types of diagrams: two for heavier scalars of mass m_1 and two for the ones with m_2 . Due to the mixing there will be a relative sign between these two “generations” of scalars. This difference cancels out the divergent part leaving us with a finite mass matrix [259]

$$(m_\nu)_{ij} = -\frac{\sin(2\alpha)}{32\pi^2} \sum_{k=1}^2 (Y_{LN})_{ik} (Y_{NR})_{kj} M_N^{(k)} \left[\frac{m_2^2 \log\left(\frac{m_2^2}{M_N^{(k)2}}\right)}{m_2^2 - M_N^{(k)2}} - \frac{m_1^2 \log\left(\frac{m_1^2}{M_N^{(k)2}}\right)}{m_1^2 - M_N^{(k)2}} \right], \quad (4.13)$$

where $M_N^{(k)}$ is the mass of the k -th heavy neutrino. To get a more insightful expression we work in the radiative Seesaw limit [246]

$$M_N^{(k)2} \gg m_0^2 \equiv \frac{m_1^2 + m_2^2}{2} \gg \Delta m_S^2. \quad (4.14)$$

After substituting in the mixing angle from (4.12) we find

$$(m_\nu)_{ij} = \sum_{k=1}^2 \frac{(Y_{LN})_{ik} (Y_{NR})_{kj}}{32\pi^2} \frac{\kappa v_H}{M_N^{(k)}} \left(\text{Log} \left(\frac{M_N^{(k)2}}{m_0^2} \right) - 1 \right), \quad (4.15)$$

where the dependence on the soft symmetry breaking coupling κ is explicit and the scaling $1/M_N$ is reminiscent of the familiar tree level Seesaw mechanism. To get a feeling for the involved scales let us estimate the neutrino mass in the single generation limit

$$m_\nu \simeq 0.1 \text{ eV} \cdot \left(\frac{Y_{LN}}{0.1} \right) \cdot \left(\frac{Y_{NR}}{0.1} \right) \cdot \left(\frac{\kappa}{1 \text{ TeV}} \right) \cdot \left(\frac{10^{11} \text{ GeV}}{M_N} \right) \cdot \left(\frac{\text{Log} \left(\frac{M_N^2}{m_0^2} \right) - 1}{\mathcal{O}(10)} \right), \quad (4.16)$$

where in the above we used $m_0 = \mathcal{O}(1 \text{ TeV})$. Constraints on this scenario from lepton flavour violation and collider searches can be found in [260]. Note that since we will investigate a different implementation of Dark matter compared to the usual Scotogenic idea, we can push the masses of the scalars and N to values (far) above the electroweak scale, avoiding all laboratory constraints.

4.4.2 Extension for radiative DM mass

We proceed by introducing four Weyl fermions which are chiral under $U(1)_{B-L}$. Usually one charges three right handed neutrinos with $Q_{B-L} = 1$ so they form a vector-like pair with the ν_L from the leptonic doublet (the e_L form a vector-like pair with e_R). However there are other anomaly free choices such as two right handed neutrinos with $Q_{B-L} = -4$ accompanied by another one with $Q_{B-L} = 5$. The idea of having chiral charges was originally put forth in [261] and applied to dark matter in [262--266]. Here we propose a new realization of this idea: Two Weyl fermions will be right handed and of equal charge Q_1 in order to form two massive Dirac fermions with ν_L . Therefore our model predicts that the third SM neutrino remains exactly massless. The remaining two fermions will be the right handed χ_3 and the left handed χ_4 , which combine to form a Dirac fermion, that will be identified with the dark matter candidate. Since we have a gauge symmetry in mind, we need to find an anomaly free set of charges. As we only consider SM singlets with chiral charges there are only two conditions for cancelling the gravitational and $U(1)_{B-L}^3$ anomalies from the Standard Model:

$$\sum_{\text{dark sector}} Q_{B-L} = -2Q_1 - Q_3 + Q_4 \stackrel{!}{=} 3 \quad (4.17)$$

$$\sum_{\text{dark sector}} Q_{B-L}^3 = -2Q_1^3 - Q_3^3 + Q_4^3 \stackrel{!}{=} 3 \quad (4.18)$$

4 Radiative keV-scale DM

Here the signs reflect the fact that only χ_4 is left handed. The system of equations is under-determined and has infinitely many solutions. In order for the same one-loop topology and soft breaking to generate the dark matter mass term $\overline{\chi}_4\chi_3 \equiv \overline{\chi}_L\chi_R$ we impose the additional condition

$$|1 + Q_1| = |Q_3 - Q_4|. \quad (4.19)$$

Without the absolute value we find no solutions. For $1 + Q_1 = -(Q_3 - Q_4)$ we find two possible solutions with irrational charges

$$Q_1 = -2, \quad Q_3 = \frac{1 - \sqrt{17}}{2}, \quad Q_4 = -\frac{1 + \sqrt{17}}{2}, \quad (4.20)$$

and

$$Q_1 = -2, \quad Q_3 = \frac{1 + \sqrt{17}}{2}, \quad Q_4 = -\frac{1 - \sqrt{17}}{2}. \quad (4.21)$$

One can see that both sets of solutions are related by exchanging $Q_3 \leftrightarrow -Q_4$. The only solution possible for 3 copies of ν_R with the same charge Q_1 would be $Q_1 = -1$ and $Q_3 = Q_4$, which would allow for a term $\overline{L}\epsilon H^\dagger \nu_R$ at tree level and hence will not be investigated further. This is why our model predicts only two massive SM neutrinos. Note that formal quantum-gravitational conjectures [267] seem to exclude abelian gauge theories with irrational charges in curved space-time. We do not consider this line of reasoning further for our purely phenomenological study.

■ ADDENDUM: After the completion of this project I realized, that irrational charges do not just lead to potential problems with quantum gravity, but with grand unified theories as well: The eigenvalues of all generators of non-abelian gauge groups are quantized as rational numbers, so our $U(1)_{B-L}$ can not arise from a broken generator like e.g. electromagnetism does in the SM. Another way to look at this is to note, that we do not gauge a compact $U(1)$, but rather the non-compact \mathbb{R} , which locally (in terms of their Lie-Algebra) look the same but have different global topology. In addition these quantum gravitational arguments would rule out the field-theoretic Stückelberg mechanism [268, 269] from an abelian Higgs model: Here one wants to decouple the radial mode of the abelian Higgs by taking the limit $v \rightarrow \infty$ while keeping the gauge boson mass $g_S Q_S v$ finite. This requires taking the limit $Q_S \rightarrow 0$ on the charge of the abelian Higgs [270], meaning that it can not be a rational number but is instead real valued. Sending the gauge coupling g_S to zero instead would just reduce the gauged symmetry to a global one as one decouples the transverse gauge fields [270]. ■

Let us emphasize that for this particle content we need a soft breaking by $|1 + Q_1| = 1$ unit. However in that case any of the previously mentioned unwanted mass terms could arise at the loop level via some number of insertions of the trilinear term. Furthermore since we break the gauge symmetry by only one unit, there will be no residual \mathcal{Z}_N symmetry that also stabilizes the dark matter. To remedy both shortcoming we resort to imposing an ad-hoc \mathcal{Z}_5 symmetry as well. The choice of an odd N was motivated by the

4.4 Appendix: The model

need to forbid bilinear terms. All the charges and representations to realize the original Dirac Scotogenic model [54, 55] with our exotic choice of $U(1)_{B-L}$ charges can be found in the table 4.1.

Let us focus on the dark matter mass now: Motivated by Zee's model [271] for neutrino masses we consider the second topology depicted in figure 4.1. We add a pair of vector-like doublets (D_L, D_R) with $Y = -1/2$ together with another pair of vector-like singlets (S_L, S_R) with $Y = 0$:

$$\mathcal{L} \supset -Y_{\chi D} \overline{\chi L} \eta \epsilon D_R - Y_{S\chi} \overline{S_L} \sigma^* \chi_R - M_D \overline{D_L} D_R - M_S \overline{S_L} S_R \quad (4.22)$$

Here we coupled the fermion χ to η, σ^* instead of η^\dagger, σ , which was the case for the active neutrinos, because we need a soft breaking by plus one unit of B-L, whereas the active neutrinos needed a breaking by -1 . Since both components of χ are $SU(2)_L$ singlets unlike for the SM leptons, we do not only need a chirality flip on the internal fermion line but an insertion of the Higgs doublet as well:

$$\mathcal{L} \supset -Y_{DS} \overline{D_L} \epsilon H^\dagger S_R - Y_{SD} \overline{S_L} H \epsilon D_R \quad (4.23)$$

These couplings are the reason why all D, S have the common B-L charge $1 + Q_3$ see table 4.1. B-L forbids all Majorana masses $\overline{S_L^c} S_L, \overline{S_R^c} S_R, \overline{\chi_L^c} \chi_L, \overline{\chi_R^c} \chi_R$ as they need a breaking by $2(1 + Q_3), 2Q_3, 2Q_4$ units. Since $Q_{3,4}$ are irrational numbers, no loop graph with an arbitrary number of soft symmetry breaking insertions by one unit can ever accidentally produce these terms. Hence we will leave $\chi_{L,R}$ uncharged under the \mathcal{Z}_5 . This automatically forbids any mass mixing between χ and the $\nu_{L,R}$ as well as the kinematically allowed radiative decay $\chi \rightarrow \nu\gamma$ or the three-body decay $\chi \rightarrow \nu\bar{\nu}\nu$. Consequently the DM candidate will be absolutely stable. All other mass terms of the schematic form $LD, DH^\dagger e_R, SN, S\nu_R, S\chi, N\chi$ are each forbidden by at least one of the symmetries or both.

The dark matter mass term from figure 4.1 depends on the mass mixing in the scalar sector as well as on the mixing between the D and S . Their mass matrix reads

$$\begin{pmatrix} \overline{S_L}, \overline{D_L^0} \end{pmatrix} \cdot \begin{pmatrix} M_S & -\frac{Y_{SD} v_H}{\sqrt{2}} \\ \frac{Y_{DS} v_H}{\sqrt{2}} & M_D \end{pmatrix} \cdot \begin{pmatrix} S_R \\ D_R^0 \end{pmatrix} \quad (4.24)$$

and we find the following eigenvalues

$$M_{1,2} = \frac{1}{2} \left(M_D + M_S \mp \sqrt{(M_D - M_S)^2 - 2v_H^2 Y_{DS} Y_{SD}} \right). \quad (4.25)$$

The diagonalization simplifies in the limit $Y_{SD} = -Y_{DS}$ and we arrive at

$$\begin{pmatrix} S_L \\ D_L^0 \end{pmatrix} = \begin{pmatrix} \cos(\beta) & \sin(\beta) \\ -\sin(\beta) & \cos(\beta) \end{pmatrix} \begin{pmatrix} (F_1)_L \\ (F_2)_L \end{pmatrix}, \quad (4.26)$$

$$\begin{pmatrix} S_R \\ D_R^0 \end{pmatrix} = \begin{pmatrix} \cos(\beta) & \sin(\beta) \\ -\sin(\beta) & \cos(\beta) \end{pmatrix} \begin{pmatrix} (F_1)_R \\ (F_2)_R \end{pmatrix}, \quad (4.27)$$

4 Radiative keV-scale DM

with a mixing angle

$$\sin(2\beta) = \frac{\sqrt{2}Y_{DS}v_H}{2\Delta M_F}, \quad \text{where} \quad \Delta M_F \equiv \frac{M_2 - M_1}{2}. \quad (4.28)$$

The dark matter mass arises due to eight loop diagrams in the mass basis. Since S_i and A_i are mass degenerate there will be only four distinct kinds of diagrams. For a fixed intermediate F_j there are two diagrams depending on $S_1(A_1)$ and $S_2(A_2)$ again with a relative sign. Consequently all divergences will cancel in the sum and the resulting DM mass is finite. For a fixed intermediate $S_i(A_i)$ there are two possible diagrams involving F_1 and F_2 , both with a relative sign due to the fermionic mass mixing. This explains the structure of the expression for the DM mass:

$$m_{\text{DM}} = -\frac{Y_{\chi D}Y_{S\chi}}{128\pi^2} \sin(2\alpha) \sin(2\beta) \sum_{j=1}^2 C_j \left[\frac{m_2^2 \log\left(\frac{m_2^2}{M_j^2}\right)}{m_2^2 - M_j^2} - \frac{m_1^2 \log\left(\frac{m_1^2}{M_j^2}\right)}{m_1^2 - M_j^2} \right] \quad (4.29)$$

with $C_2 = -C_1 = 1$. By working in the radiative Seesaw limit

$$M_F \equiv \frac{M_2 + M_1}{2} \gg m_0, \quad \Delta M_F \quad (4.30)$$

and invoking the definition of the mixing angles (4.12) and (4.28) we finally obtain

$$m_{\text{DM}} = \frac{Y_{\chi D}Y_{DS}Y_{S\chi}}{\sqrt{2}32\pi^2} \frac{\kappa v_H^2}{M_F^2} \left(\log\left(\frac{M_F^2}{m_0^2}\right) - 3 \right). \quad (4.31)$$

Note that since we generate the dark matter mass via a dimension five operator compared to the active neutrinos (see figure 4.1), whose mass is an effective dimension four operator, there is another inverse power of the heavy suppression scale M_F when compared to (4.15). Because we want our dark matter to be heavier than the neutrinos we therefore need $M_N \gg M_F$, which can be seen from the following estimate

$$m_{\text{DM}} \simeq 4 \text{ keV} \cdot \left(\frac{Y_{\chi D}}{0.1} \right) \cdot \left(\frac{Y_{DS}}{0.1} \right) \cdot \left(\frac{Y_{S\chi}}{0.1} \right) \cdot \left(\frac{\kappa}{1 \text{ TeV}} \right) \cdot \left(\frac{30 \text{ TeV}}{M_F} \right)^2 \cdot \left(\frac{\log\left(\frac{M_F^2}{m_0^2}\right) - 3}{3} \right). \quad (4.32)$$

In the above we used $m_0 = \mathcal{O}(1 \text{ TeV})$. Unlike the N which are much heavier the F and electrically charged components of D could be potentially be produced at future colliders and have a direct coupling to the SM like Higgs.

4.4.3 UV completion

In order to gauge the $U(1)_{\text{B-L}}$ symmetry and to explain the origin of the dimensionful coupling κ in the trilinear term (4.1) we introduce a second SM singlet scalar ϕ with the

4.4 Appendix: The model

charge $Q_\phi = -1 - Q_1 = 1$ without any couplings to the fermion spectrum:

$$\mathcal{L}_\phi \supset -\mu_\phi^2 |\phi|^2 - \lambda_{IV} \left(\eta^\dagger H \sigma \phi^* + \text{h.c.} \right) \quad (4.33)$$

$$- \lambda_\phi |\phi|^4 - \lambda_{H\phi} \left(H^\dagger H \right) |\phi|^2 \quad (4.34)$$

$$- \lambda_{\eta\phi} \left(\eta^\dagger \eta \right) |\phi|^2 - \lambda_{\sigma\phi} |\sigma|^2 |\phi|^2. \quad (4.35)$$

We parameterize the new scalar as

$$\phi = \frac{\phi_R^0 + v_\phi + i\phi_I^0}{\sqrt{2}}, \quad (4.36)$$

which allows us to identify $\kappa = \lambda_{IV} v_\phi \equiv \lambda_{IV} v_{\text{B-L}}$. We do not depict an insertion of this vev in figure 4.1, because the neutrino and DM mass generation only requires a non-zero value of κ irrespective of its origin in the UV. The ϕ_I^0 is the would-be-Goldstone-Boson that gets absorbed to become the longitudinal component of the massive $U(1)_{\text{B-L}}$ gauge boson that we call Z' whose mass reads

$$m_{Z'} = g_{\text{B-L}} v_{\text{B-L}}, \quad (4.37)$$

because ϕ is the only field with B-L charge that receives a vev. Direct searches at LEP place the following bound [126, 272] on the mass of a new gauge boson

$$v_{\text{B-L}} = \frac{m_{Z'}}{g_{\text{B-L}}} > 6.9 \text{ TeV} \quad @ 95\% \text{ C.L.} \quad (4.38)$$

that couples to the conventional B-L charges of the SM fermions. Searches at the LHC exclude Z' 's below $0.2 - 3.5$ TeV [273]. Since no scalar field that receives a vev is charged under both weak isospin/hypercharge or B-L there is no mass mixing between the Z and Z' bosons. However there can be gauge kinetic mixing [172], for instance generated at the loop level by self-energy graphs containing the (D_L, D_R) or η fields, which are charged under both abelian symmetries and weak isospin.

The additional scalar interactions contribute to the masses of the η^0 and σ^0 bosons by shifting the relations in (4.9) to

$$\tilde{m}_\eta^2 \rightarrow m_\eta^2 + (\lambda_{H\eta 1} + \lambda_{H\eta 2}) v_H^2 + \lambda_{\eta\phi} v_{\text{B-L}}^2, \quad (4.39)$$

$$\tilde{m}_\sigma^2 \rightarrow m_\sigma^2 + \lambda_{H\sigma} v_H^2 + \lambda_{\sigma\phi} v_{\text{B-L}}^2. \quad (4.40)$$

Additionally the mixed quartic between H and ϕ leads to mass mixing between them: First we minimize the potential in each direction and find expressions to eliminate the parameters $\mu_H^2, \mu_\phi^2 < 0$. We find that the minimum in each direction can be obtained for

$$\frac{\mu_H^2}{2} = -2\lambda_H v_H^2 - \lambda_{H\phi} v_{\text{B-L}}^2, \quad \text{and} \quad \frac{\mu_\phi^2}{2} = -2\lambda_\phi v_{\text{B-L}}^2 - \lambda_{H\phi} v_H^2 \quad (4.41)$$

and we arrive at

$$(h_R, \phi_R^0) \cdot \begin{pmatrix} 2\lambda_H v_H^2 & \frac{\lambda_{H\phi}}{2} v_H v_{\text{B-L}} \\ \frac{\lambda_{H\phi}}{2} v_H v_{\text{B-L}} & 2\lambda_\phi v_{\text{B-L}}^2 \end{pmatrix} \cdot \begin{pmatrix} h_R \\ \phi_R^0 \end{pmatrix}, \quad (4.42)$$

4 Radiative keV-scale DM

with the eigenvalues

$$m_{h,\varphi}^2 = \lambda_H v_H^2 + \lambda_\phi v_{\text{B-L}}^2 \mp \frac{1}{2} \sqrt{4\lambda_H^2 v_H^4 + 4\lambda_\phi^2 v_{\text{B-L}}^4 + v_H^2 v_{\text{B-L}}^2 (\lambda_{H\phi}^2 - 8\lambda_H \lambda_\phi)}. \quad (4.43)$$

In the limit $v_{\text{B-L}} \gg v_H$ we find at leading order

$$m_h^2 \simeq \left(2\lambda_H - \frac{\lambda_{H\phi}^2}{8\lambda_\phi} \right) v_H^2 \quad \text{and} \quad m_\varphi^2 \simeq 2\lambda_\phi v_{\text{B-L}}^2. \quad (4.44)$$

The correction to the SM like Higgs mass can be understood as a tree level threshold correction to its quartic from integrating out the heavier field [274]. The mass eigenstates are determined from

$$\begin{pmatrix} h_R \\ \phi_R^0 \end{pmatrix} = \begin{pmatrix} \cos(\gamma) & \sin(\gamma) \\ -\sin(\gamma) & \cos(\gamma) \end{pmatrix} \begin{pmatrix} h \\ \varphi \end{pmatrix} \quad (4.45)$$

with

$$\sin(2\gamma) = \frac{\lambda_{H\phi} v_H v_{\text{B-L}}}{2\Delta m_h^2}, \quad \text{where} \quad \Delta m_h^2 \equiv \frac{m_\varphi^2 - m_h^2}{2} \quad (4.46)$$

and at leading order in $v_H/v_{\text{B-L}}$ this reduces to

$$\sin(2\gamma) \simeq \frac{\lambda_{H\phi}}{2\lambda_\phi} \cdot \frac{v_H}{v_{\text{B-L}}}. \quad (4.47)$$

In the present study we will neglect this mixing completely. It is important to note that the discrete \mathcal{Z}_5 symmetry we imposed will most likely be broken by quantum gravitational effects [275--277], which is why we assume it is e.g. a residual symmetry arising from the spontaneous symmetry breaking of a gauge symmetry [278]. This larger symmetry could also connect our choice of $U(1)_{\text{B-L}}$ with the rest of the SM gauge group, e.g. by unifying it with QCD into the Pati-Salam hypercolor $SU(4)_c$ [279]. Vector-like fermions such as our singlets (N_L, N_R) and (S_L, S_R), doublets (D_L, D_R) as well as exotic vector-like down-type quarks arise in E_6 -GUTs [280, 281]. This could provide an interesting route for further completing our model in the UV as the Pati-Salam model can be embedded in $SO(10)$ which is a subgroup of E_6 .

■ ADDENDUM: The caveats about the irrational charges mentioned in the previous addendum actually prevent us from embedding our choice of $U(1)_{\text{B-L}}$ into a non-abelian group. GUTs could still work if we add additional chiral fermions so that the B-L charges become rational numbers, potentially affecting the features and phenomenology of our construction. ■

4.5 Appendix: Dark Matter

As previously mentioned our DM candidate does not mix with the active neutrinos. Hence the usually considered possibility of creating keV-scale neutrino DM via active-to-sterile oscillations [282], that can be enhanced in the presence of a chemical potential for

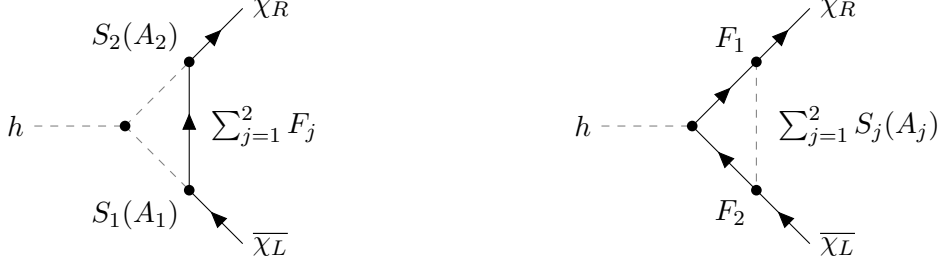


Figure 4.2: Leading order diagrams for the decay $h \rightarrow \chi_L \chi_R$ in the mass basis. See the main text for more details.

neutrinos [283], are ruled out and we have to look into other avenues to produce DM. In the following we will briefly explain why we do not consider thermal production and focus on non-thermal scenarios. To study non-thermal production of DM we assume that the reheating temperature T_{RH} of the universe is below both the masses of the particles in the loops of figure 4.1 and the mass of the B-L gauge boson Z'

$$M_N \gg M_F \gg m_0 \gg T_{\text{RH}} \quad \text{and} \quad m_{Z'} \gg T_{\text{RH}}. \quad (4.48)$$

This ensures that none of the new, potentially stable neutral particles, which are good thermal dark matter candidates, are present in the plasma. We can thus limit ourselves to the SM degrees of freedom augmented by the two ν_R and the light DM.

4.5.1 Lyman bound for FIMPs

The Lyman- α forest consists of absorption lines in the spectra of quasars due to neutral hydrogen in the intergalactic medium. It provides a window into the matter power spectrum, which contains information on the Dark matter's free-streaming scale from the time of structure formation. One can use the existing data on the Lyman- α forest to set bounds on dark matter models affecting small scale structures such as the thermally produced warm DM (WDM). Numerically challenging simulations for WDM have been performed and lead to a lower limit of $m_{\text{WDM}}^{\text{Ly-}\alpha} = 5.3 \text{ keV}$ at 95% confidence level (CL) [284, 285]. Reference [286] argued that the aforementioned bound is too strong when taking into account systematics such as assumptions about the thermal history and instead they find $m_{\text{WDM}}^{\text{Ly-}\alpha} = 1.9 \text{ keV}$ at 95% CL. In order to avoid such time consuming simulations for other DM production modes a bound mapping formalism has been devised in [287–293] and a recent reevaluation [243] found that the previously mentioned mass range $m_{\text{WDM}} \gtrsim (1.9 - 5.3) \text{ keV}$ translates into a bound on the FIMP mass of $m_{\text{FIMP}} \gtrsim (4 - 16) \text{ keV}$.

4.5.2 Out of equilibrium Higgs decays

In the following we focus on the decay $h \rightarrow \chi_L \chi_R, \chi_R \chi_L$, which is obtained from the second diagram in 4.1 by replacing one of the Higgs vevs with the radial excitation h ,

4 Radiative keV-scale DM

which leads to the two diagrams depicted in figure 4.2. By replacing both Higgs vevs one can compute the scattering process $hh \rightarrow \bar{\chi}L\chi_R, \bar{\chi}R\chi_L$, however for our first estimate we will limit ourselves to the decays. We only consider the trilinear coupling from (4.1) and neglect all the decay modes to the same chiralities (LL or RR) which occur via the quartic couplings $\lambda_{H\eta 1,2}, \lambda_{H\sigma}$, from DM mass insertions on the external lines [256], or from mass mixing in the heavy scalar or fermion sector to focus on the parameters for the DM mass. This is also why we will work to the lowest order in the mixing angles $\sin(\alpha)$ and $\sin(\beta)$ because in the mass basis there are 32 diagrams contributing and both neutrino masses were independent of the aforementioned angles in the radiative Seesaw limit. We neglect the mixing $\sin(\gamma)$ between h and φ . In this approximation with $\cos(\alpha) \simeq \cos(\beta) \simeq 1$ and $S_1 \simeq \eta_R^0, S_2 \simeq \sigma_R^0, F_1 \simeq S, F_2 \simeq D^0$ there are only four diagrams contributing. By dropping the final state DM mass we find

$$\Gamma(h \rightarrow \bar{\chi}\chi) = \Gamma(h \rightarrow \bar{\chi}L\chi_R) + \Gamma(h \rightarrow \bar{\chi}R\chi_L) = \frac{m_h}{8\pi} |f_\nu|^2. \quad (4.49)$$

The first set of graphs depicted on the left side of figure 4.2 is obtained by replacing the upper vev in 4.1 with h and only depends on $\sin(\beta)$. The amplitude is finite because it comes from a difference of terms due to the relative sign between the $F_{1,2}$ contributions. The corresponding effective Yukawa coupling is found to be at leading order in $\sin(\beta)$ from (4.12) and by making use of (4.30)

$$f_\beta = \frac{Y_{\chi D} Y_{DS} Y_{S\chi}}{\sqrt{2} 2} \frac{\kappa v_H}{M_F^2} \left(\text{Log} \left(\frac{M_F^2}{m_0^2} \right) - 2 \right). \quad (4.50)$$

Similarly the second diagram on the right side of figure 4.2 is obtained by replacing the lower vev in 4.1 with h . It is proportional to $\sin(\alpha)$ from (4.28) and finite because here the difference arises due to the relative sign of the $S_{1,2}(A_{1,2})$ contributions. The effective coupling is

$$f_\alpha = \frac{Y_{\chi D} Y_{DS} Y_{S\chi}}{\sqrt{2} 2} \frac{\kappa v_H}{M_F^2} \left(\text{Log} \left(\frac{M_F^2}{m_0^2} \right) - 3 \right). \quad (4.51)$$

In both expressions we neglected the Higgs mass. The sum of both contributions can be re-expressed by comparison with (4.31) as

$$f_\nu = f_\alpha + f_\beta = 2 \frac{m_{\text{DM}}}{v_H} \frac{\text{Log} \left(\frac{M_F^2}{m_0^2} \right) - \frac{5}{2}}{\text{Log} \left(\frac{M_F^2}{m_0^2} \right) - 3} \rightarrow 2 \frac{m_{\text{DM}}}{v_H} \quad \text{for} \quad M_F \gg m_0 \gg m_h, \quad (4.52)$$

which agrees with the EFT expectation that after EWSB the diagram on the right in figure 4.1 can be represented by an effective Weinberg-type operator [23] at energy scales below all the mediator masses

$$\mathcal{L}_{\text{EFT}} = 2 \frac{m_{\text{DM}}}{v_H^2} \bar{\chi}\chi \left(H^\dagger H \right). \quad (4.53)$$

The remainder of this section discusses how to produce DM from this effective operator and can be applied to other models that generate this operator as well. For the decay

width we find after neglecting the phase space suppression

$$\Gamma(h \rightarrow \bar{\chi}\chi) = \frac{m_h}{2\pi} \left(\frac{m_{\text{DM}}}{v_H} \right)^2 \quad (4.54)$$

and we emphasize that the only free parameter is the DM mass. The experimental limit on the branching ratio (BR) from searches for invisible Higgs decays beyond the SM is between 19% (CMS) and 26% (ATLAS) which translates to approximately $\Gamma(h \rightarrow \text{Inv.}) < 1.3 \text{ MeV}$ [213, 294, 295], implying an upper bound on the DM mass of roughly

$$m_{\text{DM}} \lesssim 2 \text{ GeV}, \quad (4.55)$$

which justifies neglecting the phase space suppression. Multiple proposed next generation collider experiments are expected to tighten the bound on the invisible BR by up to two orders of magnitude to $\text{BR}(h \rightarrow \text{Inv.}) = 0.22\%$ (FCC-ee) [296], 0.24% (CEPC) [297] and 0.26% (ILC) [298]. The corresponding bound on the DM mass would read approximately

$$m_{\text{DM}} \lesssim 170 \text{ MeV}. \quad (4.56)$$

This bound is only one order of magnitude stronger than (4.55) due to quadratic dependence of the branching ratio on the DM mass. The invisible Higgs decays lead to the strongest terrestrial bound on the DM mass, however as we will see avoiding cosmological over-production of DM from Higgs mediated scatterings firmly requires the DM mass to be below the MeV-scale see (4.91).

In the following we will limit ourselves to the era of radiation domination and make extensive use of the Hubble rate and the entropy density

$$H(T) \simeq 1.66 \sqrt{g_{*\rho}(T)} \frac{T^2}{M_{\text{Pl}}}, \quad s(T) = g_{*S}(T) \frac{2\pi^2}{45} T^3, \quad (4.57)$$

where $g_{*\rho}$ and g_{*S} are the effective number of degrees of freedom in energy and entropy respectively. Before we deal with non-thermal DM production let us take a look the thermal case first: The decay (4.54) will be in thermal equilibrium at $T = m_h$ provided that $m_{\text{DM}} \gtrsim 4.5 \text{ keV}$ (we will show this later in (4.64)). Since during radiation domination we have $\Gamma/H \sim T^{-2}$ for decays at temperatures below the mass of the decaying particle, a decay never falls out of thermal equilibrium. Consequently we need to know when the inverse decay freezes-out in order to find the decoupling temperature of χ . The corresponding rate reads at $T \ll m_h$ [299, 300]

$$\Gamma_{\text{ID}} = \frac{1}{3\zeta(3)} \sqrt{\frac{\pi}{2}} \left(\frac{m_h}{T} \right)^{\frac{3}{2}} \cdot e^{-\frac{m_h}{T}} \cdot \Gamma(h \rightarrow \bar{\chi}\chi) \quad (4.58)$$

and the phase suppression is encoded in the Boltzmann factor. Numerically we find that this interaction freezes out at $T_{\text{FO}} \gtrsim 3 \text{ GeV}$ for $m_{\text{DM}} \lesssim 2 \text{ GeV}$. Of course there is also a scattering process $hh \rightarrow \bar{\chi}\chi$, but since this requires two on shell Higgses the rate density will be double Boltzmann-suppressed below m_h typically leading to an earlier freeze-out

4 Radiative keV-scale DM

than the inverse decays. Since χ is relativistic at decoupling it would be a warm DM candidate, however it has long been known, that such a DM candidate would overclose the universe [301]

$$\Omega_{\text{DM}}^{\text{warm}} h^2 \simeq \mathcal{O}(10^6) \cdot \left(\frac{84}{g_*(T_{\text{FO}} \simeq 3 \text{ GeV})} \right) \cdot \left(\frac{m_{\text{DM}}}{1 \text{ GeV}} \right), \quad (4.59)$$

if there is no release of entropy that dilutes the relic density to the observed value. Realizing the warm DM scenario requires additional degrees of freedom in the plasma like long-lived particles that decoupled while relativistic whose decays generate the necessary entropy dilution [302]. For the sake of minimality we do not consider this idea further and focus on out-of-equilibrium-processes involving only SM states that are connected to the DM via the previously introduced BSM Yukawa and gauge interactions.

Next we investigate out of equilibrium Higgs decays. We use the notation of [303] to write down the Boltzmann equations for the DM production where $Y_{\text{DM}} \equiv \frac{n_{\text{DM}}}{s}$, with s being the entropy density and $z = \frac{m_h}{T}$

$$z H s \frac{dY_\chi}{dz} = \gamma_{h \rightarrow \bar{\chi}\chi} \frac{Y_h}{Y_h^{\text{e.q.}}} - \gamma_{\bar{\chi}\chi \rightarrow h} \frac{Y_\chi}{Y_\chi^{\text{e.q.}}} \frac{Y_{\bar{\chi}}}{Y_{\bar{\chi}}^{\text{e.q.}}}, \quad (4.60)$$

where we assumed that entropy is conserved. Note that away from thermal equilibrium the temperatures of the SM and DM baths are different so that $\gamma_{h \rightarrow \bar{\chi}\chi}$ depends on T_{SM} and $\gamma_{\bar{\chi}\chi \rightarrow h}$ is a function of T_{DM} . The freeze-in regime [82] is defined by the condition $Y_\chi \ll Y_\chi^{\text{e.q.}}$ and the same for $\bar{\chi}$. If we use the fact that the SM Higgs is kept in thermal equilibrium $Y_h \simeq Y_h^{\text{e.q.}}$ until $T_{\text{FO}} \simeq \frac{m_h}{25} \simeq 5 \text{ GeV}$ we obtain

$$z H s \frac{dY_\chi}{dz} \simeq \gamma_{h \rightarrow \bar{\chi}\chi}, \quad (4.61)$$

where the thermally averaged decay width density reads [299]

$$\gamma_{h \rightarrow \bar{\chi}\chi} = \frac{g_h m_h^2 T}{2\pi^2} K_1(z) \Gamma(h \rightarrow \bar{\chi}\chi). \quad (4.62)$$

In this context $g_h = 1$ is the spin degeneracy of the Higgs and $K_1(z)$ denotes a modified Bessel function of the first kind. To ensure that we are in the freeze-in regime the decay is not allowed to thermalize which leads to the condition

$$\frac{\Gamma(h \rightarrow \bar{\chi}\chi)}{H(T)} \Big|_{T=m_h} < 1 \quad (4.63)$$

that can be re-expressed as a bound on the DM mass

$$m_{\text{DM}} \lesssim 4.5 \text{ keV} \cdot \left(\frac{g_{*\rho}(m_h)}{100} \right)^{\frac{1}{4}}, \quad (4.64)$$

that is borderline compatible with the lower limit of the Lyman- α window. Under the assumption that there is no primordial abundance of DM we can integrate (4.62) to determine the DM abundance today at z_0

$$Y_\chi(z_0) = \mathcal{C}_h \int_{z_{\text{RH}}}^{z_0=\infty} dz \frac{z^3}{g_{*S}(z) \sqrt{g_{*\rho}(z)}} K_1(z), \quad \text{where} \quad z_{\text{RH}} = \frac{m_h}{T_{\text{RH}}} \quad (4.65)$$

and the factor \mathcal{C}_h is a short hand for all microscopic and cosmological parameters

$$\mathcal{C}_h = 1.1 \times 10^{-2} \frac{m_{\text{DM}}^2}{v_H^2} \frac{M_{\text{Pl}}}{m_h}. \quad (4.66)$$

We then use this to compute the energy density in dark matter by using the present day entropy density s_0 and the critical density ρ_c [60]

$$\Omega_{\text{DM}} h^2 = 2 \frac{m_{\text{DM}} s_0}{\rho_c} Y_\chi(z_0) \simeq 1.1 \times 10^3 \left(\frac{m_{\text{DM}}}{4 \text{keV}} \right) Y_\chi(z_0). \quad (4.67)$$

Here the factor of two arises because our DM candidate is a Dirac fermion. For a simple analytical estimate we can neglect the temperature dependence of the relativistic number of degrees of freedom in energy $g_{*\rho}(z)$ and entropy $g_{*S}(z)$ and replace them by their average values at the time of predominant dark matter production. This can be done because freeze-in production of DM is always sharply peaked around either $T \simeq m_h$ for the IR freeze-in [82, 304] or at the reheating temperature T_{RH} for UV freeze-in [305]. First let us suppose a standard big bang cosmology that corresponds to $z_{\text{RH}} \rightarrow 0$ which gives the maximally possible abundance

$$Y_\chi(z_0)^{\text{max}} \simeq \frac{4.71 \mathcal{C}_h}{g_{*S}(m_h) \sqrt{g_{*\rho}(m_h)}} \quad (4.68)$$

that corresponds to

$$h^2 \Omega_{\text{DM}} \simeq 0.12 \cdot \left(\frac{m_{\text{DM}}}{1.5 \text{keV}} \right)^3 \cdot \left(\frac{100}{g_{*S}(m_h)} \right) \cdot \sqrt{\frac{100}{g_{*\rho}(m_h)}}, \quad (4.69)$$

where we used the maximum possible number of relativistic degrees of freedom above the EW phase transition in the SM. One can see that the correct relic density [20] is obtained for a DM mass that is in conflict with the more conservative Lyman- α bound that requires $m_{\text{DM}} > 4 \text{keV}$. Since $h^2 \Omega_{\text{DM}} \sim m_{\text{DM}} Y_\chi(z_0)$ we can allow for a larger DM mass by lowering the yield $Y_\chi(z_0)$. This is most easily done by assuming $z_{\text{RH}} > 0$ which lowers the relic abundance below (4.68). In doing so we introduce a second free parameter in the form of T_{RH} . We find that we can decrease the abundance for $z_{\text{RH}} > 1$, however our fix comes with two complications: On the one hand one needs to make sure that the SM Higgs is actually thermalized after reheating. Reference [306] found that particles charged under non-abelian gauge symmetries that are produced from inflaton decays during reheating thermalize before the end of reheating (which is not an instantaneous process) provided that the fine structure constant of the gauge interaction satisfies

$$\alpha \gg \alpha_{\text{Lim}} \equiv \left(\frac{m_I}{M_{\text{Pl}}} \right)^{\frac{5}{8}} \cdot \left(\frac{\Gamma_I M_{\text{Pl}}}{m_I^3} \right)^{\frac{1}{8}}. \quad (4.70)$$

In this context m_I is the inflaton mass and Γ_I is its decay width, which we can trade for an expression involving T_{RH} (see (4.124)). We find that

$$\alpha_{\text{Lim}} \simeq 2 \times 10^{-9} \cdot \left(\frac{m_I}{1 \text{TeV}} \right)^{\frac{1}{4}} \cdot \left(\frac{T_{\text{RH}}}{1 \text{GeV}} \right)^{\frac{1}{4}} \cdot \left(\frac{g_{*\rho}(T_{\text{RH}})}{76} \right)^{\frac{1}{16}}, \quad (4.71)$$

4 Radiative keV-scale DM

which is definitely satisfied for the SM Higgs coupling to SU(2) gauge bosons where $\alpha_2 = \frac{g^2}{4\pi}$ with $g \simeq 0.64$. On the other hand the out of equilibrium condition (4.63) must be re-evaluated at $T_{\text{RH}} < m_h$ leading to

$$m_{\text{DM}} \lesssim \frac{4.5 \text{ keV}}{z_{\text{RH}}} \cdot \left(\frac{g_{*\rho}(z_{\text{RH}})}{100} \right)^{\frac{1}{4}}. \quad (4.72)$$

The necessary $z_{\text{RH}} > 1$ leads to DM masses which even violate the lower more conservative Lyman- α bound. In other words: If we tried to satisfy the Lyman- α window we would obtain a thermalized population of χ , which would actually be warm dark matter and this can only be made to work with additional processes that release enough entropy to dilute it. Since this channel leads to over-production of dark matter and the inclusion of $2 \rightarrow 2$ scattering processes will only increase the relic abundance further, we conclude that freeze-in from the SM Higgs via a Weinberg-type operator is not a viable production mode for keV-scale DM. Furthermore in order to avoid any contribution from Higgs decays we will only consider cosmologies with $T_{\text{RH}} < T_{\text{FO}} \simeq \frac{m_h}{25} \simeq 5 \text{ GeV}$. Successful BBN requires a reheating temperature of at least 4 MeV [244, 245].

4.5.3 Super WIMP contribution

Another production channel for DM is the Super WIMP scenario [307] in which the DM is produced after the thermal freeze-out of the Higgs boson from its gauge and Yukawa interactions at $T_{\text{FO}} \simeq \frac{m_h}{25}$. However the Higgs has decay modes to SM particles which are much faster than the decay to DM so the frozen out abundance of Higgses can not lead to a significant production of DM.

4.5.4 Gauge Scattering

We can also produce DM via the new gauge interaction [308, 309]. In the limit $s \ll m_{Z'}$ the cross section for interconverting DM and SM fermions f_i via Z' exchange reads for massless fermions [310]

$$\begin{aligned} \sigma(\bar{\chi}\chi \leftrightarrow \bar{f}_i f_i) &\equiv \frac{\alpha_{\chi i} s}{12\pi} \\ &= \frac{s}{12\pi} \cdot \left(\frac{g_{\text{B-L}}}{m_{Z'}} \right)^4 \cdot \left(Q(\chi_L)^2 + Q(\chi_R)^2 \right) (N_c)_i \left(Q(f_{iL})^2 + Q(f_{iR})^2 \right) \end{aligned} \quad (4.73)$$

where Q denotes the various B-L charges and N_c is a color factor which equals three for quarks and one for leptons. The above was summed and not averaged over the initial state spins. Since $m_{Z'} = g_{\text{B-L}} v_{\text{B-L}}$ the cross section is only sensitive to $v_{\text{B-L}}$ in the effective operator limit. Even though the DM mass in (4.32) formally depends on $\kappa = \lambda_{\text{IV}} v_{\text{B-L}}$ we treat m_{DM} and $v_{\text{B-L}}$ as independent parameters, because a larger $v_{\text{B-L}}$ can always be compensated by a smaller λ_{IV} or by making the fermions running in the loop heavier.

The Boltzmann equation read for $z \equiv \frac{T_{\text{RH}}}{T}$

$$zHs \frac{dY_\chi}{dz} = \sum_i \gamma_{\bar{f}_i f_i \rightarrow \bar{\chi}\chi} \frac{Y_{f_i}}{Y_{f_i}^{\text{e.q.}}} \frac{Y_{\bar{f}_i}}{Y_{\bar{f}_i}^{\text{e.q.}}} - \gamma_{\bar{\chi}\chi \rightarrow \bar{f}_i f_i} \frac{Y_\chi}{Y_\chi^{\text{e.q.}}} \frac{Y_{\bar{\chi}}}{Y_{\bar{\chi}}^{\text{e.q.}}} \quad (4.74)$$

$$\simeq \sum_i \gamma_{\bar{f}_i f_i \rightarrow \bar{\chi}\chi}, \quad (4.75)$$

where we applied the freeze-in approximation in the last step and for simplicity we compute the scattering rate densities via Maxwell Boltzmann-averaging [208, 311]

$$\begin{aligned} \gamma(a + b \rightarrow i + j + \dots) &= \langle \sigma |\vec{v}| \rangle n_a^{\text{eq.}} n_b^{\text{eq.}} \\ &= \frac{T}{32\pi^4} \int_{s_{\text{min}}}^{\infty} ds s^{\frac{3}{2}} \lambda \left(1, \frac{m_a^2}{s}, \frac{m_b^2}{s} \right) K_1 \left(\frac{\sqrt{s}}{T} \right) \sigma \end{aligned} \quad (4.76)$$

with

$$\lambda(a, b, c) \equiv (a - b - c)^2 - 4bc \quad \text{and} \quad s_{\text{min}} = \max \left[(m_a + m_b)^2, (m_i + m_j + \dots)^2 \right] \quad (4.77)$$

instead of averaging with Fermi-Dirac statistics. By neglecting the masses of the DM and SM fermions the simpler Maxwell-Boltzmann average allows us to find an analytical expression by employing the relation [311]

$$\int_0^\infty dx x^n K_1(x) = 2^{n-1} \Gamma \left(1 + \frac{n}{2} \right) \Gamma \left(\frac{n}{2} \right) \quad (4.78)$$

so that

$$\gamma(\bar{\chi}\chi \rightarrow \bar{f}_i f_i) = \gamma(\bar{f}_i f_i \rightarrow \bar{\chi}\chi) = \frac{8}{\pi^5} \alpha_{\chi i} T^8. \quad (4.79)$$

Note that while the functional forms above are the same the densities depend on the different temperatures of the SM and DM baths. The fact that both densities are equal for equal temperatures reflects the principle of detailed balance, so that the right hand side of the Boltzmann equation vanishes in thermal equilibrium [312]. Owing to our previous simplifying assumptions we will only work with relativistic fermions in the SM plasma. Annihilations from non-relativistic fermions will be Boltzmann-suppressed at $T < m_{f_i}$ and therefore less important than relativistic processes. From this we can deduce the more familiar interaction rate for relativistic SM fermions ($g_{f_i} = 2$)

$$\Gamma(\bar{f}_i f_i \rightarrow \bar{\chi}\chi) = \frac{\gamma(\bar{f}_i f_i \rightarrow \bar{\chi}\chi)}{n_{f_i}^{\text{eq.}}} = \frac{16}{3\xi(3)\pi^3} \alpha_{\chi i} T^5, \quad (4.80)$$

which agrees with the estimate based on dimensional analysis for an effective four fermion operator that leads to $\Gamma \sim T^5/v_{\text{B-L}}^4$. Our result is larger by only around 11% compared to the result [126] found by averaging over Fermi-Dirac statistics and also using massless fermions. This numerical difference agrees with the findings of [313] but we do not take percent level effects into account since what matters for freeze-in is the order of magnitude

4 Radiative keV-scale DM

of the couplings and not their precise value. In the effective operator limit the scattering rate is UV dominated so its maximum value is found at the largest available bath temperature after completion of reheating given by T_{RH} . As a consequence of our analysis for Higgs decays in 4.5.2 we will assume a reheating temperature $4 \text{ MeV} \lesssim T_{\text{RH}} \lesssim 5 \text{ GeV}$. Since the SM fermions also couple to non-abelian gauge interactions the estimate (4.71) is still approximately valid even though the SM fermions are not necessarily produced from inflaton decays. If we assume the inflaton decays to the SM like h , which definitely will be thermalized according to (4.71), and that h decays or scatters to produce the SM fermions it is plausible to expect a thermalized SM fermion bath immediately after reheating. Then in order to guarantee that we stay in the freeze-in regime the rate needs to satisfy

$$\frac{\sum_i \Gamma(\bar{f}_i f_i \rightarrow \bar{\chi} \chi)}{H(T)} \Big|_{T=T_{\text{RH}}} < 1 \quad (4.81)$$

and we can use this to constrain the B-L breaking vev to be

$$v_{\text{B-L}} \gtrsim 56.8 \text{ TeV} \cdot \left(\frac{T_{\text{RH}}}{1 \text{ GeV}} \right)^{\frac{3}{4}} \cdot \left(\frac{\sum_i N_i(T_{\text{RH}})}{11.67} \right)^{\frac{1}{4}} \cdot \left(\frac{76}{g_{* \rho}(T_{\text{RH}})} \right)^{\frac{1}{8}}, \quad (4.82)$$

which is a stronger constraint than the laboratory bound (4.37). For the above we summed over all the relativistic fermions because of the sum on the right hand side of (4.74). Moreover we used that for all SM leptons $Q_l^2 = 1$, for quarks $Q_q^2 = \frac{1}{9}$ with $N_c = 3$ colors and assumed all leptons and quarks except the top and bottom quark to be relativistic at $T_{\text{RH}} = 1 \text{ GeV}$. We compute the effective coupling of the relativistic SM fermions as

$$\begin{aligned} \sum_i N_i &\equiv \sum_i (N_c)_i \left(Q(f_{iL})^2 + Q(f_{iR})^2 \right) \\ &= 3 + 2 \sum_{l=e,\mu,\tau} \theta\left(T - \frac{m_l}{3}\right) + 2\theta(T - 200 \text{ MeV}) + \frac{2}{3} \sum_{q=t,b,c} \theta\left(T - \frac{m_q}{3}\right). \end{aligned} \quad (4.83)$$

Here we treat a fermions as relativistic as long as $E \simeq 3T > m_f$. In the above definition the first 3 stands for the SM neutrinos and the contribution from the charged leptons and quarks is multiplied by a 2 because both chiralities produce DM. We only wrote out the contributions from the heavy quarks explicitly and the term $2\theta(T - 200 \text{ MeV})$ is the contribution from u, d, s , whose mass is below the temperature of the QCD phase transition at $T_{\text{QCD}} \simeq 200 \text{ MeV}$. Below this transition all quarks hadronize and at least for a short period of temperature the light mesons are still relativistic and should be taken into account [310]. The inclusion of these particles requires the use of form-factors and we ignore them because they quickly become non-relativistic and hence the rate density becomes double-Boltzmann suppressed compared to the contributions from ν_l and e^- . Note that we can reuse this estimate to make sure that the same interaction does not equilibrate the ν_R with charge $Q_1 = -2$: The cross section (4.73) also applies to ν_R by replacing

$$Q(\chi_L)^2 + Q(\chi_R)^2 = 9 \quad \text{with} \quad Q_1^2 = 4 \quad (4.84)$$

which is valid for both possible DM charge assignments (4.20) and (4.21). Therefore the ν_R production rate is always smaller than the DM production rate so that (4.82) ensures that there is no thermal population of ν_R . We proceed by analytically solving (4.75)

$$Y_\chi(z_0) = \mathcal{C}_{\text{DM}} \int_{z_{\text{RH}}=1}^{z_0=\infty} dz \frac{\sum_i N_i(z)}{g_{*S}(z) \sqrt{g_{*\rho}(z)}} \frac{1}{z^4} \quad \text{with} \quad \mathcal{C}_{\text{DM}} = 0.32 \frac{M_{\text{Pl}} T_{\text{RH}}^3}{v_{\text{B-L}}^4}. \quad (4.85)$$

Here the reheating temperature T_{RH} acts as a UV-regulator for the effective cross section and if we were to consider $T_{\text{RH}} \rightarrow \infty$ we would need to use the full kinematic dependence of the Z' propagator to unitarize the rate. For the estimate we again replace the relativistic number of d.o.f with their values at T_{RH} (see 4.5.2) so that (4.67) evaluates to

$$\begin{aligned} \Omega_{\text{DM}} h^2 \simeq & 0.12 \cdot \left(\frac{m_{\text{DM}}}{10 \text{ keV}} \right) \cdot \left(\frac{T_{\text{RH}}}{1 \text{ GeV}} \right)^3 \cdot \left(\frac{172 \text{ TeV}}{v_{\text{B-L}}} \right)^4 \\ & \cdot \left(\frac{\sum_i N_i(T_{\text{RH}})}{11.67} \right) \cdot \left(\frac{76}{g_{*S}(T_{\text{RH}})} \right) \cdot \sqrt{\frac{76}{g_{*\rho}(T_{\text{RH}})}}. \end{aligned} \quad (4.86)$$

Note that one can not set m_{DM} to arbitrarily large values since we neglected the phase space suppression for the finite DM mass in (4.73). As a rule of thumb our results apply as long as $m_{\text{DM}} \lesssim T_{\text{RH}}$. For the numerical evaluation we use the full temperature dependence of g_{*S} and $g_{*\rho}$ by employing the fitting functions from [314], which agree up to less than one percent with the exact expressions except during the QCD phase transition and during e^+e^- annihilations, where the differences are about four percent. Figures 4.3 and 4.4 illustrate the behaviour of the DM abundance today for different values of the reheating temperature, DM mass and $v_{\text{B-L}}$ together with the observed relic abundance [20]. As previously alluded to one can see that the yield reaches its asymptotic value shortly after reheating and its final value strongly depends on T_{RH} as expected for UV freeze-in.

Before closing we would like to emphasize that the SM like Higgs can also mediate SM fermions annihilating to DM via the effective interaction in (4.53). The corresponding scattering rate density is found from (4.79)

$$\sum_{f_i} \gamma^h (\bar{f}_i f_i \rightarrow \bar{\chi} \chi) \simeq \frac{12}{\pi^5} \left(\frac{m_{\text{DM}}}{v_H} \right)^2 \sum_{f_i} \left(\frac{m_{f_i}^{\text{eff.}}(T)}{v_H} \right)^2 T^8, \quad (4.87)$$

where

$$\begin{aligned} \sum_{f_i} \left(m_{f_i}^{\text{eff.}}(T) \right)^2 \equiv & \sum_{l=e,\mu,\tau} m_l^2 \theta \left(T - \frac{m_l}{3} \right) + 3 (m_u^2 + m_d^2 + m_s^2) \theta (T - 200 \text{ MeV}) \\ & + 3 \sum_{q=t,b,c} m_q^2 \theta \left(T - \frac{m_q}{3} \right) \end{aligned} \quad (4.88)$$

encodes the couplings of the relativistic SM fermions to the Higgs in analogy with (4.83). We neglect the coupling to the active neutrinos as it scales with their mass. The Higgs

4 Radiative keV-scale DM

mediated interaction does not thermalize at reheating provided that

$$m_{\text{DM}} \lesssim 1 \text{ GeV} \cdot \left(\frac{g_{*\rho}(T_{\text{RH}})}{76} \right)^{\frac{1}{4}} \cdot \left(\frac{1 \text{ GeV}}{T_{\text{RH}}} \right)^{\frac{3}{2}}, \quad (4.89)$$

which is stronger than the bound from invisible Higgs decays (4.55). The estimate for the Higgs mediated relic abundance is straightforward and by comparing with (4.85) we arrive at

$$\frac{\Omega_{\text{DM}}^h}{\Omega_{\text{DM}}^{Z'}} \simeq \frac{3}{2} \left(\frac{v_{\text{B-L}}}{m_h} \right)^4 \left(\frac{m_{\text{DM}}}{v_H} \right)^2 \frac{\sum_{f_i} \left(\frac{m_{f_i}^{\text{eff.}}(T_{\text{RH}})}{v_H} \right)^2}{\sum_i N_i(T_{\text{RH}})}. \quad (4.90)$$

If we demand that this additional contribution is smaller than the Z' mediated one we obtain an upper limit on the DM mass of

$$m_{\text{DM}} \lesssim 3 \text{ MeV} \cdot \sqrt{\frac{\Omega_{\text{DM}}^h / \Omega_{\text{DM}}^{Z'}}{1\%}} \cdot \sqrt{\frac{\sum_i N_i(T_{\text{RH}})}{11.67}} \cdot \left(\frac{172 \text{ TeV}}{v_{\text{B-L}}} \right)^2, \quad (4.91)$$

which was evaluated at $T_{\text{RH}} = 1 \text{ GeV}$, where all charged fermions except the top and bottom quark contribute. This represents the strongest upper bound on the DM mass and is the reason why we only consider DM with typical masses at the keV-scale. We depict contours in the T_{RH} versus $v_{\text{B-L}}$ plane that reproduce the measured DM abundance today for multiple representative masses that agree with the Lyman- α bound and (4.91) in figure 4.7.

4.5.5 Dark matter phenomenology

Owing to our choice of \mathcal{Z}_5 symmetry the DM is absolutely stable and does not mix with the SM neutrinos. Consequently the DM has no radiative decay mode to a ν_L plus a photon. This decay constitutes the canonical signature of keV scale sterile neutrino DM that is being looked for via X-ray searches investigating the diffuse X-Ray background or dwarf galaxies [315--318] (see also [319] and references therein).

The coupling to the Z' and the Higgs induce velocity independent dark matter self interaction cross sections. However due to the small DM mass and $v_{\text{B-L}} \gg m_h \gg m_{\text{DM}}$ the resulting transfer cross sections [320--322] are far to small to help with the “cusp-core” and “too-big-to-fail”-problems [323--326] or even to come into conflict with bounds from the Milky way or the Bullet cluster [323, 324, 326].

The aforementioned self interactions could lead to efficient DM self scatterings which would lead to kinetic equilibrium of the DM population in the early universe. Because of the separation of scales between m_h and $v_{\text{B-L}}$ we only focus on the individual contributions and ignore the interference term. For the Higgs mediated interaction we find in the limit $s, m_{\text{DM}} \ll m_h$

$$\sigma_h(\bar{\chi}\chi \rightarrow \bar{\chi}\chi) \simeq \frac{1}{\pi} \left(\frac{m_{\text{DM}}}{v_H} \right)^4 \frac{s}{m_h^4} \quad (4.92)$$

4.5 Appendix: Dark Matter

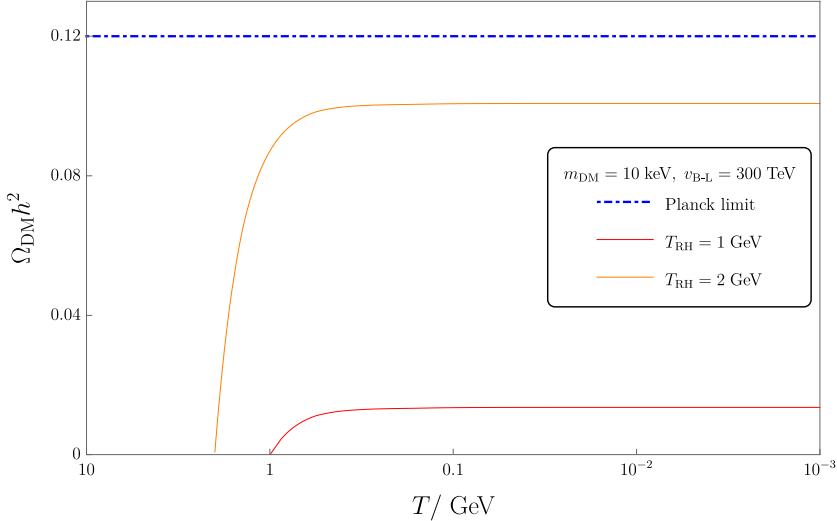


Figure 4.3: DM abundance as a function of temperature for fixed $m_{\text{DM}}, v_{\text{B-L}}$ and two different T_{RH} .

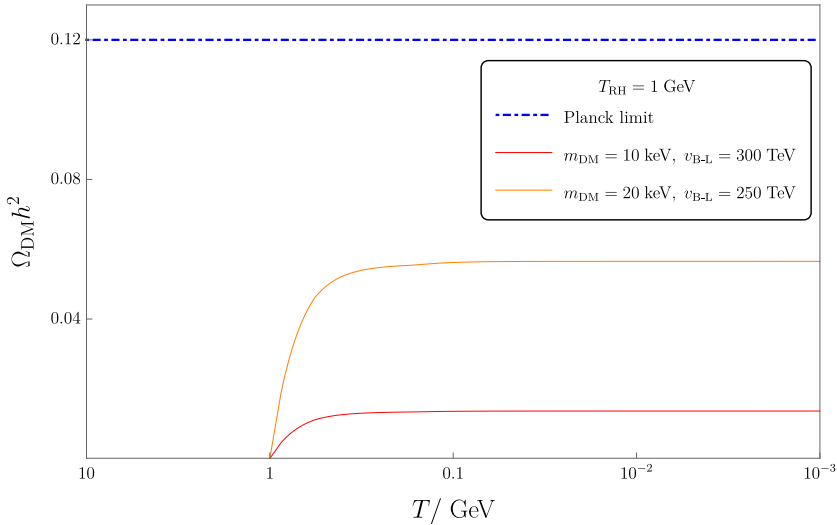


Figure 4.4: DM abundance as a function of temperature for fixed T_{RH} and two different combinations of $m_{\text{DM}}, v_{\text{B-L}}$.

and use the methods of section 4.5.4 to compute

$$\gamma_h(\bar{\chi}\chi \rightarrow \bar{\chi}\chi) \simeq \frac{24}{\pi^5} \left(\frac{m_{\text{DM}}}{v_H} \right)^4 \frac{T^8}{m_h^4}. \quad (4.93)$$

By comparing the interaction rate $\Gamma_h = \gamma_h/n_\chi$, where n_χ is the DM number density with $g_\chi = 4$ degrees of freedom, to the Hubble rate evaluated at reheating we find that the

4 Radiative keV-scale DM

DM is not in kinetic equilibrium with itself at T_{RH} as long as

$$m_{\text{DM}} \lesssim 475 \text{ MeV} \cdot \left(\frac{5 \text{ GeV}}{T_{\text{RH}}} \right)^{\frac{3}{4}} \cdot \left(\frac{g_{*}\rho(T_{\text{RH}})}{85} \right)^{\frac{1}{8}}. \quad (4.94)$$

Similarly to find $\Gamma_{Z'}(\bar{\chi}\chi \rightarrow \bar{\chi}\chi)$ we can reuse the result (4.80) by replacing the charges (see (4.83))

$$\sum_i N_i \quad \text{with} \quad Q(\chi_L)^2 + Q(\chi_R)^2 = 9. \quad (4.95)$$

The Z' mediated diagram does not equilibrate the DM with itself at reheating provided that

$$v_{\text{B-L}} \gtrsim 175 \text{ TeV} \cdot \left(\frac{T_{\text{RH}}}{5 \text{ GeV}} \right)^{\frac{3}{4}} \cdot \left(\frac{85}{g_{*}\rho(T_{\text{RH}})} \right)^{\frac{1}{8}}. \quad (4.96)$$

We conclude that scattering can lead to kinetic equilibrium of the DM at early times for certain choices of parameters. Since both rates arise from effective operators they decrease with temperature, which means that even if the DM was thermalized with itself initially it will fall out of kinetic equilibrium during the evolution of the universe.

As a consequence of the constraint (4.55) we only investigate very light DM with typical masses below 2 GeV. Since nuclear recoil experiments basically have no sensitivity for sub-GeV DM due to kinematics, there has been a growing interest in studying atomic bound state electrons as targets for direct detection of light DM [327]. In order to estimate whether these targets can be used to find our DM candidate, we compute the Higgs and Z' mediated cross sections for non-relativistic DM in the electron rest frame and expand to leading order in $v_{\text{DM}} \ll 1$:

$$\sigma_h(\chi e^- \rightarrow \chi e^-) \simeq \frac{16}{\pi} \left(\frac{m_e m_{\text{DM}}}{m_e + m_{\text{DM}}} \right)^6 \frac{v_{\text{DM}}^2}{m_h^4 v_H^4} \quad (4.97)$$

$$\simeq \begin{cases} 4 \times 10^{-71} \text{ cm}^2 \cdot \left(\frac{v_{\text{DM}}}{10^{-3}} \right)^2 & \text{for } m_{\text{DM}} \gg m_e \\ 2 \times 10^{-81} \text{ cm}^2 \cdot \left(\frac{m_{\text{DM}}}{10 \text{ keV}} \right)^6 \cdot \left(\frac{v_{\text{DM}}}{10^{-3}} \right)^2 & \text{for } m_{\text{DM}} \ll m_e \end{cases}$$

$$\sigma_{Z'}(\chi e^- \rightarrow \chi e^-) \simeq \frac{4}{\pi} \frac{m_e^4 m_{\text{DM}}^4}{(m_e + m_{\text{DM}})^6} \frac{(Q(\chi_L) + Q(\chi_R))^2}{v_{\text{B-L}}^4} v_{\text{DM}}^2 \quad (4.98)$$

$$\simeq \begin{cases} 6.5 \times 10^{-66} \text{ cm}^2 \cdot \left(\frac{10 \text{ MeV}}{m_{\text{DM}}} \right)^2 \cdot \left(\frac{v_{\text{DM}}}{10^{-3}} \right)^2 \cdot \left(\frac{967 \text{ TeV}}{v_{\text{B-L}}} \right)^4 & \text{for } m_{\text{DM}} \gg m_e \\ 3.7 \times 10^{-67} \text{ cm}^2 \cdot \left(\frac{m_{\text{DM}}}{10 \text{ keV}} \right)^4 \cdot \left(\frac{v_{\text{DM}}}{10^{-3}} \right)^2 \cdot \left(\frac{172 \text{ TeV}}{v_{\text{B-L}}} \right)^4 & \text{for } m_{\text{DM}} \ll m_e \end{cases}$$

The Higgs mediated cross section comes with two more powers of both m_e and m_{DM} compared to the Z' mediated one, because the couplings to the Higgs are proportional to the aforementioned masses. In the above we chose $v_{\text{B-L}}$ to reproduce the observed DM relic density for a given DM mass. The best current limit including form factors for bound state electrons is $\sigma \lesssim 10^{-40} \text{ cm}^2$ [328, 329]. One can see that direct detection via electrons is not a viable search strategy for our DM candidate owing to the small values of m_{DM} and the large $v_{\text{B-L}}$ necessary for freeze-in.

4.6 Appendix: Dark Radiation

The SM prediction for the number of relativistic neutrinos is [67--72]

$$N_{\text{eff.}} = 3.0440 \pm 0.0002, \quad (4.99)$$

and the small deviation from the value of 3 expected for three generations of ν_L comes from the fact that their decoupling from the SM bath is not instantaneous. Additional relativistic degrees of freedom are usually referred to as dark radiation (DR). From the observed abundance of light elements produced during Big Bang Nucleosynthesis (BBN) one infers $N_{\text{eff.}}^{\text{BBN}} = 2.95^{+0.56}_{-0.52}$ [20]. Combined analyses of the current Planck CMB data together with Baryon Acoustic oscillations (BAO) found $N_{\text{eff.}}^{\text{Planck+BAO}} = 2.99^{+0.34}_{-0.33}$ [20]. This can be recast as

$$\Delta N_{\text{eff.}}^{\text{Planck+BAO}} \simeq 0.28 @ 2\sigma \text{ C.L.} \quad (4.100)$$

Currently there is a lot experimental effort to improve this bound: The South Pole Telescope [330] and the Simons observatory [331] both aim to reach $\Delta N_{\text{eff.}} \lesssim 0.12 @ 2\sigma$ C.L. while the upcoming CMB Stage 4 (CMB-S4), experiment [332--334] and NASA's PICO proposal [335] have a sensitivity forecast of $\Delta N_{\text{eff.}} = 0.06 @ 2\sigma$ C.L. There is also the planned CORE experiment by the ESA [336] with similar goals.

4.6.1 Dark Matter as dark radiation

Since the dark matter is out of equilibrium with the SM bath, its typical momentum after production can in principle be vastly different from the temperature of the SM. Even though the DM is non-relativistic today, it might have been relativistic at the time of BBN or CMB decoupling. One can find a condition for having a relativistic DM particle at the SM bath temperature T [243]

$$m_{\text{DM}} < \frac{T_{\gamma}(t_0) \left(\frac{g_{*S}(T_{\gamma}(t_0))}{g_{*S}(T_{\text{RH}})} \right)^{\frac{1}{3}}}{a(T)} = \frac{2 \times 10^{-7} \text{ keV} \cdot \left(\frac{100}{g_{*S}(T_{\text{RH}})} \right)^{\frac{1}{3}}}{a(T)}. \quad (4.101)$$

Here $T_{\gamma}(t_0)$ is the photon temperature today and $\frac{g_{*S}(T_{\gamma}(t_0))}{g_{*S}(T_{\text{RH}})}$ is the ratio in the number of relativistic degrees of freedom in entropy today versus the number at the time of DM production, which we approximate with T_{RH} . $a(T)$ denotes the scale factor, whose value ranges from $\simeq 10^{-10}$ at the time of BBN ($T \simeq 1$ MeV) to $\simeq 10^3$ at the time of CMB decoupling ($T \simeq 1$ eV). Consequently our DM candidate can only be relativistic around BBN, but not at recombination. The contribution of the DM to $\Delta N_{\text{eff.}}$ at BBN temperatures was found to be [243, 337]

$$\Delta N_{\text{eff.}}(T_{\text{BBN}}) \simeq 3.4 \times 10^{-4} \cdot \left(\frac{\Omega_{\text{DM}} h^2}{0.12} \right) \cdot \left(\frac{10 \text{ keV}}{m_{\text{DM}}} \right) \cdot \left(\frac{100}{g_{*S}(T_{\text{RH}})} \right)^{\frac{1}{3}} \quad (4.102)$$

and is negligible compared to the expected sensitivities. Note that the above estimate relied on the FIMP being produced from a decay, however we do not expect production from scattering to significantly alter the order of magnitude of the result.

4.6.2 Right handed neutrinos as dark radiation

Due to their feeble effective Yukawa interaction with the left handed neutrinos (see (4.16)) the ν_R never equilibrate with the SM [117] and the freeze-in of the aforementioned interaction contributes an even more negligible amount of [74]

$$\Delta N_{\text{eff.}} \simeq 7.5 \times 10^{-12} \cdot \left(\frac{m_\nu}{0.1 \text{ eV}} \right)^2 \quad (4.103)$$

in standard Big Bang cosmology. Gauge annihilations of SM fermions via the Z' can also create ν_R . From section 4.5.4 we already know that if we want to produce the DM from freeze-in the ν_R production will occur in the freeze-in regime as well. The corresponding cross section is given by (4.73) under the replacement (4.84) and $\alpha_{\chi i} \rightarrow \alpha_{\nu_R i}$. We can write down the coupled Boltzmann equations for the evolution of the SM and DM energy densities [338]

$$\frac{d\rho_{\text{SM}}}{dt} + 3H(\rho_{\text{SM}} + P_{\text{SM}}) = -C_\rho, \quad (4.104)$$

$$\frac{d\rho_{\nu_R}}{dt} + 3H(\rho_{\nu_R} + P_{\nu_R}) = C_\rho, \quad (4.105)$$

where P denotes the pressure density. Adding both Boltzmann equations gives the result expected from the continuum equation

$$\sum_{i=\text{SM}, \nu_R} \frac{d\rho_i}{dt} + 3H(\rho_i + P_i) = 0. \quad (4.106)$$

Making use of the equation of state for radiation allows us to write

$$\rho_i + P_i = \frac{4}{3}\rho_i, \quad i = \text{SM}, \nu_R. \quad (4.107)$$

The right hand side of the Boltzmann equations is known as the collision term and parameterizes the energy exchange between the SM and DM baths. It can be written as [313, 339]

$$C_\rho = \sum_i \langle E\sigma |\vec{v}| \rangle_{\bar{f}_i f_i \rightarrow \bar{\nu}_R \nu_R} n_{f_i} n_{\bar{f}_i} - \langle E\sigma |\vec{v}| \rangle_{\bar{\nu}_R \nu_R \rightarrow \bar{f}_i f_i} n_{\nu_R} n_{\bar{\nu}_R}, \quad (4.108)$$

$$\simeq \sum_i \langle E\sigma |\vec{v}| \rangle_{\bar{f}_i f_i \rightarrow \bar{\nu}_R \nu_R} n_{f_i}^{\text{eq.}} n_{\bar{f}_i}^{\text{eq.}}, \quad (4.109)$$

where we neglect the back-reaction from the ν_R bath in the freeze-in approximation in the second line. The quantities $\langle E\sigma |\vec{v}| \rangle$ are functions of the respective bath temperatures and are defined completely analogous to $\langle \sigma |\vec{v}| \rangle$ in (4.76) as [208, 313, 339]

$$\begin{aligned} \delta(a + b \rightarrow i + j + \dots) &= \langle E\sigma |\vec{v}| \rangle n_a^{\text{eq.}} n_b^{\text{eq.}} \\ &= \frac{T}{64\pi^4} \int_{s_{\text{min}}}^{\infty} ds s^2 \lambda \left(1, \frac{m_a^2}{s}, \frac{m_b^2}{s} \right) \left(1 + \frac{m_a^2 - m_b^2}{2} \right) K_2 \left(\frac{\sqrt{s}}{T} \right) \sigma. \end{aligned} \quad (4.110)$$

K_2 is the modified Bessel function of the second kind, which arises compared to the K_1 in $\langle \sigma |\vec{v}| \rangle$ due to the presence of a factor of E in the thermal average. Again we use Maxwell-Boltzmann statistics instead of the correct Fermi-Dirac averaging to obtain simpler analytic results. By employing the relation

$$\int_0^\infty dx K_2(x) = 2^{n-1} \Gamma\left(\frac{n-1}{2}\right) \Gamma\left(\frac{n+3}{2}\right) \quad \text{for } n > 1 \quad (4.111)$$

we can compute the average for massless initial and final states

$$\delta(\bar{f}_i f_i \rightarrow \bar{\nu}_R \nu_R) = \delta(\bar{\nu}_R \nu_R \rightarrow \bar{f}_i f_i) = \frac{8}{\pi^5} \alpha_{\nu_R} T^9. \quad (4.112)$$

Note again that in the above one has to take into account that the rate densities depend on the different bath temperatures. The scaling of this energy exchange rate density is consistent with dimensional analysis as it scales like the rate density (4.79) for the DM abundance multiplied by another factor of T . Since we do not know the phase-space distribution function of the non-thermal ν_R we do not know their temperature so we compute their energy density directly from solving the Boltzmann equation. If we neglect the energy loss of the SM bath, which is the basis of the freeze-in scenario and assume that the SM entropy is conserved we find [74]

$$\rho_{\nu_R}(T) \simeq 2 \cdot s_{\text{SM}}(T)^{\frac{4}{3}} \int_T^{T_{\text{RH}}} d\tilde{T} \frac{s'_{\text{SM}}(\tilde{T})}{3s_{\text{SM}}(\tilde{T})^{\frac{7}{3}} H(\tilde{T})} \delta_{\bar{f}_i f_i \rightarrow \bar{\nu}_R \nu_R}(\tilde{T}) \quad (4.113)$$

in terms of the SM temperature T and use this to compute [74]

$$\Delta N_{\text{eff.}}(T) = 2 \cdot \frac{4}{7} g_{*\rho}(T) \left(\frac{10.75}{g_{*S}(T)} \right)^{\frac{4}{3}} \frac{\rho_{\nu_R}(T)}{\rho_{\text{SM}}(T)} \quad \text{with} \quad \rho_{\text{SM}}(T) = \frac{\pi^2}{30} g_{*\rho}(T) T^4, \quad (4.114)$$

where the first factor of two in (4.113) accounts for the fact that the ν_R have $g_{\nu_R} = 2$ spin polarizations and the second one in (4.114) for two generations of ν_R . At temperatures below the electron mass e^+e^- annihilations heat the SM plasma compared to the decoupled species so that by using $g_{*S}(T < m_e) = \frac{43}{11}$ we recover the more familiar formula

$$\Delta N_{\text{eff.}}(T < m_e) = 2 \cdot \frac{8}{7} \left(\frac{11}{4} \right)^{\frac{4}{3}} \frac{\rho_{\nu_R}(T)}{\rho_\gamma(T)}. \quad (4.115)$$

For the regime where the ν_R were initially in thermal equilibrium with the SM until they decoupled at T_{FO} before the ν_L decoupling one would find [20, 334]

$$\Delta N_{\text{eff.}}^{\text{eq.}} = 2 \cdot \frac{g_{\nu_R}}{2} \left(\frac{10.75}{g_{*S}(T_{\text{FO}})} \right)^{\frac{4}{3}} \quad (4.116)$$

instead. Integrating the collision term in (4.113) is straightforward and we find

$$\rho_{\nu_R}(T) = \mathcal{C}_{\nu_R}(T) \int_T^{T_{\text{RH}}} d\tilde{T} \frac{\sum_i N_i(\tilde{T}) \tilde{T}^2}{g_{*S}(\tilde{T})^{\frac{4}{3}} \sqrt{g_{*\rho}(\tilde{T})}} \quad (4.117)$$

4 Radiative keV-scale DM

with

$$\mathcal{C}_{\nu_R}(T) = 0.13 g_{*S}(T)^{\frac{4}{3}} \frac{M_{\text{Pl}} T^4}{v_{\text{B-L}}^4}. \quad (4.118)$$

Our estimate for the additional number of relativistic species is in the limit $T_{\text{RH}} \gg T$

$$\begin{aligned} \Delta N_{\text{eff.}} \simeq 1.6 \times 10^{-4} \cdot & \left(\frac{T_{\text{RH}}}{1 \text{ GeV}} \right)^3 \cdot \left(\frac{172 \text{ TeV}}{v_{\text{B-L}}} \right)^4 \\ & \cdot \left(\frac{\sum_i N_i(T_{\text{RH}})}{11.67} \right) \cdot \left(\frac{76}{g_{*S}(T_{\text{RH}})} \right)^{\frac{4}{3}} \cdot \sqrt{\frac{76}{g_{*\rho}(T_{\text{RH}})}}. \end{aligned} \quad (4.119)$$

As expected the abundance of non-thermal DR strongly depends on their production temperature T_{RH} . Note that while it seems that the above expression can lead to arbitrarily large values of $\Delta N_{\text{eff.}}$ one should keep in mind, that the present treatment relying on (4.113) breaks down as soon as one starts to violate (4.82) because the ν_R thermalize. In that case one can use (4.116) to compute $\Delta N_{\text{eff.}}$ from the freeze-out temperature and finds that it asymptotes to a value of two for two ν_R . By plugging in the lower limit on $v_{\text{B-L}}$ from the DM production being out of thermal equilibrium in (4.82) we find that the freeze-in contribution of ν_R via Z' mediated scatterings is at least a factor of five below the sensitivities of the upcoming CMB experiments

$$\Delta N_{\text{eff.}} < 1.2 \times 10^{-2} \cdot \left(\frac{85}{g_{*S}(T_{\text{RH}} = 5 \text{ GeV})} \right)^{\frac{4}{3}}. \quad (4.120)$$

We conclude that the interplay of the tiny rates $\sim v_{\text{B-L}}^{-4}$ together with the fact that we consider a cosmology with a low reheating temperature reduces the impact of ν_R and χ on $\Delta N_{\text{eff.}}$ below all current and future sensitivities. This opens up an interesting indirect way to test our model: Should observations ever point to $\Delta N_{\text{eff.}} > 0.012$ our scenario for DM production is excluded.

For the numerical evaluation of (4.113) we proceed as in section 4.5.4. The temperature dependence of $\Delta N_{\text{eff.}}$ was depicted in 4.5 and 4.6 together with the limit from Planck [20]. For better visibility of the final DR yield we chose values of $v_{\text{B-L}}$ below the bound (4.82). The curves in 4.5 demonstrate that the abundance strongly depends on the reheating temperature and 4.6 that it decreases with growing $v_{\text{B-L}}$. Both plots show how the final yield is reached shortly after reheating as was the case for DM production.

There is also a contribution to the annihilations of SM fermions to ν_R via the exchange of an SM like Higgs. The corresponding rate density reads in terms of the coupling (4.88)

$$\sum_{f_i} \delta^h(\bar{f}_i f_i \rightarrow \bar{\nu}_R \nu_R) \simeq \frac{12}{\pi^5} \left(\frac{m_\nu}{v_H} \right)^2 \sum_{f_i} \left(\frac{m_{f_i}^{\text{eff.}}(T)}{v_H} \right)^2 T^9, \quad (4.121)$$

and it does not thermalize at T_{RH} due to the tiny coupling $\propto (m_\nu/v_H)^2$. The estimate for the ratio of the resulting DR yields is equal to (4.90) under the replacement $m_{\text{DM}} \rightarrow m_\nu$. We find that we can neglect the freeze-in of $\Delta N_{\text{eff.}}$ via Higgs interactions as

$$\frac{\Delta N_{\text{eff.}}^h}{\Delta N_{\text{eff.}}^{Z'}} \simeq 10^{-17} \cdot \left(\frac{m_\nu}{0.1 \text{ eV}} \right)^2 \cdot \left(\frac{v_{\text{B-L}}}{172 \text{ TeV}} \right)^4 \cdot \left(\frac{11.67}{\sum_i N_i(T_{\text{RH}})} \right). \quad (4.122)$$

4.6 Appendix: Dark Radiation

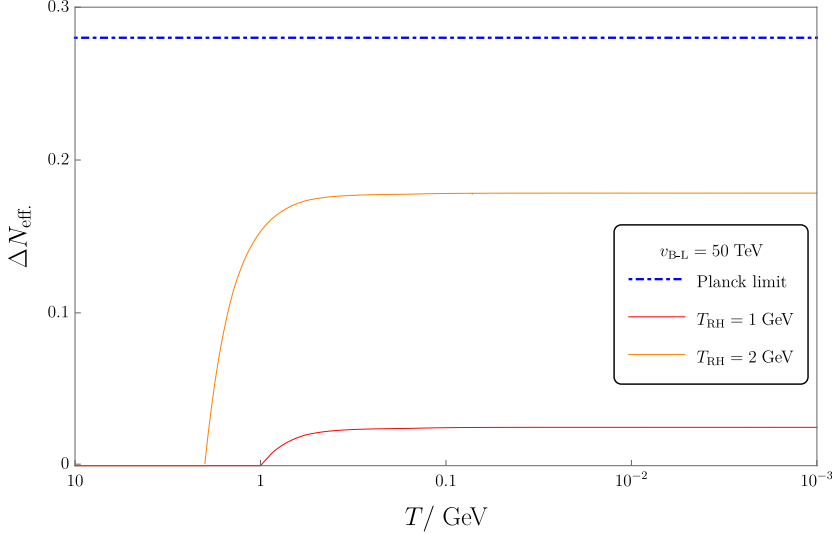


Figure 4.5: ΔN_{eff} as a function of temperature for fixed $v_{\text{B-L}}$ and two different T_{RH} .

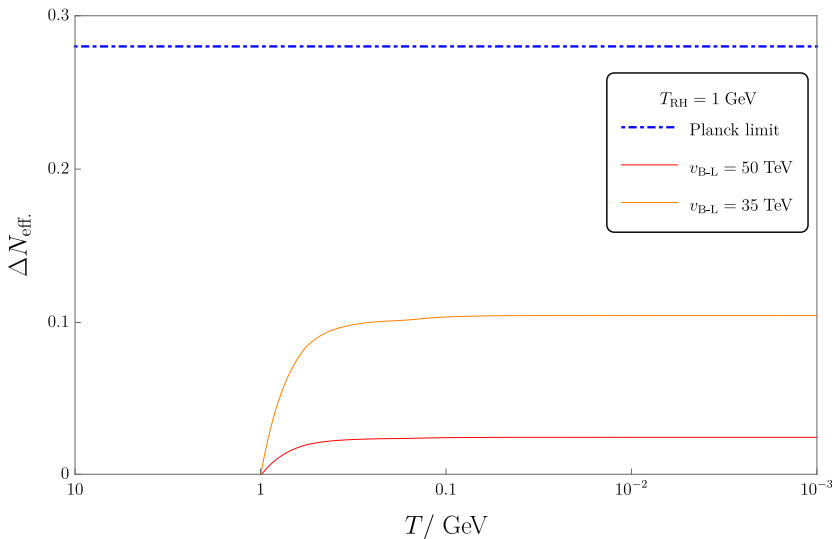


Figure 4.6: ΔN_{eff} as a function of temperature for fixed T_{RH} and two different $v_{\text{B-L}}$.

The above was evaluated at $T_{\text{RH}} = 1 \text{ GeV}$, where all charged fermions except the top and bottom quark contribute. Figure 4.7 demonstrates the available parameter space for realizing the entire DM abundance from χ s via freeze-in together with the predicted amount of dark radiation parameterized in terms of ΔN_{eff} . A few comments are in order: The gray region excluded by (4.82) has a more rugged contour because of the

4 Radiative keV-scale DM

sequence of Heaviside functions in the expression for the sum of fermion charges (4.83). Additionally there is a noticeable kink in all DM and DR contours, which occurs around the temperature of the QCD phase transition at $T_{\text{QCD}} \simeq 200 \text{ MeV}$. The physical reason for this behaviour can be found by inspecting the expressions for the DM and DR yields in (4.85) and (4.117): The integrands in both cases depend on inverse powers of $g_{*S}(T)$ and $g_{*\rho}(T)$ and the number of relativistic degrees of freedom in entropy and energy both decrease drastically when the quarks and gluons confine at T_{QCD} . To keep the relic density or $\Delta N_{\text{eff.}}$ fixed one needs to compensate this increase of the integrand by allowing for a larger value of $v_{\text{B-L}}$, hence the contours appear to be shifted to the right below T_{QCD} , which is why for illustration we chose to display a straight line at the corresponding temperature. One should not forget that the factor of $\sum_i N_i$ in both numerators also decreases sharply below T_{QCD} , but is approximately cancelled by one of the factors in the denominator leaving one factor in the denominator leading to the previously explained behaviour.

It is evident from 4.7 that the Planck constraint on $\Delta N_{\text{eff.}}$ would only be relevant for DM masses far below 4 keV, which is already excluded by the Lyman- α constraints. Moreover it is clear that producing $\Delta N_{\text{eff.}} \gtrsim 0.06$ only occurs in regions where there is either too much DM or the freeze-in approximation for DM production is not applicable because the production rates from relativistic SM fermions thermalize. Moreover we see that for larger allowed DM masses there is actually less $\Delta N_{\text{eff.}}$. The reason is simply that larger m_{DM} at constant T_{RH} require larger $v_{\text{B-L}}$ to fix the relic density, which decreases $\Delta N_{\text{eff.}} \sim v_{\text{B-L}}^{-4}$. Consequently our scenario for FIMP DM predicts only a small value of $\Delta N_{\text{eff.}}$ despite the fact that we introduce two ν_R and a rather light DM candidate.

This makes the present construction different from the cosmology of other (Dirac) neutrino mass models like e.g. the neutrino-philic Two-Higgs-Doublet model [164, 340–343] or its gauged variations such as [157, 158, 344–347] which usually feature light mediators below the EW scale that unavoidably thermalize the ν_R and themselves leading to $\Delta N_{\text{eff.}} > \mathcal{O}(0.1)$ [348, 349]. Another interesting scheme is called “Common Origin of Warm and Relativistic Decay Products” (COWaRD) [350], where DM and DR are produced together from the decay of a parent particle and the amount of $\Delta N_{\text{eff.}}$ is correlated with the warmness of DM. There a non-zero $\Delta N_{\text{eff.}}$ can help to reduce the σ_8 -tension for large scale structures [351, 352]. In a sense the COWaRD scheme is the opposite of our idea as it involves thermal DM and predicts a larger amount of DR. All of these models have in common that the more stringent limits on $\Delta N_{\text{eff.}}$ will already constrain significant amount of their parameter space or even exclude them completely. The only ways to exclude our scenario would be CMB experiments in the far future with a sensitivity to even smaller values of $\Delta N_{\text{eff.}} = \mathcal{O}(10^{-3})$ or the actual observation of a signal with $0.28 > \Delta N_{\text{eff.}} > 0.012$, which by itself would be a smoking gun for different BSM physics.

4.7 Appendix: Inflation and candidates for the inflaton

■ ADDENDUM: This section is basically an appendix, that tries to motivate a scenario

4.7 Appendix: Inflation and candidates for the inflaton

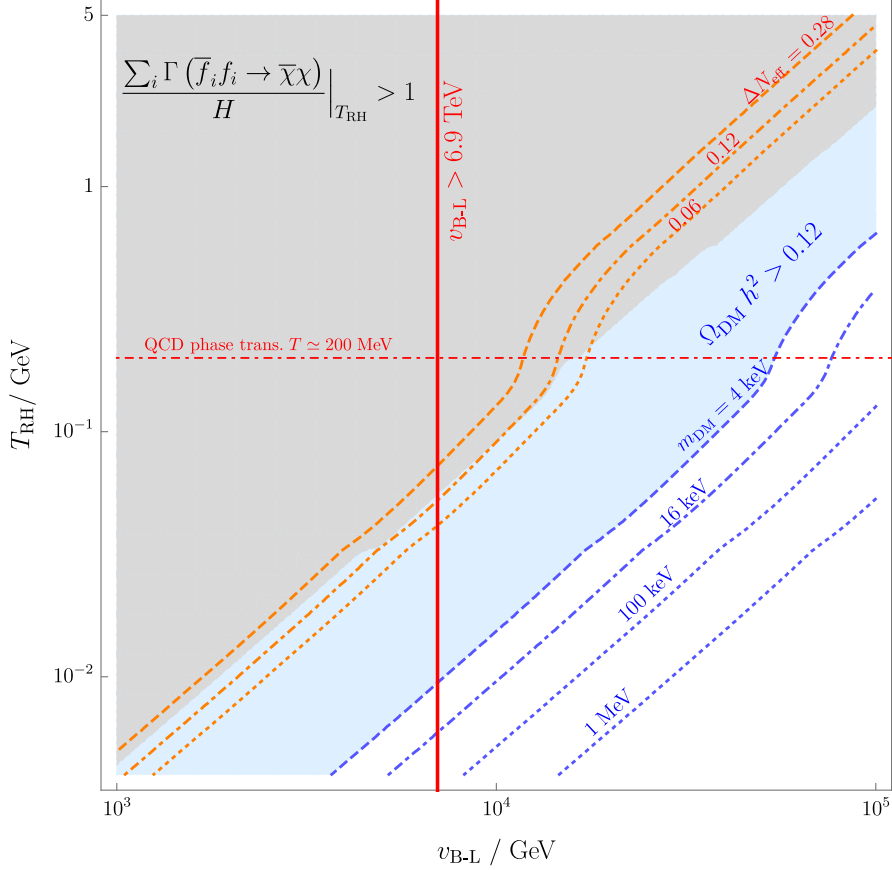


Figure 4.7: We depict the allowed combinations of the reheating temperature T_{RH} and the scale of B-L breaking $v_{\text{B-L}}$. The blue shaded area indicates where DM would overclose the universe and the blue contours reproduce the observed DM relic density for $m_{\text{DM}} \in [4, 16, 100, 10^3] \text{ keV}$. Furthermore we show the contours for generating ΔN_{eff} within the Planck bound [20], the estimated sensitivities of the South Pole Telescope [330], the Simons observatory [331] and for the CMB stage 4 experiment [332–334] as well as PICO [335]. The grey area is excluded because the interaction producing DM would equilibrate see (4.82) and searches from LEP exclude $v_{\text{B-L}} < 6.9 \text{ TeV}$ [272].

that can realize the required reheating temperature below 5 GeV. ■

The assumed production mode for DM crucially relies on a low value of the reheating temperature $4 \text{ MeV} \lesssim T_{\text{RH}} \lesssim 5 \text{ GeV}$ together with the assumption of no primordial DM abundance from e.g. inflaton decays during reheating. This puts non-trivial constraints on the explicit realization of inflation. Of course one can assume that the scalar field responsible for creating the inflationary phase of cosmic expansion is another scalar field with no couplings to the DM. However the present model already contains four different scalar multiplets so a minimal solution is to embed the inflaton into one of

them. For concreteness we will assume that the candidate field for inflation is the real component of a complex scalar field ω . Recent Planck constraints [353] disfavour monomial inflation of the form $\text{Re}(\omega)^p$ with $p > 1$ because their potential is too steep leading to a too large tensor to scalar ratio. This is why we only investigate scenarios with a non-minimal coupling of the inflaton to gravity: This scenario is known as Starobinsky-like inflation [109, 110, 354–359] and the action in the Jordan frame reads

$$\mathcal{S} = \int d^4x \sqrt{-g} \left(\frac{1}{2} M_{\text{Pl.}}^2 + \xi_\omega |\omega|^2 \right) R. \quad (4.123)$$

In this context we denote the determinant of the metric as g , the Ricci curvature scalar as R and ξ_ω is a dimensionless coupling. One can single out a scalar ω field to play the role of the inflaton by imposing that the couplings of the other scalar fields satisfy $\lambda_\omega/\xi_\omega^2 \ll \lambda_i/\xi_i^2$ [360], where the λ denote the scalar self couplings. The remaining fields will be treated as spectator fields. We will use the constraints from reheating to find the appropriate inflaton candidate in our model. Due to the presence of additional scalars besides the inflaton there is the possibility of creating isocurvature perturbations as in multi-field inflation models [361, 362], which could come into conflict with CMB bounds. Essentially the problem is that massless particles are sensitive to quantum fluctuations during inflation [363]. However large isocurvature fluctuations can be prevented if either the tree-level mass or the effective mass generated from inflaton oscillations during reheating is larger than the Hubble rate during inflation [364]. Since both η, σ have tree-level masses unconnected to any vev and potentially receive effective masses, we do not expect isocurvature perturbations in these directions. Similarly if we assume that the scale of B-L breaking $v_{\text{B-L}}$ is larger than the Hubble rate H_I during inflation and $U(1)_{\text{B-L}}$ is never restored, then the would-be-Goldstone mode φ_I corresponds to the longitudinal mode of the massive Z' and not to a massless field. Reference [360] found that in the extension of the SM with an inert doublet η housing the inflaton there are only negligible isocurvature fluctuations. A detailed investigation of these fluctuations for the full model is beyond the scope of the present study and we will be content with just outlining how inflation could be realized.

Note that we can also allow for a temperature at the end of inflation far above the MeV and GeV range if there is an additional long lived particle that dominates the energy budget of the universe. This leads to an intermediate matter dominated phase [302] which can end in a second radiation dominated epoch with a smaller temperature of the required order of magnitude.

4.7.1 The SM like Higgs

Using the SM like Higgs as the inflaton [110, 358, 359, 365–368] is a very minimal scenario see [369] for a review. The main drawback of this approach is that the measured value of the Higgs self coupling λ_H requires a rather large value of $\xi_H = \mathcal{O}(10^4)$, which might give rise to unitarity problems [370–372] at scales above M_{Pl}/ξ_H . The unitarity problem could for instance be cured by assuming a different coupling to gravity [373–375]. Another possibility is exploiting that the SM Higgs self coupling λ_H becomes very small at large

energy scales which flattens the potential and leads to $\xi = \mathcal{O}(10)$, which is known as critical Higgs inflation [376–380]. In terms of BSM physics there is also the attractive possibility to invoke additional scalars to modify the Higgs potential see e.g. [381–383]. While it would be interesting to see whether the additional scalars present in this model can solve the unitarity problem it would definitely require a dedicated analysis beyond this work. Consequently we do not consider Higgs inflation further and investigate the other scalar fields as inflaton candidates.

4.7.2 The B-L breaking singlet

The only singlet with a B-L breaking vev could be the inflaton too [384, 385]. We neglect the mixing between h and φ because the EW gauge symmetry is restored at large temperatures [386, 387] so the mixing term vanishes together with v_H . For the same reason we compute the decays to the entire doublet H and not just h . For the purpose of finding estimates we work in the regime of perturbative reheating. We assume that all additional scalars, fermions and the Z' are heavier than the inflaton so the only available decay modes are

$$\Gamma(\varphi \rightarrow H^\dagger H) = \frac{\lambda_{H\phi}^2 v_{\text{B-L}}^2}{8\pi m_\varphi}, \quad \text{and} \quad \Gamma(\varphi \rightarrow \bar{\chi}\chi) = \left(\frac{m_{\text{DM}}}{v_{\text{B-L}}}\right)^2 \frac{m_\varphi}{8\pi}, \quad (4.124)$$

where the decay width to DM is obtained from (4.50) after converting it to $\sim m_{\text{DM}}/v_H$ and replacing $v_H \rightarrow v_{\text{B-L}}$. Since the scalar will oscillate in its potential during reheating it develops an effective mass depending on its oscillation frequency and the same goes for all other scalar fields as well as the Z' since they share quartic couplings with φ . Hence requiring that (4.124) are the only available decay modes and that e.g. $\varphi \rightarrow S_1 S_2 h$ is absent amounts to a bound on the effective field dependent masses and not on the tree-level masses that we have employed so far. For the sake of simplicity this first estimate will work exclusively with the tree level masses. If we want to avoid a primordial abundance of DM the first step is to make sure that decays to SM particles dominate the reheating process

$$\text{BR} \equiv \frac{\Gamma(\varphi \rightarrow \bar{\chi}\chi)}{\Gamma(\varphi \rightarrow \bar{\chi}\chi) + \Gamma(\varphi \rightarrow H^\dagger H)} \simeq \frac{\Gamma(\varphi \rightarrow \bar{\chi}\chi)}{\Gamma(\varphi \rightarrow H^\dagger H)} = \frac{1}{\lambda_{H\phi}^2} \frac{m_{\text{DM}}^2}{v_{\text{B-L}}^2} \frac{m_\varphi^2}{v_{\text{B-L}}^2} \ll 1, \quad (4.125)$$

which sets bounds on the model parameters. Assuming $\text{BR} \ll 1$ we can determine the reheating temperature from the decay to the SM Higgses, which themselves will decay to fermions creating a hot thermal bath. In this limit the reheating temperature is found to be

$$T_{\text{RH}} = \sqrt{\frac{2}{\pi}} \left(\frac{10}{g_{*\rho}(T_{\text{RH}})} \right) \sqrt{M_{\text{Pl}} \Gamma(\varphi \rightarrow H^\dagger H)}. \quad (4.126)$$

The assumed range of reheating temperatures for DM production requires that either $\lambda_{H\phi} \ll 1$ or that $m_\varphi \gg v_{\text{B-L}}$. However the second condition can not be realized because m_φ is proportional to $v_{\text{B-L}}$ according to (4.44) and we can not make m_φ arbitrarily heavy due to the perturbativity limit $\lambda_\phi < \sqrt{4\pi}$.

4 Radiative keV-scale DM

Inflaton decays can produce DM as well and the corresponding Boltzmann equation during reheating reads [388]

$$\frac{dn_\chi}{dt} + 3Hn_\chi = \frac{\rho_\varphi}{m_\varphi} \Gamma(\varphi \rightarrow \bar{\chi}\chi), \quad \text{with} \quad H^2 = \frac{\rho_\varphi + \rho_{\text{SM}}}{3M_{\text{Pl}}^2} \quad (4.127)$$

and we denote the energy density of the non-relativistic inflaton condensate as ρ_φ . The DM yield today is found to be [388]

$$Y_\chi(T_0) \simeq \frac{3}{4} \frac{g_{*\rho}(T_{\text{RH}})}{g_{*S}(T_{\text{RH}})} \frac{T_{\text{RH}}}{m_\varphi} \text{BR} \quad (4.128)$$

and the DM energy density today can be calculated with (4.67). For simplicity we assume $g_{*\rho}(T_{\text{RH}}) \simeq g_{*S}(T_{\text{RH}})$. We trade the inflaton mass via equation (4.126) for an expression involving T_{RH} and $v_{\text{B-L}}$, where the dependence on $\lambda_{H\phi}$ in $Y_\chi(T_0)$ divides out. By using our limit on $v_{\text{B-L}}$ in (4.82) we derive an upper-limit on the relic abundance from inflaton decays

$$\Omega_{\text{DM}}^{\text{inf.}} h^2 \lesssim 0.56 \left(\frac{m_{\text{DM}}}{10 \text{ keV}} \right)^3 \cdot \left(\frac{1 \text{ GeV}}{T_{\text{RH}}} \right)^{\frac{5}{2}} \cdot \sqrt{\frac{11.67}{\sum_i N_i(T_{\text{RH}})}} \cdot \left(\frac{76}{g_{*\rho}(T_{\text{RH}})} \right)^{\frac{7}{4}}. \quad (4.129)$$

It is evident that large m_{DM} and low reheating temperatures could lead to an abundance that is larger than the FIMP one in (4.86). Demanding that the abundance from inflaton decays does not overclose the universe cuts away all the available parameter space in 4.7. There is another reason why this channel is not suited for light DM production: Since the production mode is different from both freeze-in (which requires a thermal bath) and thermal production, the phase space distribution and hence the velocity distribution of the DM will be different assuming all of DM was produced via this single channel. This manifest itself in a modified Lyman- α bound [388, 389]

$$m_{\text{DM}} \gtrsim 2 \text{ keV} \cdot \left(\frac{m_\varphi}{T_{\text{RH}}} \right) \cdot \left(\frac{m_{\text{WDM}}}{3.5 \text{ keV}} \right), \quad (4.130)$$

which was recast from the bound for thermally produced DM with $m_{\text{WDM}} \gtrsim 3.5 \text{ keV}$ [390] (which is the average of the two possible warm DM masses in section 4.5.1). If we assume that $m_\varphi = \mathcal{O}(v_{\text{B-L}})$ then we expect an inflaton with at least a TeV scale mass (see (4.38)), which is much larger than the assumed MeV-GeV reheating temperatures. Therefore the DM mass for inflaton production would be orders of magnitude larger than 2 keV and potentially violates the bound from invisible Higgs decays in (4.55) and could lead to overclosure. Thus we conclude that for our purposes φ can not be the inflaton, because it tends to produce too much DM. Therefore we assume that φ is too heavy to be produced during reheating.

4.7.3 The inert doublet or singlet scalars

As previously mentioned v_H vanishes due to the restoration of the EW symmetry at large temperatures [386, 387]. In this limit we can relate $S_1 = \eta_R^0$ as well as $S_2 = \sigma_R^0$

4.7 Appendix: Inflation and candidates for the inflaton

and consider each field as a candidate individually. Similar to Higgs inflation the inert doublet η can house the inflaton [360]. This scenario is free of the unitarity problem because the value of the η self coupling λ_η is unconstrained by phenomenology. We can not just reuse the perturbative reheating estimate (4.126) from the previous section, because without a vev there is no tree level decay to Higgses like in (4.124) or to EW gauge bosons for η_R^0 . In this model reheating occurs via quartic couplings to electroweak gauge bosons and SM Higgses [359, 360] and we assume that the Z' is too heavy to be produced. Reheating typically takes place through resonant gauge boson production which then annihilate to SM fermions. In this scenario the reheating temperature was found to be [360]

$$T_{\text{RH}}^\eta \simeq 10^{14} \text{ GeV} \lambda_\eta^{-\frac{1}{8}}. \quad (4.131)$$

Generating sub-GeV reheating temperatures is impossible in this regime, because it would require non-perturbative values of λ_η . We conclude that another reheating channel is needed and hence consider an inflaton without SM gauge interactions: σ is an SM singlet and has no vev as well. If we assume that the effective field dependent mass of the Z' is too large to be produced then creating SM Higgses via the quartic coupling $\lambda_{H\sigma}$ in (4.6) is the only possibility left. Since this process depends on the new coupling $\lambda_{H\sigma}$ instead of the known SM gauge couplings the reheating temperature will also depend on this unconstrained parameter. Subsequent decays and annihilations of the Higgs to SM states then seed the SM radiation bath. Reference [391] found that for resonant Higgs production

$$T_{\text{RH}}^{\sigma \text{ res.}} \simeq 3 \times 10^{13} \text{ GeV} \left(\frac{\lambda_\sigma}{\lambda_{H\sigma}^2} \right)^{\frac{1}{4}}. \quad (4.132)$$

The analysis [391] made the conservative assumption of having reheating occur during the quadratic phase of the potential before the quartic self-interaction of the inflaton becomes dominant, which can be expressed as $\lambda_\sigma > 0.25 \lambda_{H\sigma}$ [391]. If we drop this assumption, which [391] emphasizes is not ruled out, we can choose smaller values of $\lambda_\sigma \ll \lambda_{H\sigma}$ and can at least in principle accommodate the range $4 \text{ MeV} \lesssim T_{\text{RH}} \lesssim 5 \text{ GeV}$. The authors of [391] also found that reheating can occur in another regime if inflaton excitations annihilate into pairs of Higgs bosons leading to the estimate

$$T_{\text{RH}}^{\sigma \text{ ann.}} \simeq 9 \times 10^{13} \text{ GeV} \cdot \lambda_\sigma^{\frac{1}{4}}. \quad (4.133)$$

The conservative assumption about reheating occurring in the quadratic regime of the potential would lead to $\lambda_\sigma > 0.019$ [391], but again we need to drop this assumption and require $\lambda_\sigma \ll 1$ to obtain the phenomenologically favoured reheating temperatures. In the next section 4.8 we will introduce a decay of σ to exotic quarks, which might open up another possibility for realizing the required reheating temperature.

Let us emphasize that there are bounds from vacuum stability and perturbativity on the quartic couplings [392], but since these bounds are usually obtained in models with a simpler scalar sector it requires a dedicated study to translate them to our construction, because of e.g. threshold effects from heavy scalars [274]. Note that at some point during reheating there will be the SSB of the EW symmetry generating a coupling of σ_R^0 to the EW

gauge bosons proportional to $\sin(\alpha)$. But since the neutrino mass (4.15) does not directly depend on the mixing angle α in the radiative Seesaw limit we can make this mixing small.

If we assume that the F fermions are heavier than the σ there will be no inflaton decays to χ via the Yukawa interaction in (4.22). The only way to generate the unwanted primordial DM population would be annihilation processes of the form $\sigma_R^0 \sigma_R^0 \rightarrow \bar{\chi}\chi$ mediated by heavy F s. We do not expect this to lead to a significant DM abundance, because scattering is inefficient for non-relativistic excitations of the inflaton field and the production is suppressed by the heavy F mass. On top of that the DM production competes with the unsuppressed process for creating the SM radiation $\sigma_R^0 \sigma_R^0 \rightarrow H^\dagger H$. Since the singlet scalar might not have decay modes, we need to ensure that the inflaton becomes a subdominant component of the universe's energy budget after reheating. The additional interactions like Higgs or Z' mediated scatterings with the SM fermions could help thermalize the inflaton with the radiation bath, which is already in thermal equilibrium [306]. We conclude that the only possible inflaton candidate that is not in conflict with the cosmological DM and reheating requirements is σ_R^0 .

4.8 Appendix: Baryogenesis

■ ADDENDUM: This section is basically an appendix, that tries to motivate a Baryogenesis scenario that could work with a reheating temperature below 5 GeV. Compared to the Baryogenesis mechanisms in the next chapters this section only covers a crude sketch of a mechanism and can be skipped for the convenience of the reader. ■

The assumed low scale reheating is hard to reconcile with most known mechanisms [393--395] for Baryogenesis. Leptogenesis [116] for instance relies on producing a leptonic asymmetry that gets converted into a baryon asymmetry by electroweak sphaleron processes, which are in equilibrium only above the EW phase transition at $T_{EW} = \mathcal{O}(100 \text{ GeV})$. On top of that since the SM neutrinos do not mix with any of the heavy new neutrinos N, F we can not realize Leptogenesis via oscillations [396] as well. Thus we are left with mechanisms that do not rely on the sphaleron transition above the EW scale. One example is the spontaneous Baryogenesis [118,119] mechanism, which however needs reheating temperatures far above the assumed MeV-GeV scale window. Hence some other form of non-thermal Baryogenesis during reheating seems to be the only possibility left if we insist that the temperature at the end inflation is indeed in the previously mentioned range.

The Affleck-Dine mechanism [257] relies on baryon number charged scalars whose real and imaginary parts evolve non-trivially in time, which acts as a source term for baryon number. This scenario can in principle operate at low reheating temperatures if the initial field value of the Affleck-Dine field is very large compared to its mass. Since all of our scalars except H are charged under B-L this is an attractive possibility. For concreteness we will treat σ as the Affleck-Dine field; whether it can accommodate both Baryogenesis

and inflation at the same time like e.g. [364, 397--407] will be left for future investigation. An important ingredient is a small explicit Baryon number breaking interaction. Of course we can not break our gauged B-L explicitly but a term of the form $\lambda_{\text{AD}}(\sigma^4 + \sigma^{*4})$ could arise after the spontaneous breaking of $U(1)_{\text{B-L}}$. To do so we allow for the small \mathcal{Z}_5 breaking term

$$\mathcal{L} \subset -\lambda' (\sigma^2 \phi^2 + \text{h.c.}), \quad (4.134)$$

which after integrating out the heavy radial mode φ (we ignore the φ -Higgs mixing here) leads to an operator

$$\mathcal{L}_{\text{EFT}} \subset -\frac{\lambda'^2 v_{\text{B-L}}^2}{m_\varphi^2} (\sigma^4 + \sigma^{*4}) \quad (4.135)$$

and we can identify $\lambda_{\text{AD}} = \lambda'^2 v_{\text{B-L}}^2 / m_\varphi^2 \simeq \lambda'^2 / (2 \lambda_\phi)$ from (4.44). Quite interestingly this allows us to make λ_{AD} small just by assuming $\sqrt{\lambda'} \ll \lambda_\phi$. Since $\lambda' \rightarrow 0$ would restore the discrete symmetry the choice $\lambda' \ll 1$ is technically natural [408]. Of course assuming the existence of this operator begs the question why the other \mathcal{Z}_5 breaking interactions are absent. The last missing ingredient is a way to transmit the σ -asymmetry to the quarks. To do so we introduce a pair of heavy vector-like quarks (Q_L, Q_R) that are weak isospin singlets with the hypercharge $Y = -2/3$ ($4/3$) of the right chiral down (up) quarks. The quarks come with a B-L charge $Q_\sigma + 1/3 = -2/3$ and transform as ω^{-4} under \mathcal{Z}_5 , where $\omega = e^{\frac{2i\pi}{5}}$, so that we can realize the operators

$$\mathcal{L} \subset -Y_{Qq} \overline{Q_L} \sigma d_R - m_Q \overline{Q_L} Q_R. \quad (4.136)$$

Here d_R can in principle also be replaced with u_R ; we chose the hypercharge $-2/3$ to make the vector-like quarks resemble the down-type quarks which might help with unification [280, 281].

■ ADDENDUM: Again when it comes to unification the previously mentioned caveats apply. ■

The above interaction could also lead to inflaton mediated washout scatterings depleting the baryon asymmetry [404], which puts constraints on the coupling Y_{Qq} . In order to prevent stable exotic quarks from forming relics [409] we have to demand that $m_Q > m_\sigma$ so the Q can decay via the above operator to σu_R in the late universe. Alternatively one can also arrange for $m_\sigma > m_Q > 2m_h$ instead so that the decay of the vector-like quarks proceeds via off-shell σ as $Q_L \rightarrow \sigma^* + d_R \rightarrow 2h + d_R$; the Higgses then further decay to SM states. In the early universe the field σ receives a potentially large effective mass from inflaton oscillations during reheating so for both aforementioned cases the CP -conserving decay $\sigma \rightarrow \overline{Q_L} u_R$ would be possible and one can indeed transmit the asymmetry from the Affleck-Dine field to the quark sector. This decay could open up another interesting reheating scenario as well. In the following we will assume that T_{RH} arises either from the channels enumerated in the previous section 4.7.3 or via the aforementioned decay. An estimate for the baryon asymmetry leads to [410, 411]

$$\frac{n_B}{s} \simeq 10^{-10} \cdot \left(\frac{\lambda_{\text{AD}}}{10^{-2}} \right) \cdot \left(\frac{\sin(4\theta_i)}{0.5} \right) \cdot \left(\frac{r_i/m_\sigma}{6 \times 10^6} \right)^3 \cdot \left(\frac{r_i}{6 \times 10^9 \text{ GeV}} \right) \cdot \left(\frac{T_{\text{RH}}}{1 \text{ GeV}} \right). \quad (4.137)$$

4 Radiative keV-scale DM

Here we use the polar parameterization for σ , where r_i is the initial value of the radial component and θ_i denotes the initial angle needed for CP violation. This decomposition should not be confused with the cartesian representation from (4.7). The initial angle can not be set to arbitrarily small values in order to avoid isocurvature perturbations [405], which is why we chose $\sin(4\theta_i) \simeq 0.5$. We see that very large initial field values are needed to compensate for the low reheating temperature. Such a high field value of $r_i/m_\sigma \simeq 6 \times 10^6$ usually requires a very flat potential and could be an initial condition. Alternatively the non-minimal coupling to gravity might help to generate this field value dynamically [412]: It was found that this coupling together with the tree level mass squared creates an effective mass squared depending on the Hubble parameter. This effective mass is tachyonic at early times when $H \gg m_\sigma$ and later turns real again, which can be understood as an inverted phase transition [413, 414]. Afterwards the field, which can be visualized as an over-damped oscillator, is stuck in its previous non-trivial minimum corresponding to an initial value of [60]

$$r_i \simeq \sqrt{\frac{\xi_\sigma}{\lambda_\sigma}} m_\sigma, \quad (4.138)$$

before it starts to relax to its true minimum $\sigma = 0$ as soon as the Hubble rate satisfies $H \sim m_\sigma$ provided that $\lambda_{\text{AD}} \ll \lambda_\sigma$. From this mechanism we can deduce that a scalar self coupling of

$$\lambda_\sigma \simeq 2.8 \times 10^{-14} \cdot \xi_\sigma \cdot \left(\frac{r_i}{6 \times 10^9 \text{ GeV}} \right)^2 \cdot \left(\frac{1 \text{ TeV}}{m_\sigma} \right)^2 \quad (4.139)$$

would be required for the initial field value and a scalar mass in accord with our previous estimates (4.16) and (4.32). Note that this violates the previous assumption $\lambda_{\text{AD}} \ll \lambda_\sigma$, but we can reconcile this by assuming that the heavy φ will only be integrated out at temperatures somewhat below the inverted phase transition so that the operator (4.135) is absent initially. On the level of estimates it seems that our scalar potential can reproduce the observed baryon asymmetry, but again we stress that it requires a separate study to work out the details especially in the inflationary context and considering the radiative stability.

It is noteworthy that the operator (4.134) also sources a mass splitting $\simeq \pm \lambda' v_{\text{B-L}}^2$ between the real and imaginary parts of σ , while for the neutrino mass generation we assumed that they are mass degenerate. Under the assumption that this additional mass splitting is small compared to the overall mass scale of the $S_{1,2}(A_{1,2})$ and the mass splitting between the different generations of scalars our conclusions about the neutrino and DM masses are unchanged.

If T_{RH} is the temperature after an intermediate epoch of matter domination and the true temperature at the beginning of the first radiation dominated phase was far above the electroweak scale this allows for the other previously discussed mechanisms again. In that case the challenge is to generate enough entropy to dilute unwanted relics (such as thermally produced DM) while retaining enough baryon asymmetry [415].

4.9 Appendix: Summary

We presented an extension of the Dirac scotogenic model [54, 55] that creates the Dirac mass of a light fermionic DM candidate χ together with the active neutrino masses via one-loop diagrams. The model relied on a gauged $U(1)_{B-L}$ symmetry, whose anomaly-freedom determined the charges of the DM and two copies of ν_R . We found that our symmetry based approach predicts that only two SM neutrinos are massive Dirac fermions, whereas the third one remains exactly massless, because there is no third ν_R . In order to ensure the DM stability and to prevent unwanted operators that could affect the neutrino or DM mass generation we had to impose a separate \mathcal{Z}_5 symmetry as well. Additionally one requires an inert scalar doublet η and an inert singlet σ together with the B-L breaking scalar singlet ϕ . Moreover we had to introduce a host of vector-like fermions to generate the necessary loop diagrams. It was found that the vector-like leptons F needed for the DM masses couple to the SM Higgs and are light enough to potentially be probed by next generation collider experiments.

We then chose a minimal scenario where we assumed that only the SM degrees of freedom augmented by two ν_R and χ are present after reheating. The constraint from invisible Higgs decays enforces $m_{DM} \lesssim 2 \text{ GeV}$ and the DM mass has to be larger than $(4 - 16) \text{ keV}$ due to the Lyman- α forest. After demonstrating that thermal production and out of equilibrium Higgs decays both lead to an over-production of DM, we were able to narrow the window of the allowed reheating temperatures down to the range between about 5 GeV and 4 MeV. Consequently we analyzed the joint production of DM χ and DR ν_R from out of equilibrium annihilations of the SM fermions via the B-L gauge boson Z' . The DM mass has to be smaller than $\mathcal{O}(\text{MeV})$ in order to suppress DM production via diagrams with an intermediate SM like Higgs compared to Z' mediated scatterings. We found a potentially viable parameter space with $v_{B-L} \gtrsim \mathcal{O}(10 \text{ TeV})$ that leads to the correct observed DM abundance but predicts $\Delta N_{\text{eff.}} \lesssim 0.012$. The amount of produced dark radiation decreases with the DM mass so in a sense m_{DM} and $\Delta N_{\text{eff.}}$ are anti-correlated. This is in striking contrast to other Dirac neutrino and DM mediator models which usually predict larger $\Delta N_{\text{eff.}}$. Thus while the aforementioned models can already be tested or ruled out by tightening the observational bounds on $\Delta N_{\text{eff.}}$, only the detection of $\Delta N_{\text{eff.}} > 0.012$ could falsify our DM production scenario in the near future.

Owing to the fact that we need a very low reheating temperature and want a negligible primordial DM abundance we were able to single out the real component of the σ field to play the role of the inflaton. In addition we found a way for how the σ field can also potentially realize Affleck-Dine Baryogenesis if we introduce a small source of \mathcal{Z}_5 -breaking in the scalar potential together with a pair of vector-like down quarks. We leave a detailed study of the inflationary predictions, reheating and non-thermal Baryogenesis for future investigation.

To summarize, we introduced a new abelian gauge theory that can simultaneously explain the active neutrino and fermionic dark matter masses via loop diagrams. Our con-

4 Radiative keV-scale DM

struction produces the observed DM relic abundance together with minuscule amounts of dark radiation in the freeze-in regime and can potentially account for inflation, reheating and Baryogenesis.

4.10 Appendix: Acknowledgments

This work benefited from the use of `PackageX` [242, 416]. We would like to thank Nicolás Bernal and Andreas Trautner for helpful comments about the manuscript as well as Rahul Mehra for insightful discussions about DM direct detection using electron targets.

5 S.M.A.S.H.E.D. : Standard Model Axion Seesaw Higgs Inflation Extended for Dirac Neutrinos

5.1 Contribution and Context

The following chapter is based on the single-author publication

JCAP 11 (2022) 042, arXiv: 2207.08142 [hep-ph]

and the author of this thesis was responsible for the conception and implementation of all aspects of the publication.

The SMASH (Standard Model Axion Seesaw Higgs inflation) framework [383, 417, 418] is a minimal extension of the Standard Model with a singlet scalar, three generations of right handed neutrinos and one (or more) generation of vector-like quarks. It is essentially a combination [419] of the KSVZ axion model [420, 421] (it also works for a DFSZ [229, 422] scenario) and a Type I Seesaw [26–30, 423], where the heavy quark and neutrino masses arise from the singlet vev v_σ . The singlet scalar is also identified with the field responsible for breaking Peccei-Quinn symmetry [424] and is connected to inflation. Using only this minimal set of ingredients one can explain the strong CP problem, QCD axion dark matter, inflation and reheating from a linear combination of the Higgs and the singlet, the stability of the electroweak vacuum, neutrino masses via the Type I Seesaw and the baryon asymmetry of the universe via Leptogenesis [425]. One appealing feature of such a setup is that only involves one additional scale in the form of v_σ . The downside of introducing fermions with direct couplings to the Peccei-Quinn breaking field, whose threshold correction stabilizes the electroweak vacuum [274], is that loop corrections due to the fermions now destabilize the singlet potential unless their masses are below around 10^8 GeV. We extend SMASH by additional vector-like triplets and doublets, that are chiral under Peccei-Quinn, to generate Dirac neutrino masses instead. This sequential Seesaw allows us to keep all fermion masses below the aforementioned 10^8 GeV. Our construction uses the double suppression from integrating out two species of fermions to generate the tiny observed active neutrino mass scale via a dimension six operator. The model is free from the cosmological domain wall problem, because it has domain wall number one and in this case the network of domain walls and cosmic strings collapses under its own tension. Our scenario predicts an axion

to photon coupling that is about an order of magnitude larger than in conventional KSVZ (and DFSZ) models due to loops of the new fermions, which can be tested by current and proposed axion haloscope experiments like e.g. ORGAN or MADMAX. While the original SMASH had to invoke resonant Leptogenesis [426] to explain the baryon asymmetry of our universe due to the previously discussed upper limit in the heavy neutrino mass scale, we find that the structure of our sequential Seesaw allows one to boost the amount of CP-violation produced in triplet decays by up to six orders of magnitude without any resonant enhancement from quasi-mass-degenerate fermions. This allows us to implement a version of the Dirac Leptogenesis [117] scenario, that we study numerically. Similar to the case of decaying scalar triplets for the Majorana Type II Seesaw [427] we observe that the efficiency of the out-of-equilibrium asymmetry production can be greatly enhanced: All that is required is that the decaying particle is not self-conjugate and has multiple decay modes with different branching ratios. These conditions can be automatically satisfied in any scenario of Dirac Leptogenesis, which requires two decay modes to generate CP violation and involves e.g. Dirac fermions which are not self-conjugate and can develop an asymmetry themselves. Since both the QCD axion ($\Delta N_{\text{eff}} \simeq 0.03$) and the right handed neutrinos ($\Delta N_{\text{eff}} \simeq 0.14$ for three generations) thermalize in the early universe we predict a dark radiation abundance of $\Delta N_{\text{eff}} \simeq 0.17$ that will be tested by next generation CMB experiments and can be used to distinguish our model from either axion or Seesaw models. To summarize we introduce

- a model connecting Dirac neutrinos to the QCD axion
- a model realizing neutrino masses from a dimension six operator
- a measurable enhancement of the axion to photon coupling by one order of magnitude
- a novel non-resonant enhancement of the CP violation produced in decays
- a mechanism previously applied to Majorana scenarios that increases the efficiency of Leptogenesis
- a measurable amount of dark radiation that helps with model discrimination

5.2 Appendix: Abstract

Inspired by the S.M.A.S.H. framework we construct a model that addresses the strong CP problem, axion dark matter, inflation and Dirac neutrino masses as well as Leptogenesis. The model possesses only two dynamical scales, namely the SM breaking scale v_H and the Peccei Quinn (PQ) breaking scale v_σ . We introduce heavy vector-like quarks in the usual KSVZ fashion to implement the PQ mechanism for the strong CP problem. To generate neutrino masses via a dimension six operator scaling as $m_\nu \sim v_H^3/v_\sigma^2$ we add heavy triplet and doublet leptons, which are vector-like under the SM but chiral under PQ symmetry. The model is free from the cosmological domain wall problem and predicts an axion to photon coupling which is about an order of magnitude larger than in conventional DFSZ

and KSVZ models. Thus our scenario can be probed and potentially excluded by current and next generation axion experiments such as ORGAN or MADMAX. In addition we numerically demonstrate that our construction can generate the observed baryon asymmetry by realizing a version of the Dirac-Leptogenesis scenario. As a consequence of our neutrino mass mechanism we find that the asymmetry in triplet fermion decays can also be significantly enhanced by up to six orders of magnitude when compared to typical Seesaw scenarios without needing to invoke a resonant enhancement. In passing we note that a decaying Dirac fermion with multiple decay modes contains all the necessary ingredients required for the “quasi optimal efficiency”-scenario previously encountered in the context decaying scalar triplets. The impact of the right handed neutrinos and the axion on ΔN_{eff} is estimated and lies within current bounds.

5.3 Appendix: **Introduction**

Reductionism has been one of the most widely used approaches to building particle physics models that are supposed to address the theoretical, aesthetical and phenomenological gaps in the Standard Model (SM). For many decades the most common top-down approach consisted in unifying the SM gauge symmetries into single larger non-abelian Lie groups. This strategy led to the discovery of economical scenarios such as the Type I Seesaw-mechanism [26–30, 423] addressing both laboratory observations like neutrino masses and mixing as well as important cosmological issues such as the baryon asymmetry of the universe via Leptogenesis [425]. In more recent years the focus has shifted to bottom-up approaches realizing the wanted phenomenology often via amending the SM with only a single additional global or gauged U(1) factor. The most prominent examples of this latter category are the ν MSM [428–430], which consists of a Type I Seesaw with the lightest right handed neutrino being a good dark matter (DM) candidate, as well as the S.M.A.S.H. proposal [383, 417, 418]. Here solutions to the strong CP problem, neutrino masses, electroweak vacuum stability, dark matter, inflation and Baryogenesis via Leptogenesis are possible by combining a Type I Seesaw with a global anomalous U(1)_{PQ} Peccei-Quinn symmetry playing the role of spontaneously broken lepton number. Building on an earlier construction [419] inspired by the KSVZ [420, 421] axion model this framework identifies the mass scale of the heavy right handed neutrinos with the PQ breaking scale that in turn corresponds to the decay constant of the QCD axion (see also [431] for a similar setup where the right handed neutrino mass does not arise from PQ breaking). There also exists a class of related models based on the DFSZ [229, 422] approach see [432] for a recent example. Only two mass scales are present in the S.M.A.S.H. scenario: the electroweak breaking scale from the vacuum expectation value (vev) of the Higgs doublet scalar and the much larger vev of the PQ breaking singlet whose imaginary part is the axion. No new physics other than the PQ charged sector is needed up to the Planck scale. Most theories beyond the SM address the neutrino mass issue via mechanisms inducing parametrically light Majorana masses since this usually involves the smallest amount of new unknown coupling constants and Weyl spinors. However a priori in the absence of any experimental signal there is

no reason to focus only on Majorana neutrinos, which is why there has been renewed interest in building Dirac neutrino mass model (see [54, 55, 263, 265, 433–435] for some explicit models and [436–438] for systematic studies just to name a few). In this work we set out to extend the S.M.A.S.H. class of models for light Dirac neutrinos. We outline the particle content and the most important interactions for the low energy phenomenology in section 5.4. Section 5.6 serves a brief summary of the cosmological history and most important parameters for the original S.M.A.S.H. scenario. The main focus of this work is Dirac-Leptogenesis in section 5.7. A novel way to enhance the leptonic asymmetry parameter from heavy fermion decays is presented in subsection 5.7.3. Analytical estimates in 5.7.5 help us narrow down the relevant parameter space and we show the validity of our scenario by numerically solving the Boltzmann equations from section 5.7.6 in subsection 5.7.9. In the aforementioned section we also demonstrate that the efficacy for asymmetry production from Dirac fermions can be larger than for Majorana fermions similar to [427] for decaying scalar triplets. After estimating the amount of dark radiation in section 5.8 we summarize our findings in 5.9. Additional relevant information was collected in sections 5.4.5–5.7.7.

5.4 Appendix: The model

One way to generate tiny Dirac masses is the Type I Dirac-Seesaw scheme pioneered in [439]. In general one starts out by imposing a symmetry to forbid the tree-level Dirac neutrino mass term

$$\bar{L}\epsilon H^\dagger \nu_R \quad (5.1)$$

with $\epsilon = i\tau_2$ being the second Pauli matrix, as well as all possible Majorana masses. Then heavy vector-like SM singlet fermions coupling to both the SM leptons and ν_R are integrated out at energies below their mass scale leading to light neutrino masses from the threshold correction. Most models realize the neutrino mass via a dimension five operator similar to the Weinberg operator [440] of the schematic form $(LH)^2$ for Majorana neutrinos. Since the ν_R are SM singlets this necessitates the inclusion of a scalar singlet ϕ to form the required operator $(\bar{L}\epsilon H^\dagger)\phi\nu_R$. The vev of ϕ introduces a third scale v_ϕ apart from the SM Higgs vev v_H and the heavy mediator scale $M \gg v_\phi, v_H$. Dirac masses then scale as $m_\nu \sim v_H v_\phi / M$ and the additional parameters are the reason why these scenarios are considered to be less minimal than Majorana models. If we wish to generate this operator via PQ charged particles and a singlet scalar σ for spontaneous symmetry breaking of $U(1)_{\text{PQ}}$ there are essentially two options: One can either identify the heavy mass scale with the PQ breaking scale $M \sim v_\sigma$ as was the case for combining the Type I Seesaw with PQ symmetry in [419]. This then requires that ϕ is a third scalar field and $v_H \lesssim v_\phi \ll v_\sigma$. The other option is to identify ϕ with the PQ breaking field σ [441] and assume a separate source for the heavy vector-like fermion masses. However since cosmological and astrophysical arguments require $v_\sigma > 10^8$ GeV or even $v_\sigma \simeq 10^{11}$ GeV (see subsection 5.6.2) the mediator mass scale must be potentially close to the Planck scale even for small Yukawa couplings [441]. Our model will be able to

field	SU(3) _C	SU(2) _L	U(1) _Y	U(1) _{PQ}	generations
q_L	3	2	1/6	0	3
u_R	3	1	2/3	0	3
d_R	3	1	-1/3	0	3
L	1	2	-1/2	1	3
e_R	1	1	-1	1	3
H	1	2	1/2	0	1
$Q_L^{(1,2)}$	3	1	2/3 or -1/3	1	2
$Q_R^{(1,2)}$	3	1	2/3 or -1/3	0	2
$Q_L^{(3)}$	3	1	2/3 or -1/3	-1	1
$Q_R^{(3)}$	3	1	2/3 or -1/3	0	1
T_L	1	3	0	2	3
T_R	1	3	0	1	3
D_L	1	2	1/2	3	3
D_R	1	2	1/2	2	3
ν_R	1	1	0	3	3
σ	1	1	0	1	1

 Table 5.1: Charges and Representations under the SM gauge group and U(1)_{PQ}.

avoid these complications altogether. The key idea is that we can connect L and ν_R by integrating out two different species of vector-like fermions transforming non-trivially under the electroweak gauge symmetry. To avoid a third scale besides v_H and v_σ we will generate the required threshold correction via a dimension six operator of the schematic form $(\bar{L}\epsilon H^\dagger)(HH^\dagger)\nu_R$. The heavy fermion masses scale with v_σ and the presence of three Higgs doublets follows from the required SU(2)_L contractions. In addition to that the active neutrino masses scale as $m_\nu \sim v_H^3/v_\sigma^2$. Before we face the neutrino sector we briefly review the KSVZ-axion model, which solves the strong CP problem via heavy vector-like fermions with PQ charge.

5.4.1 KSVZ-axion

In order to implement the Peccei-Quinn solution [424, 442] to the strong CP problem in the KSVZ model [420, 421] we introduce a pair of color triplet quarks (Q_L, Q_R), which

are vector-like under the SM but chiral under PQ as well as a singlet scalar σ coupling via

$$\mathcal{L}_{\text{KSVZ}} = -Y_Q \sigma \overline{Q_L} Q_R + \text{h.c.} \quad . \quad (5.2)$$

The charges and representations under all symmetries can be found in table 5.1. The scalar potential reads

$$V(H, \sigma) = V(H) - \mu_\sigma^2 |\sigma|^2 + \lambda_\sigma |\sigma|^4 + \lambda_{\sigma H} |\sigma|^2 |H|^2, \quad (5.3)$$

with $\mu_\sigma^2 > 0$ for the SSB of PQ symmetry and $V(H)$ the SM scalar potential. We expand the singlet scalar as

$$\sigma = \frac{1}{\sqrt{2}} (v_\sigma + \rho_\sigma) e^{i \frac{a}{v_\sigma}} \quad \text{with} \quad v_\sigma \gg v_H = 246 \text{ GeV}, \quad (5.4)$$

where a denotes the axion field and we see that the exotic quarks have a mass term consisting of

$$M_Q \equiv Y_Q \frac{v_\sigma}{\sqrt{2}}. \quad (5.5)$$

After rotating the axion field away by an anomalous Peccei-Quinn transformation of the quarks [443] we can integrate them out and obtain the axion coupling to the QCD anomaly term. For $\text{SU}(2)_L$ singlets the QCD anomaly coefficient reads [444]

$$N = \sum_\psi \chi_\psi T_d(\psi), \quad (5.6)$$

where T_d is the Dynkin color index for a d -dimensional representation with $T_3(Q_L) = T_3(Q_R) = 1/2$ and χ_ψ denotes the PQ charge of the particle ψ . If we assume only one generation of exotic quarks then

$$N = \frac{1}{2} (\chi_{Q_L} - \chi_{Q_R}) = \frac{1}{2} \chi_\sigma. \quad (5.7)$$

The non-linearly realized $\text{U}(1)_{\text{PQ}}$ symmetry is explicitly broken by the non-perturbative QCD effects down to a \mathcal{Z}_{2N} once the temperature of the universe cools below the QCD phase transition at $T = \Lambda_{\text{QCD}} = \mathcal{O}(200 \text{ MeV})$. The aforementioned QCD effects manifest themselves in an effective cosine potential and thus a mass for the axion a , which dynamically relaxes to its minimum to cancel the strong CP violation [424, 442] encoded in $\theta_{\text{QCD}} + \theta_{\text{weak}}$. In this context θ_{QCD} is the topological angle of QCD and θ_{weak} is the contribution from the chiral transformations needed to diagonalize the SM quark masses. After the angular mode a relaxes in one of the $2N$ equivalent vacua, topological defects in the form of domain walls are formed from the spontaneous breaking of this discrete symmetry [445–447]. The cosmological domain wall number is given by $N_{\text{DW}} = 2N$ and stable domain walls could overclose the universe [448, 449]. The domain walls form a network with axionic strings produced during the SSB of PQ symmetry via the Kibble mechanism [450–452], and the network will in general be stable for $N_{\text{DW}} > 1$. For $N_{\text{DW}} = 1$ the network eventually decays to low momentum axions [453, 454] and

contributes to their relic density [455–457]. Pre-inflationary PQ breaking can dilute the domain walls and explicitly PQ breaking bias-terms in the scalar potential [449, 458–460] could make the domain walls decay. However we will see in section 5.6.2 that S.M.A.S.H. is only compatible with post-inflationary PQ breaking. Bias terms have to be large enough to make the domain walls decay before they dominate the energy density of the universe [461]. On the other hand, they have the drawback of contributing to the axion mass, so that one needs to ensure, that they do not spoil the PQ solution to the strong CP problem, leading to an upper limit on the corresponding coupling [461, 462]. There exists a parameter space that satisfies both conditions. The last class of solutions to the domain wall problem embeds the \mathcal{Z}_{2N} into the center of a larger continuous global or local group [463, 464]. However we prefer to avoid these complications altogether by simply normalizing the PQ charges of the quarks properly. We demand $N_{\text{DW}} = 1$, from which we deduce that $\chi_\sigma = 1$. In this scenario we have an axion decay constant of

$$f_a \equiv \frac{v_\sigma}{N_{\text{DW}}}. \quad (5.8)$$

If one wishes to incorporate more generations of exotic quarks without generating additional domain walls then one has to make sure that the QCD anomaly coefficients for the additional generations cancel each other, for example by choosing equal and opposite PQ charges for those two generations. This explains the charge assignments for the third generation of exotic quarks in 5.1. At the present stage the exotic quarks would be absolutely stable owing to their separately conserved baryon number [420]. This would lead to exotic hadrons which could also overclose the universe and are tightly constrained relative to ordinary baryons by dedicated searches [465, 466]. In order to make the exotic quarks decay we introduce a renormalizable coupling to the SM doublet quarks q_L and consider the following operators for $\chi_{Q_R} = 0$ [465, 466]

$$\mathcal{L}_{\text{decay}} = -Y_{qQ} \begin{cases} \overline{q_L} \epsilon H^\dagger Q_R & \text{for } Y_{Q_R} = \frac{2}{3} \\ \overline{q_L} H Q_R & \text{for } Y_{Q_R} = -\frac{1}{3} \end{cases} + \text{h.c.}, \quad (5.9)$$

where Y_{qQ} is a dimensionless Yukawa coupling to the SM Higgs. There will be a lower limit on the Yukawa coupling in (5.9) from demanding that decay rate (assuming $m_Q \gg m_H$)

$$\Gamma(Q \rightarrow q_L H) \simeq \frac{Y_{qQ}^2 m_Q}{16\pi} \quad (5.10)$$

is faster than the Hubble rate at the temperature $T = m_Q$ implying

$$Y_{qQ} \gtrsim 10^{-5} \sqrt{\frac{m_Q}{10^8 \text{ GeV}}}, \quad (5.11)$$

so that the abundance of vector-like quarks is actually depleted and an epoch of intermediate era of matter domination [467] from very long-lived vector-like quarks is avoided. In the above we used a value for m_Q that will be motivated in section 5.6.3. Vector-like quarks could be produced at colliders, either in pairs from a gluon or together with an

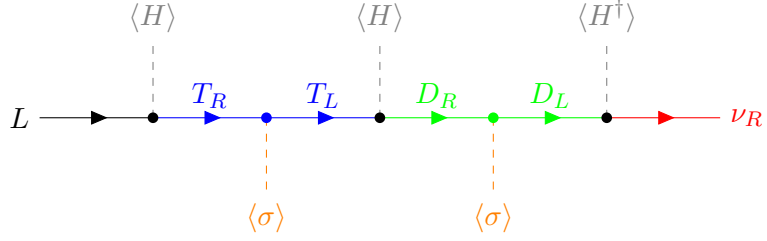


Figure 5.1: Diagrammatic representation of the dimension 6 operator giving rise to Dirac masses for the active neutrinos.

SM quark via the coupling in (5.9). Searches for new colored fermions exclude vector-like quark masses below about 1 TeV [468, 469]. The large couplings together with heavy large masses are the reason, why we expect the life-time of the vector-like quarks, if kinematically accessible at colliders, to be very short.

5.4.2 Neutrino masses

In a similar spirit we now introduce vector-like leptons as well to generate the Dirac neutrino masses in the Seesaw fashion. We give vector-like PQ charges to the SM leptons and charge ν_R in such a way that the tree level mass term $\bar{L}\epsilon H^\dagger \nu_R$ with $\epsilon = i\tau_2$ being the second Pauli matrix is absent. Since the cosmologically preferred PQ breaking scale $f_a \simeq 10^{11}$ GeV is lower than the typical Seesaw-scale (for order one Yukawas) of $M_N \simeq 10^{14}$ GeV we choose to integrate out two distinct fermions instead of a single messenger. However these two fermion species will have comparable masses so this *sequential Seesaw* depicted in figure 5.1 does not lead to a double Seesaw-mechanism [470,471]. The resulting operator for neutrino masses will have mass dimension six (see [437] for a compendium of possible Dirac dimension six operators) compared to the usual Weinberg operator at dimension five [440]. We start with introducing three generations of vector-like pairs of triplets (T_L, T_R) and doublets (D_L, D_R). The multiplets can be expanded into their components as

$$T_L \equiv \frac{T_L^a \tau^a}{2} = \begin{pmatrix} \frac{T_L^0}{\sqrt{2}} & T_L^+ \\ T_L^- & -\frac{T_L^0}{\sqrt{2}} \end{pmatrix}, \quad T_R \equiv \frac{T_R^a \tau^a}{2} = \begin{pmatrix} \frac{T_R^0}{\sqrt{2}} & T_R^+ \\ T_R^- & -\frac{T_R^0}{\sqrt{2}} \end{pmatrix} \quad (5.12)$$

and

$$D_L \equiv \begin{pmatrix} E_L^+ \\ N_L \end{pmatrix}, \quad D_R \equiv \begin{pmatrix} E_R^+ \\ -N_R \end{pmatrix}. \quad (5.13)$$

We also introduce the following notation of $\tilde{H} \equiv \epsilon H^\dagger$. A combination of chiral PQ charges, Hypercharge and non-trivial $SU(2)_L$ representations allows only the following mass

$$\mathcal{L}_{\text{mass}} = -Y_T \sigma \bar{T}_L^a T_R^a - Y_D \sigma \bar{D}_L D_R + \text{h.c.} \quad (5.14)$$

and mixing terms

$$\mathcal{L}_{\text{int}} = -Y_{LT} \bar{L} T_R^a \tau^a \tilde{H} - Y_{TD} D_R \epsilon \bar{T}_L^a \tau^a \tilde{H} - Y_{DR} \bar{D}_L H \nu_R + \text{h.c.} \quad (5.15)$$

All charges and representations for the four component spinors have been summarized in table 5.1. If we had given $D_{L,R}$ the opposite hypercharge $-1/2$ an operator of the schematic form $\bar{L} D_R \sigma^*$ would be allowed by all imposed symmetries and this operator would ruin the sequential nature of our mass generation mechanism by coupling ν_L directly to the exotic N_R neutrino with a large vev v_σ . We use triplets $T_{L,R}$ instead of singlet fermions $S_{L,R}$ because the PQ charge assignment would allow for a term $\bar{S}_L \nu_R \sigma^*$, which would also spoil the intended mass generation mechanism. Note that if one identifies our unconventional chiral choice of PQ charges with lepton number or B-L, which are usually taken to have vector-like charges normalized to ± 1 , one can understand the ‘‘Diracness’’ of the neutrinos as follows: Since σ breaks PQ symmetry by only a single unit all the renormalizable Majorana mass terms which would require breaking by two, four or six units (see table 5.1) are forbidden. This is in a similar spirit to the argument that breaking conventionally assigned lepton number or B-L by any number other than two allows only for Dirac neutrinos [263]. Of course PQ symmetry does not forbid the following non-renormalizable operators

$$\frac{c_{T_R}}{\Lambda_{\text{UV}}} (\sigma^*)^2 \bar{T}_R^c T_R^a, \quad \frac{c_{T_L}}{\Lambda_{\text{UV}}^3} (\sigma^*)^4 \bar{T}_L^c T_L^a, \quad \frac{c_{\nu_R}}{\Lambda_{\text{UV}}^5} (\sigma^*)^6 \bar{\nu}_R^c \nu_R, \quad (5.16)$$

as well as

$$\frac{c_L}{\Lambda_{\text{UV}}^3} (\sigma^*)^2 (\bar{L}^c \epsilon H) (L \epsilon H), \quad \frac{c_{D_R}}{\Lambda_{\text{UV}}^5} (\sigma^*)^4 (\bar{D}_R^c H^\dagger) (D_R H^\dagger), \quad (5.17)$$

$$\frac{c_{D_L}}{\Lambda_{\text{UV}}^7} (\sigma^*)^6 (\bar{D}_L^c H^\dagger) (D_L H^\dagger) \quad (5.18)$$

where the c_i are dimensionless Wilson-coefficients and Λ_{UV} is some mass scale above the PQ scale. Evidently the dimension five operator for T_R is the least suppressed and the mass term for the D_L at dimension eleven has the largest suppression factor due to SM gauge invariance and PQ breaking by six units. We have checked that these operators are not generated at loop level for the given particle content in field theory, but if one includes quantum gravity they might arise. Non-perturbative quantum gravitational effects could lead to a low energy effective field theory which will contain all the terms allowed by only the local gauge symmetries [444] such as the above ones. On top of that quantum gravity is expected to violate global symmetries [275–277] like PQ symmetry. These quantum gravity effects are heuristically¹ encoded in Planck-mass suppressed explicitly PQ violating operators leading to the well known ‘‘axion quality problem’’ [474–479] that could spoil the solution to the strong CP problem. PQ violating Majorana masses could arise in the same way too [480]. Since we have nothing to add to the solution of these ‘‘quality problems’’ we will assume that the

¹there might be an additional suppression factor $e^{-S_{\text{wh}}}$, where the large number S_{wh} is the wormhole action [472, 473]

Wilson coefficients of both sets of hypothetical effective operators (PQ conserving or violating) are either negligibly small or that some other mechanism prevents their existence.²

Before EWSB the triplets and doublets are decoupled and each component of an $SU(2)_L$ multiplet has a common mass set by the PQ breaking scale, which we call

$$M_T \equiv Y_T \frac{v_\sigma}{\sqrt{2}} \quad \text{and} \quad M_D \equiv Y_D \frac{v_\sigma}{\sqrt{2}}. \quad (5.19)$$

After integrating them out and applying a Fierz-transformation we find

$$\mathcal{L}_{\text{eff.}} = \frac{1}{2} Y_{LT} M_T^{-1} Y_{TD} M_D^{-1} Y_{DR} \left(\bar{L} \epsilon H^\dagger \right) \left(H H^\dagger \right) \nu_R + \text{h.c.} \quad (5.20)$$

In the one flavor approximation we find the following relation for the active neutrino mass scale after electroweak symmetry breaking (EWSB)

$$m_\nu \simeq 0.05 \text{ eV} \cdot Y_{LT} Y_{TD} Y_{DR} \cdot \left(\frac{10^9 \text{ GeV}}{M_T} \right) \cdot \left(\frac{10^8 \text{ GeV}}{M_D} \right). \quad (5.21)$$

If we choose M_T, M_D lighter than about $\mathcal{O}(10^8 \text{ GeV})$ we can maintain the light neutrino mass scale by decreasing the Yukawa coupling $Y_{LT} Y_{TD} Y_{DR}$. On the other hand the overall neutrino mass scale could be lowered too far if we chose $M_T, M_D \gg \mathcal{O}(10^8 \text{ GeV})$, which is why we work in the previously mentioned regime. Since we expect $f_a \simeq \mathcal{O}(10^{11} \text{ GeV})$ (see (5.6.2)) this means that Yukawa couplings of the T, D fields to the PQ breaking field must satisfy $Y_{T,D} \lesssim 10^{-3}$. Here there are only two dynamical scales v_H and v_σ involved in the neutrino mass generation, which comes at the price of introducing five Yukawa matrices $Y_{LT}, Y_{TD}, Y_{DR}, Y_T, Y_D$. In order to generate the two mass splitting needed to explain the neutrino oscillation data we need to introduce at least two generations of $T_{L,R}, D_{L,R}$ and in the following we will assume the existence of three such generations. We can estimate the axion decay constant

$$f_a \simeq 4 \times 10^8 \text{ GeV} \cdot \sqrt{\frac{0.1 \text{ eV}}{m_\nu}} \cdot \sqrt{\frac{Y_{LT} Y_{TD} Y_{DR}}{Y_T Y_D}} \quad (5.22)$$

as a function of the active neutrino mass. If we drop the previous assumption about the Yukawa couplings and allow all five of them to vary between $\mathcal{O}(1)$ and $\mathcal{O}(10^{-6})$ (which are the largest and smallest Yukawa couplings in the SM of the top quark and electron respectively), we find

$$0.4 \text{ GeV} \cdot \sqrt{\frac{0.1 \text{ eV}}{m_\nu}} \lesssim f_a \lesssim 4 \times 10^{14} \text{ GeV} \cdot \sqrt{\frac{0.1 \text{ eV}}{m_\nu}}. \quad (5.23)$$

²After the completion of this work reference [481] was released, in which the authors manage to avoid the PQ conserving higher dimensional operators by choosing the PQ charge of L to be a non-integer $\chi_L = 1/3$ and shifting all other fermionic charges accordingly so that $\chi_{\nu_R} = 2 + 1/3 = 7/3$. In this case the estimate for the axion to photon coupling in (5.36) remains unchanged, because the difference in PQ charge between the different chiralities (T_L, T_R) and (D_L, D_R) is still one.

The lower range of $f_a \sim 0.4 \text{ GeV}$ obtained for the extreme choice $Y_{LT} \sim Y_{TD} \sim Y_{DR} \sim 10^{-6}$ and $Y_T \sim Y_D \sim 1$ would correspond to the Weinberg-Wilczek [231, 482] axion which has been ruled out experimentally via meson decays a long time ago [483]. Furthermore astrophysical arguments based on stellar cooling demand $f_a > 10^8 \text{ GeV}$, so that the region of small $Y_{LT} \sim Y_{TD} \sim Y_{DR}$ is already excluded. Note that having such small couplings would defeat the purpose of building a rather involved Seesaw model to begin with. We depict the decay constants that would lead to a too small neutrino mass as the grey region in the figures 5.3 and 5.4, which shall be the focus of the next subsection.

5.4.3 Landau poles for the SM gauge couplings

As shown in [465, 466] the hypercharged exotic quarks with masses $5 \times 10^{11} \text{ GeV}$ do not lead to a Landau pole for the U_Y gauge coupling (or any other SM gauge coupling) below the Planck mass. Following the methods outlined in [484--486] we compute the coefficients of the two loop renormalization group equations (RGE)

$$\frac{d}{dt} \alpha_i^{-1} = a_i + \frac{b_{ij}}{4\pi} \alpha_j, \quad \text{where } \alpha_j \equiv \frac{g_j^2}{4\pi} \quad \text{and} \quad t \equiv \frac{1}{2\pi} \text{Log} \left(\frac{\mu}{m_Z} \right) \quad (5.24)$$

where $i = 1, 2, 3$ labels the gauge groups U_Y , $SU(2)_L$ and $SU(3)_c$ respectively. Here μ denotes the renormalization scale. We do not include the contribution from the Yukawa couplings for simplicity. The definitions of the constants can be found in [485, 486] and for the SM they read [484]

$$\bar{a}^{\text{SM}} = \begin{pmatrix} a_1 \\ a_2 \\ a_3 \end{pmatrix} = \begin{pmatrix} 4 + \frac{1}{10} \\ -22 + 4 + \frac{1}{6} \\ -11 + 4 \end{pmatrix} \quad (5.25)$$

as well as

$$b^{\text{SM}} = \begin{pmatrix} 0 & 0 & 0 \\ 0 & -\frac{132}{3} & 0 \\ 0 & 0 & -102 \end{pmatrix} + N_{\text{gen.}} \begin{pmatrix} \frac{19}{15} & \frac{3}{5} & \frac{44}{15} \\ \frac{1}{5} & \frac{49}{3} & 4 \\ \frac{11}{30} & \frac{3}{2} & \frac{76}{3} \end{pmatrix} + \begin{pmatrix} \frac{9}{50} & \frac{9}{10} & 0 \\ \frac{3}{10} & \frac{13}{6} & 0 \\ 0 & 0 & 0 \end{pmatrix}. \quad (5.26)$$

The first matrix comes from the gauge bosons, the second matrix measures the contribution of $N_{\text{gen.}} = 3$ generations of fermions and the last matrix arises due to the SM Higgs boson. Note that the matrix b^{SM} is transposed compared to reference [484] and we used the GUT normalization of $SU(5)$ or $SO(10)$ for the hypercharge [485]

$$Y_{\text{norm.}} = \sqrt{\frac{3}{5}} Y_{\text{SM}}. \quad (5.27)$$

Motivated by our cosmological findings we only include the lightest electroweak triplet of mass $M_T = 10^8$ GeV with $Y_{\text{SM}} = 0$ for which

$$\vec{a}_T^{\text{BSM}} = \begin{pmatrix} 0 \\ \frac{8}{3} \\ 0 \end{pmatrix}, \quad b_T^{\text{BSM}} = \begin{pmatrix} 0 & 0 & 0 \\ 0 & \frac{128}{3} & 0 \\ 0 & 0 & 0 \end{pmatrix} \quad (5.28)$$

and the doublet leptons with $Y_{\text{SM}} = -\frac{1}{2}$ at $M_D = 3 \times 10^7$ GeV for which

$$\vec{a}_D^{\text{BSM}} = \begin{pmatrix} \frac{2}{5} \\ \frac{2}{3} \\ 0 \end{pmatrix}, \quad b_D^{\text{BSM}} = \begin{pmatrix} \frac{9}{50} & \frac{9}{10} & 0 \\ \frac{3}{10} & \frac{49}{6} & 0 \\ 0 & 0 & 0 \end{pmatrix}. \quad (5.29)$$

We include the threshold effects of the heavy fermions Ψ by solving (5.24) with

$$\vec{a}^{\text{BSM}} = \vec{a}^{\text{SM}} + \Theta(\mu - M_\Psi) \vec{a}_\Psi^{\text{BSM}}, \quad b^{\text{BSM}} = b^{\text{SM}} + \Theta(\mu - M_\Psi) b_\Psi^{\text{BSM}}, \quad (5.30)$$

where Θ denotes the Heaviside function and we use the following boundary conditions [487, 488]

$$\alpha_1(m_Z) = 0.016923, \quad \alpha_2(m_Z) = 0.03374, \quad \alpha_3(m_Z) = 0.1173, \quad m_Z = 91.188 \text{ GeV}. \quad (5.31)$$

We reproduce the Landau pole in g_1 around 10^{38} GeV found for a vector-like quark with $Y = -1/3$ with a representative mass of 5×10^{11} GeV in [465, 466]. We depict the evolution of the three gauge couplings for adding the lightest triplet or doublet in 5.4.3 with the masses $M_T = 10^8$ GeV and $M_D = 3 \times 10^7$ GeV from section 5.7.9. One can observe in 5.4.3 that the Landau pole appears earlier for the lighter doublet [485]. We stopped the numerical evaluation at the Landau poles because the system of differential equations starts to exhibit singular behaviour and we can not trust our calculation for larger energies anymore. This is why the lines for the doublet in 5.4.3 terminate earlier than for the triplet. In both scenarios the potential Landau pole in g_1 manifests far above the Planck scale, so it does not affect the phenomenology of our model. Let us emphasize that this analysis only serves as a first estimate and in principle all three generations of all new species and their Yukawa interactions should be included in the running. For a more realistic estimate we include three generations of quarks with the same masses of 10^9 GeV for simplicity as well as three generations of triplets, where the two heavier ones have 10^9 GeV masses, together with three doublets, with the two heavier ones at 10^8 GeV (this range of masses was motivated in section 5.6.3). Adding the entire fermionic particle content of the model induces a Landau pole at 10^{21} GeV again in g_1 and again above the Planck scale. The landau pole appears at lower energies the more fermions we introduce because the positive coefficients in the RGEs (5.24) increase with each additional fermion [465, 466]. We conclude that our three generations of exotic fermions do not lead to phenomenologically relevant Landau Poles for the SM gauge interactions.

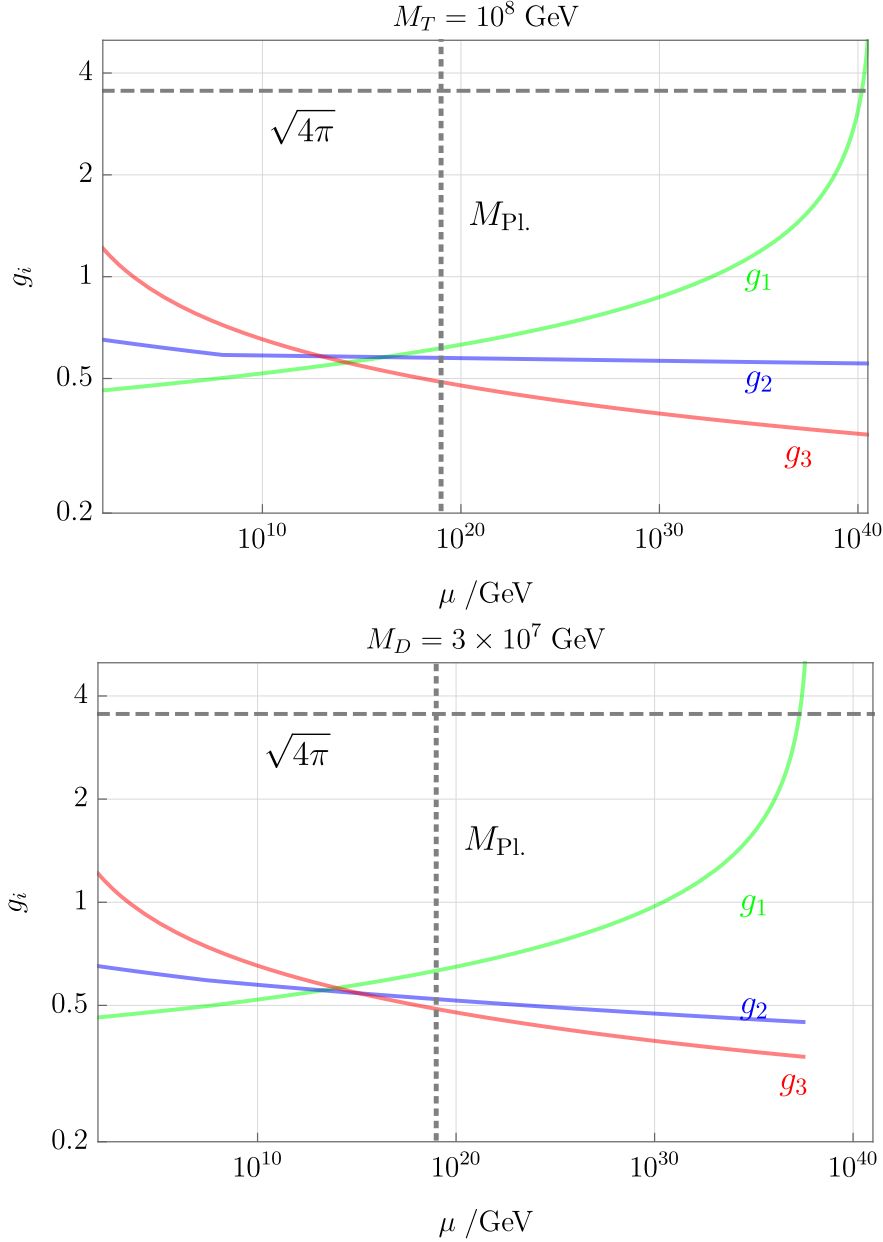


Figure 5.2: Two Loop RGE evolution of the SM gauge couplings as a function of the renormalization scale for the inclusion of a hypercharge zero $SU(2)_L$ triplet with $M_T = 10^8$ GeV (top) and a hypercharge $1/2$ $SU(2)_L$ doublet fermion with a mass of $M_D = 3 \times 10^7$ GeV (bottom).

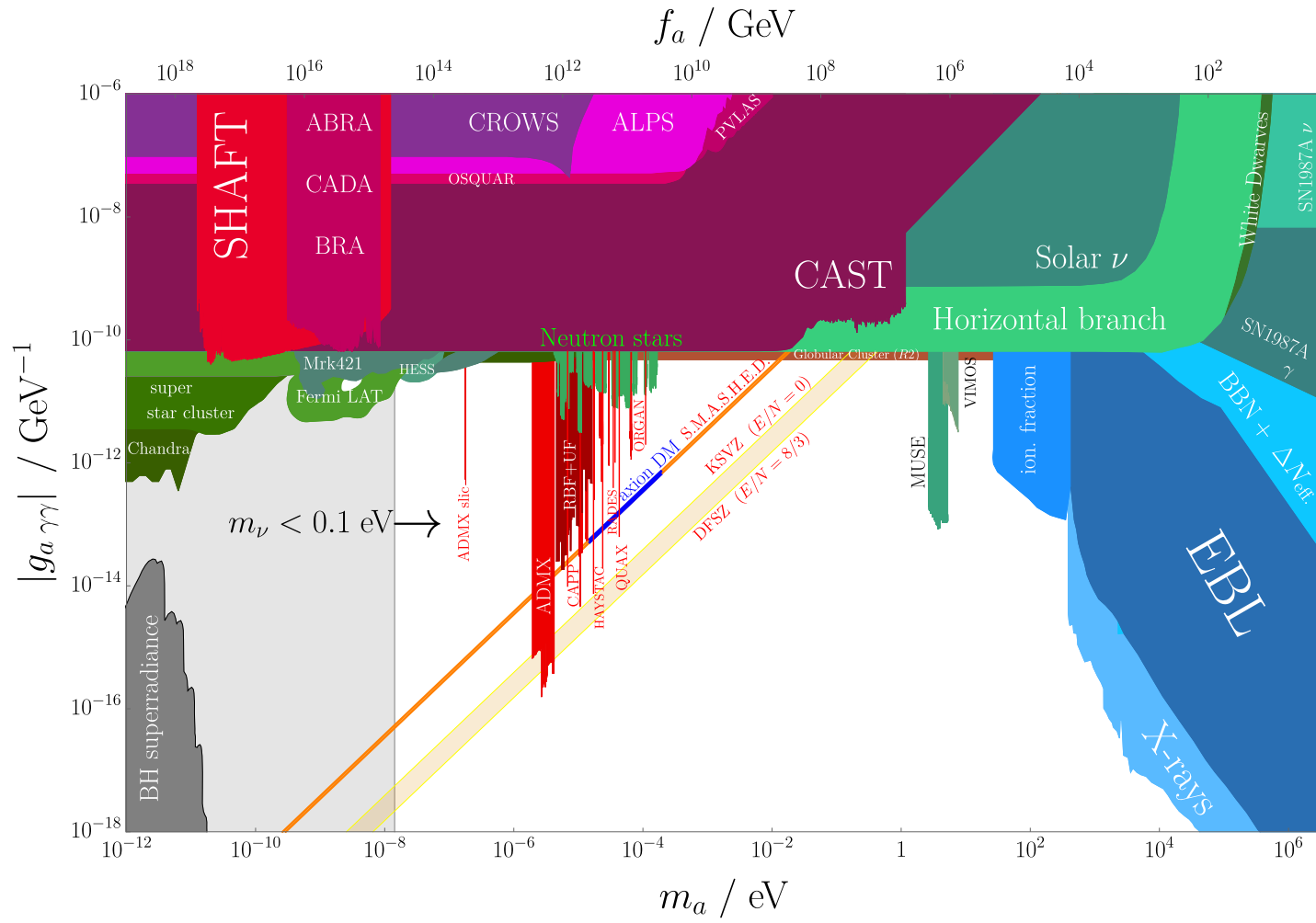


Figure 5.3: Depicted are the “S.M.A.S.H.E.D.” band in orange and the QCD-axion band for the KSVZ and DFSZ models in yellow as well as a collection of cosmological, astrophysical and laboratory constraints. The white space is allowed and in the gray area the active neutrino masses would be too small. The black arrow to the right indicates that the lower allowed limit on m_a increases for larger values of m_ν . The corresponding references can be found in section 5.4.5.

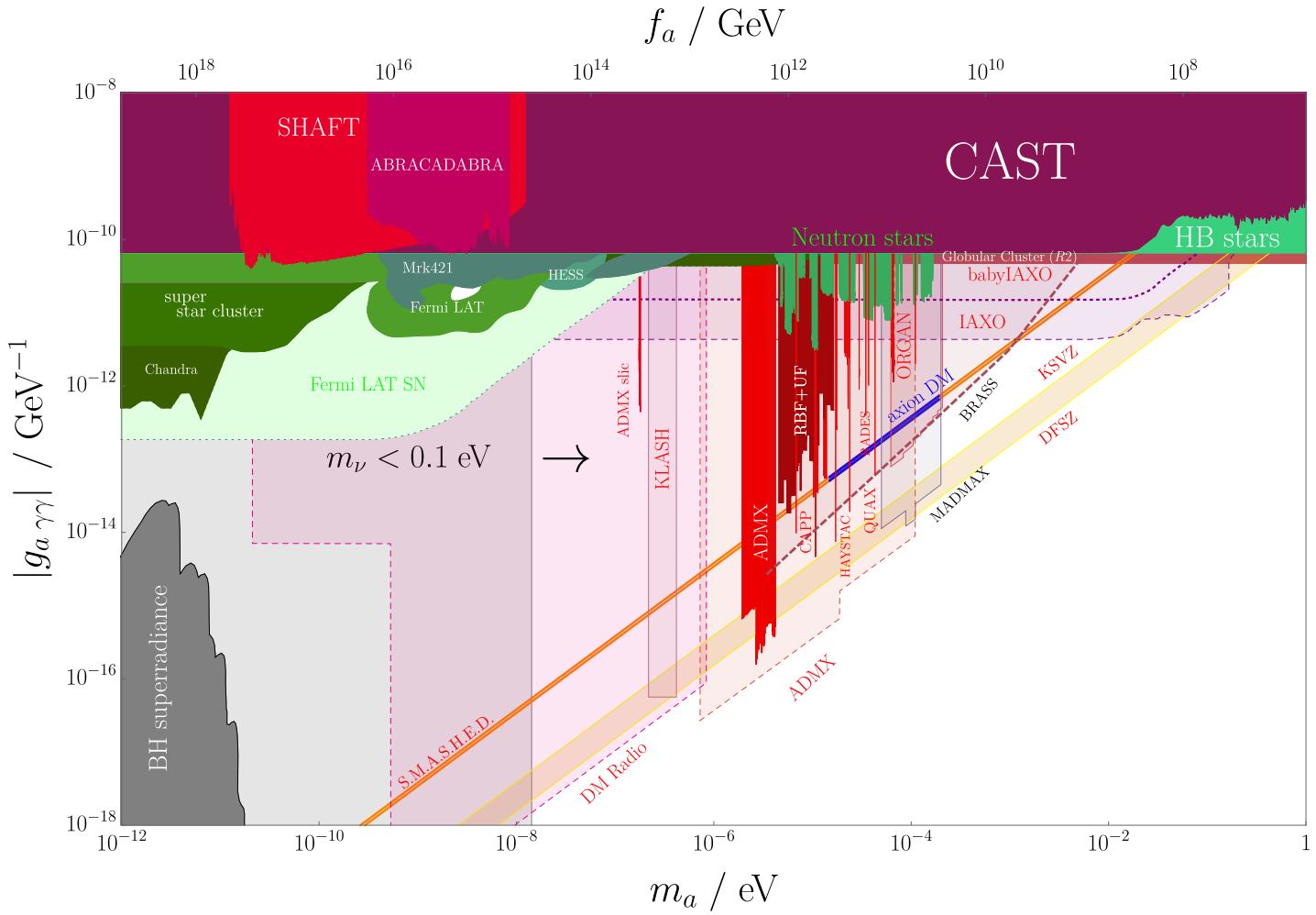


Figure 5.4: Depicted are the “S.M.A.S.H.E.D.” band in orange and the QCD-axion band for the KSVZ and DFSZ models in yellow as well as cosmological, astrophysical and laboratory constraints together with projected sensitivities. The black arrow to the right indicates that the lower allowed limit on m_a increases for larger values of m_ν . The corresponding references can be found in section 5.4.5.

5.4.4 Axion to photon coupling

The most relevant coupling for the direct detection of axions in laboratory experiments is the axion-to photon coupling, which is given by [489, 490]

$$g_{a\gamma\gamma} = \frac{\alpha}{2\pi f_a} \left(\frac{E}{N} - 1.92(4) \right), \quad (5.32)$$

where the second term represents the model-independent irreducible contribution from the axion-pion mass mixing. The color anomaly coefficient N was specified in equation (5.6) and is found to be $N = 1/2$ for this model. The electromagnetic anomaly coefficient E is defined via [444]

$$E = \sum_{\psi} \chi_{\psi} d_c(\psi) \text{Tr} (Q_{\text{EM } \psi}^2), \quad (5.33)$$

where χ_{ψ} is the PQ charge of the fermion ψ , $d_c(\psi)$ is the dimension of its color representation and $Q_{\text{EM } \psi}$ its electric charge matrix. For the original KSVZ model, where the exotic quarks have no hypercharge one finds $E/N = 0$. Since we equip them with hypercharge for cosmological reasons (see table 5.1 for their charges) their contribution reads

$$\left(\frac{E}{N} \right)_Q = 2 \cdot 3 \cdot \begin{cases} \frac{4}{9} & \text{for } Y_{Q_L} = \frac{2}{3}, \\ \frac{1}{9} & \text{for } Y_{Q_L} = -\frac{1}{3}, \end{cases} \quad (5.34)$$

where the factor of three comes from $d_c(Q_L) = 3$. Only the first generation of exotic quarks contribute since we assume the PQ charges of the second and third generations cancel each other in order to fix the domain wall number. Similarly even though the SM leptons L and e_R have electric charge, they are vector-like under PQ and do not contribute to E . As a consequence of introducing non-trivial $SU(2)_L$ representations which are chiral under PQ for neutrino mass generation we obtain an additional contribution from the T and D :

$$\left(\frac{E}{N} \right)_{T,D} = 2 \cdot 3 \cdot (2 + 1) = 18 \quad (5.35)$$

The factor of three takes the three generations of exotic leptons into account and since each triplet contains two charged fermions their contribution is twice as large as for the doublets. Consequently the model dependent part of the axion to photon coupling

$$\left(\frac{E}{N} \right)_{\text{tot}} = 18 + \begin{cases} \frac{8}{3} & \text{for } Y_{Q_L} = \frac{2}{3}, \\ \frac{2}{3} & \text{for } Y_{Q_L} = -\frac{1}{3} \end{cases} \quad (5.36)$$

is significantly larger than in conventional models such as the DFSZ I (II) scenario, where the ratio reads $8/3$ ($2/3$). Thus our neutrino mass mechanism has the additional benefit of making the axion easier to detect in laboratory experiments. Compared to other constructions in the literature this enhancement is rather small. For comparison clockwork based models such as [491--493] lead to an exponential enhancement of the coupling, a recent construction with quantized magnetic charges [494, 495] can increase the axion to photon coupling by six orders of magnitude. Mirror sector models with n

copies of the SM and PQ sectors [496, 497] can increase the axion to photon coupling as a function of n by lowering the axion mass compared to the usual QCD axion. Alternatively if one sticks to the particle content of the KSVZ model then the largest possible positive anomaly coefficient was found to be $E/N = 170/3$ [465, 466]. A recent scan over possible representations found that $E/N = -166/3$ [486] is the largest possible negative value within the range of the scan. Note that the two previously mentioned scenarios require three or eight quarks of different SM representations. We depict the experimentally allowed parameter space and a collection of limits in 5.3 together with the projections from upcoming searches in 5.4. The limits and projected limits were compiled in [498] and they can be found in section 5.4.5. The orange band dubbed “S.M.A.S.H.E.D.” corresponds to the prediction of our model. Inside this band there is a blue region called “axion DM” which reproduces the observed DM abundance for the cosmological history of the S.M.A.S.H. models and will be explained in section 5.6.2. Experiments like QUAX [499, 500] or HAYSTAC [501, 502] have already started to test the relevant parameter space depicted in blue. Other experiments like ORGAN [503, 504] or RADES [505] are close to probing the axion DM parameter space as can be seen in 5.3. When it comes to next generation experiments we find that MADMAX [506], the upgraded ADMX experiment [507–514] as well as BRASS [515] have good chances of testing the aforementioned parameter region. In section 5.4.3 we demonstrate numerically that the new heavy fermions do not lead to phenomenologically relevant Landau poles in any of the SM gauge couplings following the treatments in [484–486].

5.4.5 Collection of limits on the axion to photon coupling

Constraints on the axion to photon coupling were compiled in [498] and can be grouped into the following categories

- **Haloscopes** looking for DM axions from the galactic DM halo such as ABRACADABRA [516, 517], ADMX [507–514], BRASS [515], CAPP [518–520], DM-Radio [521], HAYSTAC [501, 502], KLASH [522], MADMAX [506], ORGAN [503, 504], QUAX [499, 500], RADES [505], RBF [523], SHAFT [524] and UF [525]
- **Helioscopes** looking for axions produced inside the sun such as CAST [526, 527], babyIAXO or IAXO [528, 529].
- **Light shining through walls (LSW)** and similar experiments such as ALPS [530, 531], CROWS [532], OSQAR [533] and PVLAS [534].
- **Cosmological probes** such as extragalactic background light (EBL), ionisation fraction, X-rays [535] or BBN and ΔN_{eff} . [536].
- (indirect) **Astrophysical bounds** such as Black hole superradiance [537], the Chandra X-ray telescope [538–541], the Fermi Large Area Telescope (LAT) [542–545], super star clusters [546], the

cosmic distance ladder [547], the HESS cherenkov telescope [548], horizontal branch stars [549], White dwarfs [550], Globular Cluster (R_2) [551], the blazar Markarian 421 (Mark 421) [552], neutron stars [553–555], observations of the solar neutrino flux [556], supernova SN 1987A [557, 558], radio telescopes [559] and optical telescopes like MUSE [560] and VIMOS [561]

5.4.6 Axion to fermion coupling

The chiral rotations that remove the phase of the singlet field σ from the mass terms induce the following derivative interactions for all PQ charged fermions Ψ with chiral charges $\chi_{L,R}$

$$\mathcal{L}_{\text{int.}} = i \frac{\partial_\mu a}{f_a} \sum_{\Psi} \bar{\Psi} \gamma^\mu \left(\frac{\chi_L + \chi_R}{2} \cdot \mathbb{1}_4 - \frac{\chi_L - \chi_R}{2} \cdot \gamma_5 \right) \Psi. \quad (5.37)$$

The only SM fermions that pick up an interaction at tree level are the three generations of charged and neutral leptons:

$$\mathcal{L}_{\text{int.}} = i \frac{\partial_\mu a}{f_a} \sum_j (\bar{e}_j \gamma^\mu e_j + \bar{\nu}_j \gamma^\mu (2 \cdot \mathbb{1}_4 + \gamma_5) \nu_j) \quad (5.38)$$

As expected the charged lepton coupling is vector-like. If we integrate the first term by parts we pick up a contribution of

$$\sum_j \partial_\mu (\bar{e}_j \gamma^\mu e_j) \quad (5.39)$$

which vanishes for on shell leptons. Of course as in the original KSVZ model a pseudoscalar coupling to will be regenerated at loop level from the axion to photon coupling in (5.32) [419]

$$g_{ae} \simeq \alpha g_{a\gamma\gamma} m_e \text{Log} \left(\frac{f_a}{m_e} \right), \quad (5.40)$$

which is dimensionless as $g_{a\gamma\gamma} \sim 1/f_a$. Here we neglected the contribution from axion pion mixing in (5.32) as it was subdominant to the inclusion of the heavy exotic fermions. One can see that this coupling $g_{ae} \simeq 3 \times 10^{-17}$ is very small due to its dependence on $\alpha m_e/f_a$. There are more one loop contributions to g_{ae} from one loop diagrams involving the other massive EW gauge bosons as well as the new exotic fermions. By recasting the result for a Majorana Type I Seesaw from [419, 562] we estimate

$$g_{ae} \simeq \frac{1}{16\pi^2} \left(\frac{m_\nu}{v_H} \right)^2 \frac{m_e}{f_a}. \quad (5.41)$$

This contributions is suppressed by both $m_e/f_a \simeq 5 \times 10^{-15}$ and $m_\nu^2/v_H^2 \simeq 10^{-25}$ so we do not consider them further. Stellar cooling arguments for the sun and red giants exclude $g_{ae} \gtrsim \mathcal{O}(10^{-13})$ [563–566], which is respected by our model. Axions could also be emitted

in laboratory experiments from the final state neutrino or charged lepton in pseudoscalar-meson decay. Since this will remove the chirality suppression of the two-body decay, these channels are sensitive probes for new physics. Existing analyses [567--570] (often) do not use the full derivative coupling in (5.38) but rely on Yukawa-interactions which are technically only valid for on-shell fermions [571, 572]. However since the full calculation can involve technical subtleties such as infrared-divergences which have to be cancelled via loop-corrections [569] we will limit ourselves to recasting the existing limits. For the emission from a neutrino line we replace the axion neutrino coupling with $g_\nu = m_\nu/f_a$. Reference [569] found that depending on the flavor-structure $g_\nu^2 < \mathcal{O}(10^{-6-7})$ which translates to

$$f_a > \mathcal{O}(10^3) \times m_\nu \quad (5.42)$$

and is not restrictive at all.

5.5 Appendix: Unification

The DFSZ [229, 230] version of the original S.M.A.S.H. framework avoids the exotic vector-like quarks by charging the SM quarks under PQ symmetry and was discussed in [418]. Since this variant of S.M.A.S.H. only requires an additional gauge singlet sterile neutrino N , one can embed the DFSZ-S.M.A.S.H. in a basic Grand Unified Theory (GUT): One can choose SU(5) [25, 573] by introducing N as an additional singlet or pick the larger SO(10) [24, 573], where N fills the 16-dimensional spinorial representation together with the other 7 Weyl spinors for one generation of the SM. For a Type I Dirac Seesaw one can also find an SO(10)-embedding by introducing the SM gauge singlet vector-like neutrinos as SO(10)-singlets [441]. In our case of S.M.A.S.H.E.D. the situation is not as straight-forward, because we introduce vector-like fermions transforming non-trivially under the SM gauge group. This is why we would need to fill additional multiplets of e.g. SO(10), which comes at the price of introducing additional fermions for anomaly cancellation. One can see, that there is no obvious GUT-embedding of our setup and further work would be required to find one.

5.6 Appendix: Cosmology of S.M.A.S.H.

We briefly recapitulate the most important aspects of the cosmological history in the S.M.A.S.H. framework [383, 417, 418].

5.6.1 Inflation and reheating

Scalar fields with a non-minimal coupling to scalar curvature [109, 110, 354--359] are chosen as the inflationary scenario. In a two field model, such as the present setup featuring the neutral component of H together with σ , the inflationary dynamics are more complicated, which is why the authors of [383, 417, 418] worked out limiting cases, in which effectively only one field is responsible for inflation. Because of the unitarity problem [370--372] for pure Higgs inflation (HI) [366--368] reference [383] considered the

inflaton to be either arising from the field σ (HSI scenario) or as a linear combination of the neutral component of H and σ (HHSI scenario). One finds the valleys of the potential, that are attractors for the inflationary trajectories, by inspecting the signs of the following quantities [383]

$$\kappa_H \equiv \lambda_{H\sigma}\xi_H - \lambda_H\xi_\sigma, \quad \kappa_\sigma \equiv \lambda_{H\sigma}\xi_\sigma - \lambda_\sigma\xi_H. \quad (5.43)$$

The relevant ranges are $\kappa_H > 0 \wedge \kappa_\sigma > 0$ (here \wedge is a logical “and”) for either HI or HSI, whereas HHSI needs $\kappa_H < 0 \wedge \kappa_\sigma < 0$. Solving the unitarity problem requires $0 < \xi_\sigma \lesssim 1$ [383] for the coupling to gravity. In this context and because of vacuum stability (see 5.6.3) for HHSI one needs a trajectory that is parametrically close to the HSI one, which can be achieved in the limit $\xi_H \ll \xi_\sigma$ [383]. Then one finds that the radial modes of the SM like Higgs and σ lead to the following inflationary trajectory [383]

$$\frac{\rho_\sigma}{\rho_H} = \sqrt{-\frac{\lambda_H}{\lambda_{H\sigma}}} + \mathcal{O}\left(\frac{\xi_H}{\xi_\sigma}\right), \quad (5.44)$$

where $\lambda_{H\sigma} < 0$ is required for HHSI [383]. On the other hand $\lambda_{H\sigma} > 0$ selects HI and HSI. In the HSI scenario non-thermal axions get produced during reheating after the non-thermal restoration of PQ symmetry (see the next subsection 5.6.2). This scenario has a reheating temperature of around 10^7 GeV that is so low that the axions never thermalize (see section 5.8.1), leading to an abundance of dark radiation $\Delta N_{\text{eff.}} \simeq 0.35 - 1.6$ [383] which is excluded by observations [20]. Therefore only the HHSI scenario is viable. In this regime the effective quartic coupling for inflation reads

$$\tilde{\lambda}_\sigma \equiv \lambda_\sigma - \frac{\lambda_{H\sigma}^2}{\lambda_H} \quad (5.45)$$

and it is bounded by [383]

$$5 \times 10^{-10} < \tilde{\lambda}_\sigma < 5 \times 10^{-13}, \quad (5.46)$$

where the upper limit comes from the amplitude of primordial scalar perturbations and the lower limit from the bound on the tensor to scalar ratio [20, 104]. Reheating occurs via damped inflaton oscillations in a quartic potential. The dominant channel is the production of EW gauge bosons from the inflaton’s SM like Higgs component during zero crossings of the oscillating condensate. The EW gauge bosons have effective inflaton dependent masses and decay efficiently to SM fermions as the gauge boson masses increase away from the crossings. During the zero crossings gauge boson production from the resulting fermion bath is also efficient. Due to their mass gain and the fact that the gauge bosons decay to fermions before they can lose this energy to the condensate again, energy is efficiently drained from the inflaton to the SM fermion bath. Production of the heavy exotic fermions occurs as well, but since their decays to SM fermions are suppressed compared to the gauge bosons, their inclusion is negligible. The reheating temperature can be estimated to be [383]

$$T_{\text{RH}} \simeq 10^9 \text{ GeV} \cdot \left(\frac{\tilde{\lambda}_\sigma}{10^{-10}}\right)^{\frac{5}{8}} \cdot \left(\frac{g^2 |\lambda_{H\sigma}| / (4\lambda_H)}{0.03}\right)^{\frac{5}{8}}, \quad (5.47)$$

where g is a shorthand for the EW gauge couplings and we used typical parameters from the analysis of [383]. A recent reevaluation [574] of the preheating dynamics revealed that one can no longer neglect the exponential growth of fluctuations of the SM like Higgs after non-thermal restoration of PQ symmetry, because there are large fluctuations in the singlet direction, whose imaginary part lowers the effective Higgs mass. The new results [574] indicate that the reheating temperature can be as large as

$$T_{\text{RH}} = (10^{12} - 10^{13}) \text{ GeV.} \quad (5.48)$$

As it turns out the critical temperature for the PQ phase transition is $T_c \simeq 0.01 f_a$ [383], which for $f_a < 10^{11}$ GeV lies below the reheating temperature in (5.48) meaning that PQ symmetry is thermally restored in the HHSI case.

5.6.2 Axion dark matter

It is well known that the cosmological evolution of the axion depends on the fate of PQ symmetry during inflation [575]. In S.M.A.S.H. one finds that PQ symmetry is non-thermally restored during preheating [383] via the growth of σ -excitations that destroy the coherence of the inflaton condensate as long as

$$f_a \lesssim 4 \times 10^{16} \text{ GeV.} \quad (5.49)$$

In case PQ symmetry was not restored only the misalignment mechanism [83–85] contributes to the axion DM abundance but this scenario leads to axion isocurvature fluctuations, which are tightly constrained [363]. Requiring the absence of these fluctuations imposes the condition [576]

$$f_a < 1.4 \times 10^{14} \text{ GeV,} \quad (5.50)$$

implying that the non-restored scenario is ruled out. In the PQ restored scenario there are contributions from both axion misalignment and the decay of the network of topological defects (made up of domain walls and axionic strings see subsection 5.4.1) [445, 453, 454, 577–580] which is unstable for $N_{\text{DW}} = 1$. The contributions from the misalignment mechanism and the decay of the topological defects fits the observed DM relic density in the regime [383]

$$3 \times 10^{10} \text{ GeV} \lesssim f_a \lesssim 1.2 \times 10^{11} \text{ GeV,} \quad (5.51)$$

which corresponds to axion masses of [383]

$$50 \mu\text{eV} \lesssim m_a \lesssim 200 \mu\text{eV}. \quad (5.52)$$

A more recent study [581] found a compatible range of masses in the window $40 \mu\text{eV} \leq m_a \leq 180 \mu\text{eV}$. In the case that the entire axion relic abundance comes from misalignment only, the precise value of the required axion mass for post-inflationary PQ breaking varies from study to study and some examples are $m_a = (14.6 \pm 0.1) \mu\text{eV}$ [582], $m_a = 18 \mu\text{eV}$ [583] and $m_a = (25.2 \pm 11.0) \mu\text{eV}$ [584]. We show the corresponding parameter space $14 \mu\text{eV} \leq m_a \leq 200 \mu\text{eV}$ for the axion to photon coupling as the blue interval labelled

“axion DM” in the orange “S.M.A.S.H.E.D.”-band in figures 5.3 and 5.4. If one abandons the cosmological history of S.M.A.S.H. and assumes a sequestered sector for inflation, then pre-inflationary PQ breaking is possible again. In that regime only the misalignment mechanism is important and depending on the arbitrary initial misalignment angle in principle all f_a inside the “S.M.A.S.H.E.D.”-band could reproduce the DM relic abundance. For the remainder of this work we will assume the S.M.A.S.H. cosmology. In our construction the axion DM could decay to neutrinos via the interaction (5.38) leading to the width

$$\Gamma(a \rightarrow \nu_l \bar{\nu}_l) = \frac{m_a}{16\pi} \left(\frac{m_{\nu_l}}{f_a} \right)^2, \quad (5.53)$$

where ν_l is the lightest neutrino with $m_a > 2 m_{\nu_l}$ and we neglected the phase space suppression from the final state neutrino masses. The condition $m_a > 2 m_{\nu_l}$ can be recast as a bound on f_a

$$f_a < 3 \times 10^7 \text{ GeV} \cdot \left(\frac{0.1 \text{ eV}}{m_{\nu_l}} \right). \quad (5.54)$$

In order to be a good DM candidate the axion lifetime needs to be longer than about 249.6 Gyr [89] which leads to the bound

$$f_a \gtrsim 600 \text{ TeV} \cdot \left(\frac{m_{\nu_l}}{0.1 \text{ eV}} \right)^{\frac{2}{3}}. \quad (5.55)$$

Since both conditions intimately rely on the unknown value of the lightest neutrino mass and not the overall neutrino mass scale, we do not depict them in figures 5.3 and 5.4. If we plug in our estimates for the lightest neutrino masses from the coming section 5.7.10 the bounds read

$$0.1 \text{ GeV} < f_a < 5 \times 10^{17} \text{ GeV} \quad \text{for} \quad m_{\nu_l} \simeq 6 \times 10^{-12} \text{ eV}, \quad (5.56)$$

$$175 \text{ GeV} < f_a < 6 \times 10^{12} \text{ GeV} \quad \text{for} \quad m_{\nu_l} \simeq 5 \times 10^{-7} \text{ eV}. \quad (5.57)$$

This agrees with the f_a required for axion DM in (5.51).

5.6.3 Vacuum stability and Leptogenesis

The S.M.A.S.H framework can also deal with the instability of the EW vacuum in the direction of the SM like Higgs by using the σ field to implement the threshold stabilization mechanism [274, 585]. Integrating out the radial mode of σ shifts the quartic coupling of the SM like Higgs to

$$\tilde{\lambda}_H \equiv \lambda_H - \frac{\lambda_{H\sigma}^2}{\lambda_\sigma} \quad (5.58)$$

at energies below m_{h_σ} . The mechanism works for typical values of $\lambda_{H\sigma}^2/\lambda_\sigma \sim 10^{-2}$ [585]. Absolute stability of the tree level vacuum requires that $\tilde{\lambda}_H > 0$ as well as $\tilde{\lambda}_\sigma > 0$ (see (5.45)) [383]. Since σ couples to the exotic quarks and leptons, RGE effects from these interactions could destabilize the scalar potential in the σ -direction if the following

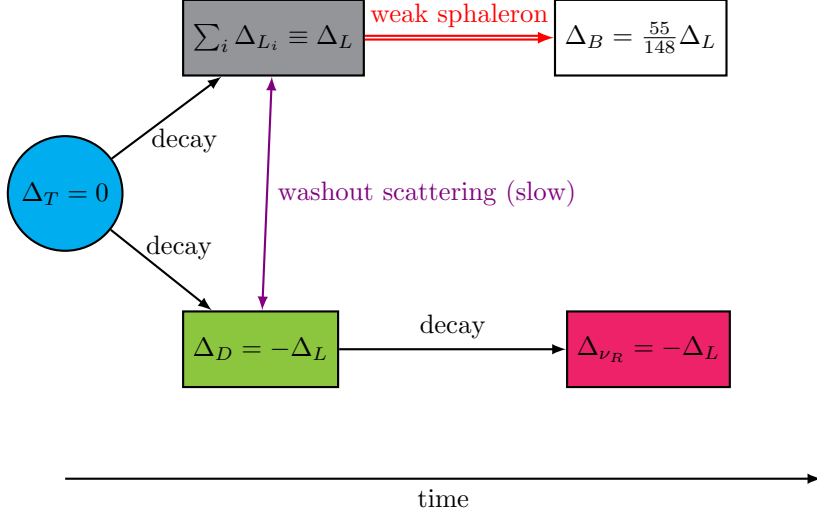


Figure 5.5: Schematic representation of our Dirac-Leptogenesis scenario.

is not satisfied (assuming a hierarchical fermion spectrum and using the triplets as a representative) [383]

$$M_T < 0.3 \cdot \lambda_\sigma^{\frac{1}{4}} \cdot f_a. \quad (5.59)$$

Setting $\lambda_\sigma \simeq 5 \times 10^{-10}$ (from (5.46)) and $f_a = 1.2 \times 10^{11}$ GeV (from (5.51)) as a first estimate would then lead to $M_T < 1.7 \times 10^8$ GeV. Since for gauge singlets such small masses would be problematic with successful Leptogenesis, which requires [586]

$$M_N \gtrsim 5 \times 10^8 \text{ GeV}, \quad (5.60)$$

the authors of [383] invoke a small amount of resonant enhancement to generate enough baryon asymmetry. As we will show in section 5.7 we do not need resonant enhancement for our model. Since we assume that the lightest triplet already has a mass of 10^8 GeV, the other triplets would not be allowed to remain heavier by a factor of 3-10 as is commonly assumed because of (5.59). Therefore we would need to include them in the cosmological analysis as well. However since the inflationary bounds in (5.46) affect only $\tilde{\lambda}_\sigma$ defined in (5.45) and not λ_σ itself, we can relax the bound (5.59) on M_T by adjusting $\lambda_{H\sigma}/\lambda_H$. To be conservative we will assume that all exotic fermion masses are bounded from above not only by f_a but by 10^9 GeV.

5.7 Appendix: Dirac-Leptogenesis in S.M.A.S.H.E.D.

5.7.1 Overview

The idea of Leptogenesis in theories without lepton number violation and Majorana masses was pioneered by [117] and applied to a plethora of proposed models in [587--601]. Since the sphalerons only freeze out around the temperature of the EW crossover,

which is far below the temperature range required for high scale Leptogenesis, we work in the limit of unbroken $SU(2)_L$. We consider the lightest triplet with a mass $M_T \simeq 10^8 \text{ GeV} \ll M_T^{(2,3)} \simeq \mathcal{O}(10^9 \text{ GeV})$ and assume that any preexisting asymmetry from the heavier triplets was washed out. Only the lightest exotic triplet and doublet fermions, hereafter denoted as T and D , are present in the plasma together with the SM. For each particle species we define

$$\Sigma_\psi \equiv \frac{n_\psi + n_{\bar{\psi}}}{s} \quad \text{and} \quad \Delta_\psi \equiv \frac{n_\psi - n_{\bar{\psi}}}{s} \quad (5.61)$$

in terms of the number densities for particles and antiparticles $n_{\psi, \bar{\psi}}$ and the entropy density s . A schematic picture of our scenario can be found in figure 5.5. The universe is initially symmetric with respect to B-L enforcing a vanishing asymmetry Δ_T in the fermionic triplets. Their decays $T \rightarrow LH$ and $T \rightarrow DH^\dagger$ generate equal and opposite asymmetries in the SM leptons L and the heavy vector-like leptons D so that $\Delta_L \equiv \sum_i \Delta_{L_i} = -\Delta_D$. Microscopically lepton number is conserved but since in the plasma the weak sphalerons couple only to the left chiral L this will be the source of lepton number violation needed for the Sakharov criteria [602]. In section 5.7.4 we explain why the asymmetry in vector-like leptons can not be transferred into a baryon asymmetry by the weak sphalerons because they do not contribute to the violation of B+L [603] via the weak interaction. Consequently only Δ_L can be converted into an asymmetry in baryons Δ_B , where the corresponding conversion factor will also be determined in the aforementioned section. Since the vector-like leptons will be heavy with masses above the EW scale they will decay to ν_R transmitting their asymmetry to these gauge singlets, which do not couple to the weak sphalerons at all. At late times we recover $\Delta_L = -\Delta_{\nu_R}$ demonstrating lepton number conservation. In order to preserve the SM lepton asymmetry until the sphalerons freeze out at the electroweak phase transition we must enforce that the $2 \rightarrow 2$ scattering processes that transform L into D are inefficient, which will be investigated in 5.7.5.

5.7.2 CP violation

The relevant Feynman diagrams for generating the CP violating interference between the tree- and one-loop-level contributions to the decay $T \rightarrow LH$ are depicted in figure 5.6. In order to have a non-vanishing imaginary part for this interference term, the Cutkosky rules [604] demand that the intermediate particles can go on shell. Therefore the decay $T \rightarrow LH$ can only violate CP if the decay channel $T \rightarrow DH^\dagger$ is also open. Consequently we must demand that $M_D < M_T$ and take both channels into account. Another consequence of our construction is that the same vertices generating the asymmetry in L also lead to an asymmetry in D as can be seen from the analogous diagrams in figure 5.7. We depicted the relevant kinematically allowed cut with a red dashed line in figures 5.6

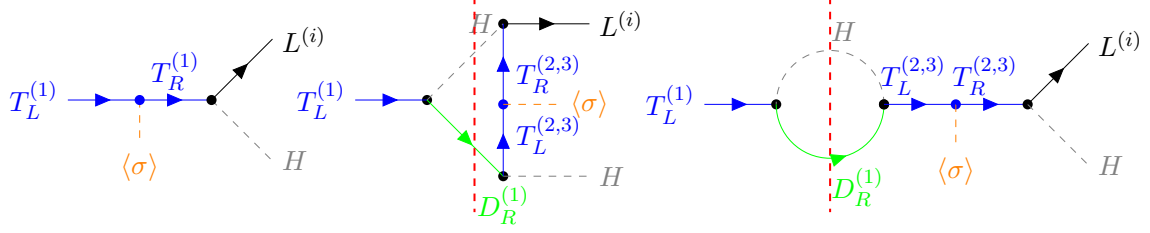


Figure 5.6: Feynman diagrams in the chiral basis for the CP violating decay of the lightest triplet fermion into SM leptons $L^{(i)}$. Internal lines intersecting the red dashed line are required to go on shell.

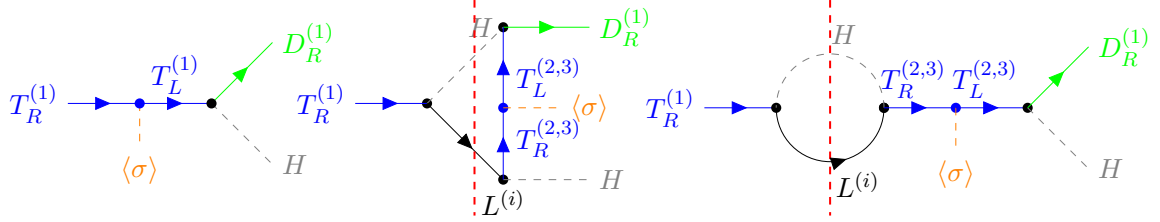


Figure 5.7: Feynman diagrams in the chiral basis for the CP violating decay of the lightest triplet fermion into the lightest exotic lepton $D^{(1)}$. Internal lines intersecting the red dashed line are required to go on shell.

and 5.7. The tree-level decay widths are determined to be

$$\Gamma(T \rightarrow LH) \equiv \sum_{\alpha, \beta} \sum_i \Gamma(T^a \rightarrow L_i^\alpha H^\beta) = \frac{M_T}{32\pi} (Y_{LT}^\dagger Y_{LT})_{11}, \quad (5.62)$$

$$\Gamma(T \rightarrow DH^\dagger) \equiv \sum_{\alpha, \beta} \Gamma(T^a \rightarrow D^\alpha H^\dagger \beta) = \frac{M_T}{32\pi} |(Y_{TD})_{11}|^2 (1 - \delta^2), \quad (5.63)$$

where we summed over all $SU(2)_L$ indices of the final states as well as SM lepton flavors i and introduced $\delta \equiv M_D^2/M_T^2$. Each component T^a with $a = 1, 2, 3$ has the same decay width. Note the phase space suppression for a massive final state fermion $\propto 1 - \delta^2$, which is different from the case for a massive final state scalar where one would have $\propto (1 - \delta)^2$ instead. Decays to the doublets D could be suppressed with respect to the leptonic mode by considering $\delta \lesssim 1$ [605]. Both triplets and doublets will receive different thermal corrections to their tree level mass owing to their different gauge interactions so the mass ratio is not constant. However we will ignore thermal effects for this analysis. We define the CP-conserving branching ratios to be

$$B_L \equiv \frac{\Gamma(T \rightarrow LH)}{\Gamma_{\text{tot.}}} = \frac{\Gamma(\bar{T} \rightarrow \bar{L}H^\dagger)}{\Gamma_{\text{tot.}}} = 1 - B_D. \quad (5.64)$$

Here we also introduced the total decay width

$$\Gamma_{\text{tot}} = \Gamma(T \rightarrow LH) + \Gamma(T \rightarrow DH^\dagger) = \Gamma(\bar{T} \rightarrow \bar{L}H^\dagger) + \Gamma(\bar{T} \rightarrow \bar{D}H) \quad (5.65)$$

in terms of the the tree-level decay widths from (5.62). Using CPT invariance together with unitarity one can show that for the matrix elements

$$|M(T \rightarrow LH)|^2 - |M(\bar{T} \rightarrow \bar{L}H^\dagger)|^2 = |M(\bar{T} \rightarrow \bar{D}H)|^2 - |M(T \rightarrow DH^\dagger)|^2, \quad (5.66)$$

holds true, which implies that the asymmetries for both channels are equal and opposite

$$\varepsilon \equiv \frac{\Gamma(T \rightarrow LH) - \Gamma(\bar{T} \rightarrow \bar{L}H^\dagger)}{2\Gamma_{\text{tot}}} = -\frac{\Gamma(T \rightarrow DH^\dagger) - \Gamma(\bar{T} \rightarrow \bar{D}H)}{2\Gamma_{\text{tot}}}, \quad (5.67)$$

because the phase-space factors divide out. Let us emphasize that the combined asymmetry of all three SM lepton flavors equals the asymmetry stored in one generation of D . We compute all imaginary parts using the Cutkosky prescription [604]. We split the asymmetry into a piece for the vertex correction and a piece for the self-energy correction (second and third diagrams in figures 5.6 and 5.7)

$$\varepsilon_{L,D} = \sum_{k \neq 1} \frac{\text{Im} \left[\left(Y_{LT}^\dagger Y_{LT} \right)_{1k} (Y_{TD})_{k1} \left(Y_{TD}^\dagger \right)_{11} \right]}{\left(Y_{LT}^\dagger Y_{LT} \right)_{11} + |(Y_{TD})_{11}|^2 (1 - \delta^2)} (I_{L,D}^V + I_{L,D}^S) \quad (5.68)$$

They read for the Lepton doublet with $x_k \equiv M_T^{(k)2}/M_T^2$

$$I_L^V = -\frac{\sqrt{x_k}}{8\pi} \left(1 - \delta - (1 + x_k) \text{Log} \left(1 + \frac{1 - \delta}{x_k} \right) \right), \quad I_L^S = \frac{\sqrt{x_k}}{8\pi} \frac{1 - \delta^2}{1 - x_k}. \quad (5.69)$$

For the D we have $I_L^V = -I_D^V$ and $I_L^S = -I_D^S$. Note that because of the Cutkosky rule both expressions rely on a D from the T decay going on-shell so they vanish for $\delta \rightarrow 1$. We checked that the asymmetry parameter for L reduces to the Type III Seesaw result [606] in the limits $\delta \rightarrow 0$ and $Y_{TD} \rightarrow Y_{LT}$:

$$I_L^V + I_L^S \Big|_{\delta=0} = -\frac{\sqrt{x_k}}{8\pi} \left(1 - (1 + x_k) \text{Log} \left(1 + \frac{1}{x_k} \right) - \frac{1}{1 - x_k} \right). \quad (5.70)$$

Unlike the case for a decaying gauge singlet, here there is a relative minus sign between the loop factors from the vertex- and self-energy-corrections [606]. The diagram involving an intermediate first generation triplet does not contribute in equation (5.68) because for $k = 1$ we find the following combination of couplings

$$\left(Y_{LT}^\dagger Y_{LT} \right)_{11} (Y_{TD})_{11} \left(Y_{TD}^\dagger \right)_{11} = \sum_{i=1}^3 \left(Y_{LT}^\dagger \right)_{1i} (Y_{LT})_{i1} |(Y_{TD})_{11}|^2 \quad (5.71)$$

$$= \sum_{i=1}^3 |(Y_{LT})_{i1}|^2 |(Y_{TD})_{11}|^2, \quad (5.72)$$

which is purely real.

5.7.3 Enhancement of the asymmetry parameter

We can find a simpler expression in the case of (infinitely) hierarchical triplets $x_k \gg 1$:

$$\varepsilon_L \simeq -\frac{1}{16\pi} \sum_{k \neq 1} \frac{\text{Im} \left[\left(Y_{LT}^\dagger Y_{LT} \right)_{1k} (Y_{TD})_{k1} \left(Y_{TD}^\dagger \right)_{11} \right]}{\left(Y_{LT}^\dagger Y_{LT} \right)_{11} + |(Y_{TD})_{11}|^2 (1 - \delta^2)} \sqrt{\frac{1}{x_k}} (1 - \delta^2), \quad (5.73)$$

which (for $\delta \ll 1$) is smaller by a factor of 3 compared to the singlet case due to relative sign between both contributions [606]. If we assume that the couplings responsible for the decay of the lightest triplet in (5.62) are real valued then we may trade them for the branching ratios to obtain

$$\varepsilon_L \simeq -\frac{M_T}{\sqrt{3} 16\pi} \sqrt{B_L B_D (1 - \delta^2)} \sum_{i=1}^3 \sum_{k \neq 1} \frac{\text{Im} [(Y_{LT})_{ik} (Y_{TD})_{k1}]}{M_T^{(k)}}, \quad (5.74)$$

where the factor of $\sqrt{3}$ takes into account that we assume the same $(Y_{LT})_{i1}$ for three generations i of SM leptons. By maximising the branching ratios $B_L = B_D = 1/2$ and neglecting the phase space suppression ($\delta \ll 1$) we find

$$\varepsilon_L \simeq -\frac{M_T}{\sqrt{3} 32\pi} \sum_{i=1}^3 \sum_{k \neq 1} \frac{\text{Im} [(Y_{LT})_{ik} (Y_{TD})_{k1}]}{M_T^{(k)}} \quad (5.75)$$

which is completely independent of the couplings for the tree level decay in (5.62). The Yukawas determining the cosmological evolution of the triplets and their out of equilibrium conditions discussed in the next section in (5.109) are therefore different from the couplings appearing in the asymmetry. Unlike in most Majorana Seesaw models we can not just use the Casas-Ibarra parametrization [607] to trade the Yukawa couplings for expressions from the available low energy neutrino data. This would allow one to set an upper bound on ε a la Davidson-Ibarra [606, 608]:

$$|\varepsilon_L| \leq \varepsilon_L^{\text{DI max}} = \frac{1}{16\pi} \frac{M_T (m_3 - m_1)}{v_H^2} < 3 \times 10^{-9} \cdot \left(\frac{M_T}{10^8 \text{ GeV}} \right) \cdot \left(\frac{m_3}{0.1 \text{ eV}} \right), \quad (5.76)$$

where m_3 and m_1 are the heaviest and lightest active neutrino respectively. This occurs since the triplet decay rate does not involve the coupling Y_{DR} to ν_R needed to reconstruct the neutrino mass matrix. Instead we find the following “effective mass” parameter

$$\tilde{m}_{i1} \equiv \sum_{k \neq 1} (Y_{LT})_{ik} (Y_{TD})_{k1} \frac{v_H^2}{M_T^{(k)}} \quad (5.77)$$

$$\simeq 60 \text{ keV} \cdot \sum_{k \neq 1} \left(\frac{|(Y_{LT})_{ik}|}{\mathcal{O}(1)} \right) \cdot \left(\frac{|(Y_{TD})_{k1}|}{\mathcal{O}(1)} \right) \cdot \left(\frac{10^9 \text{ GeV}}{M_T^{(k)}} \right) \quad (5.78)$$

playing the role of m_3 in our case. This parameter can be much larger than in the usual models, because it is missing a suppression factor of $Y_{DR} v_H / M_D$ compared to the active

neutrino mass scale. Hence we will be able to generate a significantly larger asymmetry than the $\mathcal{O}(10^{-9})$ for $M_T \simeq 10^8$ GeV without having to invoke the limit of resonant Leptogenesis where $M_T^{(1)} \approx M_T^{(2,3)}$ [426]. To quantify this enhancement we utilize our optimized asymmetry from (5.75) and decompose the Yukawa couplings into their real parts and phases:

$$|\varepsilon_L| \simeq \frac{1}{32\sqrt{3}\pi} \sum_i \sum_{k \neq 1} \frac{M_T}{M_T^{(k)}} |(Y_{LT})_{ik}| |(Y_{TD})_{k1}| |\sin((\alpha_{LT})_{ik} + (\alpha_{TD})_{k1})|. \quad (5.79)$$

Since the absolute value of the sine is bounded from above we get an upper limit of

$$|\varepsilon_L| \lesssim |\varepsilon_L^{\max}| = \frac{1}{32\sqrt{3}\pi} \sum_i \sum_{k \neq 1} \frac{M_T}{M_T^{(k)}} |(Y_{LT})_{ik}| |(Y_{TD})_{k1}| \quad (5.80)$$

$$\simeq 5.7 \times 10^{-4} \cdot \sum_i \sum_{k \neq 1} \left(\frac{M_T/M_T^{(k)}}{1/10} \right) \cdot \left(\frac{|(Y_{LT})_{ik}|}{\mathcal{O}(1)} \right) \cdot \left(\frac{|(Y_{TD})_{k1}|}{\mathcal{O}(1)} \right). \quad (5.81)$$

If we assume that the sum on the right hand side is flavor-independent and that there are no accidental cancellations we obtain an additional factor of six to that $|\varepsilon_L| \lesssim 3 \times 10^{-3}$. Note that we did not assume any resonant enhancement from the self energy diagrams for mass degenerate generations of triplets [426]. Thus our scenario provides an alternative approach to resonant Leptogenesis [426] for enhancing the asymmetry parameter. Since (5.80) depends only on the ratio of masses, we could even try to realize the neutrino masses by integrating out twice as many species of exotic fermions lowering their mass scale closer to the TeV range. We conclude that due to our sequential Seesaw needing two species of heavy mediators we were able to generate a lepton asymmetry that can potentially be up to six orders of magnitude larger than in conventional models for $M_T \simeq 10^8$ GeV. Note that this asymmetry still satisfies the perturbativity requirement $|\varepsilon_L| \ll 1$ that is assumed when deriving the semi-classical Boltzmann-equations in 5.7.6.

5.7.4 Sphaleron redistribution coefficient

Once an asymmetry in e.g. the SM leptons is created one has to take into account how this asymmetry is redistributed to the rest of the fermions and the SM Higgs via gauge and Yukawa interactions that are in equilibrium. These fast spectator processes lead to conservation laws for the individual number densities n_ψ , which for ultra-relativistic fermions (bosons) ψ (and their anti-particles $\bar{\psi}$) can be expressed in terms of their chemical potentials μ_ψ via the relation

$$n_\psi - n_{\bar{\psi}} = \frac{\mu_\psi g_\psi}{3} T^2 \begin{cases} \frac{1}{2} & \text{for fermions} \\ 1 & \text{for bosons} \end{cases}, \quad (5.82)$$

whereas for a massive particles the appropriate relation would be [609]

$$n_\psi - n_{\bar{\psi}} = \frac{\mu_\psi g_\psi}{\pi^2} T^2 F_\pm \left(\frac{m_\psi}{T} \right), \quad \text{with} \quad F_\pm(x) \equiv \int_x^\infty dy \frac{y \sqrt{y^2 - z^2} e^y}{(1 \pm e^y)^2} \quad (5.83)$$

where the + (-) applies for bosons (fermions). We will work in the regime $T_{\text{EQ}} \simeq \mathcal{O}(100 \text{ GeV}) \ll T < 10^8 \text{ GeV}$ and since we need to be above the EW phase transition for the sphaleron transition to occur we can work in the regime of unbroken electroweak symmetry where the chemical potential of the gauge bosons is $\mu_W = 0$ and components of the same multiplet have the same chemical potential [610]. For the SM we include 3 generations of q, u, d, l, e and one Higgs H . At temperatures below 10^8 GeV all SM Yukawa interactions are in equilibrium [611] and for simplicity we neglect all flavor effects and assign generation-independent chemical potentials. For the SM the appropriate conditions read [610, 612]

- hypercharge neutrality of the plasma

$$3(\mu_q + 2\mu_u - \mu_d - \mu_l - \mu_e) + 2\mu_H = 0 \quad (5.84)$$

- $\text{SU}(2)_L$ sphalerons

$$3\mu_q + \mu_l = 0 \quad \text{from} \quad \mathcal{O}_{\text{sph.}} = \Pi_{i=1}^3 l_i q_i q_i q_i \quad (5.85)$$

- $\text{SU}(3)_c$ sphalerons

$$2\mu_q - \mu - \mu_d = 0 \quad (5.86)$$

- SM Yukawa interactions

$$\mu_l - \mu_H - \mu_e = 0 \quad \text{from} \quad \bar{L}He, \quad (5.87)$$

$$\mu_q - \mu_H - \mu_d = 0 \quad \text{from} \quad \bar{Q}Hd, \quad (5.88)$$

$$\mu_q + \mu_H - \mu_u = 0 \quad \text{from} \quad \bar{Q}\tilde{H}u. \quad (5.89)$$

Note that since all Yukawa interactions equilibrate the $\text{SU}(3)_c$ sphaleron condition (5.86) becomes redundant as it is just the sum of (5.88) and (5.89). As we have six potentials and only five conditions we can express five chemical potentials in terms of a sixth. We choose the potential for the total baryon minus lepton number for three generations in the SM

$$\mu_{B-L_{\text{SM}}} = 2\mu_q + \mu_u + \mu_d - 2\mu_l - \mu_e, \quad (5.90)$$

because it is not washed out by the weak sphalerons and recover the famous relations

$$\mu_B = \frac{28}{79}\mu_{B-L_{\text{SM}}}, \quad \mu_{L_{\text{SM}}} = -\frac{51}{79}\mu_{B-L_{\text{SM}}}. \quad (5.91)$$

Next we add the additional BSM particles. We start with three gauge singlets ν_R . The previous conditions are unchanged, but since our theory conserves B-L we have to impose this on the potentials

$$\mu_{B-L_{\text{tot}}} = \mu_{B-L_{\text{SM}}} - \mu_{\nu_R} = 0, \quad (5.92)$$

which by itself would lead to [117]

$$\mu_B = \mu_{L_{\text{tot}}} = \frac{28}{79}\mu_{B-L_{\text{SM}}}. \quad (5.93)$$

However we also add the lightest two vector-like doublets (D_L, D_R) with $Y = 1/2$ and lepton number 1. The heavier doublets will be Boltzmann suppressed. We assume that the interaction $\sigma \overline{D}_L D_R$ was in equilibrium at high temperatures and since after Peccei-Quinn breaking we have $\mu_\sigma = 0$ we conclude that $\mu_{D_L} = \mu_{D_R} \equiv \mu_D$. The hypercharge neutrality condition is modified to

$$3(\mu_q + 2\mu_u - \mu_d - \mu_l - \mu_e) + 2\mu_H + 2\mu_D = 0, \quad (5.94)$$

where the factor of two for μ_H appears because the scalar Higgs has different quantum statistics compared to the fermions and the factor two for μ_D appears because of the two chiralities we add. We furthermore demand that their coupling to ν_R is in equilibrium so that there is no population of stable heavy leptons (see section 5.7.5)

$$\mu_D - \mu_H - \mu_{\nu_R} = 0 \quad \text{from} \quad \overline{D}_L H \nu_R. \quad (5.95)$$

Since the D s are leptonic doublets we expect them to couple to the weak sphaleron transition. Naively one would expect to replace μ_l the condition (5.85) with $-\mu_D$, because of the opposite hypercharge. However the pair of vector-like fermions (D_L, D_R) does not contribute to the $U(1)_{B+L} \otimes SU(2)_L^2$ anomaly. Reference [603] computed the effective sphaleron mediated operators and since the vector-like leptons do not lead to $B+L$ violation the modified sphaleron vertex will still correspond to a $\Delta(B+L) = 6$ transition like the original in (5.85) and only involves a pair of vector-like leptons

$$\mathcal{O}_{\text{sph. I}}^{\text{SM+VL}} = (\Pi_{i=1}^3 l_i q_i q_i) D_L \overline{D}_R. \quad (5.96)$$

One can see that this vertex does not lead to new constraints on the chemical potential and that the asymmetry in D can not be converted into a baryonic asymmetry. Let us continue with the conservation of the total $B-L$

$$\mu_{B-L_{\text{tot}}} = \mu_{B-L_{\text{SM}}} - \mu_{\nu_R} - \frac{4}{3}\mu_D = 0, \quad (5.97)$$

where the factor of $4/3$ arises because of the two doublets $D_{L,R}$ and there is only one generation of heavy doublets in the plasma compared to the three generations of the SM quarks, leptons and ν_R . Moreover the Boltzmann equations in section 5.7.6 respect the conservation of total lepton number see (5.134) as well. Solving the system of equations of (5.94), (5.95) and (5.97) together with the previously mentioned conditions on the SM chemical potentials we arrive at

$$\mu_B = \mu_{L_{\text{tot}}} = \frac{55}{148}\mu_{B-L_{\text{SM}}}, \quad \mu_D = \frac{201}{592}\mu_{B-L_{\text{SM}}} \quad \text{and} \quad \mu_{\nu_R} = \frac{81}{148}\mu_{B-L_{\text{SM}}}. \quad (5.98)$$

The conversion factor for generating B from $B - L_{\text{SM}}$ of $55/148 \simeq 0.37$ is only slightly larger than the SM result $28/79 \simeq 0.35$.

5.7.5 Analytical estimates

We can determine the asymmetry in SM leptons from T decays to be [303]

$$\Delta_L = 3 \cdot \kappa \cdot |\varepsilon_L| \cdot \Sigma_T (T \gg M_T), \quad (5.99)$$

where the factor of 3 comes from the three components of the decaying triplet [606] and we have

$$\Sigma_T (T \gg M_T) = 4 \cdot \frac{135\zeta(3)}{8\pi^4 g_*(T \gg M_T)} \quad (5.100)$$

with a spin degeneracy factor of 4 because T is a Dirac fermion and $g_*(T \gg M_T) = \mathcal{O}(100)$ is the effective number of degrees of freedom in entropy. Using this we find that a baryon abundance of

$$\frac{n_B}{s} = c_{\text{sph.}} \Delta_L, \quad (5.101)$$

where the sphaleron redistribution coefficient in this model is determined in equation (5.98) of section 5.7.4

$$c_{\text{sph.}} = \frac{55}{148}. \quad (5.102)$$

Using that $s = 7.04 n_\gamma$ together with conservation of n_B/s one obtains a Baryon-to photon ratio η_B today of [303]

$$\eta_B = \frac{n_B}{n_\gamma} \Big|_{\text{today}} \simeq 6.1 \times 10^{-2} \cdot \kappa \cdot |\varepsilon_L|, \quad (5.103)$$

In this context κ is the so called efficiency factor, which penalizes the triplets staying close to thermal equilibrium, as this would violate Sakharov's first condition [602]. Its functional form can be approximated as

$$\kappa \simeq \frac{\Sigma_T (T \ll M_T)}{\Sigma_T^{\text{eq.}} (T \gg M_T)} \Big|_{T=T_{\text{FO}}}, \quad (5.104)$$

where T_{FO} is the temperature at which the last interactions that changes the leptonic asymmetry freezes out. Decaying particles far away from equilibrium are still as abundant as radiation at $T_{\text{FO}} \ll M_T$ so $\Sigma_T (T_{\text{FO}} \ll M_T) \simeq \Sigma_T^{\text{eq.}} (T_{\text{FO}} \gg M_T)$ which implies $\kappa \simeq 1$ as long as they do not dominate the energy density of the universe. In case they do one can even have $\kappa \sim g_* \gg 1$ [613]. As a consequence of their weak scale gauge interactions the triplets will have an initial thermal population after reheating so that $\kappa < 1$. The penalizing effect can be seen if one considers a fully thermalized triplet with $\Sigma_T (T_{\text{FO}} \ll M_T) \simeq \Sigma_T^{\text{eq.}} (T_{\text{FO}} \ll M_T)$ which would imply $\kappa \sim e^{-\frac{M_T}{T_{\text{FO}}}} \ll 1$. If we compare our estimate to the value extracted from BBN and Planck data [90]

$$\eta_B = (6.143 \pm 0.190) \times 10^{-10} \quad (5.105)$$

we find that we need an efficiency factor of

$$\kappa \gtrsim 1.8 \times 10^{-5} \cdot \left(\frac{5.7 \times 10^{-4}}{|\varepsilon_L|} \right). \quad (5.106)$$

Efficiency parameter

The task is now to show that our model can realize a cosmological history that leads to the required value of κ . Before we do so numerically we will find the required parameters using analytical arguments. Around $T = M_T$ the distribution function of a thermalized fermion would change from its Fermi-Dirac shape to a Maxwell-Boltzmann distribution leading to the non-relativistic expressions for its number density etc. On the other hand a fermion that decoupled at $T \gg M_T$ would keep its relativistic Fermi-Dirac distribution, provided that the fermion self interactions also have decoupled. Hence $T = M_T$ is the right epoch to quantify the deviation from thermal equilibrium needed to satisfy the Sakharov conditions. We define the customary decay parameter from the decay widths in (5.62)

$$K \equiv \frac{\Gamma(T \rightarrow LH) + \Gamma(T \rightarrow DH^\dagger)}{H(T)} \Big|_{T=M_T} \quad (5.107)$$

and introduce the effective Yukawa coupling

$$Y \equiv \sqrt{\left(Y_{LT}^\dagger Y_{LT}\right)_{11} + |(Y_{TD})_{11}|^2 (1 - \delta^2)} \quad (5.108)$$

Then we re-express the Yukawa coupling in terms of the decay parameters

$$Y \simeq 4 \times 10^{-4} \cdot \sqrt{\frac{K}{100}} \cdot \left(\frac{g_*(M_T)}{100}\right)^{\frac{1}{4}} \cdot \sqrt{\frac{M_T}{10^8 \text{ GeV}}} \quad (5.109)$$

for later convenience. If the triplet had no gauge interactions the Sakharov criteria would be satisfied for an out of equilibrium decay with $K \ll 1$ implying $\kappa \simeq 1$. The efficiency for a decaying fermion with EW gauge interactions can be estimated as [606, 613]

$$\kappa \simeq \text{Min} \left(1, \frac{1}{K}, \frac{M_T}{10^{12-13} \text{ GeV}} \text{Max}(1, K) \right). \quad (5.110)$$

Since we consider $M_T \ll 10^{12} \text{ GeV}$ the efficiency will always be less than unity. In principle there are three regimes and we can understand the parametrics in terms of the last process to decouple from equilibrium:

1. Weak washout from inverse decays:

$K \ll 1$ ($Y \ll 3.5 \times 10^{-5}$) for which $\kappa \sim M_T/10^{12-13} \text{ GeV} \sim 10^{-4-5}$

The gauge interactions lead to annihilation processes $T\bar{T} \leftrightarrow WW, FF$, where W are the $SU(2)_L$ gauge bosons and $F = H, L, Q$ are the SM Higgs and Fermion doublets. Naively one would expect that this violates Sakharov's first condition, however one should not forget that the gauge scatterings will eventually drop out of equilibrium. The thermally averaged scattering rate $\Gamma(T\bar{T} \leftrightarrow WW, FF) = \gamma(T\bar{T} \leftrightarrow WW, FF)/n_T^{\text{eq}}$ can be obtained from the expression (5.143) in the section and we find

$$\frac{M_T}{T_{\text{FO}}^{\text{gaug.}}} \simeq 17 \quad \text{for} \quad M_T = 10^8 \text{ GeV}. \quad (5.111)$$

The regime $K \ll 1$, also known as the regime of weak washout from inverse decays $L_i H, DH^\dagger \rightarrow T$, corresponds to a situation where the (inverse) decays are slow when the T s freeze out from gauge interactions at typical values of $M_T/T_{\text{FO}}^{\text{gauge}} \simeq \mathcal{O}(20)$. Consequently the frozen out abundance of T s decays out of equilibrium. The factor $\kappa \sim M_T/10^{12-13} \text{ GeV} \sim 10^{-4-5}$ measures the abundance of triplets surviving the gauge annihilations.

2. Strong washout from inverse decays

$$K \gtrsim 10^5 \quad (Y \gtrsim 1.3 \times 10^{-2}) \text{ for which } \kappa \sim 1/K \lesssim 10^{-5}$$

In the regime of strong washout from inverse decays $K \gg 1$, the gauge interactions can freeze out before the inverse decays drop out of equilibrium. One can show that the approximate freeze out temperature is [303]

$$\frac{M_T}{T_{\text{FO}}^{\text{dec.}}} \simeq 5 \times \sqrt{\text{Log}(K)} \quad (5.112)$$

We find that the inverse decays freeze out after the gauge scatterings for $K \gtrsim 10^5$ and the efficiency factor corresponds to the one in the strong washout regime $\kappa \sim 1/K \lesssim 10^{-5}$ for vanilla Leptogenesis.

3. Intermediate regime

$$1 < K < 10^5 \quad (3.5 \times 10^{-5} < Y < 1.3 \times 10^{-2}) \text{ for which} \\ \kappa \sim \text{Min}(1/K, K \cdot M_T/10^{12-13} \text{ GeV})$$

In the intermediate regime there is a non-negligible amount of decays during the annihilation phase. These lead to less efficient gauge-annihilations thus creating an efficiency $\kappa \sim \text{Min}(1/K, K \cdot M_T/10^{12-13} \text{ GeV})$, which can be larger by up to a factor of K than the weak washout regime. This means that for $K \sim 100$ we get $\kappa \sim K \cdot M_T/10^{12-13} \text{ GeV} \sim 10^{-2-3}$, which is the largest enhancement possible as larger $K \gtrsim 1000$ will lead to $\kappa \sim 1/K \lesssim 10^{-3}$.

Comparing with (5.106) we conclude that the weak washout regime ($\kappa \sim 10^{-4-5}$) might be efficient enough to realize Leptogenesis, whereas the strong washout regime ($\kappa \lesssim 10^{-5}$) being less efficient by up to a factor of ten and might not work even with the largest possible asymmetries. The intermediate regime can have a larger efficacy ($\kappa \sim 10^{-2-3}$) than for weak washout so Leptogenesis will definitely work in this regime. For more precise estimates we will determine the relevant Boltzmann equations in 5.7.6 and solve them in section 5.7.9.

The numerical results of [606] for the case of Majorana triplets indicate that for the considered range of triplet masses $M_T = 10^8 \text{ GeV}$ the maximal efficiency is $\kappa_{\text{max.}} \simeq \mathcal{O}(10^{-3})$, which agrees with the previous conclusions. Note that this number was calculated for self-conjugate fermions, that also have a different washout scattering process as will be discussed in section 5.7.5. The low efficiency together with the Davidson-Ibarra bound on the asymmetry parameter in (5.76) is the reason why Majorana triplet Leptogenesis

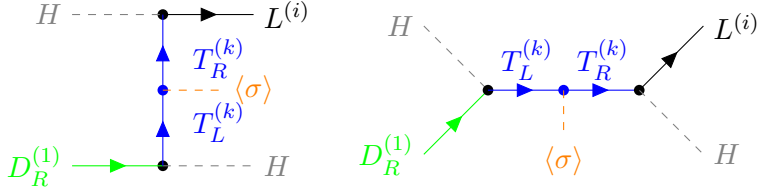


Figure 5.8: Diagrammatic representation of the relevant washout processes $DH \leftrightarrow LH$ involving leptons L and exotic leptons D . The diagrams for $L\bar{D} \leftrightarrow H\bar{H}$ are obtained via crossing symmetry.

is only possible for $M_T > 1.4 \times 10^{10}$ GeV [606]. However in section 5.7.9 we will numerically demonstrate that our Dirac-scenario is successful even for $M_T = 10^8$ GeV due to larger asymmetry parameter and the fact that the decaying particle is not self conjugate.

Additionally there could be annihilations of the triplet into the PQ scalars $T\bar{T} \leftrightarrow h_\sigma h_\sigma, a a, h_\sigma a$ [614, 615]. We find that they are slow compared to the Hubble rate at $T = M_T$ as long as

$$f_a > \mathcal{O}(10^{10} \text{ GeV}) \cdot \left(\frac{M_T}{10^8 \text{ GeV}} \right)^{\frac{3}{4}} \cdot \left(\frac{100}{g_*(M_T)} \right)^{\frac{1}{8}}, \quad (5.113)$$

which is in agreement with the parameters needed for axion DM in (5.51).

Washout scattering and heavy vector-like leptons

The defining feature of the original Dirac-Leptogenesis scenario is that the efficient conversion of the asymmetries in L into ν_R would spoil Baryogenesis, as sphalerons do not act on the ν_R . However for a coupling $\bar{L}H^\dagger\nu_R$ this only occurs much after the sphaleron freeze-out due to the tiny Yukawa coupling connecting both to the SM Higgs H [117]. In our scenario before EWSB these fermions couple to three H instead of one via the dimension six operator in (5.20) so the following three body scattering is possible

$$\Gamma(\bar{L}\nu_R \leftrightarrow HH^\dagger H) \sim \frac{1}{32\pi^2} \left(\frac{m_\nu}{v_H^3} \right)^2 T^5. \quad (5.114)$$

The above was estimated using dimensional analysis and the prefactor is an educated guess to take the three-body phase space into account. Two body annihilations of two Higgses into $\bar{\nu}_L\nu_R$ are only possible after the SM Higgs gets a vev so the sphalerons are already frozen out and this process is irrelevant for Leptogenesis. Three body annihilations decouple from the bath at around

$$T_{\text{FO}}^{2 \rightarrow 3} \simeq 2.3 \times 10^6 \text{ GeV} \cdot \left(\frac{0.1 \text{ eV}}{m_\nu} \right)^{\frac{2}{3}}, \quad (5.115)$$

where we emphasize that this is just an order of magnitude estimate. As demonstrated earlier the triplets only decouple from gauge and Yukawa interactions around

$T_{\text{FO}} \simeq M_T/\mathcal{O}(20) \simeq 5 \times 10^6 \text{ GeV}$ (see equations (5.111) and (5.112)) for any asymmetry to develop. We expect the $2 \rightarrow 3$ processes to be slow enough in this regime to disregard them compared to the next washout processes.

The scattering processes $DH \leftrightarrow LH$ depicted in figure 5.8 and $L\bar{D} \leftrightarrow HH$ are less suppressed compared to the previous process because they are two body reactions and lack the factors of Y_{DR}/M_D to form the neutrino mass. The existence of these scatterings is also required by the Cutkosky rule from the diagrams in 5.6, 5.7 and our estimate for the rate is (see (5.139) for the cross section)

$$\Gamma(L_i\bar{D} \leftrightarrow HH) \sim \Gamma(L_iH \leftrightarrow DH) \sim \frac{1}{16\pi} \left(Y_{LT} Y_{LT}^\dagger \right)_{ii} \left(Y_{TD}^\dagger Y_{TD} \right)_{11} \frac{T^3}{M_T^{(k)^2}}. \quad (5.116)$$

We demand that this rate is slow compared to the Hubble rate at $T = M_T/20$, which as explained before is the relevant temperature scale for Leptogenesis, provided that

$$(Y_{LT})_{i1} (Y_{TD})_{11} < 5 \cdot 10^{-4} \cdot \sqrt{\frac{M_T}{10^8 \text{ GeV}}} \cdot \left(\frac{g_*(M_T/25)}{100} \right)^{\frac{1}{4}}. \quad (5.117)$$

Since we assume that $M_T \gg M_D$ it may not be valid to neglect the D mass at this temperature $T \ll M_T$. If we set $Y \simeq (Y_{LT})_{i1} \simeq (Y_{TD})_{11}$ the bound implies $Y \lesssim 10^{-2}$, which is compatible with $K \lesssim 10^4$ see equation (5.109). The two benchmarks $K \ll 1$ and $K = 100$ are therefore safe from this washout process and we expect it to matter only for the region $K \sim 10^5$. For exchange of a heavier triplet $T^{(k)}$ ($k \neq 1$) the estimate changes to

$$(Y_{LT})_{ik} (Y_{TD})_{k1} < 1.5 \cdot 10^{-3} \cdot \sqrt{\frac{M_T^{(k)}/M_T}{10}} \cdot \sqrt{\frac{M_T}{10^8 \text{ GeV}}} \cdot \left(\frac{g_*(M_T/25)}{100} \right)^{\frac{1}{4}}. \quad (5.118)$$

We note that the bound (5.117) can be satisfied for the range $(Y_{LT})_{ik} \sim 0.5$ needed for the active neutrino masses in (5.21) if one considers $(Y_{TD})_{k1} \lesssim 10^{-2}$ for $k \neq 1$. Now this is devastating for the asymmetry as (5.80) gets reduced by three orders of magnitude and an efficiency of at least $\kappa \simeq 2 \times 10^{-2}$ would be needed, which might be out of reach. However so far we have assumed that the doublet D is relativistic at the temperature $M_T/20$, which does not have to be true. Since the processes $L\bar{D} \leftrightarrow HH$ and $LH \leftrightarrow DH$ require an on-shell D they are Boltzmann-suppressed at $T < M_D$ and therefore decouple exponentially with $e^{-\frac{M_D}{T}}$. The D are kept in equilibrium until $M_D/20$ by their EW gauge interactions. This leads to a quantitatively different behaviour when compared to the analogon for vanilla Leptogenesis: Here the so called $\Delta L = 2$ processes $LL \leftrightarrow HH$ and $LH \leftrightarrow \bar{L}H^\dagger$ (via an intermediate sterile neutrino N) can destroy the asymmetry in L down to temperatures of the electroweak scale. This occurs because their reaction rate densities only involve relativistic fermions as initial and final states so the rate is suppressed by a factor of $(T/M_N)^2$ [616]. We rewrite the scattering rate

using a non-relativistic number density

$$\Gamma(L_i \bar{D} \leftrightarrow HH) \sim \Gamma(L_i H \leftrightarrow DH) \quad (5.119)$$

$$\sim \frac{(Y_{LT} Y_{LT}^\dagger)_{ii} (Y_{TD}^\dagger Y_{TD})_{11}}{16\pi M_T^{(k)2}} \left(\frac{M_D T}{2\pi}\right)^{\frac{3}{2}} e^{-\frac{M_D}{T}} \quad (5.120)$$

and find that we can relax the constraint on the Yukawas down to

$$(Y_{LT})_{i1} (Y_{TD})_{11} \lesssim \mathcal{O}(0.1) \quad \text{for } \delta = \frac{M_D^2}{M_T^2} \gtrsim 0.08, \quad (5.121)$$

and similarly for $(Y_{LT})_{ik}$ $(Y_{TD})_{k1}$ both in agreement with our previous assumption $\delta \ll 1$. Therefore we need a doublet that is less than one order of magnitude lighter than the lightest triplet and for concreteness we will set $\delta = 0.1$.

Since the doublets D contain electrically neutral particles and eventually decouple from their gauge interactions, they are a good candidate for thermal WIMP dark matter. However we want to use the axion to generate the observed DM relic abundance (see section 5.6.2) and additional (meta-)stable fermions could overclose the universe. This is why we have to demand that the decays of the D to lighter particles occur rapidly enough. The most straightforward decay channel is to ν_R and total decay rate reads

$$\Gamma(D \rightarrow \nu_R H) \equiv \sum_i \Gamma(D^\alpha \rightarrow \nu_R i H^\alpha) = \frac{M_D}{16\pi} (Y_{DR} Y_{DR}^\dagger)_{11}, \quad (5.122)$$

where the rate is equal for both components of the doublets and we can also define a decay parameter

$$K_{DR} \equiv \frac{\Gamma(D \rightarrow \nu_R H)}{H(T)} \Big|_{T=M_D} \quad (5.123)$$

to see that

$$(Y_{DR})_{1i} \simeq 7 \times 10^{-4} \cdot \sqrt{\frac{K_{DR}}{10}} \cdot \left(\frac{g_*(M_D)}{100}\right)^{\frac{1}{4}} \cdot \sqrt{\frac{M_D}{3 \times 10^7 \text{ GeV}}}. \quad (5.124)$$

For the remainder of this work we set $K_{DR} = 10$.

5.7.6 Boltzmann equations

The definition of the cross sections can be found in section 5.7.7 and the parameterization for CP-violating rates densities can be found in section 5.7.8. Of central importance are the decays and inverse decays encoded in [299]

$$\gamma_{\text{tot.}} \equiv 3 \sum_T^{\text{a eq.}} \frac{K_1(z)}{K_2(z)} \Gamma_{\text{tot.}} = \frac{3g_T M_T^3}{2\pi^2 z} K_1(z) \Gamma_{\text{tot.}}, \quad (5.125)$$

where $\Gamma_{\text{tot.}}$ was defined in (5.65) and $K_{1,2}(z)$ denotes the special Bessel functions of the first and second kind. Here $\Sigma_T^{\text{eq.}} = 3 \Sigma_T^{a \text{ eq.}}$ is the total number density of all three triplet components $a = 1, 2, 3$. We used the rescaled temperature $z \equiv M_T/T$. In this context we denote the thermally averaged density of the CP-conserving decay width $\Gamma(D \rightarrow H\nu_R)$ from (5.122) as γ_{DR} and the gauge scattering rate (5.143) as γ_A . Special care needs to be taken with the inclusion of the washout scattering processes arising from the same Yukawas as the decays: The reactions $L\bar{D} \leftrightarrow HH$ occurring in the t -and u -channels can be computed by the usual methods and will be denoted as $\gamma_{T_{t+u}}$. As detailed in section 5.7.8 we need to remove the contribution of the on-shell triplet from the s -channel diagrams for the reactions $LH \leftrightarrow DH$ and their conjugates. This is necessary as the decays and inverse-decays of the intermediate on-shell triplets are already accounted for by the decay term $\propto \gamma_{\text{tot.}}$. Without this subtraction the Boltzmann equations would show unphysical behaviour such as generating asymmetries in equilibrium. One way to understand the appearance of this double counting problem is that the Boltzmann equations are essentially classical, whereas the cross sections and decay widths are computed using quantum physics. As outlined in 5.7.8 the CP-conserving rate density will be given by [427]

$$\gamma_{T_{s+t}}^{\text{sub.}} = \gamma_{T_{s+t}} - B_L B_D \gamma_{\text{tot.}}. \quad (5.126)$$

This structure can be understood by using a Breit-Wigner propagator for the unstable intermediate triplet and using the narrow width approximation for the propagator of T^a on resonance [303]

$$|D_s^a(s)|^{\text{sub.}} \equiv \left| \frac{1}{s - M_T^2 + iM_T\Gamma_{\text{tot.}}} \right|^2 - \frac{\pi\delta(s - M_T^2)}{M_T\Gamma_{\text{tot.}}}. \quad (5.127)$$

The coupling Y_{LT}^2 then reconstructs B_L . The coupling Y_{TD}^2 together with $1 - \delta^2$ arising from expanding the numerator of the matrix element for $\Gamma_{\text{tot.}}/M_T \ll 1$ reconstructs B_D . For more details consult section 5.7.7. Furthermore we only include the lightest intermediate triplet in the rates $\gamma_{T_{s+t}}^{\text{sub.}} + \gamma_{T_{t+u}}$, as the effects of the heavier triplets are suppressed by $M_T^2/M_T^{(2,3)} \lesssim 0.11$ for $M_T^{(2,3)} = (3 - 10) M_T$.

Our treatment for the asymmetry generation ignores all flavor and finite temperature effects. The impact of spectator processes responsible for washout, such as the ones from the SM lepton Yukawa couplings, is encoded in the sphaleron redistribution coefficient from section 5.7.4. We linearize the asymmetries in the small CP violating

parameter ε_L and find the following system of coupled non-linear Boltzmann equations:

$$zHs \frac{d\Sigma_T}{dz} = -2\gamma_A \left(\frac{\Sigma_T^2}{\Sigma_T^{\text{eq. 2}}} - 1 \right) - 2\gamma_{\text{tot.}} \left(\frac{\Sigma_T}{\Sigma_T^{\text{eq.}}} - 1 \right), \quad (5.128)$$

$$\begin{aligned} zHs \frac{d\Delta_T}{dz} &= -2\gamma_{\text{tot.}} \left(\frac{\Delta_T}{\Sigma_T^{\text{eq.}}} - B_L \frac{\Delta_L}{\Sigma_L^{\text{eq.}}} - B_D \frac{\Delta_D}{\Sigma_D^{\text{eq.}}} \right), \\ zHs \frac{d\Delta_L}{dz} &= 2\gamma_{\text{tot.}} \left[\varepsilon_L \left(\frac{\Sigma_T}{\Sigma_T^{\text{eq.}}} - 1 \right) + B_L \left(\frac{\Delta_T}{\Sigma_T^{\text{eq.}}} - \frac{\Delta_L}{\Sigma_L^{\text{eq.}}} \right) \right] \\ &\quad - 2 \left(\gamma_{T_{s+t}}^{\text{sub.}} + \gamma_{T_{t+u}} \right) \left(\frac{\Delta_L}{\Sigma_L^{\text{eq.}}} - \frac{\Delta_D}{\Sigma_D^{\text{eq.}}} \right), \end{aligned} \quad (5.129)$$

$$\begin{aligned} zHs \frac{d\Delta_D}{dz} &= 2\gamma_{\text{tot.}} \left[-\varepsilon_L \left(\frac{\Sigma_T}{\Sigma_T^{\text{eq.}}} - 1 \right) + B_D \left(\frac{\Delta_T}{\Sigma_T^{\text{eq.}}} - \frac{\Delta_D}{\Sigma_D^{\text{eq.}}} \right) \right] \\ &\quad + 2 \left(\gamma_{T_{s+t}}^{\text{sub.}} + \gamma_{T_{t+u}} \right) \left(\frac{\Delta_L}{\Sigma_L^{\text{eq.}}} - \frac{\Delta_D}{\Sigma_D^{\text{eq.}}} \right) - 2\gamma_{DR} \left(\frac{\Delta_D}{\Sigma_D^{\text{eq.}}} - \frac{\Delta_{\nu_R}}{\Sigma_{\nu_R}^{\text{eq.}}} \right), \end{aligned} \quad (5.130)$$

$$zHs \frac{d\Delta_{\nu_R}}{dz} = 2\gamma_{DR} \left(\frac{\Delta_D}{\Sigma_D^{\text{eq.}}} - \frac{\Delta_{\nu_R}}{\Sigma_{\nu_R}^{\text{eq.}}} \right). \quad (5.131)$$

A couple of more comments are in order: First of all it is worth pointing out that in case of thermal equilibrium $\Sigma_T = \Sigma_T^{\text{eq.}}$ and vanishing initial asymmetries $\Delta_T = \Delta_L = \Delta_D = 0$ no lepton asymmetry is produced in either channel. This is in complete accordance with Sakharov's criteria [602] and provides a useful consistency check. Since the asymmetry in D is already $\mathcal{O}(\varepsilon_L)$ it can be transmitted to the ν_R bath via CP conserving decay γ_{DR} . We do not include a Boltzmann equation for $\Sigma_L, \Sigma_D, \Sigma_{\nu_R}$ as they follow their equilibrium distributions for the relevant temperatures (see section 5.8.2 for the interactions of ν_R). In principle one should also include all scattering processes involving one gauge vertex and one of the Yukawa interactions like e.g. $T W \rightarrow LH$, $D^\dagger H$ or scattering of T with the charged SM fermions. These will be important at temperatures $T \gtrsim M_T$ because they require on shell triplets and contribute to the thermalization of T . However since we already include gauge annihilations for the thermalization and further estimated that Leptogenesis occurs far later at $T \lesssim M_T/20$ their addition is negligible.

For particles which are not self conjugate the Boltzmann equations depends on Σ and Δ so new effects are possible when compared to the equations for e.g. decaying heavy Majorana neutrinos [427]. This is why there is an equation for the asymmetry in T in (5.128), which only depends on the other asymmetries. If we add the equations for all four asymmetries we find

$$zHs \frac{d}{dz} (\Delta_T + \Delta_L + \Delta_D + \Delta_{\nu_R}) = 0. \quad (5.132)$$

This sum rule implies

$$\Delta_T(z) + \Delta_L(z) + \Delta_D(z) + \Delta_{\nu_R}(z) = \text{const.}, \quad (5.133)$$

where the constant is independent of z . For our case the appropriate initial conditions are vanishing initial asymmetries for each species so that we deduce that the constant term is actually zero. The sum rule can be represented in terms of chemical potentials

$$\mu_T + \mu_L + \mu_D + \mu_{\nu_R} = 0, \quad (5.134)$$

which can be interpreted as the conservation of the total lepton number in both the SM and PQ sectors. We find that the structure of our Boltzmann equations agrees with the ones presented in [589], which also respect lepton number conservation.

5.7.7 Cross sections and rate densities

The relevant cross sections are given in terms of the following dimensionless variables

$$\delta \equiv \left(\frac{M_D}{M_T} \right)^2, \quad x \equiv \frac{s}{M_T^2}, \quad r \equiv \sqrt{1 - \frac{4}{x}}, \quad \omega \equiv \frac{\Gamma_{\text{tot.}}}{M_T} \quad (5.135)$$

and read

- process $L\bar{D} \rightarrow HH$ possible in the $t-$ and u -channel:

$$\sigma_{t+u} = \frac{3}{8\pi M_T^2} \left(\frac{x - \delta}{x^2(1 + x - \delta)} - \frac{\text{Log}(1 + x - \delta)}{x^2(2 + x - \delta)} \right) \quad (5.136)$$

$$= \frac{3}{8\pi} \begin{cases} \frac{1}{2M_T^2} & \text{for } s \ll M_T^2 \\ \frac{1}{s} & \text{for } s \gg M_T^2 \end{cases} \quad (5.137)$$

- subtracted cross section (see section 5.7.6) for the process $LH \rightarrow DH$ possible in the $s-$ and t -channel:

$$\sigma_{s+t}^{\text{sub.}} = \frac{M_T^2}{32\pi x^2} (x^2 - \delta^2) \sum_{a=1}^3 |D_s^a(s)|^{\text{sub. 2}} \quad (5.138)$$

$$\begin{aligned} &+ \frac{3}{16\pi M_T^2 x^2} \frac{(x - \delta)((x - 1)(-2 + (x - 1)x + \delta) + (1 + x)\omega^2)}{(1 + x - \delta)((x - 1)^2 + \omega^2)} \\ &+ \frac{3}{16\pi M_T^2 x^2} \frac{(-2 + 2x + \omega^2)\text{Log}(1 + x - \delta)}{(1 - x)^2 + \omega^2} \\ &= \frac{3}{16\pi} \begin{cases} \frac{1}{2M_T^2} & \text{for } s \ll M_T^2 \\ \frac{1}{s} & \text{for } s \gg M_T^2 \end{cases} \quad (5.139) \end{aligned}$$

where for all $a = 1, 2, 3$

$$|D_s^a(s)|^{\text{sub. 2}} \equiv \left| \frac{1}{s - M_T^2 + iM_T\Gamma_{\text{tot.}}} \right|^2 - \frac{\pi\delta(s - M_T^2)}{M_T\Gamma_{\text{tot.}}}. \quad (5.140)$$

For the numerical evaluation it is convenient to carry out the thermal average of the subtracted matrix element (5.127) rather than to subtract the densities appearing

in (5.126). We follow the methods of [303] and use the following representation of the δ -distribution which decreases faster than the propagator away from the resonance

$$\delta(y) = \frac{2\rho^3}{\pi(y^2 + \rho^2)} \quad \text{with} \quad y = \frac{s}{M_T^2} - 1, \quad (5.141)$$

where $\rho \ll 1$. Since we find $\Gamma_{\text{tot.}}/M_T < 10^{-5}$ we are always in the narrow width regime and may set $\rho = \Gamma_{\text{tot.}}/M_T$ [303].

- process $T\bar{T} \rightarrow WW, F\bar{F}$, where W are the $SU(2)_L$ gauge bosons and F represents the SM fermion doublets [606]:

$$\begin{aligned} \sigma_W = & \frac{g_2^4}{\pi M_T^2 x r^2} \left(3r \left(1 + \frac{2}{x} \right) - r \left(4 + \frac{17}{x} \right) \right) \\ & + \frac{3g_2^4}{\pi M_T^2 x r^2} \left(1 + \frac{4}{x} - \frac{4}{x^2} \right) \text{Log} \left(\frac{1+r}{1-r} \right) \end{aligned} \quad (5.142)$$

For non-relativistic triplets the gauge scattering rate density can be approximately written as [617, 618]

$$\gamma(T\bar{T} \leftrightarrow WW, F\bar{F}) = 4 \times \frac{M_T T^3}{32\pi^3} e^{-2\frac{M_T}{T}} \left(c_s + 3 \frac{T}{M_T} (c_p + c_s) + \mathcal{O} \left(\frac{T^2}{M_T^2} \right) \right), \quad (5.143)$$

where we inserted a factor of four by hand to take into account that Dirac triplets have twice as many internal degrees of freedom as Majorana ones (see (5.147)). Furthermore

$$c_s = \frac{111}{8\pi} g_2^4 \quad \text{and} \quad c_p = \frac{51}{8\pi} g_2^4 \quad (5.144)$$

are the s - and p -wave coefficients from the non-relativistic velocity expansion.

5.7.8 CP-violating rate densities

γ_{tot} is the thermal average of Γ_{tot} in equation (5.65) computed via [303]

$$\gamma(\psi \rightarrow \dots) = \left(n_{\psi}^{\text{eq.}} + n_{\bar{\psi}}^{\text{eq.}} \right) \frac{K_1(z)}{K_2(z)} \Gamma(\psi \rightarrow \dots) \quad (5.145)$$

where we introduced $z \equiv m_{\psi}/T$ and $K_{1,2}(z)$ denotes the special Bessel functions of the first and second kind. The equilibrium number density of a particle ψ reads [311]

$$n_{\psi}^{\text{eq.}}(z) = g_{\psi} \frac{T^3}{\pi^2} \begin{cases} \zeta(3) & \text{for bosons with } T \gg m_{\psi}, \\ \frac{3}{4}\zeta(3) & \text{for fermions with } T \gg m_{\psi}, \\ \frac{z^2 K_2(z)}{2} & \text{for } T \ll m_{\psi}, \end{cases} \quad (5.146)$$

with g_{ψ} being the spin degeneracy of ψ . For scattering processes with a cross section σ the appropriate thermally averaged density in the Maxwell-Boltzmann approximation is

found to be [208, 311]

$$\gamma(a + b \leftrightarrow i + j + \dots) = g_a g_b \frac{T}{32\pi^4} \int_{s_{\min}}^{\infty} ds s^{\frac{3}{2}} \lambda \left(1, \frac{m_a^2}{s}, \frac{m_b^2}{s} \right) K_1 \left(\frac{\sqrt{s}}{T} \right) \sigma, \quad (5.147)$$

with $g_{a,b}$ denoting the spin degeneracies of particles a, b and

$$\lambda(a, b, c) \equiv (a - b - c)^2 - 4bc \quad (5.148)$$

together with $s_{\min} = \max \left[(m_a + m_b)^2, (m_i + m_j + \dots)^2 \right]$. We parameterize the CP-violating thermally averaged decay widths in the following way [427]

$$\gamma_{\text{eq.}}(T \rightarrow LH) = \gamma_{\text{eq.}}(\bar{L}H^\dagger \rightarrow \bar{T}) = (B_L + \varepsilon_L) \gamma_{\text{tot}} \quad (5.149)$$

$$\gamma_{\text{eq.}}(\bar{T} \rightarrow \bar{L}H^\dagger) = \gamma_{\text{eq.}}(LH \rightarrow T) = (B_L - \varepsilon_L) \gamma_{\text{tot}} \quad (5.150)$$

$$\gamma_{\text{eq.}}(T \rightarrow DH) = \gamma_{\text{eq.}}(\bar{D}H^\dagger \rightarrow \bar{T}) = (B_D - \varepsilon_L) \gamma_{\text{tot}} \quad (5.151)$$

$$\gamma_{\text{eq.}}(\bar{T} \rightarrow \bar{D}H^\dagger) = \gamma_{\text{eq.}}(DH \rightarrow T) = (B_D + \varepsilon_L) \gamma_{\text{tot}} \quad (5.152)$$

which follows from CPT invariance and the definition of ε . The CP conserving branching ratios of the decay widths are defined in (5.64). Furthermore the same branching ratios apply to the CP conserving part of $\gamma_{\text{eq.}}/\gamma_{\text{tot}}$, because the factors from the thermal averages divide out. Washout scattering mediated by T occurs at the same order in the perturbative expansion as the generation of ε . The washout rate can be decomposed into two contributions $\gamma_{T_{s+t}}$ and $\gamma_{T_{t+u}}$. Because of CPT invariance the rate densities for the following reactions only possible in the t - and u -channel have to satisfy

$$\gamma(L\bar{D} \rightarrow HH) = \gamma(H^\dagger H^\dagger \rightarrow \bar{L}D) \equiv \gamma_{T_{t+u}} \quad (5.153)$$

and the reactions possible in both the s - and t -channel satisfy

$$\gamma(\bar{D}H^\dagger \rightarrow \bar{L}H^\dagger) = \gamma(LH \rightarrow DH), \quad (5.154)$$

$$\gamma(DH \rightarrow LH) = \gamma(\bar{L}H^\dagger \rightarrow \bar{D}H^\dagger). \quad (5.155)$$

Here the s -channel contribution to the washout scattering $\gamma_{T_{s+t}}$ involves intermediate on shell T s whose decays and inverse decays are already accounted for in the Boltzmann equation. Therefore we have to perform real intermediate state (RIS) subtraction to remove the on shell contribution [299, 303, 619] which can be expressed as [303]

$$\gamma(LH \rightarrow DH)_{\text{eq.}} = \gamma_{T_{s+t}} - \gamma_{\text{eq.}}(LH \rightarrow T) \text{BR}(T \rightarrow DH), \quad (5.156)$$

$$\gamma(\bar{L}H^\dagger \rightarrow \bar{D}H^\dagger)_{\text{eq.}} = \gamma_{T_{s+t}} - \gamma_{\text{eq.}}(\bar{L}H^\dagger \rightarrow \bar{T}) \text{BR}(\bar{T} \rightarrow \bar{D}H^\dagger), \quad (5.157)$$

and we expand the CP violating branching ratios in the subtracted rates to leading order in ε_L :

$$\gamma(LH \rightarrow DH)_{\text{eq.}} = \gamma_{T_{s+t}} - B_L B_D \gamma_{\text{tot.}} + \varepsilon_L \gamma_{\text{tot.}} + \mathcal{O}(\varepsilon_L^2) \quad (5.158)$$

$$\gamma(\bar{L}H^\dagger \rightarrow \bar{D}H^\dagger)_{\text{eq.}} = \gamma_{T_{s+t}} - B_L B_D \gamma_{\text{tot.}} - \varepsilon_L \gamma_{\text{tot.}} + \mathcal{O}(\varepsilon_L^2) \quad (5.159)$$

Due to these relations we define the following object [427]

$$\gamma_{T_{s+t}}^{\text{sub.}} = \gamma_{T_{s+t}} - B_L B_D \gamma_{\text{tot.}} \quad (5.160)$$

5.7.9 Numerical results

Due to the larger number of parameters compared to standard Leptogenesis we refrain from scanning over the parameter space and rather present select benchmark points illustrating the phenomenology. To do so we integrate the Boltzmann equations between $z \equiv M_T/T \in [1/100, 100]$ and use the initial conditions that all asymmetries vanish and that Σ_T follows its equilibrium value due to its unavoidable gauge interactions for $T < 10^{12}$ GeV. For concreteness we set

$$M_T = 10^8 \text{ GeV} \quad \text{and} \quad M_D = 3 \times 10^7 \text{ GeV}, \quad (5.161)$$

which corresponds to $\delta = 0.1 \ll 1$. We will investigate the three regimes outlined in 5.7.5 and use $K = 0.01, 100$ and 10^5 as benchmark values for the decay parameter. For the most part we will consider $B_L = B_D = 1/2$ but in the strong washout regime ($K = 10^5$) we find interesting new effects for $B_L \neq B_D$. In case of $B_L = B_D$ we can vary the asymmetry parameter ε_L independently of the couplings for the tree-level decay, which are encoded in $B_{L,D}$. For the scenario $B_L \neq B_D$ we will use the parameterization $\varepsilon_L = \varepsilon_L^{\text{max.}} \sqrt{4B_L B_D(1 - \delta^2)}$ from (5.74). Additionally we take the decays of D to ν_R to be fast and fix $K_{DR} = 10$ which corresponds to $Y_{DR} = 7 \times 10^{-4}$. We use the analytical estimate in (5.143) for the gauge interactions of the triplet, which overestimates the correct rate for $z \lesssim 0.1$ by a factor of two but works excellently for the non-relativistic regime where the freeze-out occurs. The left plots in figures 5.9-5.13 show the evolution of the decay rate densities $\gamma_{L,D} \equiv B_{L,D} \gamma_{\text{tot.}}$ as well as the gauge scatterings γ_A and the washout scatterings $\gamma_{T_{s+t}}^{\text{sub.}}$, $\gamma_{T_{t+u}}^{\text{sub.}}$ divided by Hs , because that is the combination of parameters appearing in the Boltzmann equations (5.128). A value of $\gamma/Hs < 1$ is slow on cosmological time scales and the corresponding process will be inefficient.³ For all numerical benchmark points we find that the washout scatterings from $\gamma_{T_{t+u}}^{\text{sub.}}$ and $\gamma_{T_{s+t}}^{\text{sub.}}$ are always slow and orders of magnitude smaller than the smallest decay rate density (see e.g. figures 5.12 and 5.13) for $z \lesssim 50$. Hence we use $B_L B_R \gamma_{\text{tot.}}$ as a conservative estimate for the washout terms $\gamma_{T_{s+t}}^{\text{sub.}} + \gamma_{T_{t+u}}^{\text{sub.}}$, which is similar to reference [589], who employ $\gamma_{\text{tot.}}$ instead. We chose $B_L B_R \gamma_{\text{tot.}}$ as the washout scatterings are bounded from above by $\text{Min}(B_L, B_R) \gamma_{\text{tot.}}$. Since the resulting asymmetries will all be $\sim \varepsilon_L$ we rescale $\Sigma_T(z) - \Sigma_T^{\text{eq.}}(z)$ by a factor of ε_L to plot them in the same figure with the asymmetries. Additionally we rescale all leptonic asymmetries $\Delta_L, \Delta_{\nu_R}, \Delta_D, \Delta_T$ by the sphaleron redistribution coefficient from (5.101) to ease the visual comparison to the observed baryon asymmetry $\Delta_B^{\text{obs}} = \eta_B/7.04 \simeq 10^{-10}$ from (5.105).

³Note that γ/Hs has the same units as Γ/H , where Γ is the decay width or scattering rate $\Gamma \equiv \gamma/n_{\psi}^{\text{eq.}}$ for a particle ψ with equilibrium number density $n_{\psi}^{\text{eq.}}$ in the initial state. Since for non-relativistic ψ the density $n_{\psi}^{\text{eq.}}$ will be Boltzmann suppressed instead of scaling like radiation $n_{\psi}^{\text{eq.}} \sim n_{\gamma} \sim s$, the freeze-out temperature found from $\Gamma(T_{\text{FO}})/H(T_{\text{FO}}) < 1$ in section 5.7.5 will in general be different than the temperature when $\gamma/Hs < 1$.

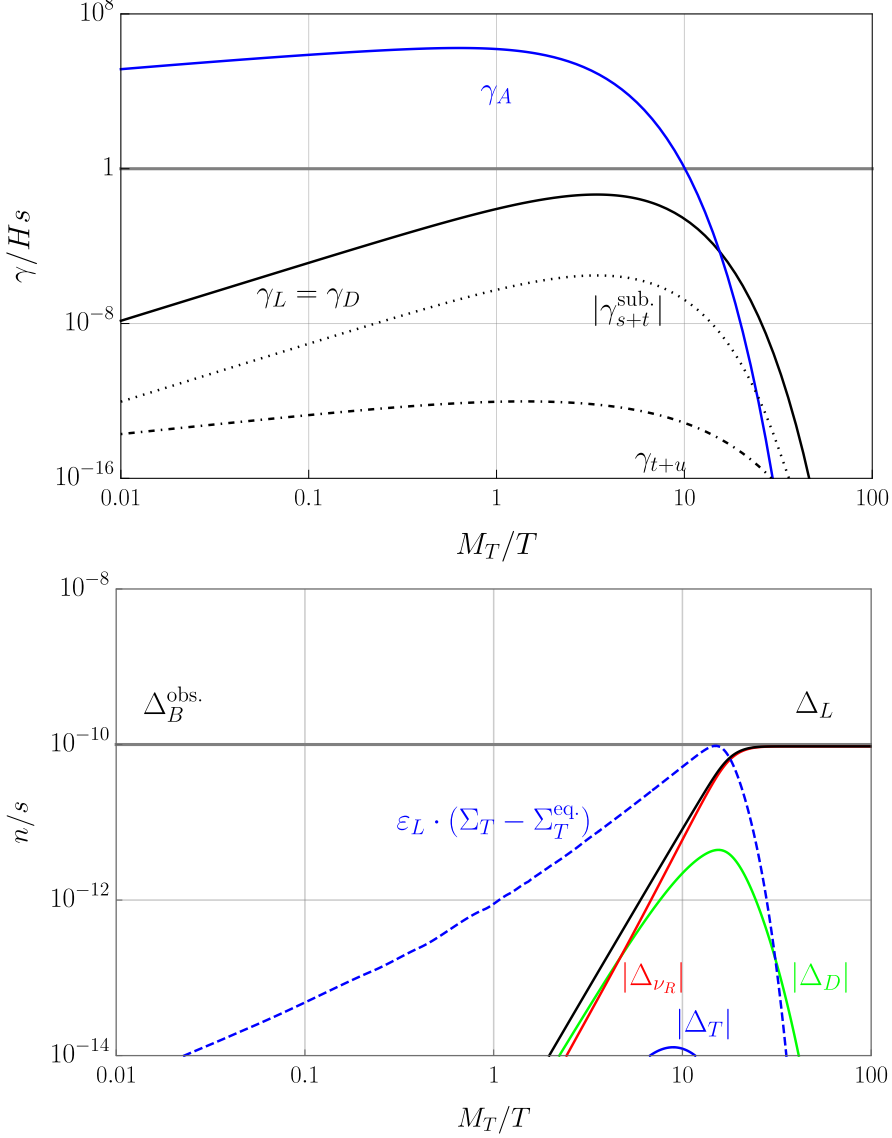


Figure 5.9: Rate densities (top) for $K = 0.01$, $B_L = B_D = 1/2$, $(Y_{LT} = Y_{TD} = 9.1 \times 10^{-6})$, $\varepsilon_L = 6.5 \times 10^{-4}$ and leptonic yields (bottom).

Weak washout regime

We fix $K = 0.01$ and $B_L = B_D = 1/2$ corresponding to $Y_{LT} = Y_{TD} = 9.1 \times 10^{-6}$. In the weak washout-regime the gauge annihilations are the last reaction to decouple from thermal equilibrium, as can be seen in the left plot of 5.9. Since decays and inverse decays are slow, washout will also be slow and the leptonic asymmetry can freeze-in [82] undisturbed. The right figure in 5.9 illustrates the evolution of the asymmetries: First around $z < 1$ equal and opposite amounts of Δ_L and Δ_D are generated. The asymmetries

track the deviation of the triplet abundance from equilibrium $\Sigma_T - \Sigma_T^{\text{eq}}$. Then the asymmetry in D is transmitted into Δ_{ν_R} via decays, which is why the corresponding red line starts later at $z \sim 5$. Since the triplet is a Dirac fermion it can develop an asymmetry itself via inverse decays of Δ_L, Δ_D . Owing to the fact that we take these decays to be slow the resulting Δ_T is small compared to the other asymmetries and the deviation from equilibrium. As the gauge interactions decouple around $z \sim 10$, the triplet abundance does not get restored from here on out and since the out-of-equilibrium decays become faster than the out-of-equilibrium gauge annihilations for $z \sim 20$, the frozen out abundance decays away, explaining the sharp decrease in the triplet abundance Σ_T at $z \gtrsim 20$. The asymmetry production asymptotes to its final value around this time as there are no more triplets left to decay. After all the triplets and doublets have decayed away only L and ν_R remain. As expected from lepton number conservation we find that the asymptotic values satisfy $\Delta_L = -\Delta_{\nu_R}$. We stop the evolution at $z = 100$ corresponding to $T = M_T/100$ long before the sphaleron decoupling because the leptonic asymmetries are conserved after the T, D have decayed. We can reproduce the observed baryon asymmetry today $\Delta_B^{\text{obs}} = \eta_B/7.04 \simeq 10^{-10}$ from (5.105) for an asymmetry parameter of $\varepsilon_L = 6.5 \times 10^{-4}$ corresponding to an efficiency of $\kappa \simeq 2 \times 10^{-5}$ from (5.106) in line with our estimate $\kappa \simeq 10^{-4-5}$.

Intermediate Regime

In this regime the decays of the triplet are not negligible during the gauge annihilation phase. Here we fix $K = 100$ and $B_L = B_D = 1/2$ corresponding to $Y_{LT} = Y_{TD} = 9.1 \times 10^{-4}$. The evolution of Δ_L is more complicated than in the weak washout-regime owing to the washout from faster inverse decays, which decouple around the same time as the gauge interactions. This is also why a larger Δ_T more comparable to $\varepsilon_L \cdot (\Sigma_T(z) - \Sigma_T^{\text{eq}}(z))$ is generated when compared to the previous benchmark. We fit the observed baryon asymmetry for $\varepsilon_L = 2.7 \times 10^{-5}$ analogous to $\kappa \simeq 4 \times 10^{-4}$. This efficiency is indeed larger by an order of magnitude than in the weak washout regime, but not quite as large as our analytical estimate from section 5.7.5.

Strong washout regime

For the strong washout regime we fix $K = 10^5$. In the first scenario we retain $B_L = B_D = 1/2$ which can be realized for $Y_{LT} = Y_{TD} = 2.9 \times 10^{-2}$. The left plot in 5.11 shows that indeed the decays are the last interaction to decouple now. Decays and inverse decays are faster than both the annihilations and the Hubble rate only for $z \sim 6 - 30$. The right plot in the same figure illustrates the evolution of the asymmetries for the maximum possible value of $\varepsilon_L = 3 \times 10^{-3}$ from (5.80). All asymmetries and $\Sigma_T - \Sigma_T^{\text{eq}}$ reach their maxima at $z \sim 6$, when the (inverse) decays overtake the gauge annihilations, and decrease afterwards. Once γ_L decouples at $z \sim 30$ the asymmetry in Δ_L approaches a constant instead of continuing to decrease. This occurs because inverse decays depleting Δ_L are slow now (and eventually there are no more triplets left to decay producing Δ_L), analogous to the well known freeze-out scenario for thermal

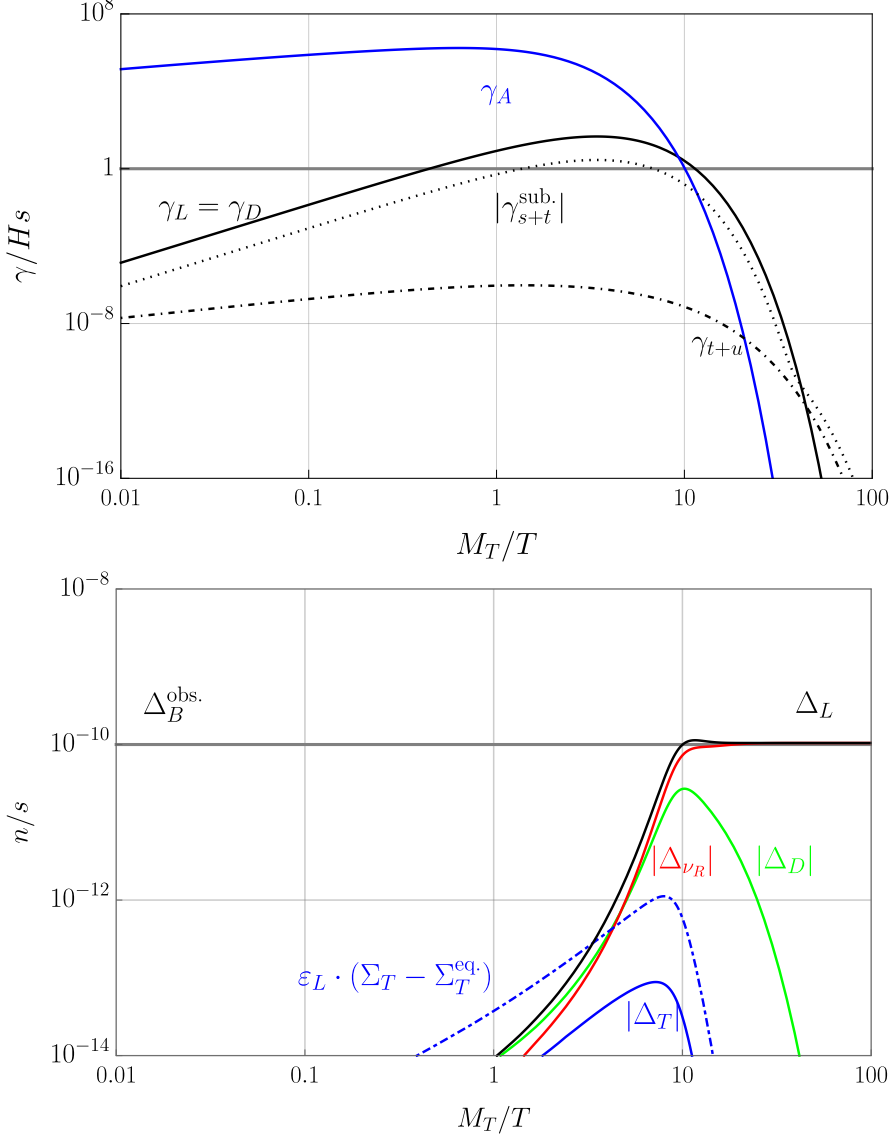


Figure 5.10: Rate densities (top) for $K = 100$, $B_L = B_D = 1/2$, $(Y_{LT} = Y_{TD} = 9.1 \times 10^{-4})$, $\varepsilon_L = 2.7 \times 10^{-5}$ and leptonic yields (bottom).

dark matter production. This is in agreement with Sakharov's conditions [602], since the lepton asymmetry would continue to decrease to zero if the inverse decays depleting them remained in equilibrium forever after $z \sim 6$. Here even for the maximum of ε_L we can not reproduce the observed baryon asymmetry. This happens because of too much washout from inverse decays and as a consequence we have a small efficacy $\kappa \sim 1/K \sim 10^{-5}$. However this is not the end for the strong washout regime. As explained in the previous subsections the larger amount of washout will produce a larger Δ_T and we will make use of this fact to obtain the required efficiency. This behaviour

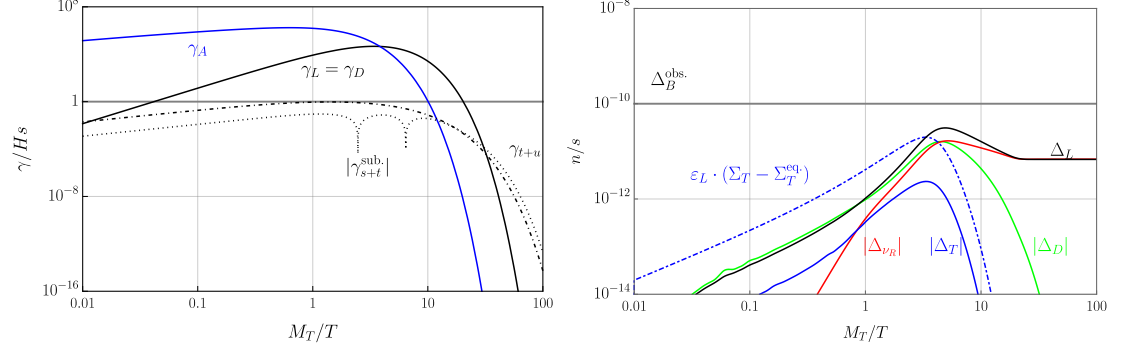


Figure 5.11: Rate densities (left) for $K = 10^5$, $B_L = B_D = 1/2$ ($Y_{LT} = Y_{TD} = 2.9 \times 10^{-2}$), $\varepsilon_L = 3 \times 10^{-3}$ and leptonic yields (right).

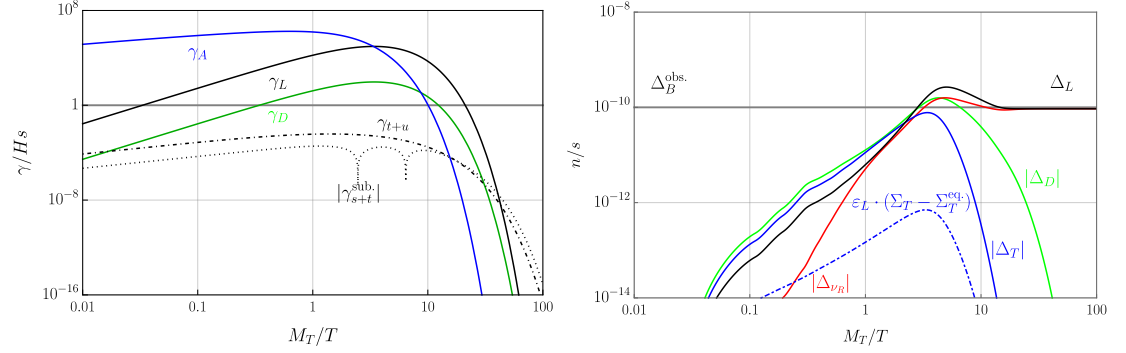


Figure 5.12: Rate densities (left) for $K = 10^5$, $B_L = 0.999$, $B_D = 10^{-3}$ ($Y_{LT} = 4.1 \times 10^{-2}$, $Y_{TD} = 1.2 \times 10^{-3}$), $\varepsilon_L = 1.7 \times 10^{-3} \sqrt{4B_L B_D(1 - \delta^2)} = 4.7 \times 10^{-5}$ and the leptonic yields (right).

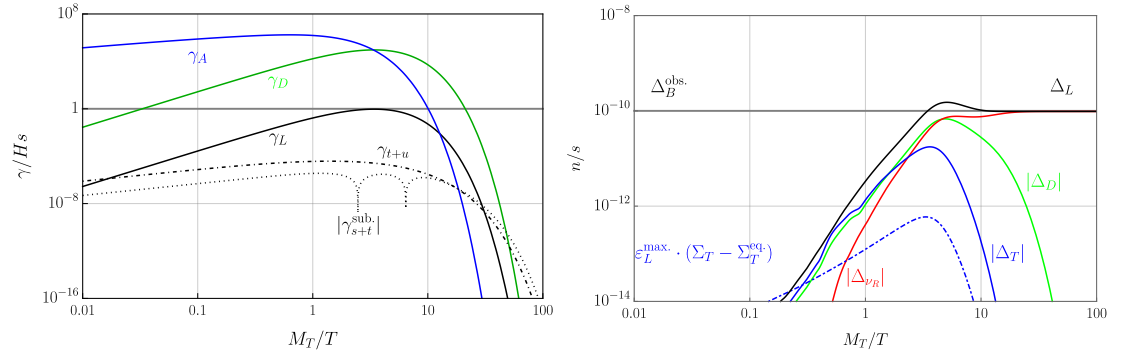


Figure 5.13: Rate densities (left) for $K = 10^5$, $B_L = 10^{-5}$, $B_D = 0.99999$ ($Y_{LT} = 1.3 \times 10^{-4}$, $Y_{TD} = 4.1 \times 10^{-2}$), $\varepsilon_L = 9 \times 10^{-5} \sqrt{4B_L B_D(1 - \delta^2)} = 2.2 \times 10^{-7}$ and the leptonic yields (right).

was first observed for decaying scalar triplets in the context of Type II Seesaw Leptogenesis [427]. The authors of [427] found that the lepton asymmetry produced by the decay

of a non-self-conjugate particle with two decays modes is washed out only if both decay modes are faster than the Hubble rate. Our previous choice $B_L = B_D$ actually leads to the most amount of washout [427]. We will demonstrate this for two concrete examples:

The first benchmark for the same decay parameter has $B_L = 0.999 \gg B_D = 10^{-3}$ implying $Y_{LT} = 4.1 \times 10^{-2}$, $Y_{TD} = 1.2 \times 10^{-3}$. The behavior depicted in the right plot of figure 5.12 can be understood as follows: First equal and opposite asymmetries in L, D are produced. However since $B_L \gg B_D$ we find that Δ_L is washed out by the fast inverse decays $LH \rightarrow T$, whereas a large Δ_D develops undisturbed. Of course the asymmetry in D is transmitted to ν_R via the fast decays. The sum rule for lepton number conservation in (5.134) then enforces that

$$\Delta_D + \Delta_{\nu_R} = -\Delta_L - \Delta_T, \quad (5.162)$$

which means that the asymmetry in the D, ν_R subsystem is compensated by an equally large asymmetry of opposite sign in the L, T subsystem. When Δ_T eventually decays it gets predominantly transferred to Δ_L again because of $B_L \gg B_D$. The baryon asymmetry is successfully generated for $\varepsilon_L = 1.7 \times 10^{-3} \sqrt{4B_L B_D(1 - \delta^2)} = 4.7 \times 10^{-5}$, where we used a value close to the maximum possible asymmetry of 3×10^{-3} . The difference to the $B_L = B_D$ case can also be understood if one notices that the triplet asymmetry in 5.11 is smaller than their deviation from equilibrium $\varepsilon_L \cdot (\Sigma_T(z) - \Sigma_T^{\text{eq.}}(z))$. For $B_L \gg B_D$ on the other hand we can see from 5.12 that Δ_T actually becomes much larger so that Δ_L starts to track its behaviour.

The second benchmark has $B_L = 10^{-5} \ll B_D = 0.99999$ implying $Y_{LT} = 1.3 \times 10^{-4}$, $Y_{TD} = 4.1 \times 10^{-2}$ and was depicted in figure 5.13: For $B_D \gg B_L$ a large initial asymmetry in L can freeze-in and is not washed out. The triplet asymmetry is predominantly produced by inverse decays $DH \rightarrow T$ now. For equal K we find that Δ_T is about an order of magnitude smaller for $B_D \gg B_L$ compared to $B_L \gg B_D$, because the inverse decay of D to T has to compete with its fast decay to ν_R . Lepton number implies that

$$\Delta_L = -\Delta_D - \Delta_{\nu_R} - \Delta_T. \quad (5.163)$$

When the triplets decay away Δ_T decays primarily to Δ_D because of $B_D \gg B_L$, and Δ_D decays to Δ_{ν_R} so again $\Delta_{\nu_R} = -\Delta_L$ is produced. Note that here we had to rescale $\Sigma_T(z) - \Sigma_T^{\text{eq.}}(z)$ by the larger $\varepsilon_L^{\text{max}}$ and not ε_L to fit it in the same plot with the other yields, since otherwise it would have been smaller than 10^{-14} . This again illustrates that Δ_T becomes the driving force for this mode instead. This benchmark fits the baryon asymmetry for $\varepsilon_L = 9 \times 10^{-5} \sqrt{4B_L B_D(1 - \delta^2)} = 2.2 \times 10^{-7}$. From this we see that the required $\varepsilon_L / \sqrt{4B_L B_D(1 - \delta^2)}$ can be made smaller the more hierarchical the branching ratios B_L/B_D are.

We conclude by noting that Dirac-Leptogenesis with a decaying fermion naturally realizes all the ingredients needed for the previously mentioned “quasi optimal efficiency”- scenario [427]: Since the decaying fermion is of Dirac nature it can have an asymmetry

itself and because of CPT and unitarity (see (5.66)) it needs to have two separate decay modes to generate the leptonic asymmetry parameter. The efficiency increases if their branching ratios are different.

5.7.10 Lightest neutrino mass

For the previously mentioned benchmarks $M_T = 10^8$ GeV and $M_D = 3 \times 10^7$ GeV we can use the Yukawa couplings Y_{LT}, Y_{TD} required for the different washout scenarios in subsection 5.7.5 to estimate the lightest neutrino mass. The third Yukawa was fixed to $Y_{DR} \simeq 7 \times 10^{-4}$ to allow for fast decays of the vector-like doublets see (5.124). Assuming no accidental flavor cancellations we find

$$m_\nu \simeq 5 \times 10^{-3} \text{ eV} \cdot Y_{LT} Y_{TD} \quad (5.164)$$

$$= \begin{cases} 6 \times 10^{-12} \text{ eV} & \text{for weak washout} & Y_{LT} \simeq Y_{TD} \simeq 3.5 \times 10^{-5}, \\ 5 \times 10^{-7} \text{ eV} & \text{for strong washout} & Y_{LT} \simeq Y_{TD} \simeq 1.3 \times 10^{-2}, \end{cases} \quad (5.165)$$

where the couplings refer only to the lightest doublet and triplet and we assumed equal branching ratios. The lightest neutrino mass eigenstate is substantially lighter than the cosmological limit on the total neutrino mass of $\sum_\nu m_\nu \lesssim 0.12$ eV [20] and can be treated as massless for all intents and purposes. This outcome is generic in Leptogenesis scenarios [249] due to the small couplings required for out of equilibrium decay.

5.8 Appendix: Dark radiation

In the SM the number of relativistic neutrinos is found to be [67–72]

$$N_{\text{eff.}} = 3.0440 \pm 0.0002, \quad (5.166)$$

where a small deviation from the value expected for three generations arises as the neutrino decoupling from the SM bath around MeV temperatures is not instantaneous. The abundance of dark radiation is typically parameterized in terms of the effective number of additional neutrinos $\Delta N_{\text{eff.}}$. The value inferred from the observed abundance of light elements produced during Big Bang Nucleosynthesis [20] is

$$N_{\text{eff.}}^{\text{BBN}} = 2.95_{-0.52}^{+0.56}. \quad (5.167)$$

Combined analyses of the current Planck CMB data together with Baryon Acoustic oscillations found [20]

$$N_{\text{eff.}}^{\text{Planck+BAO}} = 2.99_{-0.33}^{+0.34}, \quad (5.168)$$

which can be translated into

$$\Delta N_{\text{eff.}}^{\text{Planck+BAO}} \simeq 0.28. \quad (5.169)$$

The upcoming CMB Stage IV experiment [332, 333] and NASA’s PICO proposal [335] have a sensitivity forecast of

$$\Delta N_{\text{eff.}}^{\text{proj.}} = 0.06. \quad (5.170)$$

There is also the planned CORE experiment by the ESA [336] as well as the South Pole Telescope (SPT) [330] and the Simons observatory [331], which both aim to reach $\Delta N_{\text{eff.}} \lesssim 0.12$.

5.8.1 Contribution of the axion

The QCD axion does not reach thermal equilibrium via its couplings to the SM leptons: Reactions like $\nu \bar{\nu} \leftrightarrow Z a$ and $\nu e^+ \leftrightarrow W^+ a$ would only ever thermalize at temperatures far below the Z - and W^\pm -boson masses, because the rates are suppressed with m_ν^2/f_a^2 . Three body processes like $\nu \bar{\nu} \leftrightarrow \nu \bar{\nu} a$ avoid the production of heavy on-shell EW gauge bosons but are too slow to ever matter due to the previously mentioned tiny couplings. Production of two axions via $\nu \bar{\nu} \leftrightarrow a a$ is even more suppressed. References [620--622] showed that the axion decouples from its unavoidable strong interactions with the quark-gluon-plasma at

$$T_a^{\text{dec.}} \simeq 1.7 \times 10^9 \text{ GeV} \cdot \left(\frac{f_a}{10^{11} \text{ GeV}} \right)^{2.246}. \quad (5.171)$$

In the HHSI scenario PQ symmetry is broken at $T_c \simeq 0.01 f_a$ [383], which occurs after reheating for the typical range of $f_a < 10^{11} \text{ GeV}$ and the reheating temperature given by (6.77). Since both the critical temperature and the reheating temperature are larger than the decoupling temperature $T_a^{\text{dec.}}$, the axions will have had a thermal abundance in the early universe. Their contribution to the amount of dark radiation can then be estimated to be [383]

$$\Delta N_{\text{eff.}} \simeq 0.027 \cdot \left(\frac{100}{g_*(T_a^{\text{dec.}})} \right)^{\frac{4}{3}}, \quad (5.172)$$

which is an order of magnitude below the current bound of (5.169).

5.8.2 Contribution of the right handed neutrinos

The production of right handed neutrinos is driven by the Y_{DR} Yukawa coupling to the heavy doublet fields D in equation (5.15). Since the doublets have $SU(2)_L \otimes U(1)_Y$ gauge interactions they will develop a thermal abundance at high temperatures and can produce ν_R from decays and scattering. Even after the temperature drops below the lightest D mass there are still processes like $H^\dagger H \leftrightarrow \bar{\nu}_R \nu_R$ producing ν_R and keeping them in thermal equilibrium via off-shell D -exchange. On dimensional grounds we can estimate the interaction rate for the aforementioned process for $T \gg M_D$ as

$$\Gamma(T \gg M_D) \sim \frac{Y_{DR}^4 T}{16\pi} \quad (5.173)$$

and find that it comes into thermal equilibrium at a temperature of

$$T_{\text{coupl.}} \simeq 1.2 \times 10^{12} \text{ GeV} \cdot \left(\frac{Y_{DR}}{0.1} \right)^4 \cdot \sqrt{\frac{100}{g_*(T_{\text{coupl.}})}}. \quad (5.174)$$

We therefore expect a thermalized population of ν_R after reheating at around 10^9 GeV (see (5.47)). Since this process is not Boltzmann-suppressed with the heavy D -mass it can still be effective until temperatures $T \ll M_D$. In this regime we estimate the interaction rate to be

$$\Gamma(T \ll M_D) \sim \frac{Y_{DR}^4}{16\pi M_D^2} T^3, \quad (5.175)$$

where we neglected the Higgs mass and find that it drops out of thermal equilibrium at

$$T_{\text{FO}} \simeq 10 \text{ TeV} \cdot \left(\frac{0.1}{Y_{DR}} \right)^4 \cdot \left(\frac{M_D}{10^8 \text{ GeV}} \right)^2 \cdot \sqrt{\frac{g_*(T_{\text{FO}})}{100}}. \quad (5.176)$$

As this temperature is above the electroweak crossover it was self-consistent to neglect the mass of H . For a freeze-out before EWSB we can estimate the contribution of N_ν decoupled ν_R generations to the present day energy density in radiation as [348]

$$\Delta N_{\text{eff}} \simeq 3 \cdot 0.027 \cdot 2 \cdot \frac{7}{8} \cdot \left(\frac{100}{g_*(T_{\text{FO}})} \right)^{\frac{4}{3}} = 0.142. \quad (5.177)$$

We did not include the predicted asymmetry in ν_R because it is of the order of the small baryon asymmetry and negligible compared to the equilibrium abundance. Together with the contribution from the axion we have $\Delta N_{\text{eff}} \simeq 0.17$ which is allowed by current data see (5.169) and will be probed by next generation experiments. An intriguing way to make our model of Dirac neutrinos compatible with the projected sensitivity (5.170) would be to invoke additional entropy dilution after the decoupling of the right handed neutrinos, which would suppress ΔN_{eff} by a factor $\Delta > 1$. This mechanism has been used in the past to dilute the overabundance of thermalized keV-scale sterile neutrino dark matter in gauge theories [301, 623] needing $\Delta \sim 100$. Another application of entropy dilution is to bring the gravitino abundance in accordance with the reheating temperature required for vanilla Leptogenesis for $\Delta \sim 10^3 - 10^4$ [415]. The main ingredient would be a long-lived particle decaying far from equilibrium leading to an intermediate matter dominated epoch [467]. Since this particle needs to decouple while relativistic to produce sufficient entropy it should not have gauge interactions. This leaves only the radial mode of the PQ breaking field h_σ , which could be long-lived via its decays to the SM like Higgs. However the required scalar potential couplings would spoil (5.46) so that inflation and reheating in the HHSI scenario (see section 5.6.1) would cease to work. Hence we do not consider a long-lived h_σ further and treat the rather large value of $\Delta N_{\text{eff}} \simeq 0.17$ from the axion and three ν_R as an observational signature to distinguish our scenario from models involving either only a light scalar or only right handed neutrinos.

The smoking gun signature for this model would be observation of such a large ΔN_{eff} together with a signal in experiments probing the axion to photon coupling that is enhanced by an order of magnitude compared to the regular QCD axion band (see (5.36)).

5.9 Appendix: Summary

- **Dirac neutrino masses:**

We constructed Dirac neutrino mass model in the Seesaw spirit, where all heavy particles have masses from the PQ breaking scale and no new scalar besides the PQ breaking singlet is needed. To do so we introduce heavy leptons in the form of electroweak doublets D and triplets T . Unlike most models we generate the neutrino masses not via a dimension five operator but rather at dimension six. The only fundamental scales of this model are the EWSB scale v_H and the PQ scale v_σ which can be identified with the axion decay constant f_a . The lightest Dirac neutrino is approximately massless due to the Yukawa couplings required for Leptogenesis.

- **Axion to photon coupling:**

Our model involves vector-like fermion that are anomalous with respect to PQ symmetry. They boost the coupling of the QCD axions to a pair of photons by around an order of magnitude (see equation (5.36)) relative to conventional models and can be probed by current experiments such as HAYSTAC, ORGAN and QUAX or future searches by MADMAX, BRASS or ADMX. The new fermions do not lead to phenomenologically relevant Landau Poles for the SM gauge couplings.

- **preserving the attractive features of S.M.A.S.H.:** The model is compatible with the cosmological history outlined of the original S.M.A.S.H. scenario [383, 417, 418] such as successful inflation, reheating and axion DM from both misalignment and topological defect decay. Our new heavy fermions do not spoil the stability of the scalar potential.

- **Dirac-Leptogenesis:** We found an alternative for resonant Leptogenesis [426] when it comes to enhancing the leptonic asymmetry parameter ε_L in (5.80) by up to six orders of magnitude. Whereas a Majorana triplet fermion needs to have a mass of at least 10^{10} GeV our enhanced asymmetry allows for successful Leptogenesis even with 10^8 GeV masses. The phenomenology is qualitatively and quantitatively different from the case for Majorana fermions since the triplets can develop asymmetries themselves via washout processes. Choosing different branching ratios for the triplet decays to L and D allows for the “quasi optimal efficiency”-scenario first discussed for decaying scalar triplets in [427]. We identified four parameter regions that reproduce the observed baryon to photon ratio.

- **Dark radiation:**

Our setup involves an axion and three right handed neutrinos that were thermalized in the early universe producing a large value of $\Delta N_{\text{eff.}} \simeq 0.17$ which will be probed and potentially excluded by next generation CMB experiments such as CMB-S4, PICO, SPT or the Simons observatory. $\Delta N_{\text{eff.}}$ can be used to distinguish our construction from models involving only a light scalar ($\Delta N_{\text{eff.}} \simeq 0.028$) like the original S.M.A.S.H. or only right handed neutrinos ($\Delta N_{\text{eff.}} \simeq 0.142$ for three generations).

5.10 Appendix: Acknowledgements

This work benefited from the use of `PackageX` [242, 416]. We would like to thank Ciaran O'Hare for compiling the available axion limits [498] and for useful correspondence. Furthermore we are grateful to Andreas Trautner for providing valuable feedback on this manuscript.

6 The Type II Dirac Seesaw Portal to the mirror sector: Connecting neutrino masses and a solution to the strong CP problem

6.1 Contribution and Context

The following chapter is based on the single-author publication

Phys.Rev.D 106 (2022) 11, 115018, arXiv: 2209.14246 [hep-ph]

and the author of this thesis was responsible for the conception and implementation of all aspects of the publication.

In this project the aim was to develop my own version of the Type II Seesaw mechanism [32–36], which involves an electroweak triplet scalar with hypercharge $Y = 1$ (the lepton doublet has $Y = -1/2$) as the messenger that generates the active neutrino masses via a threshold correction. Such a hypercharged triplet would decompose into electrically neutral as well as singly- and doubly-charged scalar fields. The conventional expectation due to this model and the two-loop Zee-Babu model [624, 625] is that the detection of a doubly charged scalar would be circumstantial evidence for the mechanism behind Majorana neutrino masses. Following from the observation that a scalar transforming in the fundamental of two different $SU(2)$ factors, a so called bidoublet, can have the same electric charge matrix as a weak triplet, if it is also charged under an abelian symmetry that contains hypercharge, we investigated the gauge group $SU(2)_L \otimes SU(2)' \otimes U(1)_X$. This setup involves mirror copies of all SM fermions and the Higgs. Here $SU(2)' \otimes U(1)_X$ is broken down to hypercharge by the vev of the mirror Higgs H' . This model is known as the mirror sector extension of the SM [626, 627] (we do not copy QCD and hypercharge though) and is distinct from the left-right-symmetric model $SU(2)_L \otimes SU(2)_R \otimes U(1)_{B-L}$ [628–632], because we employ $SU(2)$ -singlet fermions and all mirror fermions have opposite abelian charge compared to their typical B-L charges. The neutrinos in L and the mirror neutrinos in L' are connected via the tiny induced vev of the bidoublet and we do not add any singlet neutrinos. Thus the Dirac nature of the neutrino mass is a consequence of the underlying gauge symmetry and particle spectrum. In principle there can exist couplings between SM and mirror charged leptons, but here we use an additional discrete symmetry to avoid them, meaning that the bidoublet acts as the only portal between the two sectors. A motivation behind

6 Type II Dirac Seesaw

the mirror sector construction is that it allows to solve the strong CP problem via a discrete exchange symmetry [633]. Unlike in the minimal left-right-symmetric model [634] here there is no spontaneous CP-violation from the bidoublet vev and we estimate that the two- and three-loop corrections to the strong CP angle are subleading compared to corrections from only SM fields, which already are below all current and near future limits from the neutron's electric dipole moment. Our scenario requires a high scale of $v' = (10^9 - 10^{12}) \text{ GeV}$ for the spontaneous breaking of the discrete exchange symmetry and consequently also a super-heavy bidoublet with a mass above v' . These high scales suppress the contribution of the new states to low energy lepton-flavor-violating rates and leptonic magnetic moments. The mirror electron has a mass above 20 TeV and could be detectable at next generation colliders. In order to avoid large relic abundances of electrically charged mirror particles as well as mirror hadrons in general, we have to assume that the reheating temperature is below the mass of the lightest mirror particle, also implying that there is no thermal bidoublet abundance. (The same argument also excludes dark matter from the mirror sector.) This together with the large v' automatically suppresses the production of the right handed neutrinos, which would contribute to dark radiation. There are no mirror photons or mirror gluons in our setup, whose production is typically in tension with bounds on dark radiation [635]. If there is more than one copy of the bidoublet then Dirac Leptogenesis occur from resonantly enhanced [593] decays of the lightest bidoublet during reheating. Alternatively we sketch a version of the Affleck-Dine mechanism: This mechanism would be operative if a linear combination of the electrically neutral bosons housed by the two doublets and the bidoublet plays the role of the inflaton and a certain kind of higher dimensional operator with a phase dependence is present. To summarize we introduce

- a bidoublet with the same electric charge matrix as the Majorana Type II Seesaw triplet
- a scenario where the bidoublet vev does not spoil the solution to the strong CP problem
- a cosmologically viable mirror sector
- a scenario for resonant, non-thermal Dirac Leptogenesis and potentially Affleck-Dine Dirac Leptogenesis

6.2 Appendix: Abstract

We present a version of the Type II Seesaw mechanism for parametrically small Dirac neutrino masses. Our model starts from an $SU(2)_L \otimes SU(2)' \otimes U(1)_X$ gauge extension of the Standard Model involving a sector of mirror fermions. A bidoublet scalar with a very small vacuum expectation value connects the SM leptons with their mirror counterparts and we can identify the mirror neutrino with the right-handed neutrino. Similar to the conventional Type II Seesaw, our particle spectrum features singly- and doubly-charged scalars. The strong CP problem is solved by a discrete exchange symmetry between the

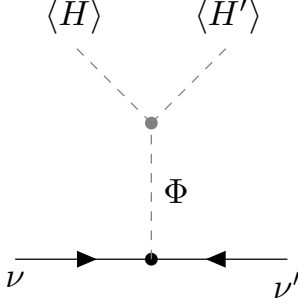


Figure 6.1: Diagrammatic representation of the Type II Dirac Seesaw mechanism. ν (ν') is embedded in the doublet l (l'). The mirror neutrino ν' plays the role of the right-chiral neutrino and the heavy scalar Φ is integrated out.

two sectors that forces the contributions of quarks and mirror quarks to the strong CP phase to cancel each other. We discuss the low-energy phenomenology, comment on the cosmological implications of this scenario and indicate how to realize successful Dirac Leptogenesis.

6.3 Appendix: Introduction

The Type II Seesaw mechanism [32–36] offers an approach to parametrically small neutrino masses, that is somewhat orthogonal to Type I Seesaw schemes involving fermionic messengers [26–30]. For Majorana neutrino masses, one needs to incorporate a weak isos triplet field with hypercharge -1 . One finds that the vacuum expectation value (vev) v_Δ of the super-heavy scalar triplet Δ with mass μ_Δ^2 is induced by the vev v of the Standard Model (SM)-like Higgs $v_\Delta \simeq \kappa v^2 / \mu_\Delta^2$, where κ is the dimensionful coupling for the term $\kappa H \Delta H$. This occurs because after H gets a vev, the aforementioned term biases the triplet potential in one direction such that a non-trivial minimum can appear despite the fact that $\mu_\Delta^2 > 0$. Since such a triplet breaks the custodial symmetry of the SM scalar potential, its vev is tightly constrained to lie below the GeV scale [636] by the observed ratio of the W^\pm and Z boson masses encoded in the ρ -parameter [637]. A typical feature of such scalar extensions for either tree- or loop-level Majorana neutrino masses [625, 638, 639] is the presence of double charged scalars whose production at colliders provides a smoking gun signature for these scenarios. As so far there is no compelling experimental or theoretical indication to consider only Majorana neutrinos, the field of Dirac model building has received renewed attention in the last years. It is possible to construct Dirac equivalents of all conventional Seesaw mechanisms [436, 640]. The usual approach for light Dirac neutrino masses is to start with a symmetry forbidding the tree-level mass term from the Standard Model (SM) Higgs doublet. Small neutrino masses at tree-level can then be realized by inducing a small vev for a new Higgs doublet [49–51, 641]. In gauge extensions of the SM like the left-right symmetric model (LRSM) $SU(2)_L \otimes SU(2)_R \otimes U(1)_{B-L}$ [628–632] or *mirror*-

6 Type II Dirac Seesaw

sector constructions [626, 627], the role of the doublet can be played by a bidoublet field [642–644], whereas in $SU(3)_C \otimes SU(3)_L \otimes U(1)_X$ models [645] Higgs triplets of $SU(3)_L$ are needed [646, 647]. In contrast to the Majorana case with its doubly-charged scalars, these scenarios feature only singly-charged ones, which are quite generic from a beyond the Standard Model (BSM) perspective. In this work we set out to close this gap by constructing a Dirac neutrino mass model with the same singly- and doubly-charged scalar spectrum as the original Type II Seesaw. The new scalar will also play an important role for Leptogenesis. Our starting point is the original mirror fermion scenario of reference [633] that was designed to solve the strong CP problem with the help of a discrete exchange symmetry. In recent years it was shown [648, 649] that one does not need to copy the entire $SU(2) \otimes U(1)$ structure of the SM, but that the gauge group of the form $SU(2)_L \otimes SU(2)' \otimes U(1)_X$ similar to the LRSM is already enough. While the proposal [648, 649] used additional singlet fermions to form a Type I Seesaw, our approach is to include the following bidoublet scalar

$$\Phi = \begin{pmatrix} \varphi_1^0 & \varphi_2^- \\ \varphi_1^- & \varphi_2^{--} \end{pmatrix} \sim (1, \mathbf{2}, \mathbf{2}, -1) \quad (6.1)$$

that couples to the SM and mirror leptons that are doublets under the two different $SU(2)$ groups via the interaction $Y_\nu l \Phi^\dagger l'$. The scalar potential contains a trilinear term involving all Higgs multiplets $\kappa H \Phi^\dagger H'$ (see (6.9) and (6.20) for the potential) that induces a small vev far below the electroweak scale

$$v_\Phi \simeq -\frac{\kappa v v'}{\sqrt{2}\mu_\Phi^2} \ll v, \quad (6.2)$$

where $\mu_\Phi \gg v, v'$ is the bare mass of Φ and v (v') the vev of H (H'). In this context we introduced the dimensionful parameter $\kappa < 0$. The neutrino mass is given by $m_\nu = Y_\nu v_\Phi / \sqrt{2}$ without the need for small Y_ν and figure 6.1 depicts a diagrammatic representation of this mechanism. After introducing the discrete symmetry and the particle spectrum in section 6.4, we deal with the vacuum structure and the bosonic masses in sections 6.5 and 6.7. The strong CP problem is the focus of section 6.8 and we demonstrate that loop corrections from the bidoublet do not spoil the symmetry-based solution to this problem. Following a brief discussion of low-energy constraints in 6.9 we consider the cosmological implications of our setup, especially for Dirac Leptogenesis in 6.10. The entire scalar potential and its minimization can be found in sections 6.6–6.6.2 together with the sufficient conditions for vacuum stability in section 6.6.3. Section 6.10.5 gives some additional details about the effective operator needed for Affleck-Dine Leptogenesis.

6.4 Appendix: The model

This solution to the strong CP problem hinges on a discrete exchange symmetry called *generalized Parity* [650] or *Higgs-Parity* [648, 649] that acts on the SM and mirror sector

field	$SU(3)_C$	$SU(2)_L$	$SU(2)'$	$U(1)_X$	\mathcal{Z}_3	generations
l	1	2	1	$-1/2$	ω^2	3
\bar{e}	1	1	1	1	ω	3
q	3	2	1	$1/6$	—	3
\bar{u}	$\bar{3}$	1	1	$-2/3$	—	3
\bar{d}	$\bar{3}$	1	1	$1/3$	—	3
H	1	2	1	$-1/2$	—	1
Φ	1	2	2	-1	—	1
l'	1	1	2	$-1/2$	ω	3
\bar{e}'	1	1	1	1	ω^2	3
q'	$\bar{3}$	1	2	$1/6$	—	3
\bar{u}'	3	1	1	$-2/3$	—	3
\bar{d}'	3	1	1	$1/3$	—	3
H'	1	1	2	$-1/2$	—	1

Table 6.1: Charges and representations for the SM and mirror sector fields as well as the bidoublet Φ . All spinors are left-chiral and we use the notation of [22]. We use $\omega \equiv e^{\frac{2\pi i}{3}}$.

(indicated by a prime) via

$$\psi(t, \vec{x}) \rightarrow i\sigma_2 \psi'^*(t, -\vec{x}), \quad (6.3)$$

where σ_2 is the second Pauli matrix contracted with the spinor index, which is absent for the bosonic fields. Note that this symmetry is distinct from the typical exchange symmetry between both sectors, as every SM matter field is interchanged with the CP-conjugate of the corresponding mirror field [651]. The symmetry exchanges the $SU(2)$ gauge fields with each other. For the gluon and the X boson the symmetry just acts on the spacetime arguments. Φ gets mapped to its own CP-conjugate. The transformation properties of all fields are summarized in table 6.1.

■ ADDENDUM: Yang-Mills theories with a topological θ -term are invariant under C [652]. This is why one can solve the strong CP-problem by either imposing CP [653,654] or P [633]. One should keep in mind, that for Weyl spinors (and without mirror fermions) C acts by exchanging e.g. the e (left-chiral electron) with \bar{e} (left chiral positron), whereas CP would map e to e^\dagger (right-chiral positron). ■

Up to the inclusion of the bidoublet this setup corresponds to model C of [648]. We use the two-component spinor formalism of [22]¹. $U(1)_X$ acts like hypercharge on all $SU(2)_L$ multiplets and $SU(2)_L \otimes SU(2)'$ singlets. Compared to the usual LRSM the abelian charges of all mirror doublets have the opposite sign, which is why we can not identify $U(1)_X$ with $U(1)_{B-L}$. It is worth pointing out that an $SU(2)_L \otimes SU(2)'$ bidoublet has exactly the same electric charge matrix as an $SU(2)_L$ triplet, so by charging it under $U(1)_X$ we obtain the desired electrically doubly charged component. The fermion sector (up to hermitian conjugates) is given by

$$\mathcal{L}_q = Y_u q H^\dagger \bar{u} + Y_d q H \bar{d} + Y'_u q' H'^\dagger \bar{u}' + Y'_d q' H' \bar{d}', \quad (6.4)$$

$$\mathcal{L}_l = Y_l l H \bar{e} + Y'_l l' H' \bar{e}', \quad (6.5)$$

$$\mathcal{L}_{\text{port.}} = Y_\nu l \Phi^\dagger l'. \quad (6.6)$$

The SM (mirror) quarks and charged leptons obtain their masses solely from the vev of H (H'). Non-observation of new colored fermion enforces a mirror scale of $v' \gtrsim 10^8$ GeV [468, 469, 650]. As a consequence of the $U(1)_X$ charge assignment there is no coupling between SM and mirror quarks and no coupling of the bidoublet to any kind of quarks. We do not add electrically neutral singlet fermions. In the lepton sector there would in principle exist three portal operators. The first one is the aforementioned coupling to Φ displayed in (6.6) and the other two $\lambda_e l H \bar{e}'$ and $\lambda'_e l' H' \bar{e}$ would mix the electrically charged SM and mirror leptons. In this study we want to focus on the Type II Dirac Seesaw portal from Φ , which is why we assume a lepton-specific \mathcal{Z}_3 symmetry (see the table 6.1) under which l, \bar{e}' transform as ω^2 and l', \bar{e} as ω with $\omega \equiv e^{\frac{2\pi i}{3}}$ that removes the terms $\propto \lambda_e, \lambda'_e$. We can estimate the masses of the Dirac neutrinos from the vev (6.2) to be

$$\frac{m_\nu}{0.1 \text{ eV}} \simeq Y_\nu \left(\frac{|\kappa|}{1 \text{ GeV}} \right) \left(\frac{v'}{10^9 \text{ GeV}} \right) \left(\frac{5 \times 10^{10} \text{ GeV}}{\mu_\Phi} \right)^2. \quad (6.7)$$

To avoid large loop corrections to the bidoublet mass we will take $|\kappa| \ll \mu_\Phi$. We choose a small value for $|\kappa|$ following the cosmological requirement for Baryogenesis in equation (6.85) of section 6.10. Setting $\kappa \rightarrow 0$ enhances the symmetry of the scalar potential [50, 655], since without the trilinear term in the potential (6.20) we can rephase each multiplet independently, which is why a small value for $|\kappa|$ is technically natural [408]. Owing to the fact that $v' \gg v$, for fixed μ_Φ we have to take a smaller $|\kappa|$ than for the Majorana Type II Seesaw in order to have a sufficiently light v_Φ . $|\kappa|$ could have a dynamical origin via the vev of an additional scalar [50, 656] and a small vev could come from another iteration of the Type II Seesaw [41, 42, 600, 641, 657]. Such a *nested Seesaw* could arise schematically from a quartic term $\phi_1 \phi_2^3$ for two additional SM gauge singlet scalars ϕ_1 and ϕ_2 , with ϕ_1 being much heavier than the vev of ϕ_2 , resulting in its induced small vev $\langle \phi_1 \rangle$ playing the role of κ . If we assume that SM and mirror

¹Arrows on fermion lines denote the chirality structure and not the flow of fermion number. A bar is part of the particle label and does not denote any kind of conjugation.

fermions have the same global B-L charge spectrum, then the mixed anomalies with the non-abelian gauge groups cancel separately for each sector. In this picture we see that the combined appearance of the terms $Y_\nu l \Phi^\dagger l'$ and $\kappa H \Phi^\dagger H'$ violates B-L by two units (as in Type II Seesaw models), because H, H' are uncharged. The gauge symmetries and particle spectrum ensure that l, l' do not pick up any Majorana mass terms allowed by $\Delta(\text{B-L}) = 2$, because they can only couple to each other via Φ , but never to themselves in the absence of scalar $\text{SU}(2)_L$ and $\text{SU}(2)'$ triplets.

6.5 Appendix: Vacuum structure

The vev of the neutral component of H' breaks $\text{SU}(2)' \otimes \text{U}(1)_X \rightarrow \text{U}(1)_Y$ and the discrete symmetry (6.3), followed by the usual electroweak symmetry breaking induced by the vev of H . Φ contributes as a small perturbation to the spontaneous symmetry breaking (SSB) of all aforementioned symmetries due to its tiny vev. We expand the multiplets into their components and assign vevs as

$$H \rightarrow \begin{pmatrix} \frac{v}{\sqrt{2}} \\ 0 \end{pmatrix}, \quad H' \rightarrow \begin{pmatrix} \frac{v'}{\sqrt{2}} \\ 0 \end{pmatrix}, \quad \Phi \rightarrow \begin{pmatrix} \frac{v_\Phi}{\sqrt{2}} & 0 \\ 0 & 0 \end{pmatrix}. \quad (6.8)$$

There are two ways to generate the phenomenologically required hierarchy $v' \gg v$ between the mirror and SM Higgs vevs: The first approach [658] is to include soft breaking of the discrete exchange symmetry in the scalar potential $\mu_1^2 |H|^2 + \mu_2^2 |H'|^2$ with $\mu_1^2 \ll \mu_2^2$. It was shown recently [659] that this soft breaking leads to two-loop contributions to the strong CP phase $\bar{\theta}$ (see section 6.8) in the original *universal Seesaw* model by [658] regenerating the $\bar{\theta}$ angle that was cancelled at tree-level. As of now there exists no similar analysis on the impact of soft breaking for the class of mirror sector models we are employing, so to be conservative we do not use this scheme. A second mechanism was presented by [648] that relies on tuning the quartic couplings of the scalar potential in section 6.6 and the details will be discussed in section 6.6.1: If the mixed quartic coupling λ' in the potential

$$V \supset \lambda' H^\dagger H H'^\dagger H' + \kappa (H \Phi^\dagger H' + H'^\dagger \Phi H^\dagger) \quad (6.9)$$

(see (6.18) and (6.20) for the full potential) is set to zero, the scalar potential develops an unbroken custodial $\text{SU}(4)$ symmetry and one can view the lighter SM-like Higgs as the Goldstone-boson of this accidental symmetry. This idea is similar to the situation in the *Twin-Higgs* model [651], where asymmetric vacua with $v \neq v'$ also require explicit breaking of an accidental custodial $\text{SU}(4)$ [660]. However in those models the equivalent of the exchange symmetry (6.3) is typically softly broken as well [660], whereas here the breaking is only spontaneous. The field H' has a mass $-\mu_H^2 < 0$ and obtains the vev $v' \simeq \mu_H / \sqrt{\lambda_H}$. After integrating out H' one finds that the potential for H reads

$$\lambda' v'^2 H^\dagger H + \lambda' \left(1 + \frac{2\lambda'}{\lambda_H}\right) (H^\dagger H)^2 \quad (6.10)$$

6 Type II Dirac Seesaw

and for spontaneous symmetry breaking one requires $\lambda' < 0$. Further $|\lambda'| \ll 1$ is needed for the phenomenologically required hierarchy $v \ll v'$. The second term in the above is the self-coupling of H modified by the finite threshold correction from integrating out H' [274]. In [648] a real v needs a small $\lambda' < 0$ at the high scale $\mu = v'$, which is why in this construction, v' is identified with the electroweak instability scale

$$v' \simeq (10^9 - 10^{12}) \text{ GeV}. \quad (6.11)$$

RGE effects dominated by the top quark Yukawa then drive the Higgs self-coupling λ_h to its positive $\mathcal{O}(0.1)$ value at low energies. Once we add a bidoublet in (6.9) and integrate it out we find that

$$\lambda'_{\text{eff}} \equiv \lambda' - \frac{\kappa^2}{\mu_\Phi^2}. \quad (6.12)$$

plays the role of λ' . The smallness and sign of this mixed quartic could be understood as the result of the threshold correction [274] from Φ , but since we actually have $\kappa^2/\mu_\Phi^2 \simeq m_\nu \kappa / (Y_\nu v v') \ll 1$ the correction to λ' is completely negligible. As it turns out, the tree level potential is not enough for the correct vacuum structure and to induce $v \neq 0$ we actually need to include quantum corrections [649, 661, 662] from the one-loop Coleman-Weinberg potential [663]. This contribution, again dominated by the top quark, generates quartic scalar terms with a coupling $c_1 < 0$ (see section 6.6.1 for details). This results in a Higgs mass and self coupling of [661]

$$m_h \simeq \sqrt{-\left(\lambda'_{\text{eff}} - \frac{c_1}{2}\right) v'}, \quad \lambda_h(\mu = v') = \frac{c_1}{16} \lesssim 0. \quad (6.13)$$

A shortcoming of this approach is that one needs the fine-tuning $\lambda'_{\text{eff}} \simeq c_1/2$ of order $\mathcal{O}(v^2/v'^2)$ for the hierarchy $v' \gg v$ [648] ($\lambda'_{\text{eff}} < 0$ for a real v). In section 6.6.2 we demonstrate that the v_Φ in the Type II Seesaw regime does not spoil the desired vacuum structure. As far as naturalness is concerned, the small vev v_Φ in (6.2) is technically natural [408] and one may argue along the lines of [648, 651], that the hierarchy between v and v' does not lead to a separate hierarchy problem besides the usual one. Of course here will be loop corrections from the heavy Φ , which could be cured by compositeness or supersymmetry at the bidoublet mass scale $\mu_\Phi > 10^{10}$ GeV. If we consider the vevs v_i to have phases β_i then gauge transformations with the transformation parameters $\omega, \omega', \omega_X$ shift the phases to be² [664]

$$\beta \rightarrow \beta + \frac{1}{2}(\omega - \omega_X), \quad \beta' \rightarrow \beta' + \frac{1}{2}(\omega' - \omega_X), \quad (6.14)$$

$$\beta_\Phi \rightarrow \beta_\Phi + \frac{1}{2}(\omega + \omega') - \omega_X. \quad (6.15)$$

If we set β, β' locally to zero this induces the shift $\beta_\Phi \rightarrow \beta_\Phi - \beta - \beta'$ for the phase of v_Φ . The minimization conditions of the scalar potential enforce that

$$0 = \frac{\partial V}{\partial \beta} = \frac{\partial V}{\partial \beta'} = -\frac{\partial V}{\partial \beta_\Phi} = \frac{\kappa v v' v_\Phi}{\sqrt{2}} \sin(\beta_\Phi - \beta - \beta'), \quad (6.16)$$

²Note the slight abuse of notation for the passive gauge transformations.

which implies that the physical phase for the vev v_Φ is zero. In other words, there is no spontaneous CP violation [665] in this model. The exchange symmetry (6.3) only enforces $Y_\nu = Y_\nu^\dagger$, so the PMNS Dirac phase would come from this matrix if the charged lepton Yukawa Y_l were purely real.

6.6 Appendix: Full Scalar Potential

The most general scalar potential satisfying the discrete exchange symmetry of [648, 649] defined in (6.3) reads:

$$V_\Phi = \mu_\Phi^2 \text{Tr} (\Phi^\dagger \Phi) + \lambda_\Phi \text{Tr} (\Phi^\dagger \Phi)^2 \quad (6.17)$$

$$V_H = -\mu_H^2 (H^\dagger H + H'^\dagger H') + \lambda_H (H^\dagger H + H'^\dagger H')^2 + \lambda' H^\dagger H H'^\dagger H' \quad (6.18)$$

$$V_{H\Phi} = \kappa (H\Phi^\dagger H' + H'^\dagger \Phi H^\dagger) + \lambda_{H\Phi} (H\Phi^\dagger \Phi H^\dagger + H'^\dagger \Phi \Phi^\dagger H') \quad (6.19)$$

$$+ \alpha_{H\Phi} (H^\dagger H + H'^\dagger H') \text{Tr} (\Phi^\dagger \Phi) \quad (6.20)$$

The scalar sector involving only H, H' in (6.18) has an approximate, global SU(4) custodial symmetry so that we can embed the doublets in its fundamental representation

$$\mathcal{H} \equiv \begin{pmatrix} H \\ H' \end{pmatrix}. \quad (6.21)$$

Using this parameterization it is evident, that the terms $\propto \lambda', \kappa$ in (6.18) and (6.20) explicitly violate the custodial SU(4) symmetry. We take $\mu_\Phi^2 \gg \mu_H^2 > 0$. All couplings are real as a consequence of the discrete exchange symmetry (6.3) and because Φ has an abelian charge under $U(1)_X$. If the bidoublet was uncharged, the potential would depend on both Φ and $\tilde{\Phi} \equiv -\sigma_2 \Phi^* \sigma_2$ leading to explicit CP-violation via terms like

$$\alpha_{H\Phi 2} (H^\dagger H \text{Tr} (\tilde{\Phi}^\dagger \Phi) + H'^\dagger H' \text{Tr} (\tilde{\Phi} \Phi^\dagger)) + \text{h.c.} \quad (6.22)$$

with a complex coupling $\alpha_{H\Phi 2}$. For the charged bidoublet case loop diagrams do not regenerate the explicit CP-violating scalar couplings unlike the case of the minimal LRSM [666].

6.6.1 Minimization of the scalar potential: Original Higgs-Parity model

Here we explore the minima of the scalar potential in the electrically neutral directions. For the other directions see the next section 6.6.3. We begin our discussion of the minimization of the scalar potential in (6.17)-(6.20) by introducing the notation

$$v_H \equiv \sqrt{v^2 + v'^2}, \quad \sin(\phi) \equiv \frac{v}{v_H}, \quad \cos(\phi) \equiv \frac{v'}{v_H}. \quad (6.23)$$

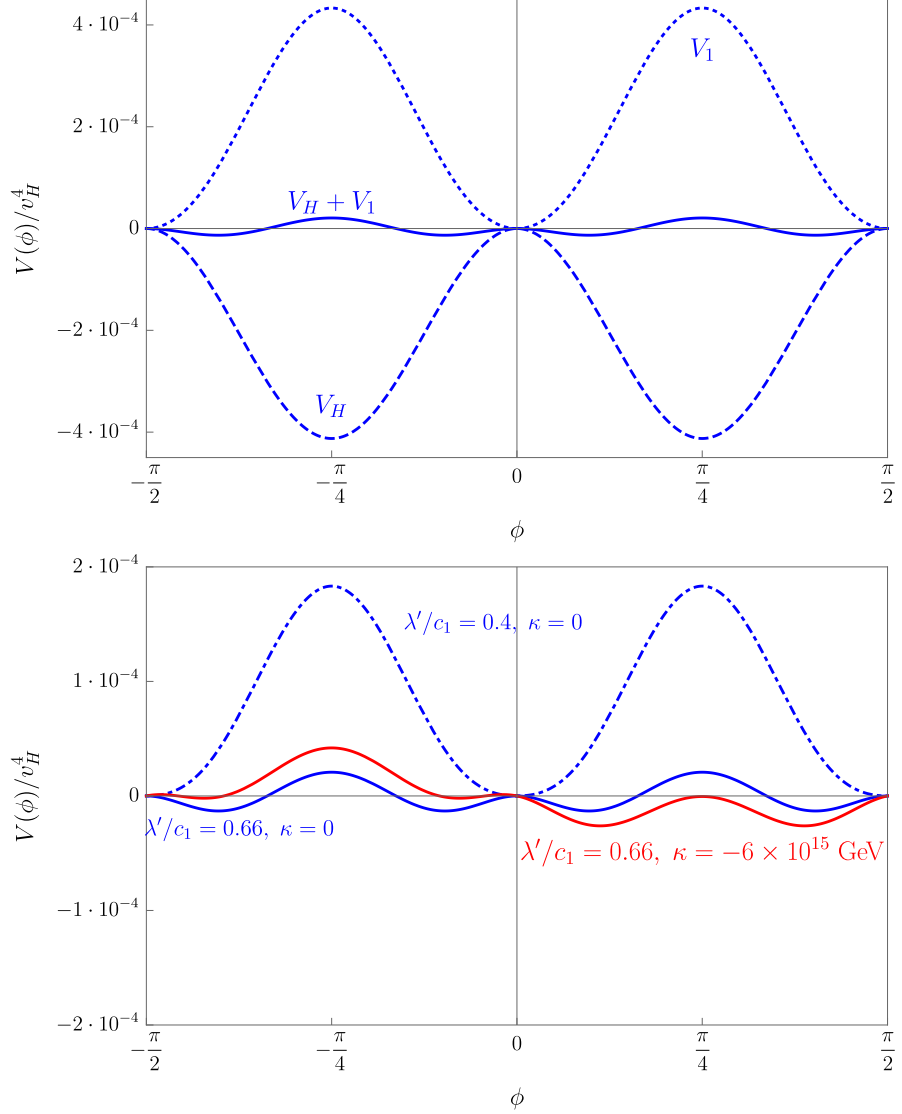


Figure 6.2: Plot of the contributions to the scalar potential without a bidoublet (*top*) and with a bidoublet (*bottom*). For the sake of visibility and illustration we chose $v_H = 10^{10}$ GeV, $v_\Phi = 1$ GeV, $c_1 = -10^{-2}$ and $\kappa = -6 \times 10^{15}$ GeV, which do not correspond to phenomenologically viable parameters. On the left hand side we fixed $\lambda'/c_1 = 0.66$ and we varied this combination of parameters on the right hand side. Note that we scaled the vertical axis differently in both plots. Realistic parameters would lead to minima at $|\phi| \simeq 10^{-7} - 10^{-10}$ and in practise the phenomenologically required small value of $|\kappa|$, e.g. $|\kappa| < 10$ GeV from (6.85) in the main text, only has a negligible impact on the value of ϕ .

The phenomenologically required vacuum structure is $v' \neq 0 \gg v \neq 0$. This together with $v \neq v'$ implies that $\phi \in (0, \frac{\pi}{4})$. For the observed value of $v = 246$ GeV and the

6.6 Appendix: Full Scalar Potential

required $v' \simeq (10^9 - 10^{12})$ GeV (see (6.11)) we have $0 < \phi \simeq 10^{-7} - 10^{-10} \ll 1$ and $v_H \simeq v'$.

First we will summarize the results of [648, 649] for the scalar potential involving only H and H' , before discussing the impact of the bidoublet. The vacuum potential reads

$$V_H = \frac{v_H^2}{32} (-16\mu_H^2 + v_H^2 (8\lambda_H + \lambda'(1 - \cos(4\phi)))) \quad (6.24)$$

and the minimization conditions are found to be

$$\frac{\partial V_H}{\partial v_H} = \frac{v_H}{8} (-8\mu_H^2 + v_H^2 (8\lambda_H + \lambda'(1 - \cos(4\phi)))) , \quad (6.25)$$

$$\frac{\partial V_H}{\partial \phi} = \frac{v_H^4}{8} \lambda' \sin(4\phi) . \quad (6.26)$$

The second condition has the solutions $\phi = (0, \pi/2, \pi/4)$ corresponding to $(v = 0, v' = 0, v = v')$, where in the first (second) case we have $v' \neq 0$ ($v \neq 0$). This essentially happens, because the potential for ϕ has periodicity of $\pi/2$ and a reflection symmetry [661] owing to the Higgs-parity defined in (6.3). While the custodial-symmetry-breaking and Higgs Parity conserving interaction $\lambda' H^\dagger H H'^\dagger H'$ allows us to find an asymmetric vacuum with $v = 0$ and $v' \neq 0$, it does not suffice in order to also break the electroweak gauge symmetry. To realize $v \neq 0$ we need a separate source of custodial symmetry violation, that slightly tilts the potential even further. Yukawa and gauge interactions break the custodial symmetry explicitly and these effects are communicated to the scalar potential via quantum corrections encoded in the one-loop Coleman-Weinberg potential [663]

$$V_1 = c_1 \left(\left(H^\dagger H \right)^2 \log \left(\frac{|H|}{\mu} \right) + \left(H'^\dagger H' \right)^2 \log \left(\frac{|H'|}{\mu} \right) \right) , \quad (6.27)$$

$$c_1 \equiv -\frac{3}{8\pi^2} Y_t^4 + \frac{3}{128\pi^2} (g^2 + g'^2)^2 + \frac{3}{64\pi} g^4 . \quad (6.28)$$

The negative contribution from the top quark Yukawa is the dominant one, which is why $c_1 < 0$. If we plug in the values of the Yukawa and gauge couplings around the weak scale as an estimate we find $|c_1| < 10^{-2}$. In terms of the parameterization (6.23) this potential reads for a renormalization scale of $\mu = v_H$ [661]

$$V_1 = c_1 v_H^4 (\cos(\phi)^4 \log(\cos(\phi)) + \sin(\phi)^4 \log(\sin(\phi))) \quad (6.29)$$

$$= \frac{c_1 v_H^4}{4} \left(\frac{25 - 24 \log(2)}{96} \cos(4\phi) - \frac{1}{240} \cos(8\phi) - \frac{1}{2240} \cos(12\phi) \right) \quad (6.30)$$

$$- \frac{c_1 v_H^4}{4} \left(\frac{1}{10080} \cos(16\phi) + \mathcal{O}(\cos(20\phi)) \right) . \quad (6.31)$$

Following [661] we only include the terms up to 8ϕ as we find the rest to be negligible due to numerically small coefficients. A partial cancellation between the $\cos(4\phi)$ terms in (6.24) and (6.31) will allow us to find a viable solution $0 < \phi \ll \frac{\pi}{4}$. This is also why

6 Type II Dirac Seesaw

we only display the leading order coefficients of a Fourier expansion in $\cos(n 4\phi)$ with $n \in \mathbb{N}$. The new minimization conditions are found to be

$$\frac{\partial V}{\partial v_H} = \frac{1}{480} (60v_H (-8\mu_H^2 + v_H^2 (8\lambda_H + \lambda'))) \quad (6.32)$$

$$- \frac{1}{480} (v_H^3 (5 \cos(4\phi) (12\lambda' + c_1(24 \log(2) - 25)) - 2c_1 \cos(8\phi))), \quad (6.33)$$

$$\frac{\partial V}{\partial \phi} = \frac{v_H^4}{480} (60\lambda' + 8c_1 \cos(4\phi) + 5c_1(24 \log(2) - 25)) \sin(4\phi). \quad (6.34)$$

When solving for ϕ one has two solutions: Either $\sin(4\phi) = 0$, which implies the solutions $\phi = (0, \pi/2, \pi/4)$ for the unwanted set of either partially unbroken or symmetric vacua. Else, the second factor in (6.34) has to be zero itself for a solution with non-zero $\phi \ll 1$. We can solve this equation to find the required λ' for a minimum, that can accommodate the input parameter ϕ

$$\lambda' = \frac{c_1}{60} (125 - 60 \log(4) - 8 \cos(4\phi)) \stackrel{\phi \ll 1}{\simeq} 0.56 c_1, \quad (6.35)$$

and substitute this into the first minimization condition to obtain

$$v_H = \frac{\mu_H}{\sqrt{\lambda_H + \frac{c_1}{16} \left(\frac{645}{10} - 4 \log(2) - \frac{4}{15} \cos(4\phi) + \frac{1}{15} \cos(8\phi) \right)}} \quad (6.36)$$

$$\stackrel{\phi \ll 1}{\simeq} \frac{4\sqrt{10}\mu_H}{\sqrt{160\lambda_H + c_1(41 - 40 \log(2))}} \stackrel{|c_1| \ll 1}{\simeq} \frac{\mu_H}{\sqrt{\lambda_H}}. \quad (6.37)$$

The Higgs mass and self coupling at the scale $\mu = v_H$ are found to be [661]

$$m_h^2 \simeq - \left(\lambda' - \frac{c_1}{2} \right) v_H^2, \quad \text{and} \quad \lambda_h(\mu = v_H) = \frac{c_1}{16} \lesssim 0. \quad (6.38)$$

The lightness of m_h with respect to the high scale $v_H \simeq v'$ is related to the tuning $\lambda' \simeq c_1/2 \lesssim 0$ [649] in (6.35), which manifests the previously mentioned partial cancellation. If λ'/c_1 stays between 0.5 and 0.81, the unwanted values with $\phi = (0, \pi/4)$ are actually maxima of the scalar potential, as can be seen from its second derivative [661]. The sign of ϕ is in general undefined and the solution to (6.34) reads

$$\phi = \pm \frac{1}{4} \arccos \left(\frac{5}{8} \left(25 - 24 \log(2) - 12 \frac{\lambda'}{c_1} \right) \right), \quad (6.39)$$

which is a consequence of the reflection symmetry of the potential. Since a physically sound vev must satisfy $v > 0$, we have to impose $\phi > 0$. We illustrate the previously discussed partial cancellation between the tree level potential V_H and the Coleman-Weinberg terms V_1 on the left side of figure 6.2. One can see that there are two symmetric non-zero minima with $|\phi| < \pi/4$. On the right hand side of the aforementioned figure we plotted the potential for different choices of λ'/c_1 and one can clearly observe that the non-zero values of $|\phi| < \pi/4$ require $\lambda'/c_1 \gtrsim 1/2$. For the plots we used unrealistic parameters for the sake of being able to see the minima of ϕ between 0 and $\pm\pi/4$. Realistic parameters would lead to minima at $|\phi| \simeq 10^{-7} - 10^{-10}$.

6.6.2 Minimization of the scalar potential: Inclusion of the bidoublet

Next we introduce the couplings to the bidoublet

$$V_\Phi = \frac{v_\Phi^2}{2} \left(\mu_\Phi^2 + \frac{\lambda_\Phi}{2} v_\Phi^2 \right), \quad V_{H\Phi} = v_\Phi v_H^2 \left(\frac{v_\Phi}{4} (\alpha_{H\Phi} + \lambda_{H\Phi}) + \frac{\kappa}{2\sqrt{2}} \sin(2\phi) \right), \quad (6.40)$$

where we see that only the trilinear term $\propto \kappa$ depends on ϕ and thus violates the custodial symmetry. Furthermore, since this term is $\propto \sin(2\phi)$ the scalar potential for ϕ no longer has the periodicity $\pi/2$. The modified minimization conditions read

$$\begin{aligned} \frac{\partial V}{\partial v_H} &= \frac{1}{480} (60v_H (-8\mu_H^2 + v_H^2 (8\lambda_H + \lambda'))) \\ &\quad - \frac{1}{480} (v_H^3 (5 \cos(4\phi) (12\lambda' + c_1(24 \log(2) - 25)) + 2c_1 \cos(8\phi))) \\ &\quad + \frac{v_\Phi v_H}{2} (v_\Phi (\alpha_{H\Phi} + \lambda_{H\Phi}) + \sqrt{2}\kappa \sin(2\phi)), \end{aligned} \quad (6.41)$$

$$\frac{\partial V}{\partial v_\Phi} = v_\Phi (\mu_\Phi^2 + \lambda_\Phi v_\Phi^2 + (\alpha_{H\Phi} + \lambda_{H\Phi}) v_H^2) + \frac{v_H^2}{2\sqrt{2}} \kappa \sin(2\phi), \quad (6.42)$$

$$\begin{aligned} \frac{\partial V}{\partial \phi} &= \frac{v_H^4}{480} (60\lambda' + 8c_1 \cos(4\phi) + 5c_1(24 \log(2) - 25)) \sin(4\phi) \\ &\quad + \frac{v_H^4}{480} \left(120\sqrt{2} \frac{v_\Phi \kappa}{v_H^2} \frac{1}{\sin(2\phi)} \right) \sin(4\phi). \end{aligned} \quad (6.43)$$

The required λ' for values of $\phi \neq (0, \pi/2, \pi/4)$ that minimize the potential in the ϕ -direction is found to be

$$\lambda' = \frac{c_1}{60} (125 - 60 \log(4) - 8 \cos(4\phi)) - 2\sqrt{2} \frac{v_\Phi \kappa}{v_H^2} \frac{1}{\sin(2\phi)} \quad (6.44)$$

$$\stackrel{\phi \ll 1}{\simeq} 0.56 c_1 - \frac{\sqrt{2}}{\phi} \frac{v_\Phi \kappa}{v_H^2}. \quad (6.45)$$

Note that the trilinear term $v_\Phi \kappa v_H^2 \sin(2\phi)$ in (6.40) breaks the reflection symmetry and biases the vacuum in the direction $\phi > 0$ ($\phi < 0$) for $\kappa < 0$ ($\kappa > 0$) (analogous to the sign of v_Φ for a Type II Seesaw). However in practise this contribution is suppressed as $v_\Phi \kappa / v_H^2$ compared to $V_H + V_1$, so that we would need to take large (and phenomenologically excluded) values of κ to select a sign for ϕ . This was illustrated on the right side of figure 6.2 and one sees the deeper minimum $\phi > 0$ for the unrealistically large $\kappa = -6 \times 10^{15} \text{ GeV} \neq 0$ in red. The next paragraphs explain, why we can not make $|\kappa|$ arbitrarily large and phenomenologically we need a small value of $|\kappa| < 10 \text{ GeV}$ (see (6.85) in the main text) anyway. We find that v_H is determined to be

$$v_H = 4 \frac{\sqrt{30\mu_H^2 - 15v_\Phi (v_\Phi (\alpha_{H\Phi} + \lambda_{H\Phi}) + \sqrt{2}\kappa \sin(2\phi))}}{\sqrt{60(8\lambda_H + \lambda') - 2c_1 \cos(8\phi) - 5 \cos(4\phi) (12\lambda' + c_1(24 \log(2) - 25))}}. \quad (6.46)$$

6 Type II Dirac Seesaw

If the first term $30\mu_H^2$ dominates over the contribution $\propto v_\Phi^2, v_\Phi \kappa$, the previously determined minimum in (6.36) is still valid. Once the contribution $\propto v_\Phi^2, v_\Phi \kappa$ takes over, a deeper minimum starts to appear and the vev v_H is actually induced by v_Φ (instead of the other way around for a Type II Seesaw). To study the implications of v_Φ on ϕ, v_H requires finding, which value of v_Φ solves (6.42). If we were to switch off all bidoublet couplings to the other scalars and set $\mu_\Phi^2 < 0$, we expect $v_\Phi = |\mu_\Phi|/\sqrt{\lambda_\Phi}$ as usual. Generally speaking this relation will be modified by the vevs of the other Higgses as well, because the the trilinear coupling κ and the full solution to (6.42) can only be found numerically. In the following we either fix v_Φ via the Type II Seesaw scheme used in the main text, or use it as a free parameter in order to find the conditions for unwanted symmetric or deeper minima.

Induced bidoublet vev a la Type II Seesaw

Here we take the vev v_Φ to be induced by v_H . This means, we assume $\mu_\Phi^2 > 0$ and furthermore, that $\mu_\Phi^2 \gg \lambda_\Phi v_\Phi^2 + (\alpha_{H\Phi} + \lambda_{H\Phi}) v_H^2$, so that (6.42) is approximately solved by

$$v_\Phi \simeq -\frac{\kappa v_H^2}{2\sqrt{2}\mu_\Phi^2} \sin(2\phi) = -\frac{\kappa v v'}{\sqrt{2}\mu_\Phi^2}. \quad (6.47)$$

In the limit $|\kappa| \ll v_H \ll \mu_\Phi$ this vev will essentially be the smallest scale in the potential. The value of λ' required for a given ϕ in (6.44) then reads

$$\lambda'_{\text{eff.}} \equiv \lambda' - \frac{\kappa^2}{\mu_\Phi^2} = \frac{c_1}{60} (125 - 60 \log(4) - 8 \cos(4\phi)) \stackrel{\phi \ll 1}{\simeq} 0.56 c_1. \quad (6.48)$$

We see, that integrating out the super-heavy bidoublet just shifts the coupling λ' via a threshold correction, as was mentioned above of (6.12) in the main text. Since we expect $|\kappa| \ll \mu_\Phi$ by many orders of magnitude (see (6.7) and the discussion below), it is safe to take $\lambda'_{\text{eff.}} \simeq \lambda'$ and the previously determined minimum for ϕ in (6.35) is still valid. In order to avoid deeper minima than v_H in (6.36) we have to require that the numerator in (6.46) satisfies

$$2\mu_H^2 \gg v_\Phi \left(v_\Phi (\alpha_{H\Phi} + \lambda_{H\Phi}) + \sqrt{2}\kappa \sin(2\phi) \right) \simeq \frac{\kappa^2 v_H^2}{2\mu_\Phi^2} \sin(2\phi)^2, \quad (6.49)$$

where we used $\mu_\Phi^2 \gg (\alpha_{H\Phi} + \lambda_{H\Phi}) v_H^2$ in the last step. Expanding for small ϕ and setting $v_H \simeq \mu_H/\sqrt{\lambda_H}$ turns this into

$$\lambda_H \gg \phi^2 \frac{\kappa^2}{\mu_\Phi^2}. \quad (6.50)$$

Since we assume $\lambda_H = \mathcal{O}(1)$ and again stress that $\phi, |\kappa|/\mu_\Phi \ll 1$, we do not need to worry about deeper minima for v_H with the super-light v_Φ we consider in (6.47).

General bidoublet vev

As discussed earlier, it is in general not possible, to obtain a full analytic expression for v_Φ . This is why, we take it as a free parameter and in the following make no assumption about its relative size compared to v_H , μ_Φ and κ . Inspecting (6.44) reveals, that the $1/\sin(2\phi)$ factor can become large for the required small $\phi \ll 1$ and if it is not cancelled by $v_\Phi\kappa/v_H^2$, it might happen, that this term becomes larger than the perturbative limit for λ' of 4π . We therefore require that

$$\left| 0.56 c_1 - \frac{\sqrt{2}}{\phi} \frac{v_\Phi \kappa}{v_H^2} \right| < 4\pi, \quad (6.51)$$

where the absolute value takes into account the in general undetermined sign of κ and the fact that $c_1 < 0$. Assuming the bidoublet contribution is larger than the Coleman-Weinberg piece $\propto c_1$, one finds that this condition implies

$$v_\Phi |\kappa| < 2\sqrt{2}\pi v v'. \quad (6.52)$$

In other words, if we make $v_\Phi |\kappa|$ larger than the input parameters $v v'$, then the corrections from the bidoublet vev will spoil the partial cancellation between the λ' and the Coleman-Weinberg terms $\propto c_1$ responsible for the correct asymmetric vacuum $v \neq 0 \ll v'$. The $\sin(2\phi)$ term coming from the coupling to the bidoublet in (6.40) is responsible for this effect, since the aforementioned partial cancellation involves the $\cos(4\phi)$ terms. This is in agreement with the findings of [648], who arrived at the conclusion, that the vev of an additional bidoublet can not contribute significantly to electroweak symmetry breaking. Consequently we are forced to have a small $v_\Phi |\kappa|$. Avoiding a deeper minimum from (6.46) than the v_H in (6.36) requires

$$\mu_H^2 \gg \frac{1}{\sqrt{2}} v_\Phi \kappa \sin(2\phi), \quad (6.53)$$

where we assumed that $\alpha_{H\Phi} + \lambda_{H\Phi}$ is negligible so that we can focus on κ . This bound can be re-expressed as

$$v_\Phi |\kappa| \ll \frac{\lambda_H}{\sqrt{2}} \frac{v'^3}{v}. \quad (6.54)$$

We find that this constraint is weaker than (6.52) for $v \ll v'$, meaning that taking $v_\Phi |\kappa|$ to be large will first destroy the misalignment of vacua (leading to $v = v'$ or $v = 0$) before it leads to deeper minima in v' . The smallness of the induced v_Φ in the Type II Seesaw of (6.47) automatically avoids these problems in the limit $|\kappa| \ll \mu_\Phi$.

6.6.3 Sufficient conditions for vacuum stability

For vacuum stability at large field values only the quartic terms are important. Following reference [667] we define

$$r^2 \equiv H^\dagger H + H'^\dagger H' + \text{Tr}(\Phi^\dagger \Phi), \quad (6.55)$$

$$r^2 \cos(\gamma) \equiv H^\dagger H + H'^\dagger H', \quad r^2 \sin(\gamma) \equiv \text{Tr}(\Phi^\dagger \Phi), \quad (6.56)$$

$$x \equiv \frac{H^\dagger H H'^\dagger H'}{(H^\dagger H + H'^\dagger H')^2}, \quad y \equiv \frac{H\Phi^\dagger \Phi H^\dagger + H'\Phi\Phi^\dagger H'}{(H^\dagger H + H'^\dagger H') \text{Tr}(\Phi^\dagger \Phi)}. \quad (6.57)$$

One can show that

$$0 \leq x \leq \frac{1}{2}, \quad 0 \leq y \leq 1. \quad (6.58)$$

Using this parameterization we employ the co-positivity criteria of [668] to find

$$\lambda_\Phi > 0, \quad \lambda_H + x\lambda' > 0, \quad \alpha_{H\Phi} + y\lambda_{H\Phi} + 2\sqrt{\lambda_\Phi(\lambda_H + x\lambda')} > 0. \quad (6.59)$$

Note that x, y may not be independent parameters [669], however we will ignore this complication for our first estimate. This is the reason why we only find the sufficient but not the necessary criteria for vacuum stability. A more refined analysis along the lines of [669–671] is required to treat the general case. Our preliminary investigation did not find deeper electric charge-breaking minima compared to the charge-conserving ones in (6.8), which can occur for models with trilinear scalar couplings [672], and we do not expect them due to the smallness of the trilinear coupling κ (see the previous paragraph and the discussion below (6.7)). A full numerical analysis is beyond the scope of this work.

6.7 Appendix: Scalar and Gauge Bosons

The scalar spectrum consists of three CP even neutral scalars $h, h', h_\Phi = \sqrt{2} \text{Re}(\varphi_1^0)$ and one CP odd scalar $a_\Phi = \sqrt{2} \text{Im}(\varphi_1^0)$ with the masses

$$m_h \simeq \sqrt{2\lambda_h} v, \quad m_{h'} \simeq \sqrt{2\lambda_H} v', \quad (6.60)$$

$$m_{h_\Phi} \simeq m_{a_\Phi} \simeq \mu_\Phi, \quad (6.61)$$

where we used the low energy value $\lambda_h \simeq 0.129$ for the self-coupling of the SM like Higgs. h, h' mix primarily with each other via their quartic interaction and the small mixing angle is approximately $1/2(1 + \lambda'_{\text{eff}}/\lambda_H)v/v'$. The dominant source of mixing between h (h') and h_Φ comes from the trilinear term and is $\simeq \kappa v'(v)/\mu_\Phi^2$. The same expression holds for the mixing between the “would-be-Nambu-Goldstone-bosons”(NGB)of the Z (Z') gauge bosons (see the end of this section) with a_Φ . Additionally there are

two singly-charged scalars $\varphi_1^\pm, \varphi_2^\pm$ and one doubly-charged scalar $\varphi_2^{\pm\pm}$ present. Their approximately degenerate masses read

$$m_{\varphi_1^\pm} \simeq m_{\varphi_2^\pm} \simeq m_{\varphi_2^{\pm\pm}} \simeq \mu_\Phi. \quad (6.62)$$

There is also mixing between φ_1^\pm (φ_2^\pm) and the “would-be-NGB” of the charged gauge bosons W^\pm (W'^\pm) of the order of $\simeq \kappa v'(v)/\mu_\Phi^2$. When it comes to the charged gauge bosons we obtain

$$m_W = \frac{g}{2} \sqrt{v^2 + v_\Phi^2}, \quad m_{W'} = \frac{g}{2} \sqrt{v'^2 + v_\Phi^2}. \quad (6.63)$$

There is no mass mixing between the charged gauge bosons at tree-level since Φ only has one vev [673]. Mixing could arise from loop diagrams involving the tree-level mixing between the electrically charged SM and mirror leptons in (6.6), which we have set to zero via another discrete symmetry. In the neutral gauge boson sector we find in addition to the massless photon that

$$m_Z \simeq \frac{g \sqrt{v^2 + v_\Phi^2}}{2 \cos(\theta_W)}, \quad m_{Z'} \simeq \frac{g \cos(\theta_W)^2}{2 \cos(2\theta_W)} v', \quad (6.64)$$

where we employed the weak mixing angle defined in (6.65). It is evident that the bidoublet vev contributes with the same strength to m_W and m_Z , which means that the SM prediction for the electroweak ρ -parameter [637, 674] defined as $\rho \equiv m_W^2/(m_Z^2 \cos(\theta_W)^2)$ is unchanged. To understand why, note that after the SSB of $SU(2)' \otimes U(1)_X$ down to $U(1)_Y$, the multiplet Φ decomposes into two $SU(2)_L$ doublets $\Phi_1 \equiv (\varphi_1^0, \varphi_1^-)^t$ with $Y = -1/2$ and $\Phi_2 \equiv (\varphi_2^-, \varphi_2^{--})^t$ with $Y = -3/2$. Since only the neutral component of Φ_1 develops a vev the contribution of Φ to the SM gauge boson masses reduces to the one in a Two-Higgs-doublet model. This is why at tree-level our model does not modify the ρ -parameter and it can not help to address the tentative tension in the W^\pm boson mass reported by the CDF collaboration [675]. Moreover, unlike for the electroweak triplet needed for the conventional Type II Seesaw, here the ρ -parameter does not force the small vev to be below the GeV-scale [636]. In principle, there could also be one-loop gauge boson self-energy diagrams with e.g. h_Φ and φ_1^\pm running in the loop [676]. The shift in the relevant electroweak precision observables [677, 678] will roughly depend on their mass splitting via $(m_{h_\Phi}^2 - m_{\varphi_1^\pm}^2)/\mu_\Phi^2$. However, since we assume all mass splittings to be small compared to the largest scale in the scalar potential μ_Φ^2 and since the contribution will essentially decouple for large bidoublet masses, our model can not help ameliorate the CDF tension [675]. When it comes to the mixing between the neutral gauge bosons the situation simplifies in the limit $v_\Phi \rightarrow 0$: There are only two mixing angles required. The electroweak mixing angle is defined via³ [658]

$$\frac{g_X}{g} = \frac{\sin(\theta_W)}{\sqrt{\cos(2\theta_W)}} \quad (6.65)$$

³The discrete exchange symmetry requires the $SU(2)' \otimes SU_L(2)$ couplings g', g to be equal at high scales and we neglect the differences in their RGE running here.

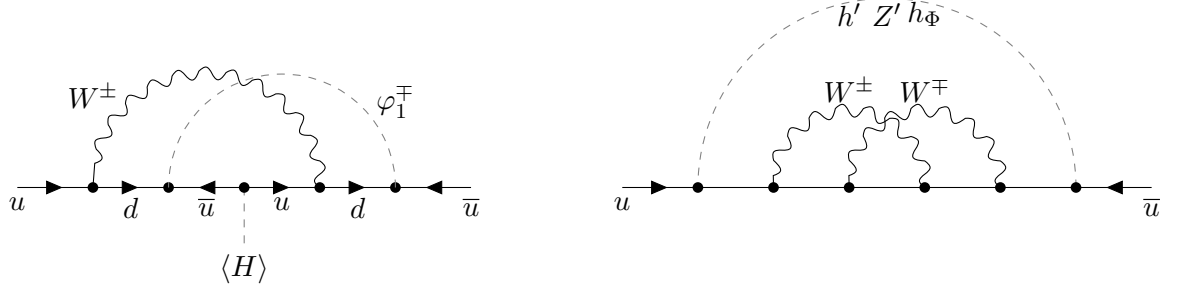


Figure 6.3: Two- (left) and three-loop (right) Feynman diagrams leading to phases in the quark mass matrices contributing to $\bar{\theta} = \theta_{\text{chir.}}$ in this model. h', Z', h_Φ and φ_1^\pm only couple to the SM quarks via suppressed mixing. For the three-loop diagrams we did not indicate the internal chirality structure and the labels of the internal quark fields, because for h, h_Φ there is a mass insertion $\propto \langle H \rangle$ after the first vertex and in the Z' case there is the same kind of insertion before the sixth vertex.

and the angle between the physical Z, Z' [658] reads

$$\sin(\gamma) = \frac{\sin(\theta_W)^2 \sqrt{\cos(2\theta_W)}}{\cos(\theta_W)^4} \left(\frac{v}{v'} \right)^2. \quad (6.66)$$

Turning on v_Φ only leads to a sub-dominant modifications of the angle γ as long as $v_\Phi \ll v$.

6.8 Appendix: Strong CP problem

The physical CP violating parameter $\bar{\theta} = \theta_{\text{QCD}} + \theta_{\text{chir.}}$ is conventionally split into the contribution of the QCD theta-term and the part $\theta_{\text{chir.}} = \arg(\det(M_u M_d))$ arising from the up- and down-type quark mass matrices M_u, M_d . Following from the fact that the topological vacuum selection parameter θ_{QCD} arises because of non-perturbative QCD dynamics and due to its origin as the coefficient of a non-vanishing surface term [679], one might argue that θ_{QCD} is unlike all other dimensionless parameters of the SM such as gauge or Yukawa couplings and more akin to a boundary condition. In the SM, the electroweak part $\theta_{\text{chir.}}$ only receives finite loop corrections at three-loop order and diverges at seven loops [680], which is fundamentally different from e.g. the hierarchy problem of the Higgs mass. In recent years, a new perspective on the strong CP problem has emerged [681, 682] that relies on a careful analysis of the boundary condition for the path integral and the infinite spacetime volume limit, suggesting that the strong CP violation disappears for the mathematically correct order of limits. In the present work we take the smallness of $\bar{\theta}$ at face value and follow the UV symmetry based BSM approach [633, 653, 654, 658, 683, 684] to “explain” its tiny value. For recent work that

directly ties the smallness of $\bar{\theta}$ to a different Dirac neutrino mass generation mechanism see [685].

6.8.1 Tree level

Owing to the fact that the discrete exchange symmetry defined in (6.3) imposes $\theta_{\text{QCD}} = 0$ we only need to care about the quark contribution. Following reference [648] there could exist a dimension six operator allowed by the discrete exchange symmetry in (6.3)

$$\frac{c_6}{\Lambda_{\text{UV}}^2} \left(H^\dagger H - H'^\dagger H' \right) G_{\mu\nu} \tilde{G}^{\mu\nu} \quad (6.67)$$

that regenerates θ_{QCD} after the H' obtains a vev. This leads to the requirement of $v' < 10^{13}$ GeV for a cut-off scale of $\Lambda_{\text{UV}} = M_{\text{Pl}}$ and order one Wilson coefficient c_6 , to stay within the observational bound of $\bar{\theta} < 10^{-10}$ [686–689]. For the given particle content this operator is not realized at the loop level. The mass matrix for either up-type or down-type quarks in the basis (q', \bar{q}) and $(q, \bar{q}')^t$ with $q = u, d$, where we have suppressed generation indices, reads

$$M_q = \begin{pmatrix} 0 & Y'_q \frac{v'}{\sqrt{2}} \\ Y_q \frac{v}{\sqrt{2}} & 0 \end{pmatrix}. \quad (6.68)$$

Because the exchange symmetry (6.3) sets $Y'_q = Y_q^*$ [648]

$$\arg(\det(M_q)) = -\frac{vv'}{2} \arg(\det(Y_q) \det(Y'_q)) \quad (6.69)$$

vanishes, meaning that the SM and mirror sector phases cancel each other out [633]. Since neither Y_q nor Y'_q are required to be real, they source the CKM phase for the SM and mirror sector and one does not need a separate sector to do so unlike in the case for Nelson-Barr models [653, 654]. The presence of the bidoublet field does not change this picture as it does not couple to quarks. Reference [690] demonstrated that integrating out the heavy mirror quarks does not generate phases for the SM quark Yukawas via RGE effects.

6.8.2 Loop level

So far we have only worked at tree-level. Radiative corrections to the quark masses at one-loop level all turn out to be real valued. Two-loop diagrams with two W^\pm running in the loops have the correct complex couplings from the CKM matrix but the wrong chirality structure [680]. That leaves us with two options: Either we replace one of the W^\pm with the charged scalar φ_1^\pm , that couples to quarks via its mixing with the “would-be-NGB” of the W^\pm , and add a mass insertion for the right-chirality structure (see the left diagram in figure 6.3)

$$\theta^{(2)} \simeq \frac{\alpha}{\pi} \left(\frac{\kappa v'}{\mu_\Phi^2} \right)^2 \frac{m_q^2}{m_W^2} \frac{m_q^2}{\mu_\Phi^2}, \quad (6.70)$$

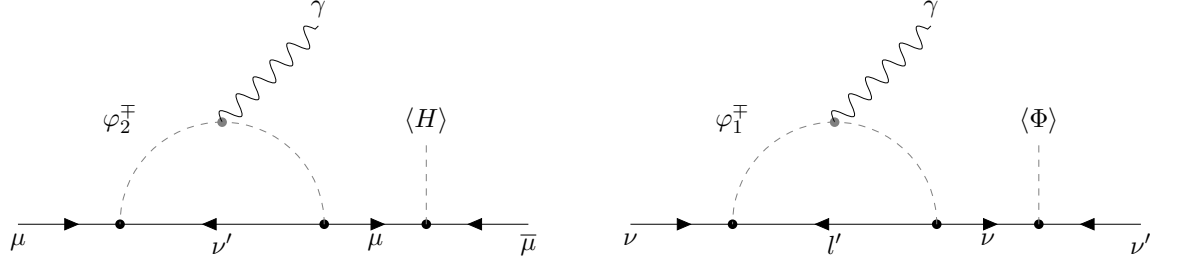


Figure 6.4: One-loop Feynman diagrams contributing to the magnetic moments of the muon (*left*) and neutrinos (*right*). The photon line in the second diagram can be attached to the electrically charged mirror lepton inside the loop as well. For this diagram the mass insertion can also appear on the incoming line, so that we get a second set of diagrams with l, φ_2^\mp running in the loop.

or we add a third loop with a neutral boson [680] depicted on the right in figure 6.3

$$\theta^{(3)} \simeq \left(\frac{\alpha}{\pi}\right)^3 \left(\frac{m_q^2}{m_W^2}\right)^3 \begin{cases} \left(\frac{v}{v'}\right)^2 \frac{m_q^2}{m_{h'}^2} & (h'), \\ \left(\frac{v}{v'}\right)^4 \frac{m_q^2}{m_W^2} \frac{m_q^2}{m_{Z'}^2} & (Z'), \\ \left(\frac{\kappa v'}{\mu_\Phi^2}\right)^2 \frac{m_q^2}{\mu_\Phi^2} & (h_\Phi). \end{cases} \quad (6.71)$$

In the above estimates we have dropped order one and loop factors. m_q^2 must be a combination of two different quark masses due to CKM unitarity and α denotes the fine-structure constant. All of the above contributions are negligibly small due to large BSM mediator masses and small mixing angles. For instance the factor $\kappa v'/\mu_\Phi^2 \simeq m_\nu/(Y_\nu v) \simeq 10^{-12}$ for $Y_\nu = \mathcal{O}(1)$ appearing for the bidoublet scalars is already sufficient to suppress the loop diagrams below the current experimental bounds of $\bar{\theta} < 10^{-10}$ [686–689] and the small ratio v/v' achieves the same. Leptonic loops involving the Y_ν coupling occur at even higher orders and are even more negligible. Consequently we find that the leading contribution arises from purely SM effects at three loops (two virtual W^\pm and one virtual gluon) and reads $\bar{\theta} \simeq \mathcal{O}(10^{-16})$ [680] which corresponds to an electric dipole moment of the neutron of about $\mathcal{O}(10^{-31})$ e cm [680]. Unfortunately this is still out of reach for current and future experiments, that are expected to probe dipole moments down to $\mathcal{O}(10^{-27})$ e cm [691–693].

6.9 Appendix: Low-energy phenomenology

Tree-level exchange of φ_2^- leads to a BSM contribution to muon decay of [224]

$$\Gamma(\mu^- \rightarrow \sum_{i,j} e^- \nu_i'^\dagger \nu_j') \simeq \frac{1}{6144\pi^3} \frac{m_\mu^5}{\mu_\Phi^4} \sum_{i,j} \left| (Y_\nu)_{\mu i} (Y_\nu)^*_{e j} \right|^2, \quad (6.72)$$

which modifies the Michel-parameters (ρ, δ, ξ) [694, 695] encoding the angular and energy distribution of the decay relative to the SM. Using the methods of [696] we find that $\rho = \xi\delta = 3/4\delta = 3/16|g_S|^2$ when compared to the SM where the number on the right hand side is one. In this context we have defined

$$g_S \equiv \frac{v^2}{2\mu_\Phi^2} \sum_{i,j} (Y_\nu)_{\mu i} (Y_\nu)_{\mu j}^*, \quad (6.73)$$

which is currently constrained to be smaller than 0.55 [697, 698] not imposing any stringent limits on our scenario with super-heavy scalars. Note that the previous bound was derived using left-chiral neutrinos scattering off charged leptons [698–702], whereas our decay involves the ν' of opposite chirality, so we expect that the limit on g_S in our model would be even weaker due to additional neutrino mass insertions.

6.9.1 Dipole moments and lepton flavor violation

Loops involving φ_2^\pm generate a correction to the magnetic dipole moment of the muon depicted in the left diagram of figure 6.4 of

$$\Delta a_\mu \simeq \frac{e}{96\pi} \left(\frac{m_\mu}{\mu_\Phi} \right)^2 \sum_{j=e,\mu,\tau} (Y_\nu)_{\mu j} (Y_\nu)_{\mu j}^*. \quad (6.74)$$

Here, there is no chiral enhancement inside the loop and the correct chirality structure is obtained from a mass insertion on the external legs (see figure 6.4), hence the dependence on m_μ . For masses of $\mu_\Phi \simeq 10^{10}$ GeV (see (6.7)), the shift in the magnetic moment is of $\mathcal{O}(10^{-36})$, which is far too small to explain the deviation of $\Delta a_\mu = (251 \pm 59) \times 10^{-11}$ observed by the BNL [703] and FNL [704] collaborations. We can reuse this result to estimate the full transition dipole form factor and find the partial width [705]

$$\frac{\text{BR}(\mu \rightarrow e\gamma)}{8 \times 10^{-8}} \simeq \alpha \left(\frac{v}{\mu_\Phi} \right)^4 \left| \sum_{j=e,\mu,\tau} (Y_\nu)_{\mu j} (Y_\nu)_{ej}^* \right|^2. \quad (6.75)$$

Compared to the present experimental limit of $\text{BR}(\mu \rightarrow e\gamma) < 4.2 \times 10^{-13}$ [706] set by the MEG collaboration and the future projection of 6×10^{-14} from MEG II [707], our scenario leads to branching ratios of $\mathcal{O}(10^{-40})$ for the μ_Φ in (6.7) and is therefore not excluded. Since the bidoublet only connects leptons and mirror leptons, the process $\mu^- \rightarrow e^- e^+ e^-$ occurs via a penguin diagram with the same dipole form factor as before so we can estimate $\text{BR}(\mu^- \rightarrow e^- e^+ e^-) \simeq 7 \times 10^{-3} \text{BR}(\mu \rightarrow e\gamma)$ [708], which is compatible with the current bound $\text{BR}(\mu^- \rightarrow e^- e^+ e^-) < 10^{-12}$ from [709] and the projected sensitivity of $\mathcal{O}(10^{-15})$ of the Mu3e experiment [710]. The analogous decays of τ leptons are typically less constrained and also do not set any significant bounds on our scenario. Similarly we can estimate the neutrino magnetic moment, where there are two diagrams involving the coupling of φ_1^\pm (φ_2^\pm) to ν (ν') depicted on the right side of figure 6.4:

$$(\mu_\nu)_{ii} = \frac{\mu_B}{16\pi^2} \frac{m_e(m_\nu)_i}{\mu_\Phi^2} \sum_{j=e,\mu,\tau} (Y_\nu)_{ij} (Y_\nu)_{ij}^* \quad (6.76)$$

Both diagrams contribute with the same strength as φ_1^\pm and φ_2^\pm are mass degenerate, see (6.62). Here the factor of m_e does not arise from any chirality enhancement but rather from the definition of the Bohr magneton $\mu_B \equiv e/(2m_e)$. Again we observe mass insertions on the external legs (see figure 6.4) for the right-chirality structure explaining the m_ν dependence. The most stringent limit on neutrino magnetic moments of $\mu_\nu < 6.3 \times 10^{-12} \mu_B$ comes from the XENONnT experiment [711] and our estimate for the aforementioned masses reads $\mu_\nu \simeq \mathcal{O}(10^{-36}) \mu_B$, far below the bound.

■ ADDENDUM: Note that if we were to discard the solution to the strong CP problems and the mirror quarks all-together, then we could lower v' and consequently μ_Φ , which might lead to observable rates for the previously mentioned processes. ■

6.9.2 Collider bounds

The singly-charged scalars $\varphi_{1,2}^\pm$ have to be heavier than $\mathcal{O}(100 \text{ GeV})$ to escape direct production at colliders [712--715]. If we were to turn on the couplings $\propto \lambda_e, \lambda'_e$ between the charged SM and mirror leptons the $\varphi_2^{\pm\pm}$ could produce same-sign di-lepton signatures, similar to the canonical Type II Seesaw. Current collider searches [716] place a bound of $m_{\varphi_2^{\pm\pm}} > 800 \text{ GeV}$ and a future 100 TeV proton-proton collider could probe masses up to 4.5 TeV [717]. In this scenario, the exchange of the neutral h_Φ can induce a contact interaction between the SM leptons, which evades the LEP bound [718] due to the large μ_Φ and potentially small mixing between SM and mirror leptons. For the smallest allowed $v' \simeq 10^9 \text{ GeV}$, we find that the mirror electron (see the discussion above (6.77) in the next section) would have a mass of $\simeq 2 \text{ TeV}$, potentially accessible at colliders.

6.10 Appendix: Cosmology

6.10.1 Reheating

In the early universe the discrete exchange symmetry in (6.3) is spontaneously broken by the vev of the heavy doublet H' , leading to the presence of topological defects, which can overclose the universe if they are stable [449, 450, 719]. There exist basically two remedies for this conundrum: One may either include small bias terms [449, 720] in the scalar potential, explicitly breaking the discrete symmetry and thereby leading to domain wall decay. The explicit breaking might then manifest [659] as a contribution to $\bar{\theta}$ at low energies similar to the soft breaking discussed in section 6.5. Alternatively [93], if the domain walls are formed before or during the exponential expansion phase of cosmic inflation, they will be diluted by the expansion of spacetime. The second scenario requires that the symmetry is broken before or during inflation and does not get restored afterwards, which can be satisfied for a reheating temperature of $T_{\text{RH}} < v'$ [721]. Since the discrete exchange symmetry relates the SM and mirror Yukawas, we expect a similar mass spectrum in the mirror sector up to factors of v'/v of course. This means that, as long as we turn off the lepton-mirror lepton mixing in (6.6) via the \mathcal{Z}_3 symmetry in table 6.1, the mirror electron e' is the lightest stable electrically charged particle of the mirror sector. To avoid the stringent bounds [722--725] on the number density of such charged

thermal relics [726], we require the reheating temperature to be

$$T_{\text{RH}} < m_{e'} \simeq 2 \times 10^{-6} \cdot v', \quad (6.77)$$

corresponding to $T_{\text{RH}} < 2 \times (10^3 - 10^6)$ GeV for $v' = (10^9 - 10^{12})$ GeV. Of course there are also mirror quarks, with the lightest quark having a mass of $m_u' = m_u v' / v \simeq 2 \times 10^{-5} v'$ one order of magnitude above (6.77). Reference [649] found that the mirror quark masses actually run faster compared to the mirror leptons owing to their color charge, leading to a situation where the lightest mirror quarks u', d' are almost mass degenerate with e' for $v' \gg 10^{11}$ GeV. Consequently relic abundances of colored mirror fermions are also avoided by the previously determined reheating temperature. Reheating could either occur from the dynamics of the oscillating inflaton condensate or from a second unrelated epoch of intermediate matter domination [467]. Alternatively one might consider asymmetric reheating scenarios [635, 727], in which the SM and mirror sectors are reheated to different temperatures. This could happen if the particle responsible for reheating decays preferentially to the SM instead of the mirror sector.

■ ADDENDUM: In hindsight I realized that asymmetric reheating would not work for this construction since both the SM and mirror sector couple to the same QCD and (the symmetric components) would rapidly equilibrate. ■

As a consequence of the large hierarchy between v and v' , the mirror neutrinos never equilibrate with the SM plasma via gauge or Yukawa interactions and are only produced via freeze-in [74, 338].

6.10.2 Dark Radiation

Since the present setup only doubles the SU(2) gauge group of the SM, without introducing a second U(1), there is no dark photon. Thus the associated problem of large amounts of dark radiation from mirror neutrinos and a dark photon, that typically plagues mirror sector models [635], is absent. For $2 \rightarrow 2$ scattering producing ν' from the SM, h_Φ exchange is completely negligible due to its large mass. Z exchange via $Z - Z'$ mixing (see (6.66)) leads to

$$\frac{\Delta N_{\text{eff.}}}{\mathcal{O}(10^{-14})} \simeq \left(\frac{10^9 \text{ GeV}}{v'} \right)^4 \begin{cases} \left(\frac{T_{\text{RH}}}{100 \text{ GeV}} \right)^3 & (T_{\text{RH}} \lesssim v), \\ 0.1 \cdot \left(\frac{1 \text{ TeV}}{T_{\text{RH}}} \right) & (T_{\text{RH}} \gg v), \end{cases} \quad (6.78)$$

and we find that out-of-equilibrium Z decays to two ν' would give $\Delta N_{\text{eff.}} \simeq 10^{-15} (10^9 \text{ GeV}/v')^4$. These yields are at least two orders of magnitude smaller than the contribution $\Delta N_{\text{eff.}} \simeq 7.5 \times 10^{-12}$ from out-of-equilibrium Higgs decays [74], provided that $T_{\text{RH}} \gtrsim m_h$, and Higgs mediated scattering leads to $\Delta N_{\text{eff.}} < 10^{-10}$.

6.10.3 Leptogenesis from decays

Seesaw mechanisms are often invoked to realize Baryogenesis via the Leptogenesis mechanism [425]. For the standard out-of-equilibrium decay scenario it has long been

known that scalar triplet Leptogenesis [427] requires at least two triplets or insertions of heavy neutrinos to generate the required CP violation. Otherwise there would be no imaginary part in the interference term between the tree-level decay and its one-loop self-energy and vertex corrections. This conclusion also holds for Dirac Seesaw models [642, 728] and we could consider the channel $\Phi \rightarrow ll'$, which also requires $\Phi \rightarrow HH'$ for the asymmetry generation via self-energy graphs [642, 728] for at least two different bidoublets. The tree level decay widths of each bidoublet read (with suppressed generation indices)

$$\Gamma(\Phi \rightarrow ll') = \frac{Y_\nu^2}{8\pi} \mu_\Phi, \quad \Gamma(\Phi \rightarrow HH') = \frac{\kappa^2}{32\pi \mu_\Phi}. \quad (6.79)$$

We emphasize that the low reheating temperature in (6.77) is in tension with the high scale $> \mathcal{O}(10^{10} \text{ GeV})$ bidoublet mass, which is why non-thermal Leptogenesis [729] would be required. As an example we consider reheating via perturbative decays of an inflaton with mass $m_I > 2\mu_\Phi$, decaying to both SM particles and bidoublets. The inflaton's total decay width Γ_I is related to the reheating temperature via $T_{\text{RH}} \sim \sqrt{\Gamma_I M_{\text{Pl}}}$. One finds that the baryon asymmetry normalized to entropy at the end of reheating would be given by [730]

$$\frac{n_B}{s} \simeq -\frac{42}{79} \varepsilon \text{BR}_I \frac{T_{\text{RH}}}{m_I}. \quad (6.80)$$

Here $\text{BR}_I < 1$ denotes the branching ratio of inflaton decays to bidoublets and ε is the previously mentioned CP violating decay parameter depending on the mass spectrum of the different bidoublet generations [642].

■ ADDENDUM: Here we implicitly assume that the lifetime of the bidoublet is shorter than the typical timescale for the thermalization of the weak and mirror gauge interactions, so that the bidoublets decay out of equilibrium. ■

As for all Dirac Leptogenesis scenarios [117], equal and opposite asymmetries in l and l' are produced. If the $\text{SU}(2)'$ sphalerons are fast during or after the asymmetry generation, then the asymmetry in l' will be transferred into a mirror baryon asymmetry, which will be equal and opposite to the baryon asymmetry produced via $\text{SU}(2)_L$ sphalerons from the l asymmetry. Since there is no direct interaction coupling baryons to mirror baryons, the respective asymmetries will not equilibrate to zero and remain separately conserved. For a hierarchical bidoublet spectrum with the lightest mass μ_Φ one finds that the CP violating decay parameter reads [427, 642]

$$\varepsilon < \frac{r \sqrt{\text{BR}_l \text{BR}_H}}{8\pi} \frac{m_\nu \mu_\Phi}{v v'}, \quad (6.81)$$

where $r \equiv \mu_\Phi/\mu_\Phi^{(2)} < 1$ is the ratio of the lightest and next heavier bidoublet masses, $\text{BR}_{l,H}$ are the branching ratios for both decay modes in (6.79) and m_ν is the heaviest active neutrino mass. A typical value for equal branching fractions and $\mu_\Phi = 10 v'$ is

$\varepsilon \simeq 10^{-13}$, which is smaller than for the Type II Seesaw result [427] due to the additional v/v' suppression. For a hierarchical bidoublet spectrum we find

$$\left| \frac{n_B}{s} \right|^{\text{hier.}} < 10^{-23} \left(\frac{\text{BR}_I}{1\%} \right) \left(\frac{m_\nu}{0.1\text{eV}} \right) \left(\frac{2\mu_\Phi r}{m_I} \right) \left(\frac{T_{\text{RH}}}{10^{-6} v'} \right) \quad (6.82)$$

being far too small to explain the observed value of $n_B/s \simeq 8 \times 10^{-11}$ [311]. Therefore we have to invoke a resonant enhancement of the self-energy diagrams [426, 731--736] via assuming that μ_Φ and the next heavier mass $\mu_\Phi^{(2)}$ are nearly degenerate $|\mu_\Phi^{(2)} - \mu_\Phi| \ll \mu_\Phi^{(2)} \simeq \mu_\Phi$ ($r \simeq 1$). This scenario enhances the previous estimate for ε by a factor of [426, 736]

$$\frac{\rho}{\rho^2 + \delta^2} \gg 1, \quad \text{with} \quad \rho \equiv 1 - r^2, \quad \delta \equiv \frac{\Gamma_{\text{tot.}}}{\mu_\Phi}. \quad (6.83)$$

The above expression is regulated by the total decay width of the bidoublet $\Gamma_{\text{tot.}}$, which is the sum of the rates in (6.79). We assume both bidoublets to have comparable decay rates. A sizeable enhancement requires $\rho \sim \delta \ll 1$ and hence $Y_\nu^2 + \kappa^2/(4\mu_\Phi^2) \ll 8\pi$. The decay width to Higgses is automatically small for $\kappa \ll \mu_\Phi$, but we may have to make Y_ν small by hand, which would require a larger v_Φ for this scenario to fit m_ν . Note that this small $\Gamma_{\text{tot.}} \ll \mu_\Phi$ does not necessarily force ε to be small, as this parameter depends only on the branching ratios $\text{BR}_l \text{BR}_H = \Gamma(\Phi \rightarrow ll')\Gamma(\Phi \rightarrow HH')/\Gamma_{\text{tot.}}^2 \leq 1/4$ and not on the absolute widths. Of course we can not make the decay width arbitrarily small, or else the decay will take place after inflationary reheating during an epoch where the bidoublets dominate the energy density of the universe. In this regime (6.80) still holds with the replacement $T_{\text{RH}}/m_I \rightarrow T_{\text{dec.}}/\mu_\Phi$ [737], where $T_{\text{dec.}}$ is the reheating temperature after the second matter dominated epoch. The enhancement factor of ε is bounded from above by the perturbativity requirement $\varepsilon \ll 1$ assumed in the derivation of the Boltzmann equations, where one linearizes in the chemical potentials [303, 311]. The precise value of ε depends on the details of the active neutrino mass spectrum such as almost degenerate masses [606], which is why we use ε as a free parameter. Employing the kinematic condition $m_I > 2\mu_\Phi$ and (6.77) to eliminate T_{RH}/m_I in (6.80) lets us determine that there is indeed a parameter range reproducing the observed baryon asymmetry

$$\left| \frac{n_B}{s} \right|^{\text{res.}} < 10^{-10} \left(\frac{\varepsilon}{0.05} \right) \left(\frac{\text{BR}_I}{5\%} \right) \left(\frac{50}{\mu_\Phi/v'} \right). \quad (6.84)$$

To obtain this result we had to set ε close to its perturbative limit, which implies highly degenerate bidoublets with $|\mu_\Phi^{(2)} - \mu_\Phi|/\mu_\Phi \simeq 10^{-12}$. We further had to assume only a small hierarchy between v' and μ_Φ to accommodate the inflaton decaying mostly to other SM particles implying $\text{BR}_I \ll 1$.

6.10.4 Inflationary Affleck-Dine Leptogenesis

Alternatively, the coherent rotation in field space of a complex scalar field with lepton number during inflation facilitates Leptogenesis via the Affleck-Dine mechanism [257]. In

this picture, the Sakharov conditions [602] are realized via the initial phase of the scalar field providing C and CP violation and deviations from thermal equilibrium appear in the form of a large field amplitude during cosmic inflation. The last ingredient is baryon number violation, that arises from lepton number violation in the scalar potential and gets transmitted to the SM leptons so that afterwards it gets converted into baryon number via the B+L violating $SU(2)_L$ sphaleron vertex. The authors of [405, 738] put forth a very economical framework unifying Higgs inflation [378] and the conventional Type II Seesaw. Motivated by [405, 738], we will assume that the inflaton is a linear combination of the neutral fields h, h' and $h_\Phi + ia_\Phi \equiv \rho_\Phi e^{i\phi}$ after giving all scalar multiplets a non-minimal coupling to gravity [109]. Note that identifying the Affleck-Dine field with the inflaton is just a particularly convenient example for generating the required large initial field value and there exist other scenarios [739, 740], where the large field value is dynamically realized without this identification. Following the discussion at the end of section 6.4, we assign the B-L charge of two to Φ and treat the $\kappa H\Phi^\dagger H'$ term as an explicit B-L breaking by two units. Since the field value of the inflaton approaches the Planck scale during inflation, the trilinear scalar term is subdominant compared to other Planck-scale suppressed effective operators and will only matter when the field value has decreased due to the cosmic expansion. Even worse, during reheating, the trilinear coupling can lead to oscillations of the scalar condensate instead of a rotation, manifesting as an oscillation in the lepton asymmetry spoiling the mechanism unless we set [405, 738]

$$|\kappa| < 10^{-18} M_{\text{Pl}} \simeq \mathcal{O}(10 \text{ GeV}). \quad (6.85)$$

This bound is far stronger than the most naive estimate for $|\kappa|$ using the sub-eV-scale vev v_Φ in (6.2) and $\mu_\Phi < M_{\text{Pl}}$ together with v' in (6.11)

$$|\kappa| < 10^{-6} M_{\text{Pl}} \left(\frac{v_\Phi}{m_\nu} \right) \left(\frac{10^{12} \text{ GeV}}{v'} \right), \quad (6.86)$$

that is compatible with our previous assumption $|\kappa| \ll \mu_\Phi$. Additionally, for the asymmetry generation, an operator of dimension larger than four is needed so that the produced lepton number is conserved during reheating [405, 738]. Consequently, we consider the following dimension five operator

$$\frac{\lambda_5}{M_{\text{Pl}}} \left(H\Phi^\dagger H' \pm H'^\dagger \Phi H^\dagger \right) \left(H^\dagger H \pm H'^\dagger H' \right), \quad (6.87)$$

which conserves the discrete exchange symmetry if both signs are the same. The origin of this operator will be elucidated in section 6.10.5. If we have opposite signs in both brackets, the operator violates the discrete exchange symmetry explicitly and we might be able to use it as a bias term to remove the domain walls. In the following we stick to the symmetry-conserving case and use plus signs following [405, 738] so that the dimension five term is $\propto \cos(\phi)$. Up to mixing angles between the scalars during inflation and order one factors the lepton asymmetry at the end of inflation turns out to be [405, 738]

$$n_{L \text{ end}} \simeq -2 \lambda_5 \rho_{\text{end}}^3 \frac{\sin(\phi_0)}{\sqrt{3\tilde{\lambda}}}, \quad (6.88)$$

where the factor of two takes the B-L charge of Φ into account, $\tilde{\lambda}$ is the effective quartic self-coupling of the inflaton, $\rho_{\text{end}} \simeq \mathcal{O}(M_{\text{Pl}})$ the field value of the inflaton at the end of inflation and ϕ_0 is the initial phase of $\rho_{\Phi} e^{i\phi}$. Taking into account the redshifting of the lepton asymmetry during reheating and the sphaleron redistribution coefficient, one finds that the baryon to photon ratio today can be explained for $\lambda_5 \sin(\phi_0) / \sqrt{3\tilde{\lambda}} \simeq \mathcal{O}(10^{-16})$ [405, 738]. Evidently, small values of λ_5 and ϕ_0 are needed which also suppress isocurvature fluctuations [405, 738] and a small λ_5 is necessary anyway to not spoil inflation from the non-minimal coupling. We assume a thermalized bidoublet after reheating. In order to efficiently transmit the asymmetry from the bidoublet to the leptons we have to require that the decay width $\Gamma(\Phi \rightarrow ll')$ is larger than the decay width to scalars $\Gamma(\Phi \rightarrow HH')$ leading to

$$\mu_{\Phi} < 10^{21} \text{ GeV} Y_{\nu}^2 \left(\frac{v'}{10^9 \text{ GeV}} \right) \left(\frac{0.1 \text{ eV}}{m_{\nu}} \right). \quad (6.89)$$

Moreover the interaction $\Phi \leftrightarrow HH'$ should be out of equilibrium and we estimate that $\Gamma(HH' \rightarrow \Phi)|_{T=\mu_{\Phi}} \simeq \Gamma(\Phi \rightarrow HH')|_{T=\mu_{\Phi}}$ is slower than the Hubble rate $H(T)$ at $T = \mu_{\Phi}$ as long as

$$v_{\Phi} < 10 \text{ MeV} \left(\frac{v'}{10^9 \text{ GeV}} \right) \sqrt{\frac{5 \times 10^{10} \text{ GeV}}{\mu_{\Phi}}}. \quad (6.90)$$

Of course we also need to ensure that the process $ll' \leftrightarrow HH'$ via off-shell Φ does not thermalize, which sets a weaker bound compared to (6.89)

$$\mu_{\Phi} < 10^{25} \text{ GeV} \left(\frac{v'}{10^9 \text{ GeV}} \right)^2 \left(\frac{0.1 \text{ eV}}{m_{\nu}} \right)^2. \quad (6.91)$$

Let us note that the cosmological history in [405, 738] has an inflationary reheating temperature of $\mathcal{O}(10^{14} \text{ GeV})$, which is in conflict with the requirement (6.77) for the absence of charged mirror leptons and quarks. That means we either need an additional mechanism to suppress reheating the mirror sector via asymmetric reheating [635, 727] or simply a different scenario, where Φ is not the inflaton and its large initial field value has a different origin during inflation [739, 740]. That way we can sequester the asymmetric reheating from the Affleck-Dine dynamics.

■ ADDENDUM: See one of the previous addenda for why asymmetric reheating would not actually help in this scenario. ■

Before we close, we would like to mention that there exists no obvious dark matter candidate in this model: The neutral component of Φ can decay to neutrinos or gauge bosons and will in general not be long-lived enough due its large mass. The heavy H', Z' are also not long-lived enough as they couple to all fermions (via mixing). Stable mirror quarks could form electrically neutral dark mesons after the QCD phase transition [741], however here we assume that the mirror sector is never populated to begin with or heavily diluted (see (6.77)). Therefore dark matter has to come from a separate dark sector.

6.10.5 Origin of the dimension five operator for Affleck-Dine Leptogenesis

The discrete exchange symmetry conserving effective operator in (6.87) (same signs in each bracket) can be realized by including a real singlet either even ($\sigma(t, \vec{x}) \rightarrow \sigma(t, -\vec{x})$) or odd ($\sigma(t, \vec{x}) \rightarrow -\sigma(t, -\vec{x})$) under the symmetry (6.3). This adds the following terms to the scalar potential

$$V_\sigma = \mu_\sigma^2 \sigma^2 + \lambda_{3\sigma} \sigma^3 + \lambda_{4\sigma} \sigma^4, \quad (6.92)$$

$$V_{\text{int.}} = \kappa_\sigma \sigma \left(H^\dagger H \pm H'^\dagger H' \right) + \lambda_{\sigma H \Phi H'} \sigma \left(H \Phi^\dagger H' \pm H'^\dagger \Phi H \right) \quad (6.93)$$

$$+ \lambda_{H\sigma} \sigma^2 \left(H^\dagger H + H'^\dagger H' \right) + \lambda_{\Phi\sigma} \sigma^2 \text{Tr} \left(\Phi^\dagger \Phi \right), \quad (6.94)$$

where the $+(-)$ sign applies to the even (odd) case and furthermore the term $\lambda_{3\sigma} \sigma^3$ is absent for odd σ . Note that all of the above couplings are real. If we assume the σ mass is the largest in the potential, we find after integrating it out, that the effective coupling in (6.87) is given by

$$\frac{\lambda_5}{M_{\text{Pl}}} \simeq \frac{\lambda_{\sigma H \Phi H'} \kappa_\sigma}{|\mu_\sigma|^2}. \quad (6.95)$$

In order for this operator to be present during the inflationary stage, where the inflaton can approach Planck scale field values, we have to impose $|\mu_\sigma| \simeq \mathcal{O}(M_{\text{Pl}})$. A vev for σ is not required to generate the right operator. For completeness let us consider the implications of a vev for the real σ :

- **even case:** Since the scalar σ is even, the discrete exchange symmetry remains unbroken and v_σ simply shifts $\mu_\Phi^2 \rightarrow \mu_\Phi^2 + \lambda_{\Phi\sigma} v_\sigma^2$, $-\mu_H^2 \rightarrow -\mu_H^2 + \kappa_\sigma v_\sigma + \lambda_{H\sigma} v_\sigma^2$ as well as $\kappa \rightarrow \kappa + \lambda_{\sigma H \Phi H'} v_\sigma$. Since we expect v_σ to be very large we require small couplings in order to not shift the scales too much.
- **odd case:** In this scenario σ is a pseudo-scalar that spontaneously breaks the discrete exchange symmetry and leads to different mass terms $-\mu_H^2 \pm \kappa_\sigma v_\sigma$ for H, H' effectively realizing the softly-broken parity scenario of [658] for $v' \gg v$ mentioned in section 6.5. On top of that when it comes to CP the minimum of the scalar potential will be different from (6.16) and we find spontaneous CP violation with an angle for v_Φ of

$$\beta_\Phi - \beta - \beta' = \arctan \left(\frac{\lambda_{\sigma H \Phi H'} v_\sigma}{\sqrt{2} \kappa} \right). \quad (6.96)$$

This phase is negligible for the solution to the strong CP problem in section 6.8, because the field Φ has no direct couplings to quarks and leptonic insertions occur only at very large and thus heavily suppressed loop orders. In the symmetry-odd case there could arise a dimension five operator similar to (6.67) [721]

$$\frac{c_5^g}{\Lambda_{\text{UV}}} \sigma G_{\mu\nu} \tilde{G}^{\mu\nu}, \quad (6.97)$$

or a correction to the quark Yukawas in (6.4) of the form [721]

$$\frac{c_5^u}{\Lambda_{\text{UV}}} i\sigma \left(Y_u q H^\dagger \bar{u} + Y'_u q' H'^\dagger \bar{u}' \right) + \frac{c_5^d}{\Lambda_{\text{UV}}} i\sigma \left(Y_d q H \bar{d} + Y'_d q' H' \bar{d}' \right) + \text{h.c.}, \quad (6.98)$$

which for a Planck-scale cut-off Λ_{UV} need to satisfy $c_5^{g,u,d} v_\sigma < 10^9 \text{ GeV}$ [721] in order to comply with the experimental bound of $\bar{\theta} < 10^{-10}$ [686–689].

The effective operator in (6.87) with different signs in each bracket, violating the discrete exchange symmetry, could arise from non-perturbative quantum gravitational effects, which are expected [275–277] to explicitly break all global symmetries that are not residual symmetries of gauge symmetries.

6.11 Appendix: Conclusion

We have presented a high scale Dirac neutrino mass model in the Type II Seesaw spirit, that has the same scalar spectrum of neutral, singly- and doubly-charged scalars as the original Majorana Type II Seesaw. This idea was implemented by introducing a bidoublet scalar in a mirror sector model with the gauge group $SU(2)_L \otimes SU(2)' \otimes U(1)_X$, where we identify the mirror neutrinos as the Dirac partners of the SM neutrinos. It was shown that the bidoublet is compatible with the discrete symmetry based solution to the strong CP problem, which was the motivation behind the mirror sector to begin with. The super-heavy bidoublet does not lead to any observable signatures for collider or other terrestrial experiments. However it might have played a role in the early universe as the source of the matter-antimatter asymmetry via either the non-thermal decay scenario or Affleck-Dine Dirac Leptogenesis.

6.12 Appendix: Acknowledgments

We are grateful to Andreas Trautner and Alessandro Valenti for many useful comments including, but not limited to, subtle aspects of discrete symmetries as well as to Saurabh Nangia for valuable feedback on earlier iterations of this manuscript. This work benefited from the use of `PackageX` [242, 416] and we sincerely hope that this tool and its codebase will live on in one way or another.

7 Impact of high-scale Seesaw and Leptogenesis on inflationary tensor perturbations as detectable gravitational waves

7.1 Contribution and Context

The following chapter is based on the publication

JHEP 05 (2023) 172, arXiv: 2301.05672 [hep-ph]

in collaboration with Dr. Anish Ghoshal (AG). AG had the initial idea for the project, supplied relevant literature and suggested computing the signal-to-noise ratio as well as incorporating dark matter into our setup. MB worked out the details for Leptogenesis and dark matter production, digitized most of the plots for gravitational wave detectors and CMB experiments, made all of the plots in the paper and wrote almost the entire manuscript. MB also worked out the conditions under which the gravitational wave signal from phase transitions and topological defects would be absent and, motivated by a suggestion from AG, checked, if this scenario could produce observable amounts of dark radiation.

In this chapter we do not construct a new model but rather we chose to work with the most basic prototype for small neutrino masses: The Type I Seesaw [26–30, 423]. The Davidson-Ibarra bound [608] for a hierarchical right handed neutrino (RHN) mass spectrum requires a mass above 10^8 GeV in order to explain the observed baryon asymmetry via the Leptogenesis mechanism [116], which is also known as high scale Leptogenesis. As a consequence of the large RHN mass this scenario is particularly hard to test in laboratory experiments and our only indirect handle on the associated mass scale would come from e.g. virtual RHN mediating neutrinoless-double-beta-decay [19]. Of course there exist scenarios based on resonant enhancement of self-energy graphs [426] or Leptogenesis from oscillations [396] that are actually testable at our energy scales [742], but here we tried to come up with a way to learn more about the high scale scenario. To do so we employ gravitational wave astronomy, which might provide a window into the dynamics of the early universe. While there exist ample amounts of literature about gravitational waves produced from the phase transitions and topological defects [743–752] that are present in models for the masses of the RHNs themselves, here we take a complementary approach: If no new degrees of freedom apart from the RHN are added to the SM below the Planck

scale, then the usually discussed GW signatures from phase transitions and topological defects are absent. Even if such a phase transition took place in the early universe, there would be no observational trace left, if it happened before inflation and the underlying symmetry was never restored during inflation or reheating. Instead of producing a new stochastic gravitational wave background, we study the dilution or distortion of the primordial gravitational wave background expected from cosmic inflation due to the decays of very-long lived RHN. The idea is that an initially thermal RHN population starts to dominate the energy density of the universe after they become non-relativistic. Gravitational waves that enter during this intermediate matter-dominated phase are than damped compared to horizon crossing during radiation domination. This damping can also be understood from the entropy released during the out-of-equilibrium RHN decay, which dilutes the baryon asymmetry too. Putting these ingredients together we obtain a modified Davidson-Ibarra bound and deduce that the frequency above which inflationary gravitational waves would be affected lies above ca. 0.1 Hz. Here we assume a value of the tensor to scalar ratio, which is not too far below the current bound of $r < 0.036$ [104]. In order to analyze the detection prospects we compute the signal-to-noise ratio for various interferometers like e.g. AEDGE, BBO, DECIGO, EINSTEIN TELESCOPE or LISA. In our analysis we take the spectral tilt as a free parameter and vary it between zero and 0.5. We further extend this simple framework by a singlet fermion and a singlet scalar and we focus on the fermion as a dark matter candidate, that gets produced together with the lepton asymmetry from RHN decays. To summarize we

- showed that Leptogenesis might leave a trace in the inflationary tensor mode background at frequencies above 0.1 Hz
- quantified the detection prospects for numerous gravitational wave detectors
- included a minimal extension for dark matter

7.2 Appendix: Abstract

We discuss the damping of inflationary gravitational waves (GW) that re-enter the horizon before or during an epoch, where the energy budget of the universe is dominated by an unstable right handed neutrino (RHN), whose out of equilibrium decay releases entropy. Starting from the minimal Standard Model extension, motivated by the observed neutrino mass scale, with nothing more than 3 RHN for the Seesaw mechanism, we discuss the conditions for high scale Leptogenesis assuming a thermal initial population of RHN. We further address the associated production of potentially light non-thermal dark matter and a potential component of dark radiation from the same RHN decay. One of our main findings is that the frequency, above which the damping of the tensor modes is potentially observable, is completely determined by successful Leptogenesis and a Davidson-Ibarra type bound to be at around 0.1 Hz. To quantify the detection prospects of this GW background for various proposed interferometers such as AEDGE, BBO, DECIGO, EINSTEIN TELESCOPE or LISA we compute the *signal-to-noise ratio* (SNR). This allows us to investigate the viable parameter space of our model, spanned by the

mass of the decaying RHN $M_1 \gtrsim 2.4 \times 10^8 \text{ GeV} \cdot \sqrt{2 \times 10^{-7} \text{ eV}/\tilde{m}_1}$ (for Leptogenesis) and the effective neutrino mass parameterizing its decay width $\tilde{m}_1 < 2.9 \times 10^{-7} \text{ eV}$ (for RHN matter domination). Thus gravitational wave astronomy is a novel way to probe both the Seesaw and the Leptogenesis scale, which are completely inaccessible to laboratory experiments in high scale scenarios.

7.3 Appendix: Introduction

The standard model (SM) of particle physics predicts that the neutrinos are massless, but due to the observation of neutrino oscillations for solar [753–760], atmospheric [761, 762] and reactor [10, 12, 763, 764] neutrinos we now know that they are massive and the flavor states mix due to the propagation of multiple mass eigenstates. Moreover the β -decay experiment KATRIN [18] has provided us with the first direct limit of the neutrino mass scale $m_\nu < 0.8 \text{ eV}$. Cosmology offers an indirect probe of this scale and demands that the sum of all neutrino masses satisfies $\sum_i m_{\nu_i} < 0.12 \text{ eV}$ [133, 765] in order to be consistent with the predictions for the Cosmic Microwave Background (CMB) radiation, Large scale structure (LSS) formation and Big Bang Nucleosynthesis (BBN). The accelerated expansion at the beginning of the universe provided by cosmic inflation, which was postulated in order to solve the horizon and the flatness problems and is responsible for quantum generation of the primordial fluctuations seeding the large scale structure of the universe, is thought to be driven by a scalar field known as the inflaton (see [112] for a review). In this paper, we will be concerned with the primordial Gravitational Waves (GW) background of such inflationary origin [766–768] (see [769] for a review on this topic). These inflationary GWs can act as a logbook of the expansion history of our universe throughout its entire evolution [770–777]. Particularly, the detailed time evolution of the Hubble rate during the expansion determines the transfer function that describes how gravitational waves at different frequencies are red-shifted to the present day. This property turns primordial GWs into a powerful tool that grants access to the thermal history of our universe prior to BBN. Primordial GWs offer, *e.g.* an opportunity to measure the reheating temperature after inflation [744, 778–784]. Similarly, with help of these inference can be drawn of the equation of state during the quark-hadron phase transition in quantum chromodynamics [785, 786] or constrain properties of the hidden sectors beyond the Standard Model (BSM) of particle physics [787, 788].

The observed baryon asymmetry of the universe (BAU) is longstanding puzzle in particle physics and cosmology [133, 488]. While the universe is expected to start in a matter-antimatter symmetric phase, any primordial asymmetry set due to the initial conditions is expected to get diluted by the exponential expansion phase during cosmic inflation. The BAU is often quoted in terms of the baryon to photon ratio measurement which, according to the latest Planck 2018 data, is given by [133]

$$\eta_B = \frac{n_B - n_{\bar{B}}}{n_\gamma} = 6.1 \times 10^{-10} \quad (7.1)$$

and agrees with the value extracted from BBN [90] as well. Similar to the BAU, there has been another question related to the presence of a mysterious, non-luminous form of matter, popularly known as dark matter (DM), giving rise to approximately 26% of the energy density in the present universe. In terms of density parameter Ω_{DM} and $h = H_0/(100 \text{ km s}^{-1}\text{Mpc}^{-1})$ with H_0 being the observed present day Hubble parameter, the current DM abundance is conventionally reported to be [133]

$$\Omega_{DM}h^2 = 0.120 \pm 0.001 \quad (7.2)$$

at 68% CL. Apart from cosmological evidence, the presence of DM has also been suggested by several astrophysical implications [81, 789, 790]. While none of the standard model particles satisfy the criteria of a particle DM candidate, the SM also does not satisfy the criteria to dynamically generate the observed BAU, known as Sakharov's conditions [113], in adequate amounts. This has led to several BSM possibilities offering intriguing solutions to these puzzles: The Type I Seesaw mechanism [26–30, 423], where the SM is augmented with three right handed SM gauge singlet neutrinos (RHN), may explain both the observed neutrino masses (from neutrino oscillation experiments) as well as the baryon asymmetry of the universe via first generating an asymmetry in the dark leptonic sector [116, 303, 734, 791, 792] and subsequently getting transferred to the visible baryonic sector via the electroweak sphaleron transitions [114]. Among the BSM proposals for DM, the weakly interacting massive particle (WIMP) [62] produced as a thermal relic is perhaps the most widely studied one (see [793] for a review). However due to the absence of any WIMP related signals in nuclear and electron recoil DM direct detection experiments, there has been growing interest in other (non-thermal) production modes: some examples are the well-known super-WIMP scenario [307], where frozen out WIMP decays to the actual DM, FIMPs [82] (see [304] for a review) that have such tiny couplings to the SM plasma that they never thermalize, or non-thermal production from inflaton decays [794] during the process of the formation of the radiation bath known as reheating. In Leptogenesis models the RHN might also have the decay modes to other SM singlets that can be good DM candidates [795, 796], which is why we will adopt this framework. Since the RHN decays out-of-thermal equilibrium the DM will be non-thermal.

We will demonstrate that the same RHN decay responsible for both the generation of the primordial baryon asymmetry via Leptogenesis, as well as the production of non-thermal dark matter and a possible component of dark radiation, leaves its vestige on the primordial spectrum of inflationary GWs. In particular we consider an epoch of intermediate matter domination [62, 301, 302] from the lightest RHN, which decouples from the plasma while relativistic and is very long-lived compared to the characteristic time scale of the cosmic expansion. Since the decay occurs far away from thermal equilibrium it will release a large amount of entropy, which dilutes the energy density of primordial GWs that enter the horizon before the decay.

Although the Seesaw mechanism ties Leptogenesis to the observed light neutrino masses,

the mechanism itself is notoriously difficult to test in laboratory based experiments, as the heavy right-handed neutrino mass scale has to be above $\gtrsim 10^9$ GeV (see [619]). One should keep in mind that this bound can be evaded, see for example [426] and with some fine tuning, it is also possible to bring down the scale of the non-resonant thermal Leptogenesis to as low as 10^6 GeV [797]. However indirect tests for high scale Leptogenesis of course exist as well. These are primarily based on neutrino-less double beta decay scenarios [19, 798], meson decay scenarios [799–801], and via CP violation in the neutrino oscillation [802, 803], the structure of the leptonic mixing matrix [804], or via considering theoretical constraints from the demand of the SM Higgs vacuum does not become unstable in early universe [805, 806]. Therefore, it is necessary, although very challenging to find newer and complementary tests of such heavy neutrino Seesaw physics and consequently the Leptogenesis mechanism. Recently it has been proposed to complement these indirect tests with the observations of GWs of primordial origin such as that from cosmic strings [750], domain walls [807] and other topological defects [752] or from nucleating and colliding vacuum bubbles [808, 809], graviton bremmstrahlung [810] and primordial black holes [811, 812]. These previous studies on GW [743–752] focused on the stochastic GW background from the dynamics of the scalar field, whose vacuum expectation value is responsible for the RHN mass, whereas (when it comes to Leptogenesis) we only extend the SM by adding nothing more than three RHNs with hard mass terms. In order to ensure a thermal population of the lightest RHN, which can not be established by the Yukawa couplings we consider, we have to assume that the RHNs are produced from inflaton decays or additional gauge interactions. In this paper we propose the imprint of the RHN decay on the inflationary first-order tensor perturbations as a novel probe of the minimal high-scale Leptogenesis mechanism.

The paper is organized as follows: In the subsection 7.4.1 of section 7.4 we discuss the Seesaw model, then how the decay of the lightest right handed neutrino (RHN) leads to an intermediate era of matter domination in 7.4.2, and we elaborate on the generation of baryon asymmetry via Leptogenesis from the decay of the lightest RHN in 7.4.3. We also discuss the production of non-thermal dark matter and dark radiation from such heavy RHN decays in 7.4.4. In section 7.5 we discuss the generation and propagation of inflationary tensor perturbations as Gravitational Wave signals and show how RHN decays leave their imprint on the GW spectrum. We discuss the GW detection prospects in 7.6.1 of section 7.6 and translate such experimental sensitivities into the reach for probing the parameter space and scale of Leptogenesis via computing the *signal-to-noise ratio* (SNR) in 7.6.2. We end with the conclusions in section 7.7.

7.4 Appendix: Decays of a long-lived RHN

7.4.1 Type I Seesaw mechanism

We start with a conventional Type I Seesaw [26--30,423] with three right handed neutrinos N

$$\mathcal{L} = \lambda \bar{L}(i\sigma_2)H^\dagger N + \frac{M_N}{2} \bar{N^c}N + \text{h.c.}, \quad (7.3)$$

where σ_2 is the second Pauli matrix and assume without loss of generality that the symmetric right handed neutrino (RHN) mass matrix is diagonal

$$M_N = \text{diag}(M_1, M_2, M_3), \quad (7.4)$$

without making any assumptions about the mass spectrum yet. After Integrating out the RHN and electroweak symmetry breaking with $\langle H \rangle \equiv v = 174 \text{ GeV}$ the active neutrino mass matrix reads at leading order in the Seesaw expansion

$$m_\nu = -m_D \cdot M_N^{-1} \cdot m_D^t = \text{diag}(m_1, m_2, m_3), \quad \text{with } m_D \equiv \lambda v \ll M_N. \quad (7.5)$$

Using the Casas-Ibarra parameterization in the basis where the charged lepton mass matrix is diagonal one finds [607]

$$\lambda = \frac{1}{v} \cdot M_N^{\frac{1}{2}} \cdot R \cdot m_\nu^{\frac{1}{2}} \cdot U_{\text{PMNS}}^\dagger, \quad (7.6)$$

where U_{PMNS} is the leptonic equivalent of the CKM matrix. R describes the mixing and CP-violation in the RHN sector and is expressed as a complex, orthogonal matrix that reads

$$R \equiv \text{diag}(\pm 1, \pm 1, \pm 1) \cdot R^{(23)}(z_{23}) \cdot R^{(13)}(z_{13}) \cdot R^{(12)}(z_{12}) \quad (7.7)$$

in terms of 2×2 rotation matrices $R^{(ij)}$ in the ij -plane with an angle z_{ij} .

7.4.2 Conditions for intermediate matter domination

The lightest RHN N_1 has the tree level decay width summed over all SM lepton flavours of

$$\Gamma_1 \equiv \Gamma(N_1 \rightarrow LH, \bar{L}H^\dagger) = \frac{|\lambda\lambda^\dagger|_{11}}{8\pi} M_1. \quad (7.8)$$

For $T \gg M_j$ the decay in the plasma is suppressed by a time dilation factor of M_1/T [299], which goes to one for $T \leq M_1$. It is customary to define the effective neutrino mass mediated by N_1

$$\tilde{m}_1 \equiv \frac{|\lambda\lambda^\dagger|_{11} v^2}{M_1} = \sum_i m_i |R_{1i}|^2, \quad (7.9)$$

7.4 Appendix: Decays of a long-lived RHN

which appears when comparing the decay rate to the characteristic time scale of cosmic expansion $H(T)^{-1}$, where $H(T)$ is the Hubble rate during radiation domination

$$K_1 \equiv \frac{\Gamma_1}{2H(T)} \Big|_{T=M_1} = \frac{\tilde{m}_1}{2 \times 10^{-3} \text{ eV}}. \quad (7.10)$$

This effective mass only coincides with the physical mass ($\tilde{m}_j = m_j$) for $R_{ji} = 0, \forall i \neq j$. A small effective mass \tilde{m}_1 implies that N_1 is weakly coupled to other two RHN. One can show that this effective mass is larger than the lightest active neutrino mass [813]

$$\tilde{m}_1 > \text{Min} [m_\nu]. \quad (7.11)$$

We find that the N_1 decays after it has become non-relativistic ($K_1 \ll 1$) as long as

$$\tilde{m}_1 \ll 2 \times 10^{-3} \text{ eV}. \quad (7.12)$$

The energy density of the non-relativistic RHN redshifts slower than radiation, so it overtakes the radiation component and becomes the dominant contribution to the energy budget of the universe at [737]

$$T_{\text{dom.}} = \frac{7}{4} \frac{M_1}{g_*(T_{\text{dom.}})} \simeq 2\% M_1, \quad (7.13)$$

where we used that the number of relativistic degrees of freedom above the electroweak crossover is $g_*(T_{\text{dom.}}) = \mathcal{O}(100)$. Once $\Gamma_1 = H(T_{\text{dec.}})$ the intermediate epoch of matter domination ends and the decays of N_1 to relativistic particles begin a new epoch of radiation domination with a starting temperature of

$$T_{\text{dec.}} = 3 \times 10^8 \text{ GeV} \sqrt{\frac{\tilde{m}_1}{10^{-6} \text{ eV}}} \left(\frac{M_1}{10^{10} \text{ GeV}} \right) \left(\frac{106.75}{g_*(T_{\text{dec.}})} \right)^{\frac{1}{4}}. \quad (7.14)$$

The decay takes place after the onset of early matter domination for [737]

$$\tilde{m}_1 < 2.9 \times 10^{-7} \text{ eV}. \quad (7.15)$$

If \tilde{m}_1 is larger than this number, there will be no era of intermediate RHN matter domination and consequently the decays of the N_1 will not produce enough entropy to lead to an appreciable dilution of the inflationary tensor mode background (see the following discussion in section 7.5.1). This bound implies together with (7.11) that the lightest active neutrino mass has to be smaller than $2.9 \times 10^{-7} \text{ eV}$ meaning that for normal-ordering (NO) we consider the following neutrino spectrum [814]

$$m_1 \simeq 0, \quad m_2 \simeq \sqrt{\Delta m_{\text{sol.}}^2} \simeq 8.6 \times 10^{-3} \text{ eV}, \quad m_3 \simeq \sqrt{\Delta m_{\text{sol.}}^2 + \Delta m_{\text{atm.}}^2} \simeq 0.05 \text{ eV}. \quad (7.16)$$

For the inverted ordering (IO) we would instead have a quasi-degenerate spectrum [814]

$$m_1 \simeq \sqrt{|\Delta m_{\text{sol.}}^2 + \Delta m_{\text{atm.}}^2|} \simeq 0.0492 \text{ eV}, \quad m_2 \simeq \sqrt{|\Delta m_{\text{atm.}}^2|} \simeq 0.05 \text{ eV}, \quad m_3 \simeq 0. \quad (7.17)$$

Above we used the results of the global fit to neutrino oscillation data [4] including the atmospheric data from Super-Kamiokande [5, 6]:

$$\text{NO: } \Delta m_{\text{sol.}}^2 = 7.42_{-0.20}^{+0.21} \times 10^{-5} \text{ eV}, \quad \Delta m_{\text{atm.}}^2 = 2.517_{-0.028}^{+0.026} \times 10^{-3} \text{ eV}, \quad (7.18)$$

$$\text{IO: } \Delta m_{\text{sol.}}^2 = 7.42_{-0.20}^{+0.21} \times 10^{-5} \text{ eV}, \quad \Delta m_{\text{atm.}}^2 = -2.498_{-0.028}^{+0.028} \times 10^{-3} \text{ eV}. \quad (7.19)$$

The duration of the intermediate matter dominated era can be expressed in terms of the number of e -foldings

$$N_e = \log \left(\frac{a(T_{\text{dec.}})}{a(T_{\text{dom.}})} \right) \simeq \log \left(\frac{25.4}{g_*(T_{\text{dom.}})} \left(\frac{v^2}{\tilde{m}_1 M_{\text{Pl}}} \right)^{\frac{2}{3}} \right), \quad (7.20)$$

$$\simeq \begin{cases} 0.3 & \text{for } \tilde{m}_1 = 2 \times 10^{-7} \text{ eV}, \\ 5 & \text{for } \tilde{m}_1 = 2 \times 10^{-10} \text{ eV}, \end{cases} \quad (7.21)$$

where we used that during matter domination $a \sim H^{-2/3}$ together with $H(T_{\text{dec.}}) = \Gamma_1$ and $H(T_{\text{dom.}}) \sim T_{\text{dom.}}^2/M_{\text{Pl}}$ at the transition from radiation to matter domination.

Throughout this work we assume an initial equilibrium distribution for N_1 . For small Yukawa couplings giving rise to $\tilde{m}_1 < 10^{-3}$ eV [737] the interactions in (7.3) do not suffice to establish equilibrium in the radiation dominated plasma after inflationary reheating at T_{RH} . Hence our scenario precludes thermal Leptogenesis and is sensitive to the initial conditions of the radiation bath. This is why we assume the initial population of RHN is produced by additional interactions such as couplings to the inflaton φ [815] like *e.g.*

$$Y_{\varphi N} \varphi \overline{N^c} N, \quad (7.22)$$

for a production during reheating, or new gauge bosons from *e.g.* GUTs [24, 573] or gauged B-L [301]. Concentrating on the case of a $U(1)_{\text{B-L}}$ gauge boson with mass $m_{Z'} = g_{\text{B-L}} v_{\text{B-L}} > T_{\text{RH}}$ as an example, the scattering rate of N_1 with the SM quarks and leptons via off-shell Z' would read approximately

$$\Gamma_{\text{scat.}} \simeq \frac{g_{\text{B-L}}^4 T^5}{m_{Z'}^4} = \frac{T^5}{v_{\text{B-L}}^4}. \quad (7.23)$$

This interaction freezes-out while the N_1 are still relativistic ($T_{\text{FO}} > 10M_1$) as long as

$$v_{\text{B-L}} > 7 \times 10^{11} \text{ GeV} \cdot \left(\frac{M_1}{7.5 \times 10^8 \text{ GeV}} \right)^{\frac{3}{4}} \cdot \left(\frac{106.75}{g_{*\rho}(T_{\text{FO}})} \right)^{\frac{1}{8}}. \quad (7.24)$$

The impact of the underlying $U(1)_{\text{B-L}}$ breaking on stochastic GWs is briefly explained in section 7.5.2.

■ **ADDENDUM:** One might wonder why we assume a thermal initial population of RHN instead of assuming that RHNs produced from inflaton decays immediately dominate the energy budget of the universe, which would allow for larger values of \tilde{m}_1 that are also

compatible with Leptogenesis. The reason is that the RHN produced from inflationary reheating become more and more short-lived for larger \tilde{m}_1 , which implies that the RHN reheating temperature $T_{\text{dec.}}$ becomes closer to the inflationary reheating temperature T_{RH} , so eventually we would not be able to distinguish between both epochs by only using the damping of the tensor modes. ■

7.4.3 Non-thermal Leptogenesis

We assume the inflationary reheating dynamics satisfy $M_2, M_3 > T_{\text{max}} > M_1$ so that we can focus on the decays of the lightest RHN N_1 . In this context we defined $T_{\text{max}} > T_{\text{RH}}$ as the largest temperature during the epoch of inflationary reheating [816–818], which ends with a radiation bath of the temperature T_{RH} . Alternatively, if one assumes only $M_2, M_3 \gtrsim (3 - 10) \times M_1$, the population of $N_{2,3}$ will have decayed away long before N_1 decays, as a consequence of their larger Yukawa couplings needed to explain the observed neutrino masses. Further we assume there is no primordial lepton asymmetry *e.g.* from the decays of $N_{2,3}$. Since the N_1 are too weakly coupled, they would not be able to erase this preexisting asymmetry [819]. However for realistic light neutrino masses the $N_{2,3}$ will be in the strong washout regime $\tilde{m}_{2,3} > 10^{-3}$ eV, so that inverse decays $LH \rightarrow N_{2,3}$ destroy a large portion of the asymmetry produced by the decays of $N_{2,3}$. The lepton asymmetry $n_{\text{B-L}}/s$, defined in terms of the number density of leptons minus anti-leptons normalized to the entropy density s , can be converted into a baryon asymmetry via the electroweak sphaleron process. For the RHN dominated scenario one finds a baryon asymmetry of [737]

$$\frac{n_{\text{B}}}{s} = \frac{3}{4} c_{\text{sph.}} \cdot \varepsilon_1 \cdot \frac{T_{\text{dec.}}}{M_1} \cdot \omega. \quad (7.25)$$

The parameter ε_1 denotes the CP-violating decay parameter encoding the amount of leptonic asymmetry produced per decay of N_1 . The sphaleron redistribution coefficient is found to be $c_{\text{sph.}} = 28/79$ [610] and the term ω , that will be determined later in this paragraph, parameterizes the washout of the lepton asymmetry. Our analysis is different from the more commonly studied case of non-thermal Leptogenesis immediately after inflationary reheating [729, 730], where $T_{\text{dec.}}/M_1$ would have to be replaced with T_{RH}/m_φ with m_φ being the inflaton mass, because here the RHN decay takes place much later, after it had time to dominate the energy budget of the universe. The factor of $T_{\text{dec.}}/M_1 < 2\%$ comes from n_N/s , which can be obtained from energy conservation ($\rho_{\text{tot.}} = M_1 n_N$ before the decay) leading to

$$n_N = \frac{\pi^2}{30} g_{*\rho}(T_{\text{dec.}}) \frac{T_{\text{dec.}}^4}{M_1} \quad (7.26)$$

and can be understood as the entropy dilution from the N_1 reheating: The dimensionless dilution factor from the entropy produced by the instantaneous¹ out-of-equilibrium decay

¹Reference [820] goes beyond this approximation and also deals with the case of a decaying particle whose temperature is different from the SM bath.

of the dominating RHN N_1 [62, 301, 302] reads

$$\Delta \equiv \frac{s(T_{\text{dec.}})a^3(T_{\text{dec.}})}{s(T_{\text{RH}})a^3(T_{\text{RH}})} = \left(1 + 2.95 \left(\frac{2\pi^2 \langle g_*(T) \rangle}{45} \right)^{\frac{1}{3}} \frac{\left(\frac{n_N^i}{s} M_1 \right)^{\frac{4}{3}}}{(M_{\text{Pl.}} \Gamma_1)^{\frac{2}{3}}} \right)^{\frac{3}{4}} \quad (7.27)$$

$$(\text{for } \Delta \gg 1) \quad \simeq 18.4 \cdot \sqrt{\frac{10^{-10} \text{ eV}}{\tilde{m}_1}} \left(\frac{106.75}{g_*(T_{\text{dec.}})} \right)^{\frac{3}{4}}. \quad (7.28)$$

In this context we denote the average of $g_*(T)$ over the decay period as $\langle g_*(T) \rangle$ and we assume that $\langle g_*(T) \rangle \simeq g_*(T_{\text{dec.}})$. To obtain the second line we assumed for the initial abundance n_N^i/s that N_1 decoupled from the plasma while relativistic to maximize the amount of entropy produced [301], see also (7.24). For hierarchical RHN spectrum ($M_3 > M_2 > M_1$) the decay parameter from the interference between tree-level and one-loop vertex- and self-energy-corrections is found to be [606]

$$|\varepsilon_1|^{\text{hier.}} = \sum_{i \neq 1} \frac{3}{16\pi} \frac{M_1}{M_i} \frac{\text{Im} \left((\lambda \lambda^\dagger)_{1i} \right)}{|\lambda \lambda^\dagger|_{11}} = \frac{3}{16\pi} \frac{M_1}{v^2} \frac{\sum_i m_i^2 \text{Im} (R_{1i}^2)}{\sum_j m_j |R_{1j}|^2} < \varepsilon_{\text{max}}, \quad (7.29)$$

where the upper limit (for normal ordered neutrino masses) reads [608]

$$\varepsilon_{\text{max}} = \frac{3}{16\pi} \frac{M_1}{v^2} (m_3 - m_1). \quad (7.30)$$

It is worth mentioning that while the small required value of \tilde{m}_1 in (7.14) necessitates small values of $|R_{1i}|^2$, this does not automatically force $|\varepsilon_1|^{\text{hier.}}$ to be tiny, since this quantity depends only on a ratio of squared R -matrix elements. For completeness let us mention that for a degenerate spectrum with $M_3 > M_2 \simeq M_1$ the self-energy graph gets resonantly enhanced and the estimate gets modified as [606]

$$|\varepsilon_1|^{\text{degen.}} = \varepsilon_{\text{max}} \cdot \frac{S_2 \cdot m_3 - m_1}{m_3 - m_1}, \quad \text{where} \quad S_2 \equiv \frac{M_2}{2\Gamma_2} \quad \text{as long as} \quad M_2 - M_1 = \frac{\Gamma_2}{2}. \quad (7.31)$$

We estimate the baryonic asymmetry for a general value of ε_1

$$\frac{n_B}{s} \simeq 0.15 \cdot \frac{\sqrt{\tilde{m}_1 M_{\text{pl.}}}}{v} \cdot \varepsilon_1 \cdot \omega, \quad (7.32)$$

$$\simeq 8.75 \times 10^{-11} \cdot \sqrt{\frac{\tilde{m}_1}{2 \times 10^{-7} \text{ eV}}} \cdot \left(\frac{\varepsilon_1 \cdot \omega}{2.4 \times 10^{-8}} \right), \quad (7.33)$$

where we chose \tilde{m}_1 for matter domination according to (7.15). One can compute the observed n_B/s from the baryon-to-photon-ratio in (7.1) by making use of $s \simeq 7.04 n_\gamma$. The required mass M_1 for the hierarchical spectrum can be obtained from (7.30)

$$M_1 \gtrsim 2.44 \times 10^8 \text{ GeV} \cdot \left(\frac{n_B/s}{8.75 \times 10^{-11}} \right) \cdot \sqrt{\frac{2 \times 10^{-7} \text{ eV}}{\tilde{m}_1}} \cdot \left(\frac{0.05 \text{ eV}}{m_3 - m_1} \right) \cdot \left(\frac{1}{\omega} \right) \quad (7.34)$$

and depends intimately on the details of the active neutrino mass spectrum. Note that unlike the usual Davidson-Ibarra bound $M_1 \gtrsim 10^9$ GeV [608] our estimate depends on the parameter \tilde{m}_1 due to the entropy produced in the RHN decay. It is not surprising that this bound can be slightly lower than the Davidson-Ibarra limit, as the out-of-equilibrium RHN abundance at $T_{\text{dec.}}$ can be larger than the typically assumed relativistic thermal yield. Fitting M_1, \tilde{m}_1 to the baryon asymmetry of the universe leads to $T_{\text{dec.}} \gtrsim 3.3 \times 10^6$ GeV [821] and the condition $M_1 > T_{\text{dec.}}$ is always satisfied for the range of \tilde{m}_1 we consider (see the discussion above (7.15)). It is important to point out that our present treatment ignores flavour effects [611,822--824] such as the charged lepton Yukawa interactions being fast compared to the Hubble scale at different temperatures. These effects can change the asymmetry and consequently the Davidson-Ibarra bound by order one numbers [824] and are expected to be most relevant in the strong washout regime $\tilde{m}_1 > 10^{-3}$ eV [822] not applicable here. Now let us take into account the washout of the asymmetry instantaneously produced at $T_{\text{dec.}}$. Because the universe transitions back to a second phase of radiation domination at $T_{\text{dec.}}$, we can reuse the standard estimates for washout. Since the inverse decay requires an on-shell N_1 it gets Boltzmann-suppressed and scales as [619]

$$\Gamma_{\text{ID}} \sim \Gamma_1 e^{-\frac{M_1}{T}}. \quad (7.35)$$

Consequently for $T < T_{\text{dec.}} < M_1$ we can neglect the washout from inverse decays. That leaves the scattering processes $LL \leftrightarrow H^\dagger H^\dagger$ and $LH \leftrightarrow \bar{L}H^\dagger$ via intermediate RHNs N_j ($j = 1, 2, 3$). Here one does not include the resonant contribution from on-shell N_1 , as they are already included in the decay term of the Boltzmann equations [303] and the masses of $N_{2,3}$ are not kinematically accessible. For $T \ll M_1$ the scattering term can be expressed as [619]

$$\Delta W \equiv \frac{2 \times 10^{-6}}{z^2} \cdot \left(\frac{M_1}{2.5 \times 10^8 \text{ GeV}} \right) \cdot \left(\frac{\overline{m}_\nu}{0.05 \text{ eV}} \right)^2, \quad (7.36)$$

where

$$z \equiv \frac{M_1}{T}, \quad \text{and} \quad \overline{m}_\nu \equiv \sqrt{3m_1^2 + 2\Delta m_{\text{sol.}}^2 + \Delta m_{\text{atm.}}^2} \quad (7.37)$$

implying

$$\omega \simeq \exp \left(- \int_{z_{\text{dec.}}}^{\infty} dz \Delta W \right) \quad (7.38)$$

$$\simeq \exp \left(-2.7 \times 10^{-9} \cdot \left(\frac{M_1}{2.5 \times 10^8 \text{ GeV}} \right) \cdot \left(\frac{\overline{m}_\nu}{0.05 \text{ eV}} \right)^2 \cdot \sqrt{\frac{\tilde{m}_1}{2 \times 10^{-7} \text{ eV}}} \right). \quad (7.39)$$

In the above we used equations (7.16) and (7.17) for the sum of neutrino masses \overline{m}_ν . This process is negligible, if the absolute value of the exponent is $\lesssim 0.1$ [825], which corresponds to the bound

$$M_1 < 2.3 \times 10^{16} \text{ GeV} \cdot \left(\frac{0.05 \text{ eV}}{\overline{m}_\nu} \right)^2 \cdot \sqrt{\frac{2 \times 10^{-7} \text{ eV}}{\tilde{m}_1}}, \quad (7.40)$$

compatible with the findings of [303], indicating that our parameter space (see (7.34)) will be save from any kind of washout: $\omega \simeq 1$.

■ ADDENDUM: We corrected a typo in the above expressions compared to the published version, which erroneously contained a factor of \overline{m}_ν instead of the correct \overline{m}_ν^2 , which marginally changes the bound on M_1 from 9×10^{15} GeV to 2.3×10^{16} GeV without affecting our conclusions. ■

7.4.4 Dark Matter and Dark Radiation Co-genesis

Dark Matter could be included in Seesaw models via a lightest RHN with keV-scale masses [428, 429] produced via either active-to-sterile oscillations [282, 283] or gauge interactions [301]. The neutrino mass mediated by a keV-scale N_1 as DM is expected to be smaller than $\mathcal{O}(10^{-5}$ eV) [428]. Since then N_2 would have to play the role of the decaying particle for Leptogenesis and we would have to require the associated effective neutrino mass to be below $\mathcal{O}(10^{-7}$ eV) for matter domination (see (7.15)), we would not be able to explain both of the observed neutrino mass splittings in (7.16) and (7.17). Consequently we consider an additional particle as the DM. The out-of-equilibrium decay of a heavy N_1 to this particle might then populate the dark matter abundance. A schematic model for this purpose consists of adding a gauge singlet Majorana fermion ψ and a real singlet scalar σ , either of which (or both) could play the role of dark matter a priori. This approach was first considered in reference [795] for the context of asymmetric dark matter and later in [796] for the case of CP-conserving decays to DM. The relevant couplings are

$$\mathcal{L} \supset y N\sigma\psi + m_\psi \overline{\psi}^c \psi + V(H, \sigma). \quad (7.41)$$

For the sake of minimality we assumed that ψ is a Majorana fermion. It might as well be a Dirac fermion, if we were to introduce a vector-like partner for it. We assume a general renormalizable scalar potential $V(H, \sigma)$ for the real scalar σ and that $M_1 \gg m_\psi + m_\sigma$. Additionally all portal couplings are presumed to be small enough to prevent thermal abundances of ψ, σ in the early universe. The decay width of N_1 to $\psi\sigma$ reads

$$\Gamma_\psi \equiv \Gamma(N_1 \rightarrow \psi\sigma) = \frac{|yy^\dagger|_{11}}{16\pi} M_1, \quad (7.42)$$

where the factor of 1/2 compared to (7.8) arises because this decay has singlets and not doublets in the final state. We define

$$\text{BR}_\psi = \frac{\Gamma_\psi}{\Gamma_1 + \Gamma_\psi} \quad \text{and} \quad \text{BR}_L = \frac{\Gamma_1}{\Gamma_1 + \Gamma_\psi}. \quad (7.43)$$

The discussion in section 7.4.2 assumed that Γ_1 was the leading decay mode of N_1 determining the temperature $T_{\text{dec.}}$ at the end of the matter dominated phase in (7.14).

7.4 Appendix: Decays of a long-lived RHN

Generally speaking this temperature should be calculated from $\text{Max}[\Gamma_1, \Gamma_\psi]$ instead. In order to use the parameter region from section 7.4.2 we will set $\text{BR}_L \geq \text{BR}_\psi$. In the following we will assume that ψ is the DM, because as long as σ does not receive a vev [795] it has only a suppressed decay mode to $\nu_L \sigma$ for $m_\psi > m_\sigma$ via $\nu_L - N$ mixing, that will be discussed in a moment. Its yield is different from the typical Freeze-in approach [82, 826] since the decaying RHN is not in thermal equilibrium with the rest of the bath anymore. It also differs from the super-WIMP [307], because the RHN is relativistic at decoupling unlike the non-relativistic WIMP that decays to DM. For our case one finds [794, 827]

$$\frac{n_\psi}{s} = \text{BR}_\psi \frac{n_N}{s} = \frac{3}{4} \text{BR}_\psi \frac{T_{\text{dec.}}}{M_1}, \quad (7.44)$$

from which we deduce that

$$\Omega_\psi h^2 \simeq 0.12 \cdot \left(\frac{m_\psi}{170 \text{ keV}} \right) \cdot \left(\frac{\text{BR}_\psi}{5 \times 10^{-4}} \right) \cdot \sqrt{\frac{\tilde{m}_1}{2 \times 10^{-7} \text{ eV}}}. \quad (7.45)$$

One can see that the DM abundance only constraints the product $m_\psi \text{BR}_\psi$ and we use it as a free parameter in the upcoming sections about gravitational waves instead of just m_ψ . For small branching fractions our scenario leads to light dark matter. Fermionic DM is only gravitationally bound to the DM halo of our galaxy if $m_\psi \gtrsim \mathcal{O}(100 \text{ eV})$ [828]. In order to comply with bounds from structure formation, that constrain the free-streaming scale of dark matter, we have to demand that [243]

$$m_\psi \gtrsim \mathcal{O}(10 \text{ keV}). \quad (7.46)$$

Both of these constraints illustrate why we need $\text{BR}_\psi \ll \text{BR}_L$, which translates to $y_1 \ll \lambda_{1i}$. In the regime $m_\sigma < m_\psi$ the following decay from $\nu_L - N_{1,2,3}$ mixing after electroweak symmetry breaking becomes kinematically allowed [829] and we assume that $m_\sigma \ll m_\psi$:

$$\Gamma(\psi \rightarrow \nu_L \sigma) = \frac{|yy^\dagger|_{11}}{16\pi} \sum_{i,j} \frac{\lambda_{ji} \lambda_{ij}^\dagger}{M_j^2} \frac{v^2}{m_\psi} \simeq \frac{m_\psi \text{BR}_\psi}{8\pi} \frac{\tilde{m}_1 \sum_i m_i}{v^2} \frac{M_1}{M_{2,3}} \quad (7.47)$$

Here we summed over the final state lepton flavors, which together with the sum over all three RHNs and making the approximation of factoring out one power of $M_{2,3}$, allows us to trade the λ -couplings of the active neutrino masses via the Seesaw-relation (7.5). Equation (7.43) lets us trade the y -couplings for BR_ψ and \tilde{m}_1 in the limit $\text{BR}_\psi \ll \text{BR}_L$. Data on baryon acoustic oscillations and structure formation requires a lifetime $\tau_\psi = 1/\Gamma(\psi \rightarrow \nu_L \sigma)$ for DM decaying to dark radiation of $\tau_\psi > (249.6 - 268.8) \times 10^9 \text{ yr}$ [89] depending on the exact dataset used. The resulting bound for $\tau_\psi > 250 \times 10^9 \text{ yr}$ reads

$$m_\psi \text{BR}_\psi < 1.8 \times 10^{-2} \text{ eV} \cdot \left(\frac{2 \times 10^{-7} \text{ eV}}{\tilde{m}_1} \right) \cdot \left(\frac{0.05 \text{ eV}}{\sum_i m_i} \right) \cdot \left(\frac{M_{2,3}/M_1}{3} \right) \quad (7.48)$$

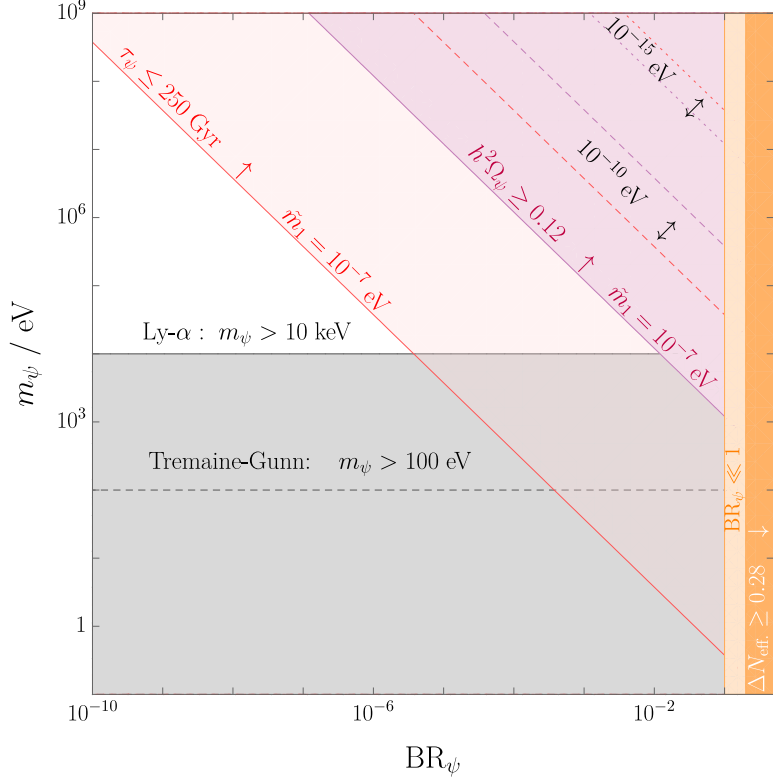


Figure 7.1: Parameter space for the dark matter mass m_ψ versus the branching ratio BR_ψ of the RHN decay to dark matter. Contours with (straight, dashed, dotted) lines correspond to $\tilde{m}_1 = (10^{-7}, 10^{-10}, 10^{-15})$ eV. The purple contours reproduce the observed dark matter relic abundance and above the contour the abundance would be too large (for fixed \tilde{m}_1). The gray regions are excluded because of unsuccessful structure formation (Lyman- α) and dark matter not being gravitationally bound (Tremaine-Gunn). On the red contours for the DM lifetime from $\psi \rightarrow \nu_L \sigma$ is equal to the observational limit and in the colored region above (for fixed \tilde{m}_1) the lifetime would be too small. This excludes the lines with $\tilde{m}_1 = (10^{-7}, 10^{-10})$ eV, meaning that here only $\tilde{m}_1 = 10^{-15}$ eV is viable for DM. Note that lifetime bound disappears for $m_\psi < m_\sigma$, in which case the entire purple region is allowed. The area in light orange is excluded by our assumption $BR_\psi \ll BR_L \simeq 1$ and the orange region would be excluded, if the real scalar also produced in the RHN decay was stable and light enough to be dark radiation (see the discussion below (7.53)).

and is compatible with the relic density (7.45) for

$$\tilde{m}_1 < 9.7 \times 10^{-15} \text{ eV} \cdot \left(\frac{0.12}{\Omega_\psi h^2} \right)^2. \quad (7.49)$$

We depict the allowed parameter space in figure 7.1. Once can see that the parameters $\tilde{m}_1 = (10^{-7}, 10^{-10})$ eV violate the lifetime constraint, because for each constant \tilde{m}_1 the purple relic abundance iso-contour line is above the red line for $\tau_\psi = 250 \times 10^9$ yr. The only viable parameter point in this plot has $\tilde{m}_1 = 10^{-15}$ eV in agreement with (7.49), because here the lifetime iso-contour is above the line for the relic density and we find dark matter close to the GeV-scale. The previous limits only apply for $m_\psi > m_\sigma$. In general the scalar σ couples to the SM Higgs through the following terms

$$V(H, \sigma) \supset \lambda_{\sigma H} \sigma^2 |H|^2 + (\kappa \sigma + \text{h.c.}) |H|^2. \quad (7.50)$$

For $m_\sigma > m_h$ it could decay to the SM Higgs. If this is kinematically forbidden, there could be decay modes lighter SM fermions such as *e.g.* the electron $\sigma \rightarrow e^+ e^- e^+ e^-$ via off-shell SM Higgs bosons. In case σ has no vev these decays require the κ coupling. If σ is too light to decay to SM states or the couplings $\lambda_{H\sigma}$ and κ are very small, then the relic abundance of σ survives until today. In this case and assuming that $\lambda_{H\sigma}$ and κ are small enough to avoid thermalization with the SM plasma, the non-thermal σ could still exist in the form of dark radiation. Its energy density is found from $n_\sigma = n_\psi = \text{BR}_\psi n_N$ to be [830]

$$\rho_\sigma(T_{\text{dec.}}) = \frac{\pi^2}{30} g_*(T_{\text{dec.}}) \text{BR}_\psi \frac{\sqrt{m_\sigma^2 + \left(\frac{M_1}{2}\right)^2}}{M_1} T_{\text{dec.}}^4. \quad (7.51)$$

and we compute the abundance of dark radiation, conventionally parameterized as the number of additional neutrinos as [74] assuming again that $M_1 \gg m_\sigma$:

$$\Delta N_{\text{eff.}} = \frac{4}{7} \cdot g_{*\rho}(T_{\text{dec.}}) \cdot \left(\frac{10.75}{g_{*S}(T_{\text{dec.}})} \right)^{\frac{4}{3}} \cdot \frac{\rho_\sigma(T_{\text{dec.}})}{\rho_{\text{SM}}(T_{\text{dec.}})} \quad (7.52)$$

$$\simeq 0.06 \cdot \left(\frac{\text{BR}_\psi}{4\%} \right) \cdot \left(\frac{106.75}{g_{*S}(T_{\text{dec.}})} \right)^{\frac{4}{3}} \cdot \left(\frac{g_*(T_{\text{dec.}})}{106.75} \right) \quad (7.53)$$

We see that σ would lead to too much dark radiation compared with the current Planck bound $\Delta N_{\text{eff.}}^{\text{Planck+BAO}} \simeq 0.28$ [20] unless we make the branching ratio BR_ψ , which also controls the DM production, smaller than about 20% (see figure 7.1). However we saw previously that BR_ψ can be far below a percent for heavy enough DM, which is why we do not necessarily expect observable dark radiation. BBN sets a bound of $\Delta N_{\text{eff.}}^{\text{BBN}} \simeq 0.4$ [831]. The projected sensitivities of upcoming experiments read $\Delta N_{\text{eff.}}^{\text{proj.}} = 0.014$ for CMB-HD [832], $\Delta N_{\text{eff.}}^{\text{proj.}} = 0.05$ for CMB-Bharat [833], $\Delta N_{\text{eff.}}^{\text{proj.}} = 0.06$ for CMB Stage IV [332, 333] and NASA's PICO mission [335] or $\Delta N_{\text{eff.}} \lesssim 0.12$ for CORE [336], the South Pole Telescope [330] as well as the Simons observatory [331]. Before closing let us emphasize again that σ only counts as dark radiation when it is very light and stable or long-lived.

7.5 Appendix: Gravitational Waves

7.5.1 Distortion of the inflationary tensor mode spectrum

We assume primordial inflation ended in an epoch of reheating, creating a Standard Model plasma of radiation with an initial temperature T_{RH} set by the reheating dynamics. Gravitational waves produced during inflation first leave the horizon and have constant amplitudes while outside the horizon. After they re-enter the horizon the amplitude becomes damped. The power spectrum of gravitational waves (GWs) today can be written as a function of the wave-number $k = 2\pi f$ with f being the frequency

$$\Omega_{\text{GW}}(k) = \frac{1}{12} \left(\frac{k}{a_0 H_0} \right)^2 P_T(k), \quad (7.54)$$

where $a_0 = 1$ and $H_0 \simeq 2.2 \times 10^{-4} \text{ Mpc}^{-1}$ [834] are the scale factor and expansion rate today and P_T denotes the spectrum of tensor modes. It is parameterized in terms of the primordial power spectrum from inflation $P_T^{\text{prim.}}$

$$P_T(k) = T_T^2(k) P_T^{\text{prim.}}(k) \quad (7.55)$$

as well as a transfer function $T_T^2(k)$. This transfer function describes the propagation of GWs h_{ij} in the Friedmann-Lemaitre-Robertson-Walker background

$$h_{ij}'' + 2aHh_{ij}' - \Delta h_{ij} = 0, \quad (7.56)$$

where primes denote derivatives with respect to conformal time, after the horizon re-entry at a temperature of T_{in} that depends on the wave-number via [780]

$$T_{\text{in}} = 5.8 \times 10^6 \text{ GeV} \cdot \left(\frac{106.75}{g_*(T_{\text{in}})} \right)^{\frac{1}{6}} \left(\frac{k}{10^4 \text{ Mpc}^{-1}} \right). \quad (7.57)$$

The inflationary tensor power spectrum is conventionally parameterized in terms of its amplitude A_T and its spectral index n_T at the pivot scale $k_* = 0.05 \text{ Mpc}^{-1}$ [353]

$$P_T^{\text{prim.}}(k) = A_T(k_*) \left(\frac{k}{k_*} \right)^{n_T}. \quad (7.58)$$

This amplitude is related to the scalar power spectrum $P_\xi(k_*) = 2.0989 \times 10^{-9}$ [353] via the tensor-to-scalar-ratio $r < 0.035$ [835]

$$A_T(k_*) = r P_\xi(k_*). \quad (7.59)$$

Observations of the cosmic microwave background only constrain the scalar spectral index to be $n_S = 0.9649 \pm 0.0042$ [353], which is why we take n_T as a constant free parameter. The case of $n_T > 0$ (< 0) is known as a blue-tilted (red-tilted) spectrum. Standard single field slow-roll inflation predicts a red-tilted spectrum, as the tensor spectral index n_T satisfies the so-called consistency relation $n_T = -r/8$ [836], however

this does not rule out the possibilities of a blue-tilted spectrum, which is well motivated in various scenarios including *e.g.* string gas cosmology [837], super-inflation models [838], G-inflation [839], non-commutative inflation [840, 841], particle production during inflation [842, 843], and several others [844]. Here we will also seek to investigate such scenarios from the perspective of models of the early universe and Leptogenesis.

■ ADDENDUM: Saturating the current limit on r leads to $n_T = -4 \times 10^{-3}$ for single field inflation. Visually the corresponding plots are pretty much indistinguishable from the case of $n_T = 0$. ■

An epoch of early or intermediate matter domination would change the transfer function compared to the standard case of radiation domination, and hence the expansion of the background is imprinted in the damping of the gravitational wave amplitude. References [774, 780, 781, 845--847] computed this transfer function numerically and found a compact analytical expression with a fitting function $F(k)$

$$T_T^2(k) = \Omega_m^2 \left(\frac{g_*(T_{\text{in}})}{g_*^0} \right) \left(\frac{g_{*S}^0}{g_{*S}(T_{\text{in}})} \right)^{\frac{4}{3}} \left(\frac{3j_1(z_k)}{z_k} \right)^2 F(k) \quad (7.60)$$

in terms of the total matter density $\Omega_m = 0.31$, the first spherical Bessel function $j_1(z_k)$ and $z_k \equiv k \tau_0$ with $\tau_0 = 2/H_0$ [834] being the conformal time today. The factors of the relativistic degrees of freedom encode the expansion of the universe and we use the fitting functions of reference [847] for $g_*(T_{\text{in}})$ and $g_{*S}(T_{\text{in}})$ with the present day values $g_*^0 = 3.36$ and $g_{*S}^0 = 3.91$, whereas the Bessel function describes the damping of the gravitational wave amplitude after horizon re-entry. In the limit $z_k \gg 1$, which always holds for the frequencies we are interested in,

$$k \tau_0 \simeq 6 \times 10^{15} \left(\frac{f}{10^{-3} \text{ Hz}} \right), \quad (7.61)$$

we can trade the oscillatory $j_1(z_k)$ for $1/(\sqrt{2}z_k)$. Note that in references [781, 847] the correct limiting behavior was mentioned for the wrong limit $z_k \ll 1$ (for which one would obtain $j_1(z_k) \sim z_k$ instead). We employ the most recent results of [847] for the fitting function $F(k)$. Without intermediate matter domination it reads

$$F(k)_{\text{standard}} = T_1^2 \left(\frac{k}{k_{\text{eq.}}} \right) T_2^2 \left(\frac{k}{k_{\text{RH}}} \right), \quad (7.62)$$

whereas including an epoch of RHN domination leads to

$$F(k)_{\text{IMD}} = T_1^2 \left(\frac{k}{k_{\text{eq.}}} \right) T_2^2 \left(\frac{k}{k_{\text{dec.}}} \right) T_3^2 \left(\frac{k}{k_{\text{dec. S}}} \right) T_2^2 \left(\frac{k}{k_{\text{RH S}}} \right). \quad (7.63)$$

Here we introduce

$$k_{\text{eq.}} = 7.1 \times 10^{-2} \text{ Mpc}^{-1} \cdot \Omega_m h^2, \quad (7.64)$$

$$k_{\text{dec.}} = 1.7 \times 10^{14} \text{ Mpc}^{-1} \left(\frac{g_{*S}(T_{\text{dec.}})}{g_{*S}^0} \right)^{\frac{1}{6}} \left(\frac{T_{\text{dec.}}}{10^7 \text{ GeV}} \right), \quad (7.65)$$

$$k_{\text{RH}} = 1.7 \times 10^{14} \text{ Mpc}^{-1} \left(\frac{g_{*S}(T_{\text{RH}})}{g_{*S}^0} \right)^{\frac{1}{6}} \left(\frac{T_{\text{RH}}}{10^7 \text{ GeV}} \right), \quad (7.66)$$

$$k_{\text{dec. S}} = k_{\text{dec.}} \Delta^{\frac{2}{3}}, \quad (7.67)$$

$$k_{\text{RH S}} = k_{\text{RH}} \Delta^{-\frac{1}{3}}, \quad (7.68)$$

where all quantities with a subscript (superscript) “0” are evaluated today and we set $h = 0.7$. The entropy dilution factor Δ was defined in (7.27) and the fit functions read

$$T_1^2(x) = 1 + 1.57x + 3.42x^2, \quad (7.69)$$

$$T_2^2(x) = (1 - 0.22x^{\frac{3}{2}} + 0.65x^2)^{-1}, \quad (7.70)$$

$$T_3^2(x) = 1 + 0.59x + 0.65x^2. \quad (7.71)$$

Physically T_1 describes the transition from a radiation dominated phase to a matter dominated epoch and T_2 the case of going from matter domination to radiation domination. T_3 has the same physical interpretation as T_1 but allows for a better numerical fit [847]. One deduces from the wave-number $k_{\text{dec.}} = 2\pi f_{\text{sup.}}$ at the time of RHN decay in (7.65) that the gravitational wave spectrum gets suppressed by the entropy dilution for frequencies above

$$f_{\text{sup.}} \simeq 2.7 \times 10^{-10} \text{ Hz} \left(\frac{T_{\text{dec.}}}{10 \text{ MeV}} \right), \quad (7.72)$$

$$\simeq 9 \times 10^{-2} \text{ Hz} \cdot \left(\frac{n_B/s}{8.75 \times 10^{-11}} \right) \cdot \left(\frac{0.05 \text{ eV}}{m_3 - m_1} \right) \cdot \left(\frac{106.75}{g_*(T_{\text{dec.}})} \right)^{\frac{1}{4}}, \quad (7.73)$$

where in the last line we fixed M_1 via equation (7.34) to reproduce the observed baryon asymmetry, which means that all the RHN decay at $T_{\text{dec.}} = 3.3 \times 10^6 \text{ GeV}$ hence the constant $f_{\text{sup.}}$. The suppression factor of the power spectrum is [770]

$$R_{\text{sup.}} = \frac{\Omega_{\text{GW}}^{\text{IMD}}}{\Omega_{\text{GW}}^{\text{standard}}} \simeq \frac{1}{\Delta^{\frac{4}{3}}}, \quad (7.74)$$

which depends only on \tilde{m}_1 via Δ in (7.28). Here $\Omega_{\text{GW}}^{\text{IMD}}$ was computed from (7.63) and takes the intermediate matter domination (IMD) from the RHN into account, whereas $\Omega_{\text{GW}}^{\text{standard}}$ from (7.62) appears in the absence of RHN domination.

7.5.2 Other GW sources

So far, when it comes to gravitational waves, most studies involving the Seesaw mechanism have focused on the dynamics of *e.g.* the $U(1)_{\text{B-L}}$ breaking, which underlies the RHN

Majorana masses in unified gauge theories [24,573]. The dynamics of the scalar responsible for breaking this gauge symmetry can source a separate stochastic gravitational wave background by means of a first order [745, 746, 748, 749] or second order [744, 747, 750] phase transition as well as via the formation of a network of cosmic strings [743, 750--752] via the Kibble mechanism [848]. If the phase transition or the formation of topological defects happens before inflation - and the symmetry is never (non-)thermally restored - any trace of the B-L transition will be diluted away due to the exponential expansion of space-time. The symmetry is broken throughout inflation and reheating if [849]

$$v_{\text{B-L}} > \text{Max} \left[\frac{H_I}{2\pi}, T_{\text{max.}} \right], \quad (7.75)$$

where the first term is the Gibbons-Hawking temperature [850] in terms of the Hubble rate during inflation H_I and the second term the maximum temperature during reheating [816--818], which can be drastically larger than the temperature of the radiation bath at the end of reheating T_{RH} . Since $T_{\text{max.}}$ depends on the reheating scenario, the best we can do to get an estimate on $v_{\text{B-L}}$ is to assume that $H_I/(2\pi) > T_{\text{max.}}$ and saturate the current CMB-limit on $H_I \lesssim 2.5 \times 10^{14} \text{ GeV}$ [77] leading to

$$v_{\text{B-L}} \gtrsim 4 \times 10^{13} \text{ GeV}. \quad (7.76)$$

This further motivates why we consider high scale Leptogenesis. Moreover this bound is compatible with the condition (7.24) for a thermalized population of N_1 from B-L gauge scatterings. Also note that one could even consider a case, where no additional degrees of freedom except the RHN are added to the SM below the Planck scale, so that there would be no source for the stochastic GW background (in this case the initial thermal RHN abundance would have to come from inflaton decays). Consequently our high scale scenario without a stochastic GW background, being essentially independent of the dynamics of the $\text{U}(1)_{\text{B-L}}$ transition and the associated scalar, can be viewed as complementary to the existing analyses.

7.5.3 Detectors and signal-to-noise ratio

We display the (expected) sensitivity curves for a variety of existing and proposed experiments that can be grouped in terms of

- **ground based interferometers:** LIGO/VIRGO [851--856], aLIGO/aVIRGO [857--860], AION [861--864], EINSTEIN TELESCOPE (ET) [865, 866], COSMIC EXPLORER (CE) [867, 868],
- **space based interferometers:** LISA [869, 870], BBO [871--873], DECIGO, U-DECIGO [774, 874--878], AEDGE [861, 879], μ -ARES [880]
- **recasts of star surveys:** GAIA/THEIA [881],
- **pulsar timing arrays (PTA):** SKA [882--884], EPTA [885--887], NANOGRAV [888--892]

- **CMB polarization:** Planck 2018 [77] and BICEP 2/ Keck [893] computed by [894], LITEBIRD [895],
- **CMB spectral distortions:** PIXIE, SUPER-PIXIE [896,897], VOYAGER2050 [898]

Interferometers measure displacements in terms of a so called dimensionless strain-noise $h_{\text{GW}}(f)$ that is related to the GW amplitude and can be converted into the corresponding energy density [881]

$$\Omega_{\text{exp}}(f)h^2 = \frac{2\pi^2 f^2}{3H_0^2} h_{\text{GW}}(f)^2 h^2, \quad (7.77)$$

with $H_0 = h \times 100 \text{ (km/s)/Mpc}$ being the Hubble rate today. We compute the signal-to-noise ratio (SNR) for a given or projected experimental sensitivity $\Omega_{\text{exp}}(f)h^2$ in order to assess the detection probability of the primordial GW background via the following prescription [899, 900]

$$\text{SNR} \equiv \sqrt{\tau \int_{f_{\text{min}}}^{f_{\text{max}}} df \left(\frac{\Omega_{\text{GW}}(f)h^2}{\Omega_{\text{exp}}(f)h^2} \right)^2}, \quad (7.78)$$

where $h = 0.7$ and $\tau = 4$ years is the observation time. For this analysis we consider $\text{SNR} \geq 10$ as the detection threshold.

7.5.4 Dark radiation bounds from BBN and CMB decoupling

The energy density in gravitational waves should be smaller than the limit on dark radiation encoded in $\Delta N_{\text{eff.}}$ from Big Bang Nucleosynthesis and CMB observations (see the discussion below (7.53) for bounds and projections on $\Delta N_{\text{eff.}}$) [901]

$$\int_{f_{\text{min}}}^{f=\infty} \frac{df}{f} \Omega_{\text{GW}}(f)h^2 \leq 5.6 \times 10^{-6} \Delta N_{\text{eff.}}. \quad (7.79)$$

The lower limit of the integration is $f_{\text{min}} \simeq 10^{-10} \text{Hz}$ for BBN and $f_{\text{min}} \simeq 10^{-18} \text{Hz}$ for the CMB. In practice, when *e.g.* plotting many GW spectra simultaneously, and as a first estimate we neglect the frequency dependence to constrain the energy density of the peak for a given spectrum

$$\Omega_{\text{GW}}^{\text{Peak}} h^2 \leq 5.6 \times 10^{-6} \Delta N_{\text{eff.}}. \quad (7.80)$$

7.5.5 Impact of free-streaming particles

As shown in the seminal work [902] and expanded upon in *e.g.* [903–906], there is a damping effect on the GW amplitude from free-streaming particles whose mean free path is larger than the Hubble scale. Free streaming particles such as the active neutrinos, the RHN, additional sources of dark radiation or gravitational waves themselves contribute to anisotropic stress-energy tensor and can reduce the primordial GW amplitude by up to 35.6% [902]. In this work we neglect this effect to focus on the damping from the RHN induced matter dominated epoch as a first estimate, since percent level effects will only become relevant once we have actual data.

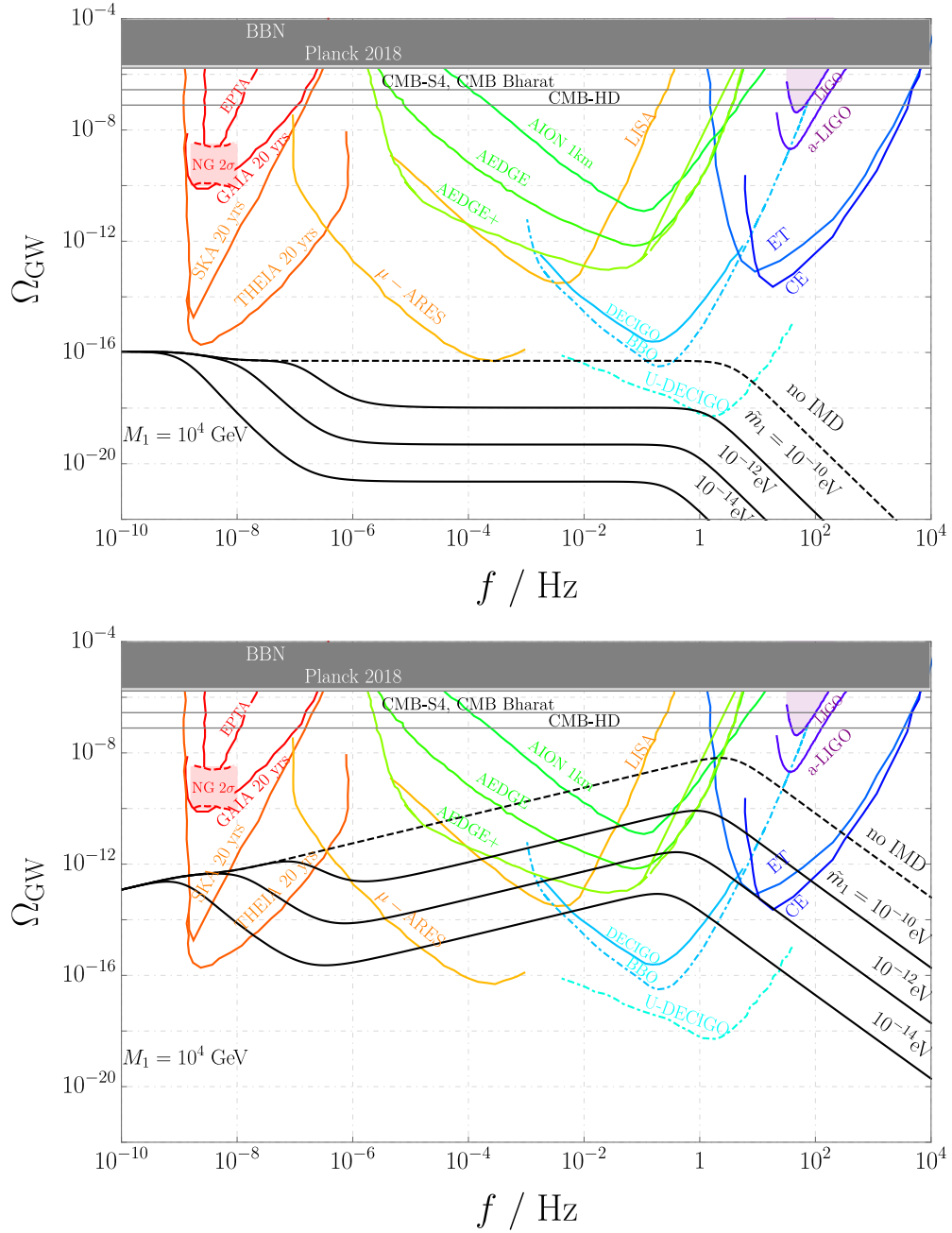


Figure 7.2: Example GW spectra for $T_{\text{RH}} = 10^8 \text{ GeV}$, $M_1 = 10^4 \text{ GeV}$ and $n_T = 0$ (top) as well as $n_T = 0.5$ (bottom). Here we varied $\tilde{m}_1 = (10^{-10}, 10^{-12}, 10^{-14}) \text{ eV}$ and “no IMD” refers to the scenario without RHN domination.

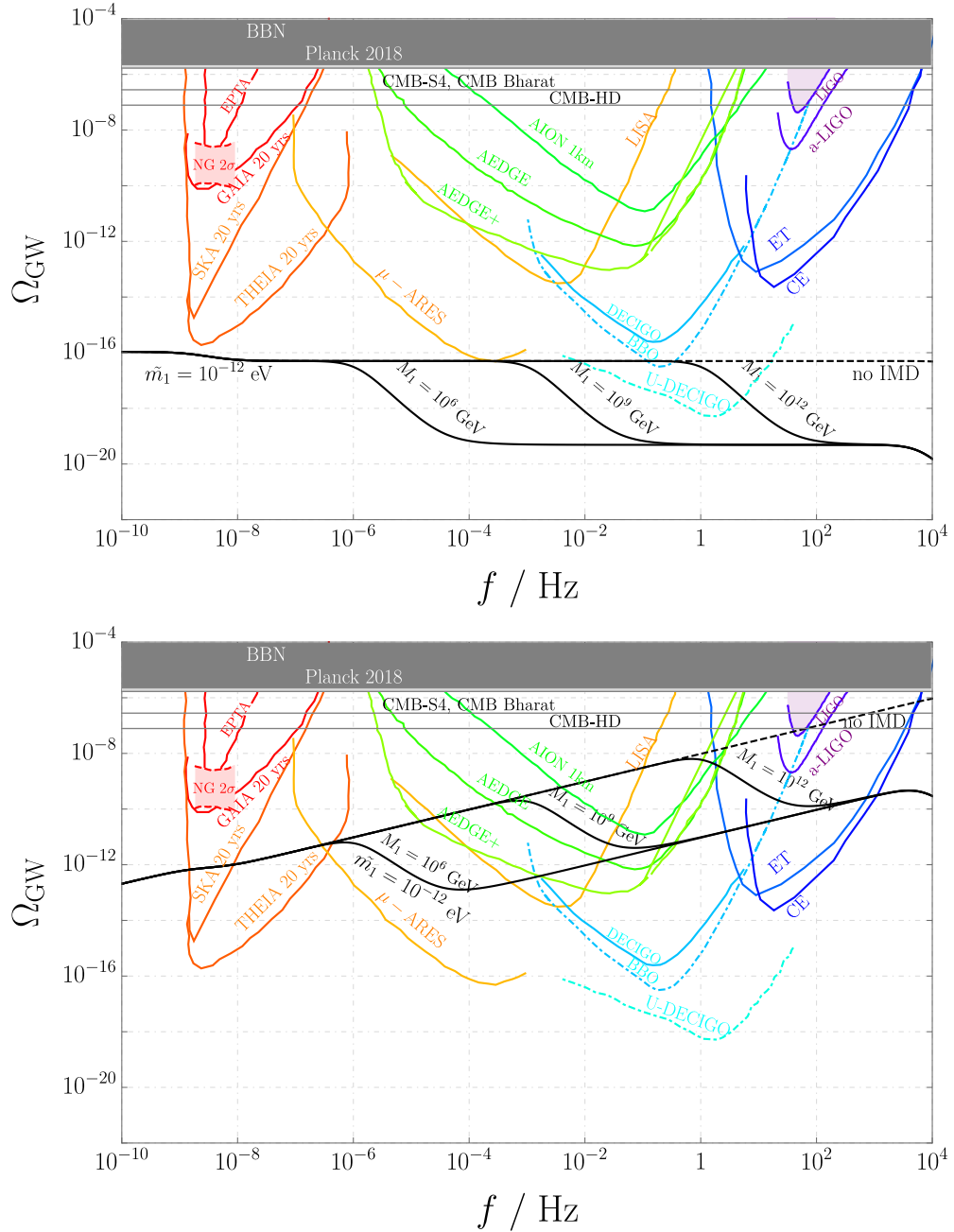


Figure 7.3: Example spectra for $T_{\text{RH}} = 10^{12} \text{ GeV}$, $\tilde{m}_1 = 10^{-12} \text{ eV}$ and $n_T = 0$ (top) as well as $n_T = 0.5$ (bottom). Here we varied $M_1 = (10^6, 10^9, 10^{12}) \text{ GeV}$ and “no IMD” refers to the scenario without RHN domination.

7.6 Appendix: Results

7.6.1 General results

In the following we fix $r = 0.035$ [835] and vary the reheating temperature as well as M_1, \tilde{m}_1 together with $n_T \geq 0$. We depict some example spectra in figures 7.2 and 7.3, where we reproduced the figures from reference [907]. We depict the constraints from LIGO/VIRGO [851--856] and NANOGRAV [888--892] observations, the CMB as well as BBN as shaded regions in our plots 7.2-7.6. It is important to note that the depicted projection for the sensitivity of U-DECIGO [774, 874--878] is optimistic, but we do not employ the most optimistic case known as U-DECIGO-CORR, which assumes that the noise of the instrument is only given by the irreducible quantum noise [875] and should therefore treated as a hypothetical best case scenario. The proposal for BBO [871--873] is also a bit speculative, because it is supposed to eventually succeed the currently planned LISA mission [869, 870]. To remind the reader of these potential caveats we depict the sensitivities for U-DECIGO and BBO with dashed-dotted lines in the figures 7.2-7.6. The plots in figures 7.4 and 7.5 depict the case where we fix M_1 as function of \tilde{m}_1 according to (7.34) in order to reproduce the observed baryon asymmetry via Leptogenesis. In the aforementioned plot we also depict which values of $m_\psi \text{BR}_\psi$ would be needed according to (7.45) to fit the dark matter relic abundance for a given \tilde{m}_1 . The labels “no IMD” in 7.2, 7.3 and “no intermediate matter dom.” in 7.4-7.5 refer to the scenario without RHN domination computed from (7.62), where the only dilution arises from inflationary reheating. One can clearly see in 7.4 and 7.5 that the primordial tensor modes get diluted by the entropy released in the RHN decay for frequencies above $f_{\text{sup.}} \simeq 0.1$ Hz, see (7.73). Furthermore one can observe in 7.4-7.6 that there is second break in the spectra at frequencies larger than $f_{\text{sup.}} \sim T_{\text{dec.}}$. This is due to the inflationary reheating at T_{RH} and since our scenario is defined by the regime $T_{\text{dec.}} < M_1 < T_{\text{RH}}$ the second break occurs at a larger frequency. The same figures also show a small subleading suppression of frequencies larger than $\mathcal{O}(10^{-9}$ Hz), which is due to the entropy released in the QCD phase transition [786]. Irrespective of the value of n_T , one can deduce from 7.2-7.6 that LITEBIRD [895] will already probe the inflationary tensor modes in the $(10^{-16} - 10^{-18})$ Hz range. For $n_T = 0$ we find that U-DECIGO [774, 874--878] has the best chance to distinguish our entropy suppressed spectra from the standard case without RHN domination depicted by the dashed line in 7.4. In case neither BBO [871--873] nor U-DECIGO [774, 874--878] detect the tensor mode background expected from inflation, this does not have to rule out primordial gravitational waves and could be a tell-tale sign of scenarios with entropy dilution, such as ours. In the next section we will analyze this in terms of the SNR. The case of $n_T = 0.5$ without RHN domination would start to be probed by the dark radiation bounds in (7.80) from BBN [831] and Planck [20] (see the dashed line in 7.5) and is only borderline compatible with the existing LIGO/VIRGO [851--856] observations. An attempt to explain the recent anomaly in the 12.5-year dataset [892] of the NANOGRAV collaboration [888--891] with primordial tensor modes would require an extremely large $n_T \simeq 0.85$. The challenge is then to have enough entropy dilution to comply with the dark radiation and LIGO/VIRGO bounds. We

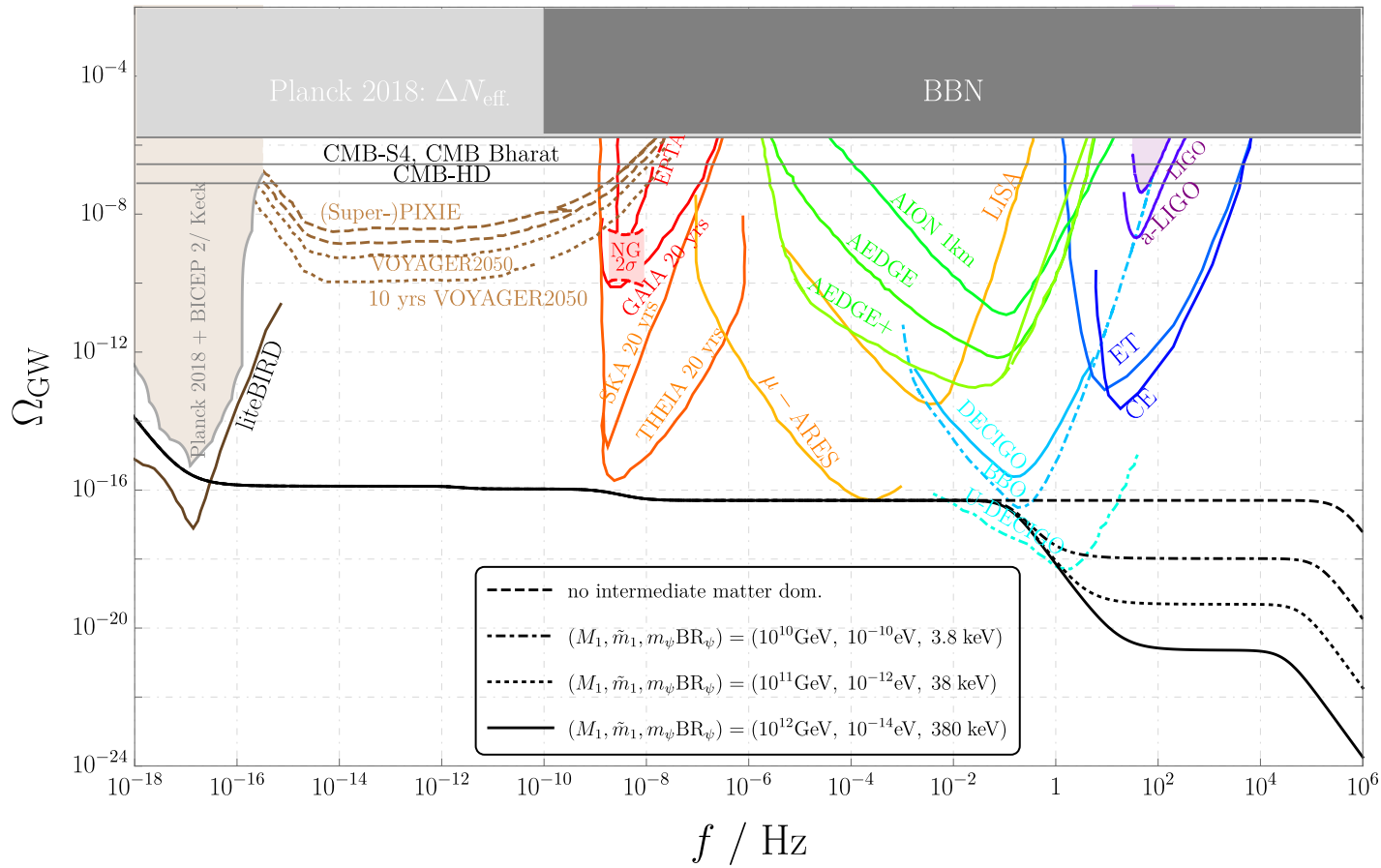


Figure 7.4: We fix M_1 as a function of $\tilde{m}_1 = (10^{-10}, 10^{-12}, 10^{-14})$ eV for successful Leptogenesis and set $T_{\text{RH}} = 10^{13}$ GeV, $n_T = 0$. Furthermore we show which value of $m_\psi \text{BR}_\psi$ would be required for a given \tilde{m}_1 to generate the observed dark matter relic abundance.

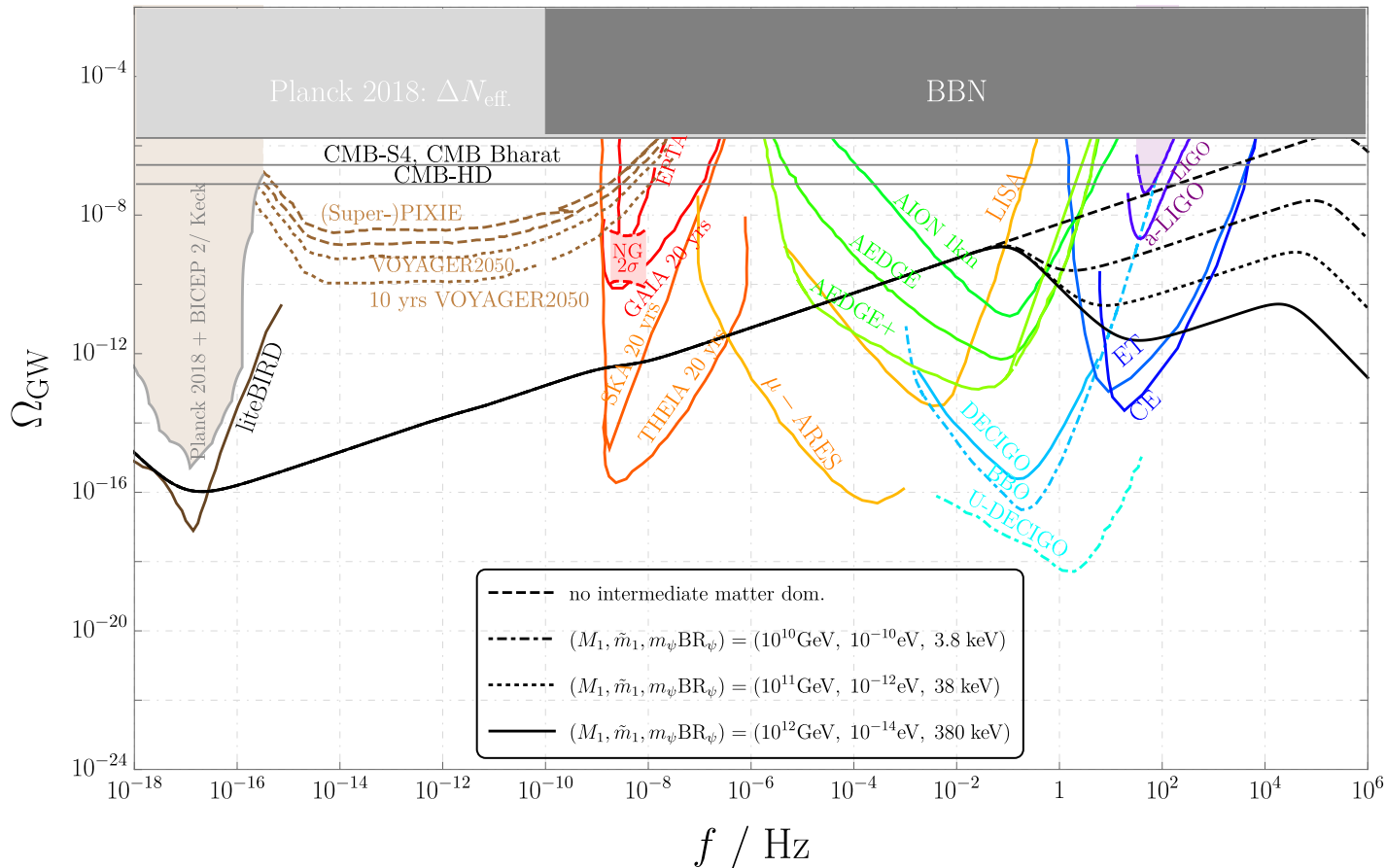


Figure 7.5: We fix M_1 as a function of $\tilde{m}_1 = (10^{-10}, 10^{-12}, 10^{-14})$ eV for successful Leptogenesis and set $T_{\text{RH}} = 10^{13}$ GeV, $n_T = 0.5$. Furthermore we show which value of $m_\psi \text{BR}_\psi$ would be required for a given \tilde{m}_1 to generate the observed dark matter relic abundance.

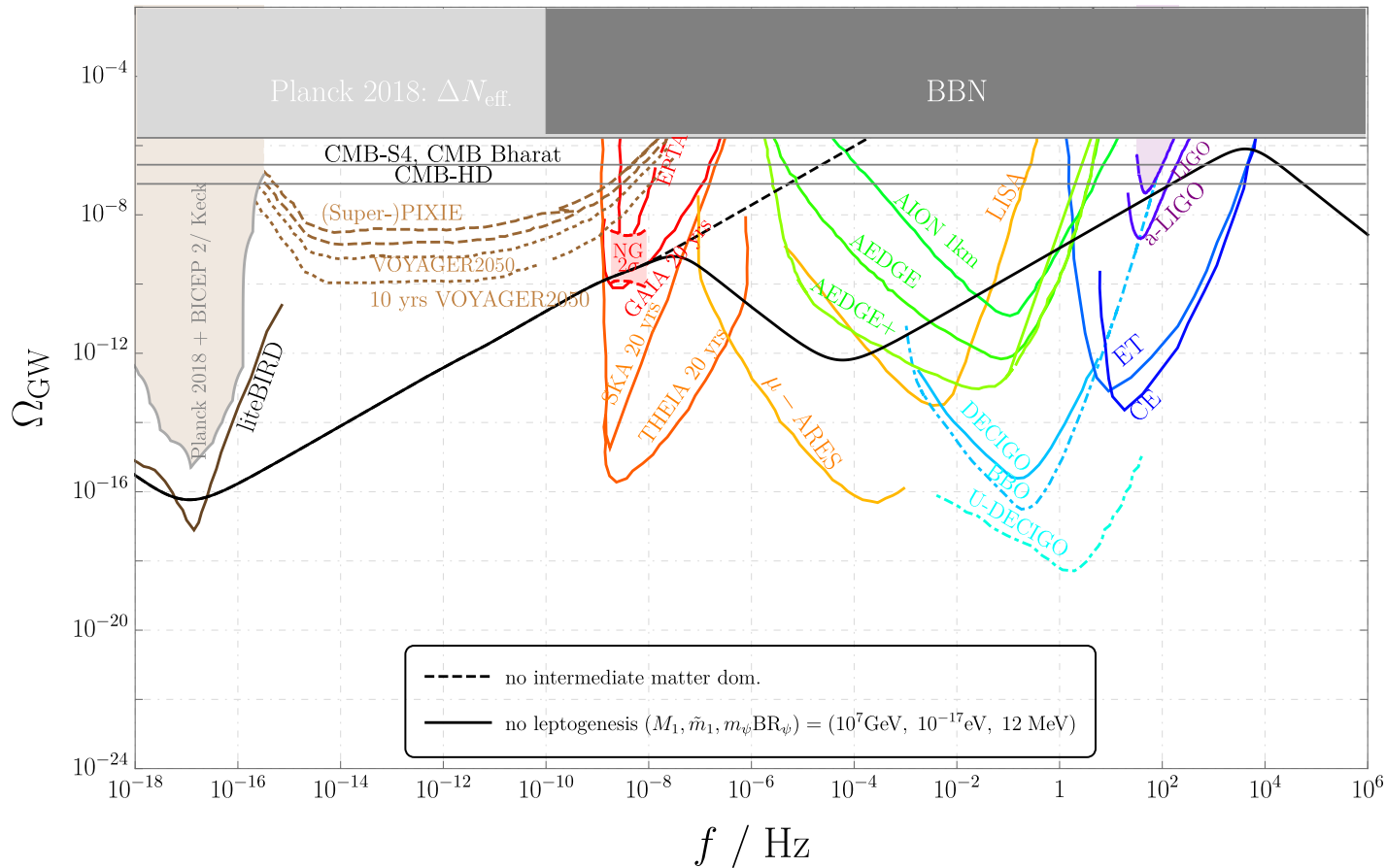


Figure 7.6: We fix $M_1 = 10^7 \text{ GeV}$, $\tilde{m}_1 = 10^{-17} \text{ eV}$, $T_{\text{RH}} = 5 \times 10^{12} \text{ GeV}$ and $n_T = 0.85$ to fit the NANOGRAV anomaly [892]. Furthermore we show the value of $m_\psi \text{BR}_\psi = 12 \text{ MeV}$ required for the given \tilde{m}_1 to generate the observed dark matter relic abundance.

depict a spectrum for $M_1 = 10^7$ GeV, $\tilde{m}_1 = 10^{-17}$ eV that could be the source of the anomaly in figure 7.6 for the case without Leptogenesis. The reason for abandoning Leptogenesis is simply that with such a large n_T the peak of the GW energy density at the typical frequency $f_{\text{sup.}} = 0.1$ Hz (before the dilution kicks in) will already be far too large to comply with the dark radiation bounds. Therefore one needs a spectrum where the damping (which is only proportional to \tilde{m}_1 see (7.74)) occurs at lower decay temperatures and hence lower frequencies (set by both M_1 and \tilde{m}_1 see (7.14)). This is why we chose a value of $M_1 = 10^7$ GeV below the Leptogenesis bound in (7.34). On top of that we set $T_{\text{RH}} = 5 \times 10^{12}$ GeV, so that the GWs at large frequencies beyond LIGO/VIRGO do not come into tension with the dark radiation bound due to the damping from inflationary reheating. These estimates illustrate, why we would need a rather contrived scenario and we do not pursue the aforementioned anomaly further in this work.

7.6.2 Signal-to-noise ratio

We use the SNR defined in (7.78) to determine the region in the M_1 versus \tilde{m}_1 parameter space, where a detection of primordial gravitational waves can be claimed for a SNR threshold of ten over four years of observation time. For $n_T = 0$ we find that BBO [871--873], μ -ARES [880] and U-DECIGO [774, 874--878] are the most relevant experiments that have a chance of probing the primordial GW background, as can be deduced from figure 7.4. For $n_T > 0$ there are a lot more experiments that can probe our GW spectra, which is why we focus on AEDGE [861, 879], BBO [871--873], the EINSTEIN TELESCOPE (ET) [865, 866] and LISA [869, 870]. Of course there are also other currently developed experiments, such as the radio telescope SKA [882--884], that become relevant for $n_T > 0$. The parameter space for $n_T = 0$ was displayed in 7.7, whereas figure 7.8 showcases $n_T = 0.1$, 0.2 and 0.9 the cases of $n_T = 0.3$, 0.5. The region in (7.34) that leads to the observed baryon asymmetry via Leptogenesis was shaded in gray. For $n_T = 0.1$ one can conclude from the left plot in figure 7.8 that the SNR threshold for ET [865, 866] will start to probe the edge of the parameter space for Leptogenesis in the regime $\tilde{m}_1 \lesssim 10^{-11}$ eV. For $n_T > 0$ we see in 7.8-7.9 that AEDGE [861, 879], BBO [871--873] and LISA [869, 870] probe the entire parameter space for Leptogenesis. We impose the following constraints in figures 7.7-7.9: Successful BBN requires that the RHN decay temperature in (7.14) is at least 10 MeV [244, 245], which was depicted as a brown region. RHN with masses above 10^{14} GeV could destabilize the electroweak vacuum [908, 909]. We do not show the bound $M_1 \lesssim 10^7$ GeV [910--913] from the naturalness of the Higgs mass under corrections from its couplings to the RHN, as it would basically exclude our entire parameter space in (7.34). The last bound comes from the observed neutrino masses: Due to the perturbativity of the RHN Yukawa coupling $\lambda_{ij} < \sqrt{4\pi}$ and the need to reproduce at least one mass eigenstate with $m_\nu = 0.05$ eV we find that $M_2 \lesssim 3.8 \times 10^{15}$ GeV. This together with our assumption that $M_2 > 3M_1$ means that we have to require at least $M_1 \lesssim 10^{15}$ GeV. In all plots we fixed $T_{\text{RH}} = 10^{16}$ GeV so that even the heaviest N_1 allowed by the previous considerations would be present in the plasma. As mentioned in the previous section we find that U-DECIGO [774, 874--878] is the best candidate to

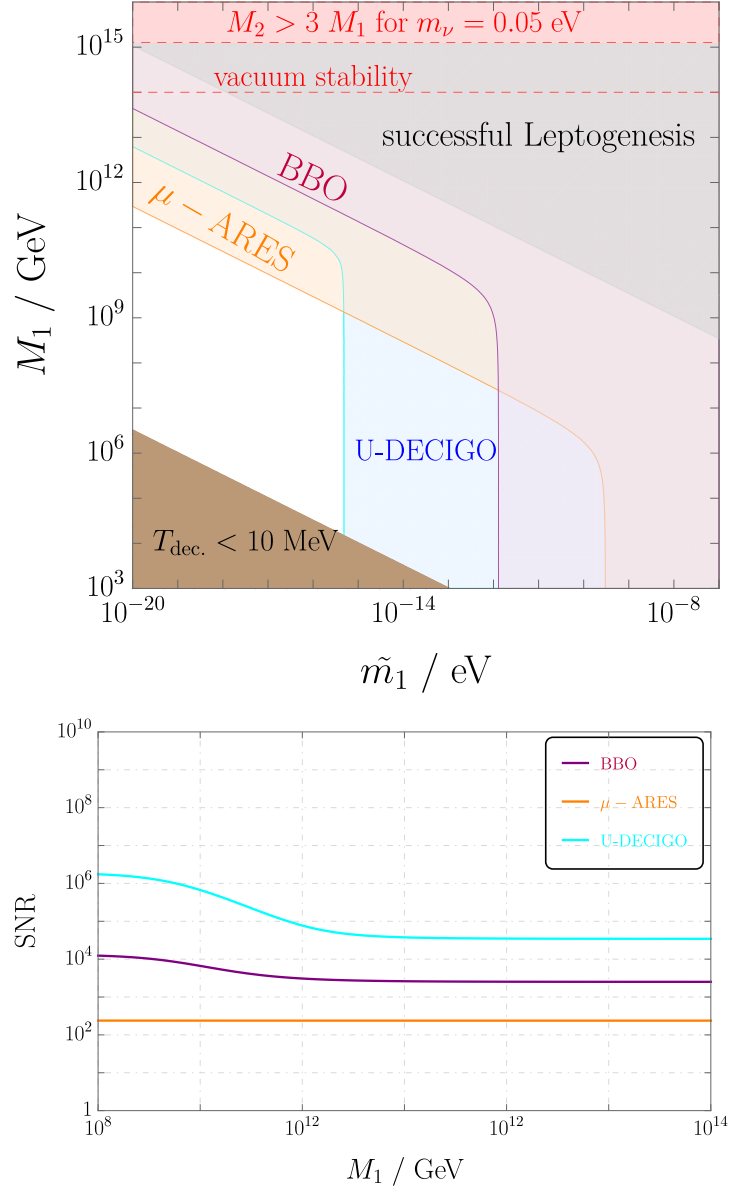


Figure 7.7: Parameter space in the M_1 versus \tilde{m}_1 plane with contours for $\text{SNR} = 10$ (top) and SNR as a function of M_1 , where \tilde{m}_1 was fixed for Leptogenesis via (7.34) (bottom). In both plots we fixed $T_{\text{RH}} = 10^{16} \text{ GeV}$, $n_T = 0$. See the main text for details on the constraints. The SNR is larger than 10 in the colored regions. Note that the colored lines from the experiments do not correspond to constraints, but to projections of future sensitivities.

test our setup compared to the case with no decaying RHN for $n_T = 0$. A future non-

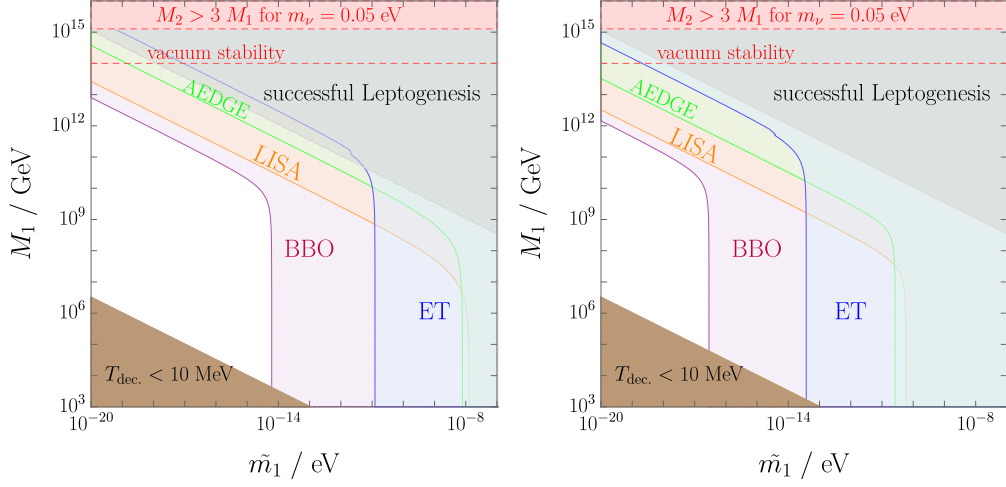


Figure 7.8: Parameter space in the M_1 versus \tilde{m}_1 plane with contours for $\text{SNR} = 10$ for $n_T = 0.1$ (left) and $n_T = 0.2$ (right). In both plots we fixed $T_{\text{RH}} = 10^{16}$ GeV. See the main text for details on the constraints. The SNR is larger than 10 in the colored regions. Note that the colored lines from the experiments do not correspond to constraints, but to projections of future sensitivities.

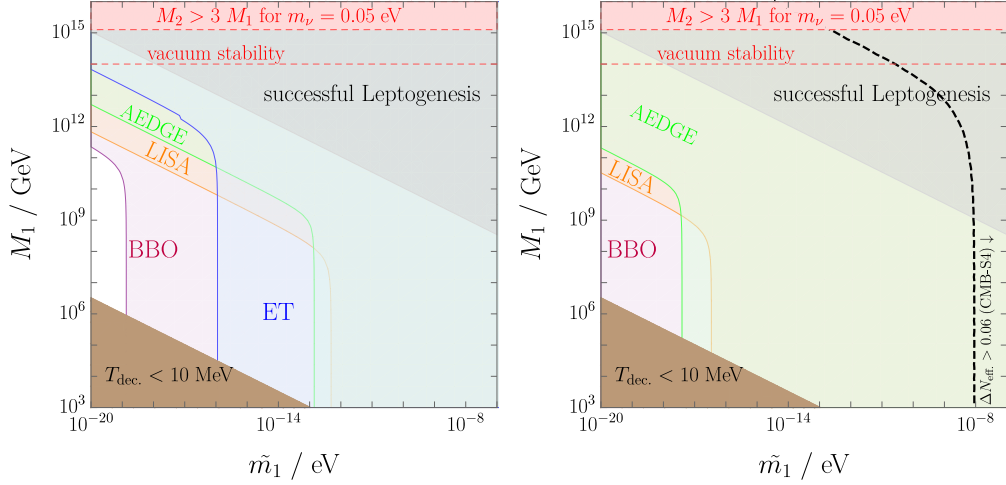


Figure 7.9: Parameter space in the M_1 versus \tilde{m}_1 plane with contours for $\text{SNR} = 10$ for $n_T = 0.3$ (left) and $n_T = 0.5$ (right). In both plots we fixed $T_{\text{RH}} = 10^{16}$ GeV. See the main text for details on the constraints. The SNR is larger than 10 in the colored regions. Note that the colored lines from the experiments do not correspond to constraints, but to projections of future sensitivities.

observation of the inflationary tensor mode spectrum could be explained by a decaying N_1 with $\tilde{m}_1 < 10^{-14}$ eV and a mass of $M_1 \gtrsim 10^4$ GeV (the precise number depends

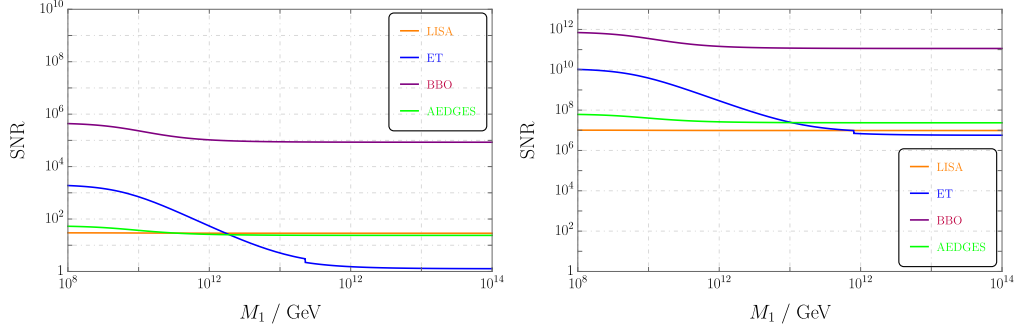


Figure 7.10: SNR as a function of M_1 , where \tilde{m}_1 was fixed for Leptogenesis via (7.34) with $n_T = 0.1$ (left) and $n_T = 0.5$ (right). In both plots we fixed $T_{\text{RH}} = 10^{16}$ GeV

on the BBN bound on the RHN decay temperature of at least 10 MeV). By fixing \tilde{m}_1 as a function of M_1 for Leptogenesis via (7.34) we plot the SNR as a function of M_1 on the right side of 7.7. Here the SNR for μ -ARES [880] is constant because the peak of its sensitivity is situated at a frequency below $f_{\text{sup.}} \simeq 0.1$ Hz and it is therefore blind to the entropy damping. For cosmologies with $n_T > 0$ we find that the SNR for U-DECIGO [774,874--878] is always larger than 10 in the depicted parameter space, which is why we focus on different detectors. BBO [871--873] is a promising candidate for a detection of primordial GWs with both $n_T = 0$ and $n_T > 0$ (compare the plots in 7.7 and 7.8, 7.9). For $n_T \gtrsim 0.5$ the dark radiation bound becomes important again and we show the contour $\Delta N_{\text{eff}}^{\text{proj.}} = 0.06$ for CMB Stage IV [332,333] computed via (7.79) on the right side of figure 7.9. For completeness we display the SNR as a function of M_1 (with \tilde{m}_1 fixed by Leptogenesis (7.34)) for $n_T = 0.1, 0.5$ in figure 7.10.

7.7 Appendix: Conclusions and Discussions

We focused on the minimal Seesaw model, which adds only three right handed neutrinos (RHN) to the SM, and demonstrated that an epoch of right handed neutrino domination, with a Yukawa coupling corresponding to $\tilde{m}_1 < 2.9 \times 10^{-7}$ eV, can realize Baryogenesis via Leptogenesis for a mass of $M_1 \gtrsim 2.4 \times 10^8$ GeV $\sqrt{2 \times 10^{-7}}$ eV/ \tilde{m}_1 (see (7.34)). Since the effective mass is \tilde{m}_1 is too small for a thermal RHN population, we had to assume a different production channel via either inflaton decays or B-L gauge scatterings for the initial RHN abundance. Furthermore such a small \tilde{m}_1 requires that one of the SM neutrinos is approximately massless compared to the other two. The amplitude of gravitational waves that re-enter the horizon before the end of the RHN matter dominated epoch is damped by a factor proportional to the entropy released in the RHN decay. We discussed the detection possibilities of primordial GWs and computed the signal-to-noise ratio for various detectors such as AEDGE [861,879], BBO [871--873], DECIGO [774,874--878], EINSTEIN TELESCOPE [865,866], LISA [869,870] or μ -ARES [880] as well as for several spectral tilts $n_T \geq 0$ of the tensor mode spectrum. Additionally we determined the regions in the M_1 versus \tilde{m}_1 parameter space in which the signal-

to-noise ratio (SNR) is larger than ten over a four year observational period in the figures 7.7-7.9. Our main finding is that high scale Leptogenesis can have an observable imprint on the gravitational waves from inflation. Further we discussed under which conditions our scenario leads to the dominant GW signal. Since fixing M_1 as a function of \tilde{m}_1 for successful Leptogenesis by saturating the maximum of the CP-violating decay parameter ε_1 for a hierarchical spectrum (see (7.30)) completely determines the RHN decay temperature to be $T_{\text{dec.}} \simeq 3.3 \times 10^6 \text{ GeV}$, we find a constant characteristic frequency of $f_{\text{sup.}} \simeq 0.1 \text{ Hz}$ (see (7.73) and figures 7.4-7.5), above which the suppression of the GW amplitude manifests itself. The same RHN can also have a second potentially suppressed decay mode to a stable fermion ψ , that is responsible for the dark matter abundance, if the product of the DM mass and the branching fraction of the RHN decay to DM satisfies $m_\psi \text{BR}_\psi \simeq 85 \text{ eV} \cdot \sqrt{2 \times 10^{-7} \text{ eV}/\tilde{m}_1}$. In order for the dark matter to be heavy enough for successful structure formation ($m_\psi > \mathcal{O}(10 \text{ keV})$) for fixed \tilde{m}_1 we typically need a small branching ratio $\text{BR}_\psi \ll 1$. Such a small branching fraction can also suppress the amount of BSM dark radiation $\Delta N_{\text{eff.}} \simeq 0.06 \cdot (\text{BR}_\psi/4\%)$, that could potentially be generated, if the scalar produced together with ψ is very light and survives until today. This particular scenario leads to GeV-scale DM decaying to dark radiation and SM neutrinos, which necessitates $\tilde{m}_1 < 9.7 \times 10^{-15} \text{ eV}$ in order to have DM with a large enough lifetime on cosmological scales and the right relic abundance.

7.8 Appendix: Acknowledgements

We would like to thank Bowen Fu, Stephen King, Alessandro Strumia and Andreas Trautner for useful comments on the manuscript.

8 Diraxiogenesis

8.1 Contribution to the project

The following chapter is based on unpublished material and the author of this thesis was responsible for the conception and implementation of all aspects of the project. A refined version of this chapter will be uploaded to a preprint server in the weeks after the submission of this thesis.

8.2 Introduction

Condensates of scalar fields, either elementary or composite, play an important role in our understanding of fermion and gauge boson mass generation. Apart from the celebrated Higgs mechanism these condensates also allow for the possibility of explaining either the observed dark matter relic abundance or the matter anti-matter asymmetry. Some of the earliest proposals for Baryogenesis focused on the dynamics of oscillating scalar bosons [914]. With the advent of inflationary cosmology [93] it was realized that the vacuum expectation value (vev) of such a field can undergo a large excursion during the quasi de-Sitter phase of the early universe [915]. The requirement for this is the existence of a very flat or almost vanishing scalar potential, which is naturally realized in supersymmetric field theories such as the MSSM. About 300 of these flat directions, that only receive their masses from supersymmetry breaking and higher dimensional effective operators or radiative corrections, are known [412, 916]. This prompted the development of the Affleck-Dine mechanism [917], where the large effective vev generates the baryon asymmetry from a (potentially Planck scale) suppressed baryon number violating scalar interaction. To transfer this asymmetry from the scalar sector to the baryons typically involves decays of the condensate to thermal bath particles, which can be automatically included if the flat direction is responsible for inflation and the subsequent era of reheating (see e.g. [401] for a recent example).

While the aforementioned scenario adheres to well known Sakharov-conditions [113] relying on CPT-conservation, there exist a class of scenarios in which CPT is spontaneously broken in the plasma of the early universe [119, 918]: The Pseudo-Nambu-Goldstone boson (PNGB) θ of an abelian symmetry, such as e.g. baryon number, oscillates in a cosine-potential. The required large field value is given by the amplitude of its oscillations, which can be at most 2π times the decay constant f of the field, typically requiring a rather large f , see e.g. [919]. Since the baryon asymmetry in these models is proportional to the oscillation frequency of the PNGB $\dot{\theta}$, which is related to its mass, one typically

also needs masses around [119, 918] or far above the electroweak scale [919] making these proposals hard to test in laboratory experiments. Consult also reference [920] for a review and [921] for a systematic treatment of this scenario. The charge from the oscillating PNGB is transferred to the fermions ψ in the plasma via a (schematic) derivative coupling $(\partial_\mu \theta) \bar{\psi} \gamma^\mu \psi$, which reduces to $\dot{\theta} \bar{\psi} \gamma^0 \psi$ for a homogeneous and isotropic PNGB field. Following from the fact that this only time-dependent term breaks Lorentz symmetry spontaneously in the early universe plasma, one can deduce that CPT is also spontaneously violated, hence the name of this scenario.

A new approach pioneered by [922] essentially combines the two aforementioned proposals with the phenomenologically attractive QCD axion [229, 230, 232, 923–926]. Here one can have large decay constants f_a and an observable PNGB whose mass is inversely proportional to f_a , making the scenario potentially testable. A large field excursion of the radial mode of the complex scalar that houses the PNGB angle, known as the *Saxion*, can be used to convert its oscillatory motion in the early universe into a coherent rotation with $\dot{\theta} \neq 0$. The rotation in the axion direction couples to the QCD anomaly and induces chiral asymmetries for the quarks via the QCD sphaleron, which gets reprocessed into a B+L asymmetry via the electroweak sphaleron process. On top of that one can use the axion field velocity for a new scenario of dark matter known as kinetic misalignment [740, 927] (see also [928]), unlike the conventional misalignment which works under the assumption of negligible velocity [929]. However this comes with the drawback of overproducing dark matter if one fixes the baryon asymmetry to its observed value [922]. This conclusion can be avoided if the electroweak phase transition is modified [922], one introduces additional sphalerons from e.g. a gauged $SU(2)_R$ [930], one takes the chiral plasma instability into account [931] or the axion possesses very large couplings to the weak anomaly [932]. The basic scenario can also work for more generic axion-like particles [933], very heavy QCD axions [934] or with multiple scalars [935]. Additionally there can be rich gravitational wave signatures [936–941]. Another way to make Axiogenesis viable is to directly produce a B-L asymmetry instead of B+L via additional processes such as lepton number violating scatterings mediated by heavy Majorana neutrinos, known under the name of "Lepto-axiogenesis" [942–944], or R-parity violating (RPV) supersymmetry [945] (see reference [946] for a review on RPV).

In this work we follow the Lepto-axiogenesis route and try to explain the origin of the PNGB and the effective B-L violation from the same source. To this end we abandon the traditional QCD axion and focus on the PNGBs associated with neutrino mass generation. While the corresponding particle for Majorana neutrinos with the fitting name Majoron [947] has been widely studied [948], we choose to focus on the case of Dirac neutrinos. We call the associated PNGB *Diraxion*. The idea is that we produce equal and opposite asymmetries in the Standard Model leptons and the right handed singlet neutrinos due to B-L conservation, which never get equilibrated [117]. The electroweak sphaleron process is only sensitive to the the lepton doublet so effectively $(B-L)_{\text{SM}}$ is violated in the plasma and can be converted into a baryon asymmetry. A similar idea albeit with a QCD axion has been pursued in [949] for the case of composite right

handed neutrinos. However due to the unspecified UV nature of the non-perturbative mechanism behind the right handed neutrino formation the authors can only use the temperature from when on $(B-L)_{\text{SM}}$ is conserved as a free parameter. Our scenario relies on calculable, perturbative models realizing parametrically small Dirac neutrino masses from threshold corrections in the Seesaw spirit. We discuss the three possible cases for these Dirac Seesaws and show that the singlet scalar that appears in all those constructions can house the Saxion and Diraxion. Similar to the original spontaneous Baryogenesis proposal [119], we will assume that the underlying global symmetry is only broken by a higher dimensional operator responsible for both the Diraxion mass and converting the Saxion oscillation into a Diraxion rotation. Our scenario is inspired by models combining scalar field Leptogenesis with neutrino mass generation such as spontaneous Leptogenesis from a very heavy oscillating Majoron [950] or inflationary Affleck-Dine Leptogenesis from the Type II Seesaw [405, 738]. Unlike these models we predict sub-eV PNGBs and are able to explain the dark matter relic abundance via kinetic misalignment [927] or parametric resonance [951, 952]. Another recent construction [953] also involves Dirac neutrinos and the Affleck Dine mechanism leading to asymmetric dark matter. This proposal requires additional scalars and soft symmetry breaking for neutrino mass generation, which are absent for the Dirac Seesaws. If our setup is only responsible for Baryogenesis, dark radiation in the ν_R component can be produced with an amount of $\Delta N_{\text{eff.}} \lesssim 0.028$. Alternatively if we reproduce the dark matter relic abundance, the Diraxion can be heavy and metastable enough for decays to neutrinos, leading to a discovery potential in next generation experiments investigating the cosmic neutrino background. Requiring the cogenesis of the baryon asymmetry together with dark matter on the other hand leads to unobservably small $\Delta N_{\text{eff.}}$ and too light or long-lived Diraxions. While isocurvature fluctuations in baryons and dark matter are a generic prediction of this kind of scenario, we find that our setup also produces dark radiation isocurvature modes that are correlated with the previously mentioned ones, as they are all induced by Saxion oscillations. Since the Diraxion only has suppressed two-loop couplings to photons we do not expect any signal in axion haloscopes or helioscopes. In our scenario we find slightly heavier Saxions than for Lepto-Axiogenesis [942] with masses around the GeV scale, which can be tested in collider experiments and rare decays of heavier mesons.

The relevant parameter space of our analysis is spanned by the Diraxion mass m_a , the Saxion mass m_S , the Diraxion decay constant today f_a , the initial Saxion field value S_i as well as the domain wall number N , which coincides with the mass dimension of the non-renormalizable operator responsible for the Diraxion mass. We can eliminate f_a by requiring that the interaction of the Saxion with the thermal bath is slow, which is equivalent to fixing the amount of right handed neutrino dark radiation produced via Freeze-In. Successful Saxion thermalization from the Higgs portal interaction is viable for $S_i \lesssim 0.1 M_{\text{Pl}}$. In order to keep the Diraxion light enough we fix $N = 6$. This allows us to predict the masses m_a and m_S for successful cogenesis of the baryon asymmetry and dark matter relic abundance.

model	field	SU(3) _C	SU(2) _L	U(1) _Y	U(1) _D	generations
all	ν_R	1	1	0	-1	3
all	σ	1	1	0	1	1
Type I	N_L	1	1	0	0	3
Type I	N_R	1	1	0	0	3
Type II	η	1	2	1/2	1	1
Type III-a	T_L	1	3	0	0	3
Type III-a	T_R	1	3	0	0	3
Type III-b	D_L	1	2	-1/2	-1	3
Type III-b	D_R	1	2	-1/2	-1	3
Type III	Δ	1	3	0	1	1

Table 8.1: Charges and Representations under the SM gauge group and U(1)_D.

Section 8.3 gives an overview over the family of Dirac Seesaws together with the details about the Saxion and Diraxion. We illustrate the cosmological evolution leading to Saxion oscillations and ultimately a coherent rotation in the Diraxion direction in section 8.4. Dirac-Lepto-Axiogenesis is the subject of section 8.5. Dark Matter and Dark Radiation are the topics of sections 8.6 and 8.7 respectively. Estimates of the Dark Matter and Dark Radiation isocurvature perturbations can be found in 8.8. Section 8.9 describes the required Saxion thermalization to avoid overclosure and excessive amounts of Dark Radiation. We discuss our findings for the regions of parameter space that realize both Leptogenesis and dark matter in 8.10 before we conclude in 8.11.

8.3 Models

8.3.1 Dirac Weinberg operator

The famous dimension five Weinberg operator $(\bar{L}\tilde{H})(L^c i\sigma_2 H)$ with $\tilde{H} \equiv i\sigma_2 H^\dagger$ is the only gauge invariant combination of SM fields that generates a Majorana mass for the left chiral neutrinos [440]. However it has long been known that by adding gauge singlet right chiral neutrinos ν_R together with a singlet scalar σ one can realize a analogue of the Weinberg operator for Dirac neutrinos

$$\mathcal{L}_5 = \frac{c_\nu}{\Lambda_{\text{UV}}} \bar{L}\tilde{H} \sigma \nu_R, \quad (8.1)$$

where c_ν is a dimensionless Wilson-coefficient that appears together with a UV cut-off-scale $\Lambda_{\text{UV}} \gg v_H$ and $v_H \equiv 246 \text{ GeV}$ is the vacuum expectation value (vev) of the neutral

component of the SM Higgs field. After σ condenses with the vev v_σ the above operator represents a neutrino mass

$$m_\nu = c_\nu \frac{v_\sigma}{\Lambda_{\text{UV}}} v_H, \quad (8.2)$$

and the required suppression of the neutrino mass scale needs $\Lambda_{\text{UV}} \gg v_H, v_\sigma$ for order one c_ν . The coupling of ν_R to the SM like Higgs via the operator

$$Y_D \bar{L} \tilde{H} \nu_R + \text{h.c.} \quad (8.3)$$

can be forbidden by invoking a global $U(1)_D$, under which the SM is uncharged and no mixed anomalies appear. To form the Weinberg-Operator then requires that the charges of ν_R and σ satisfy

$$Q_D[\nu_R] + Q_D[\sigma] = 0. \quad (8.4)$$

To ensure the absence of any perturbatively (in field theory) or non-perturbatively (from quantum gravity) generated Majorana mass terms for the SM neutrinos or heavy messenger fermions, we assume either an unbroken global symmetry like lepton number as a residual symmetry from a larger gauge symmetry, or a gauged symmetry like $U(1)_{B-L}$, which can give rise to Dirac masses depending on the choice of charges and the breaking pattern. In the following sections we discuss the tree-level UV-completions of the operator in (8.1). We will not concern ourselves too much with the details of the aforementioned symmetry for the absence of Majorana masses such as anomaly cancellation etc. Instead we focus on the cosmological evolution of the global $U(1)_D$ breaking.

8.3.2 The three Dirac Seesaws

Here we introduce the three tree-level UV-completions to the Weinberg operator in (8.1) and focus on the heavy new messenger fields whose threshold corrections lead to the tiny observed active neutrino masses. A systematic study of tree- and one-loop-level UV completions can be found in [436, 954].

Type I

The most basic Dirac Seesaw [48] was discovered shortly after the more well known Majorana-Seesaw [26–30, 423] and its phenomenology was explored in [589]. The mechanism requires nothing more than at least two generations of super-heavy, electrically neutral vector-like fermions $N_{L,R}$ and the field content and charges can be found in table 8.1.

$$\mathcal{L}^I = Y_L \bar{L} \tilde{H} N_R + Y_R \bar{N}_L \sigma \nu_R + M_N \bar{N}_L N_R. \quad (8.5)$$

We assume that their masses M_N are not connected to $U(1)_D$ and a global or gauged $U(1)_{B-L}$ to be responsible for the absence of any Majorana masses. A diagrammatic representation of the mass generation mechanism was depicted on the left of figure 8.1.

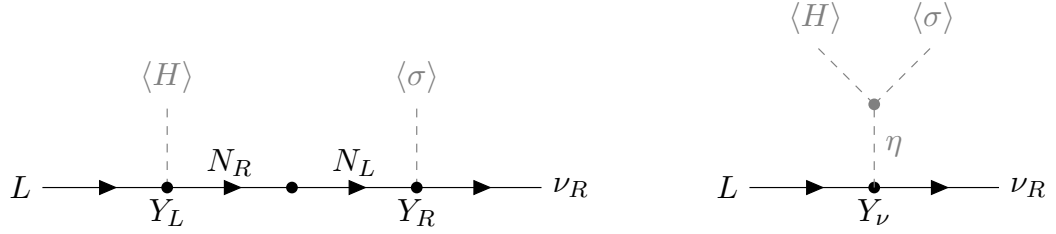


Figure 8.1: Diagrammatic representation of the dimension 5 operators for the Type I Dirac Seesaw (left) and Type II Dirac Seesaw (right) giving rise to Dirac masses for the active neutrinos. For the Type II case one could also consider an additional insertion of σ not depicted here.

After integrating $N_{L,R}$ out, the light neutrino masses in the single flavor approximation read

$$m_\nu^I \simeq Y_L Y_R \frac{v_\sigma}{2M_N} v_H, \quad (8.6)$$

where $Y_L v_H, Y_R v_\sigma \ll M_N$ was assumed and we can estimate

$$m_\nu^I \simeq 0.05 \text{ eV} \cdot Y_L Y_R \cdot \left(\frac{v_\sigma}{4 \text{ TeV}} \right) \cdot \left(\frac{10^{16} \text{ GeV}}{M_N} \right), \quad (8.7)$$

where we chose M_N around the grand unification scale for illustration. Keeping M_N fixed we can accommodate larger v_σ by making the Yukawa couplings $Y_L Y_R$ smaller. This variant of the Seesaw can be embedded in the grand unified theories based on SU(5) [48] or SO(10) [441]. For example in the SO(10) case this comes with the drawback of spoiling matter unification: N_R fills up the 16-dimensional spinorial representation together with the rest of the SM fermions and ν_R, N_L have to be added as additional gauge singlets. A simpler UV-completion based on U(1)_{B-L} consists of giving all leptons L, ν_R, N_L, N_R vector-like charges normalized to one implying that B-L can be gauged and then breaking it via the vev of a scalar φ with charge $|Q_{B-L}[\varphi]| > 2$ [263], which has no direct couplings to fermions. This automatically forbids all renormalizable and effective operators leading to Majorana masses.

Type II

Instead of fermionic messengers fields that mix with the active neutrinos, for a Type II Seesaw one instead tilts a scalar potential slightly, to generate a tiny vev for a much heavier scalar field [32–36]. The first version of this mechanism applied to Dirac neutrinos was considered by [49] in the context of a two-Higgs-doublet model with a soft mass term $\mu^2 \eta^\dagger H$, where we introduced a new doublet η that is a copy of the SM like doublet, but charged under U(1)_D so that it couples to ν_R

$$\mathcal{L}^{II} = Y_\nu \bar{L} \tilde{\eta} \nu_R + \text{h.c.} \quad (8.8)$$

This scenario was UV-completed in [50, 51, 641] by adding a singlet scalar σ whose vev generates the soft mass term: The scalar potential can contain the following two terms

$$V^{\text{II}} \subset \begin{cases} \kappa \sigma H \eta^\dagger + \text{h.c.} & \text{if } Q_D[\nu_R] = -1, \\ \lambda_4 \sigma^2 H \eta^\dagger + \text{h.c.} & \text{if } Q_D[\nu_R] = -1/2, \end{cases} \quad (8.9)$$

where we fixed $Q_D[\sigma] = 1$ in both cases and one can observe that the scalar potential is identical to the two possible choices for the DFSZ axion model [229, 230]. Note that these terms do not induce a mass for the Imaginary component of σ , which becomes evident after diagonalizing the mass matrix for all pseudoscalars [50]. In the following we focus on the term $\propto \kappa$ which is linear in σ , because this allows us to discuss all Dirac Seesaw variants via the same effective operator (8.1). All required fields and charges can be found in table 8.1. If we assume that the positive μ_η^2 is the largest scale in the scalar potential then the aforementioned trilinear term will induce a tiny vev

$$v_\eta \simeq \frac{v_H}{\sqrt{2}} \frac{\kappa v_\sigma}{\mu_\eta^2} \quad (8.10)$$

that lies below the electroweak scale for $\kappa v_\sigma \ll \mu_\eta^2$ and can naturally accommodate the observed neutrino mass scale

$$m_\nu^{\text{II}} \simeq Y_\nu \frac{\kappa v_\sigma}{2\mu_\eta^2} v_H \quad (8.11)$$

without needing a small Yukawa coupling Y_ν . A corresponding Feynman diagram can be found on the right hand side of 8.1. The Type II Seesaw scheme comes with an additional suppression factor κ/μ_η when compared to the fermionic Type I Seesaw (for $M_N \simeq \mu_\eta$), which is why for the same v_σ the neutral component of the η -doublet can be made lighter than the vectorlike neutrinos N . An estimate illustrates the interplay of the various scales

$$m_\nu^{\text{II}} \simeq 0.05 \text{ eV} \cdot Y_\nu \cdot \left(\frac{\kappa}{100 \text{ GeV}} \right) \cdot \left(\frac{v_\sigma}{400 \text{ TeV}} \right) \cdot \left(\frac{10^{10} \text{ GeV}}{\mu_\eta} \right)^2. \quad (8.12)$$

This scenario is the most straightforward to further UV-complete in terms of a gauged $U(1)_{\text{B-L}}$ since all gravitational and cubic anomalies will vanish, if one adds no other fermions than three generation of ν_R with the same canonical lepton number $Q_{\text{B-L}}[L] = -1$ as L . Renormalizable and effective Majorana masses for L , ν_R can then be forbidden if the scalar φ dominantly responsible for the $U(1)_{\text{B-L}}$ -breaking has a charge $|Q_{\text{B-L}}[\varphi]| > 2$ [263].

Type III

The Type III Dirac Seesaw scenario is defined by the presence of a hypercharge-less scalar iso-triplet Δ . In the first case, which we call Type III-a, Δ has no couplings to SM fields and only interacts with ν_R and the right chiral component of a vector-like fermion triplet $T_{L,R}$ [52]

$$\mathcal{L}^{\text{III (a)}} = Y_L \bar{L} H T_R + Y_R \bar{T}_L \Delta \nu_R + M_T \bar{T}_L T_R + \text{h.c.}, \quad (8.13)$$

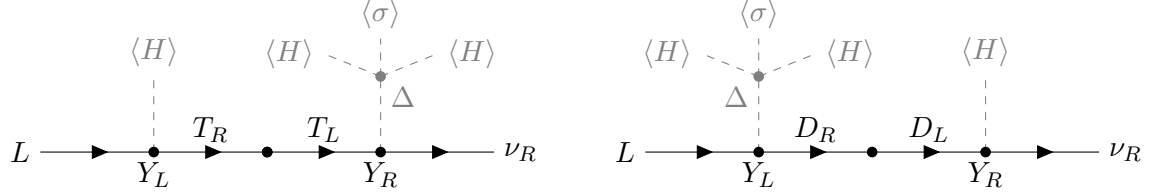


Figure 8.2: Diagrammatic representation of the dimension 5 operators for the Type III-a Dirac Seesaw (*left*) involving new triplet fermions and Type III-b Dirac Seesaw (*right*) involving new doublet fermions, both giving rise to Dirac masses for the active neutrinos.

which was shown on the left of figure 8.2. Alternatively for the Type III-b model depicted on the right of 8.2, one may consider a direct coupling of Δ to L by introducing vector-like doublet leptons $D_{L,R}$ [53]

$$\mathcal{L}^{\text{III (b)}} = Y_L \overline{L} \Delta D_R + Y_R \overline{D}_L \tilde{H} \nu_R + M_D \overline{D}_L D_R + \text{h.c.} . \quad (8.14)$$

For both models all fields and charges were compiled in 8.1. Since an iso-triplet scalar will spoil the custodial symmetry of the SM scalar potential, its vev modifies the SM ρ -parameter [637, 674] to be [52, 53]

$$\rho - 1 = 8 \frac{v_\Delta^2}{v_H^2}. \quad (8.15)$$

The observed masses of the electroweak gauge bosons force $\rho \equiv m_W^2/(m_Z^2 \cos(\theta_W)^2)$ to be close to one, which requires v_Δ at or below the GeV-scale [636]. Indeed one of the motivations for this scenario is the observed deviation in the W -boson mass reported by the CDF collaboration [675], which can be stated in terms of the electroweak precision observable [677, 678] known as the T -parameter [53]

$$T \equiv \frac{\rho - 1}{\alpha} = 0.17 \pm 0.020899. \quad (8.16)$$

The CDF-tension can then be explained by [52]

$$v_\Delta \simeq 4 \text{ GeV}. \quad (8.17)$$

Such a low vev typically implies that the electrically neutral component of Δ has to be below the weak scale as well, which can phenomenologically challenging¹ similarly to the light scalar in neutrino-philic Two-Higgs-doublet models [164, 340--343]. On top of that the pseudoscalar component of Δ playing the role of the Diraxion can

¹If we assume that the neutral component of Δ is the Saxion, then the bound from Saxion isocurvature fluctuations would even require $m_{\Delta^0} \ll v_\Delta$ by many orders of magnitude.

typically have anomalous couplings to the weak $SU(2)_L$ gauge bosons, implying a different phenomenology compared to the case, where the Diraxion comes from an SM singlet. To avoid these problems we add an additional scalar singlet σ . An attractive way to generate a small v_Δ while keeping the components of Δ ultra-heavy is the inclusion of a Type II suppression for v_Δ , completely analogous to the mechanism for a small v_η in the previous paragraph 8.3.2. The relevant scalar potential reads

$$V^{\text{III}} \subset \lambda_4 \sigma^* H^\dagger \Delta H + \text{h.c.} \quad (8.18)$$

and one finds [53]

$$v_\Delta \simeq \frac{\lambda_4}{2} \frac{v_H^2 v_\sigma}{\mu_\Delta^2}, \quad (8.19)$$

which is suppressed compared to the electroweak scale as long as $\lambda_4 v_H v_\sigma \ll \mu_\Delta^2$. The required parameters turn out to be

$$v_\Delta \simeq 4 \text{ GeV} \cdot \left(\frac{\lambda_4}{0.3} \right) \cdot \left(\frac{v_\sigma}{10^8 \text{ GeV}} \right) \cdot \left(\frac{470 \text{ TeV}}{\mu_\Delta} \right)^2. \quad (8.20)$$

Thus these versions of the Type III Dirac Seesaw correspond to the class of “nested Seesaws” [41, 42, 600, 641, 657] with a built in double suppression from the heavy T or D masses and the tiny value of v_Δ

$$m_\nu^{\text{III}} \simeq Y_L Y_R \frac{v_\Delta}{2M_F} v_H, \quad \text{with} \quad M_F = \begin{cases} M_T & \text{for case (a)} \\ M_D & \text{for case (b)} \end{cases}. \quad (8.21)$$

The heavy fermion masses M_F can be estimated from

$$m_\nu^{\text{III}} \simeq 0.05 \text{ eV} \cdot Y_L Y_R \cdot \left(\frac{v_\Delta}{4 \text{ GeV}} \right) \cdot \left(\frac{10^{13} \text{ GeV}}{M_F} \right) \quad (8.22)$$

and as expected the vector-like iso-multiplet fermions $F = D, T$ are lighter than the singlet fermions N from the Type I Dirac Seesaw due to the additional suppression from the scalar sector. If we make no assumption about the value of v_Δ we find that the observed neutrino mass scale would require $M_F \simeq \mu_\Delta \simeq 10^8 \text{ GeV}$ for order one couplings Y_L, Y_R, λ_4 and $v_\sigma = 10^6 \text{ GeV}$. A straightforward way to UV complete these models in terms of a gauged $U(1)_{\text{B-L}}$ is to assume that the fermions are vector-like under both the SM gauge group as well as B-L.

8.3.3 Saxon

The singlet scalar field has a renormalizable potential

$$V_\sigma = \lambda_\sigma \left(|\sigma|^2 - v_\sigma^2 \right)^2, \quad (8.23)$$

where we minimized the potential by balancing the tachyonic mass squared $-|\mu_\sigma|^2 < 0$ against the quartic coupling λ_σ to define the nontrivial vev $v_\sigma \equiv |\mu_\sigma|/\sqrt{2\lambda_\sigma}$. One can decompose the scalar field as

$$\sigma = \frac{S + v_\sigma}{\sqrt{2}} e^{i\frac{\theta}{N}}, \quad \text{with} \quad \frac{\theta}{N} \equiv \frac{a}{\langle S \rangle}, \quad (8.24)$$

where we anticipated that during inflation the radial mode will be displaced from its true vacuum $\langle S \rangle = v_\sigma$

$$\langle S \rangle = \begin{cases} \gg v_\sigma & \text{early universe} \\ v_\sigma & \text{today} \end{cases}. \quad (8.25)$$

Apart from the SM and ν_R the particle spectrum will contain a massive scalar state S called the **Saxion**, whose mass squared reads

$$m_S^2 \equiv 2\lambda_\sigma v_\sigma^2. \quad (8.26)$$

The **Saxion** couplings were summarized in section 8.3.4.

8.3.4 **Saxion Couplings**

The relevant couplings of the **Saxion** to the SM fields can be parameterized as

$$\mathcal{L}_{\text{ferm.}} = Y_{S\nu} S \bar{\nu}\nu + \sum_{\psi=l,q} Y_{S\psi} S \bar{\psi}\psi \quad (8.27)$$

$$\mathcal{L}_{\text{bos.}} = \frac{\lambda_\sigma}{4} S^4 + \frac{\lambda_{\sigma H}}{4} S^2 h^2 + g_{S\gamma\gamma} S F_{\mu\nu} F^{\mu\nu}. \quad (8.28)$$

Apart from the interaction with the neutrinos given by

$$Y_{S\nu} = \frac{m_\nu}{N f_a} \quad (8.29)$$

all other interactions originate from **Saxion-Higgs** mixing or loop diagrams.

Couplings from **Saxion-Higgs** mixing

The **Saxion-Higgs** mixing angle reads

$$\tan(2\theta_{SH}) \equiv 2\lambda_{\sigma H} \frac{v_H N f_a}{m_h^2 - m_S^2}, \quad (8.30)$$

where $m_h = 125$ GeV is the mass of the SM like Higgs. The coupling to charged leptons and quarks ψ is given by

$$Y_{S\psi} \equiv \sin(\theta_{SH}) \frac{m_\psi}{v_H}. \quad (8.31)$$

The on-loop Higgs di-photon coupling also leads to a Saxion-photon coupling in terms of the fine structure constant α [955, 956]

$$g_{S\gamma\gamma} \equiv \frac{\sin(\theta_{SH})\alpha}{2\pi v_H} \left(\frac{N_c Q_t^2}{3} - \frac{7}{4} \right), \quad (8.32)$$

where the first term in parentheses is the contribution from the top-quark with $N_c = 3$ colors and an electric charge $Q_t = 2/3$ and the second term is due to the W -boson. Here the Saxion only couples to the strongly interacting quarks and gluons, or equivalently the hadronic sector, via mass mixing with the Higgs. This is the reason why strong limits [957] from light Saxion emission via couplings to nucleons inside SN1987A are absent.

Loop induced couplings

The Saxion can also obtain one- and two-loop couplings to SM fermions and photons respectively via similar diagrams as the Diraxion in 8.3.7. However since these couplings are suppressed by at least m_ν^2/v_H^2 , we take them to be negligible compared to the couplings from Saxion-Higgs mixing. Note that for Saxion masses below the QCD confinement scale $\mathcal{O}(100 \text{ MeV})$ we would need to replace the quarks running in the photonic loops with hadrons [562, 958], which is beyond the scope of this work.

8.3.5 Diraxion

The most important ingredient of our scenario is the pseudoscalar Nambu-Goldstone-Boson (NGB) a of the $U(1)_D$ symmetry, also known as the Diron [48] or Dirac [50, 51], which can be understood of the Dirac equivalent of the well-known Majoron [947]. Quantum effects like instantons or classical explicit breaking of the underlying global symmetry can generate a mass for a turning it into a Pseudo-NGB (PNGB), provided that its mass is parametrically below v_σ and m_S . In analogy to arguably the most well studied PNGB, the QCD-axion [229, 230, 232, 923–926], we will call this CP-odd scalar the “Diraxion”. This PNGB will not couple to any SM fermions and does not have any anomalies with the SM gauge group. Global symmetries like our $U(1)_D$ are expected to be broken by non-perturbative quantum gravitational effects [275–277], as can be seen from wormhole arguments. Heuristically these effects are encoded in Planck-scale suppressed non-renormalizable operators, that explicitly violate a given symmetry. Furthermore, if we also want to use the same operator to induce a “kick” in the angular Diraxion direction from the Saxion oscillation, we need an operator with dimension larger than five [942]. While we normalized the number of units by which the vev of σ breaks the global symmetry to be $Q_D[\sigma] = 1$, the explicit breaking will in general occur with a different number of units and consequently we have to deal with a degenerate vacuum. The most straight-forward way to see this, is to consider a potential of the form

$$c_N \sigma^N + \text{h.c.} = |c_N| \frac{S^N}{\sqrt{2}^N} \cos \left(\frac{N a}{v_\sigma} + \delta \right), \quad \text{with} \quad \delta \equiv \text{Arg}(c_N) \quad (8.33)$$

which implies that the Diraxion decay constant is not v_σ but instead

$$f_a \equiv \frac{v_\sigma}{N}, \quad (8.34)$$

where N is the vacuum degeneracy factor also known as the Domain-Wall number and we define

$$\theta \equiv \frac{a}{f_a}. \quad (8.35)$$

One can deduce that the above interaction is invariant under an unbroken residual discrete \mathcal{Z}_N symmetry, where σ transforms as ω with $\omega^N = 1$. This mismatch between spontaneous and explicit breaking will have considerable implications for cosmology since it can lead to long-lived domain walls that might overclose the universe [448, 449]. However domain walls can be attached to cosmic strings from e.g. the $U(1)_D$ breaking and the resulting hybrid defect will be unstable for $N = 1$ [453, 454]. Furthermore even for $N > 1$ one can use the same effective operator responsible for the Diraxion mass to induce domain wall decays to Diraxions [959]. We begin with the simplest effective operator imaginable with more than five singlet fields

$$N = d > 5 : \quad V_D = c_d \frac{\sigma^d}{M_{\text{Pl}}^{d-4}} + \text{h.c.}, \quad m_a^2 \equiv \frac{d^4}{\sqrt{2}^{d-2}} |c_d| \left(\frac{d f_a}{M_{\text{Pl}}} \right)^{d-4} f_a^2, \quad (8.36)$$

and one can see that the Diraxion mass will automatically be suppressed compared to f_a without needing a small dimensionless coefficient $c_d^{(i)}$ as long as $f_a \ll M_{\text{Pl}}$ and $d > 4$. This approach comes with the downside of having a potentially large number of domain walls $N = d > 5$. In section 8.6.3 it will be explained why our setup is also viable for domain wall numbers larger than one. Hence for simplicity we will only consider the operator in equation (8.36) for the rest of this paper as it relates two of the free parameters N and d . More operators and a way to generate a specific value of N can be found in section 8.3.6. One can estimate e.g. for $N = 6$ that

$$m_a \simeq 9 \text{ keV} \cdot \sqrt{c_6} \cdot \left(\frac{N}{6} \right) \cdot \left(\frac{N f_a}{10^6 \text{ GeV}} \right)^2, \quad (8.37)$$

however it turns out that we need a Diraxion mass between 10^{-3} eV and 1 eV, which would require a tiny coefficient c_6 . An exponential suppression of the Wilson-coefficient due to a large wormhole action [472, 473] might accomplish this. Alternatively we illustrate in section 8.3.6 how the required effective operator could arise from a second scalar field φ , that we assume is charged under a gauged $U(1)_{\text{B-L}}$, which is responsible for the absence of Majorana masses. One such operator is

$$c_8 \frac{\sigma^6 \varphi^{*2}}{M_{\text{Pl}}^4} + \text{h.c.} \quad (8.38)$$

and the required charges read $Q_{\text{B-L}}[\sigma] = 3$, $Q_{\text{B-L}}[\varphi] = 9$. Here we assume that φ has no direct couplings to the Seesaw messenger fields. For the Diraxion mass we find in this scenario that

$$m_a \simeq 0.1 \text{ eV} \cdot \sqrt{c_8} \cdot \left(\frac{N}{6} \right) \cdot \left(\frac{v_{\text{B-L}}}{10^9 \text{ GeV}} \right) \cdot \left(\frac{N f_a}{10^6 \text{ GeV}} \right)^2. \quad (8.39)$$

If we also charge σ under B-L then we have to use more complicated chiral charge assignments than just ± 1 for the fermion fields in order to forbid Majorana masses and to avoid gauge anomalies. Since this will typically involve additional anomaly cancelling fermions, we refrain from writing down the explicit UV-completions.

8.3.6 Higher dimensional operator from a second scalar field

The domain wall problem can be remedied by considering another effective operator constructed from σ and its conjugate that essentially reduces to a tadpole, where the operator dimension reads $d = 5 + 2n$ with $n > 0$

$$N^{(ii)} = 1 : \quad V_{\not{D}}^{(ii)} = c_d^{(ii)} \frac{|\sigma|^{2(2+n)} \sigma}{M_{\text{Pl}}^{2n+1}} + \text{h.c.}, \quad m_a^2 {}^{(ii)} \equiv \frac{2}{\sqrt{2}^{2n+5}} \left| c_d^{(ii)} \right| \left(\frac{f_a}{M_{\text{Pl}}} \right)^{2n+1} f_a^2 \quad (8.40)$$

and the domain wall number is unity for all choices of n . Alternatively one can switch on multiple effective operators with different dimensions d of lowest common denominator one so that no residual \mathcal{Z}_N symmetry remains intact [960]. However this comes at the price of having at least two sources for the Diraxion mass. One can actually engineer a scenario where the desired operator dimension appears due to an accidental symmetry after the spontaneous breaking of an additional gauge symmetry such as e.g. $U(1)_{\text{B-L}}$, hypercharge or a linear combination of them. We assume a particle spectrum and charge assignment to cancel all gauge anomalies. Let us concentrate on the case of $U(1)_{\text{B-L}}$ since this symmetry can have the additional benefit of prohibiting Majorana masses. A second scalar singlet φ with a vev $v_\varphi \gg v_\sigma$ dominantly breaks the local symmetry, under which the scalars have charges $Q_{\text{B-L}}[\varphi]$ and $Q_{\text{B-L}}[\sigma]$ with lowest common denominator one. The only gauge invariant operators of dimension $d = n_\phi + n_\sigma > n_\phi + 5$ then read [961, 962]

$$N^{(iii)} : \quad V_{\not{D}}^{(iii)} = c_d^{(iii)} \frac{\varphi^{* n_\varphi} \sigma^{n_\sigma}}{M_{\text{Pl}}^{n_\sigma + n_\varphi - 4}} + \text{h.c.}, \quad m_a^2 {}^{(iii)} \equiv \frac{2 N_{\text{glob.}}^{n_\sigma}}{\sqrt{2}^{n_\sigma + n_\varphi}} \left| c_d^{(iii)} \right| \frac{v_\sigma^{n_\sigma - 2} v_\varphi^{n_\varphi}}{M_{\text{Pl}}^{n_\sigma + n_\varphi - 4}} \quad (8.41)$$

and the gauge charges must satisfy

$$n_\sigma Q_{\text{B-L}}[\sigma] - n_\varphi Q_{\text{B-L}}[\varphi] = 0. \quad (8.42)$$

After φ condenses we see that the potential has an accidental \mathcal{Z}_{n_σ} symmetry, that can be understood as a remnant of the original gauge symmetry. The Diraxion mass then depends on its decay constant and the second larger vev v_φ . When it comes to the domain

wall issue the situation is more complicated due to the presence of two symmetries: Once φ gets a vev local strings from the $U(1)_{B-L}$ breaking are formed. Afterwards when σ condenses global strings from the breaking of $U(1)_D$ are formed. However σ also carries a gauge charge, so the local $U(1)_{B-L}$ string obtains a defect in v_σ , and the winding number $\omega_\sigma^{(\varphi)}$ of σ around the local string is determined from the minimization of the system's kinetic energy leading to² [961, 962]

$$N^{(iii)} = \begin{cases} |n_\sigma| & \text{global} \\ \text{Min} \left| n_\varphi - \omega_\sigma^{(\varphi)} n_\sigma \right| & \text{local} \end{cases}. \quad (8.43)$$

The important point is that the system of domain walls and two types of strings will be unstable if *either* of the domain wall numbers is one [961, 962]. Since we need $n_\sigma > 5$ for Axiogenesis [942] this leaves the two choices $n_\varphi = 1$, $\omega_\sigma^{(\varphi)} = 0$ or $n_\varphi \neq 1$, $\omega_\sigma^{(\varphi)} = (n_\varphi - 1)/n_\sigma$. A non-trivial winding number $\omega_\sigma^{(\varphi)}$ implies mixed anomalies between $U(1)_D$ and $U(1)_{B-L}$. Since the gauge symmetry is assumed to be abelian, this does not lead to non-perturbative contributions from instantons to the Diraxion mass. On the other hand, if $U(1)_{B-L}$ is embedded into a larger non-abelian group such as the Pati-Salam hypercolor $SU(4)_c$ [279], these unwanted effects reappear and might be even compounded by small size UV-instantons [963, 964], which could limit the possible UV-completions of our setup. The dynamics of φ in the early universe can be neglected as long as

$$\sqrt{|\lambda_{\sigma\varphi}|} S_i > \text{Max} \left[T_{\text{RH}}, T_{\text{max}}, \frac{H_I}{2\pi} \right]. \quad (8.44)$$

As long as $\lambda_{\sigma\varphi} < 0$ there is no danger of restoring the B-L symmetry via the large vev S_i .

8.3.7 Diraxion couplings

The Diraxion only has tree-level derivative couplings to ν_R as well as the heavy BSM fermions and scalars. Here we focus on the low energy couplings to SM particles and ν_R .

Derivative Couplings

From the Saxion kinetic term we find that the Diraxion-Saxion coupling reads

$$\mathcal{L} = \frac{(S + N f_a)^2}{2} \partial_\mu \theta \partial^\mu \theta. \quad (8.45)$$

We then remove the phase of σ by a field definition of the fields charged under $U(1)_D$, which leads to derivative couplings from their kinetic terms. At low energies only ν_R is in the plasma so we focus on its couplings

$$\mathcal{L} = c_{\nu_R} \partial_\mu \theta \overline{\nu_R} \gamma^\mu \nu_R, \quad (8.46)$$

²Here we assumed that v_σ wraps once around the global string and v_φ winds once around the local string

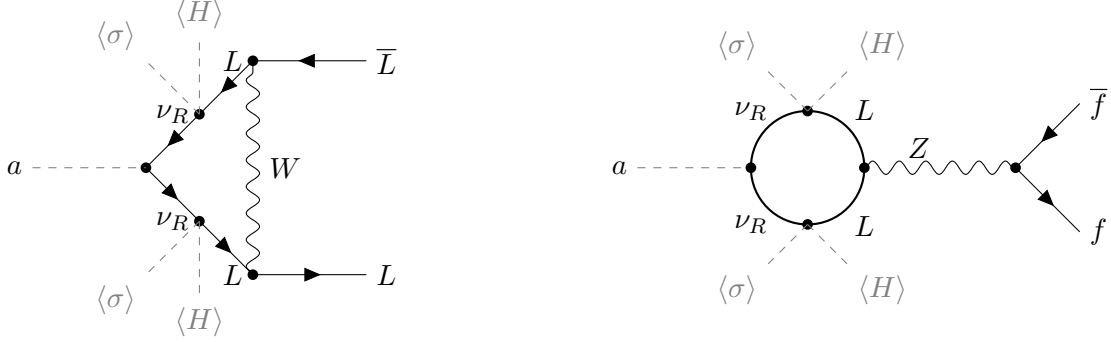


Figure 8.3: One loop diagrams for the coupling of the Diraxion to SM fermions involving two insertions of the Dirac Weinberg operator. The first diagram generates a coupling to the lepton doublet only, whereas the second one involves all fermions $f = L, e_R, Q, u_R, d_R$.

which read

$$c_{\nu_R} = \begin{cases} \frac{1}{N} - \alpha^2 & \text{Type I, III-a} \\ \frac{1}{N} & \text{Type II, III-b} \end{cases}, \quad \text{with} \quad \alpha \equiv \frac{Y_R}{\sqrt{2}} \begin{cases} v_\sigma/M_N & \text{Type I} \\ v_\Delta/M_T & \text{Type III-a} \end{cases}. \quad (8.47)$$

The couplings for the Type I and Type III-a Seesaw are reduced [933], because here the ν_R with charge $Q_D[\nu_R] = -1$ mix with N_R and T_R of charge $Q_D[N_R] = Q_D[T_R] = 0$. For the Type II Seesaw there are no additional fermions for ν_R to mix with and the D_R for a Type III-b Seesaw have the same charge $Q_D[T_R] = -1$ as ν_R . However for Type III-b there is also the mass mixing between D_R and L with $Q_D[L] = 0$ that induces a derivative coupling $c_{\nu_L} = \alpha^2$ for L . Such a coupling of the Diraxion to a fermion with hypercharge might be interesting as it can lead to chiral hypermagnetic instabilities [931]. It is evident that the parameter $\alpha \ll 1$ due to the heavy messenger fermions, which is why in practise we will take $c_{\nu_R} \simeq 1/N$ for all Seesaws and $c_{\nu_L} \simeq 0$ for Type III-b. The effective coupling for the production of a single on shell Diraxion from a neutrino line is given by

$$g_{a\nu} = c_{\nu_R} \frac{m_\nu}{f_a} \simeq 5 \times 10^{-17} \cdot \left(\frac{m_\nu}{0.05 \text{ eV}} \right) \cdot \left(\frac{10^6 \text{ GeV}}{N f_a} \right). \quad (8.48)$$

Limits from SN1987A on the energy loss and deleptonization exclude $10^{-12} \lesssim g_{a\nu} \lesssim 10^{-5}$ [965--967] and for larger couplings the Diraxion would remain trapped inside the supernova. Meson decays exclude only $g_{a\nu} \gtrsim 10^{-3}$ [569]. It is obvious from (8.48) that our setup is compatible with these bounds.

Loop induced couplings

The Diraxion only couples to SM quarks and leptons via the one-loop diagrams in 8.3 and here we recast the results of [562, 958] obtained for a Majoron in a conventional

Type I Seesaw. For us the pseudo-scalar coupling to electrons is the most relevant and it turns out to be

$$g_{ae} \simeq \frac{1}{16\pi^2} \frac{m_e}{v_H} \frac{m_\nu^2}{N f_a} \simeq 10^{-37} \cdot \left(\frac{m_\nu}{0.05 \text{ eV}} \right)^2 \cdot \left(\frac{10^6 \text{ GeV}}{N f_a} \right). \quad (8.49)$$

Stellar cooling arguments from the sun as well as red giants exclude $g_{ae} \gtrsim 10^{-13}$ [563–566], which is not in conflict with our scenario. By closing the charged fermion line and attaching two photons to the one-loop diagrams depicted in 8.3, we obtain the two-loop Diraxion-photon coupling. Since our choice of $U(1)_D$ symmetry has no mixed anomalies with the SM gauge sector, the resulting coupling will be proportional to m_a^2/m_ψ^2 [562], where m_ψ is the mass of the fermion running in the loop. Consequently the dominant contribution comes from the electrons being the lightest SM fermion and it reads [562, 958]

$$|g_{a\gamma\gamma}| \simeq \frac{\alpha}{64\pi^3 N f_a} \left(\frac{m_\nu}{v_H} \right)^2 \left(\frac{m_a}{m_e} \right)^2 \simeq \frac{10^{-52}}{\text{GeV}} \cdot \left(\frac{m_\nu}{0.05 \text{ eV}} \right)^2 \cdot \left(\frac{10^6 \text{ GeV}}{N f_a} \right) \cdot \left(\frac{m_a}{10 \text{ meV}} \right)^2. \quad (8.50)$$

In contrast to the case of a QCD axion the above has no contribution from mixing with the pions, as the Diraxion has no tree-level coupling to quarks. Due to their dependence on the tiny neutrino masses squared we find that these couplings are below all relevant constraints.

8.4 Two-field dynamics

8.4.1 Equations of motion

The coupled equations of motion for the Saxion S and the Diraxion θ for the case of $N = 1$ are given by [939]

$$\dot{S} + 3H\dot{S} + \frac{\partial V_\sigma}{\partial S} + \frac{\partial V_\phi}{\partial S} - S\dot{\theta}^2 = 0, \quad (8.51)$$

$$S\ddot{\theta} + 3HS\dot{\theta} + \frac{1}{S} \frac{\partial V_\phi}{\partial \theta} + 2\dot{S}\dot{\theta} = 0. \quad (8.52)$$

8.4.2 Initial Saxion field value

We consider a radial mode whose vev is displaced during inflation from its minimum as $S_i \gg N f_a$ and treat S_i as the initial condition for the evolution of the Saxion. Here we present two ways to induce the displacement of the Saxion field value during inflation, and in section 8.4.2 we also discuss a way to avoid or relax the isocurvature constraints. In the following we take the initial field value S_i as a free parameter and $m_S(S_i)^2 \simeq 3\lambda_\sigma S_i^2$ denotes the effective mass squared for a quartic potential

$$m_S(S_i)^2 \equiv \frac{3}{2} m_S^2 \left(\frac{S_i}{N f_a} \right)^2, \quad (8.53)$$

where we defined the Saxion mass squared in our vacuum today to be m_S^2 . The complex singlet scalar is assumed to be a spectator field during inflation.

Quantum fluctuations

It has been long known [968--976] that scalar fields with very shallow potentials undergo large field excursions during inflation as a consequence of quantum fluctuations. We can take this potentially large field value as an initial condition S_i for the Saxon field. When the Hubble rate during inflation H_I is much larger than the effective mass, quantum fluctuations grow the expectation value of S . The field excursion of S can be determined from the variance $\langle S^2 \rangle$ of the Starobinsky-Yokoyama distribution [915]

$$S_i \simeq \sqrt{\langle S^2 \rangle} = \left(\frac{1}{4\pi^2} \right)^{\frac{1}{4}} \sqrt{\frac{N f_a}{m_S}} H_I, \quad (8.54)$$

where m_S is the bare mass defined in (8.26). From this it becomes apparent, why a large field excursion S_i demands a very flat potential, meaning a small m_S .

Non-minimal coupling to gravity

While quantum fluctuations required $m_S(S_i) \ll H_I$ a non minimal coupling to gravity can lead to a Hubble dependent mass $m_S(S_i) \simeq H_I$. This kind of mass term was first suggested in the context of supersymmetry breaking from finite energy density effects [412, 739] in the early universe. The same net effect can be generated by coupling the singlet scalar to the Ricci scalar

$$V \supset c_R R |\sigma|^2, \quad (8.55)$$

whose value for a Friedmann-Lemaitre-Robertson-Walker metric depends on the equation of state of the dominant energy density driving the cosmic expansion [977]

$$R = -3(1 - 3\omega)H^2 = \begin{cases} -3H^2 & \text{for MD} \quad (\omega = 0) \\ 0 & \text{for RD} \quad (\omega = \frac{1}{3}) \\ -12H^2 & \text{for infl.} \quad (\omega = -1) \end{cases}. \quad (8.56)$$

The idea is to balance this tachyonic mass squared during inflation against the quartic term $\lambda_\sigma S^4/4$, which requires $c_R > 0$. In order to have $m_S(S_i)^2 = -H_I^2$ we take $c_R = 1/12$ and find

$$S_i = \sqrt{2} \left(\frac{N f_a}{m_S} \right) H_I. \quad (8.57)$$

The Saxon remains stuck in this value even at the onset of radiation domination because of the equilibrium between the Hubble friction and the slope of the potential [978--980]. Before we close let us note that an epoch of intermediate matter domination after inflation with $R = -3H^2$, such as e.g. the well motivated curvaton scenario [981--983], could also be used to induce the large field value, which would be entirely free from inflationary isocurvature perturbations. The absence of fluctuations during inflation requires an effective mass during inflation that is larger than H_I , which could be realized via the couplings to the inflaton introduced in the next subsection 8.4.2.

Initial field value from a coupling to the Inflaton

A second way to generate a Hubble dependent mass contains one (or more) coupling(s) to the inflaton field χ that could take the following forms

$$V(\sigma) \supset c_1 \frac{|\chi|^{2m} |\sigma|^{2n}}{M_{\text{Pl}}^{2(m+n)-4}}, \quad c_2 \frac{V(\chi) |\sigma|^2}{M_{\text{Pl}}^2}, \quad c_3 \frac{(\partial_\mu \chi \partial^\mu \chi) |\sigma|^2}{M_{\text{Pl}}^2}, \quad (8.58)$$

that were suggested by references [984–986], [987] and [988] respectively. One can understand the effect of these couplings by focusing e.g. on the second term and using the Friedmann equation to eliminate $V(\chi)$ for slow roll inflation, which implies an effective mass squared $3c_2 H_I^2$. In general the idea is, that the large initial field value χ_i of the slowly rolling inflaton field sources an effective mass term that is initially larger than the Hubble rate $m_S(\chi_i) > H_I$. As the inflaton field decreases the effective mass will become smaller than the Hubble rate after N_{last} e-folds of inflation (counted from the end of inflation) so that quantum fluctuations can push S to the value (we assume $m_S < H_I$) [984–986]

$$S_i \simeq \sqrt{\langle S^2 \rangle} = \frac{\sqrt{N_{\text{last}}}}{2\pi} H_I. \quad (8.59)$$

That implies that isocurvature fluctuations will not be produced before N_{last} . Observations by the Planck and WMAP collaborations only constrain isocurvature modes whose momenta are below the pivot scale $k_* = 0.1 \text{ Mpc}^{-1}$ [353]. The matter power spectrum extracted from Lyman- α data is only sensitive to perturbations at scales of $0.2 \text{ Mpc}^{-1} \lesssim k \lesssim 10 \text{ Mpc}^{-1}$ [989]. If the Saxion fluctuation has comoving momenta $k \geq 10 \text{ Mpc}^{-1}$, current experiments do not set a limit on the isocurvature power spectrum. Reference [986] determined the required value of N_{last} to be

$$N_{\text{last}} \lesssim 46.4 - \text{Log} \left(\frac{k}{10 \text{ Mpc}^{-1}} \right) + \frac{1}{3} \text{Log} \left(\frac{H_I}{10^{13} \text{ GeV}} \right) + \frac{1}{3} \text{Log} \left(\frac{T_{\text{RH}}}{10^{12} \text{ GeV}} \right), \quad (8.60)$$

where we suppressed subleading terms depending on the temperature today and number of relativistic degrees of freedom. Determining the evolution of the effective mass from the evolution of χ and checking whether N_{last} is realizable, requires specifying an inflationary model and a dedicated analysis beyond this work. It is important to note that we chose only effective couplings between the inflaton and the singlet scalar in (8.58) in order to not destabilize the flat inflaton potential too much [987] and to avoid additional, potentially large, contributions to the energy density of the universe [987]. The second and third operator in the above are motivated by scenarios where the inflaton is protected by a shift symmetry [105], that is only explicitly broken by $V(\chi)$. Consequently these operators do not introduce a new source of shift symmetry breaking.

8.4.3 Saxon oscillation

The Hubble rate during radiation domination and instantaneous reheating (RH), which corresponds to matter domination,

$$H(T) = \frac{\pi^2 g_*(T)}{90 M_{\text{Pl}}} \cdot \begin{cases} T^2 & T < T_{\text{RH}} \\ T^4/T_{\text{RH}}^2 & T \geq T_{\text{RH}} \end{cases} \quad (8.61)$$

in terms of the number of relativistic degrees of freedom g_* . The radial mode starts oscillating with a frequency $m_S(S_i)$ when $3H(T_{\text{osc.}}) = m_S(S_i)$ which determines for radiation domination

$$T_{\text{osc.}} = \left(\frac{135}{8\pi^3 g_*(T_{\text{osc.}})} \right)^{\frac{1}{4}} \sqrt{M_{\text{Pl}} m_S} \sqrt{\frac{S_i}{N f_a}} \quad (8.62)$$

$$\simeq 9.5 \times 10^{14} \text{ GeV} \cdot \sqrt{\frac{m_S}{1 \text{ GeV}}} \cdot \sqrt{\frac{10^6 \text{ GeV}}{N f_a}} \cdot \sqrt{\frac{S_i}{0.1 M_{\text{Pl}}}}. \quad (8.63)$$

The oscillation occurs after reheating ($T_{\text{osc.}} < T_{\text{RH}}$) as long as

$$m_S < \frac{8\pi^3 g_*(T_{\text{osc.}})}{135} \frac{N f_a}{S_i} \frac{T_{\text{RH}}^2}{M_{\text{Pl}}} \simeq 1.1 \text{ GeV} \cdot \left(\frac{N f_a}{10^6 \text{ GeV}} \right) \cdot \left(\frac{0.1 M_{\text{Pl}}}{S_i} \right) \cdot \left(\frac{T_{\text{RH}}}{10^{15} \text{ GeV}} \right)^2. \quad (8.64)$$

For a quartic potential during radiation domination the field value $S \sim 1/a$ redshifts like radiation as a function of temperature for $S > N f_a$

$$S(T > T_S) = S_i \frac{T}{T_{\text{osc.}}}. \quad (8.65)$$

After the Saxon starts to relax to its minimum $S = N f_a$ at the temperature

$$T_S \equiv T_{\text{osc.}} \frac{N f_a}{S_i} \simeq 950 \text{ GeV} \cdot \sqrt{\frac{m_S}{1 \text{ GeV}}} \cdot \sqrt{\frac{N f_a}{10^6 \text{ GeV}}} \cdot \sqrt{\frac{0.1 M_{\text{Pl}}}{S_i}} \quad (8.66)$$

the potential is dominated by the constant mass term in (8.26) and the field value of the now non-relativistic condensate redshifts as

$$S(T \leq T_S) = N f_a \left(\frac{T}{T_S} \right)^{\frac{3}{2}}. \quad (8.67)$$

For oscillations before the completion of reheating we find

$$T_{\text{osc.}}^{\text{RH}} = \left(\frac{135}{8\pi^3 g_*(T_{\text{osc.}})} \right)^{\frac{1}{8}} \left(M_{\text{Pl}} m_S \frac{S_i}{N f_a} \right)^{\frac{1}{4}} \sqrt{T_{\text{RH}}} \quad (8.68)$$

$$\simeq 1.5 \times 10^{15} \text{ GeV} \cdot \left(\frac{m_S}{5 \text{ GeV}} \right)^{\frac{1}{4}} \cdot \left(\frac{10^6 \text{ GeV}}{N f_a} \right)^{\frac{1}{4}} \cdot \left(\frac{S_i}{0.1 M_{\text{Pl}}} \right)^{\frac{1}{4}} \cdot \sqrt{\frac{T_{\text{RH}}}{10^{15} \text{ GeV}}}. \quad (8.69)$$

instead. During reheating we find the scaling law $S \sim 1/a \sim T^{8/3}$ because during matter domination $T \sim 1/a^{3/8}$. For most of our parameter space T_S is below T_{RH} , so the estimate in (8.66) applies with $T_{\text{osc.}}^{\text{RD}}$ replaced by T_{RH} and $S(T_{\text{RH}})$ obtained from the previous scaling. We can also compute the number density of the oscillating and thereby non-relativistic Saxion condensate

$$n_S \equiv \frac{m_S(S)}{2} S^2, \quad (8.70)$$

which follows from its energy density $\rho_S = V_\sigma(S) = m_S n_S$. We want the evolution of the cosmological background to proceed as usual, which is why we demand that there is no period of inflation due the large Saxion field value [990]

$$V_\sigma(S_i) < 3H^2(T_{\text{osc.}})^2 M_{\text{Pl}}^2. \quad (8.71)$$

By making use of $m_S(S_i) = 3H(T_{\text{osc.}})$ we find that this implies [740, 939]

$$S_i < 2M_{\text{Pl}}. \quad (8.72)$$

The evolution of the Saxion field during radiation domination, its energy density and its equation of state parameter ω_S can be summarized by the following scaling relations

$$S \sim \begin{cases} a^{-1} & , \quad \rho_S \equiv \frac{m_S(S)^2}{2} S^2 \sim \begin{cases} a^{-4} & , \quad \omega_S = \begin{cases} \frac{1}{3} & \text{for } S \gg N f_a \\ 0 & \text{for } S \simeq N f_a \end{cases} \\ a^{-3} & , \end{cases} \end{cases} \quad (8.73)$$

In this work we assume that the masses of all additional particles are given by their tree-level expressions and do not get modified due to the large initial field value S_i . Specifically this means that

$$S_i < \begin{cases} M_N/Y_R & \text{Type I} \\ \mu_\eta^2/\kappa & \text{Type II} \\ \mu_\Delta^2/(\lambda_4 v_H) & \text{Type III} \end{cases}, \quad (8.74)$$

If this condition was violated ν_R and N_L would form a Dirac fermion of mass $Y_R S_i$ or H , η would mix strongly. Furthermore we impose that the heavy messenger fields are not present in the plasma at any point in time

$$\text{Max} \left(T_{\text{osc.}}, T_{\text{RH}}, T_{\text{max}}, \frac{H_I}{2\pi} \right) < \begin{cases} M_N & \text{Type I} \\ \mu_\eta & \text{Type II} \\ \mu_\Delta, M_F & \text{Type III} \end{cases}, \quad (8.75)$$

where $H_I/(2\pi)$ is the Gibbons-Hawking temperature during inflation [850], T_{RH} the radiation bath temperature at the end of reheating and

$$T_{\text{max}} \equiv \beta \sqrt{\sqrt{\frac{3}{8\pi}} H_I M_{\text{Pl}}}, \quad \text{with } \beta \in [0, 1] \quad (8.76)$$

the maximum temperature during reheating [816, 991], which can be much larger than T_{RH} . Note that it will in general be hard to satisfy (8.75) for the Type III scenario due to the smallness of $\mu_\Delta \simeq \mathcal{O}(100\text{TeV})$ (see equation (8.19)) unless we assume a low Hubble scale during inflation and a small reheating temperature. As long as (8.75) is satisfied the Saxon will not receive a thermal mass of the order YT , where Y is a Yukawa or the square root of quartic coupling from (8.74). However since the heavy η or Δ coupling to σ have electroweak gauge interactions, integrating them out can potentially modify the logarithmic running of the weak gauge couplings manifesting itself in a so called thermal logarithmic potential [992, 993]

$$V_{\text{Log.}}(T) = c_W \alpha_W^2 T^4 \log\left(\frac{S^2}{T^2}\right). \quad (8.77)$$

Here c_W is a model-dependent coefficient from the couplings of η, Δ to σ . Demanding that this correction is subdominant to the quartic potential, so that the Saxon oscillates around its mass in (8.53), leads to the condition

$$S_i > \alpha_W \sqrt{\frac{c_W}{g_*(T_{\text{osc.}})}} M_{\text{Pl.}} \simeq 10^{16} \text{ GeV} \cdot \sqrt{c_W} \cdot \left(\frac{\alpha_W}{1/100}\right) \cdot \sqrt{\frac{100}{g_*(T_{\text{osc.}})}}. \quad (8.78)$$

To be conservative we will take $S_i > 10^{16}$ GeV throughout this work. Note that this bound will be absent for the Type I Seesaw, because the heavy vectorlike neutrinos have no weak gauge couplings. In section 8.8.3 we investigate the one loop quantum corrections to the Saxon quartic.

8.4.4 Generating the Diraxion rotation

We assume that the global symmetry is spontaneously broken with a vev S_i during inflation that is significantly larger than today. Due to this vev, Planck scale suppressed explicit symmetry breaking will be active. As longs as the mass of the angular mode (during inflation) is small compared to the radial mode, we can consider $U(1)_D$ as an approximate symmetry (during inflation). The explicit breaking then becomes irrelevant as the vev relaxes to its true vacuum at Nf_a today. During inflation the Diraxion will have a mass

$$m_a(S_i)^2 \equiv m_a^2 \left(\frac{S_i}{Nf_a}\right)^{N-2}. \quad (8.79)$$

In order for our description in terms of an approximate $U(1)_D$ symmetry to apply we require that the Diraxion mass during inflation is smaller than the Saxon mass in (8.53) [934], which leads to

$$m_a < m_S \left(\frac{Nf_a}{S}\right)^{\frac{N-4}{2}}. \quad (8.80)$$

For $N = 4$ this would reduce to the requirement for the PNGB mass compared to the mass for the Higgs scalar of the underlying symmetry $m_a < m_S$. We further deduce that

we can not take N to be arbitrarily large in order not to spoil the previous relation. Next one defines the charge yield or asymmetry of the scalar condensate as

$$n_\theta \equiv \frac{\dot{\theta} S^2}{N^2}, \quad (8.81)$$

which is conserved as long as there are no interactions that explicitly violate the underlying global $U(1)_D$ symmetry. One can understand the fact that only a rotating condensate can carry a charge compared to an oscillating one from the observation that an oscillation is a superposition of two rotations in opposite directions [994]. The Planck suppressed effective operators in $V_{\mathcal{D}}$ of section 8.3.5, that are responsible for generating the Diraxion mass, convert a part of the oscillatory motion of the radial mode into a velocity for the angle. After the radial mode has decreased via redshifting and eventually settled to its minimum, the Planck suppressed operators σ^N become negligible for $N > 5$ [942]. The corresponding equation of motion reads [942]

$$\dot{n}_\theta + 3Hn_\theta = \frac{i}{N} \left(\sigma^* \frac{\partial V_{\mathcal{D}}}{\partial \sigma^*} - \sigma \frac{\partial V_{\mathcal{D}}}{\partial \sigma} \right), \quad (8.82)$$

$$= \frac{2|c^{(i)}|}{\sqrt{2}^N} \frac{S_i^N}{M_{\text{Pl}}^{N-4}} \sin(\theta + \delta). \quad (8.83)$$

Due to the redshifting of S the majority of the asymmetry is produced at the start of the Saxion oscillations over one Hubble time $t \simeq 1/H(T_{\text{osc.}}) \simeq 3/m_S(S_i)$ [740] and we find

$$n_\theta(T_{\text{osc.}}) \simeq \frac{\dot{n}_\theta(T_{\text{osc.}})}{m_S(S_i)} = \frac{6|c^{(i)}|}{\sqrt{2}^N} \left(\frac{S_i}{M_{\text{Pl}}} \right)^{N-4} \frac{S_i^4}{m_S(S_i)} \sin(\theta_i + \delta). \quad (8.84)$$

Here θ_i is the initial angle of the Diraxion also known as the misalignment angle. It is customary (see e.g. [78, 410]) to define the eccentricity parameter ε [922, 942]

$$\varepsilon \equiv \frac{n_\theta m_S(S_i)}{V_\sigma(S_i)} = \frac{24}{N^2} \left(\frac{m_a}{m_S} \right)^2 \left(\frac{S_i}{N f_a} \right)^{N-4} \sin(\theta_i + \delta) \simeq \frac{12}{N} \frac{\partial V_{\mathcal{D}}/\partial S}{\partial V_\sigma/\partial S}, \quad (8.85)$$

where we made use of the definition of the Diraxion mass in (8.36) and the Saxion mass in (8.53). The last approximate equality holds for $\sin(\theta_i + \delta) \simeq \mathcal{O}(1)$, which suppresses axion isocurvature perturbations [942] (see section 8.8). This parameter $\varepsilon \leq 1$ has the following physical interpretation: An orbit with $\varepsilon = 1$ corresponds to a perfectly circular rotation, whereas $\varepsilon = 0$ for a pure oscillation in the Saxion direction. Our scenario is different from the case of QCD-Axiogenesis [922] because here the “kick” in the angular direction and the Diraxion mass originate from the same operator, so that we can in principle choose $\varepsilon \simeq 1$. For a quartic potential and a QCD axion this is in general not possible [740], because of the axion quality problem from the Planck suppressed operators, which can shift the minimum of the QCD axion to too large angles compared to the limit from the neutron’s electric dipole moment. However for $\varepsilon = 1$ two complications arise: On the one hand we can no longer neglect $V_{\mathcal{D}}$ compared to the quartic term when

determining the Saxion mass and initial field value, so our present description based on (8.53) breaks down. Additionally for larger V_{ϕ} one can no longer neglect the angular gradient compared to the Hubble friction, so that the Diraxion stops being overdamped and starts to relax to the minimum of its potential given by (see also the discussion in section 8.8.1)

$$\frac{\partial V_{\phi}}{\partial \theta} \Big|_{\theta_i} \sim -m_a(S_i)^2 S_i^2 \sin(\theta_i + \delta) \stackrel{!}{=} 0. \quad (8.86)$$

If the Diraxion is trapped in such a vacuum, the rotation of the condensate will not occur or be significantly damped [942], which is why we demand $\varepsilon < 1$

$$m_a < \frac{N}{2\sqrt{6}} \left(\frac{N f_a}{S_i} \right)^{\frac{N-4}{2}} m_S. \quad (8.87)$$

This condition intuitively means that the Diraxion should not start oscillating before the Saxion [942], which is nothing more than the requirement $m_a(S_i) < m_S(S_i)$ we already imposed in (8.80) to have a Pseudo-Nambu-Goldstone boson, hence the bounds being the same up to a prefactor. Both conditions automatically make sure that Diraxion is in motion [934] since its velocity $\dot{\theta} \simeq m_S(S)$ is always larger than its mass $m_a(S)$. In a quartic potential the angular and radial modes redshift as radiation for $S \gg N f_a$ ($\omega_S = \omega_{\theta} = 1/3$). For cosmological reasons that will be elaborated upon in section 8.9, the Saxion needs to be thermalized and will typically loose its energy to the SM plasma. After the damping of the Saxion oscillations only the angular rotation, which is now perfectly circular, remains. The angular rotation is stable because of $U(1)_D$ -charge conservation. It minimizes the free energy [922] and can loose energy to thermal bath via interactions with particles charged under $U(1)_D$ leading to the production of fermionic asymmetries. However as long as the Noether charge of the condensate $\dot{\theta} S^2$ is larger than the typically produced fermionic asymmetry $\dot{\theta} T^2$, it is energetically favoured for the rotating condensate to retain most of its charge compared to the production of fermions. This requirement can be expressed as [922, 995]

$$N f_a \gg T_S, \quad (8.88)$$

where T_S defined in (8.66) is the temperature at which the Saxion reaches its minimum $S = N f_a$. This condition implies that $T_{\text{osc.}} \ll S_i$ for a quartic potential with the oscillation temperature from (8.62) and it can be expressed as

$$\frac{m_S}{N f_a} \ll \sqrt{\frac{8\pi^3 g_*(T_{\text{osc.}})}{135}} \frac{S_i}{M_{\text{Pl}}} \lesssim 14.5 \cdot \sqrt{\frac{g_*(T_{\text{osc.}})}{100}} \quad (8.89)$$

which is not a strong constraint compared to the limits from isocurvature in section 8.8.1. The tilt in the angular direction responsible for the Diraxion mass can also lead to washout by converting Diraxions into Saxions, who scatter of the plasma with a rate Γ_S defined in sections 8.5.1 and 8.9. The resulting rate for the angular mode is then

suppressed by a factor of $m_a(S_i)^4/m_S(S_i)^4$ leading to a rate of [934]

$$\Gamma_a \simeq \left(\frac{m_a}{m_S}\right)^4 \left(\frac{Nf_a}{S_i}\right)^{2(N-4)} \Gamma_S, \quad (8.90)$$

which is too suppressed to matter compared to Γ_S . Once it thermalizes and reaches $S = Nf_a$ the Saxion behaves as non-relativistic matter ($\omega_S = 0$) and the Diraxion has the equation of state of kination $\omega_\theta = 1$, because only the kinetic energy of the remaining circular rotation is left, which is why then $\varepsilon = 1$. We can summarize the evolution of the angular field by the following scaling relations

$$\dot{\theta} \sim \begin{cases} a^{-1} \\ a^{-3} \end{cases}, \quad \rho_\theta \equiv \frac{\dot{\theta}^2}{2} S^2 \sim \begin{cases} a^{-4} \\ a^{-6} \end{cases}, \quad \omega_\theta = \begin{cases} \frac{1}{3} & \text{for } S \gg Nf_a \\ 1 & \text{for } S \simeq Nf_a \end{cases}. \quad (8.91)$$

During the time when S approaches Nf_a and redshifts as $S \sim 1/a^{3/2}$ before settling in its minimum we have a constant $\dot{\theta} \sim a^0$. We further define the conserved charge yield n_θ/s for an oscillation starting during radiation domination with $T_{\text{osc.}} < T_{\text{RH}}$

$$Y_\theta^{\text{RD}} \equiv \frac{n_\theta(T_{\text{osc.}})}{s(T_{\text{osc.}})}. \quad (8.92)$$

If the oscillation starts before the end of reheating $T_{\text{osc.}} > T_{\text{RH}}$ we need a different adiabatic invariant than n_θ/s , because entropy is not conserved during reheating. Instead one normalizes $n_\theta \sim 1/a^3$ to the energy density of the non-relativistic inflaton $\rho_{\text{inf.}} \sim n_{\text{inf.}} \sim 1/a^3$ [740, 942]

$$Y_\theta^{\text{RH}} \equiv \frac{n_\theta(T_{\text{RH}})}{s(T_{\text{RH}})} = \frac{n_\theta}{\rho_{\text{inf.}}} \Big|_{T=T_{\text{osc.}}} \cdot \frac{\rho_{\text{inf.}}}{s} \Big|_{T=T_{\text{RH}}} = \frac{n_\theta(T_{\text{osc.}})}{s(T_{\text{RH}})} \cdot \left(\frac{T_{\text{RH}}}{T_{\text{osc.}}}\right)^8. \quad (8.93)$$

After Saxion thermalization, where $\varepsilon \rightarrow 1$, and while the Saxion still approaches its minimum Nf_a one finds that the equations of motion for θ reduce to the balance between the radial potential gradient and the centripetal force $S(\dot{\theta}/N)^2$ [931]

$$\dot{\theta}^2 = \frac{N^2}{S} \frac{\partial V(S)}{\partial S} = N^2 m_S(S)^2. \quad (8.94)$$

Note that the energy density in the rotation $\rho_\theta = \varepsilon \rho_S$ (with $\rho_S = V_\sigma(S_i)$) does not affect the condition of having less energy in the condensate than the radiation bath leading to (8.71), because the Diraxion energy originates from the Saxion oscillation, whose energy decreases to $(1 - \varepsilon)\rho_S$ after the kick in the angular direction. As a consequence of the oscillations for $\varepsilon \ll 1$ the quantities S and $\dot{\theta}$ will not be constant in time and oscillate themselves around their minimum and maximum values during one cycle

$$S_{\text{min}} \equiv \varepsilon S, \quad \dot{\theta}_{\text{max}} = \frac{Nm_S(S)}{\varepsilon}, \quad (8.95)$$

which can be obtained from the conservation of charge and energy

$$n_\theta = \varepsilon m_S(S) S_{\text{max}}^2, \quad \rho_S + \rho_\theta = m_S(S)^2 S_{\text{max}}^2, \quad (8.96)$$

where S_{\max} denotes the maximum field value during a cycle and we identify

$$S_{\max}(T_{\text{osc.}}) = S_i. \quad (8.97)$$

The Diraxion velocity is as large as $\dot{\theta}_{\max}$ for a time scale $\Delta t \simeq 1/\dot{\theta}_{\max}$. If we compute the cycle average of $\dot{\theta}$ over a time scale $t_S \equiv 1/m_S(S)$ we find that [942]

$$\langle \dot{\theta} \rangle \simeq \frac{\Delta t}{t_S} \dot{\theta}_{\max} = N m_S(S). \quad (8.98)$$

More refined analytical [939] and numerical [942] calculations have confirmed that $\langle \dot{\theta} \rangle = N m_S(S)$ is indeed an attractor solution, meaning that $\langle \dot{\theta} \rangle$ is independent of ε in practise [942]. In the above expression for m_S we slightly abuse notation by denoting the root-mean-square $\sqrt{\langle S^2 \rangle}$ of the Saxion amplitude with the same symbol as its (oscillating) field value S . If parametric resonance from Saxion oscillations occurs (see section 8.6.5) the average of $\dot{\theta}$ gets reduced and one finds [942]

$$\langle \dot{\theta} \rangle = \varepsilon N m_S(S). \quad (8.99)$$

Note that reference [942] employs a different parameterization of ε , that determines the frequency ω of the coherent motion from the full potential $V = V_\sigma + V_\phi$

$$\varepsilon \equiv \frac{n_\theta}{N \omega S_{\max}^2}, \quad \text{with} \quad \omega \equiv \sqrt{\frac{1}{S} \frac{\partial V(S)}{\partial S}} \Big|_{S_{\max}} \quad \text{and} \quad n_S = \frac{\dot{S}^2}{\omega} \Big|_{S_{\max}}. \quad (8.100)$$

Formally this parameterization coincides with our choice of ε in (8.85) only for $\varepsilon \ll 1$. For simplicity we keep using (8.85) and demand $\varepsilon \ll 1$. We assume that $\dot{\theta}$ and consequently $\dot{\theta}_{\max}$ changes only adiabatically, meaning slower than the time scale of the plasma $1/T$, which is why we impose $\dot{\theta}_{\max} < T_{\text{osc.}}$ [942] leading to

$$m_a > 0.24 \sqrt{N} \cdot \begin{cases} g_*(T_{\text{osc.}})^{\frac{1}{8}} m_S \left(\frac{m_S}{M_{\text{Pl}}} \right)^{\frac{1}{4}} \left(\frac{N f_a}{S_i} \right)^{\frac{2N-9}{4}} & \text{RD} \\ g_*(T_{\text{osc.}})^{\frac{1}{16}} \sqrt{N} \frac{m_S^{\frac{11}{8}}}{M_{\text{Pl}}^{\frac{1}{8}} T_{\text{RH}}^{\frac{1}{4}}} \left(\frac{N f_a}{S_i} \right)^{\frac{4N-17}{8}} & \text{RH} \end{cases}. \quad (8.101)$$

Additionally we assume that the Saxion field value is always the largest energy scale in the plasma $S_{\min} = \varepsilon S_i > T_{\text{osc.}}$ [942] from which we find

$$m_a > 0.19 N \cdot \begin{cases} \frac{1}{g_*(T_{\text{osc.}})^{\frac{1}{8}}} \frac{m_S^{\frac{5}{4}} M_{\text{Pl}}^{\frac{1}{4}}}{\sqrt{S_i}} \left(\frac{N f_a}{S_i} \right)^{\frac{2N-9}{4}} & \text{RD} \\ \frac{1}{g_*(T_{\text{osc.}})^{\frac{1}{16}}} \frac{m_S^{\frac{9}{8}} M_{\text{Pl}}^{\frac{1}{8}} T_{\text{RH}}^{\frac{1}{4}}}{\sqrt{S_i}} \left(\frac{N f_a}{S_i} \right)^{\frac{4N-19}{8}} & \text{RH} \end{cases} \quad (8.102)$$

and one observes that both bounds are comparable in strength. These bounds are weakest for $N = 5$ due to an approximate cancellation in the exponent of $N f_a/S_i$, and get stronger for larger N . For reference we will take $N = 6$ throughout this paper.

8.5 Dirac-Lepto-Axiogenesis

8.5.1 Dissipation coefficient from Dirac Weinberg operator

The Saxon only couples to the thermal bath via its mixed quartic with the Higgs or the non-renormalizable Dirac Weinberg operator. A proper determination of the relevant dissipation coefficient [996, 997] for our scenario would involve two-loop thermal self energy diagrams [998], which is why we resort to dimensional analysis. The Saxon can scatter via the reactions $HS \rightarrow \bar{L}\nu_R$, $LS \rightarrow H^\dagger\nu_R$ or decay as $S \rightarrow \bar{L}H^\dagger\nu_R$, where we assumed a vanishing thermal abundance of ν_R and put the non-thermal S in the initial state. Due to time-dilation effects [299] the decay will only be relevant for $m_S(S) < T$, which is why we add both contributions as

$$\Gamma_S(S) \equiv \frac{1}{16\pi} \left(\frac{\sum m_\nu^2}{v_H^2} \right) \left(\frac{S}{Nf_a} \right)^2 (2T + m_S(S)). \quad (8.103)$$

The scaling is similar to the interaction of two Higgsinos with two Saxes considered in [944] and can be understood as follows: The matrix element involves one insertion of S and the factor $m_\nu/(v_H N f_a)$ from the coefficient of the Dirac Weinberg operator. After squaring the matrix element to obtain the rate one can use dimensional analysis to find the remaining factor of $2T$ for the two scattering modes or $m_S(S)$ for the decay. One should keep in mind that the rate depends on the time-dependent field value S and not on its amplitude S_{\max} [999]. After thermalization of S the rate reduces to

$$\Gamma_L(T) \equiv \frac{1}{16\pi} \left(\frac{\sum m_\nu^2}{v_H^2} \right) \frac{2T^3 + m_S^3}{(Nf_a)^2}, \quad (8.104)$$

and the overall rate for $T > m_S(S)$ differs only by a factor of $v_H^2/(Nf_a)^2$ from the result for Majorana neutrinos. We always find that $m_S(S) \ll T$ for $S \gg Nf_a$ because $m_S(S_i) = 3H(T_{\text{osc}}) \ll T_{\text{osc}}$, which is why the Saxon decay is negligible above T_S .

8.5.2 Chemical potentials and Boltzmann equation

The derivative coupling of the spatially homogeneous Diraxion $\partial_\mu \theta \bar{\nu}_R \gamma^\mu \nu_R$ defined in (8.47) can be thought of as inducing an effective chemical potential for the right chiral neutrinos [119, 918, 1000]

$$\mu_{\nu_R}^{\text{eff.}} \equiv c_{\nu_R} \dot{\theta}. \quad (8.105)$$

As pointed out in [1001–1003] and more recently in [1004] however this derivative coupling does not lead to actual splittings in the single particle energies of particles and anti-particles, which is why it is not an actual chemical potential. A more accurate way to think about the effect of $\dot{\theta}$ is to treat it as a background field that shifts the dispersion relation of the particles coupling to it $E = \sqrt{p^2 + m^2} \rightarrow \sqrt{p^2 + m^2} \mp c_{\nu_R} \dot{\theta}$ [1001–1003] with a (minus) plus sign for (anti-)particles in analogy to explicit CPT-violation in the form of different masses for particles and antiparticles, see e.g. [1005]. Since the

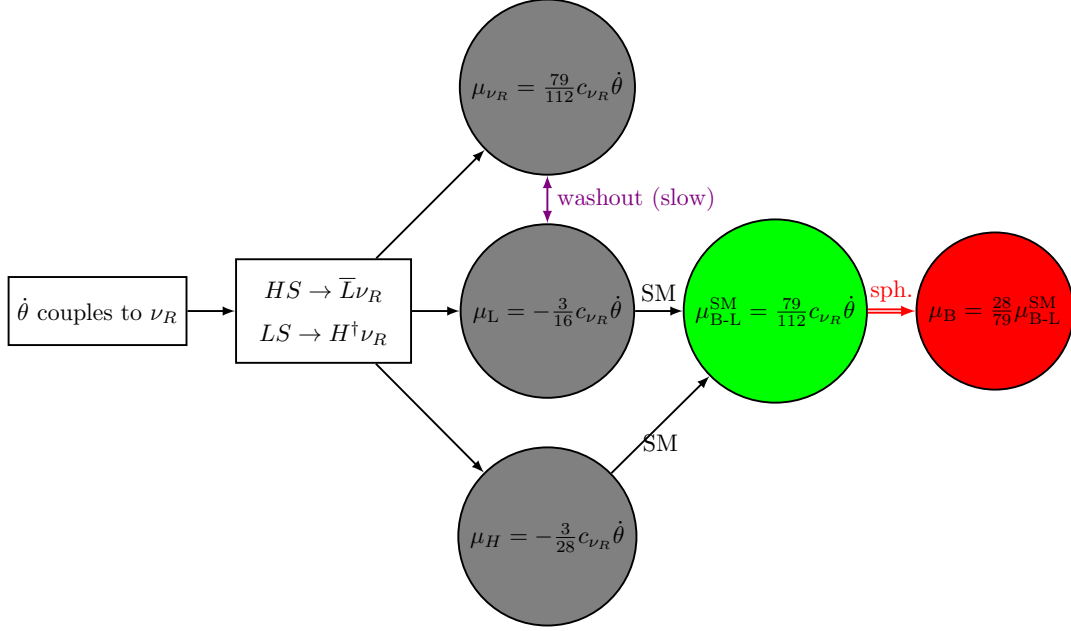


Figure 8.4: Schematic representation of the reaction chain for generating a chemical potential in baryons. The arrows labelled “SM” indicate the network of equilibrated Standard Model Yukawa and gauge interactions. The red arrow labelled “sph.” stands for the $B+L$ violating electroweak sphaleron process. Time progresses from left to right.

background field $\dot{\theta} \neq 0$ spontaneously violates CPT in the plasma, this scenario is known as spontaneous Baryogenesis [119, 918] and we do not need to worry about the Sakharov conditions [602], which assume CPT-conservation. If the Dirac Weinberg operator leads to reactions $HS \rightarrow \bar{L}\nu_R$, $HL \rightarrow S\nu_R$ or $S \rightarrow \bar{L}\nu_R H^\dagger$ in equilibrium, then the chemical potentials satisfy

$$\mu_L - \mu_H + \mu_{\nu_R} + c_{\nu_R} \dot{\theta} = 0, \quad (8.106)$$

where we used that the real valued Saxion has no chemical potential. The same result can be obtained without making reference to the effective chemical potential $\mu_{\nu_R}^{\text{eff}}$: Suppose we work in the basis, where we do not remove the phase of the Dirac Weinberg operator $m_\nu / (v_H N f_a) e^{i\theta(t)}$ and hence have no derivative couplings of the Diraxion to ν_R . The time dependent phase in the aforementioned coupling does not enter the matrix element but rather it modifies the delta distributions encoding energy-momentum-conservation by also taking the effect of the slowly varying background field into account [950]. For e.g. $HS \rightarrow \bar{L}\nu_R$ one would find $E_H + E_S = E_L + E_{\nu_R} - c_{\nu_R} \dot{\theta}$ [1001--1003] and via the collision term of the Boltzmann equation³ one is then lead to the same equation for the

³The energy and chemical potential enter the phase space distribution functions with opposite signs e.g. $f_i \sim \exp((-E_i + \mu_i)/T)$ for a non-relativistic particle i .

chemical potentials as in (8.106). We now also impose the conservation of the total B-L, which might be gauged in the UV and is responsible for the Dirac nature of neutrinos,

$$2\mu_Q + \mu_u + \mu_d - 2\mu_L - \mu_e - \mu_{\nu_R} \equiv \mu_{\text{B-L}}^{\text{SM}} - \mu_{\nu_R} = 0. \quad (8.107)$$

Here the actual chemical potential μ_{ν_R} appears, because as previously discussed $c_{\nu_R}\dot{\theta}$ only contributes to scattering processes involving ν_R . Next, if we impose the conservation of hypercharge, take all SM Yukawa and gauge interactions to be fast (see e.g. appendix C in [1006]) and treat all flavors the same, then the network of chemical reaction implies that in equilibrium

$$\mu_B^{\text{eq.}} = \frac{28}{79}\mu_{\text{B-L}}^{\text{SM eq.}}, \quad \text{with} \quad \mu_{\text{B-L}}^{\text{SM eq.}} = \mu_{\nu_R}^{\text{eq.}} = \frac{79}{112}c_{\nu_R}\dot{\theta}. \quad (8.108)$$

The relation between $\mu_B^{\text{eq.}}$ and $\mu_{\text{B-L}}^{\text{SM eq.}}$ is given by the standard value 28/79 [115, 612] for the sphaleron redistribution coefficient. By employing the relation $n_i = \mu_i/6T^2$ between asymmetries and chemical potential for a fermionic particle i and using the principle of detailed balance we can immediately write down the Boltzmann equation for $n_{\text{B-L}}^{\text{SM}}$

$$\frac{d}{dt} n_{\text{B-L}}^{\text{SM}} + 3H n_{\text{B-L}}^{\text{SM}} = -\Gamma_S(S) \left(n_{\text{B-L}}^{\text{SM}} - \frac{79}{672}c_{\nu_R}\dot{\theta}T^2 \right) \quad (8.109)$$

in terms of the dissipation coefficient $\Gamma_S(S)$ defined in (8.103). Our mechanism is similar to the case of Dirac-Leptogenesis [117] in the sense that total lepton number vanishes and we produce equal asymmetries ($n_{\text{B-L}}^{\text{SM}} = n_{\nu_R}$) in the left- and right-chiral leptons. These leptonic asymmetries are never equilibrated because in the following we take Γ_S to be slow for $S \gg Nf_a$. Once $S \simeq Nf_a$ we recover the usual Yukawa interaction with the Higgs from the Dirac Weinberg operator, which is always slow due to the smallness of the effective Yukawa coupling m_ν/v_H [117]. The B+L-violating sphaleron transition only acts on the doublet of left-chiral leptons and converts $n_{\text{B-L}}^{\text{SM}}$ into the observed baryon asymmetry. A sketch of the scenario can be found in figure 8.4.

8.5.3 Baryon Asymmetry

We rewrite (8.109) in terms of the dimensionless yield $n_{\text{B-L}}^{\text{SM}}/s$, which is conserved in the comoving volume as long as entropy is conserved

$$\frac{d}{dt} \frac{n_{\text{B-L}}^{\text{SM}}}{s} = -\Gamma_S(S) \left(\frac{n_{\text{B-L}}^{\text{SM}}}{s} - \frac{79}{672} \frac{c_{\nu_R}\dot{\theta}T^2}{s} \right) \quad (8.110)$$

Solving (8.110) is in general complicated by the fact that our problem has two intrinsic time-scales: The expansion rate of the universe and the oscillation frequency $m_S(S)$. Since our dissipation coefficient is given in terms of an effective operator, it will be UV-dominated and hence we expect the baryon asymmetry to be predominantly produced at $T_{\text{osc.}}$. By definition we have $3H(T_{\text{osc.}}) = m_S(S_i)$ at this point in time, which simplifies the problem. The last complication is the fact that the production rate $\Gamma_S(S)$ depends

on the oscillating field value, which is why we need to average over one cycle of oscillations. Reference [942] solved (8.110) numerically (see appendix E of the aforementioned reference) and provided analytical arguments to understand the resulting abundances given by

$$\left\langle \frac{n_{\text{B-L}}^{\text{SM}}}{s} \right\rangle \simeq \frac{79}{672} \frac{c_{\nu_R} N \langle \dot{\theta} \rangle T_{\text{osc.}}^2}{s} \cdot \begin{cases} 1 & \Gamma_S(S_i) \gg \frac{m_S(S_i)}{\varepsilon^3} \\ \varepsilon \left(\frac{\Gamma_S(S_i)}{m_S(S_i)} \right)^{\frac{1}{3}} & m_S(S_i) \ll \Gamma_S(S_i) \ll \frac{m_S(S_i)}{\varepsilon^3} \\ 2\varepsilon & \Gamma_S(S_i) \ll m_S(S_i) \end{cases} \quad (8.111)$$

The first result can be understood as follows [942]: In order for $\langle n_{\text{B-L}}^{\text{SM}} \rangle / s$ to track its equilibrium value, $\dot{\theta}$ needs to be close to its maximum $\dot{\theta}_{\text{max}} = m_S(S_i)/\varepsilon > m_S(S_i)$. However due to the conservation of the condensate charge $n_{\theta} = \varepsilon m_S(S_i) S_i^2$ we find that this only occurs when S is at its minimum for a cycle given by $S_{\text{min}} = \varepsilon S_i$ (see (8.95)). For a field-dependent interaction it was found in [942], that the charge transfer from the condensate to the plasma is only efficient if the transfer rate is larger than the frequency of the coherent motion, which for this case reads

$$\Gamma_S(S_{\text{min}}) \sim \varepsilon^2 S_i^2 \gg \dot{\theta}_{\text{max}} = \frac{m_S(S_i)}{\varepsilon} \quad (8.112)$$

and reduces to the condition $\Gamma_S(S_i) \gg m_S(S_i)/\varepsilon^3$ displayed in (8.111). However if we take e.g. $\varepsilon = 0.1$ then this implies that $\Gamma_S(S_i)$ would have to be a thousand times faster than the Hubble rate at the beginning of the oscillations. We discuss in section 8.9.1 how this is potentially problematic. The next regime $m_S(S_i) \ll \Gamma_S(S_i) \ll m_S(S_i)/\varepsilon^3$ suffers from the same drawback. Since $\Gamma_S(S_{\text{min}})$ is now too small to track $\dot{\theta}_{\text{max}}$, the transfer can only be relevant when S is close to its maximum value $S_{\text{max}}(T_{\text{osc.}}) = S_i$. Once S decreases from its maximum during a cycle and $\dot{\theta}$ increases, $\langle n_{\text{B-L}}^{\text{SM}} / s \rangle$ stops tracking $\dot{\theta} T^2 / s$ as soon as $\dot{\theta}$ reaches the value $\dot{\theta}_d \simeq \varepsilon \Gamma_S(S_i)^{\frac{2}{3}} m_S(S_i)^{\frac{1}{3}}$ at which it stays for a time of $\Delta t_d \simeq \Gamma_S(S_i)^{-\frac{1}{3}} m_S(S_i)^{-\frac{2}{3}}$ so that the average over a time scale $t_S = 1/m_S(S_i)$ becomes [942]

$$\langle \dot{\theta} \rangle = \frac{\Delta t_d}{t_S} \dot{\theta}_d = \varepsilon m_S(S_i) \left(\frac{\Gamma_S(S_i)}{m_S(S_i)} \right)^{\frac{1}{3}}. \quad (8.113)$$

Rotation during Radiation domination

To be conservative we focus on the regime $\Gamma_S(S_i) \ll m_S(S_i) \simeq 3H(T_{\text{osc.}})$, which can be thought of as Freeze-In production [82] in contrast to the previous two cases, which are akin to thermal Freeze-Out. We average the Boltzmann equation in (8.110) over a time scale larger than $t_S = 1/m_S(S_i)$ and factor out the S -dependence of the rate by employing (8.103) and (8.104) to rewrite $\Gamma_S = \Gamma_L \cdot (S/T)^2$ leading to

$$\left\langle \frac{d}{dt} \frac{n_{\text{B-L}}^{\text{SM}}}{s} \right\rangle = -\Gamma_L(T) \left(\left\langle \frac{n_{\text{B-L}}^{\text{SM}}}{s} \right\rangle \frac{\langle S^2 \rangle}{T^2} - \frac{79}{672} \frac{c_{\nu_R} \langle \dot{\theta} S^2 \rangle}{s} \right). \quad (8.114)$$

Because θ and S move together coherently in the broken phase, we have to average them together as $\langle \dot{\theta}S^2 \rangle$ (unless parametric resonance occurs). For $\Gamma_S(S_i) \ll m_S(S_i)$ it follows that S evolves much faster than $n_{\text{B-L}}^{\text{SM}}/s$, which is why we can set $\left\langle \frac{d}{dt} \frac{n_{\text{B-L}}^{\text{SM}}}{s} \right\rangle = 0$ [942] and thus solve for $\langle n_{\text{B-L}}^{\text{SM}}/s \rangle$ from the vanishing of the parenthesis above. To do so we make use of the charge conservation [942]

$$Nn_\theta = \frac{1}{N} \langle \dot{\theta}S^2 \rangle = \varepsilon n_S = \varepsilon m_S(S) \langle S^2 \rangle \quad (8.115)$$

and obtain $\langle n_{\text{B-L}}^{\text{SM}}/s \rangle \sim \langle \dot{\theta}S^2 \rangle / \langle S^2 \rangle = \varepsilon N m_S(S_i)$, which explains the factor of ε in the last line of (8.111) and the factor of two comes from matching to the previous two solutions. However $\left\langle \frac{d}{dt} \frac{n_{\text{B-L}}^{\text{SM}}}{s} \right\rangle = 0$ can also be obtained from $\Gamma_S \rightarrow 0$ and we expect [82] the Freeze-In abundance to vanish if the production rate goes to zero (there is only an upper limit on Γ_S in the third line of (8.111)). Therefore we write

$$\left\langle \frac{n_B}{s} \right\rangle \simeq \frac{c_{\nu_R} N}{24} \cdot \frac{\Gamma_S(S_i)}{H(T_{\text{osc.}})} \cdot \frac{\varepsilon m_S(S_i) T_{\text{osc.}}^2}{s(T_{\text{osc.}})} \quad (8.116)$$

$$= \frac{c_{\nu_R} N^2}{24} \cdot \frac{\Gamma_S(S_i)}{H(T_{\text{osc.}})} \cdot \left(\frac{T_{\text{osc.}}}{S_i} \right)^2 \cdot Y_\theta^{\text{RD}}, \quad (8.117)$$

where in the last line we used the charged yield during radiation domination defined in (8.92). The same result can also be found from dropping the back-reaction term $\propto \langle n_{\text{B-L}}^{\text{SM}}/s \rangle$ in (8.114) and considering the amount of asymmetry produced $\langle n_{\text{B-L}}/s \rangle \simeq 1/H \cdot d/dt \langle n_{\text{B-L}}/s \rangle$ over one Hubble time $1/H$ together with the charge conservation in (8.115). One can observe that the resulting asymmetry is suppressed by both $\varepsilon < 1$ and $\Gamma_S/H \ll 1$ compared to the scenario for a very efficient charge transfer $\Gamma_S(S_i) \gg m_S(S_i)/\varepsilon^3$, which also justifies neglecting the back-reaction. By using the scaling relations for the redshift of S one can deduce that during radiation domination we have $m_S(S) \sim S \sim T$ and $\Gamma_S/H \sim S^2/T \sim T$ leading to $\langle n_B/s \rangle \sim T$, which means that the produced asymmetry is indeed UV dominated. We deviate from [942] by writing our result in terms of $m_S(S_i)$ instead of $\langle \dot{\theta} \rangle$ for the following reason: Typically one has $\langle \dot{\theta} \rangle = m_S(S_i)$ at the beginning of oscillations, except when parametric resonance from Saxion oscillations takes place (see section 8.6.5), where one obtains $\langle \dot{\theta} \rangle = \varepsilon m_S(S_i)$ instead. However our asymmetry is sourced by $\langle \dot{\theta}S^2 \rangle$ and not just $\langle \dot{\theta} \rangle$, so no additional factor of ε arises. The net effect of parametric resonance is that the radial and angular fields will not move coherently anymore due to the non-thermal symmetry restoration, which simply means that we can separate the averages $\langle \dot{\theta}S^2 \rangle = \langle \dot{\theta} \rangle \langle S^2 \rangle$ [942].⁴ The baryon asymmetry differs from the result for Majorana Lepto-Axiogenesis [942] in two aspects: On the one hand our asymmetry always depends on ε due to the linear coupling to S and on the other hand the ratio Γ_S/H is parametrically different from the suppression factor Γ_L/H found in the Majorana scenario. The order of magnitude and sign of the asymmetry will be determined by the first oscillation [919, 984, 985]. If we plug in the

⁴Using this together with the charge conservation (8.115) then readily implies $\langle \dot{\theta} \rangle = \varepsilon m_S(S_i)$.

out-of-equilibrium condition for successful Freeze-In $\Gamma_S(S_i) \ll m_S(S_i) = 3H(T_{\text{osc.}})$ we obtain an upper limit on the produced asymmetry

$$\left\langle \frac{n_B}{s} \right\rangle \ll \frac{c_{\nu_R} N^2}{8} \cdot \left(\frac{T_{\text{osc.}}}{S_i} \right)^2 \cdot Y_\theta, \quad (8.118)$$

in terms of the charge yield of the condensate. Since the above is much less⁵ than n_θ/s , it was valid to neglect the back-reaction of the asymmetry production on the condensate; Leptogenesis will not evaporate the condensate. The produced leptonic asymmetry is not washed out, because the Dirac Weinberg operator is the only coupling connecting ν_R to the bath and we take it to be slow throughout the evolution of the universe. Once the Saxion settles at its minimum $N f_a$ the Dirac Weinberg operator reduces to the Yukawa coupling of the neutrinos with the SM like Higgs, which never equilibrates [117]. To estimate the baryon asymmetry we eliminate f_a via the condition $\Gamma_S(S_i)/H(T_{\text{osc}}) < 1$

$$f_a = 2 \times 10^6 \text{ GeV} \cdot \left(\frac{0.1}{\Gamma_S(S_i)/H(T_{\text{osc}})} \right)^{\frac{2}{3}} \cdot \left(\frac{\sum m_\nu^2}{(0.05 \text{ eV})^2} \right)^{\frac{2}{3}} \cdot \left(\frac{S_i}{0.1 M_{\text{Pl}}} \right) \cdot \left(\frac{100 \text{ MeV}}{m_S} \right)^{\frac{1}{3}} \quad (8.119)$$

and obtain the following $Y_B = n_B/s$ for $N = 6$

$$\frac{Y_B}{8 \times 10^{-11}} \simeq \left(\frac{m_a}{10^{-3} \text{ eV}} \right)^2 \cdot \left(\frac{100 \text{ MeV}}{m_S} \right)^{\frac{2}{3}} \cdot \left(\frac{\Gamma_S(S_i)/H(T_{\text{osc}})}{0.1} \right)^{\frac{8}{3}} \cdot \left(\frac{(0.05 \text{ eV})^2}{\sum m_\nu^2} \right)^{\frac{5}{3}}. \quad (8.120)$$

The baryon asymmetry only depends on the ratio S_i/f_a , so the dependence on S_i divides out when inserting (8.119).

Rotation during Reheating

In the above we assumed that the oscillation occurs during radiation domination. For the opposite case of $T_{\text{osc.}} > T_{\text{RH}}$ we have production during reheating, where entropy is not conserved. Thus n_B/s is not the correct adiabatic invariant anymore and we have to use $\langle n_B \rangle / \rho_{\text{inf}}$ evaluated at production multiplied with ρ_{inf}/s evaluated at reheating. In this context ρ_{inf} denotes the energy density of the non-relativistic inflaton. During the matter dominated reheating phase we have $T \sim 1/a^{3/8}$ and a Hubble rate of $H \sim T^4$. By using the Friedmann equation $\rho_{\text{inf.}} = 3M_{\text{Pl}}^2 H^2$ we find that $\rho_{\text{inf.}} \sim T^8$. The scaling of the asymmetry could be different depending on whether the Saxion settles to its minimum $N f_a$ during ($T_{\text{osc.}} > T_S > T_{\text{RH}}$) or after reheating ($T_{\text{osc.}} > T_{\text{RH}} > T_S$). For $T_{\text{RH}} > T_S$ we find that $m_S(S) \sim S \sim 1/a \sim T^{8/3}$ and $\Gamma_S(S)/H \sim S^2/T^3 \sim T^{7/3}$ implying $\langle n_B \rangle / \rho_{\text{inf.}} \sim 1/T$. In the second regime $T_{\text{RH}} < T_S$ we have $S = N f_a = \text{const.}$ so conservation of the Noether charge $\dot{\theta} N^2 f_a^2$ implies $\langle \dot{\theta} \rangle \sim 1/a^3 \sim T^8$. Further we find $\Gamma_S/H \sim T f_a^2/T^4 \sim 1/T^3$ resulting in $\langle n_B \rangle / \rho_{\text{inf.}} \sim 1/T$. Both regimes redshift the same,

⁵This assumes that $S_i > T_{\text{osc.}}/\sqrt{N}$, which is valid throughout our parameter space and we used $c_{\nu_R} \simeq 1/N$.

because they depend on $\langle \dot{S}^2 \rangle \sim n_\theta$, which always redshifts as $1/a^3$ no matter if S is at or above Nf_a . During reheating the asymmetry is always IR-dominated and gets predominantly generated at T_{RH} , which is why we can evaluate $\langle n_B/s \rangle$ at reheating. This is unlike the usual case for Lepto-Axiogenesis, where one would find $\langle n_B \rangle / \rho_{\text{inf}} \sim T$ for $T_S > T_{\text{RH}}$ [942]. We arrive at

$$\left\langle \frac{n_B}{s} \right\rangle \simeq \frac{c_{\nu_R} N}{24} \cdot \frac{\Gamma_S(S_{\text{RH}})}{H(T_{\text{RH}})} \cdot \frac{\varepsilon m_S(S_{\text{RH}}) T_{\text{RH}}^2}{s(T_{\text{RH}})} \quad (8.121)$$

$$= \frac{c_{\nu_R} N^2}{24} \cdot \frac{\Gamma_S(S_i)}{H(T_{\text{osc.}}^{\text{RH}})} \cdot \left(\frac{T_{\text{osc.}}^{\text{RH}}}{S_i} \right)^2 \cdot \left(\frac{T_{\text{osc.}}^{\text{RH}}}{T_{\text{RH}}} \right) \cdot Y_\theta^{\text{RH}}, \quad (8.122)$$

where in the second line we used the charge yield for reheating defined in (8.93) as well as the scaling laws to relate the field value at reheating S_{RH} and S_i , which restores the factor of $\Gamma_S(S_i)/H(T_{\text{osc.}}) \ll 1$ ⁶. Note that the above is not enhanced by $T_{\text{osc.}} > T_{\text{RH}}$ because $Y_\theta^{\text{RH}} \sim T_{\text{RH}}^8/T_{\text{osc.}}^8$. We eliminate f_a via the condition $\Gamma_S(S_i)/H(T_{\text{osc.}}^{\text{RH}}) < 1$

$$f_a = 9.9 \times 10^5 \text{ GeV} \cdot \left(\frac{0.1}{\Gamma_S(S_i)/H(T_{\text{osc.}}^{\text{RH}})} \right)^{\frac{4}{5}} \cdot \left(\frac{\sum m_\nu^2}{(0.05 \text{ eV})^2} \right)^{\frac{4}{5}} \cdot \left(\frac{S_i}{0.1 M_{\text{Pl.}}} \right) \cdot \left(\frac{100 \text{ MeV}}{m_S} \right)^{\frac{3}{5}} \cdot \left(\frac{T_{\text{RH}}}{10^{13} \text{ GeV}} \right)^{\frac{2}{5}} \quad (8.123)$$

to find

$$\frac{Y_B}{8 \times 10^{-11}} \simeq \left(\frac{m_a}{10^{-3} \text{ eV}} \right)^2 \cdot \left(\frac{40 \text{ MeV}}{m_S} \right)^{\frac{6}{5}} \cdot \left(\frac{\Gamma_S(S_i)/H(T_{\text{osc.}}^{\text{RH}})}{0.1} \right)^{\frac{12}{5}} \cdot \left(\frac{(0.05 \text{ eV})^2}{\sum m_\nu^2} \right)^{\frac{7}{5}}. \quad (8.124)$$

8.6 Dark Matter

8.6.1 Dark Matter decay

The Diraxion is only a good dark matter candidate if it is sufficiently long-lived. Its main decay mode is to neutrinos, followed by a subleading mode to photons via a two-loop coupling and the width is given by [960]

$$\Gamma(a \rightarrow \bar{\nu}\nu) \simeq \frac{m_a}{16\pi} \frac{\sum_\nu m_\nu^2}{N^2 f_a^2} \sqrt{1 - 4 \frac{\sum_\nu m_\nu^2}{m_a^2}}, \quad (8.125)$$

where we estimated the phase space suppression in the single flavor approximation. Since the coupling is dependent on the absolute neutrino masses $\sum_\nu m_\nu^2$ we take the lightest neutrino mass to be zero so that

$$\sum_\nu m_\nu^2 \simeq \begin{cases} (0.05 \text{ eV})^2 & \text{for NH} \\ (0.1 \text{ eV})^2 & \text{for IH} \end{cases}, \quad (8.126)$$

⁶For $T_{\text{RH}} < T_S$ the scattering rate is IR dominated and we should demand $\Gamma_S(S_{\text{RH}})/H(T_{\text{RH}}) \ll 1$ instead. However in practise we typically find that $T_{\text{RH}} > T_S$ so we ignore this additional complication.

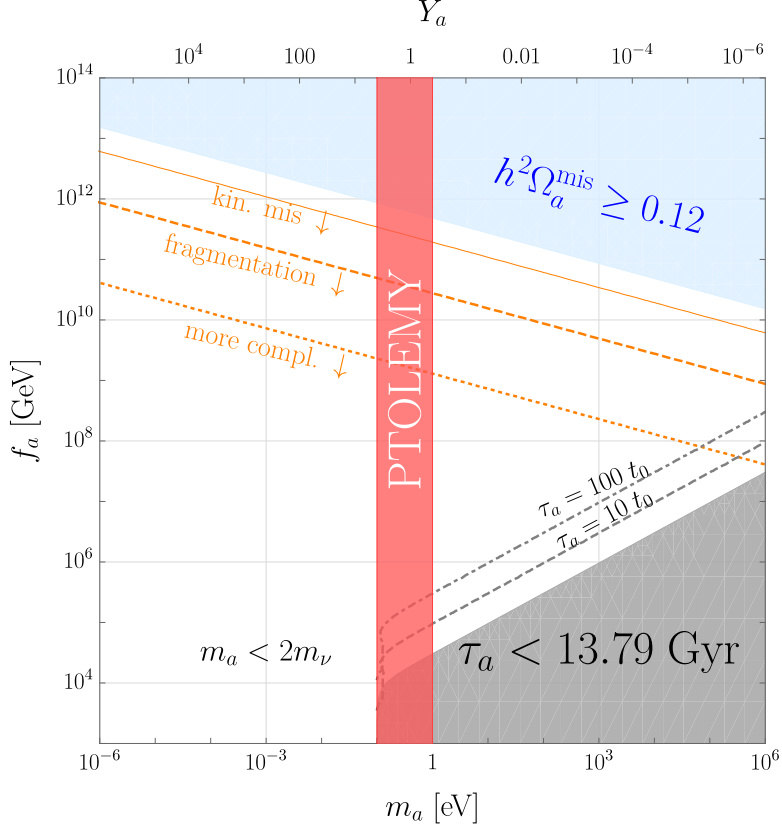


Figure 8.5: Allowed parameter space for Diraxion dark matter, that is stable enough on cosmological time scales.

where NH (IH) denotes the normal (inverted) hierarchy of neutrino masses. Throughout this work we focus on the normal hierarchy. Normalized to the age of the universe $t_0 \simeq 13.79$ Gyr we obtain

$$\tau = 1/\Gamma(a \rightarrow \bar{\nu}\nu) \simeq 30 t_0 \cdot \left(\frac{(0.05 \text{ eV})^2}{\sum_\nu m_\nu^2} \right) \cdot \left(\frac{1 \text{ eV}}{m_a} \right) \cdot \left(\frac{N f_a}{10^6 \text{ GeV}} \right)^2. \quad (8.127)$$

There is no appreciable bound from the Diraxion to photon decay via the two-loop coupling in, as the rate would be suppressed by the free factors $(m_a/v_H)^2$, $(m_\nu/N f_a)^4$ and $(m_a/m_e)^4$. The limit on the life-time of Diraxion dark matter was depicted in black in figure 8.5. Experiments such as PTOLEMY [1007, 1008] aimed at detecting the cosmic neutrino background could potentially detect [1009, 1010] the neutrinos produced in decays of dark matter with masses between 0.1 eV and 1 eV for lifetimes between $(10 - 100) t_0$ [960]. We show the corresponding parameter region colored in red in figure 8.5. While standard misalignment and decays of topological defects (blue region in 8.5) works only for too large values of f_a compared to the detectable region, we will see that kinetic misalignment (see the orange lines in the aforementioned plot together with 8.6.4)

and parametric resonance in 8.6.5 could both reproduce the relic abundance for much smaller f_a and could potentially be probed by PTOLEMY.

8.6.2 Standard Misalignment

First we discuss the conventional misalignment mechanism, which operates when the kinetic energy of the Diraxion is smaller than its potential barrier. We will state the precise conditions for this at the end of this subsection and in the next one. During inflation the Diraxion is trapped in its initial angle $\theta_{\text{inf.}} = \pi/2 - \delta$ by the Hubble friction (see section 8.8.1). The QCD axion dark matter literature usually employs an axion potential of the form $1 - \cos(\theta)$ unlike our choice of $\cos(\theta)$ from (8.36). The constant piece is irrelevant for dark matter and the correct sign can be obtained by defining $\theta_i = \theta_{\text{inf.}} \pm \pi$, where we take the plus sign for concreteness. However since the Diraxion is light during inflation, its initial angle will receive corrections from quantum fluctuations giving rise to isocurvature perturbations [991]

$$\langle \theta_i^2 \rangle = \left(\delta - \frac{3\pi}{2} \right)^2 + \left(\frac{H_I}{2\pi S_i} \right)^2. \quad (8.128)$$

Using $H_I \simeq 6 \times 10^{13} \text{ GeV}$ and $10^{16} \text{ GeV} < S_i < 10^{19} \text{ GeV}$ one can deduce that $10^{-5} < H_I/(2\pi) < 10^{-2}$, indicating that we can not take the initial misalignment angle to be arbitrarily small. However parametric resonance occurs (see 8.6.5) for most of our parameter space and it has the effect of randomizing the initial misalignment angle, so that the estimate from post-inflationary symmetry breaking with an average angle of $\pi/\sqrt{3}$ applies [942]. Since this angle is much larger than the contribution from the fluctuations we take

$$\sqrt{\langle \theta_i^2 \rangle} \simeq \frac{\pi}{\sqrt{3}} \quad (8.129)$$

in the following. The Diraxion oscillates around the minimum of its cosine potential (8.33), which reduces to the Diraxion mass m_a^2 in the small angle limit. During radiation domination oscillations start at the temperature

$$T_{\text{osc.}}^a = \left(\frac{45}{4\pi^3 g_*(T_{\text{osc.}})} \right)^{\frac{1}{4}} \sqrt{M_{\text{Pl}} m_a} \simeq 27 \text{ TeV} \cdot \left(\frac{100}{g_*(T_{\text{osc.}})} \right)^{\frac{1}{4}} \cdot \sqrt{\frac{m_a}{1 \text{ eV}}} \quad (8.130)$$

The energy density from these coherent oscillations with an amplitude $\sqrt{\langle \theta_i^2 \rangle} f_a$ is

$$\rho_a^{\text{mis.}}(T_{\text{osc.}}^a) = \frac{\langle \theta_i^2 \rangle m_a^2 f_a^2}{2}, \quad (8.131)$$

which normalized to the entropy density reads [933]

$$\frac{\rho_a^{\text{mis.}}(T_{\text{osc.}}^a)}{s(T_{\text{osc.}}^a)} \simeq \frac{2.4}{g_*(T_{\text{osc.}}^a)^{\frac{1}{4}}} \frac{\sqrt{m_a} \langle \theta_i^2 \rangle f_a^2}{M_{\text{Pl}}^{\frac{3}{2}}} \quad (8.132)$$

and the relic abundance is found to be

$$\Omega_a^{\text{mis.}} h^2 = \frac{\rho_a^{\text{mis.}}(T_{\text{osc.}}^a)}{s(T_{\text{osc.}}^a)} \cdot \frac{s_0}{\rho_c} h^2 \quad (8.133)$$

$$\simeq 0.12 \cdot \sqrt{\frac{m_a}{1 \text{ eV}}} \cdot \left(\frac{\langle \theta_i^2 \rangle}{\pi^2/3} \right) \cdot \left(\frac{f_a}{5 \times 10^{11} \text{ GeV}} \right)^2 \cdot \left(\frac{100}{g_*(T_{\text{osc.}}^a)} \right)^{\frac{1}{4}} \quad (8.134)$$

in terms of the the critical density $\rho_c = 3/(8\pi G_N)H_0^2$, the Hubble rate today $H_0 \equiv h \cdot 100 \text{ km/s Mpc}^{-1}$ with $h \simeq 0.7$ and the entropy density today s_0 related via $\rho_c/(s_0 h^2) \simeq 3.6 \text{ eV}$. The corresponding parameter space was displayed in figure 8.5. Since we are typically interested in $f_a = \mathcal{O}(10^6 - 10^7 \text{ GeV})$, one can deduce that standard misalignment can not be responsible for the observed dark matter relic abundance.

8.6.3 Topological Defect decay

Cosmic strings are formed via the Kibble mechanism [848, 1011, 1012], when the underlying $U(1)_D$ symmetry is spontaneously broken down to \mathcal{Z}_N . Detailed numerical simulations of the cosmic strings decaying to axions e.g. [455, 456, 581, 583, 584, 1013--1026] typically have large uncertainties and often disagree with each other, see e.g. [1027] for a recent overview. This is why we resort to simple order of magnitude estimates. Cosmic strings are characterized by their string tension or energy by unit length [1028]

$$\mu_{\text{str.}} = \pi(N f_a)^2 \text{Log} \left(\frac{m_S}{\sqrt{\xi} H} \right), \quad (8.135)$$

where ξ is a dimensionless length parameter that needs to be determined from numerical simulations. Following reference [455] we take $\xi \simeq 1$ and note that this parameter could very well be larger. Cosmic strings have a core diameter $d \sim 1/m_S$ and typical distances of $L \sim 1/H$, which acts as a regulator for global strings. We obtain the energy density via dividing the string tension by an area, which is given by the typical Hubble volume $4/3\pi \cdot 1/H^3$ over the string separation $1/H$ to be

$$\rho_{\text{str.}} \simeq \frac{3}{4}\pi \text{Log} \left(\frac{m_S}{\sqrt{\xi} H} \right) H^2 (N f_a)^2. \quad (8.136)$$

Apart from cosmic strings there is a second type of defect that might be formed: When the Diraxion oscillates at $T_{\text{osc.}}^a$ and settles into one of its N degenerate minima the residual \mathcal{Z}_N is explicitly broken. Consequently domain walls, whose energy density interpolates between the different vacua, will be formed around the time of $T_{\text{osc.}}^a$. A similar argument can be made for the case of kinetic misalignment: Since the Diraxion start its oscillation near the top of the potential, even a small fluctuation could lead it to fall into one of the available minima [942]. However these effects typically only occur for scenarios where the global $U(1)_D$ symmetry is broken after inflation: The observable universe consists of many patches with randomly distributed, different values of θ_i [1029] and domain walls separating different patches. Our scenario on the other hand involves (spontaneous and explicit [1030]) symmetry breaking during inflation, so one would

expect a uniform θ_i throughout the observable universe [1029]. However this does not guarantee the absence of domain walls. Parametric resonance (see section 8.6.5) grows fluctuations and the resulting large fluctuations facilitate a non-thermal restoration of the $U(1)_D$ symmetry [1031–1037] so that the angular field becomes randomized instead of being stuck in its value θ_{inf} . (see the beginning of 8.6.2). Once the fluctuations are smaller than f_a , the $U(1)_D$ symmetry is broken again with different initial angles for each Hubble patch leading to domain wall formation at $T_{\text{osc.}}^a$ [942]. If the condensate was thermalized before parametric resonance can occur, this outcome could be avoided. However as we argue in section 8.9.1, such an early thermalization is not possible from the Dirac Weinberg operator, as this UV-dominated rate would dampen the oscillation too much before a rotation could be induced. The only way out is to consider the Seesaw messenger fields as bath particles, which is the scenario sketched in 8.9.2. Since the symmetry is restored only to be broken again, cosmic strings will also form and the resulting hybrid network of decays can decay for $N = 1$ [1038, 1039]. A second reason to expect domain walls is that the isocurvature fluctuations can experience a power law growth [740]: Due to the isocurvature fluctuations the different patches that make up our visible universe start with different initial velocities $\dot{\theta}_i$ and evolve to different field values. By the time $T_{\text{osc.}}^a$, when the Diraxion mass becomes cosmologically relevant, domain walls will form to interpolate between the different θ . The surface tension or energy via unit area of a domain wall reads [1020]

$$\sigma_{\text{DW}} = 8m_a f_a^2 \quad (8.137)$$

and one finds the energy density from the ratio of the surface density over the typical length scale. For a Hubble volume $4/3\pi \cdot 1/H^3$ and a typical surface area of $4\pi^2 \cdot 1/H^2$ the result is

$$\rho_{\text{DW}} \simeq 24Hm_a f_a^2. \quad (8.138)$$

The network collapses under its tension when [1028]

$$H_{\text{dec.}} = \frac{\mu_{\text{str.}}}{\sigma_{\text{DW}}} = \frac{8}{\pi N^2} \text{Log} \left(\frac{m_S}{H_{\text{dec.}}} \right)^{-1} m_a. \quad (8.139)$$

As long as $\text{Log}(m_S/H_{\text{dec.}}) \gtrsim 8/(3\pi N^2)$ we find that $H_{\text{dec.}} \lesssim 3m_a$ which means that the axions produced from the hybrid defect decay are as cold as the ones produced in the conventional misalignment scenario [1028]. For a QCD axion it was found that the logarithm can be as large as 70 [1027], so the previous conclusion is likely to hold true. Since the domain walls are expected to form at $H \simeq 3m_a$ and decay around the same epoch, they do not have time to dominate the energy budget of the universe. We find that the total energy density of the produced Diraxions

$$\rho_{\text{str. Wall}} = \frac{48}{\pi} \left(4 + \frac{1}{\pi} \right) \text{Log} \left(\frac{m_S}{H_{\text{dec.}}} \right)^{-1} m_a^2 (N f_a)^2 \quad (8.140)$$

is comparable to the conventional misalignment contribution 8.131. For $N \neq 1$ we have more than one domain wall and the system of walls can decay via the explicit symmetry

breaking encoded in the Diraxion mass from (8.36) [959]. For group theoretical solutions to the domain wall problem see [463, 464]. The explicit symmetry breaking potential or bias term $V_{\mathcal{D}}$ induces a different energy for each of the N vacua and the pressure difference between neighboring vacua is proportional to

$$\Delta V = V_{\mathcal{D}}(\theta = 0) - V_{\mathcal{D}}\left(\theta = \frac{2\pi}{N}\right) = m_a^2 f_a^2 \left(\cos(\delta) - \cos\left(\delta + \frac{2\pi}{N}\right)\right) \quad (8.141)$$

and the domain wall collapses if the pressure difference is larger than the domain wall tension implying

$$H_{\text{bias}} = \frac{\Delta V}{\sigma_{\text{DW}}} = \frac{m_a}{8} \left(\cos(\delta) - \cos\left(\delta + \frac{2\pi}{N}\right)\right). \quad (8.142)$$

Since again $H_{\text{bias}} \simeq m_a$ this scenario produces sufficiently cold Diraxions and the walls decay right after their formation. The resulting energy density is given by (8.138) evaluated at H_{bias} and multiplied by N to take the fact into account that more than one domain wall decays. In terms of the energy density one finds [459]

$$\rho_{\text{bias}} = 3N \left(\cos(\delta) - \cos\left(\delta + \frac{2\pi}{N}\right)\right) m_a^2 f_a^2, \quad (8.143)$$

which is of comparable size to the previous abundance (8.140) and the misalignment contribution (8.131) unless N is so large that $2\pi/N$ is negligible compared to δ . We conclude that topological defects do not pose a cosmological problem in our scenario and their effect on the relic density is essentially the same as standard misalignment. Since we focus on decay constants in the $\mathcal{O}(10^6 \text{ GeV} - 10^7 \text{ GeV})$ range, we find that these contributions are negligible compared to the Kinetic Misalignment and Parametric resonance scenarios encountered in the next sections.

8.6.4 Kinetic Misalignment and fragmentation

If the Diraxion velocity $\dot{\theta}$ is larger than $2m_a$ [933] the rolling pseudoscalar will get trapped in its cosine potential later than for conventional misalignment. As a consequence of its large kinetic energy it does not just probe the harmonic part of its potential (small angles) but instead can start near the hilltop. Due to these effects one obtains the dark matter yield [927] from (8.92) and (8.93)

$$Y_a = 2Y_\theta, \quad (8.144)$$

where the factor of two, found numerically in [927] and analytically in [1040], encodes the enhancement from the anharmonicity. This mechanism reproduces the observed relic abundance for [933]

$$\Omega_a^{\text{KM}} h^2 = 0.12 \cdot \left(\frac{m_a}{1 \text{ eV}}\right) \cdot \left(\frac{Y_\theta}{0.4}\right) \quad (8.145)$$

$$\simeq 0.12 \cdot \begin{cases} \left(\frac{m_a}{0.01 \text{ eV}}\right)^3 \cdot \left(\frac{270 \text{ MeV}}{m_S}\right)^{\frac{5}{2}} \cdot \left(\frac{S_i}{0.1 M_{\text{Pl}}}\right)^{\frac{7}{2}} \cdot \left(\frac{10^7 \text{ GeV}}{f_a}\right)^{\frac{3}{2}} & \text{RD} \\ \left(\frac{m_a}{0.01 \text{ eV}}\right)^3 \cdot \left(\frac{140 \text{ MeV}}{m_S}\right)^3 \cdot \left(\frac{S_i}{0.1 M_{\text{Pl}}}\right)^3 \cdot \left(\frac{10^7 \text{ GeV}}{f_a}\right) \cdot \left(\frac{T_{\text{RH}}}{10^{13} \text{ GeV}}\right) & \text{RH,} \end{cases} \quad (8.146)$$

where we used $N = 6$ together with (8.92) and (8.93) for our estimate. We show the required value of Y_θ as a function of m_a on the upper axis in 8.5. Fixing the ratio f_s/S_i via the relations (8.119) and (8.123) together with explaining the observed baryon asymmetry via Dirac Lepto-Axiogenesis (see (8.120) and (8.124)) allows us to estimate the required Diraxion and Saxion masses for DM from kinetic misalignment:

$$m_a = \begin{cases} 0.1 \text{ eV} \cdot \left(\frac{0.01}{\Gamma_S(S_i)/H(T_{\text{osc}})} \right)^{\frac{7}{3}} \cdot \left(\frac{\sum m_\nu^2}{(0.05 \text{ eV})^2} \right)^{\frac{4}{3}} \cdot \left(\frac{S_i}{0.1 M_{\text{Pl}}} \right)^{\frac{2}{3}} & \text{RD} \\ 0.66 \text{ eV} \cdot \left(\frac{0.01}{\Gamma_S(S_i)/H(T_{\text{osc}})} \right)^4 \cdot \left(\frac{\sum m_\nu^2}{(0.05 \text{ eV})^2} \right)^2 \cdot \left(\frac{S_i}{0.1 M_{\text{Pl}}} \right)^2 \cdot \left(\frac{10^{13} \text{ GeV}}{T_{\text{RH}}} \right) & \text{RH} \end{cases} \quad (8.147)$$

$$m_S = \begin{cases} 11.5 \text{ GeV} \cdot \left(\frac{0.01}{\Gamma_S(S_i)/H(T_{\text{osc}})} \right)^3 \cdot \left(\frac{\sum m_\nu^2}{(0.05 \text{ eV})^2} \right)^{\frac{3}{2}} \cdot \left(\frac{S_i}{0.1 M_{\text{Pl}}} \right)^2 & \text{RD} \\ 14 \text{ GeV} \cdot \left(\frac{0.01}{\Gamma_S(S_i)/H(T_{\text{osc}})} \right)^{\frac{14}{3}} \cdot \left(\frac{\sum m_\nu^2}{(0.05 \text{ eV})^2} \right)^{\frac{13}{6}} \cdot \left(\frac{S_i}{0.1 M_{\text{Pl}}} \right)^{\frac{10}{3}} \cdot \left(\frac{10^{13} \text{ GeV}}{T_{\text{RH}}} \right) & \text{RH} \end{cases} \quad (8.148)$$

The Diraxion gets trapped in its potential at the temperature [1040]

$$T_* \simeq 0.23 \text{ GeV} \cdot \left(\frac{100}{g_*(T_*)} \right)^{\frac{1}{3}} \cdot \left(\frac{m_a}{10 \text{ meV}} \right)^{\frac{2}{3}} \cdot \left(\frac{f_a}{10^6 \text{ GeV}} \right)^{\frac{2}{3}} \cdot \left(\frac{0.12}{\Omega_a h^2} \right)^{\frac{1}{3}} \quad (8.149)$$

defined as the time when the Diraxion's kinetic and potential energy coincide. Kinetic misalignment occurs for $T_* < T_{\text{osc}}^a$ and one finds that this implies [1040]

$$f_a < 6 \times 10^{11} \text{ GeV} \cdot \left(\frac{g_*(T_*)}{100} \right)^{\frac{1}{8}} \cdot \left(\frac{10 \text{ meV}}{m_a} \right)^{\frac{1}{4}} \cdot \sqrt{\frac{\Omega_a h^2}{0.12}}. \quad (8.150)$$

Since the Diraxion scans its potential for a long time, parametric resonance from the Diraxion self-interactions becomes possible leading to a fragmentation of the zero mode condensate into higher momentum excitations. Parametric resonance was first discussed in the context of (p)reheating [100, 1041]. This effect was then applied to the study of relaxions and axions from monodromy [1042–1044] and recently to kinetic misalignment in [1040]. The basic idea is that the mass term for the higher momentum fluctuations a_k is time dependent and acts like the external force for a driven oscillator [934]

$$\ddot{a}_k + \left(k^2 + m_a^2 \cos(\dot{\theta}t) \right) a_k = 0. \quad (8.151)$$

In the limit $\dot{\theta} \gg m_s$ one finds a narrow resonance band around the momentum $k \simeq \dot{\theta}/2$ with a relative width $\Delta k/k \simeq m_a^2/\dot{\theta}^2$ and that the fluctuations are produced with a rate $\Gamma_{a \text{ PR}} \simeq m_a^4/\dot{\theta}^3$ [1044]. It turns out that the Diraxion abundance including fluctuations coincides with the zero mode estimate in (8.144) [937], which can be understood by noting that the characteristic energy scale of both processes is $\dot{\theta}$ [930]. Fragmentation can even lead to a slight enhancement of the relic abundance, because the zero mode redshifting as $\rho_\theta \sim 1/a^6$ is converted into fluctuations that redshift slower than $1/a^6$ [1040]. As a

rule of thumb fragmentation is more important for smaller decay constants [1040]:

$$f_a < \left(\frac{g_*(T_*)}{100} \right)^{\frac{1}{8}} \cdot \left(\frac{10 \text{ meV}}{m_a} \right)^{\frac{1}{4}} \cdot \sqrt{\frac{\Omega_a h^2}{0.12}} \cdot \begin{cases} 8.79 \times 10^{10} \text{ GeV} & \text{weak frag.} \\ 4.39 \times 10^{10} \text{ GeV} & \text{complete frag.} \\ 2.25 \times 10^{10} \text{ GeV} & \text{more complic.} \end{cases} \quad (8.152)$$

One can show that the condensate does not fragment completely as long as $f_a < 8.79 \times 10^{10} \text{ GeV}$ [1040], meaning that most of its energy density is still in the zero mode and the fragmentation ends after the trapping has taken place. Complete fragmentation occurs before the trapping can take place [1040] and implies $f_a < 4.39 \times 10^{10} \text{ GeV}$. The analysis of [1040] breaks down if the backreaction of the fluctuations on the zero mode occurs before the onset of fragmentation, which can be expressed as $m_a/H(T_*) < \mathcal{O}(10^3 - 10^4)$ corresponding to $f_a < 2.25 \times 10^{10} \text{ GeV}$. This does not mean that the corresponding parameter space is excluded, just that a more complicated analysis e.g. a lattice study is needed. The aforementioned regions in which kinetic misalignment and fragmentation take place are shown as orange lines in figure 8.5. Since the typical momenta produced during parametric resonance can be much larger than the Diraxion mass, the fluctuations will be less cold than the zero mode oscillations. We need to ensure that the dark matter matter redshifts enough so that it is sufficiently cold by the time of matter-radiation equality. Reference [1040] found that the momentum modes $m_a a(T_*)$, with $a(T_*) \sim 1/T_*$ the scale factor at the trapping temperature, undergo the most efficient growth from parametric resonance. The warmness bound on the dark matter velocity reads [390, 1045]

$$v_{a \text{ eq.}} \simeq \frac{m_a \cdot a(T_*)/a_{\text{eq.}}}{m_a} \lesssim 2 \times 10^{-4}. \quad (8.153)$$

implying $T_* \gtrsim 5 \times 10^3 T_{\text{eq.}} \simeq 5 \text{ keV}$ and

$$f_a > 9.3 \times 10^{-2} \text{ GeV} \cdot \sqrt{\frac{g_*(T_*)}{100}} \cdot \left(\frac{10 \text{ meV}}{m_a} \right) \cdot \sqrt{\frac{\Omega_a h^2}{0.12}}, \quad (8.154)$$

which is hardly constraining. One should also take into account that, if the field is still not trapped at the time of Big Bang Nucleosynthesis (BBN) then its energy density scaling as $\rho_\theta \sim 1/a^6$, which is different from ordinary dark radiation $\sim 1/a^4$, could modify the expansion history of the universe and alter the produced light element abundances. This condition $T_* \gtrsim 20 \text{ keV}$ leads to the bound [1040]

$$f_a > 8.1 \times 10^{-2} \text{ GeV} \cdot \left(\frac{10 \text{ meV}}{m_a} \right) \cdot \left(\frac{\Omega_a h^2}{0.12} \right), \quad (8.155)$$

comparable to the structure formation one.

8.6.5 Parametric Resonance from Saxion oscillations

The non-perturbative process of Parametric resonance [100, 1041] is analogous to stimulated emission and can also be driven by the Saxion oscillations [951, 952]. One finds that the oscillating zero mode of the Saxion field is rapidly converted into higher momentum Saxion and Diraxion fluctuations. Production of QCD axion dark radiation from Saxion parametric resonance was studied in [383, 417]. The fluctuations in the angular mode can be produced because both equations of motions in section 8.4.1 are coupled as long as $S > N f_a$. Since the energy density in the fluctuations is comparable to the one in the zero mode, these large fluctuations will lead to an effective mass squared for the radial mode that is positive, hence the original $U(1)_D$ symmetry gets non-thermally restored [1031–1037]. Once the amplitude of the fluctuations redshifts below f_a the symmetry is broken again. Saxion fluctuations will later be thermalized and only the rotation together with the Diraxion fluctuations will remain. It was found that the transfer from the condensate into the higher momentum modes begins shortly after the start of the oscillations and for a quartic potential during radiation (matter) domination it ends at around $S \simeq 10^{-2}(10^{-4})S_i$ [1035, 1037, 1046], when the backreaction from scattering of the fluctuations with the condensate and themselves becomes important. Parametric resonance from Saxion oscillations requires a violation of the adiabaticity condition $|m_S(S_i)/m_S(S_i)^2| < 1$ which can be translated into the condition [740]

$$\varepsilon < 0.8 . \quad (8.156)$$

During parametric resonance comparable amounts of Saxion and Diraxion fluctuations are produced [740]

$$n_S \sim n_\theta \sim \frac{V_\sigma(S_i)}{m_S(S_i)}, \quad (8.157)$$

which is why the abundance of Diraxion fluctuations is formally equivalent to the result for kinetic misalignment under the replacement $\varepsilon \rightarrow 1/2$ in the definitions of the yields (8.92) and (8.93). We estimate that

$$\Omega_a^{\text{PR}} h^2 \simeq 0.12 \cdot \begin{cases} \left(\frac{m_a}{0.01 \text{ eV}}\right) \cdot \sqrt{\frac{500 \text{ MeV}}{m_S}} \cdot \left(\frac{S_i}{0.1 M_{\text{Pl}}}\right)^{\frac{3}{2}} \cdot \sqrt{\frac{10^7 \text{ GeV}}{f_a}} & \text{RD} \\ \left(\frac{m_a}{0.01 \text{ eV}}\right) \cdot \left(\frac{500 \text{ MeV}}{m_S}\right) \cdot \left(\frac{S_i}{0.1 M_{\text{Pl}}}\right) \cdot \left(\frac{10^7 \text{ GeV}}{f_a}\right) \cdot \left(\frac{T_{\text{RH}}}{10^{13} \text{ GeV}}\right) & \text{RH}, \end{cases} \quad (8.158)$$

where we used $N = 6$ together with (8.92) and (8.93). We can determine the Diraxion and Saxion mass by eliminating f_a/S_i via (8.119), (8.123) and demanding successful

Dirac-Lepto-Axiogenesis:

$$m_a = \begin{cases} 0.11 \text{ eV} \cdot \left(\frac{0.01}{\Gamma_S(S_i)/H(T_{\text{osc}})} \right)^3 \cdot \left(\frac{\sum m_\nu^2}{(0.05 \text{ eV})^2} \right)^2 \cdot \left(\frac{S_i}{0.1 M_{\text{Pl}}} \right)^2 & \text{RD} \\ 0.05 \text{ eV} \cdot \left(\frac{0.01}{\Gamma_S(S_i)/H(T_{\text{osc}})} \right)^{\frac{12}{5}} \cdot \left(\frac{\sum m_\nu^2}{(0.05 \text{ eV})^2} \right)^{\frac{16}{10}} \cdot \left(\frac{S_i}{0.1 M_{\text{Pl}}} \right)^{\frac{6}{5}} \cdot \left(\frac{T_{\text{RH}}}{10^{13} \text{ GeV}} \right)^{\frac{1}{5}} & \text{RH} \end{cases} \quad (8.159)$$

$$m_S = \begin{cases} 14 \text{ GeV} \cdot \left(\frac{0.01}{\Gamma_S(S_i)/H(T_{\text{osc}})} \right)^5 \cdot \left(\frac{\sum m_\nu^2}{(0.05 \text{ eV})^2} \right)^{\frac{7}{2}} \cdot \left(\frac{S_i}{0.1 M_{\text{Pl}}} \right)^6 & \text{RD} \\ 11.5 \text{ GeV} \cdot \left(\frac{0.01}{\Gamma_S(S_i)/H(T_{\text{osc}})} \right)^2 \cdot \left(\frac{\sum m_\nu^2}{(0.05 \text{ eV})^2} \right)^{\frac{3}{2}} \cdot \left(\frac{S_i}{0.1 M_{\text{Pl}}} \right)^2 \cdot \left(\frac{T_{\text{RH}}}{10^{13} \text{ GeV}} \right) & \text{RH} \end{cases} \quad (8.160)$$

Owing to the fact that the relativistic fluctuations are produced with momenta $k \sim \dot{\theta}(S_i) \sim m_S(S_i)$ warmness constraints become relevant again: Even though the fluctuations are produced with much larger momenta compared to the fragmentation from Diraxion self-interactions, the non-perturbative production occurs much earlier at $T_{\text{osc}} \gg T_*$ so in principle the fluctuations have enough time to redshift sufficiently. The constraint on the velocity is [390, 1045]

$$v_a(T = 1 \text{ eV}) \simeq \frac{k_a(T = 1 \text{ eV})}{m_a} \lesssim 2 \times 10^{-4} \quad (8.161)$$

and we estimate the momentum $k_a(T = 1 \text{ eV})$ at matter-radiation equality $T_{\text{eq.}} \simeq 1 \text{ eV}$ following [740, 942]: Since $n_a \sim k_a^3 \sim 1/a^3$ one deduces that n_a/k_a^3 is an adiabatic invariant. From $k_a \sim m_S(S)$ and $n_a \sim m_S(S)S^2$ we obtain

$$\frac{n_a}{k_a^3} \simeq \frac{1}{3} \left(\frac{N f_a}{m_S} \right)^2. \quad (8.162)$$

With this expression we trade the momenta for $n_a(T = 1 \text{ eV})$ from the yield (8.145) that reproduces the dark matter relic abundance and find

$$m_S < 0.28 \text{ MeV} \cdot \left(\frac{v_a(T = 1 \text{ eV})}{2 \times 10^{-4}} \right)^{\frac{3}{2}} \cdot \left(\frac{m_a}{10 \text{ meV}} \right)^2 \cdot \sqrt{\frac{0.12}{\Omega_a^{\text{PR}} h^2}} \cdot \left(\frac{N f_a}{10^6 \text{ GeV}} \right). \quad (8.163)$$

One can see that the parameter region for DM from parametric resonance and Dirac-Lepto-Axiogenesis requires larger m_S and is thus only viable with early thermalization (see section 8.9.1).

8.7 Dark Radiation

The Standard Model prediction for the amount of non-photonic radiation is conventionally expressed as an effective number of neutrinos given by $N_{\text{eff.}} = 3.0432 \pm 0.0002$ [67--73]. Additional dark radiation would shift this number by [74]

$$\Delta N_{\text{eff.}}(T) = \frac{4}{7} g_{*\rho}(T) \left(\frac{10.75}{g_{*S}(T)} \right)^{\frac{4}{3}} \frac{\rho_{\text{DR}}(T)}{\rho_{\text{SM}}(T)} \quad \text{with} \quad \rho_{\text{SM}}(T) = \frac{\pi^2}{30} g_{*\rho}(T) T^4. \quad (8.164)$$

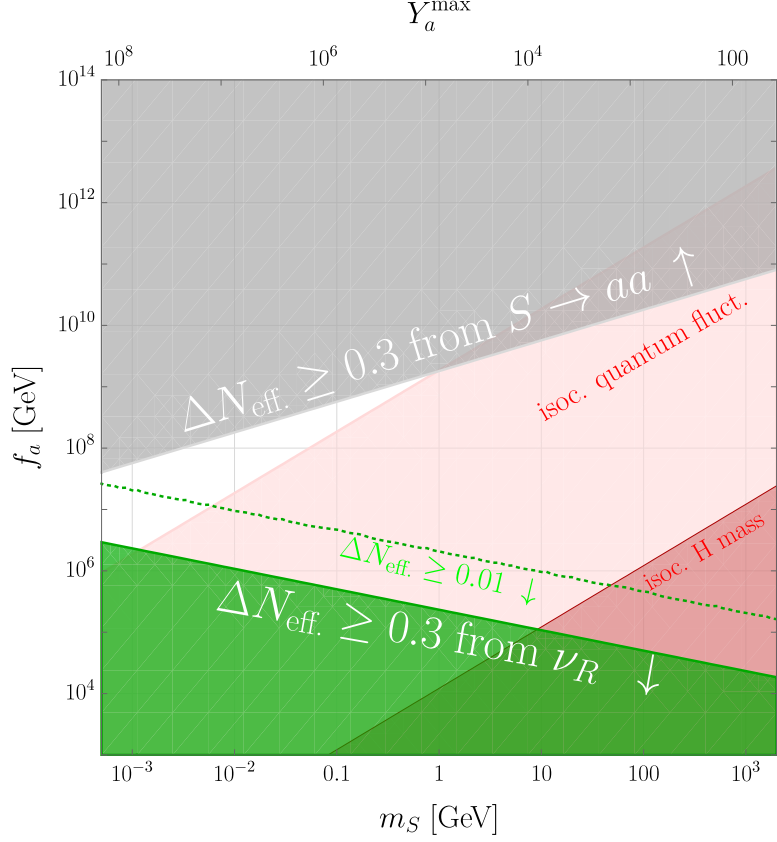


Figure 8.6: Saxion parameter space for the isocurvature and dark radiation constraints.

Current limits from BBN and the Planck data together with baryon acoustic oscillations (BAO) read [20]

$$N_{\text{eff}}^{\text{BBN}} = 2.97_{-0.54}^{+0.58}, \quad N_{\text{eff}}^{\text{Planck+BAO}} = 2.99_{-0.33}^{+0.34}, \quad (8.165)$$

which amounts to $\Delta N_{\text{eff.}}^{\text{Planck+BAO}} \simeq 0.28$. A sensitivity of $\Delta N_{\text{eff.}} \lesssim 0.12$ could be reached by next generation experiments such as COrE [336], Euclid [1047], SPT-3G [330] or the Simons observatory [331]. CMB-S4 [332, 333] and PICO [335] could even reach down to $\Delta N_{\text{eff.}} \simeq 0.06$ and CMB-HD might probe $\Delta N_{\text{eff.}} \simeq 0.014$ [832].

8.7.1 Freeze-In scattering from Dirac Weinberg operator

We estimate the energy density of ν_R as follows

$$\rho_{\nu_R} \simeq \langle E_{\nu_R} \rangle \cdot 2 \cdot 3 \cdot n_{\nu_R} \quad (8.166)$$

where the factor of two counts the helicity states and the three comes from the number of generations. The typical energy of a ν_R produced out of thermal equilibrium reads

$$\langle E_{\nu_R} \rangle = \text{Max}(2.5 T, m_S(S)). \quad (8.167)$$

Freeze-in from a thermal bath leads to typical momenta of $2.5 T$ [289], whereas production from an non-thermal condensate involves momenta of the order of the oscillation frequency $m_S(S)$ (see section 8.6.5). Since we have $m_S(S) \ll T$ (see section 8.5.1) we take $\langle E_{\nu_R} \rangle \simeq 2.5 T$. As argued in section 8.5.3 the Dirac Weinberg operator will only operate in the Freeze-in regime, which is why we can simplify the Boltzmann equation for the right handed neutrino abundance in terms of the thermally averaged cross sections $\langle \sigma |v| \rangle$ and the equilibrium number densities

$$\frac{d}{dt} n_{\nu_R} + 3H n_{\nu_R} \simeq \left(\langle \sigma |v| \rangle_{LS \rightarrow H^\dagger \nu_R} n_L^{\text{eq.}} + \langle \sigma |v| \rangle_{HS \rightarrow \bar{L} \nu_R} n_H^{\text{eq.}} \right) n_S \simeq \frac{7}{6} \Gamma_S(S) n_L^{\text{eq.}}, \quad (8.168)$$

where we made use of the definition of the dissipation coefficient (8.103) and used $n_H^{\text{eq.}}/n_L^{\text{eq.}} = 4/3$. It is straightforward to find the number density frozen-in [74, 338] over a Hubble time $1/H$ and from that

$$\rho_{\nu_R}(T) \simeq \frac{35}{2} \cdot \frac{\Gamma_S(S)}{H(T)} \cdot n_L^{\text{eq.}}(T) T \quad (8.169)$$

The scaling relations from 8.5.3 reveal that the energy density UV-dominated during radiation domination since $\rho_{\nu_R}/\rho_{\text{SM}}$ scales like T . Consequently the production is peaked at the beginning of the oscillations. For production during radiation domination we obtain

$$\Delta N_{\text{eff.}} \simeq 0.01 \cdot \left(\frac{\sum_\nu m_\nu^2}{(0.05 \text{ eV})^2} \right) \cdot \sqrt{\frac{100 \text{ MeV}}{m_S}} \cdot \left(\frac{S_i}{5 \times 10^{15} \text{ GeV}} \right)^{\frac{3}{2}} \cdot \left(\frac{10^5 \text{ GeV}}{N f_a} \right)^{\frac{3}{2}} \quad (8.170)$$

If the oscillations occur before the completion of reheating, we have to take into account that the entropy of the decaying inflaton heats the SM plasma compared to the decoupled⁷ ν_R . Another way to come to the same conclusion is the fact that ρ_{SM} is only conserved after reheating⁸. Since $\rho_{\nu_R} \sim 1/a^4$ and the non-relativistic inflaton energy density redshifts as $\rho_{\text{inf.}} \sim 1/a^3$ we are lead to consider $\rho_{\nu_R}/\rho_{\text{inf.}}^{4/3}$ as an invariant, which scales as $(1/T^{13/3}, 1/T^{29/3})$ for $(T_{\text{osc.}} > T_{\text{RH}} > T_S, T_{\text{osc.}} > T_S > T_{\text{RH}})$. This implies that production is IR dominated and mostly occurs at T_{RH}

$$\frac{\rho_{\nu_R}(T_{\text{RH}})}{\rho_{\text{SM}}(T_{\text{RH}})} \simeq \frac{35}{2} \cdot \frac{\Gamma_S(S_i)}{H(T_{\text{osc.}}^{\text{RH}})} \cdot \left(\frac{T_{\text{RH}}}{T_{\text{osc.}}^{\text{RH}}} \right)^{\frac{7}{3}} \cdot \frac{n_L^{\text{eq.}}(T_{\text{RH}}) T_{\text{RH}}}{\rho_{\text{SM}}(T_{\text{RH}})}, \quad (8.171)$$

where we used the scaling relations to restore $\Gamma_S(S_i)/H(T_{\text{osc.}}) \ll 1$ and focused on the regime $T_{\text{osc.}} > T_{\text{RH}} > T_S$ where $\Gamma_S(S)/H(T) \sim T^{7/3}$, because we typically find that the Saxon reaches its minimum after reheating. The amount of dark radiation is

$$\Delta N_{\text{eff.}} \lesssim 2 \times 10^{-5} \cdot \left(\frac{\sum_\nu m_\nu^2}{(0.05 \text{ eV})^2} \right) \cdot \left(\frac{S_i}{5 \times 10^{15} \text{ GeV}} \right)^2 \cdot \left(\frac{10^5 \text{ GeV}}{N f_a} \right)^2 \cdot \left(\frac{10^{15} \text{ GeV}}{T_{\text{RH}}} \right), \quad (8.172)$$

⁷We assume no coupling of the inflaton to ν_R .

⁸The sum $\rho_{\text{SM}} + \rho_{\text{inf.}}$ is always conserved. Reheating starts out from $\rho_{\text{SM}} = 0$, $\rho_{\text{inf.}} \neq 0$ and ends with $\rho_{\text{SM}} \simeq \rho_{\text{inf.}}$

where we eliminated m_S using (8.64) to make sure the oscillation starts before the completion of reheating. Comparing equations (8.170) and (8.172) reveals that typically less dark radiation is produced for oscillations during reheating due to the entropy dilution in (8.171). For both scenarios we find an upper limit of

$$\Delta N_{\text{eff.}} = 0.028 \cdot \left(\frac{\Gamma_S(T_{\text{osc.}})/H(T_{\text{osc.}})}{0.1} \right) \cdot \left(\frac{100}{g_*(T_{\text{osc.}})} \right)^{\frac{4}{3}}, \quad (8.173)$$

where $g_*(T_{\text{osc.}})$ has to be replaced with $g_*(T_{\text{RH}})$ for production before the end of reheating. Fixing f_a via equations (8.119) and (8.123) is equivalent to fixing the amount of dark radiation produced from Freeze-In. The above value for the dark radiation abundance is only a factor of two away from the projected sensitivity of CMB-S4 [332, 333], and PICO [335]. CMB-HD [832] would have sufficient sensitivity to probe this scenario. The regions corresponding to observable $\Delta N_{\text{eff.}}$ from ν_R produced via scattering can be found in green in figure 8.6, where we made use of (8.119).

8.7.2 Out-of-equilibrium Saxion decays

The Saxion can decay to Diraxions via its derivative coupling in (8.45) with a width [830]

$$\Gamma(S \rightarrow aa) = \frac{1}{32\pi} \frac{m_S^3}{(Nf_a)^2} \quad (8.174)$$

and to neutrinos with a decay width, that is given by the expression (8.125) for the decays of Diraxion to neutrinos under the replacement $m_a \rightarrow m_S$. The decay to Diraxions is the dominant mode because $m_S^2 > 2 \sum_\nu m_\nu^2$. Non-thermalized Saxions could basically produce an arbitrarily large $\Delta N_{\text{eff.}}$, which is why we require Saxion thermalization (see section 8.9). The thermalized Saxions decouple at T_D and could decay out of equilibrium to Diraxions at a later time $T_{\text{dec.}} < T_D$

$$T_{\text{dec.}} = \frac{0.08}{g_*(T_{\text{dec.}})^{\frac{1}{4}}} \frac{\sqrt{m_S^3 M_{\text{Pl}}}}{Nf_a} \simeq 1.52 \text{ GeV} \cdot \left(\frac{m_S}{1 \text{ GeV}} \right)^{\frac{3}{2}} \cdot \left(\frac{10^6 \text{ GeV}}{Nf_a} \right) \cdot \left(\frac{10.75}{g_*(T_{\text{dec.}})} \right)^{\frac{1}{4}}. \quad (8.175)$$

Its energy density at T_D reads $\rho_S(T_D) = m_S T_D^3 \zeta(3)/\pi^2$ and since $\rho_S \sim n_S \sim 1/a^3$ it redshifts to $\rho_S(T_{\text{dec.}}) = \rho_S(T_D) (g_*(T_{\text{dec.}}) T_{\text{dec.}}^3) / (g_*(T_D) T_D^3)$. Using this together with the definition of $T_{\text{dec.}}$ one finds that [942]

$$\Delta N_{\text{eff.}} \simeq 0.25 \cdot \sqrt{\frac{10 \text{ MeV}}{m_S}} \cdot \left(\frac{Nf_a}{10^8 \text{ GeV}} \right) \cdot \left(\frac{100}{g_*(T_D)} \right) \cdot \left(\frac{10.75}{g_*(T_{\text{dec.}})} \right)^{\frac{1}{12}}. \quad (8.176)$$

The current bound $\Delta N_{\text{eff.}} < 0.28$ [20] excludes $Nf_a > 10^8 \text{ GeV} \cdot \sqrt{m_S/10 \text{ MeV}}$. This bound is not very restrictive to our scenario due to the absence of stellar cooling constraints, which exclude $f_a < 10^8 \text{ GeV}$ for a QCD axion. We showcase this bound as the gray area in figure 8.6. However the above estimate only holds when the Saxion

decouples from the thermal bath while relativistic. In section 8.9.4 we show that for late thermalization the Saxion can stay in thermal equilibrium until it becomes non-relativistic and hence Boltzmann-suppressed. Furthermore one can see from 8.6 that the channels for Diraxion and ν_R dark radiation exist in different regions of parameter space and only overlap for Saxion masses below the MeV-scale.

8.8 Isocurvature perturbations

Since both the Saxion and the Diraxion are light during inflation we expect that quantum fluctuations imprint on them and lead to isocurvature modes [363, 1048–1050]. For a quartic potential the typical time-scale over which S relaxes to its minimum Nf_a is given by $t_{\text{Relax}} \simeq 1/m_S(S)$ [984, 985]. In order for the radial mode to remain stuck in its large initial field value until after inflation, we have to demand that the relaxation time is larger than age of the universe $t \simeq 1/H_I$ after inflation with a Hubble rate H_I . The corresponding condition

$$m_S(S) \leq H_I \quad (8.177)$$

immediately implies that there will be isocurvature fluctuations in the Saxion direction, which is typical for Affleck-Dine scenarios.

8.8.1 Dark Matter and Baryon isocurvature

First we investigate dark matter and baryon isocurvature modes. The gauge invariant entropy perturbation reads [363]

$$\mathcal{S}_a = \frac{\delta(n_a/s)}{n_a/s} = \frac{\delta Y_\theta}{Y_\theta} \quad (8.178)$$

and we compute the amplitude of the isocurvature power spectrum following reference [740] assuming that the Diraxion makes up the whole of dark matter:

$$\mathcal{P}_a(k_*) = \left\langle \left(\frac{\delta Y_\theta}{Y_\theta} \right)^2 \right\rangle = \left(\frac{1}{Y_\theta} \frac{\partial Y_\theta}{\partial \theta} \right)^2 \langle \delta \theta_i^2 \rangle + \left(\frac{1}{Y_\theta} \frac{\partial Y_\theta}{\partial S} \right)^2 \langle \delta S_i^2 \rangle \quad (8.179)$$

We find the amplitude of the baryon isocurvature perturbations by an analogous calculation

$$\mathcal{P}_B(k_*) = \left\langle \left(\frac{\delta Y_B}{Y_B} \right)^2 \right\rangle = \left(\frac{1}{Y_B} \frac{\partial Y_B}{\partial \theta} \right)^2 \langle \delta \theta_i^2 \rangle + \left(\frac{1}{Y_B} \frac{\partial Y_B}{\partial S} \right)^2 \langle \delta S_i^2 \rangle. \quad (8.180)$$

In the above we defined the fluctuations in the angular and radial modes in terms of the Hubble rate during inflation to be

$$\sqrt{\langle \delta \theta_i^2 \rangle} \equiv \frac{H_I}{2\pi S_i}, \quad \sqrt{\langle \delta S_i^2 \rangle} \equiv \frac{H_I}{2\pi}. \quad (8.181)$$

CMB observations [353] at the pivot scale $k_* = 0.05 \text{ Mpc}^{-1}$ determined the power spectrum of the adiabatic perturbations to be $P_\zeta(k_*) \simeq 2.2 \times 10^{-9}$ and they constrain

$$\beta_{\text{iso}} \equiv \frac{\mathcal{P}_a(k_*)}{\mathcal{P}_a(k_*) + \mathcal{P}_\zeta(k_*)} < 0.038, \quad (8.182)$$

which implies

$$\mathcal{P}_a(k_*) < \frac{\beta_{\text{iso}}}{1 - \beta_{\text{iso}}} \mathcal{P}_\zeta(k_*) \simeq 8.7 \times 10^{-11}. \quad (8.183)$$

By rescaling the bound on $\mathcal{P}_a(k_*)$ to the observed baryon abundance and using $h^2 \Omega_B = 0.0224$ as well as $h^2 \Omega_a = 0.12$ [20] we find [78]

$$\mathcal{P}_B(k_*) < \left(\frac{\Omega_a}{\Omega_B} \right)^2 \cdot \frac{\beta_{\text{iso}}}{1 - \beta_{\text{iso}}} \mathcal{P}_\zeta(k_*) \simeq 2.5 \times 10^{-9}. \quad (8.184)$$

Let us first deal with the contribution from the Diraxion fluctuations: Since only ε depends on the angle θ , we find that the usual and kinetic misalignment scenarios are relevant; parametric resonance depends only the initial Saxion number density. Furthermore we deduce from equations (8.116) and (8.121) that in our scenario the baryon asymmetry always depends on ε . Consequently we find for kinetic misalignment and Baryogenesis that

$$\frac{1}{Y_\theta} \frac{\partial Y_\theta}{\partial \theta} = \frac{1}{Y_B} \frac{\partial Y_B}{\partial \theta} = \frac{1}{\varepsilon} \frac{\partial \varepsilon}{\partial \theta} = \cot(\theta_i + \delta) \quad (8.185)$$

where we used (8.85) for the last equality. If we choose $\theta_i + \delta = \pm\pi/2$ the cosine vanishes and there will be no perturbations in the Diraxion direction [920]. The Diraxion will be stuck in this value due to the Hubble friction. Hence we have to assume that the Diraxion is not aligned with the minimum of its potential which would instead enforce from equation (8.86) $\partial V_D / \partial \theta \sim \sin(\theta_i + \delta) = 0$. For conventional misalignment the amplitude of the dark matter isocurvature spectrum is given by the standard expression [951] with f_a replaced by S_i

$$\mathcal{P}_a^{\text{mis.}}(k_*) = \frac{4}{\langle \theta_i^2 \rangle} \left(\frac{H_I}{2\pi S_i} \right)^2, \quad (8.186)$$

where $\langle \theta_i^2 \rangle$ was defined in (8.128). Since parametric resonance will randomize the angle we take $\langle \theta_i^2 \rangle \simeq \pi^2/3$ [942] and find

$$\frac{m_S}{N f_a} < \begin{cases} 4.5 \times 10^{-10} & \text{quant. fluct.} \\ 7.5 \times 10^{-5} & H\text{-mass from } R \end{cases}, \quad (8.187)$$

where the first line fixes S_i via quantum fluctuations and in the second line it is induced from a Hubble-dependent mass term (see sections 8.4.2 and 8.4.2 respectively). For our parameter space with smaller f_a regular misalignment can not be responsible for the

majority of the dark matter relic abundance and the previous bounds disappear.

In the following we only have to deal with the Saxion isocurvature perturbations: Using the definition of the charge yields in (8.92) and (8.93) together with the definition of ε in (8.85) we obtain for kinetic misalignment that [740]

$$\mathcal{P}_a(k_*) = \frac{(N-x)^2}{4\pi^2} \frac{H_I^2}{S_i^2}, \quad \text{with} \quad x = \begin{cases} \frac{5}{2} & \text{RD} \\ 3 & \text{RH} \end{cases}. \quad (8.188)$$

For parametric resonance we deduce from (8.92) and (8.93) that [740]

$$\mathcal{P}_a(k_*) = \frac{1}{4\pi^2} \frac{H_I^2}{S_i^2} \cdot \begin{cases} \frac{9}{4} & \text{RD} \\ 1 & \text{RH} \end{cases}. \quad (8.189)$$

One can see that the spectra for parametric resonance correspond to the ones for kinetic misalignment under the replacement $N \rightarrow 4$, because here the relic abundance is induced from the Saxion potential $V_\sigma \sim S^4$ and not the Diraxion potential $V_{\mathcal{D}} \sim S^N$ [740]. For the baryonic perturbations we find using (8.116) and (8.121)

$$\mathcal{P}_B(k_*) = \frac{(N-y)^2}{4\pi^2} \frac{H_I^2}{S_i^2}, \quad \text{with} \quad y = \begin{cases} 2 & \text{RD} \\ \frac{5}{2} & \text{RH} \end{cases}. \quad (8.190)$$

We focus on the bound for the dark matter perturbations, since the limit is slightly stronger than for baryons. Our result for the scenario in section 8.4.2, where S_i originates from quantum fluctuations, reads

$$\frac{m_S}{Nf_a} < \frac{5.4 \times 10^{-10}}{(N-x)^2} \quad (8.191)$$

and the case of a Hubble-dependent mass from the Ricci scalar in section 8.4.2 is constrained to be

$$\frac{m_S}{Nf_a} < \frac{8.2 \times 10^{-5}}{N-x}. \quad (8.192)$$

The corresponding regions were drawn in red in figure 8.6 and we see that for the case of quantum fluctuations inducing S_i , most of the interesting parameter space would be excluded. In section 8.8.3 we demonstrate under which conditions the Dirac Seesaw models do not induce radiative corrections that violate the aforementioned bounds. The large hierarchy between m_S and Nf_a is the main drawback of using a quartic potential. This problem can be avoided in supersymmetric models such as [942--945], where the approximately quadratic scalar potential arises from supersymmetry breaking via soft masses in a two field model [1051], dimensional transmutation from the RGE running of soft masses [1052] or loop corrections in gauge mediated supersymmetry breaking [1053] in single field models.

8.8.2 Dark Radiation isocurvature

We define the gauge invariant perturbation in the dark radiation fluid via the relation [1054]

$$\mathcal{S}_{\text{DR}} = \frac{3}{4} \frac{\delta(\rho_{\nu_R}/\rho_{\text{SM}})}{\rho_{\nu_R}/\rho_{\text{SM}}} = \frac{3}{4} \frac{\delta \Delta N_{\text{eff.}}}{\Delta N_{\text{eff.}}}, \quad (8.193)$$

where we made use of the fact that the photons are adiabatic with respect to the perturbations in the SM plasma to trade ρ_γ for ρ_{SM} . The amplitude of the dark radiation isocurvature spectrum reads

$$\mathcal{P}_{\text{DR}}(k_*) = \left\langle \left(\frac{\delta \Delta N_{\text{eff.}}}{\Delta N_{\text{eff.}}} \right)^2 \right\rangle = \left(\frac{1}{\Delta N_{\text{eff.}}} \frac{\partial \Delta N_{\text{eff.}}}{\partial S} \right)^2 \langle \delta S_i^2 \rangle \quad (8.194)$$

and we already used the fact that $\Delta N_{\text{eff.}}$ does not depend on θ in our model, see e.g. (8.170) and (8.172). Dark radiation isocurvature leads to a spatial variation of $\Delta N_{\text{eff.}}$ compared to its spatial average $\Delta \bar{N}_{\text{eff.}}$ [1054]

$$\Delta N_{\text{eff.}} \simeq \Delta \bar{N}_{\text{eff.}} \left(1 + \frac{4}{3} \sqrt{\mathcal{P}(k_*)_{\text{DR}}} \right). \quad (8.195)$$

A spatially varying $\Delta N_{\text{eff.}}$ would lead to spatially varying abundances of light elements produced during BBN. Reference [1054] sets constraints on this effect by making use of the ${}^4\text{He}/\text{D}$ data extracted from local galaxies [1055] and measurements of D/H obtained from high-redshift Lyman- α absorption systems [76], which correspond to a pivot scale of $k_* \simeq 1 \text{ Mpc}^{-1}$ and they obtain the limit

$$\mathcal{P}_{\text{DR}}(k_*) < \frac{0.17}{\Delta \bar{N}_{\text{eff.}}^2}. \quad (8.196)$$

CMB data with $k_* \simeq 0.1 \text{ Mpc}^{-1}$ can be used to set constraints of isocurvature modes in the left-chiral SM neutrinos, which can be recast as a bound on dark radiation [1054]

$$\mathcal{P}_{\text{DR}}(k_*) < 10^{-10} \left(\frac{N_{\text{eff.}}}{\Delta \bar{N}_{\text{eff.}}} \right)^2. \quad (8.197)$$

The authors of [1056] recast CMB data with variable $\Delta N_{\text{eff.}}$, updating a similar study [1057] based on WMAP data, and their bound reads

$$\mathcal{P}_{\text{DR}}(k_*) < \frac{2 \times 10^{-8}}{\Delta N_{\text{eff.}}^2} \quad (8.198)$$

For simplicity we neglect the correlation between the dark matter and dark radiation isocurvature perturbations, which both inherit the fluctuations from S . By setting $N_{\text{eff.}} \simeq 3$ one can see that the bound (8.197) is about an order of magnitude stronger

than (8.198), so to be conservative we use (8.197) to set limits on the amplitude of the power spectrum

$$\mathcal{P}_{\text{DR}}(k_*) = \frac{H_I^2}{S_i^2} \cdot \begin{cases} 0.032 & \text{RD} \\ 2.4 \times 10^{-3} & \text{RH} \end{cases} \quad (8.199)$$

From this result and for $N_{\text{eff.}} \simeq 3.045 + \Delta N_{\text{eff.}}$ with $\Delta N_{\text{eff.}} = 0.028$ from (8.173) we can deduce that for S_i from quantum fluctuations (see section 8.4.2)

$$\frac{m_S}{N f_a} < \begin{cases} 7.5 \times 10^{-6} & \text{RD} \\ 10^{-4} & \text{RH} \end{cases} \quad (8.200)$$

and for S_i from a Hubble-dependent mass (see section 8.4.2)

$$\frac{m_S}{N f_a} < \begin{cases} 9.7 \times 10^{-3} & \text{RD} \\ 3.5 \times 10^{-2} & \text{RH} \end{cases} \quad (8.201)$$

These limits are sub-leading to the ones from dark matter isocurvature in (8.191) and (8.192).

8.8.3 One Loop corrections

Since isocurvature perturbations typically require a tiny Saxion quartic coupling λ_σ

$$\lambda_\sigma = \frac{m_S^2}{2N^2 f_a^2} < \begin{cases} 9.1 \times 10^{-21} & \text{quant. fluct.} \\ 2.1 \times 10^{-10} & H\text{-mass from } R \end{cases} \quad (8.202)$$

where we used the bounds in (8.191) as well as (8.192) and set $N - x = 3.5$ for the strongest limit, we have to check that radiative corrections to this parameter and to m_S are under control. Here we write out only the finite pieces of the loop corrections and neglect logarithmic factors. The mixed quartic coupling with the SM like Higgs, the scalar doublet η for the Type II scenario, or the triplet Δ in the Type III Seesaw induce corrections of [383]

$$\delta m_S^{(H)2} = -\frac{\lambda_{H\sigma}^2}{8\pi^2} (N f_a)^2, \quad \delta m_S^{(\eta)2} = -\frac{\lambda_{\eta\sigma}^2}{8\pi^2} (N f_a)^2, \quad \delta m_S^{(\Delta)2} = -\frac{\lambda_{\Delta\sigma}^2}{8\pi^2} (N f_a)^2, \quad (8.203)$$

where the minus signs take into account that at tree level $m_S^2 < 0$, as well as

$$\delta \lambda_\sigma^{(H)} = \frac{\lambda_{H\sigma}^2}{16\pi^2}, \quad \delta \lambda_\sigma^{(\eta)} = \frac{\lambda_{\eta\sigma}^2}{16\pi^2}, \quad \delta \lambda_\sigma^{(\Delta)} = \frac{\lambda_{\Delta\sigma}^2}{16\pi^2}. \quad (8.204)$$

We find that for both kinds of corrections the mixed quartic couplings need to satisfy

$$|\lambda_{H\sigma}|, |\lambda_{\eta\sigma}|, |\lambda_{\Delta\sigma}| < \begin{cases} 1.2 \times 10^{-9} & \text{quant. fluct.} \\ 1.8 \times 10^{-4} & H\text{-mass from } R \end{cases} \quad (8.205)$$

For the one-loop correction from the $N_L - \nu_R$ loop in the Type I Seesaw we can recycle the result for a Majorana Seesaw [912, 913], because only one chirality of N runs in the loop

$$\delta m_S^{(I)2} = \frac{Y_R^2}{8\pi^2} M_N^2, \quad \delta\lambda_\sigma^{(I)} \simeq -\frac{5}{32\pi^2} Y_R^4. \quad (8.206)$$

Both contributions come with a minus sign from the closed fermion loop, which for the two-point function was already absorbed in the definition of $m_S^2 < 0$. The bound from the correction to the negative m_S^2 can be re-expressed by using the Type I Seesaw relation in (8.6) as

$$M_N < \sqrt{Y_L} \cdot \left(\frac{N}{6}\right) \cdot \left(\frac{f_a}{10^6 \text{ GeV}}\right) \cdot \left(\frac{(0.05 \text{ eV})^2}{\sum m_\nu^2}\right)^{\frac{1}{4}} \cdot \begin{cases} 4.6 \times 10^8 \text{ GeV} & \text{quant. fluct.} \\ 1.8 \times 10^{11} \text{ GeV} & H\text{-mass from } R \end{cases} \quad (8.207)$$

and the one from the quartic is given by

$$M_N < Y_L \cdot \left(\frac{N}{6}\right) \cdot \left(\frac{f_a}{10^6 \text{ GeV}}\right) \cdot \sqrt{\frac{(0.05 \text{ eV})^2}{\sum m_\nu^2}} \cdot \begin{cases} 8.1 \times 10^{14} \text{ GeV} & \text{quant. fluct.} \\ 3.2 \times 10^{17} \text{ GeV} & H\text{-mass from } R \end{cases} \quad (8.208)$$

It is evident that the bound on M_N from the correction to m_S^2 is the stronger one and would lead to values of M_N that are in conflict with our cosmological assumptions in (8.74) and (8.75), so that the heavy N could be produced from the plasma. On the other hand the bound from the correction to the quartic is compatible with our choices of e.g. $T_{RH} = (10^{14} - 10^{15}) \text{ GeV}$. One way to avoid this conclusion is to assume that there is an accidental cancellation between the corrections $\delta m_S^{(I)2}$ and $\delta m_S^{(H)2}$ assuming e.g. $\lambda_{H\sigma}^2 < 0$. This would lead to

$$M_N \simeq 1.8 \times 10^{13} \text{ GeV} \cdot \sqrt{Y_L} \cdot \sqrt{|\lambda_{H\sigma}|} \cdot \left(\frac{N}{6}\right) \cdot \left(\frac{f_a}{10^6 \text{ GeV}}\right) \cdot \left(\frac{(0.05 \text{ eV})}{\sum m_\nu^2}\right), \quad (8.209)$$

which is still too small for our purposes. However we can ameliorate this problem by assuming the simultaneous presence of two or more different Dirac Seesaws.

The trilinear term connecting σ, η and H in the Type II Dirac Seesaw induces

$$\delta m_S^{(II)2} = -\frac{1}{16\pi^2} \kappa^2, \quad \delta\lambda_\sigma^{(II)} \simeq \frac{1}{16\pi^2} \frac{\kappa^4}{\mu_\eta^4}, \quad (8.210)$$

where we eliminate κ by using the Type II Seesaw relation in (8.11) and set a bound on μ_η . The limit from the correction to m_S is given by

$$\mu_\eta < \sqrt{Y_\nu} \cdot \left(\frac{N}{6}\right) \cdot \left(\frac{f_a}{10^6 \text{ GeV}}\right) \cdot \left(\frac{(0.05 \text{ eV})^2}{\sum m_\nu^2}\right)^{\frac{1}{4}} \begin{cases} 3.3 \times 10^8 \text{ GeV} & \text{quant. fluct.} \\ 1.3 \times 10^{11} \text{ GeV} & H\text{-mass from } R \end{cases} \quad (8.211)$$

and is stronger than the bound from the correction to the quartic

$$\mu_\eta < Y_\nu \cdot \left(\frac{N}{6} \right) \cdot \left(\frac{f_a}{10^6 \text{ GeV}} \right) \cdot \sqrt{\frac{(0.05 \text{ eV})^2}{\sum m_\nu^2}} \cdot \begin{cases} 5.1 \cdot 10^{13} \text{ GeV} & \text{quant. fluct.} \\ 2 \times 10^{16} \text{ GeV} & H\text{-mass from } R \end{cases}. \quad (8.212)$$

We observe that the limit from $\delta m_S^{(\text{II}) 2}$ enforces values of μ_η , which can be problematic in the context of equations (8.74) and (8.75), just like for M_N in the Type I scenario. If both the Type I and Type II Seesaw are responsible for Dirac neutrino masses, which is known as a Hybrid-Seesaw [44, 45], their one loop corrections could cancel each other as long as

$$M_N \simeq \frac{1}{2} \sqrt{\frac{Y_L}{Y_\nu}} \mu_\eta, \quad (8.213)$$

owing to the fact that the bosonic and fermionic contributions have different signs. In this case the bounds from the quartic in (8.208) and (8.212) also get weakened and by using the previous relation we find that

$$\lambda_\sigma^{(\text{I})} + \lambda_\sigma^{(\text{II})} \simeq \frac{1}{32\pi^2} \left(\frac{m_\nu}{v_H N f_a} \right)^4 \left(\frac{1}{Y_\nu^2} - \frac{5}{4Y_L^2} \right) \frac{M_N^4}{Y_L^2}, \quad (8.214)$$

which can be arbitrarily small depending on Y_L, Y_ν .

Analogously we find for the quartic term connecting σ, Δ and H for both versions of the Type III Seesaw

$$\delta m_S^{(\text{III}) 2} = \frac{\lambda_4^2}{16\pi^2} (v_H^2 + v_\Delta^2), \quad \delta \lambda_\sigma^{(\text{III})} \simeq \frac{\lambda_4^4}{64\pi^2} \left(\frac{v_H^4}{\mu_\Delta^4} + \frac{v_\Delta^4}{m_h^4} \right), \quad (8.215)$$

where there are two contributions each, because we can either have just H or H and Δ running in the loop. With the relation (8.20) for v_Δ in mind one sees that the first term for the correction to m_S^2 and the second term for the correction of λ_σ are the leading ones and the limits read

$$\lambda_4 < \left(\frac{N}{6} \right) \cdot \left(\frac{f_a}{10^6 \text{ GeV}} \right) \cdot \begin{cases} 3 \times 10^{-5} & \text{quant. fluct.} \\ 4.4 & H\text{-mass from } R \end{cases} \quad (8.216)$$

as well as

$$\lambda_4 < \left(\frac{4 \text{ GeV}}{v_\Delta} \right) \cdot \begin{cases} 1.5 \times 10^{-3} & \text{quant. fluct.} \\ 0.6 & H\text{-mass from } R \end{cases}. \quad (8.217)$$

As was discussed below (8.208) and (8.212), the new degrees of freedom in the Type III scenario even without the aforementioned range of v_Δ are typically so light that we can not avoid their presence in the plasma anyway, which will be exploited in section 8.9.2.

8.9 Thermalization

The Saxion only couples to the bath via the Dirac Weinberg operator, leading to a UV-dominated rate (8.103), and the mixed quartic coupling with the Higgs, that leads to a IR-dominated rate to be discussed in the next subsection. We need to ensure that the Saxion is thermalized to avoid the overproduction of dark radiation or relic Saxions.

8.9.1 Early Thermalization

If the Dirac Weinberg operator is supposed to be fast at early times $T \lesssim T_{\text{osc.}}$ to thermalize the Saxions, it would be already fast at $T_{\text{osc.}}$. As we saw in section 8.5.3, an efficient charge transfer from the condensate to the bath would require a rate $\Gamma_S(T_{\text{osc.}})$ that is a thousand times faster than the Hubble rate for $\varepsilon = 0.1$. Such a large dissipation rate would naively lead to immediate evaporation of the condensate. Reference [999] however showed that since the dissipation rate depends on the oscillating field value (and not the amplitude) and further since it is the coefficient of \dot{S} in the equation of motion (see section 8.4.1 for the coupled equations of motion for both fields)

$$\ddot{S} + (3H + \Gamma_S) \dot{S} + \frac{\partial V_\sigma}{\partial S} = S \dot{\theta}^2 \quad (8.218)$$

it vanishes twice every period: Once when $\Gamma_S \sim S^2 = 0$ and once when $\dot{S} = 0$. The authors of [999] found from numerical simulations that such a term $\Gamma_S \sim S^2$ does not quickly evaporate the condensate, but instead leads to stronger damping of the amplitude than Hubble friction alone. The backreaction of particle production on an oscillating condensate can be captured by multiplying the amplitude with a factor of $\exp(-\Gamma_S/H)$ [1058]. A stronger decrease of the amplitude at early times could however decrease the amount of angular rotation produced during the first couple oscillations in (8.84). We also expect that the additional friction from the coupling to the thermal bath would delay the commencement of the oscillations until $m_S(S) \simeq \sqrt{\Gamma_S(S) H}$ [1059], which is below the usual oscillation temperature defined in (8.62). Since the production rate Γ_S depends on T , the baryon asymmetry production would consequently be even more inefficient. Studies of oscillating QCD axions with additional friction from a thermal bath [1059, 1060] also find that the oscillations are damped and delayed. We conclude that early thermalization via an effective operator is not necessarily viable and requires a dedicated numerical simulation. Reference [944] considers thermalization of Saxions with Higgsinos via an effective operator similar to (8.103) and avoids the aforementioned problem in the following way: The Higgsino mass gets a correction from the same coupling leading to the thermalization operator and the Higgsinos only become kinematically accessible at some time after the start of the oscillations. We sketch a scenario based on using the potentially light triplet scalar in the Type III Dirac Seesaw (see 8.3.2) in section 8.9.2. Early thermalization before the Saxion has reached $N f_a$ has the appealing advantage that the Diraxion gets automatically thermalized as well [942] as a consequence of their coupled equations of motion in section 8.4.1, which removes the warmness-bound for parametric resonance dark matter in (8.163).

8.9.2 Early Thermalization from Type III Dirac Seesaw

To realize early thermalization, that occurs some time after the initiation of oscillations, but still early enough to thermalize the parametric resonance Diraxions, we need a particle with a thermal abundance and a renormalizable coupling to S , such as the iso-triplet Δ from the Type III scenario 8.3.2, which may be much lighter than the other new degrees of freedom (see (8.20)). Early thermalization could proceed as follows: Δ is relativistic and rapidly scatters with the bath due to its gauge interactions. For this to stay true we need to ensure that the corrections to the triplet mass squared $\lambda_{H\Delta} S_i^2$ (tree level) and $\lambda_4^2/(16\pi^2) S_i^2$ (one-loop) stay below $T_{\text{osc.}}^2$, which has typical values of $\mathcal{O}(10^{15} \text{ GeV})$ for successful cogenesis. This implies that

$$\lambda_{H\Delta} < 10^{-6} \cdot \left(\frac{0.1 M_{\text{Pl}}}{S_i} \right)^2 \cdot \left(\frac{T_{\text{osc.}}}{10^{15} \text{ GeV}} \right)^2, \quad (8.219)$$

$$\lambda_4 < 10^{-2} \cdot \left(\frac{0.1 M_{\text{Pl}}}{S_i} \right) \cdot \left(\frac{T_{\text{osc.}}}{10^{15} \text{ GeV}} \right). \quad (8.220)$$

In general the Saxion may also receive a thermal mass from its coupling to Δ . The thermal mass is smaller than the tree level mass as long as

$$\text{Max}(\lambda_{H\Delta}, \lambda_4) < \left(\frac{S_i}{0.1 M_{\text{Pl}}} \right) \cdot \left(\frac{10^{15} \text{ GeV}}{T_{\text{osc.}}} \right) \cdot \begin{cases} 10^{-6} & \text{quant. fluct.} \\ 0.1 & H\text{-mass from } R \end{cases}. \quad (8.221)$$

We expect interaction rate between triplets and Saxions to scale as⁹ e.g. $\Gamma \sim \text{Max}[\lambda_{H\Delta}^2, \lambda_4^2] S^2/T$ [996, 997] so that during radiation domination $\Gamma/H \sim S^2/T^3 \sim 1/T$, which is IR dominated. Hence the scattering with Δ can be taken to be slow when the oscillations start implying $T_{\text{th.}} < T_{\text{osc.}}$ and further

$$\text{Max}(\lambda_{H\Delta}, \lambda_4) < 1.4 \times 10^{-3} \cdot \left(\frac{0.1 M_{\text{Pl}}}{S_i} \right) \cdot \left(\frac{T_{\text{osc.}}}{10^{15} \text{ GeV}} \right)^2. \quad (8.222)$$

The thermalization rate peaks while the Δ are relativistic and then rapidly decreases once they are Boltzmann-suppressed. In order to avoid warmness bounds on the Diraxion abundance from parametric resonance, thermalization during radiation domination needs to occur before the Saxion field value has reached $S \simeq 10^{-2} S_i$ [1035, 1037, 1046], hence we require $T_{\text{th.}} > 0.01 T_{\text{osc.}}$, from which

$$\text{Max}(\lambda_{H\Delta}, \lambda_4) > 1.4 \times 10^{-4} \cdot \left(\frac{0.1 M_{\text{Pl}}}{S_i} \right) \cdot \left(\frac{T_{\text{osc.}}}{10^{15} \text{ GeV}} \right)^2 \quad (8.223)$$

follows. Comparing this to (8.219) and (8.220) reveals that only λ_4 is large enough for thermalization, which is not in conflict with either the attractive features of the Type III scenario presented in 8.3.2 or the isocurvature bounds in (8.216) and (8.217) (at

⁹Here for simplicity we ignore the factor of $\alpha_2(T)^2$ that would appear with the coupling $\lambda_{H\Delta}$, see (8.224).

$$S_i = 0.1 M_{\text{Pl}}, \quad \sum m_\nu^2 = (0.05 \text{ eV})^2, \quad \Delta N_{\text{eff.}} = 0.028$$

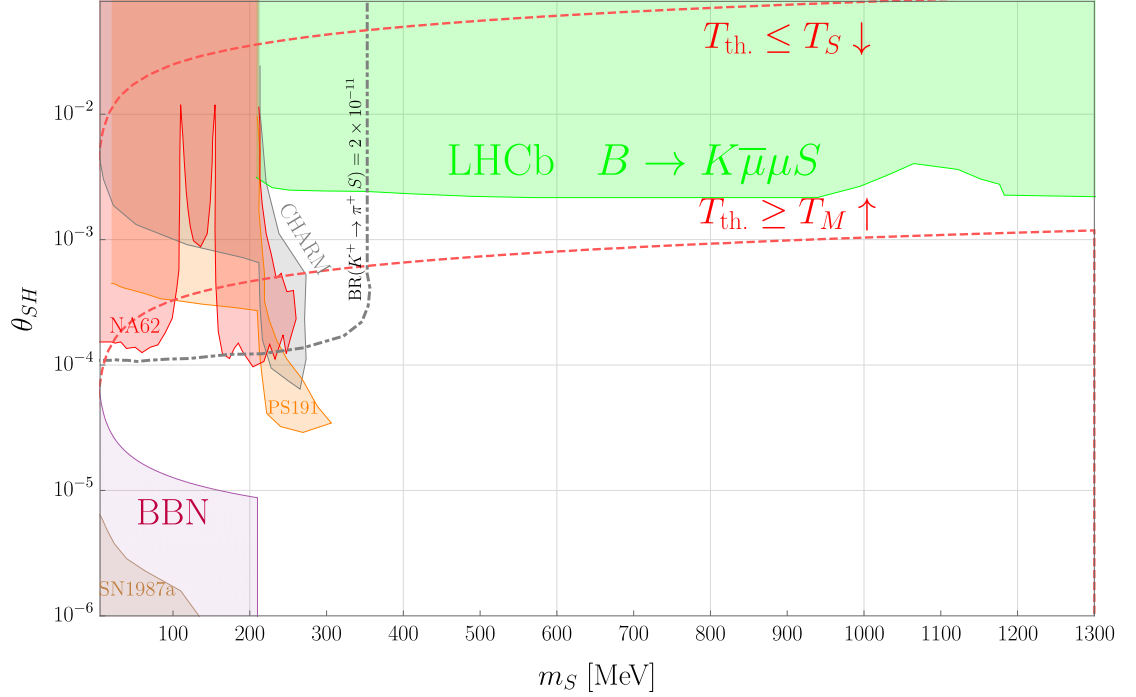


Figure 8.7: Parameter space for successful thermalization compared to current experimental and astrophysical limits on the production of scalars. The line labelled $T_{\text{th.}} \geq T_M$ would be in the excluded region for $S_i > 0.1 M_{\text{Pl}}$. If we decrease $\Delta N_{\text{eff.}}$ the red dotted lines move upwards. The dotted line for the Kaon branching ratio was obtained from [1061] and the LHCb constraint continues (with small interruptions) until below 5 GeV. Equation (8.239) leads to the purple BBN bound from light Saxion decays to electrons below the muon threshold.

least for the Hubble induced Saxion field value). Since Δ is charged under the $U(1)_D$ symmetry, its interactions with the condensate can transmit a fraction of the Noether charge into an asymmetry of Δ . Reference [935] considers the charge transfer between rotating condensates in detail. The asymmetry in Δ is then converted via its Yukawa couplings (essentially the same reactions as in 8.5.1 but with S replaced by Δ) into an asymmetry of the left chiral leptons that gets reprocessed into a baryon asymmetry via the sphalerons. Once Δ becomes Boltzmann suppressed we can integrate it out and recover the Weinberg operator.

8.9.3 Late Thermalization

Here we adopt the thermalization scenario of references [740, 942, 952], which utilizes the mixed quartic coupling between the singlet scalar and the SM Higgs and summarize the

required parameter space. The Saxion can thermalize via the processes $SH \leftrightarrow HZ, HW$ and the corresponding rate is [740, 942]

$$\Gamma_{S,H} = \lambda_{\sigma H}^2 \alpha_2(T)^2 \frac{(S + N f_a)^2}{T}, \quad (8.224)$$

where we take the weak fine structure constant to be $\alpha_2(T) \simeq 1/30$. The isocurvature constraints from section 8.8.3 require that

$$\lambda_{\sigma H} < \begin{cases} 1.2 \times 10^{-9} & \text{quant. fluct.} \\ 1.8 \times 10^{-4} & H\text{-mass from } R \end{cases}. \quad (8.225)$$

Laboratory searches for light scalars constrain the mixing angle θ_{SH} between the Saxion and the Higgs. This angle is defined in section (8.30) and in the small angle approximation together with $m_S \ll m_h$ we can re-express it as

$$\theta_{SH} \simeq \lambda_{\sigma H} \cdot \frac{v_H N f_a}{m_h^2}. \quad (8.226)$$

Higgs to invisible decays constrain $\lambda_{SH} < 0.01$ [1062]. We also use the limits from Kaon decays at NA62 [1063–1065], recasts of PS191 data [1066] as well as a recast [1067] of old CHARM data [1068], which are relevant for Saxion masses below about 300 MeV. Additionally we employ the bounds from displaced vertex searches of B-meson decays $B \rightarrow K \bar{\mu} \mu S$ at LHCb [1069, 1070] which are sensitive below around 5 GeV. For heavier singlets there exists a LEP search [1071] for the process $e^+ e^- \rightarrow Z^* S$, which only excludes $\theta_{SH} \gtrsim 0.1$. For an overview of the existing laboratory constraints consult [1061, 1072]. The bounds from SN1987A on light scalars were recently reevaluated in [1073].

Thermalization during radiation domination

Below T_S the Saxion redshifts like non-relativistic matter $S = N f_a (T/T_S)^{3/2}$ and would lead to an era of matter domination starting at a temperature

$$T_M \simeq \frac{4.8}{g_*(T_M)^{\frac{1}{4}}} \left(\frac{S_i}{M_{\text{Pl}}} \right)^{\frac{3}{2}} \sqrt{m_S N f_a} \quad (8.227)$$

$$\simeq 63 \text{ GeV} \cdot \left(\frac{10}{g_*(T_M)} \right)^{\frac{1}{4}} \cdot \sqrt{\frac{m_S}{1 \text{ GeV}}} \cdot \sqrt{\frac{N f_a}{10^6 \text{ GeV}}} \cdot \left(\frac{S_i}{0.1 M_{\text{Pl}}} \right)^{\frac{3}{2}}, \quad (8.228)$$

if it was not thermalized beforehand. During radiation domination we find that $\Gamma_{S,H}/H \sim 1/T$ so thermalization is IR dominated. The thermalization temperature is found to be

$$T_{\text{th}} \simeq \frac{0.27}{g_*(T_{\text{th}})^{\frac{1}{6}}} M_{\text{Pl}}^{\frac{1}{3}} (N f_a)^{\frac{2}{3}} \lambda_{\sigma H}^{\frac{2}{3}} \simeq 45.7 \text{ TeV} \cdot \left(\frac{\theta_{SH}}{10^{-3}} \right)^{\frac{2}{3}} \cdot \left(\frac{100}{g_*(T_{\text{th}})} \right)^{\frac{1}{6}}. \quad (8.229)$$

To avoid complications from the oscillatory effective masses of the Higgs for $S \gg Nf_a$ we work in the limit $T_{\text{th}} < T_S$ [740] with T_S defined in (8.66), which implies

$$\theta_{SH} < 1.1 \times 10^{-5} \cdot \left(\frac{m_S}{1 \text{ GeV}} \right)^{\frac{3}{4}} \cdot \left(\frac{Nf_a}{10^6 \text{ GeV}} \right)^{\frac{3}{4}} \cdot \left(\frac{0.1 M_{\text{Pl.}}}{S_i} \right)^{\frac{3}{4}}. \quad (8.230)$$

The condition $T_{\text{th}} > T_M$ on the other hand leads to

$$\theta_{SH} > 2.2 \times 10^{-8} \cdot \left(\frac{m_S}{1 \text{ GeV}} \right)^{\frac{3}{4}} \cdot \left(\frac{Nf_a}{10^6 \text{ GeV}} \right)^{\frac{3}{4}} \cdot \left(\frac{S_i}{0.1 M_{\text{Pl.}}} \right)^{\frac{9}{4}}. \quad (8.231)$$

One should keep in mind that the SM like Higgs has to be as abundant as radiation for this process to work, which is why we require $T_{\text{th}} > m_h = 125 \text{ GeV}$

$$\theta_{SH} > 1.4 \times 10^{-7} \cdot \left(\frac{g_*(T_{\text{th}})}{100} \right)^{\frac{1}{4}}. \quad (8.232)$$

The Higgs could also receive a mass correction from its coupling to S namely $\Delta m_H^2 \simeq 2\lambda_{\sigma H} Nf_a S$, where we dropped the S^2 term following [740, 942], because it is expected to be subdominant for $T < T_S$ owing to $S = Nf_a(T/T_S)^{\frac{3}{2}} < Nf_a$. Demanding that $T_{\text{th}} > \Delta m_H$ gives an upper bound

$$\theta_{SH} < 0.35 \cdot \left(\frac{m_S}{1 \text{ GeV}} \right)^{\frac{9}{8}} \cdot \left(\frac{10^6 \text{ GeV}}{Nf_a} \right)^{\frac{3}{8}} \cdot \left(\frac{0.1 M_{\text{Pl.}}}{S_i} \right)^{\frac{9}{8}}. \quad (8.233)$$

Additionally we need to ensure that the Saxion does not receive a large thermal correction from its coupling to the abundant Higgses $m_S(S_i) > \sqrt{\lambda_{\sigma H}} T_{\text{osc.}}$ which can be cast as

$$\theta_{SH} < 2.6 \times 10^{-2} \cdot \left(\frac{m_S}{1 \text{ GeV}} \right) \cdot \left(\frac{S_i}{0.1 M_{\text{Pl.}}} \right). \quad (8.234)$$

The bounds in (8.230) and (8.231) are the strongest thermalization constraints and we depict them in figure 8.7 by fixing f_a/S_i via (8.119), which explains the dependence on $\sum m_\nu^2$ and $\Delta N_{\text{eff.}}$. We find that all the available parameter space would be excluded by the constraints from meson decays unless we take $S_i \lesssim 0.1 M_{\text{Pl.}}$. Furthermore for this initial field value we have to require that $\Delta N_{\text{eff.}} > 2.8 \times 10^{-3}$, or else our entire parameter space would be excluded by LHCb. The original Lepto-Axiogenesis parameter space for a quartic potential involves Saxion masses that typically lie below the GeV-scale, whereas we will show in (8.10) that our Saxion can be heavier.

Thermalization during reheating

For the case where the oscillations begin before the completion of reheating our analysis finds that typically $T_S < T_{\text{RH}}$ which together with $T_{\text{th}} < T_S$ leads to the conclusion that thermalization will again proceed during radiation domination. Still we need to demand that $m_S(S_i) > \sqrt{\lambda_{\sigma H}} T_{\text{osc.}}^{\text{RH}}$

$$\theta_{SH} < 0.25 \cdot \left(\frac{m_S}{1 \text{ GeV}} \right)^{\frac{3}{2}} \cdot \sqrt{\frac{10^6 \text{ GeV}}{Nf_a}} \cdot \left(\frac{S_i}{0.1 M_{\text{Pl.}}} \right)^{\frac{3}{2}} \cdot \left(\frac{10^{14} \text{ GeV}}{T_{\text{RH}}} \right). \quad (8.235)$$

For our parameter space this constraint is subdominant compared to (8.230) and (8.231).

8.9.4 Thermalized Saxon decays

In section 8.7.2 we showed that a significant part of the parameter space would be excluded by dark radiation constraints if the thermalized Saxon decayed long after their decoupling from the bath. Hence we require that the Saxon are in thermal equilibrium when they become non-relativistic. The mixing with the SM like Higgs allows for the following decay modes to the light SM leptons

$$\Gamma(S \rightarrow \bar{l}l) \simeq \frac{\theta_{SH}^2}{8\pi} \left(\frac{m_l}{v_H} \right)^2 m_S \left(1 - \frac{4m_l^2}{m_S^2} \right)^{\frac{3}{2}} \quad \text{with } l = e, \mu, \quad (8.236)$$

where we neglect the phase space suppression for our first estimate and the corresponding decay temperature reads

$$T_{\text{dec}} = \frac{0.15}{g_*(T_{\text{dec}})^{\frac{1}{4}}} \lambda_{\sigma H} \frac{\sqrt{m_S M_{\text{Pl}}} N f_a m_l}{m_h^2} \quad (8.237)$$

$$\simeq \left(\frac{\theta_{SH}}{10^{-6}} \right) \cdot \left(\frac{10}{g_*(T_{\text{dec}})} \right)^{\frac{1}{4}} \cdot \begin{cases} 0.2 \text{ MeV} \cdot \sqrt{\frac{m_S}{100 \text{ MeV}}}, & m_S < 2m_\mu \simeq 200 \text{ MeV} \\ 97 \text{ MeV} \cdot \sqrt{\frac{m_S}{250 \text{ MeV}}}, & m_S \geq 2m_\mu \simeq 200 \text{ MeV} \end{cases} \quad (8.238)$$

BBN will not be affected if the Saxon decay before the neutrino decoupling at $T = 2 \text{ MeV}$ implying

$$\theta_{SH} > 2 \times 10^{-5} \cdot \sqrt{\frac{100 \text{ MeV}}{m_S}}, \quad m_S < 2m_\mu \simeq 200 \text{ MeV}. \quad (8.239)$$

This limit was depicted in figure 8.7. Additionally the Saxon need to be Boltzmann-suppressed when the SM neutrinos decouple, because else at $T < T_{\text{dec}}$ the Saxon are still kept in equilibrium via decays and inverse decays to electrons and inject entropy into the SM plasma. This process would heat only the SM bath so the already decoupled neutrinos are cooled leading to a reduction in ΔN_{eff} [1074]. Reference [740] obtained that the lower bound $\Delta N_{\text{eff}} < -0.44$ [90] is only compatible with (see also [1075] for a similar analysis involving heavy QCD axions)

$$m_S > 4 \text{ MeV}. \quad (8.240)$$

As it turns out our scenario typically requires Saxon with masses around the GeV-scale (see sections 8.6.4 and 8.6.5), which means that on the one hand decays to mesons are possible and on the other that the Saxon would be Boltzmann-suppressed at BBN. The decay to SM fermions ψ is the dominant mode compared to Diraxion final states as long as

$$\theta_{SH} \frac{m_\psi}{v_H} > \frac{m_S}{2N f_a}. \quad (8.241)$$

From the isocurvature limits (8.191) and (8.192) one can deduce that the right hand side in the above is of $\mathcal{O}(10^{-5} - 10^{-11})$, which is much smaller than the coupling to SM states for GeV-scale Saxon.

8.9.5 Maximum Yield

The thermalization temperature allows us to determine an upper limit on the charge yield [942, 944, 945]

$$Y_\theta < Y_\theta^{\max} \equiv \frac{3}{4} \frac{T_{\text{th}}}{m_S} \quad (8.242)$$

where we used $T_{\text{th}} < T_S$ so that the result only depends on m_S . This relation can be understood as follows: During thermalization the energy density of the oscillations $\rho_S = (1 - \varepsilon)m_S n_S$ is dumped into the bath [939] and only the pure rotation will remain. The entropy density released during thermalization is found from the first law of thermodynamics to be $s_f \sim \rho_S/T_{\text{th}}$ and consequently we obtain for the dimensionless dilution factor

$$\Delta \equiv \frac{s_f a^3(T_f)}{s a^3(T)} \sim (1 - \varepsilon) \frac{m_S}{T_{\text{th}}} Y_\theta \quad (8.243)$$

that leads to $Y_\theta/\Delta \sim T_{\text{th}}/m_S$. The entropy generation is maximal for the case of Saxion domination, for which an equal sign in (8.242) would apply. We express the maximum charge yield in terms of the mixing angle $\theta_{SH} < 3 \times 10^{-3}$ by using (8.229) together with (8.242). On the upper axis of figure 8.6 one can read off the value of Y_θ^{\max} for a given m_S .

8.10 Discussion

Late Saxion thermalization via the Higgs portal requires $S_i \lesssim 0.1 M_{\text{Pl}}$ (see the plot 8.7) and for concreteness we saturate this value. This leads to a high oscillation temperature for the Saxion in (8.62) and (8.68), which is why we typically need reheating temperatures above around 10^{14} GeV, which could be seen as a drawback of our scenario compared to Leptogenesis or Lepto-Axiogenesis [942], that both work for reheating temperatures as low as 10^9 GeV [608]. Thermalization with $S_i = 0.1 M_{\text{Pl}}$ is only viable as long as $\Delta N_{\text{eff.}} > 2.8 \times 10^{-3}$ for Saxions around the GeV-scale. To ensure that the processes encoded in Γ_S never thermalize, we fix f_a/S_i via equations (8.119) (radiation domination) and (8.123) (during reheating), which is equivalent to fixing the amount of ν_R dark radiation produced in (8.173). We find that we typically need $\Gamma_S(S_i)/H(T_{\text{osc}}) < 0.1$ to avoid $\varepsilon > 1$ (see (8.80) and (8.87)), so the upper limit on $\Delta N_{\text{eff.}}$ is never saturated and our cogenesis setup does not lead to observable amounts of dark radiation. For $N = 5$ the bounds from the self-consistency criteria in (8.101) and (8.102) would be the most relaxed, however we find that cogenesis of the baryon asymmetry and dark matter would take place in regions with $m_a = \mathcal{O}(\text{keV})$. While we can generate the correct relic abundance in this regime, dark matter will not be long-lived enough due to its decay to neutrinos (see (8.127) for the lifetime). Hence we fix $N = 6$ for the rest of our analysis, which leads to stable enough Diraxions with $m_a = \mathcal{O}(\text{meV} - \text{eV})$. The downside of this parameter range of N and S_i is that we find ourselves in a region, where the warmness constraint (8.163) on parametric resonance dark matter will always be

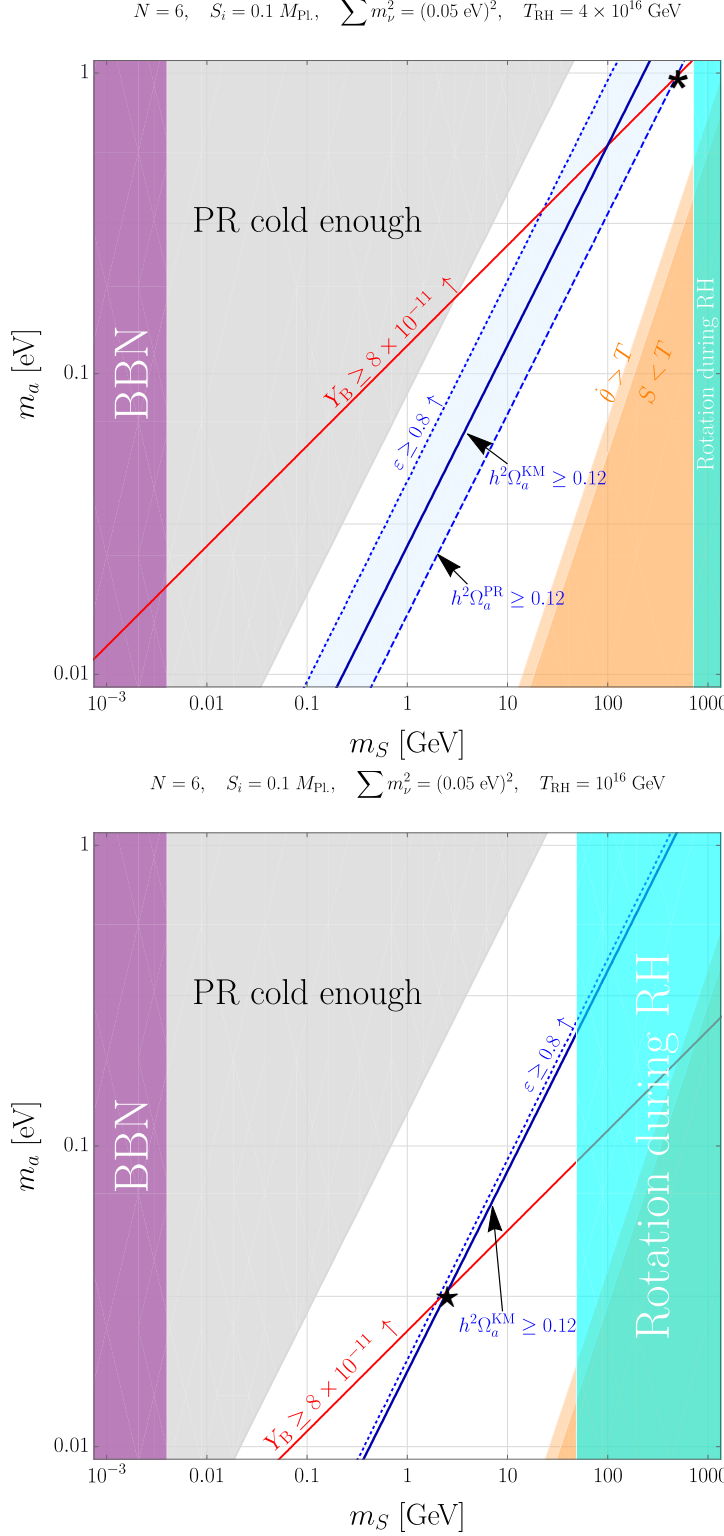


Figure 8.8: In the *upper* plot we fixed $\Delta N_{\text{eff.}} = 1.4 \times 10^{-3}$ and the point marked with a star corresponds to $(m_S, m_a, f_a) = (500 \text{ GeV}, 1 \text{ eV}, 1.1 \times 10^6 \text{ GeV})$. Here the Diraxion has a lifetime of 4×10^4 in units of the age of our universe. In the *lower* plot we fixed $\Delta N_{\text{eff.}} = 5 \times 10^{-3}$ and the point marked with a ~~star~~ corresponds to $(m_S, m_a, f_a) = (1.8 \text{ GeV}, 28 \text{ meV}, 3 \times 10^6 \text{ GeV})$.

$$N = 6, \quad S_i = 0.1 M_{\text{Pl}}, \quad \sum m_\nu^2 = (0.05 \text{ eV})^2, \quad T_{\text{RH}} = 2 \times 10^{15} \text{ GeV}$$

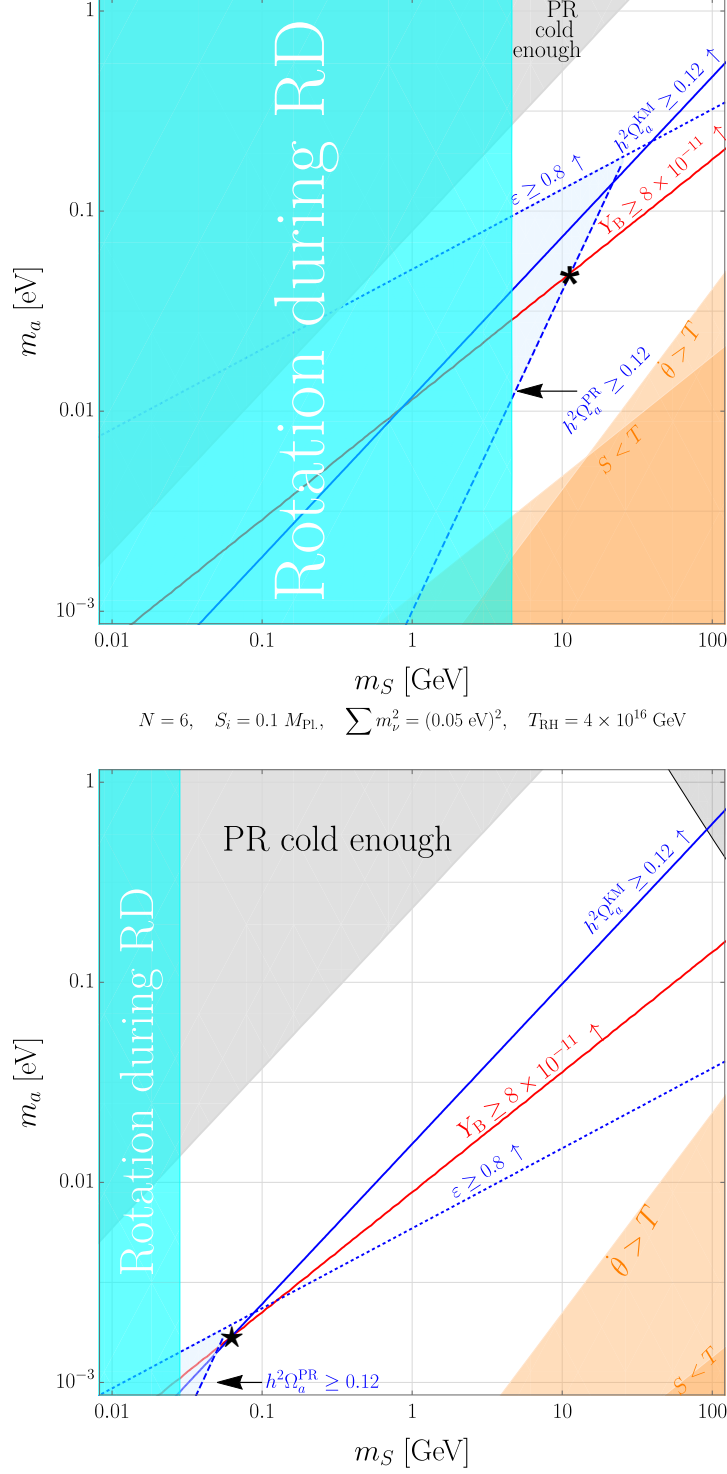


Figure 8.9: In the *upper* plot we fixed $\Delta N_{\text{eff.}} = 4 \times 10^{-3}$ and the point marked with a star corresponds to $(m_S, m_a, f_a) = (11.2 \text{ GeV}, 50 \text{ meV}, 2.2 \times 10^6 \text{ GeV})$ with $\epsilon = 0.1$. In the *lower* plot we fixed $\Delta N_{\text{eff.}} = 0.014$ and the point marked with a star corresponds to $(m_S, m_a, f_a) = (63 \text{ MeV}, 1.5 \text{ meV}, 6 \times 10^7 \text{ GeV})$ with $\epsilon = 0.4$.

violated. Thus we either have to invoke a scenario for early thermalization of the coupled Saxion-Diraxion system as sketched for the Type III Dirac Seesaw in 8.9.2 or tune the eccentricity parameter ε defined in (8.85) close to $\varepsilon \simeq 0.8$ (consult section 8.6.5 for details).

In figures 8.8 and 8.9 we plot the baryon asymmetry as red line and the dark matter relic abundance from kinetic misalignment as a blue line. Both quantities are overproduced above their respective lines. Parametric resonance dark matter is possible in the blue shaded region surrounded by the blue dashed line indicating $\Omega_a^{\text{PR}} h^2 \gtrsim 0.12$ and the dotted line for $\varepsilon = 0.8$. Inbetween these lines dark matter from parametric resonance is overproduced. Our parameter space for oscillations during radiation domination (reheating) can be seen in figure 8.8 (8.9). In the gray shaded area parametric resonance dark matter would be cold enough and in the orange regions we begin to violate the self-consistency criteria $\dot{\theta} < T$ from (8.101) and $S > T$ from (8.102). The purple region is excluded by neutrino cooling from too light Saxions during BBN, see (8.240). In the cyan area of figure 8.8 (8.9) the Saxion oscillation would take place during reheating (radiation domination) as described by equation (8.64). The first panel in 8.8 shows a point $(m_S, m_a, f_a) = (500 \text{ GeV}, 1 \text{ eV}, 1.1 \times 10^6 \text{ GeV})$, which would work with early thermalized parametric resonance. While m_a is of the right order of magnitude to be detected by PTOLEMY [1007, 1008] via decays to neutrinos [1009, 1010] its lifetime of about about 4×10^4 times the age of the universe is far too large, so there would be no appreciable number of produced neutrinos. Note that here we can have $\Delta N_{\text{eff.}} < 2.8 \times 10^{-3}$ because the Saxion mass is around 100 GeV and thus not constrained by B-meson decays. The second panel in the same figure shows a point $(m_S, m_a, f_a) = (1.8 \text{ GeV}, 28 \text{ meV}, 3 \times 10^6 \text{ GeV})$, where cogenesis with kinetic misalignment is possible for $\varepsilon \simeq 0.8$. While this point is allowed by the limits in (8.80) and (8.87), here the S_i -dependent Diraxion mass $m_a(S_i)$ starts to become comparable in magnitude to the initial Saxion mass $m_S S(S_i)$, which might potentially hinder the onset of the coherent rotation.

This conclusion can be somewhat ameliorated for rotations during reheating as depicted in 8.9: Again the upper panel showcases a point $(m_S, m_a, f_a) = (11.2 \text{ GeV}, 50 \text{ meV}, 2.2 \times 10^6 \text{ GeV})$ that would work with early thermalization for parametric resonance dark matter. This panel also demonstrates that kinetic misalignment and parametric resonance scale differently during reheating, which can also be deduced by comparing the second line of (8.145) with the second line of (8.158). One finds that the relic abundance for parametric resonance scales with f_a/S_i and becomes independent of S_i after one uses (8.123). The different scaling allows us to find the point $(m_S, m_a, f_a) = (63 \text{ MeV}, 1.5 \text{ meV}, 6 \times 10^7 \text{ GeV})$ depicted in the lower panel of 8.9, where the lines for the baryon asymmetry and kinetic misalignment meet for $\varepsilon \simeq 0.4$. The required Saxion mass of 63 MeV is however excluded, if thermalization is supposed to occur via the Higgs portal, see figure 8.7.

For our parameter space of interest we find that $f_a \simeq (10^6 - 10^7) \text{ GeV}$, which means that regular misalignment and topological defect decay can at most only contribute a tiny fraction of the DM relic abundance. Inspection of 8.5 reveals that for these values of f_a and kinetic misalignment one expects a completely fragmented Diraxion, so in principle

a lattice study is needed. Consequently the Diraxion will not be a zero mode condensate for either production from parametric resonance or kinetic misalignment. As argued in the beginning of this section, we find $\Delta N_{\text{eff.}} < 0.028$ in the regions, where we can explain both the observed baryon asymmetry and dark matter. A detection of a larger amount of dark radiation by next generation experiments would exclude only the cogenesis scenario. Thus such a detection would imply that this construction can be responsible for *either* Baryogenesis or the origin of dark matter.

8.11 Conclusion

- **The Diraxion originating from the Dirac Seesaw:**

We showed that all three versions of the Dirac Seesaw mechanism automatically provide us with a PNGB that we call the Diraxion, whose cosmological implications have previously not been analyzed. While we assume a global $U(1)_D$ symmetry in order to forbid couplings of ν_R to the SM Higgs, we also require a separate (gauged) $U(1)_{B-L}$ to forbid Majorana masses.

- **Parameter space:**

Our parameter space is spanned by the Diraxion and Saxon masses m_a, m_S together with the initial Saxon field value S_i and the Saxon vev today $N f_a$, where N is the domain wall number. Thermalization fixes $S_i \lesssim 0.1 M_{\text{Pl}}$ and we can eliminate f_a by demanding that the Saxon does not have fast interactions with the bath, which also fixes the amount of right handed neutrino dark radiation. Throughout this work we use $N = 6$ to keep the Diraxion light enough. These inputs allow us to determine the values of m_a, m_S for generating the correct dark matter abundance together with the right baryon asymmetry.

- **Diraxion rotation and Dirac-Leptogenesis:**

The Diraxion is accompanied by a radial mode called the Saxon, whose vev can undergo a large excursion during inflation and which oscillates in the early universe. We discuss three ways of inducing this large vev with a Hubble-dependent mass during inflation being the least excluded (see figure 8.6). If the Diraxion mass comes from a higher dimensional operator, it can convert a part of the Saxon's oscillatory motion into a coherent rotation around the bottom of the scalar potential in the angular direction. This rotation is thermodynamically stable and can act as a background field enabling spontaneous Baryogenesis via Dirac-Leptogenesis from the Dirac Weinberg operator. We find that we need a dimension six operator to do so. If this operator involves additional insertions of the $U(1)_{B-L}$ -breaking scalar, we can also generate the cosmologically required mass scale $m_a = \mathcal{O}(\text{meV} - \text{eV})$ without assuming a small Wilson coefficient.

- **Dark Matter:**

After Saxon thermalization the Diraxion rotation survives and could be responsible for the dark matter relic abundance via the kinetic misalignment mechanism.

Additionally fluctuations of the Diraxion can be produced via parametric resonance from the Saxion oscillation. There is no domain wall problem in this construction, because domain walls can immediately decay to Diraxions either via a string-wall network with a single domain wall or for more domain walls via the well known bias-term from the Diraxion mass. Both contributions are comparable to the relic abundance from standard misalignment, which is negligible for our range of decay constants $f_a \simeq (10^6 - 10^7)$ GeV. Our parameter space with $m_S = \mathcal{O}(100 \text{ MeV} - 100 \text{ GeV})$ suffers from too warm Diraxions from parametric resonance, which is why we either need thermalization from additional degrees of freedom in the bath, present e.g. in the Type III Dirac Seesaw, or a region where $\varepsilon \simeq 0.4$ (0.8) for oscillations during reheating (radiation domination). This implies that the initial Diraxion is comparable in size to the initial Saxion mass, which brings our scenario closer to the mechanisms relying on heavy axion oscillations like e.g. [919, 950].

- **Isocurvature constraints:**

Dark matter and baryon isocurvature constraints enforce a value of m_S that is very small compared to the $U(1)_D$ breaking scale Nf_a . We showed that one-loop corrections do not upset this tuning. This comes with the price that the heavy messenger fields responsible for the Dirac Weinberg operator could be potentially light enough to be present in the plasma, so the description in terms of the Dirac Weinberg operator breaks down. To avoid this we assume an accidental cancellation between the one loop corrections to m_S^2 from the heavy Dirac fermion N for the Type I Seesaw and the heavy doublet η for the Type II Seesaw (see (8.213)). Thus our scenario is a Hybrid-Seesaw [44, 45] and each contribution could be responsible for sourcing one of the two mass splittings observed in neutrino oscillation experiments implying that only one generation of N would be needed. The messenger fields for the two versions of the Type III Dirac Seesaw are usually much lighter than N , η so a separate study is needed to investigate their cosmological evolution and impact on the presented mechanism.

- **Dark Radiation:**

This setup can produce ν_R dark radiation with $2.8 \times 10^{-3} \leq \Delta N_{\text{eff.}} \leq 0.028$, where the lower limit applies for Saxion masses below around 5 GeV due to thermalization via the Higgs portal. While explaining both the baryon asymmetry and dark matter relic abundance involves smaller values of $\Delta N_{\text{eff.}}$, fixing only one observable allows us to generate more dark radiation and to saturate the previous upper limit. Consequently we can use next generation measurements of $\Delta N_{\text{eff.}}$ to test which cosmological history is realized in this framework. Our work predicts dark radiation isocurvature correlated with the dark matter and baryon isocurvature fluctuations, potentially detectable as neutrino isocurvature modes in the CMB.

- **Signatures:**

The Diraxion has no direct coupling to SM fields and its connection to charged fermions or photons arises only at one or two loops respectively. If we only fix the

observed dark matter abundance, we find parameter regions where the Diraxion can decay to neutrinos while being long-lived enough on cosmological time scales, see figure 8.5. In the future this could be detectable [1009, 1010] with cosmic neutrino background searches [1007, 1008]. Our Saxion is typically predicted to heavier than for Lepto-Axiogenesis, which could be used experimentally distinguish these two scenarios. It could be produced by (heavy) meson decays and collider experiments as depicted in figure 8.7.

- **Extensions and Outlook:**

It would be worthwhile to consider **(a)** the case of thermalized, lighter messenger fields for all Dirac Seesaws, **(b)** a supersymmetric set-up to ameliorate the strong isocurvature bounds on the non-supersymmetric quartic potential and **(c)** whether the Saxion could play the role of the inflaton, so Saxion thermalization is automatically obtained from successful reheating. Since each of these aspects constitutes a substantial modification of our analysis, we leave them for future investigation.

9 Conclusion

Let us close by summarizing all the different ideas collected in this manuscript: We first discuss the symmetry structure for the models at hand and then we focus on the predictions for Baryogenesis and the nature of dark matter. The last paragraphs deals with the various observational signatures and predictions for the amount of dark radiation encoded in ΔN_{eff} .

Chapters 3, 4 and 6 involve gauge extensions of the Standard Model either by additional abelian or non-abelian groups. In contrast to that the QCD-axion model in chapter 5 or the Diraxion from the Dirac Seesaws in chapter 8 rely on global symmetries such as Peccei-Quinn symmetry or our $U(1)_D$. Our work on the Type I Seesaw in chapter 7 does not rely on any underlying symmetry structure.

When it comes to the nature and origin of neutrino masses, our models cover a wide range of possibilities: The Type I Seesaw in chapter 7 is literally the textbook example for how to realize parametrically small active neutrino masses from messenger fields in the form of three generations of right chiral neutrinos with large Majorana masses. On the other hand the model for the Hubble tension in chapter 3 does not generate the observed neutrino mass scale and only leads to mixing between the active neutrinos and our additional hidden Dirac neutrino, which is allowed to have a hard tree level mass since it is vector-like under the new gauge symmetry. Chapter 4 demonstrates that it is possible to source both the active neutrino and dark matter masses from one-loop diagrams involving inert scalars and the SM like Higgs together with new vector-like fermions. Here a gauge symmetry is responsible for the prediction that only two of the SM neutrinos are massive and an additional discrete symmetry forbids Majorana masses. In chapter 5 we challenge the conventional notion that neutrino masses arise at dimension five in effective field theory by constructing an explicit realization for the dimension six operator $(\bar{L}\epsilon H^\dagger)(H H^\dagger)\nu_R$, which is the lowest dimensional operator for Dirac neutrino masses involving only the SM like Higgs scalar H . This sequential Seesaw involves the exchange of heavy triplet fermions without hypercharge and heavy doublets with the opposite hypercharge of the SM lepton doublet L . All new fermions are vector-like under the SM but chiral under Peccei-Quinn symmetry, which is why they receive their masses from the scalar singlet spontaneously breaking this global symmetry. One of the attractive features of such a construction is that we can relax the mass scale of the messenger fields down to the 10^8 GeV scale, which helps with keeping the vacuum for the singlet scalar stable. Another pathway to small Dirac neutrino masses is presented in the mirror sector model of chapter 6: Here we copy the SM fermion sector and the neutrinos in L pair up with the mirror neutrinos ν' embedded in the

9 Conclusion

mirror lepton doublet L' . This is facilitated by the inclusion of a bidoublet scalar of mass μ_Φ , that couples to both the lepton doublets as well as to the SM Higgs and its mirror counterpart H' . We find that the tiny neutrino mass scale can arise from demanding that $\mu_\Phi \gg v'$, where $v' = (10^9 - 10^{12})$ GeV is the vev of the neutral component in H' and $\mu_\Phi \gg \kappa$, where κ is the dimensionful coupling of the dimension three operator $H\Phi^\dagger H'$. Here the Diracness of neutrinos follows from the gauge symmetry and choice of particle content. We present an overview over the conventional tree-level mechanisms for Dirac neutrino masses known as the Dirac Seesaws in chapter 8. Here we can explain the smallness of the neutrino mass scale by either integrating out vector-like fermions (Type I Dirac Seesaw), a heavy doublet scalar (Type II Dirac Seesaw) or a triplet scalar together with either vector-like doublet or triplet fermions (Type III Dirac Seesaw). A novel $U(1)_D$ forbids a direct coupling between the right handed neutrinos and H , whereas an additional global or gauged $U(1)_{B-L}$ prevents Majorana mass terms for any kind of fermion.

Generating the baryon asymmetry of our universe via the Leptogenesis mechanism is another focus of this work: We review the basic ingredients for conventional Leptogenesis from a Type I Majorana Seesaw in chapter 7 and then focus on the non-thermal scenario: Here an initially thermal right handed neutrino eventually comes to dominate the energy density of our universe leading to an epoch of early matter domination before decaying far out of equilibrium. A less well known scenario goes by the name of Dirac Leptogenesis and does not rely on microscopic lepton number violation. The S.M.A.S.H.E.D. model in chapter 5 allows for novel effects in this scenario by allowing us to boost the CP-violation produced in the out-of-equilibrium decays by up to six orders of magnitude. Additionally we point out that decaying Dirac fermions feature all the requirements for the “quasi-optimal-efficiency”-scenario previously encountered for triplet scalars in the Majorana Type II Seesaw: The decaying particles are not self-conjugate, meaning that they can develop an asymmetry themselves, and have two decay modes (required by CP violation) with different branching ratios, so that one channel can be protected from washout (which branching ratio is larger does not matter here due to conservation of B-L). The bidoublet in chapter 6 can also have decay modes that fit into the Dirac Leptogenesis scenario, if there are two or more copies of this multiplet present in the spectrum. As a consequence of the low reheating temperature required to avoid large relic abundances of mirror electrons and mirror hadrons, Leptogenesis has to occur during reheating, which is also known as non-thermal Leptogenesis. Additionally we have to invoke a tiny mass splitting between the different bidoublet generations in order to have enough resonant enhancement needed to match the observed baryon to photon ratio. Near the end of chapter 6 we further sketch a non-thermal production mechanism for the baryon asymmetry from the dynamics of the bidoublet condensate. Such dynamics based on the Affleck-Dine mechanism are discussed in far more detail for the Dirac Seesaws of chapter 8. Here the same non-trivial scalar field dynamics can account for both Dirac Leptogenesis as well as dark matter. We call this scenario “Diraxogenesis”.

When it comes to dark matter we have two examples of potentially light (above the keV scale) fermionic dark matter in chapters 4 and 7. QCD axions produced from

misalignment and the decay of the cosmic-string-domain-wall-network are invoked in 5. Diraxiogenesis relies on Diraxions (essentially axion like particles) predominantly produced via kinetic mialignment or parametric resonance. Due to the smallness of the Diraxion-decay constant f_a the conventional misalignment and topological defect decay are only subleading contributions to the relic density.

Before we finish this paragraph we would like to point out the ways to potentially observe our models and how to discriminate them from other proposed SM extensions: The self-interacting neutrino model of chapter 3 involves a Z' with a mass of 25 eV as well as an eV-scale hidden neutrino, which could facilitate the decaying sterile neutrino solution to the long-standing MiniBooNE anomaly. On top of that the scenario provides us with GeV-TeV scale charged and pseudo-scalar Higgs bosons, which could appear at the next generation of colliders. Our radiative dark matter mass model in chapter 4 predicts TeV-scale vector-like leptons that could be accompanied by vector-like quarks. Here no detectable amount of dark radiation is generated, which could provide an indirect way to exclude our setup. S.M.A.S.H.E.D. from chapter 5 enhances the axion to photon coupling by an order of magnitude, which provides a clear experimental target accessible by haloscopes such as ORGAN or MADMAX. When it comes to dark radiation we predict a value of $\Delta N_{\text{eff}} = 0.17$, with contributions of $\Delta N_{\text{eff}} = 0.14$ from three generations of right handed neutrino and $\Delta N_{\text{eff}} = 0.03$ from the QCD axion. The mirror sector model in chapter 6 is hard to test due to the presence of multiple hierarchical energy scales far above the electroweak scale. However the mirror electrons could be as light as 20 TeV, which again could be in the reach of future collider experiments. No appreciable amount of right handed neutrino dark radiation is produced via freeze-in for the the associated cosmology. The purpose of chapter 7 was to demonstrate that gravitational wave astronomy could be a probe of the dynamics of high scale sterile neutrinos in the early universe. We predict that successful Leptogenesis should lead to a damped inflationary gravitational wave spectrum, potentially observable with BBO or U-DECIGO. This of course assumes that a tensor-to-scalar ratio not too far below its current limit of 0.036 will be observed in the cosmic microwave background by searches for primordial B-modes. The same setup can produce observable amounts dark radiation if dark matter is around the GeV scale. Diraxionogenesis predicts right handed neutrino dark radiation of $\Delta N_{\text{eff}} \lesssim 0.028$ and the Diraxion dark matter might be observable by experiments such as PTOLEMY via its decay to neutrinos. As it turns out these signatures only appear if we fix either the baryon asymmetry of the universe or dark matter. To explain both requires too weakly coupled right handed neutrinos and too long lived Diraxions. Isocurvature constraints force the scalar known as the Saxon to be at or below the GeV-scale, so that one could hope to find in heavy meson decays at e.g. LHCb.

We have demonstrated that Dirac neutrinos are a viable alternative to the conventionally invoked Majorana neutrinos. The structures underlying parametrically small neutrino masses allow for a rich phenomenology and novel insights into early universe physics. The hope that underpins these theoretical efforts is that they might provide

9 Conclusion

some clues for previously unexplored experimental signatures and that they could be testable with next generation cosmic microwave background probes. At the very least we hope to have convinced the reader that adding light right handed neutrinos to the Standard Model is not automatically excluded by cosmology.

List of Figures

2.1	Diagrammatic representation of the Type I Seesaw (<i>left</i>) and the Type II Seesaw (<i>right</i>). The Type III Seesaw has the same Feynman diagram as the Type I Seesaw if one replaces the SM gauge singlets $\bar{\nu}$ with hyperchargeless weak triplets T	5
2.2	Plot of the anisotropic temperature power spectrum as function of the multipole moment ℓ , which corresponds to the angular separation taken from [20].	8
2.3	Impact of varying the curvature parameter (a), the dark energy density (b), the baryon energy density (c) and the total matter energy density (d) on the acoustic peaks of the CMB temperature power spectrum taken from reference [63].	9
3.1	Thermally averaged four-neutrino interaction rate relative to the Hubble rate as a function of Temperature for $m_{Z'} = 25$ eV and two different values of the Z' width.	23
3.2	Allowed region (blank) in the $\tan \gamma$ – (μ/v_h) plane. The region is independent of any other free parameters as long as $\lambda_{HS}, \lambda_{34} \ll \mathcal{O}(10^{-2})$ (for definiteness, we have chosen scalar potential parameters as $\lambda_{HS} = 0.001$, $\lambda_3 = 0.002$, $\lambda_4 = 0.003$, $\lambda_\Phi = 0.3$, $\lambda_S = 0.4$, $\lambda_{\Phi S} = 0.5$). The Hubble tension can be resolved in the entire allowed region. We show equilines of the corresponding hidden neutrino mass M for benchmark parameters $\varepsilon_m = 0.05$, $g_X = 2 \times 10^{-3}$, and $y = 6 \times 10^{-5}(6 \times 10^{-3})$. In the orange region $M < m_\nu$ (for $y = 6 \times 10^{-5}$) which is inconsistent with our assumptions. . .	30
4.1	Feynman diagrams in the gauge basis responsible for the creation of the neutrino and dark matter (χ) Dirac masses at the one loop level.	38
4.2	Leading order diagrams for the decay $h \rightarrow \bar{\chi}_L \chi_R$ in the mass basis. See the main text for more details.	47
4.3	DM abundance as a function of temperature for fixed m_{DM} , $v_{\text{B-L}}$ and two different T_{RH}	57
4.4	DM abundance as a function of temperature for fixed T_{RH} and two different combinations of m_{DM} , $v_{\text{B-L}}$	57
4.5	ΔN_{eff} as a function of temperature for fixed $v_{\text{B-L}}$ and two different T_{RH} . .	63
4.6	ΔN_{eff} as a function of temperature for fixed T_{RH} and two different $v_{\text{B-L}}$. .	63

List of Figures

4.7	We depict the allowed combinations of the reheating temperature T_{RH} and the scale of B-L breaking $v_{\text{B-L}}$. The blue shaded area indicates where DM would overclose the universe and the blue contours reproduce the observed DM relic density for $m_{\text{DM}} \in [4, 16, 100, 10^3] \text{ keV}$. Furthermore we show the contours for generating ΔN_{eff} within the Planck bound [20], the estimated sensitivities of the South Pole Telescope [330], the Simons observatory [331] and for the CMB stage 4 experiment [332–334] as well as PICO [335]. The grey area is excluded because the interaction producing DM would equilibrate see (4.82) and searches from LEP exclude $v_{\text{B-L}} < 6.9 \text{ TeV}$ [272].	65
5.1	Diagrammatic representation of the dimension 6 operator giving rise to Dirac masses for the active neutrinos.	82
5.2	Two Loop RGE evolution of the SM gauge couplings as a function of the renormalization scale for the inclusion of a hypercharge zero $\text{SU}(2)_L$ triplet with $M_T = 10^8 \text{ GeV}$ (<i>top</i>) and a hypercharge 1/2 $\text{SU}(2)_L$ doublet fermion with a mass of $M_D = 3 \times 10^7 \text{ GeV}$ (<i>bottom</i>).	87
5.3	Depicted are the “S.M.A.S.H.E.D.” band in orange and the QCD-axion band for the KSVZ and DFSZ models in yellow as well as a collection of cosmological, astrophysical and laboratory constraints. The white space is allowed and in the gray area the active neutrino masses would be too small. The black arrow to the right indicates that the lower allowed limit on m_a increases for larger values of m_ν . The corresponding references can be found in section 5.4.5.	88
5.4	Depicted are the “S.M.A.S.H.E.D.” band in orange and the QCD-axion band for the KSVZ and DFSZ models in yellow as well as cosmological, astrophysical and laboratory constraints together with projected sensitivities. The black arrow to the right indicates that the lower allowed limit on m_a increases for larger values of m_ν . The corresponding references can be found in section 5.4.5.	89
5.5	Schematic representation of our Dirac-Leptogenesis scenario.	97
5.6	Feynman diagrams in the chiral basis for the CP violating decay of the lightest triplet fermion into SM leptons $L^{(i)}$. Internal lines intersecting the red dashed line are required to go on shell.	99
5.7	Feynman diagrams in the chiral basis for the CP violating decay of the lightest triplet fermion into the lightest exotic lepton $D^{(1)}$. Internal lines intersecting the red dashed line are required to go on shell.	99
5.8	Diagrammatic representation of the relevant washout processes $DH \leftrightarrow LH$ involving leptons L and exotic leptons D . The diagrams for $L\bar{D} \leftrightarrow H\bar{H}$ are obtained via crossing symmetry.	108
5.9	Rate densities (<i>top</i>) for $K = 0.01$, $B_L = B_D = 1/2$, ($Y_{LT} = Y_{TD} = 9.1 \times 10^{-6}$), $\varepsilon_L = 6.5 \times 10^{-4}$ and leptonic yields (<i>bottom</i>).	117
5.10	Rate densities (<i>top</i>) for $K = 100$, $B_L = B_D = 1/2$, ($Y_{LT} = Y_{TD} = 9.1 \times 10^{-4}$), $\varepsilon_L = 2.7 \times 10^{-5}$ and leptonic yields (<i>bottom</i>).	119

5.11 Rate densities (<i>left</i>) for $K = 10^5$, $B_L = B_D = 1/2$ ($Y_{LT} = Y_{TD} = 2.9 \times 10^{-2}$), $\varepsilon_L = 3 \times 10^{-3}$ and leptonic yields (<i>right</i>).	120
5.12 Rate densities (<i>left</i>) for $K = 10^5$, $B_L = 0.999$, $B_D = 10^{-3}$ ($Y_{LT} = 4.1 \times 10^{-2}$, $Y_{TD} = 1.2 \times 10^{-3}$), $\varepsilon_L = 1.7 \times 10^{-3} \sqrt{4B_L B_D (1 - \delta^2)} = 4.7 \times 10^{-5}$ and the leptonic yields (<i>right</i>).	120
5.13 Rate densities (<i>left</i>) for $K = 10^5$, $B_L = 10^{-5}$, $B_D = 0.99999$ ($Y_{LT} = 1.3 \times 10^{-4}$, $Y_{TD} = 4.1 \times 10^{-2}$), $\varepsilon_L = 9 \times 10^{-5} \sqrt{4B_L B_D (1 - \delta^2)} = 2.2 \times 10^{-7}$ and the leptonic yields (<i>right</i>).	120
6.1 Diagrammatic representation of the Type II Dirac Seesaw mechanism. ν (ν') is embedded in the doublet l (l'). The mirror neutrino ν' plays the role of the right-chiral neutrino and the heavy scalar Φ is integrated out.	129
6.2 Plot of the contributions to the scalar potential without a bidoublet (<i>top</i>) and with a bidoublet (<i>bottom</i>). For the sake of visibility and illustration we chose $v_H = 10^{10}$ GeV, $v_\Phi = 1$ GeV, $c_1 = -10^{-2}$ and $\kappa = -6 \times 10^{15}$ GeV, which do not correspond to phenomenologically viable parameters. On the left hand side we fixed $\lambda'/c_1 = 0.66$ and we varied this combination of parameters on the right hand side. Note that we scaled the vertical axis differently in both plots. Realistic parameters would lead to minima at $ \phi \simeq 10^{-7} - 10^{-10}$ and in practise the phenomenologically required small value of $ \kappa $, e.g. $ \kappa < 10$ GeV from (6.85) in the main text, only has a negligible impact on the value of ϕ	136
6.3 Two- (<i>left</i>) and three-loop (<i>right</i>) Feynman diagrams leading to phases in the quark mass matrices contributing to $\bar{\theta} = \theta_{\text{chir}}$ in this model. h' , Z' , h_Φ and φ_1^\pm only couple to the SM quarks via suppressed mixing. For the three-loop diagrams we did not indicate the internal chirality structure and the labels of the internal quark fields, because for h , h_Φ there is a mass insertion $\propto \langle H \rangle$ after the first vertex and in the Z' case there is the same kind of insertion before the sixth vertex.	144
6.4 One-loop Feynman diagrams contributing to the magnetic moments of the muon (<i>left</i>) and neutrinos (<i>right</i>). The photon line in the second diagram can be attached to the electrically charged mirror lepton inside the loop as well. For this diagram the mass insertion can also appear on the incoming line, so that we get a second set of diagrams with l, φ_2^\mp running in the loop.	146

7.1	Parameter space for the dark matter mass m_ψ versus the branching ratio BR_ψ of the RHN decay to dark matter. Contours with (straight, dashed, dotted) lines correspond to $\tilde{m}_1 = (10^{-7}, 10^{-10}, 10^{-15})$ eV. The purple contours reproduce the observed dark matter relic abundance and above the contour the abundance would be too large (for fixed \tilde{m}_1). The gray regions are excluded because of unsuccessful structure formation (Lyman- α) and dark matter not being gravitationally bound (Tremaine-Gunn). On the red contours for the DM lifetime from $\psi \rightarrow \nu_L \sigma$ is equal to the observational limit and in the colored region above (for fixed \tilde{m}_1) the lifetime would be too small. This excludes the lines with $\tilde{m}_1 = (10^{-7}, 10^{-10})$ eV, meaning that here only $\tilde{m}_1 = 10^{-15}$ eV is viable for DM. Note that lifetime bound disappears for $m_\psi < m_\sigma$, in which case the entire purple region is allowed. The area in light orange is excluded by our assumption $\text{BR}_\psi \ll \text{BR}_L \simeq 1$ and the orange region would be excluded, if the real scalar also produced in the RHN decay was stable and light enough to be dark radiation (see the discussion below (7.53))	170
7.2	Example GW spectra for $T_{\text{RH}} = 10^8$ GeV, $M_1 = 10^4$ GeV and $n_T = 0$ (<i>top</i>) as well as $n_T = 0.5$ (<i>bottom</i>). Here we varied $\tilde{m}_1 = (10^{-10}, 10^{-12}, 10^{-14})$ eV and “no IMD” refers to the scenario without RHN domination.	177
7.3	Example spectra for $T_{\text{RH}} = 10^{12}$ GeV, $\tilde{m}_1 = 10^{-12}$ eV and $n_T = 0$ (<i>top</i>) as well as $n_T = 0.5$ (<i>bottom</i>). Here we varied $M_1 = (10^6, 10^9, 10^{12})$ GeV and “no IMD” refers to the scenario without RHN domination.	178
7.4	We fix M_1 as a function of $\tilde{m}_1 = (10^{-10}, 10^{-12}, 10^{-14})$ eV for successful Leptogenesis and set $T_{\text{RH}} = 10^{13}$ GeV, $n_T = 0$. Furthermore we show which value of $m_\psi \text{BR}_\psi$ would be required for a given \tilde{m}_1 to generate the observed dark matter relic abundance.	180
7.5	We fix M_1 as a function of $\tilde{m}_1 = (10^{-10}, 10^{-12}, 10^{-14})$ eV for successful Leptogenesis and set $T_{\text{RH}} = 10^{13}$ GeV, $n_T = 0.5$. Furthermore we show which value of $m_\psi \text{BR}_\psi$ would be required for a given \tilde{m}_1 to generate the observed dark matter relic abundance.	181
7.6	We fix $M_1 = 10^7$ GeV, $\tilde{m}_1 = 10^{-17}$ eV, $T_{\text{RH}} = 5 \times 10^{12}$ GeV and $n_T = 0.85$ to fit the NANOGRAV anomaly [892]. Furthermore we show the value of $m_\psi \text{BR}_\psi = 12$ MeV required for the given \tilde{m}_1 to generate the observed dark matter relic abundance.	182
7.7	Parameter space in the M_1 versus \tilde{m}_1 plane with contours for $\text{SNR} = 10$ (<i>top</i>) and SNR as a function of M_1 , where \tilde{m}_1 was fixed for Leptogenesis via (7.34) (<i>bottom</i>). In both plots we fixed $T_{\text{RH}} = 10^{16}$ GeV, $n_T = 0$. See the main text for details on the constraints. The SNR is larger than 10 in the colored regions. Note that the colored lines from the experiments do no correspond to constraints, but to projections of future sensitivities. . .	184

7.8	Parameter space in the M_1 versus \tilde{m}_1 plane with contours for $\text{SNR} = 10$ for $n_T = 0.1$ (<i>left</i>) and $n_T = 0.2$ (<i>right</i>). In both plots we fixed $T_{\text{RH}} = 10^{16}$ GeV. See the main text for details on the constraints. The SNR is larger than 10 in the colored regions. Note that the colored lines from the experiments do no correspond to constraints, but to projections of future sensitivities.	185
7.9	Parameter space in the M_1 versus \tilde{m}_1 plane with contours for $\text{SNR} = 10$ for $n_T = 0.3$ (<i>left</i>) and $n_T = 0.5$ (<i>right</i>). In both plots we fixed $T_{\text{RH}} = 10^{16}$ GeV. See the main text for details on the constraints. The SNR is larger than 10 in the colored regions. Note that the colored lines from the experiments do no correspond to constraints, but to projections of future sensitivities.	185
7.10	SNR as a function of M_1 , where \tilde{m}_1 was fixed for Leptogenesis via (7.34) with $n_T = 0.1$ (<i>left</i>) and $n_T = 0.5$ (<i>right</i>). In both plots we fixed $T_{\text{RH}} = 10^{16}$ GeV	186
8.1	Diagrammatic representation of the dimension 5 operators for the Type I Dirac Seesaw (<i>left</i>) and Type II Dirac Seesaw (<i>right</i>) giving rise to Dirac masses for the active neutrinos. For the Type II case one could also consider an additional insertion of σ not depicted here.	194
8.2	Diagrammatic representation of the dimension 5 operators for the Type III-a Dirac Seesaw (<i>left</i>) involving new triplet fermions and Type III-b Dirac Seesaw (<i>right</i>) involving new doublet fermions, both giving rise to Dirac masses for the active neutrinos.	196
8.3	One loop diagrams for the coupling of the Diraxion to SM fermions involving two insertions of the Dirac Weinberg operator. The first diagram generates a coupling to the lepton doublet only, whereas the second one involves all fermions $f = L, e_R, Q, u_R, d_R$	203
8.4	Schematic representation of the reaction chain for generating a chemical potential in baryons. The arrows labelled “SM” indicate the network of equilibrated Standard Model Yukawa and gauge interactions. The red arrow labelled “sph.” stands for the B+L violating electroweak sphaleron process. Time progresses from left to right.	215
8.5	Allowed parameter space for Diraxion dark matter, that is stable enough on cosmological time scales.	221
8.6	Saxion parameter space for the isocurvature and dark radiation constraints.	230
8.7	Parameter space for successful thermalization compared to current experimental and astrophysical limits on the production of scalars. The line labelled $T_{\text{th.}} \geq T_M$ would be in the excluded region for $S_i > 0.1 M_{\text{Pl}}$. If we decrease ΔN_{eff} , the red dotted lines move upwards. The dotted line for the Kaon branching ratio was obtained from [1061] and the LHCb constraint continues (with small interruptions) until below 5 GeV. Equation (8.239) leads to the purple BBN bound from light Saxion decays to electrons below the muon threshold.	242
		261

List of Figures

8.8 In the *upper* plot we fixed $\Delta N_{\text{eff.}} = 1.4 \times 10^{-3}$ and the point marked with a star corresponds to $(m_S, m_a, f_a) = (500 \text{ GeV}, 1 \text{ eV}, 1.1 \times 10^6 \text{ GeV})$. Here the Diraxion has a lifetime of 4×10^4 in units of the age of our universe. In the *lower* plot we fixed $\Delta N_{\text{eff.}} = 5 \times 10^{-3}$ and the point marked with a star corresponds to $(m_S, m_a, f_a) = (1.8 \text{ GeV}, 28 \text{ meV}, 3 \times 10^6 \text{ GeV})$ 247

8.9 In the *upper* plot we fixed $\Delta N_{\text{eff.}} = 4 \times 10^{-3}$ and the point marked with a star corresponds to $(m_S, m_a, f_a) = (11.2 \text{ GeV}, 50 \text{ meV}, 2.2 \times 10^6 \text{ GeV})$ with $\varepsilon = 0.1$. In the *lower* plot we fixed $\Delta N_{\text{eff.}} = 0.014$ and the point marked with a star corresponds to $(m_S, m_a, f_a) = (63 \text{ MeV}, 1.5 \text{ meV}, 6 \times 10^7 \text{ GeV})$ with $\varepsilon = 0.4$ 248

List of Tables

3.1	New fields and their charges under Lorentz, SM gauge, new $U(1)_X$ gauge symmetry as well as under global Lepton number (S=Scalar, RH=right-handed Weyl fermion, V=vector).	24
4.1	Charges and representations for all particles participating in the neutrino or dark matter mass generation. The integers n in the fifth column are an abbreviation for ω^n , where $\omega = e^{\frac{2i\pi}{5}}$	39
5.1	Charges and Representations under the SM gauge group and $U(1)_{PQ}$. . .	79
6.1	Charges and representations for the SM and mirror sector fields as well as the bidoublet Φ . All spinors are left-chiral and we use the notation of [22]. We use $\omega \equiv e^{\frac{2\pi i}{3}}$	131
8.1	Charges and Representations under the SM gauge group and $U(1)_D$. . .	192

Bibliography

- [1] M. Mukerjee, *Profile: Yoichiro Nambu in 1995*, *Scientific American* (1995) .
- [2] L. Wolfenstein, *Neutrino Oscillations in Matter*, *Phys. Rev. D* **17** (1978) 2369.
- [3] S.P. Mikheev and A.Y. Smirnov, *Resonant amplification of neutrino oscillations in matter and solar neutrino spectroscopy*, *Nuovo Cim. C* **9** (1986) 17.
- [4] I. Esteban, M.C. Gonzalez-Garcia, M. Maltoni, T. Schwetz and A. Zhou, *The fate of hints: updated global analysis of three-flavor neutrino oscillations*, *JHEP* **09** (2020) 178 [2007.14792].
- [5] SUPER-KAMIOKANDE collaboration, *Solar neutrino measurements in super-Kamiokande-I*, *Phys. Rev. D* **73** (2006) 112001 [hep-ex/0508053].
- [6] SUPER-KAMIOKANDE collaboration, *Evidence for an oscillatory signature in atmospheric neutrino oscillation*, *Phys. Rev. Lett.* **93** (2004) 101801 [hep-ex/0404034].
- [7] KamLAND collaboration, *First results from KamLAND: Evidence for reactor anti-neutrino disappearance*, *Phys. Rev. Lett.* **90** (2003) 021802 [hep-ex/0212021].
- [8] DAYA BAY collaboration, *Observation of electron-antineutrino disappearance at Daya Bay*, *Phys. Rev. Lett.* **108** (2012) 171803 [1203.1669].
- [9] RENO collaboration, *Observation of Reactor Electron Antineutrino Disappearance in the RENO Experiment*, *Phys. Rev. Lett.* **108** (2012) 191802 [1204.0626].
- [10] DOUBLE CHOOZ collaboration, *Indication of Reactor $\bar{\nu}_e$ Disappearance in the Double Chooz Experiment*, *Phys. Rev. Lett.* **108** (2012) 131801 [1112.6353].
- [11] P. Harrison, D. Perkins and W. Scott, *Tri-bimaximal mixing and the neutrino oscillation data*, *Phys. Lett.* **B530** (2002) 167 [hep-ph/0202074].
- [12] T2K collaboration, *Indication of Electron Neutrino Appearance from an Accelerator-produced Off-axis Muon Neutrino Beam*, *Phys. Rev. Lett.* **107** (2011) 041801 [1106.2822].
- [13] MINOS collaboration, *Improved search for muon-neutrino to electron-neutrino oscillations in MINOS*, *Phys. Rev. Lett.* **107** (2011) 181802 [1108.0015].

Bibliography

- [14] NOvA collaboration, *First Measurement of Neutrino Oscillation Parameters using Neutrinos and Antineutrinos by NOvA*, *Phys. Rev. Lett.* **123** (2019) 151803 [1906.04907].
- [15] Z. Maki, M. Nakagawa and S. Sakata, *Remarks on the unified model of elementary particles*, in *11th International Conference on High-energy Physics*, pp. 663–666, 1962.
- [16] B. Pontecorvo, *Neutrino Experiments and the Problem of Conservation of Leptonic Charge*, *Zh. Eksp. Teor. Fiz.* **53** (1967) 1717.
- [17] U. Rahaman and S.K. Raut, *On the tension between the latest NOvA and T2K data*, *Eur. Phys. J. C* **82** (2022) 910 [2112.13186].
- [18] KATRIN collaboration, *Direct neutrino-mass measurement with sub-electronvolt sensitivity*, *Nature Phys.* **18** (2022) 160 [2105.08533].
- [19] J. Schechter and J.W.F. Valle, *Neutrinoless Double beta Decay in $SU(2) \times U(1)$ Theories*, *Phys. Rev. D* **25** (1982) 2951.
- [20] PLANCK collaboration, *Planck 2018 results. VI. Cosmological parameters*, *Astron. Astrophys.* **641** (2020) A6 [1807.06209].
- [21] S. Roy Choudhury and S. Hannestad, *Updated results on neutrino mass and mass hierarchy from cosmology with Planck 2018 likelihoods*, *JCAP* **07** (2020) 037 [1907.12598].
- [22] H.K. Dreiner, H.E. Haber and S.P. Martin, *Two-component spinor techniques and Feynman rules for quantum field theory and supersymmetry*, *Phys. Rept.* **494** (2010) 1 [0812.1594].
- [23] S. Weinberg, *Baryon- and lepton-nonconserving processes*, *Phys. Rev. Lett.* **43** (1979) 1566.
- [24] H. Fritzsch and P. Minkowski, *Unified interactions of leptons and hadrons*, *Ann. Phys.* **93** (1975) 193.
- [25] H. Georgi and S.L. Glashow, *Unity of All Elementary Particle Forces*, *Phys. Rev. Lett.* **32** (1974) 438.
- [26] T. Yanagida, *Horizontal gauge symmetry and masses of neutrinos*, *Conf. Proc. C* **7902131** (1979) 95.
- [27] T. Yanagida, *Horizontal Symmetry and Masses of Neutrinos*, *Progress of Theoretical Physics* **64** (1980) 1103 [<https://academic.oup.com/ptp/article-pdf/64/3/1103/5394376/64-3-1103.pdf>].
- [28] P. Minkowski, $\mu \rightarrow e\gamma$ at a Rate of One Out of 10^9 Muon Decays?, *Phys. Lett. B* **67** (1977) 421.

- [29] M. Gell-Mann, P. Ramond and R. Slansky, *Complex Spinors and Unified Theories*, *Conf. Proc. C* **790927** (1979) 315 [[1306.4669](#)].
- [30] R.N. Mohapatra and G. Senjanović, *Neutrino mass and spontaneous parity nonconservation*, *Phys. Rev. Lett.* **44** (1980) 912.
- [31] E. Ma, *Pathways to naturally small neutrino masses*, *Phys. Rev. Lett.* **81** (1998) 1171 [[hep-ph/9805219](#)].
- [32] G. Lazarides, Q. Shafi and C. Wetterich, *Proton Lifetime and Fermion Masses in an $SO(10)$ Model*, *Nucl. Phys. B* **181** (1981) 287.
- [33] J. Schechter and J.W.F. Valle, *Neutrino Masses in $SU(2) \times U(1)$ Theories*, *Phys. Rev. D* **22** (1980) 2227.
- [34] R.N. Mohapatra and G. Senjanovic, *Neutrino Masses and Mixings in Gauge Models with Spontaneous Parity Violation*, *Phys. Rev. D* **23** (1981) 165.
- [35] T.P. Cheng and L.-F. Li, *Neutrino masses, mixings, and oscillations in $su(2) \times u(1)$ models of electroweak interactions*, *Phys. Rev. D* **22** (1980) 2860.
- [36] C. Wetterich, *Neutrino Masses and the Scale of B-L Violation*, *Nucl. Phys. B* **187** (1981) 343.
- [37] R. Foot, H. Lew, X.G. He and G.C. Joshi, *Seesaw Neutrino Masses Induced by a Triplet of Leptons*, *Z. Phys. C* **44** (1989) 441.
- [38] R.N. Mohapatra, *Mechanism for Understanding Small Neutrino Mass in Superstring Theories*, *Phys. Rev. Lett.* **56** (1986) 561.
- [39] R. Mohapatra and J. Valle, *Neutrino Mass and Baryon Number Nonconservation in Superstring Models*, *Phys. Rev. D* **34** (1986) 1642.
- [40] M. Malinsky, J.C. Romao and J.W.F. Valle, *Novel supersymmetric $SO(10)$ seesaw mechanism*, *Phys. Rev. Lett.* **95** (2005) 161801 [[hep-ph/0506296](#)].
- [41] P.-H. Gu, H.-J. He, U. Sarkar and X.-m. Zhang, *Double Type-II Seesaw, Baryon Asymmetry and Dark Matter for Cosmic e^\pm Excesses*, *Phys. Rev. D* **80** (2009) 053004 [[0906.0442](#)].
- [42] P.-H. Gu, *Double type II seesaw mechanism accompanied by Dirac fermionic dark matter*, *Phys. Rev. D* **101** (2020) 015006 [[1907.10019](#)].
- [43] I. Picek and B. Radovcic, *Novel TeV-scale seesaw mechanism with Dirac mediators*, *Phys. Lett. B* **687** (2010) 338 [[0911.1374](#)].
- [44] C. Wetterich, *Natural maximal muon-neutrino - tau-neutrino mixing*, *Phys. Lett. B* **451** (1999) 397 [[hep-ph/9812426](#)].

Bibliography

- [45] S.-L. Chen, M. Frigerio and E. Ma, *Hybrid seesaw neutrino masses with $A(4)$ family symmetry*, *Nucl. Phys. B* **724** (2005) 423 [[hep-ph/0504181](#)].
- [46] K.S. Babu and R.N. Mohapatra, *A Solution to the Strong CP Problem Without an Axion*, *Phys. Rev. D* **41** (1990) 1286.
- [47] Y. Cai, J. Herrero-García, M.A. Schmidt, A. Vicente and R.R. Volkas, *From the trees to the forest: a review of radiative neutrino mass models*, *Front. in Phys.* **5** (2017) 63 [[1706.08524](#)].
- [48] M. Roncadelli and D. Wyler, *Naturally Light Dirac Neutrinos in Gauge Theories*, *Phys. Lett. B* **133** (1983) 325.
- [49] E. Ma, *Naturally small seesaw neutrino mass with no new physics beyond the TeV scale*, *Phys. Rev. Lett.* **86** (2001) 2502 [[hep-ph/0011121](#)].
- [50] C. Bonilla and J.W.F. Valle, *Naturally light neutrinos in Dirac model*, *Phys. Lett. B* **762** (2016) 162 [[1605.08362](#)].
- [51] C. Bonilla, J.M. Lamprea, E. Peinado and J.W.F. Valle, *Flavour-symmetric type-II Dirac neutrino seesaw mechanism*, *Phys. Lett. B* **779** (2018) 257 [[1710.06498](#)].
- [52] O. Popov and R. Srivastava, *The Triplet Dirac Seesaw in the View of the Recent CDF-II W Mass Anomaly*, [2204.08568](#).
- [53] D. Borah, S. Mahapatra, D. Nanda and N. Sahu, *Type II Dirac seesaw with observable ΔN_{eff} in the light of W-mass anomaly*, *Phys. Lett. B* **833** (2022) 137297 [[2204.08266](#)].
- [54] P.-H. Gu and U. Sarkar, *Radiative Neutrino Mass, Dark Matter and Leptogenesis*, *Phys. Rev. D* **77** (2008) 105031 [[0712.2933](#)].
- [55] Y. Farzan and E. Ma, *Dirac neutrino mass generation from dark matter*, *Phys. Rev. D* **86** (2012) 033007 [[1204.4890](#)].
- [56] N. Arkani-Hamed and Y. Grossman, *Light active and sterile neutrinos from compositeness*, *Phys. Lett. B* **459** (1999) 179 [[hep-ph/9806223](#)].
- [57] N. Arkani-Hamed, S. Dimopoulos, G.R. Dvali and J. March-Russell, *Neutrino masses from large extra dimensions*, *Phys. Rev. D* **65** (2001) 024032 [[hep-ph/9811448](#)].
- [58] T. Gherghetta, *Dirac neutrino masses with Planck scale lepton number violation*, *Phys. Rev. Lett.* **92** (2004) 161601 [[hep-ph/0312392](#)].
- [59] P.J. Fox, A.E. Nelson and N. Weiner, *Dirac gaugino masses and supersoft supersymmetry breaking*, *JHEP* **08** (2002) 035 [[hep-ph/0206096](#)].

- [60] V.A. Rubakov and D.S. Gorbunov, *Introduction to the Theory of the Early Universe: Hot big bang theory*, World Scientific, Singapore (2017), 10.1142/10447.
- [61] D.S. Gorbunov and V.A. Rubakov, *Introduction to the theory of the early universe: Cosmological perturbations and inflationary theory*, World Scientific (2011), 10.1142/7873.
- [62] E.W. Kolb and M.S. Turner, *The Early Universe*, vol. 69, Westview Press (1990), 10.1201/9780429492860.
- [63] W. Hu and S. Dodelson, *Cosmic Microwave Background Anisotropies*, *Ann. Rev. Astron. Astrophys.* **40** (2002) 171 [[astro-ph/0110414](#)].
- [64] D.J. Fixsen, *The Temperature of the Cosmic Microwave Background*, *apj* **707** (2009) 916 [[0911.1955](#)].
- [65] COBE collaboration, *Structure in the COBE differential microwave radiometer first year maps*, *Astrophys. J. Lett.* **396** (1992) L1.
- [66] WMAP collaboration, *First year Wilkinson Microwave Anisotropy Probe (WMAP) observations: Determination of cosmological parameters*, *Astrophys. J. Suppl.* **148** (2003) 175 [[astro-ph/0302209](#)].
- [67] N.Y. Gnedin and O.Y. Gnedin, *Cosmological neutrino background revisited*, *Astrophys. J.* **509** (1998) 11 [[astro-ph/9712199](#)].
- [68] G. Mangano, G. Miele, S. Pastor, T. Pinto, O. Pisanti and P.D. Serpico, *Relic neutrino decoupling including flavor oscillations*, *Nucl. Phys. B* **729** (2005) 221 [[hep-ph/0506164](#)].
- [69] P.F. de Salas and S. Pastor, *Relic neutrino decoupling with flavour oscillations revisited*, *JCAP* **07** (2016) 051 [[1606.06986](#)].
- [70] J. Froustey, C. Pitrou and M.C. Volpe, *Neutrino decoupling including flavour oscillations and primordial nucleosynthesis*, *JCAP* **12** (2020) 015 [[2008.01074](#)].
- [71] K. Akita and M. Yamaguchi, *A precision calculation of relic neutrino decoupling*, *JCAP* **08** (2020) 012 [[2005.07047](#)].
- [72] J.J. Bennett, G. Buldgen, P.F. De Salas, M. Drewes, S. Gariazzo, S. Pastor et al., *Towards a precision calculation of N_{eff} in the Standard Model II: Neutrino decoupling in the presence of flavour oscillations and finite-temperature QED*, *JCAP* **04** (2021) 073 [[2012.02726](#)].
- [73] M. Cielo, M. Escudero, G. Mangano and O. Pisanti, *N_{eff} in the Standard Model at NLO is 3.043*, [2306.05460](#).
- [74] X. Luo, W. Rodejohann and X.-J. Xu, *Dirac neutrinos and N_{eff} . Part II. The freeze-in case*, *JCAP* **03** (2021) 082 [[2011.13059](#)].

Bibliography

- [75] C.D. Kreisch, F.-Y. Cyr-Racine and O. Doré, *The Neutrino Puzzle: Anomalies, Interactions, and Cosmological Tensions*, 1902.00534.
- [76] E. Aver, K.A. Olive and E.D. Skillman, *The effects of $He\,I\,\lambda 10830$ on helium abundance determinations*, *JCAP* **07** (2015) 011 [1503.08146].
- [77] PLANCK collaboration, *Planck 2018 results. X. Constraints on inflation*, *Astron. Astrophys.* **641** (2020) A10 [1807.06211].
- [78] K. Harigaya, A. Kamada, M. Kawasaki, K. Mukaida and M. Yamada, *Affleck-Dine Baryogenesis and Dark Matter Production after High-scale Inflation*, *Phys. Rev. D* **90** (2014) 043510 [1404.3138].
- [79] A.G. Riess, S. Casertano, W. Yuan, J.B. Bowers, L. Macri, J.C. Zinn et al., *Cosmic Distances Calibrated to 1% Precision with Gaia EDR3 Parallaxes and Hubble Space Telescope Photometry of 75 Milky Way Cepheids Confirm Tension with Λ CDM*, *Astrophys. J. Lett.* **908** (2021) L6 [2012.08534].
- [80] N. Schöneberg, G. Franco Abellán, A. Pérez Sánchez, S.J. Witte, V. Poulin and J. Lesgourges, *The H_0 Olympics: A fair ranking of proposed models*, *Phys. Rept.* **984** (2022) 1 [2107.10291].
- [81] F. Zwicky, *Die Rotverschiebung von extragalaktischen Nebeln*, *Helv. Phys. Acta* **6** (1933) 110.
- [82] L.J. Hall, K. Jedamzik, J. March-Russell and S.M. West, *Freeze-In Production of FIMP Dark Matter*, *JHEP* **03** (2010) 080 [0911.1120].
- [83] J. Preskill, M.B. Wise and F. Wilczek, *Cosmology of the invisible axion*, *Physics Letters B* **120** (1983) 127.
- [84] L. Abbott and P. Sikivie, *A cosmological bound on the invisible axion*, *Physics Letters B* **120** (1983) 133.
- [85] M. Dine and W. Fischler, *The not-so-harmless axion*, *Physics Letters B* **120** (1983) 137.
- [86] L. Hui, J.P. Ostriker, S. Tremaine and E. Witten, *On the hypothesis that cosmological dark matter is composed of ultra-light bosons*, 1610.08297.
- [87] S. Tremaine and J.E. Gunn, *Dynamical Role of Light Neutral Leptons in Cosmology*, *Phys. Rev. Lett.* **42** (1979) 407.
- [88] B. Audren, J. Lesgourges, G. Mangano, P.D. Serpico and T. Tram, *Strongest model-independent bound on the lifetime of Dark Matter*, *JCAP* **12** (2014) 028 [1407.2418].
- [89] T. Simon, G. Franco Abellán, P. Du, V. Poulin and Y. Tsai, “Constraining decaying dark matter with BOSS data and the effective field theory of large-scale structures.” 3, 2022.

- [90] B.D. Fields, K.A. Olive, T.-H. Yeh and C. Young, *Big-Bang Nucleosynthesis after Planck*, *JCAP* **03** (2020) 010 [[1912.01132](#)].
- [91] S. Koren, *A Cosmological Lithium Solution from Discrete Gauged Baryon Minus Lepton Number*, [2204.01750](#).
- [92] A. Matsumoto et al., *EMPRESS. VIII. A New Determination of Primordial He Abundance with Extremely Metal-poor Galaxies: A Suggestion of the Lepton Asymmetry and Implications for the Hubble Tension*, *Astrophys. J.* **941** (2022) 167 [[2203.09617](#)].
- [93] A.H. Guth, *The Inflationary Universe: A Possible Solution to the Horizon and Flatness Problems*, *Phys. Rev. D* **23** (1981) 347.
- [94] J. Preskill, *Cosmological Production of Superheavy Magnetic Monopoles*, *Phys. Rev. Lett.* **43** (1979) 1365.
- [95] A.D. Linde, *A New Inflationary Universe Scenario: A Possible Solution of the Horizon, Flatness, Homogeneity, Isotropy and Primordial Monopole Problems*, *Phys. Lett. B* **108** (1982) 389.
- [96] A. Albrecht and P.J. Steinhardt, *Cosmology for Grand Unified Theories with Radiatively Induced Symmetry Breaking*, *Phys. Rev. Lett.* **48** (1982) 1220.
- [97] A.D. Linde, *Chaotic Inflation*, *Phys. Lett. B* **129** (1983) 177.
- [98] A.D. Linde, *Hybrid inflation*, *Phys. Rev. D* **49** (1994) 748 [[astro-ph/9307002](#)].
- [99] D. Baumann, *Inflation*, in *Theoretical Advanced Study Institute in Elementary Particle Physics: Physics of the Large and the Small*, pp. 523–686, 2011, DOI [[0907.5424](#)].
- [100] L. Kofman, A.D. Linde and A.A. Starobinsky, *Towards the theory of reheating after inflation*, *Phys. Rev. D* **56** (1997) 3258 [[hep-ph/9704452](#)].
- [101] E.R. Harrison, *Fluctuations at the threshold of classical cosmology*, *Phys. Rev. D* **1** (1970) 2726.
- [102] Y.B. Zeldovich, *A Hypothesis, unifying the structure and the entropy of the universe*, *Mon. Not. Roy. Astron. Soc.* **160** (1972) 1P.
- [103] SPTPOL COLLABORATION collaboration, *Detection of b-mode polarization in the cosmic microwave background with data from the south pole telescope*, *Phys. Rev. Lett.* **111** (2013) 141301.
- [104] BICEP2, KECK ARRAY collaboration, *Improved Constraints on Cosmology and Foregrounds from BICEP2 and Keck Array Cosmic Microwave Background Data with Inclusion of 95 GHz Band*, *Phys. Rev. Lett.* **116** (2016) 031302 [[1510.09217](#)].

Bibliography

- [105] K. Freese, J.A. Frieman and A.V. Olinto, *Natural inflation with pseudo - Nambu-Goldstone bosons*, *Phys. Rev. Lett.* **65** (1990) 3233.
- [106] G.R. Dvali, Q. Shafi and R.K. Schaefer, *Large scale structure and supersymmetric inflation without fine tuning*, *Phys. Rev. Lett.* **73** (1994) 1886 [[hep-ph/9406319](#)].
- [107] M. Drees and Y. Xu, *Small field polynomial inflation: reheating, radiative stability and lower bound*, *JCAP* **09** (2021) 012 [[2104.03977](#)].
- [108] M. Drees and Y. Xu, *Large field polynomial inflation: parameter space, predictions and (double) eternal nature*, *JCAP* **12** (2022) 005 [[2209.07545](#)].
- [109] A. Starobinsky, *A new type of isotropic cosmological models without singularity*, *Physics Letters B* **91** (1980) 99.
- [110] F.L. Bezrukov and M. Shaposhnikov, *The Standard Model Higgs boson as the inflaton*, *Phys. Lett. B* **659** (2008) 703 [[0710.3755](#)].
- [111] R. Kallosh, A. Linde and D. Roest, *Superconformal Inflationary α -Attractors*, *JHEP* **11** (2013) 198 [[1311.0472](#)].
- [112] J. Martin, C. Ringeval and V. Vennin, *Encyclopædia Inflationaris*, *Phys. Dark Univ.* **5-6** (2014) 75 [[1303.3787](#)].
- [113] A.D. Sakharov, *Violation of CP Invariance, C asymmetry, and baryon asymmetry of the universe*, *Pisma Zh. Eksp. Teor. Fiz.* **5** (1967) 32.
- [114] V. Kuzmin, V. Rubakov and M. Shaposhnikov, *On the Anomalous Electroweak Baryon Number Nonconservation in the Early Universe*, *Phys.Lett.* **B155** (1985) 36.
- [115] J.A. Harvey and M.S. Turner, *Cosmological baryon and lepton number in the presence of electroweak fermion number violation*, *Phys.Rev.* **D42** (1990) 3344.
- [116] M. Fukugita and T. Yanagida, *Baryogenesis Without Grand Unification*, *Phys. Lett. B* **174** (1986) 45.
- [117] K. Dick, M. Lindner, M. Ratz and D. Wright, *Leptogenesis with Dirac neutrinos*, *Phys. Rev. Lett.* **84** (2000) 4039 [[hep-ph/9907562](#)].
- [118] A.G. Cohen and D.B. Kaplan, *Thermodynamic generation of the baryon asymmetry*, *Physics Letters B* **199** (1987) 251.
- [119] A.G. Cohen and D.B. Kaplan, *Spontaneous Baryogenesis*, *Nucl. Phys. B* **308** (1988) 913.
- [120] M. Berbig, *A model for long ranged neutrino self-interactions*, Master's thesis, Bethe Center for Theoretical Physics, Physics Institute, Bonn University, 2019.

- [121] S. Bashinsky and U. Seljak, *Neutrino perturbations in CMB anisotropy and matter clustering*, *Phys. Rev. D* **69** (2004) 083002 [[astro-ph/0310198](#)].
- [122] S. Roy Choudhury, S. Hannestad and T. Tram, *Updated constraints on massive neutrino self-interactions from cosmology in light of the H_0 tension*, *JCAP* **03** (2021) 084 [[2012.07519](#)].
- [123] T. Brinckmann, J.H. Chang and M. LoVerde, *Self-interacting neutrinos, the Hubble parameter tension, and the cosmic microwave background*, *Phys. Rev. D* **104** (2021) 063523 [[2012.11830](#)].
- [124] C.D. Kreisch et al., *The Atacama Cosmology Telescope: The Persistence of Neutrino Self-Interaction in Cosmological Measurements*, [2207.03164](#).
- [125] M. Escudero and S.J. Witte, *A CMB Search for the Neutrino Mass Mechanism and its Relation to the H_0 Tension*, [1909.04044](#).
- [126] J. Heeck, *Unbroken $B - L$ symmetry*, *Phys. Lett. B* **739** (2014) 256 [[1408.6845](#)].
- [127] J. Venzor, G. Garcia-Arroyo, A. Pérez-Lorenzana and J. De-Santiago, *Resonant neutrino self-interactions and the H_0 tension*, [2303.12792](#).
- [128] A.G. Riess et al., *A 2.4% Determination of the Local Value of the Hubble Constant*, *Astrophys. J.* **826** (2016) 56 [[1604.01424](#)].
- [129] A.G. Riess, S. Casertano, W. Yuan, L.M. Macri and D. Scolnic, *Large Magellanic Cloud Cepheid Standards Provide a 1% Foundation for the Determination of the Hubble Constant and Stronger Evidence for Physics beyond Λ CDM*, *Astrophys. J.* **876** (2019) 85 [[1903.07603](#)].
- [130] W.L. Freedman et al., *The Carnegie-Chicago Hubble Program. VIII. An Independent Determination of the Hubble Constant Based on the Tip of the Red Giant Branch*, [1907.05922](#).
- [131] S. Birrer et al., *H0LiCOW - IX. Cosmographic analysis of the doubly imaged quasar SDSS 1206+4332 and a new measurement of the Hubble constant*, *Mon. Not. Roy. Astron. Soc.* **484** (2019) 4726 [[1809.01274](#)].
- [132] K.C. Wong et al., *H0LiCOW XIII. A 2.4% measurement of H_0 from lensed quasars: 5.3 σ tension between early and late-Universe probes*, [1907.04869](#).
- [133] PLANCK collaboration, *Planck 2018 results. VI. Cosmological parameters*, *Astron. Astrophys.* **641** (2020) A6 [[1807.06209](#)].
- [134] F. Köhlinger et al., *KiDS-450: The tomographic weak lensing power spectrum and constraints on cosmological parameters*, *Mon. Not. Roy. Astron. Soc.* **471** (2017) 4412 [[1706.02892](#)].

Bibliography

- [135] S. Joudaki et al., *KiDS-450 + 2dFLenS: Cosmological parameter constraints from weak gravitational lensing tomography and overlapping redshift-space galaxy clustering*, *Mon. Not. Roy. Astron. Soc.* **474** (2018) 4894 [1707.06627].
- [136] S. Joudaki et al., *KiDS+VIKING-450 and DES-Y1 combined: Cosmology with cosmic shear*, 1906.09262.
- [137] BOSS collaboration, *The clustering of galaxies in the completed SDSS-III Baryon Oscillation Spectroscopic Survey: cosmological analysis of the DR12 galaxy sample*, *Mon. Not. Roy. Astron. Soc.* **470** (2017) 2617 [1607.03155].
- [138] O.H.E. Philcox, M.M. Ivanov, M. Simonović and M. Zaldarriaga, *Combining Full-Shape and BAO Analyses of Galaxy Power Spectra: A 1.6% CMB-independent constraint on H_0* , 2002.04035.
- [139] DES collaboration, *Dark Energy Survey Year 1 results: Cosmological constraints from cosmic shear*, *Phys. Rev.* **D98** (2018) 043528 [1708.01538].
- [140] DES collaboration, *Dark Energy Survey Year 1 Results: A Precise H_0 Estimate from DES Y1, BAO, and D/H Data*, *Mon. Not. Roy. Astron. Soc.* **480** (2018) 3879 [1711.00403].
- [141] DES collaboration, *Dark Energy Survey Year 1 Results: Measurement of the Baryon Acoustic Oscillation scale in the distribution of galaxies to redshift 1*, *Mon. Not. Roy. Astron. Soc.* **483** (2019) 4866 [1712.06209].
- [142] HSC collaboration, *Cosmology from cosmic shear power spectra with Subaru Hyper Suprime-Cam first-year data*, *Publ. Astron. Soc. Jap.* **71** (2019) 43 [1809.09148].
- [143] M.H. Abdullah, A. Klypin and G. Wilson, *Cosmological Constraint on Ω_m and σ_8 from Cluster Abundances using the GalWCat19 Optical-Spectroscopic SDSS Catalog*, 2002.11907.
- [144] E. Di Valentino, A. Melchiorri and J. Silk, *Planck evidence for a closed Universe and a possible crisis for cosmology*, *Nat. Astron.* (2019) [1911.02087].
- [145] E. Di Valentino, A. Melchiorri and J. Silk, *Cosmic Discordance: Planck and luminosity distance data exclude Λ CDM*, 2003.04935.
- [146] N. Schöneberg, J. Lesgourgues and D.C. Hooper, *The BAO+BBN take on the Hubble tension*, *JCAP* **1910** (2019) 029 [1907.11594].
- [147] L. Knox and M. Millea, *The Hubble Hunter's Guide*, 1908.03663.
- [148] J. Sakstein and M. Trodden, *Early dark energy from massive neutrinos -- a natural resolution of the Hubble tension*, 1911.11760.

- [149] L. Verde, T. Treu and A.G. Riess, *Tensions between the Early and the Late Universe*, in *Nature Astronomy* **2019**, 2019, DOI [1907.10625].
- [150] F.-Y. Cyr-Racine and K. Sigurdson, *Limits on Neutrino-Neutrino Scattering in the Early Universe*, *Phys. Rev.* **D90** (2014) 123533 [1306.1536].
- [151] M. Archidiacono and S. Hannestad, *Updated constraints on non-standard neutrino interactions from Planck*, *JCAP* **1407** (2014) 046 [1311.3873].
- [152] L. Lancaster, F.-Y. Cyr-Racine, L. Knox and Z. Pan, *A tale of two modes: Neutrino free-streaming in the early universe*, *JCAP* **1707** (2017) 033 [1704.06657].
- [153] I.M. Oldengott, T. Tram, C. Rampf and Y.Y.Y. Wong, *Interacting neutrinos in cosmology: exact description and constraints*, *JCAP* **1711** (2017) 027 [1706.02123].
- [154] M. Park, C.D. Kreisch, J. Dunkley, B. Hadzhiyska and F.-Y. Cyr-Racine, Λ *CDM or self-interacting neutrinos: How CMB data can tell the two models apart*, *Phys. Rev.* **D100** (2019) 063524 [1904.02625].
- [155] F. Forastieri, M. Lattanzi and P. Natoli, *Constraints on secret neutrino interactions after Planck*, *JCAP* **1507** (2015) 014 [1504.04999].
- [156] F. Forastieri, M. Lattanzi and P. Natoli, *Cosmological constraints on neutrino self-interactions with a light mediator*, *Phys. Rev.* **D100** (2019) 103526 [1904.07810].
- [157] Y. Farzan and J. Heeck, *Neutrinoophilic nonstandard interactions*, *Phys. Rev. D* **94** (2016) 053010 [1607.07616].
- [158] Y. Farzan and M. Tortola, *Neutrino oscillations and Non-Standard Interactions*, *Front. in Phys.* **6** (2018) 10 [1710.09360].
- [159] P.B. Denton, Y. Farzan and I.M. Shoemaker, *Activating the fourth neutrino of the 3+1 scheme*, *Phys. Rev.* **D99** (2019) 035003 [1811.01310].
- [160] S. Weinberg, *Baryon and Lepton Nonconserving Processes*, *Phys. Rev. Lett.* **43** (1979) 1566.
- [161] R.N. Mohapatra, *New contributions to neutrinoless double-beta decay in supersymmetric theories*, *Phys. Rev.* **D34** (1986) 3457.
- [162] E. Bertuzzo, S. Jana, P.A.N. Machado and R. Zukanovich Funchal, *Neutrino Masses and Mixings Dynamically Generated by a Light Dark Sector*, *Phys. Lett.* **B791** (2019) 210 [1808.02500].
- [163] P.S.B. Dev and A. Pilaftsis, *Minimal Radiative Neutrino Mass Mechanism for Inverse Seesaw Models*, *Phys. Rev.* **D86** (2012) 113001 [1209.4051].

Bibliography

- [164] S. Gabriel and S. Nandi, *A New two Higgs doublet model*, *Phys. Lett. B* **655** (2007) 141 [[hep-ph/0610253](#)].
- [165] S. Baek and T. Nomura, *Dark matter physics in neutrino specific two Higgs doublet model*, *JHEP* **03** (2017) 059 [[1611.09145](#)].
- [166] E. Bertuzzo, P.A.N. Machado, Z. Tabrizi and R. Zukanovich Funchal, *A Neutrinophilic 2HDM as a UV Completion for the Inverse Seesaw Mechanism*, *JHEP* **11** (2017) 004 [[1706.10000](#)].
- [167] T. Nomura and H. Okada, *Hidden $U(1)$ gauge symmetry realizing a neutrinophilic two-Higgs-doublet model with dark matter*, *Phys. Rev. D* **97** (2018) 075038 [[1709.06406](#)].
- [168] S. Baek, A. Das and T. Nomura, *Scalar dark matter search from the extended ν THDM*, *JHEP* **05** (2018) 205 [[1802.08615](#)].
- [169] U.K. Dey, N. Nath and S. Sadhukhan, *Non-Standard Neutrino Interactions in a Modified ν 2HDM*, *Phys. Rev. D* **98** (2018) 055004 [[1804.05808](#)].
- [170] J. Beacham et al., *Physics Beyond Colliders at CERN: Beyond the Standard Model Working Group Report*, *J. Phys. G* **47** (2020) 010501 [[1901.09966](#)].
- [171] P. Galison and A. Manohar, *TWO Z's OR NOT TWO Z's?*, *Phys. Lett. B* **136** (1984) 279.
- [172] B. Holdom, *Two $U(1)$'s and Epsilon Charge Shifts*, *Phys. Lett. 166B* (1986) 196.
- [173] M. Baumgart, C. Cheung, J.T. Ruderman, L.-T. Wang and I. Yavin, *Non-Abelian Dark Sectors and Their Collider Signatures*, *JHEP* **04** (2009) 014 [[0901.0283](#)].
- [174] K. Babu, A. Friedland, P. Machado and I. Mocioiu, *Flavor Gauge Models Below the Fermi Scale*, *JHEP* **12** (2017) 096 [[1705.01822](#)].
- [175] J. Redondo, *Atlas of solar hidden photon emission*, *JCAP* **07** (2015) 024 [[1501.07292](#)].
- [176] T. Gherghetta, J. Kersten, K. Olive and M. Pospelov, *Evaluating the price of tiny kinetic mixing*, *Phys. Rev. D* **100** (2019) 095001 [[1909.00696](#)].
- [177] A. de Gouvêa and A. Kobach, *Global Constraints on a Heavy Neutrino*, *Phys. Rev. D* **93** (2016) 033005 [[1511.00683](#)].
- [178] D.A. Bryman and R. Shrock, *Improved Constraints on Sterile Neutrinos in the MeV to GeV Mass Range*, *Phys. Rev. D* **100** (2019) 053006 [[1904.06787](#)].
- [179] D.A. Bryman and R. Shrock, *Constraints on Sterile Neutrinos in the MeV to GeV Mass Range*, *Phys. Rev. D* **100** (2019) 073011 [[1909.11198](#)].

- [180] P.D. Bolton, F.F. Deppisch and P. Bhupal Dev, *Neutrinoless double beta decay versus other probes of heavy sterile neutrinos*, *JHEP* **03** (2020) 170 [1912.03058].
- [181] S. Antusch and O. Fischer, *Non-unitarity of the leptonic mixing matrix: Present bounds and future sensitivities*, *JHEP* **10** (2014) 094 [1407.6607].
- [182] E. Fernandez-Martinez, J. Hernandez-Garcia and J. Lopez-Pavon, *Global constraints on heavy neutrino mixing*, *JHEP* **08** (2016) 033 [1605.08774].
- [183] M. Dentler, Á. Hernández-Cabezudo, J. Kopp, P.A.N. Machado, M. Maltoni, I. Martinez-Soler et al., *Updated Global Analysis of Neutrino Oscillations in the Presence of eV-Scale Sterile Neutrinos*, *JHEP* **08** (2018) 010 [1803.10661].
- [184] R. Laha, B. Dasgupta and J.F. Beacom, *Constraints on New Neutrino Interactions via Light Abelian Vector Bosons*, *Phys. Rev.* **D89** (2014) 093025 [1304.3460].
- [185] K.C.Y. Ng and J.F. Beacom, *Cosmic neutrino cascades from secret neutrino interactions*, *Phys. Rev.* **D90** (2014) 065035 [1404.2288].
- [186] K. Ioka and K. Murase, *IceCube PeV-EeV neutrinos and secret interactions of neutrinos*, *PTEP* **2014** (2014) 061E01 [1404.2279].
- [187] M. Bustamante, C.A. Rosenstroem, S. Shalgar and I. Tamborra, *Bounds on secret neutrino interactions from high-energy astrophysical neutrinos*, 2001.04994.
- [188] N. Blinov, K.J. Kelly, G.Z. Krnjaic and S.D. McDermott, *Constraining the Self-Interacting Neutrino Interpretation of the Hubble Tension*, *Phys. Rev. Lett.* **123** (2019) 191102 [1905.02727].
- [189] V. Brdar, M. Lindner, S. Vogl and X.-J. Xu, *Revisiting Neutrino Self-Interaction Constraints from Z and τ decays*, 2003.05339.
- [190] A. de Gouvêa, P.B. Dev, B. Dutta, T. Ghosh, T. Han and Y. Zhang, *Leptonic Scalars at the LHC*, 1910.01132.
- [191] K.-F. Lyu, E. Stamou and L.-T. Wang, *Self-interacting neutrinos: solution to Hubble tension versus experimental constraints*, 2004.10868.
- [192] K.M. Belotsky, A.L. Sudarikov and M. Khlopov, *Constraint on anomalous 4nu interaction*, *Phys. Atom. Nucl.* **64** (2001) 1637.
- [193] A.P. Lessa and O.L.G. Peres, *Revising limits on neutrino-Majoron couplings*, *Phys. Rev.* **D75** (2007) 094001 [[hep-ph/0701068](#)].
- [194] NA48/2 collaboration, *Testing LFV measuring the ratio $R(K)$ between the branching ratio of $K^\pm \rightarrow e^\pm \nu(\gamma)$ and $K^\pm \rightarrow \mu^\pm \nu(\gamma)$ in NA48/2 experiment: Measurement and perspectives*, *Nucl. Phys. Proc. Suppl.* **169** (2007) 205.

Bibliography

- [195] P. Bakhti and Y. Farzan, *Constraining secret gauge interactions of neutrinos by meson decays*, *Phys. Rev.* **D95** (2017) 095008 [[1702.04187](#)].
- [196] J.A. Dror, R. Lasenby and M. Pospelov, *New constraints on light vectors coupled to anomalous currents*, *Phys. Rev. Lett.* **119** (2017) 141803 [[1705.06726](#)].
- [197] J.A. Dror, R. Lasenby and M. Pospelov, *Dark forces coupled to nonconserved currents*, *Phys. Rev.* **D96** (2017) 075036 [[1707.01503](#)].
- [198] P. Bakhti, Y. Farzan and M. Rajaei, *Secret interactions of neutrinos with light gauge boson at the DUNE near detector*, *Phys. Rev. D* **99** (2019) 055019 [[1810.04441](#)].
- [199] J.A. Dror, R. Lasenby and M. Pospelov, *Light vectors coupled to bosonic currents*, *Phys. Rev.* **D99** (2019) 055016 [[1811.00595](#)].
- [200] M. Bahraminasr, P. Bakhti and M. Rajaei, *Sensitivities to secret neutrino interaction at FASER ν* , [2003.09985](#).
- [201] J.A. Dror, *Discovering leptonic forces using non-conserved currents*, [2004.04750](#).
- [202] C.D. Carone, *Double beta decay with vector majorons*, *Phys. Lett.* **B308** (1993) 85 [[hep-ph/9302290](#)].
- [203] M. Agostini et al., *Results on $\beta\beta$ decay with emission of two neutrinos or Majorons in ^{76}Ge from GERDA Phase I*, *Eur. Phys. J.* **C75** (2015) 416 [[1501.02345](#)].
- [204] K. Blum, Y. Nir and M. Shavit, *Neutrinoless double-beta decay with massive scalar emission*, *Phys. Lett.* **B785** (2018) 354 [[1802.08019](#)].
- [205] T. Brune and H. Päs, *Massive Majorons and constraints on the Majoron-neutrino coupling*, *Phys. Rev.* **D99** (2019) 096005 [[1808.08158](#)].
- [206] F.F. Deppisch, L. Graf, W. Rodejohann and X.-J. Xu, *Neutrino Self-Interactions and Double Beta Decay*, [2004.11919](#).
- [207] E.W. Kolb and M.S. Turner, *Supernova SN 1987a and the Secret Interactions of Neutrinos*, *Phys. Rev.* **D36** (1987) 2895.
- [208] P. Gondolo and G. Gelmini, *Cosmic abundances of stable particles: Improved analysis*, *Nucl. Phys.* **B360** (1991) 145.
- [209] G. Arcadi, O. Lebedev, S. Pokorski and T. Toma, *Real Scalar Dark Matter: Relativistic Treatment*, *JHEP* **08** (2019) 050 [[1906.07659](#)].
- [210] O. Lebedev and T. Toma, *Relativistic Freeze-in*, *Phys. Lett.* **B798** (2019) 134961 [[1908.05491](#)].

- [211] N. Blinov and G. Marques-Tavares, *Interacting radiation after Planck and its implications for the Hubble Tension*, 2003.08387.
- [212] PARTICLE DATA GROUP collaboration, *Review of Particle Physics*, *Phys. Rev. D* **98** (2018) 030001.
- [213] M. Cepeda et al., *Report from Working Group 2: Higgs Physics at the HL-LHC and HE-LHC*, *CERN Yellow Rep. Monogr.* **7** (2019) 221 [1902.00134].
- [214] ATLAS collaboration, *Search for invisible Higgs boson decays with vector boson fusion signatures with the ATLAS detector using an integrated luminosity of 139 fb^{-1}* .
- [215] M. Carena, A. de Gouvea, A. Freitas and M. Schmitt, *Invisible Z boson decays at $e+e-$ colliders*, *Phys. Rev. D* **68** (2003) 113007 [hep-ph/0308053].
- [216] ATLAS collaboration, *Search for charged Higgs bosons decaying into top and bottom quarks at $\sqrt{s} = 13$ TeV with the ATLAS detector*, *JHEP* **11** (2018) 085 [1808.03599].
- [217] CMS collaboration, *Search for a charged Higgs boson decaying into top and bottom quarks in events with electrons or muons in proton-proton collisions at $\sqrt{s} = 13$ TeV*, *JHEP* **01** (2020) 096 [1908.09206].
- [218] ALEPH, DELPHI, L3, OPAL, LEP collaboration, *Search for Charged Higgs bosons: Combined Results Using LEP Data*, *Eur. Phys. J. C* **73** (2013) 2463 [1301.6065].
- [219] ALEPH collaboration, *Search for scalar leptons in $e+e-$ collisions at center-of-mass energies up to 209-GeV*, *Phys. Lett. B* **526** (2002) 206 [hep-ex/0112011].
- [220] OPAL collaboration, *Search for anomalous production of dilepton events with missing transverse momentum in $e+e-$ collisions at $s^{**}(1/2) = 183$ -Gev to 209-GeV*, *Eur. Phys. J. C* **32** (2004) 453 [hep-ex/0309014].
- [221] L3 collaboration, *Search for scalar leptons and scalar quarks at LEP*, *Phys. Lett. B* **580** (2004) 37 [hep-ex/0310007].
- [222] DELPHI collaboration, *Searches for supersymmetric particles in $e+e-$ collisions up to 208-GeV and interpretation of the results within the MSSM*, *Eur. Phys. J. C* **31** (2003) 421 [hep-ex/0311019].
- [223] CMS collaboration, *Searches for electroweak production of charginos, neutralinos, and sleptons decaying to leptons and W, Z, and Higgs bosons in pp collisions at 8 TeV*, *Eur. Phys. J. C* **74** (2014) 3036 [1405.7570].
- [224] K.S. Babu, P.S.B. Dev, S. Jana and A. Thapa, *Non-Standard Interactions in Radiative Neutrino Mass Models*, *JHEP* **03** (2020) 006 [1907.09498].

Bibliography

- [225] W. Grimus, L. Lavoura, O.M. Ogreid and P. Osland, *A Precision constraint on multi-Higgs-doublet models*, *J. Phys.* **G35** (2008) 075001 [[0711.4022](#)].
- [226] GFITTER GROUP collaboration, *The global electroweak fit at NNLO and prospects for the LHC and ILC*, *Eur. Phys. J.* **C74** (2014) 3046 [[1407.3792](#)].
- [227] P.D. Group, P.A. Zyla, R.M. Barnett, J. Beringer, O. Dahl, D.A. Dwyer et al., *Review of Particle Physics, Progress of Theoretical and Experimental Physics* **2020** (2020) [<https://academic.oup.com/ptep/article-pdf/2020/8/083C01/34673722/ptaa104.pdf>].
- [228] B.W. Lee, C. Quigg and H.B. Thacker, *Weak Interactions at Very High-Energies: The Role of the Higgs Boson Mass*, *Phys. Rev. D* **16** (1977) 1519.
- [229] A.R. Zhitnitsky, *On Possible Suppression of the Axion Hadron Interactions. (In Russian)*, *Sov. J. Nucl. Phys.* **31** (1980) 260.
- [230] M. Dine, W. Fischler and M. Srednicki, *A Simple Solution to the Strong CP Problem with a Harmless Axion*, *Phys. Lett. B* **104** (1981) 199.
- [231] S. Weinberg, *A new light boson?*, *Phys. Rev. Lett.* **40** (1978) 223.
- [232] F. Wilczek, *Problem of Strong p and t Invariance in the Presence of Instantons*, *Phys. Rev. Lett.* **40** (1978) 279.
- [233] L. Vecchi, *Light sterile neutrinos from a late phase transition*, *Phys. Rev.* **D94** (2016) 113015 [[1607.04161](#)].
- [234] S. Böser, C. Buck, C. Giunti, J. Lesgourgues, L. Ludhova, S. Mertens et al., *Status of Light Sterile Neutrino Searches*, *Prog. Part. Nucl. Phys.* **111** (2020) 103736 [[1906.01739](#)].
- [235] M. Dentler, I. Esteban, J. Kopp and P. Machado, *Decaying Sterile Neutrinos and the Short Baseline Oscillation Anomalies*, [1911.01427](#).
- [236] A. de Gouvêa, O.L.G. Peres, S. Prakash and G.V. Stenico, *On The Decaying-Sterile Neutrino Solution to the Electron (Anti)Neutrino Appearance Anomalies*, [1911.01447](#).
- [237] R.S.L. Hansen and S. Vogl, *Thermalizing sterile neutrino dark matter*, *Phys. Rev. Lett.* **119** (2017) 251305 [[1706.02707](#)].
- [238] H.-J. He, Y.-Z. Ma and J. Zheng, *Resolving Hubble Tension by Self-Interacting Neutrinos with Dirac Seesaw*, [2003.12057](#).
- [239] F. Staub, *SARAH 4 : A tool for (not only SUSY) model builders*, *Comput. Phys. Commun.* **185** (2014) 1773 [[1309.7223](#)].
- [240] T. Hahn, *Generating Feynman diagrams and amplitudes with FeynArts 3*, *Comput. Phys. Commun.* **140** (2001) 418 [[hep-ph/0012260](#)].

- [241] T. Hahn and M. Perez-Victoria, *Automatized one loop calculations in four-dimensions and D-dimensions*, *Comput. Phys. Commun.* **118** (1999) 153 [[hep-ph/9807565](#)].
- [242] H.H. Patel, *Package-X: A Mathematica package for the analytic calculation of one-loop integrals*, *Comput. Phys. Commun.* **197** (2015) 276 [[1503.01469](#)].
- [243] Q. Decant, J. Heisig, D.C. Hooper and L. Lopez-Honorez, *Lyman- α constraints on freeze-in and superWIMPs*, *JCAP* **03** (2022) 041 [[2111.09321](#)].
- [244] M. Kawasaki, K. Kohri and N. Sugiyama, *MeV scale reheating temperature and thermalization of neutrino background*, *Phys. Rev.* **D62** (2000) 023506 [[astro-ph/0002127](#)].
- [245] S. Hannestad, *What is the lowest possible reheating temperature?*, *Phys. Rev. D* **70** (2004) 043506 [[astro-ph/0403291](#)].
- [246] E. Ma, *Verifiable radiative seesaw mechanism of neutrino mass and dark matter*, *Phys. Rev. D* **73** (2006) 077301 [[hep-ph/0601225](#)].
- [247] E. Ma, *Common origin of neutrino mass, dark matter, and baryogenesis*, *Mod. Phys. Lett. A* **21** (2006) 1777 [[hep-ph/0605180](#)].
- [248] J. Kubo, E. Ma and D. Suematsu, *Cold Dark Matter, Radiative Neutrino Mass, $\mu \rightarrow e\gamma$, and Neutrinoless Double Beta Decay*, *Phys. Lett. B* **642** (2006) 18 [[hep-ph/0604114](#)].
- [249] T. Hambye, K. Kannike, E. Ma and M. Raidal, *Emanations of Dark Matter: Muon Anomalous Magnetic Moment, Radiative Neutrino Mass, and Novel Leptogenesis at the TeV Scale*, *Phys. Rev. D* **75** (2007) 095003 [[hep-ph/0609228](#)].
- [250] E. Molinaro, C.E. Yaguna and O. Zapata, *FIMP realization of the scotogenic model*, *JCAP* **07** (2014) 015 [[1405.1259](#)].
- [251] A. Dedes, D. Karamitros and A. Pilaftsis, *Radiative Light Dark Matter*, *Phys. Rev. D* **95** (2017) 115037 [[1704.01497](#)].
- [252] D. Borah and R. Adhikari, *Common Radiative Origin of Active and Sterile Neutrino Masses*, *Phys. Lett. B* **729** (2014) 143 [[1310.5419](#)].
- [253] R. Adhikari, D. Borah and E. Ma, *Common Origin of Active and Sterile Neutrino Masses with Dark Matter*, [1411.4602](#).
- [254] R. Adhikari, D. Borah and E. Ma, *New U(1) Gauge Model of Radiative Lepton Masses with Sterile Neutrino and Dark Matter*, *Phys. Lett. B* **755** (2016) 414 [[1512.05491](#)].

Bibliography

- [255] T. Yanagida, *Proceedings: Workshop on the Unified Theories and the Baryon Number in the Universe: Tsukuba, Japan, February 13-14, 1979*, .
- [256] E. Ma and V. De Romeri, *Radiative seesaw dark matter*, *Phys. Rev. D* **104** (2021) 055004 [[2105.00552](#)].
- [257] I. Affleck and M. Dine, *A new mechanism for baryogenesis*, *Nuclear Physics B* **249** (1985) 361.
- [258] E. Ma, *Leptonic Source of Dark Matter and Radiative Majorana or Dirac Neutrino Mass*, *Phys. Lett. B* **809** (2020) 135736 [[1912.11950](#)].
- [259] P. Escribano, M. Reig and A. Vicente, *Generalizing the Scotogenic model*, *JHEP* **07** (2020) 097 [[2004.05172](#)].
- [260] S.-Y. Guo and Z.-L. Han, *Observable Signatures of Scotogenic Dirac Model*, *JHEP* **12** (2020) 062 [[2005.08287](#)].
- [261] J.C. Montero and V. Pleitez, *Gauging $U(1)$ symmetries and the number of right-handed neutrinos*, *Phys. Lett. B* **675** (2009) 64 [[0706.0473](#)].
- [262] B.L. Sánchez-Vega, J.C. Montero and E.R. Schmitz, *Complex Scalar DM in a $B-L$ Model*, *Phys. Rev. D* **90** (2014) 055022 [[1404.5973](#)].
- [263] E. Ma and R. Srivastava, *Dirac or inverse seesaw neutrino masses with $B - L$ gauge symmetry and S_3 flavor symmetry*, *Phys. Lett. B* **741** (2015) 217 [[1411.5042](#)].
- [264] B.L. Sánchez-Vega and E.R. Schmitz, *Fermionic dark matter and neutrino masses in a $B-L$ model*, *Phys. Rev. D* **92** (2015) 053007 [[1505.03595](#)].
- [265] E. Ma, N. Pollard, R. Srivastava and M. Zakeri, *Gauge $B - L$ Model with Residual Z_3 Symmetry*, *Phys. Lett. B* **750** (2015) 135 [[1507.03943](#)].
- [266] S. Patra, W. Rodejohann and C.E. Yaguna, *A new $B - L$ model without right-handed neutrinos*, *JHEP* **09** (2016) 076 [[1607.04029](#)].
- [267] T. Banks and N. Seiberg, *Symmetries and Strings in Field Theory and Gravity*, *Phys. Rev. D* **83** (2011) 084019 [[1011.5120](#)].
- [268] E.C.G. Stueckelberg, *Interaction energy in electrodynamics and in the field theory of nuclear forces*, *Helv. Phys. Acta* **11** (1938) 225.
- [269] E.C.G. Stueckelberg, *Interaction forces in electrodynamics and in the field theory of nuclear forces*, *Helv. Phys. Acta* **11** (1938) 299.
- [270] J. Heeck, *Neutrinos and Abelian Gauge Symmetries*, Ph.D. thesis, Heidelberg U., 2014.

- [271] A. Zee, *A Theory of Lepton Number Violation, Neutrino Majorana Mass, and Oscillation*, *Phys. Lett. B* **93** (1980) 389.
- [272] M. Carena, A. Daleo, B.A. Dobrescu and T.M.P. Tait, *Z' gauge bosons at the fermilab tevatron*, *Phys. Rev. D* **70** (2004) 093009.
- [273] ATLAS collaboration, *Search for high-mass dilepton resonances in pp collisions at $\sqrt{s} = 8$ TeV with the ATLAS detector*, *Phys. Rev. D* **90** (2014) 052005 [1405.4123].
- [274] J. Elias-Miro, J.R. Espinosa, G.F. Giudice, H.M. Lee and A. Strumia, *Stabilization of the Electroweak Vacuum by a Scalar Threshold Effect*, *JHEP* **06** (2012) 031 [1203.0237].
- [275] S. Coleman, *Why there is nothing rather than something: A theory of the cosmological constant*, *Nuclear Physics B* **310** (1988) 643.
- [276] S.B. Giddings and A. Strominger, *Loss of incoherence and determination of coupling constants in quantum gravity*, *Nuclear Physics B* **307** (1988) 854.
- [277] G. Gilbert, *Wormhole-induced proton decay*, *Nuclear Physics B* **328** (1989) 159.
- [278] F.J. Wegner, *Duality in generalized ising models and phase transitions without local order parameters*, *Journal of Mathematical Physics* **12** (1971) 2259 [<https://doi.org/10.1063/1.1665530>].
- [279] J.C. Pati and A. Salam, *Lepton number as the fourth "color"*, *Phys. Rev. D* **10** (1974) 275.
- [280] F. Gürsey, P. Ramond and P. Sikivie, *A universal gauge theory model based on $e6$* , *Physics Letters B* **60** (1976) 177.
- [281] Q. Shafi, *$E6$ as a unifying gauge symmetry*, *Physics Letters B* **79** (1978) 301.
- [282] S. Dodelson and L.M. Widrow, *Sterile-neutrinos as dark matter*, *Phys. Rev. Lett.* **72** (1994) 17 [hep-ph/9303287].
- [283] X.-D. Shi and G.M. Fuller, *A New dark matter candidate: Nonthermal sterile neutrinos*, *Phys. Rev. Lett.* **82** (1999) 2832 [astro-ph/9810076].
- [284] M. Viel, G.D. Becker, J.S. Bolton and M.G. Haehnelt, *Warm dark matter as a solution to the small scale crisis: New constraints from high redshift Lyman- α forest data*, *Phys. Rev. D* **88** (2013) 043502 [1306.2314].
- [285] N. Palanque-Delabrouille, C. Yèche, N. Schöneberg, J. Lesgourgues, M. Walther, S. Chabanier et al., *Hints, neutrino bounds and WDM constraints from SDSS DR14 Lyman- α and Planck full-survey data*, *JCAP* **04** (2020) 038 [1911.09073].

Bibliography

- [286] A. Garzilli, O. Ruchayskiy, A. Magalich and A. Boyarsky, *How warm is too warm? Towards robust Lyman- α forest bounds on warm dark matter*, [1912.09397](#).
- [287] K.J. Bae, A. Kamada, S.P. Liew and K. Yanagi, *Light axinos from freeze-in: production processes, phase space distributions, and Ly- α forest constraints*, *JCAP* **01** (2018) 054 [[1707.06418](#)].
- [288] R. Murgia, A. Merle, M. Viel, M. Totzauer and A. Schneider, *”Non-cold” dark matter at small scales: a general approach*, *JCAP* **11** (2017) 046 [[1704.07838](#)].
- [289] J. Heeck and D. Teresi, *Cold keV dark matter from decays and scatterings*, *Phys. Rev. D* **96** (2017) 035018 [[1706.09909](#)].
- [290] S. Boulebnane, J. Heeck, A. Nguyen and D. Teresi, *Cold light dark matter in extended seesaw models*, *JCAP* **04** (2018) 006 [[1709.07283](#)].
- [291] I. Baldes, Q. Decant, D.C. Hooper and L. Lopez-Honorez, *Non-Cold Dark Matter from Primordial Black Hole Evaporation*, *JCAP* **08** (2020) 045 [[2004.14773](#)].
- [292] G. Ballesteros, M.A.G. Garcia and M. Pierre, *How warm are non-thermal relics? Lyman- α bounds on out-of-equilibrium dark matter*, *JCAP* **03** (2021) 101 [[2011.13458](#)].
- [293] F. D’Eramo and A. Lenoci, *Lower mass bounds on FIMP dark matter produced via freeze-in*, *JCAP* **10** (2021) 045 [[2012.01446](#)].
- [294] ATLAS collaboration, *Search for invisible Higgs boson decays in vector boson fusion at $\sqrt{s} = 13$ TeV with the ATLAS detector*, *Phys. Lett. B* **793** (2019) 499 [[1809.06682](#)].
- [295] ATLAS COLLABORATION collaboration, *Search for invisible Higgs boson decays with vector boson fusion signatures with the ATLAS detector using an integrated luminosity of 139 fb^{-1}* , .
- [296] J. de Blas et al., *Higgs Boson Studies at Future Particle Colliders*, *JHEP* **01** (2020) 139 [[1905.03764](#)].
- [297] Y. Tan et al., *Search for invisible decays of the Higgs boson produced at the CEPC*, *Chin. Phys. C* **44** (2020) 123001 [[2001.05912](#)].
- [298] A. Ishikawa, *Search for invisible decays of the Higgs boson at the ILC*, *PoS LeptonPhoton2019* (2019) 147 [[1909.07537](#)].
- [299] E.W. Kolb and S. Wolfram, *Baryon Number Generation in the Early Universe*, *Nucl. Phys. B* **172** (1980) 224.
- [300] W. Buchmuller, R.D. Peccei and T. Yanagida, *Leptogenesis as the origin of matter*, *Ann. Rev. Nucl. Part. Sci.* **55** (2005) 311 [[hep-ph/0502169](#)].

- [301] F. Bezrukov, H. Hettmansperger and M. Lindner, *keV sterile neutrino Dark Matter in gauge extensions of the Standard Model*, *Phys. Rev. D* **81** (2010) 085032 [[0912.4415](#)].
- [302] R.J. Scherrer and M.S. Turner, *Decaying particles do not ‘heat up’ the universe*, *Phys. Rev. D* **31** (1985) 681.
- [303] G.F. Giudice, A. Notari, M. Raidal, A. Riotto and A. Strumia, *Towards a complete theory of thermal leptogenesis in the SM and MSSM*, *Nucl. Phys. B* **685** (2004) 89 [[hep-ph/0310123](#)].
- [304] N. Bernal, M. Heikinheimo, T. Tenkanen, K. Tuominen and V. Vaskonen, *The Dawn of FIMP Dark Matter: A Review of Models and Constraints*, *Int. J. Mod. Phys. A* **32** (2017) 1730023 [[1706.07442](#)].
- [305] F. Elahi, C. Kolda and J. Unwin, *UltraViolet Freeze-in*, *JHEP* **03** (2015) 048 [[1410.6157](#)].
- [306] K. Harigaya and K. Mukaida, *Thermalization after/during Reheating*, *JHEP* **05** (2014) 006 [[1312.3097](#)].
- [307] J.L. Feng, A. Rajaraman and F. Takayama, *Superweakly interacting massive particles*, *Phys. Rev. Lett.* **91** (2003) 011302 [[hep-ph/0302215](#)].
- [308] S. Khalil and O. Seto, *Sterile neutrino dark matter in B - L extension of the standard model and galactic 511-keV line*, *JCAP* **10** (2008) 024 [[0804.0336](#)].
- [309] A. Das, S. Goswami, V. K. N. and T.K. Poddar, *Freeze-in sterile neutrino dark matter in a class of U(1)' models with inverse seesaw*, [2104.13986](#).
- [310] V. Barger, P. Langacker and H.-S. Lee, *Primordial nucleosynthesis constraints on Z' properties*, *Phys. Rev. D* **67** (2003) 075009 [[hep-ph/0302066](#)].
- [311] S. Davidson, E. Nardi and Y. Nir, *Leptogenesis*, *Phys. Rept.* **466** (2008) 105 [[0802.2962](#)].
- [312] R.T. D’Agnolo and J.T. Ruderman, *Light Dark Matter from Forbidden Channels*, *Phys. Rev. Lett.* **115** (2015) 061301 [[1505.07107](#)].
- [313] M. Escudero Abenza, *Precision early universe thermodynamics made simple: N_{eff} and neutrino decoupling in the Standard Model and beyond*, *JCAP* **05** (2020) 048 [[2001.04466](#)].
- [314] O. Wantz and E.P.S. Shellard, *Axion Cosmology Revisited*, *Phys. Rev. D* **82** (2010) 123508 [[0910.1066](#)].
- [315] A.D. Dolgov and S.H. Hansen, *Massive sterile neutrinos as warm dark matter*, *Astropart. Phys.* **16** (2002) 339 [[hep-ph/0009083](#)].

Bibliography

- [316] K. Abazajian, G.M. Fuller and W.H. Tucker, *Direct detection of warm dark matter in the X-ray*, *Astrophys. J.* **562** (2001) 593 [[astro-ph/0106002](#)].
- [317] A. Boyarsky, A. Neronov, O. Ruchayskiy and M. Shaposhnikov, *Constraints on sterile neutrino as a dark matter candidate from the diffuse x-ray background*, *Mon. Not. Roy. Astron. Soc.* **370** (2006) 213 [[astro-ph/0512509](#)].
- [318] J.W. den Herder, A. Boyarsky, O. Ruchayskiy, K. Abazajian, C. Frenk, S. Hansen et al., *The search for decaying Dark Matter*, *arXiv e-prints* (2009) arXiv:0906.1788 [[0906.1788](#)].
- [319] M. Drewes et al., *A White Paper on keV Sterile Neutrino Dark Matter*, *JCAP* **01** (2017) 025 [[1602.04816](#)].
- [320] J.L. Feng, M. Kaplinghat and H.-B. Yu, *Halo Shape and Relic Density Exclusions of Sommerfeld-Enhanced Dark Matter Explanations of Cosmic Ray Excesses*, *Phys. Rev. Lett.* **104** (2010) 151301 [[0911.0422](#)].
- [321] S. Tulin, H.-B. Yu and K.M. Zurek, *Beyond Collisionless Dark Matter: Particle Physics Dynamics for Dark Matter Halo Structure*, *Phys. Rev. D* **87** (2013) 115007 [[1302.3898](#)].
- [322] F. Kahlhoefer, K. Schmidt-Hoberg and S. Wild, *Dark matter self-interactions from a general spin-0 mediator*, *JCAP* **08** (2017) 003 [[1704.02149](#)].
- [323] M. Vogelsberger, J. Zavala and A. Loeb, *Subhaloes in self-interacting galactic dark matter haloes*, *Monthly Notices of the Royal Astronomical Society* **423** (2012) 3740–3752 [[1201.5892](#)].
- [324] M. Rocha, A.H.G. Peter, J.S. Bullock, M. Kaplinghat, S. Garrison-Kimmel, J. Onorbe et al., *Cosmological Simulations with Self-Interacting Dark Matter I: Constant Density Cores and Substructure*, *Mon. Not. Roy. Astron. Soc.* **430** (2013) 81 [[1208.3025](#)].
- [325] J. Zavala, M. Vogelsberger and M.G. Walker, *Constraining self-interacting dark matter with the milky way’s dwarf spheroidals*, *Monthly Notices of the Royal Astronomical Society: Letters* **431** (2013) L20–L24 [[1211.6426](#)].
- [326] A.H.G. Peter, M. Rocha, J.S. Bullock and M. Kaplinghat, *Cosmological Simulations with Self-Interacting Dark Matter II: Halo Shapes vs. Observations*, *Mon. Not. Roy. Astron. Soc.* **430** (2013) 105 [[1208.3026](#)].
- [327] R. Essig, T. Volansky and T.-T. Yu, *New Constraints and Prospects for sub-GeV Dark Matter Scattering off Electrons in Xenon*, *Phys. Rev. D* **96** (2017) 043017 [[1703.00910](#)].
- [328] XENON collaboration, *Light Dark Matter Search with Ionization Signals in XENON1T*, *Phys. Rev. Lett.* **123** (2019) 251801 [[1907.11485](#)].

- [329] XENON collaboration, *Emission of Single and Few Electrons in XENON1T and Limits on Light Dark Matter*, 2112.12116.
- [330] SPT-3G collaboration, *SPT-3G: A Next-Generation Cosmic Microwave Background Polarization Experiment on the South Pole Telescope*, *Proc. SPIE Int. Soc. Opt. Eng.* **9153** (2014) 91531P [1407.2973].
- [331] SIMONS OBSERVATORY collaboration, *The Simons Observatory: Science goals and forecasts*, *JCAP* **02** (2019) 056 [1808.07445].
- [332] K. Abazajian et al., *CMB-S4 Science Case, Reference Design, and Project Plan*, 1907.04473.
- [333] K.N. Abazajian and M. Kaplinghat, *Neutrino physics from the cosmic microwave background and large-scale structure*, *Annual Review of Nuclear and Particle Science* **66** (2016) 401 [<https://doi.org/10.1146/annurev-nucl-102014-021908>].
- [334] CMB-S4 collaboration, *CMB-S4 Science Book, First Edition*, 1610.02743.
- [335] NASA PICO collaboration, “PICO: Probe of Inflation and Cosmic Origins.” 3, 2019.
- [336] CORE collaboration, *Exploring cosmic origins with CORE: Survey requirements and mission design*, *JCAP* **04** (2018) 014 [1706.04516].
- [337] S.-P. Li, X.-Q. Li, X.-S. Yan and Y.-D. Yang, *Simple estimate of BBN sensitivity to light freeze-in dark matter*, *Phys. Rev. D* **104** (2021) 115007 [2106.07122].
- [338] X. Luo, W. Rodejohann and X.-J. Xu, *Dirac neutrinos and N_{eff}* , *JCAP* **06** (2020) 058 [2005.01629].
- [339] A. Biswas, D. Borah and D. Nanda, *Light Dirac neutrino portal dark matter with observable ΔN_{eff}* , *JCAP* **10** (2021) 002 [2103.05648].
- [340] F. Wang, W. Wang and J.M. Yang, *Split two-Higgs-doublet model and neutrino condensation*, *Europhys. Lett.* **76** (2006) 388 [hep-ph/0601018].
- [341] M. Sher and C. Triola, *Astrophysical Consequences of a Neutrinophilic Two-Higgs-Doublet Model*, *Phys. Rev. D* **83** (2011) 117702 [1105.4844].
- [342] S. Zhou, *Comment on astrophysical consequences of a neutrinophilic 2HDM*, *Phys. Rev. D* **84** (2011) 038701 [1106.3880].
- [343] S.M. Davidson and H.E. Logan, *Dirac neutrinos from a second Higgs doublet*, *Phys. Rev. D* **80** (2009) 095008 [0906.3335].
- [344] P.B. Denton, Y. Farzan and I.M. Shoemaker, *Activating the fourth neutrino of the 3 + 1 scheme*, *Phys. Rev. D* **99** (2019) 035003.

Bibliography

- [345] M. Berbig, S. Jana and A. Trautner, *The Hubble tension and a renormalizable model of gauged neutrino self-interactions*, *Phys. Rev. D* **102** (2020) 115008 [2004.13039].
- [346] A. Bally, S. Jana and A. Trautner, *Neutrino self-interactions and XENON1T electron recoil excess*, *Phys. Rev. Lett.* **125** (2020) 161802 [2006.11919].
- [347] S.-P. Li, X.-Q. Li, X.-S. Yan and Y.-D. Yang, *Effective neutrino number shift from keV-vacuum neutrinoophilic 2HDM*, 2202.10250.
- [348] K.N. Abazajian and J. Heeck, *Observing Dirac neutrinos in the cosmic microwave background*, *Phys. Rev. D* **100** (2019) 075027 [1908.03286].
- [349] P. Fileviez Pérez, C. Murgui and A.D. Plascencia, *Neutrino-Dark Matter Connections in Gauge Theories*, *Phys. Rev. D* **100** (2019) 035041 [1905.06344].
- [350] M.A. Buen-Abad, R.T. Co and K. Harigaya, *Common Origin of Warm Dark Matter and Dark Radiation*, *JCAP* **12** (2020) 024 [1911.13267].
- [351] M. Douspis, L. Salvati and N. Aghanim, *On the Tension between Large Scale Structures and Cosmic Microwave Background*, *PoS EDSU2018* (2018) 037 [1901.05289].
- [352] R.C. Nunes and S. Vagnozzi, *Arbitrating the S8 discrepancy with growth rate measurements from redshift-space distortions*, *Mon. Not. Roy. Astron. Soc.* **505** (2021) 5427 [2106.01208].
- [353] PLANCK collaboration, *Planck 2018 results. X. Constraints on inflation*, *Astron. Astrophys.* **641** (2020) A10 [1807.06211].
- [354] D.S. Salopek, J.R. Bond and J.M. Bardeen, *Designing density fluctuation spectra in inflation*, *Phys. Rev. D* **40** (1989) 1753.
- [355] R. Fakir and W.G. Unruh, *Improvement on cosmological chaotic inflation through nonminimal coupling*, *Phys. Rev. D* **41** (1990) 1783.
- [356] D.I. Kaiser, *Primordial spectral indices from generalized einstein theories*, *Phys. Rev. D* **52** (1995) 4295.
- [357] E. Komatsu and T. Futamase, *Complete constraints on a nonminimally coupled chaotic inflationary scenario from the cosmic microwave background*, *Phys. Rev. D* **59** (1999) 064029.
- [358] F.L. Bezrukov, A. Magnin and M. Shaposhnikov, *Standard Model Higgs boson mass from inflation*, *Phys. Lett. B* **675** (2009) 88 [0812.4950].
- [359] F. Bezrukov, D. Gorbunov and M. Shaposhnikov, *On initial conditions for the Hot Big Bang*, *JCAP* **06** (2009) 029 [0812.3622].

- [360] S. Choubey and A. Kumar, *Inflation and Dark Matter in the Inert Doublet Model*, *JHEP* **11** (2017) 080 [1707.06587].
- [361] D.I. Kaiser and E.I. Sfakianakis, *Multifield Inflation after Planck: The Case for Nonminimal Couplings*, *Phys. Rev. Lett.* **112** (2014) 011302 [1304.0363].
- [362] K. Schutz, E.I. Sfakianakis and D.I. Kaiser, *Multifield Inflation after Planck: Isocurvature Modes from Nonminimal Couplings*, *Phys. Rev. D* **89** (2014) 064044 [1310.8285].
- [363] M. Beltran, J. Garcia-Bellido and J. Lesgourges, *Isocurvature bounds on axions revisited*, *Phys. Rev. D* **75** (2007) 103507 [hep-ph/0606107].
- [364] D. Bettoni and J. Rubio, *Quintessential Affleck-Dine baryogenesis with non-minimal couplings*, *Phys. Lett. B* **784** (2018) 122 [1805.02669].
- [365] F. Bezrukov and M. Shaposhnikov, *Standard Model Higgs boson mass from inflation: Two loop analysis*, *JHEP* **07** (2009) 089 [0904.1537].
- [366] J. Garcia-Bellido, J. Rubio, M. Shaposhnikov and D. Zenhausern, *Higgs-Dilaton Cosmology: From the Early to the Late Universe*, *Phys. Rev. D* **84** (2011) 123504 [1107.2163].
- [367] A.O. Barvinsky, A.Y. Kamenshchik and A.A. Starobinsky, *Inflation scenario via the Standard Model Higgs boson and LHC*, *JCAP* **11** (2008) 021 [0809.2104].
- [368] A.O. Barvinsky, A.Y. Kamenshchik, C. Kiefer, A.A. Starobinsky and C. Steinwachs, *Asymptotic freedom in inflationary cosmology with a non-minimally coupled Higgs field*, *JCAP* **12** (2009) 003 [0904.1698].
- [369] J. Rubio, *Higgs inflation*, *Front. Astron. Space Sci.* **5** (2019) 50 [1807.02376].
- [370] R.N. Lerner and J. McDonald, *Higgs Inflation and Naturalness*, *JCAP* **04** (2010) 015 [0912.5463].
- [371] C.P. Burgess, H.M. Lee and M. Trott, *Comment on Higgs Inflation and Naturalness*, *JHEP* **07** (2010) 007 [1002.2730].
- [372] M.P. Hertzberg, *On Inflation with Non-minimal Coupling*, *JHEP* **11** (2010) 023 [1002.2995].
- [373] A. Escrivà and C. Germani, *Beyond dimensional analysis: Higgs and new Higgs inflations do not violate unitarity*, *Phys. Rev. D* **95** (2017) 123526 [1612.06253].
- [374] J. Fumagalli, S. Mooij and M. Postma, *Unitarity and predictiveness in new Higgs inflation*, *JHEP* **03** (2018) 038 [1711.08761].
- [375] T. Tenkanen, *Minimal Higgs inflation with an R^2 term in Palatini gravity*, *Phys. Rev. D* **99** (2019) 063528 [1901.01794].

Bibliography

- [376] Y. Hamada, H. Kawai and K.-y. Oda, *Minimal Higgs inflation*, *PTEP* **2014** (2014) 023B02 [1308.6651].
- [377] Y. Hamada, H. Kawai, K.-y. Oda and S.C. Park, *Higgs Inflation is Still Alive after the Results from BICEP2*, *Phys. Rev. Lett.* **112** (2014) 241301 [1403.5043].
- [378] F. Bezrukov and M. Shaposhnikov, *Higgs inflation at the critical point*, *Phys. Lett. B* **734** (2014) 249 [1403.6078].
- [379] Y. Hamada, H. Kawai, K.-y. Oda and S.C. Park, *Higgs inflation from Standard Model criticality*, *Phys. Rev. D* **91** (2015) 053008 [1408.4864].
- [380] M. Drees and Y. Xu, *Overshooting, Critical Higgs Inflation and Second Order Gravitational Wave Signatures*, *Eur. Phys. J. C* **81** (2021) 182 [1905.13581].
- [381] G.F. Giudice and H.M. Lee, *Unitarizing Higgs Inflation*, *Phys. Lett. B* **694** (2011) 294 [1010.1417].
- [382] F. Kahlhoefer and J. McDonald, *WIMP Dark Matter and Unitarity-Conserving Inflation via a Gauge Singlet Scalar*, *JCAP* **11** (2015) 015 [1507.03600].
- [383] G. Ballesteros, J. Redondo, A. Ringwald and C. Tamarit, *Standard Model—axion—seesaw—Higgs portal inflation. Five problems of particle physics and cosmology solved in one stroke*, *JCAP* **08** (2017) 001 [1610.01639].
- [384] N. Okada, M.U. Rehman and Q. Shafi, *Non-Minimal B-L Inflation with Observable Gravity Waves*, *Phys. Lett. B* **701** (2011) 520 [1102.4747].
- [385] W. Buchmuller, V. Domcke and K. Schmitz, *Spontaneous B-L Breaking as the Origin of the Hot Early Universe*, *Nucl. Phys. B* **862** (2012) 587 [1202.6679].
- [386] D.A. Kirzhnits, *Weinberg model in the hot universe*, *JETP Lett.* **15** (1972) 529.
- [387] D. Kirzhnits and A. Linde, *Macroscopic consequences of the weinberg model*, *Physics Letters B* **42** (1972) 471.
- [388] N. Bernal and Y. Xu, *Polynomial inflation and dark matter*, *Eur. Phys. J. C* **81** (2021) 877 [2106.03950].
- [389] I. Masina, *Dark matter and dark radiation from evaporating primordial black holes*, *Eur. Phys. J. Plus* **135** (2020) 552 [2004.04740].
- [390] V. Iršič et al., *New Constraints on the free-streaming of warm dark matter from intermediate and small scale Lyman- α forest data*, *Phys. Rev. D* **96** (2017) 023522 [1702.01764].
- [391] R.N. Lerner and J. McDonald, *Distinguishing Higgs inflation and its variants*, *Phys. Rev. D* **83** (2011) 123522 [1104.2468].

- [392] R.N. Lerner and J. McDonald, *Gauge singlet scalar as inflaton and thermal relic dark matter*, *Phys. Rev. D* **80** (2009) 123507 [0909.0520].
- [393] M. Yoshimura, *Origin of Cosmological Baryon Asymmetry*, *Phys. Lett. B* **88** (1979) 294.
- [394] S. Weinberg, *Cosmological Production of Baryons*, *Phys. Rev. Lett.* **42** (1979) 850.
- [395] J.N. Fry, K.A. Olive and M.S. Turner, *Hierarchy of Cosmological Baryon Generation*, *Phys. Rev. Lett.* **45** (1980) 2074.
- [396] E.K. Akhmedov, V.A. Rubakov and A.Y. Smirnov, *Baryogenesis via neutrino oscillations*, *Phys. Rev. Lett.* **81** (1998) 1359 [hep-ph/9803255].
- [397] Y.-Y. Charng, D.-S. Lee, C.N. Leung and K.-W. Ng, *Affleck-Dine Baryogenesis, Split Supersymmetry, and Inflation*, *Phys. Rev. D* **80** (2009) 063519 [0802.1328].
- [398] M.P. Hertzberg and J. Karouby, *Baryogenesis from the Inflaton Field*, *Phys. Lett. B* **737** (2014) 34 [1309.0007].
- [399] M.P. Hertzberg and J. Karouby, *Generating the Observed Baryon Asymmetry from the Inflaton Field*, *Phys. Rev. D* **89** (2014) 063523 [1309.0010].
- [400] N. Takeda, *Inflatonic baryogenesis with large tensor mode*, *Phys. Lett. B* **746** (2015) 368 [1405.1959].
- [401] J.M. Cline, M. Puel and T. Toma, *Affleck-Dine inflation*, *Phys. Rev. D* **101** (2020) 043014 [1909.12300].
- [402] J.M. Cline, M. Puel and T. Toma, *A little theory of everything, with heavy neutral leptons*, *JHEP* **05** (2020) 039 [2001.11505].
- [403] C.-M. Lin and K. Kohri, *Inflaton as the Affleck-Dine Baryogenesis Field in Hilltop Supernatural Inflation*, *Phys. Rev. D* **102** (2020) 043511 [2003.13963].
- [404] A. Lloyd-Stubbs and J. McDonald, *A Minimal Approach to Baryogenesis via Affleck-Dine and Inflaton Mass Terms*, *Phys. Rev. D* **103** (2021) 123514 [2008.04339].
- [405] N.D. Barrie, C. Han and H. Murayama, *Affleck-Dine Leptogenesis from Higgs Inflation*, *Phys. Rev. Lett.* **128** (2022) 141801 [2106.03381].
- [406] R.N. Mohapatra and N. Okada, *Unified model for inflation, pseudo-Goldstone dark matter, neutrino mass, and baryogenesis*, *Phys. Rev. D* **105** (2022) 035024 [2112.02069].
- [407] R.N. Mohapatra and N. Okada, *Neutrino Mass from Affleck-Dine Leptogenesis and WIMP Dark Matter*, 2201.06151.

Bibliography

- [408] G. 't Hooft, *Naturalness, chiral symmetry, and spontaneous chiral symmetry breaking*, *NATO Sci. Ser. B* **59** (1980) 135.
- [409] M.L. Perl, E.R. Lee and D. Loomba, *Searches for fractionally charged particles*, *Annual Review of Nuclear and Particle Science* **59** (2009) 47 [<https://doi.org/10.1146/annurev-nucl-121908-122035>].
- [410] K. Harigaya, T. Hayakawa, M. Kawasaki and M. Yamada, *Cosmology with a Heavy Polonyi Field*, *JCAP* **06** (2016) 015 [[1601.02140](https://arxiv.org/abs/1601.02140)].
- [411] K. Harigaya, *Nambu-Goldstone Affleck-Dine Baryogenesis*, *JHEP* **08** (2019) 085 [[1906.05286](https://arxiv.org/abs/1906.05286)].
- [412] M. Dine, L. Randall and S.D. Thomas, *Baryogenesis from flat directions of the supersymmetric standard model*, *Nucl. Phys. B* **458** (1996) 291 [[hep-ph/9507453](https://arxiv.org/abs/hep-ph/9507453)].
- [413] S. Weinberg, *Gauge and Global Symmetries at High Temperature*, *Phys. Rev. D* **9** (1974) 3357.
- [414] P. Langacker and S.-Y. Pi, *Magnetic monopoles in grand unified theories*, *Phys. Rev. Lett.* **45** (1980) 1.
- [415] J. Hasenkamp and J. Kersten, *Leptogenesis, Gravitino Dark Matter and Entropy Production*, *Phys. Rev. D* **82** (2010) 115029 [[1008.1740](https://arxiv.org/abs/1008.1740)].
- [416] H.H. Patel, *Package-X 2.0: A Mathematica package for the analytic calculation of one-loop integrals*, *Comput. Phys. Commun.* **218** (2017) 66 [[1612.00009](https://arxiv.org/abs/1612.00009)].
- [417] G. Ballesteros, J. Redondo, A. Ringwald and C. Tamarit, *Unifying inflation with the axion, dark matter, baryogenesis and the seesaw mechanism*, *Phys. Rev. Lett.* **118** (2017) 071802 [[1608.05414](https://arxiv.org/abs/1608.05414)].
- [418] G. Ballesteros, J. Redondo, A. Ringwald and C. Tamarit, *Several Problems in Particle Physics and Cosmology Solved in One SMASH*, *Front. Astron. Space Sci.* **6** (2019) 55 [[1904.05594](https://arxiv.org/abs/1904.05594)].
- [419] M. Shin, *Light Neutrino Masses and Strong CP Problem*, *Phys. Rev. Lett.* **59** (1987) 2515.
- [420] J.E. Kim, *Weak-interaction singlet and strong CP invariance*, *Phys. Rev. Lett.* **43** (1979) 103.
- [421] M. Shifman, A. Vainshtein and V. Zakharov, *Can confinement ensure natural cp invariance of strong interactions?*, *Nuclear Physics B* **166** (1980) 493.
- [422] M. Dine, W. Fischler and M. Srednicki, *A simple solution to the strong cp problem with a harmless axion*, *Physics Letters B* **104** (1981) 199.

- [423] S.L. Glashow, *The Future of Elementary Particle Physics, NATO Sci. Ser. B* **61** (1980) 687.
- [424] R.D. Peccei and H.R. Quinn, *CP conservation in the presence of pseudoparticles*, *Phys. Rev. Lett.* **38** (1977) 1440.
- [425] M. Fukugita and T. Yanagida, *Baryogenesis without grand unification*, *Physics Letters B* **174** (1986) 45.
- [426] A. Pilaftsis and T.E.J. Underwood, *Resonant leptogenesis*, *Nucl. Phys. B* **692** (2004) 303 [[hep-ph/0309342](#)].
- [427] T. Hambye, M. Raidal and A. Strumia, *Efficiency and maximal CP-asymmetry of scalar triplet leptogenesis*, *Phys. Lett. B* **632** (2006) 667 [[hep-ph/0510008](#)].
- [428] T. Asaka, S. Blanchet and M. Shaposhnikov, *The nuMSM, dark matter and neutrino masses*, *Phys. Lett. B* **631** (2005) 151 [[hep-ph/0503065](#)].
- [429] T. Asaka and M. Shaposhnikov, *The ν MSM, dark matter and baryon asymmetry of the universe*, *Phys. Lett. B* **620** (2005) 17 [[hep-ph/0505013](#)].
- [430] M. Shaposhnikov and I. Tkachev, *The nuMSM, inflation, and dark matter*, *Phys. Lett. B* **639** (2006) 414 [[hep-ph/0604236](#)].
- [431] A. Salvio, *A Simple Motivated Completion of the Standard Model below the Planck Scale: Axions and Right-Handed Neutrinos*, *Phys. Lett. B* **743** (2015) 428 [[1501.03781](#)].
- [432] A.H. Sopov and R.R. Volkas, “VISH ν : a unified solution to five SM shortcomings with a protected electroweak scale.” 6, 2022.
- [433] E. Ma and R. Srivastava, *Dirac or inverse seesaw neutrino masses from gauged B-L symmetry*, *Mod. Phys. Lett. A* **30** (2015) 1530020 [[1504.00111](#)].
- [434] E. Ma, *$U(1)_\chi$ and Seesaw Dirac Neutrinos*, *Letters in High Energy Physics* (2018) [[1811.09645](#)].
- [435] S. Centelles Chuliá, E. Ma, R. Srivastava and J.W.F. Valle, *Dirac Neutrinos and Dark Matter Stability from Lepton Quarticity*, *Phys. Lett. B* **767** (2017) 209 [[1606.04543](#)].
- [436] S. Centelles Chuliá, R. Srivastava and J.W.F. Valle, *Seesaw roadmap to neutrino mass and dark matter*, *Phys. Lett. B* **781** (2018) 122 [[1802.05722](#)].
- [437] S. Centelles Chuliá, R. Srivastava and J.W.F. Valle, *Seesaw Dirac neutrino mass through dimension-six operators*, *Phys. Rev. D* **98** (2018) 035009 [[1804.03181](#)].
- [438] S. Centelles Chuliá, R. Cepedello, E. Peinado and R. Srivastava, *Systematic classification of two loop $d = 4$ Dirac neutrino mass models and the Diracness-dark matter stability connection*, *JHEP* **10** (2019) 093 [[1907.08630](#)].

Bibliography

- [439] M. Roncadelli and D. Wyler, *Naturally light dirac neutrinos in gauge theories*, *Physics Letters B* **133** (1983) 325.
- [440] S. Weinberg, *Baryon- and lepton-nonconserving processes*, *Phys. Rev. Lett.* **43** (1979) 1566.
- [441] E. Peinado, M. Reig, R. Srivastava and J.W.F. Valle, *Dirac neutrinos from Peccei–Quinn symmetry: A fresh look at the axion*, *Mod. Phys. Lett. A* **35** (2020) 2050176 [1910.02961].
- [442] R.D. Peccei and H.R. Quinn, *Constraints Imposed by CP Conservation in the Presence of Instantons*, *Phys. Rev. D* **16** (1977) 1791.
- [443] K. Fujikawa, *On the Evaluation of Chiral Anomaly in Gauge Theories with Gamma(5) Couplings*, *Phys. Rev. D* **29** (1984) 285.
- [444] L. Di Luzio, M. Giannotti, E. Nardi and L. Visinelli, *The landscape of QCD axion models*, *Phys. Rept.* **870** (2020) 1 [2003.01100].
- [445] A. Vilenkin and A.E. Everett, *Cosmic strings and domain walls in models with goldstone and pseudo-goldstone bosons*, *Phys. Rev. Lett.* **48** (1982) 1867.
- [446] A. Vilenkin, *Cosmic strings and domain walls*, *Physics Reports* **121** (1985) 263.
- [447] A. Vilenkin and E.P.S. Shellard, *Cosmic Strings and Other Topological Defects*, Cambridge University Press (7, 2000).
- [448] W.H. Press, *Spontaneous production of the zel'dovich spectrum of cosmological fluctuations*, *Physica Scripta* **21** (1980) 702.
- [449] P. Sikivie, *Axions, domain walls, and the early universe*, *Phys. Rev. Lett.* **48** (1982) 1156.
- [450] T.W.B. Kibble, *Topology of cosmic domains and strings*, *Journal of Physics A: Mathematical and General* **9** (1976) 1387.
- [451] T.W.B. Kibble, G. Lazarides and Q. Shafi, *Walls bounded by strings*, *Phys. Rev. D* **26** (1982) 435.
- [452] T. Kibble, *Some implications of a cosmological phase transition*, *Physics Reports* **67** (1980) 183.
- [453] A. Vilenkin, *Cosmic strings*, *Phys. Rev. D* **24** (1981) 2082.
- [454] R. Davis, *Cosmic axions from cosmic strings*, *Physics Letters B* **180** (1986) 225.
- [455] T. Hiramatsu, M. Kawasaki, K. Saikawa and T. Sekiguchi, *Production of dark matter axions from collapse of string-wall systems*, *Phys. Rev. D* **85** (2012) 105020 [1202.5851].

- [456] M. Gorgetto, E. Hardy and G. Villadoro, *Axions from Strings: the Attractive Solution*, *JHEP* **07** (2018) 151 [[1806.04677](#)].
- [457] A. Vaquero, J. Redondo and J. Stadler, *Early seeds of axion miniclusters*, *Journal of Cosmology and Astroparticle Physics* **2019** (2019) 012.
- [458] S.M. Barr and J.E. Kim, *New confining force solution of the qcd axion domain-wall problem*, *Phys. Rev. Lett.* **113** (2014) 241301.
- [459] M. Reig, *On the high-scale instanton interference effect: axion models without domain wall problem*, *JHEP* **08** (2019) 167 [[1901.00203](#)].
- [460] A. Caputo and M. Reig, *Cosmic implications of a low-scale solution to the axion domain wall problem*, *Phys. Rev. D* **100** (2019) 063530 [[1905.13116](#)].
- [461] P. Sikivie, *Axion Cosmology*, *Lect. Notes Phys.* **741** (2008) 19 [[astro-ph/0610440](#)].
- [462] M. Kawasaki and K. Nakayama, *Axions: Theory and Cosmological Role*, *Ann. Rev. Nucl. Part. Sci.* **63** (2013) 69 [[1301.1123](#)].
- [463] G. Lazarides and Q. Shafi, *Axion models with no domain wall problem*, *Physics Letters B* **115** (1982) 21.
- [464] S. Barr, D. Reiss and A. Zee, *Families, the invisible axion, and domain walls*, *Physics Letters B* **116** (1982) 227.
- [465] L. Di Luzio, F. Mescia and E. Nardi, *Redefining the Axion Window*, *Phys. Rev. Lett.* **118** (2017) 031801 [[1610.07593](#)].
- [466] L. Di Luzio, F. Mescia and E. Nardi, *Window for preferred axion models*, *Phys. Rev. D* **96** (2017) 075003 [[1705.05370](#)].
- [467] R.J. Scherrer and M.S. Turner, *Decaying Particles Do Not Heat Up the Universe*, *Phys. Rev. D* **31** (1985) 681.
- [468] CMS collaboration, *Search for vector-like T and B quark pairs in final states with leptons at $\sqrt{s} = 13$ TeV*, *JHEP* **08** (2018) 177 [[1805.04758](#)].
- [469] ATLAS collaboration, *Combination of the searches for pair-produced vector-like partners of the third-generation quarks at $\sqrt{s} = 13$ TeV with the ATLAS detector*, *Phys. Rev. Lett.* **121** (2018) 211801 [[1808.02343](#)].
- [470] R.N. Mohapatra, *Mechanism for understanding small neutrino mass in superstring theories*, *Phys. Rev. Lett.* **56** (1986) 561.
- [471] R.N. Mohapatra and J.W.F. Valle, *Neutrino mass and baryon-number nonconservation in superstring models*, *Phys. Rev. D* **34** (1986) 1642.

Bibliography

- [472] R. Kallosh, A.D. Linde, D.A. Linde and L. Susskind, *Gravity and global symmetries*, *Phys. Rev. D* **52** (1995) 912 [[hep-th/9502069](#)].
- [473] R. Alonso and A. Urbano, *Wormholes and masses for Goldstone bosons*, *JHEP* **02** (2019) 136 [[1706.07415](#)].
- [474] H.M. Georgi, L.J. Hall and M.B. Wise, *Grand unified models with an automatic *peccei-quinn* symmetry*, *Nuclear Physics B* **192** (1981) 409.
- [475] M. Dine and N. Seiberg, *String theory and the strong *cp* problem*, *Nuclear Physics B* **273** (1986) 109.
- [476] S.M. Barr and D. Seckel, *Planck-scale corrections to axion models*, *Phys. Rev. D* **46** (1992) 539.
- [477] M. Kamionkowski and J. March-Russell, *Planck-scale physics and the *peccei-quinn* mechanism*, *Physics Letters B* **282** (1992) 137.
- [478] R. Holman, S.D.H. Hsu, T.W. Kephart, E.W. Kolb, R. Watkins and L.M. Widrow, *Solutions to the strong *CP* problem in a world with gravity*, *Phys. Lett. B* **282** (1992) 132 [[hep-ph/9203206](#)].
- [479] S. Ghigna, M. Lusignoli and M. Roncadelli, *Instability of the invisible axion*, *Physics Letters B* **283** (1992) 278.
- [480] A. de Gouvea and J.W.F. Valle, *Minimalistic neutrino mass model*, *Phys. Lett. B* **501** (2001) 115 [[hep-ph/0010299](#)].
- [481] J.T. Penedo, Y. Reyimuaji and X. Zhang, “Axionic Dirac seesaw and electroweak vacuum stability.” 8, 2022.
- [482] F. Wilczek, *Problem of strong *p* and *t* invariance in the presence of instantons*, *Phys. Rev. Lett.* **40** (1978) 279.
- [483] W.A. Bardeen, R.D. Peccei and T. Yanagida, *CONSTRAINTS ON VARIANT AXION MODELS*, *Nucl. Phys. B* **279** (1987) 401.
- [484] M.E. Machacek and M.T. Vaughn, *Two-loop renormalization group equations in a general quantum field theory: (i). wave function renormalization*, *Nuclear Physics B* **222** (1983) 83.
- [485] L. Di Luzio, R. Gröber, J.F. Kamenik and M. Nardecchia, *Accidental matter at the LHC*, *JHEP* **07** (2015) 074 [[1504.00359](#)].
- [486] V. Plakkot and S. Hoof, *Anomaly ratio distributions of hadronic axion models with multiple heavy quarks*, *Phys. Rev. D* **104** (2021) 075017 [[2107.12378](#)].
- [487] L.N. Mihaila, J. Salomon and M. Steinhauser, *Renormalization constants and beta functions for the gauge couplings of the Standard Model to three-loop order*, *Phys. Rev. D* **86** (2012) 096008 [[1208.3357](#)].

[488] PARTICLE DATA GROUP collaboration, *Review of Particle Physics*, *PTEP* **2020** (2020) 083C01.

[489] D.B. Kaplan, *Opening the axion window*, *Nuclear Physics B* **260** (1985) 215.

[490] M. Srednicki, *Axion Couplings to Matter. 1. CP Conserving Parts*, *Nucl. Phys. B* **260** (1985) 689.

[491] M. Farina, D. Pappadopulo, F. Rompineve and A. Tesi, *The photo-philic QCD axion*, *JHEP* **01** (2017) 095 [[1611.09855](https://arxiv.org/abs/1611.09855)].

[492] T. Higaki, K.S. Jeong, N. Kitajima and F. Takahashi, *The QCD Axion from Aligned Axions and Diphoton Excess*, *Phys. Lett. B* **755** (2016) 13 [[1512.05295](https://arxiv.org/abs/1512.05295)].

[493] T. Higaki, K.S. Jeong, N. Kitajima and F. Takahashi, *Quality of the Peccei-Quinn symmetry in the Aligned QCD Axion and Cosmological Implications*, *JHEP* **06** (2016) 150 [[1603.02090](https://arxiv.org/abs/1603.02090)].

[494] A.V. Sokolov and A. Ringwald, *Photophilic hadronic axion from heavy magnetic monopoles*, *JHEP* **06** (2021) 123 [[2104.02574](https://arxiv.org/abs/2104.02574)].

[495] A.V. Sokolov and A. Ringwald, “Electromagnetic Couplings of Axions.” 5, 2022.

[496] A. Hook, *Solving the Hierarchy Problem Discretely*, *Phys. Rev. Lett.* **120** (2018) 261802 [[1802.10093](https://arxiv.org/abs/1802.10093)].

[497] L. Di Luzio, B. Gavela, P. Quilez and A. Ringwald, *An even lighter QCD axion*, *JHEP* **05** (2021) 184 [[2102.00012](https://arxiv.org/abs/2102.00012)].

[498] C. O’Hare, “cajohare/axionlimits: Axionlimits.” <https://cajohare.github.io/AxionLimits/>, July, 2020. 10.5281/zenodo.3932430.

[499] D. Alesini et al., *Galactic axions search with a superconducting resonant cavity*, *Phys. Rev. D* **99** (2019) 101101 [[1903.06547](https://arxiv.org/abs/1903.06547)].

[500] D. Alesini et al., *Search for invisible axion dark matter of mass $m_a = 43 \mu\text{eV}$ with the QUAX-- $a\gamma$ experiment*, *Phys. Rev. D* **103** (2021) 102004 [[2012.09498](https://arxiv.org/abs/2012.09498)].

[501] HAYSTAC collaboration, *Results from phase 1 of the HAYSTAC microwave cavity axion experiment*, *Phys. Rev. D* **97** (2018) 092001 [[1803.03690](https://arxiv.org/abs/1803.03690)].

[502] HAYSTAC collaboration, *A quantum-enhanced search for dark matter axions*, *Nature* **590** (2021) 238 [[2008.01853](https://arxiv.org/abs/2008.01853)].

[503] B.T. McAllister, G. Flower, E.N. Ivanov, M. Goryachev, J. Bourhill and M.E. Tobar, *The ORGAN Experiment: An axion haloscope above 15 GHz*, *Phys. Dark Univ.* **18** (2017) 67 [[1706.00209](https://arxiv.org/abs/1706.00209)].

Bibliography

- [504] A. Quiskamp, B.T. McAllister, P. Altin, E.N. Ivanov, M. Goryachev and M.E. Tobar, *Direct search for dark matter axions excluding alp cogenesis in the 63- to 67- μ eV range with the organ experiment*, *Science Advances* **8** (2022) eabq3765 [<https://www.science.org/doi/pdf/10.1126/sciadv.abq3765>].
- [505] CAST collaboration, *First results of the CAST-RADES haloscope search for axions at 34.67 μ eV*, *JHEP* **21** (2020) 075 [2104.13798].
- [506] S. Beurthey et al., “MADMAX Status Report.” 3, 2020.
- [507] S.J. Asztalos, G. Carosi, C. Hagmann, D. Kinion, K. van Bibber, M. Hotz et al., *SQUID-Based Microwave Cavity Search for Dark-Matter Axions*, *Phys. Rev. Lett.* **104** (2010) 041301 [0910.5914].
- [508] I. Stern, *ADMX Status*, *PoS ICHEP2016* (2016) 198 [1612.08296].
- [509] ADMX collaboration, *A Search for Invisible Axion Dark Matter with the Axion Dark Matter Experiment*, *Phys. Rev. Lett.* **120** (2018) 151301 [1804.05750].
- [510] ADMX collaboration, *Extended Search for the Invisible Axion with the Axion Dark Matter Experiment*, *Phys. Rev. Lett.* **124** (2020) 101303 [1910.08638].
- [511] ADMX collaboration, *Search for Invisible Axion Dark Matter in the 3.3–4.2 μ eV Mass Range*, *Phys. Rev. Lett.* **127** (2021) 261803 [2110.06096].
- [512] ADMX collaboration, *Piezoelectrically Tuned Multimode Cavity Search for Axion Dark Matter*, *Phys. Rev. Lett.* **121** (2018) 261302 [1901.00920].
- [513] C. Bartram et al., *Dark Matter Axion Search Using a Josephson Traveling Wave Parametric Amplifier*, 10, 2021.
- [514] N. Crisosto, P. Sikivie, N.S. Sullivan, D.B. Tanner, J. Yang and G. Rybka, *ADMX SLIC: Results from a Superconducting LC Circuit Investigating Cold Axions*, *Phys. Rev. Lett.* **124** (2020) 241101 [1911.05772].
- [515] D.H. et al., “BRASS experiment.”.
- [516] J.L. Ouellet et al., *First Results from ABRACADABRA-10 cm: A Search for Sub- μ eV Axion Dark Matter*, *Phys. Rev. Lett.* **122** (2019) 121802 [1810.12257].
- [517] C.P. Salemi et al., *Search for Low-Mass Axion Dark Matter with ABRACADABRA-10 cm*, *Phys. Rev. Lett.* **127** (2021) 081801 [2102.06722].
- [518] S. Lee, S. Ahn, J. Choi, B.R. Ko and Y.K. Semertzidis, *Axion Dark Matter Search around 6.7 μ eV*, *Phys. Rev. Lett.* **124** (2020) 101802 [2001.05102].
- [519] J. Jeong, S. Youn, S. Bae, J. Kim, T. Seong, J.E. Kim et al., *Search for Invisible Axion Dark Matter with a Multiple-Cell Haloscope*, *Phys. Rev. Lett.* **125** (2020) 221302 [2008.10141].

- [520] CAPP collaboration, *First Results from an Axion Haloscope at CAPP around 10.7 μ eV*, *Phys. Rev. Lett.* **126** (2021) 191802 [2012.10764].
- [521] D.M.R. collaboration, “Dark Matter Radio.”
- [522] D. Alesini, D. Babusci, D. Di Gioacchino, C. Gatti, G. Lamanna and C. Ligi, “The KLASH Proposal.” 7, 2017.
- [523] S. DePanfilis, A.C. Melissinos, B.E. Moskowitz, J.T. Rogers, Y.K. Semertzidis, W.U. Wuensch et al., *Limits on the abundance and coupling of cosmic axions at 4.5 μ eV*, *Phys. Rev. Lett.* **59** (1987) 839.
- [524] A.V. Gramolin, D. Aybas, D. Johnson, J. Adam and A.O. Sushkov, *Search for axion-like dark matter with ferromagnets*, *Nature Phys.* **17** (2021) 79 [2003.03348].
- [525] C. Hagmann, P. Sikivie, N.S. Sullivan and D.B. Tanner, *Results from a search for cosmic axions*, *Phys. Rev. D* **42** (1990) 1297.
- [526] CAST collaboration, *An Improved limit on the axion-photon coupling from the CAST experiment*, *JCAP* **04** (2007) 010 [hep-ex/0702006].
- [527] CAST collaboration, *New CAST Limit on the Axion-Photon Interaction*, *Nature Phys.* **13** (2017) 584 [1705.02290].
- [528] I. Shilon, A. Dudarev, H. Silva and H.H.J. ten Kate, *Conceptual Design of a New Large Superconducting Toroid for IAXO, the New International AXion Observatory*, *IEEE Transactions on Applied Superconductivity* **23** (2013) 4500604 [1212.4633].
- [529] S.-F. Ge, K. Hamaguchi, K. Ichimura, K. Ishidoshiro, Y. Kanazawa, Y. Kishimoto et al., *Supernova-scope for the Direct Search of Supernova Axions*, *JCAP* **11** (2020) 059 [2008.03924].
- [530] K. Ehret et al., *New ALPS Results on Hidden-Sector Lightweights*, *Phys. Lett. B* **689** (2010) 149 [1004.1313].
- [531] M.D. Ortiz et al., *Design of the ALPS II optical system*, *Phys. Dark Univ.* **35** (2022) 100968 [2009.14294].
- [532] M. Betz, F. Caspers, M. Gasior, M. Thumm and S.W. Rieger, *First results of the CERN Resonant Weakly Interacting sub-eV Particle Search (CROWS)*, *Phys. Rev. D* **88** (2013) 075014 [1310.8098].
- [533] OSQAR collaboration, *New exclusion limits on scalar and pseudoscalar axionlike particles from light shining through a wall*, *Phys. Rev. D* **92** (2015) 092002 [1506.08082].

Bibliography

- [534] F. Della Valle, A. Ejlli, U. Gastaldi, G. Messineo, E. Milotti, R. Pengo et al., *The PVLAS experiment: measuring vacuum magnetic birefringence and dichroism with a birefringent Fabry-Perot cavity*, *Eur. Phys. J. C* **76** (2016) 24 [1510.08052].
- [535] D. Cadamuro and J. Redondo, *Cosmological bounds on pseudo Nambu-Goldstone bosons*, *JCAP* **02** (2012) 032 [1110.2895].
- [536] P.F. Depta, M. Hufnagel and K. Schmidt-Hoberg, *Robust cosmological constraints on axion-like particles*, *JCAP* **05** (2020) 009 [2002.08370].
- [537] V.M. Mehta, M. Demirtas, C. Long, D.J.E. Marsh, L. McAllister and M.J. Stott, “Superradiance Exclusions in the Landscape of Type IIB String Theory.” 11, 2020.
- [538] D. Wouters and P. Brun, *Constraints on Axion-like Particles from X-Ray Observations of the Hydra Galaxy Cluster*, *Astrophys. J.* **772** (2013) 44 [1304.0989].
- [539] C.S. Reynolds, M.C.D. Marsh, H.R. Russell, A.C. Fabian, R. Smith, F. Tombesi et al., *Astrophysical limits on very light axion-like particles from chandra grating spectroscopy of NGC 1275*, *The Astrophysical Journal* **890** (2020) 59.
- [540] J. Sisk-Reynés, J.H. Matthews, C.S. Reynolds, H.R. Russell, R.N. Smith and M.C.D. Marsh, *New constraints on light axion-like particles using Chandra transmission grating spectroscopy of the powerful cluster-hosted quasar H1821+643*, *Monthly Notices of the Royal Astronomical Society* **510** (2021) 1264 [<https://academic.oup.com/mnras/article-pdf/510/1/1264/41916805/stab3464.pdf>].
- [541] C. Dessert, A.J. Long and B.R. Safdi, *No evidence for axions from chandra observation of the magnetic white dwarf re j0317-853*, *Phys. Rev. Lett.* **128** (2022) 071102.
- [542] FERMI-LAT collaboration, *Search for Spectral Irregularities due to Photon-Axionlike-Particle Oscillations with the Fermi Large Area Telescope*, *Phys. Rev. Lett.* **116** (2016) 161101 [1603.06978].
- [543] M. Meyer, M. Giannotti, A. Mirizzi, J. Conrad and M.A. Sánchez-Conde, *Fermi Large Area Telescope as a Galactic Supernovae Axionscope*, *Phys. Rev. Lett.* **118** (2017) 011103 [1609.02350].
- [544] M. Meyer and T. Petrushevska, *Search for Axionlike-Particle-Induced Prompt γ -Ray Emission from Extragalactic Core-Collapse Supernovae with the Fermi Large Area Telescope*, *Phys. Rev. Lett.* **124** (2020) 231101 [2006.06722].
- [545] F. Calore, P. Carenza, C. Eckner, T. Fischer, M. Giannotti, J. Jaeckel et al., *3d template-based fermi-lat constraints on the diffuse supernova axion-like particle background*, *Phys. Rev. D* **105** (2022) 063028.

- [546] C. Dessert, J.W. Foster and B.R. Safdi, *X-ray Searches for Axions from Super Star Clusters*, *Phys. Rev. Lett.* **125** (2020) 261102 [2008.03305].
- [547] M.A. Buen-Abad, J. Fan and C. Sun, *Constraints on axions from cosmic distance measurements*, *JHEP* **02** (2022) 103 [2011.05993].
- [548] H.E.S.S. collaboration, *Constraints on axionlike particles with H.E.S.S. from the irregularity of the PKS 2155-304 energy spectrum*, *Phys. Rev. D* **88** (2013) 102003 [1311.3148].
- [549] A. Ayala, I. Domínguez, M. Giannotti, A. Mirizzi and O. Straniero, *Revisiting the bound on axion-photon coupling from Globular Clusters*, *Phys. Rev. Lett.* **113** (2014) 191302 [1406.6053].
- [550] M.J. Dolan, F.J. Hiskens and R.R. Volkas, *Constraining axion-like particles using the white dwarf initial-final mass relation*, *JCAP* **09** (2021) 010 [2102.00379].
- [551] M.J. Dolan, F.J. Hiskens and R.R. Volkas, “Advancing Globular Cluster Constraints on the Axion-Photon Coupling.” 7, 2022.
- [552] H.-J. Li, J.-G. Guo, X.-J. Bi, S.-J. Lin and P.-F. Yin, *Limits on axion-like particles from Mrk 421 with 4.5-year period observations by ARGO-YBJ and Fermi-LAT*, *Phys. Rev. D* **103** (2021) 083003 [2008.09464].
- [553] J.W. Foster, Y. Kahn, O. Macias, Z. Sun, R.P. Eatough, V.I. Kondratiev et al., *Green Bank and Effelsberg Radio Telescope Searches for Axion Dark Matter Conversion in Neutron Star Magnetospheres*, *Phys. Rev. Lett.* **125** (2020) 171301 [2004.00011].
- [554] J. Darling, *New Limits on Axionic Dark Matter from the Magnetar PSR J1745-2900*, *Astrophys. J. Lett.* **900** (2020) L28 [2008.11188].
- [555] R.A. Battye, J. Darling, J.I. McDonald and S. Srinivasan, *Towards robust constraints on axion dark matter using PSR J1745-2900*, *Phys. Rev. D* **105** (2022) L021305 [2107.01225].
- [556] N. Vinyoles, A. Serenelli, F.L. Villante, S. Basu, J. Redondo and J. Isern, *New axion and hidden photon constraints from a solar data global fit*, *JCAP* **2015** (2015) 015 [1501.01639].
- [557] J. Jaeckel, P.C. Malta and J. Redondo, *Decay photons from the axionlike particles burst of type II supernovae*, *Phys. Rev. D* **98** (2018) 055032 [1702.02964].
- [558] A. Caputo, G. Raffelt and E. Vitagliano, *Muonic boson limits: Supernova redux*, *Phys. Rev. D* **105** (2022) 035022.
- [559] B.D. Blout, E.J. Daw, M.P. Decowski, P.T.P. Ho, L.J. Rosenberg and D.B. Yu, *A radio telescope search for axions*, *The Astrophysical Journal* **546** (2001) 825.

Bibliography

- [560] M. Regis, M. Taoso, D. Vaz, J. Brinchmann, S.L. Zoutendijk, N.F. Bouché et al., *Searching for light in the darkness: Bounds on ALP dark matter with the optical MUSE-faint survey*, *Phys. Lett. B* **814** (2021) 136075 [2009.01310].
- [561] D. Grin, G. Covone, J.-P. Kneib, M. Kamionkowski, A. Blain and E. Jullo, *A Telescope Search for Decaying Relic Axions*, *Phys. Rev. D* **75** (2007) 105018 [astro-ph/0611502].
- [562] C. Garcia-Cely and J. Heeck, *Neutrino Lines from Majoron Dark Matter*, *JHEP* **05** (2017) 102 [1701.07209].
- [563] N. Viaux, M. Catelan, P.B. Stetson, G. Raffelt, J. Redondo, A.A.R. Valcarce et al., *Particle-physics constraints from the globular cluster M5: Neutrino Dipole Moments*, *Astron. Astrophys.* **558** (2013) A12 [1308.4627].
- [564] M. Giannotti, I.G. Irastorza, J. Redondo, A. Ringwald and K. Saikawa, *Stellar Recipes for Axion Hunters*, *JCAP* **10** (2017) 010 [1708.02111].
- [565] J. Isern, E. García-Berro, S. Torres, R. Cojocaru and S. Catalán, *Axions and the luminosity function of white dwarfs: the thin and thick discs, and the halo*, *MNRAS* **478** (2018) 2569 [1805.00135].
- [566] O. Straniero, I. Dominguez, M. Giannotti and A. Mirizzi, *Axion-electron coupling from the RGB tip of Globular Clusters*, *arXiv e-prints* (2018) arXiv:1802.10357 [1802.10357].
- [567] V.D. Barger, W.-Y. Keung and S. Pakvasa, *Majoron Emission by Neutrinos*, *Phys. Rev. D* **25** (1982) 907.
- [568] Y.G. Aditya, K.J. Healey and A.A. Petrov, *Searching for super-WIMPs in leptonic heavy meson decays*, *Phys. Lett. B* **710** (2012) 118 [1201.1007].
- [569] P.S. Pasquini and O.L.G. Peres, *Bounds on Neutrino-Scalar Yukawa Coupling*, *Phys. Rev. D* **93** (2016) 053007 [1511.01811].
- [570] J.A. Gallo, A.W.M. Guerrera, S. Peñaranda and S. Rigolin, *Leptonic meson decays into invisible ALP*, *Nucl. Phys. B* **979** (2022) 115791 [2111.02536].
- [571] G. Raffelt and D. Seckel, *Bounds on exotic-particle interactions from sn1987a*, *Phys. Rev. Lett.* **60** (1988) 1793.
- [572] G.G. Raffelt, *Stars as laboratories for fundamental physics: The astrophysics of neutrinos, axions, and other weakly interacting particles*, University of Chicago Press (5, 1996).
- [573] H. Georgi, *The State of the Art—Gauge Theories*, *AIP Conf. Proc.* **23** (1975) 575.

- [574] A. Ringwald and C. Tamarit, *Revealing the cosmic history with gravitational waves*, *Phys. Rev. D* **106** (2022) 063027.
- [575] M.S. Turner and F. Wilczek, *Inflationary axion cosmology*, *Phys. Rev. Lett.* **66** (1991) 5.
- [576] M. Fairbairn, R. Hogan and D.J.E. Marsh, *Unifying inflation and dark matter with the Peccei-Quinn field: observable axions and observable tensors*, *Phys. Rev. D* **91** (2015) 023509 [[1410.1752](#)].
- [577] A. Vilenkin and T. Vachaspati, *Radiation of goldstone bosons from cosmic strings*, *Phys. Rev. D* **35** (1987) 1138.
- [578] D. Harari and P. Sikivie, *On the evolution of global strings in the early universe*, *Physics Letters B* **195** (1987) 361.
- [579] R. Davis and E. Shellard, *Do axions need inflation?*, *Nuclear Physics B* **324** (1989) 167.
- [580] D.H. Lyth, *Estimates of the cosmological axion density*, *Physics Letters B* **275** (1992) 279.
- [581] M. Buschmann, J.W. Foster, A. Hook, A. Peterson, D.E. Willcox, W. Zhang et al., *Dark matter from axion strings with adaptive mesh refinement*, *Nature Commun.* **13** (2022) 1049 [[2108.05368](#)].
- [582] E. Berkowitz, M.I. Buchhoff and E. Rinaldi, *Lattice QCD input for axion cosmology*, *Phys. Rev. D* **92** (2015) 034507 [[1505.07455](#)].
- [583] L. Fleury and G.D. Moore, *Axion dark matter: strings and their cores*, *JCAP* **01** (2016) 004 [[1509.00026](#)].
- [584] M. Buschmann, J.W. Foster and B.R. Safdi, *Early-Universe Simulations of the Cosmological Axion*, *Phys. Rev. Lett.* **124** (2020) 161103 [[1906.00967](#)].
- [585] O. Lebedev, *On Stability of the Electroweak Vacuum and the Higgs Portal*, *Eur. Phys. J. C* **72** (2012) 2058 [[1203.0156](#)].
- [586] W. Buchmüller, P. Di Bari and M. Plümacher, *Cosmic microwave background, matter - antimatter asymmetry and neutrino masses*, *Nucl. Phys.* **B643** (2002) 367 [[hep-ph/0205349](#)].
- [587] H. Murayama and A. Pierce, *Realistic Dirac leptogenesis*, *Phys. Rev. Lett.* **89** (2002) 271601 [[hep-ph/0206177](#)].
- [588] M. Boz and N.K. Pak, *Dirac Leptogenesis and anomalous $U(1)$* , *Eur. Phys. J. C* **37** (2004) 507.

Bibliography

- [589] D.G. Cerdeno, A. Dedes and T.E.J. Underwood, *The Minimal Phantom Sector of the Standard Model: Higgs Phenomenology and Dirac Leptogenesis*, *JHEP* **09** (2006) 067 [[hep-ph/0607157](#)].
- [590] B. Thomas and M. Toharia, *Phenomenology of Dirac neutrino genesis in split supersymmetry*, *Phys. Rev. D* **73** (2006) 063512 [[hep-ph/0511206](#)].
- [591] B. Thomas and M. Toharia, *Lepton flavor violation and supersymmetric Dirac leptogenesis*, *Phys. Rev. D* **75** (2007) 013013 [[hep-ph/0607285](#)].
- [592] E.J. Chun and P. Roy, *Dirac Leptogenesis in extended nMSSM*, *JHEP* **06** (2008) 089 [[0803.1720](#)].
- [593] A. Bechinger and G. Seidl, *Resonant Dirac leptogenesis on throats*, *Phys. Rev. D* **81** (2010) 065015 [[0907.4341](#)].
- [594] M.-C. Chen, J. Huang and W. Shepherd, *Dirac Leptogenesis with a Non-anomalous $U(1)'$ Family Symmetry*, *JHEP* **11** (2012) 059 [[1111.5018](#)].
- [595] K.-Y. Choi, E.J. Chun and C.S. Shin, *Dark matter asymmetry in supersymmetric Dirac leptogenesis*, *Phys. Lett. B* **723** (2013) 90 [[1211.5409](#)].
- [596] J. Heeck, *Leptogenesis with Lepton-Number- Violating Dirac Neutrinos*, *Phys. Rev. D* **88** (2013) 076004 [[1307.2241](#)].
- [597] D. Borah and A. Dasgupta, *Common Origin of Neutrino Mass, Dark Matter and Dirac Leptogenesis*, *JCAP* **12** (2016) 034 [[1608.03872](#)].
- [598] P.-H. Gu, *Peccei-Quinn symmetry for Dirac seesaw and leptogenesis*, *JCAP* **07** (2016) 004 [[1603.05070](#)].
- [599] P.-H. Gu, “Radiative Dirac neutrino mass, DAMPE dark matter and leptogenesis.” 11, 2017.
- [600] P.-H. Gu, *Leptogenesis with testable Dirac neutrino mass generation*, *Phys. Lett. B* **805** (2020) 135411 [[1907.09443](#)].
- [601] D. Mahanta and D. Borah, *Low scale Dirac leptogenesis and dark matter with observable ΔN_{eff}* , *Eur. Phys. J. C* **82** (2022) 495 [[2101.02092](#)].
- [602] A.D. Sakharov, *Violation of CP in variance, casymmetry, and baryon asymmetry of the universe*, *Soviet Physics Uspekhi* **34** (1991) 392.
- [603] D.G. Cerdeño, P. Reimitz, K. Sakurai and C. Tamarit, *$B + L$ violation at colliders and new physics*, *JHEP* **04** (2018) 076 [[1801.03492](#)].
- [604] R.E. Cutkosky, *Singularities and discontinuities of feynman amplitudes*, *Journal of Mathematical Physics* **1** (1960) 429 [<https://doi.org/10.1063/1.1703676>].

- [605] P.-H. Gu and U. Sarkar, *Pathways to testable leptogenesis*, *Mod. Phys. Lett. A* **25** (2010) 501 [0811.0956].
- [606] T. Hambye, Y. Lin, A. Notari, M. Papucci and A. Strumia, *Constraints on neutrino masses from leptogenesis models*, *Nucl. Phys. B* **695** (2004) 169 [hep-ph/0312203].
- [607] J.A. Casas and A. Ibarra, *Oscillating neutrinos and $\mu \rightarrow e, \gamma$* , *Nucl. Phys. B* **618** (2001) 171 [hep-ph/0103065].
- [608] S. Davidson and A. Ibarra, *A Lower bound on the right-handed neutrino mass from leptogenesis*, *Phys. Lett. B* **535** (2002) 25 [hep-ph/0202239].
- [609] H. Dreiner and G. Ross, *Sphaleron erasure of primordial baryogenesis*, *Nuclear Physics B* **410** (1993) 188.
- [610] J.A. Harvey and M.S. Turner, *Cosmological baryon and lepton number in the presence of electroweak fermion-number violation*, *Phys. Rev. D* **42** (1990) 3344.
- [611] E. Nardi, Y. Nir, J. Racker and E. Roulet, *On Higgs and sphaleron effects during the leptogenesis era*, *JHEP* **01** (2006) 068 [hep-ph/0512052].
- [612] S.Y. Khlebnikov and M.E. Shaposhnikov, *Melting of the Higgs vacuum: Conserved numbers at high temperature*, *Phys. Lett. B* **387** (1996) 817 [hep-ph/9607386].
- [613] A. Strumia, *Baryogenesis via leptogenesis*, in *Les Houches Summer School on Theoretical Physics: Session 84: Particle Physics Beyond the Standard Model*, 8, 2006 [hep-ph/0608347].
- [614] P. Langacker, R.D. Peccei and T. Yanagida, *Invisible Axions and Light Neutrinos: Are They Connected?*, *Mod. Phys. Lett. A* **1** (1986) 541.
- [615] S. Hannestad and G. Raffelt, *Constraining invisible neutrino decays with the cosmic microwave background*, *Phys. Rev. D* **72** (2005) 103514 [hep-ph/0509278].
- [616] R. Barbieri, P. Creminelli, A. Strumia and N. Tetradis, *Baryogenesis through leptogenesis*, *Nucl. Phys. B* **575** (2000) 61 [hep-ph/9911315].
- [617] M. Cirelli, A. Strumia and M. Tamburini, *Cosmology and Astrophysics of Minimal Dark Matter*, *Nucl. Phys. B* **787** (2007) 152 [0706.4071].
- [618] A. Strumia, *Sommerfeld corrections to type-II and III leptogenesis*, *Nucl. Phys. B* **809** (2009) 308 [0806.1630].
- [619] W. Buchmuller, P. Di Bari and M. Plumacher, *Leptogenesis for pedestrians*, *Annals Phys.* **315** (2005) 305 [hep-ph/0401240].

Bibliography

- [620] E. Masso, F. Rota and G. Zsembinszki, *On axion thermalization in the early universe*, *Phys. Rev. D* **66** (2002) 023004 [[hep-ph/0203221](#)].
- [621] P. Graf and F.D. Steffen, *Thermal axion production in the primordial quark-gluon plasma*, *Phys. Rev. D* **83** (2011) 075011 [[1008.4528](#)].
- [622] A. Salvio, A. Strumia and W. Xue, *Thermal axion production*, *JCAP* **01** (2014) 011 [[1310.6982](#)].
- [623] T. Asaka, M. Shaposhnikov and A. Kusenko, *Opening a new window for warm dark matter*, *Phys. Lett. B* **638** (2006) 401 [[hep-ph/0602150](#)].
- [624] T.P. Cheng and L.-F. Li, *Neutrino Masses, Mixings and Oscillations in $SU(2) \times U(1)$ Models of Electroweak Interactions*, *Phys. Rev. D* **22** (1980) 2860.
- [625] K.S. Babu, *Model of 'Calculable' Majorana Neutrino Masses*, *Phys. Lett. B* **203** (1988) 132.
- [626] R. Foot, H. Lew and R.R. Volkas, *Possible consequences of parity conservation*, *Mod. Phys. Lett. A* **7** (1992) 2567.
- [627] R. Foot and R.R. Volkas, *Neutrino physics and the mirror world: How exact parity symmetry explains the solar neutrino deficit, the atmospheric neutrino anomaly and the LSND experiment*, *Phys. Rev. D* **52** (1995) 6595 [[hep-ph/9505359](#)].
- [628] J.C. Pati and A. Salam, *Lepton Number as the Fourth Color*, *Phys. Rev. D* **10** (1974) 275.
- [629] R.N. Mohapatra and J.C. Pati, *A Natural Left-Right Symmetry*, *Phys. Rev. D* **11** (1975) 2558.
- [630] G. Senjanović and R.N. Mohapatra, *Exact left-right symmetry and spontaneous violation of parity*, *Phys. Rev. D* **12** (1975) 1502.
- [631] R.N. Mohapatra and G. Senjanovic, *Neutrino Mass and Spontaneous Parity Violation*, *Phys. Rev. Lett.* **44** (1980) 912.
- [632] N.G. Deshpande, J.F. Gunion, B. Kayser and F.I. Olness, *Left-right symmetric electroweak models with triplet Higgs*, *Phys. Rev. D* **44** (1991) 837.
- [633] S.M. Barr, D. Chang and G. Senjanović, *Strong cp problem and parity*, *Phys. Rev. Lett.* **67** (1991) 2765.
- [634] N.G. Deshpande, J.F. Gunion, B. Kayser and F. Olness, *Left-right-symmetric electroweak models with triplet higgs field*, *Phys. Rev. D* **44** (1991) 837.
- [635] N. Craig, S. Koren and T. Trott, *Cosmological Signals of a Mirror Twin Higgs*, *JHEP* **05** (2017) 038 [[1611.07977](#)].

- [636] S. Kanemura and K. Yagyu, *Radiative corrections to electroweak parameters in the Higgs triplet model and implication with the recent Higgs boson searches*, *Phys. Rev. D* **85** (2012) 115009 [[1201.6287](#)].
- [637] M.J.G. Veltman, *Second Threshold in Weak Interactions*, *Acta Phys. Polon. B* **8** (1977) 475.
- [638] A. Zee, *Quantum Numbers of Majorana Neutrino Masses*, *Nucl. Phys. B* **264** (1986) 99.
- [639] M. Gustafsson, J.M. No and M.A. Rivera, *Predictive Model for Radiatively Induced Neutrino Masses and Mixings with Dark Matter*, *Phys. Rev. Lett.* **110** (2013) 211802 [[1212.4806](#)].
- [640] E. Ma and O. Popov, *Pathways to Naturally Small Dirac Neutrino Masses*, *Phys. Lett. B* **764** (2017) 142 [[1609.02538](#)].
- [641] P.-H. Gu, *Double type-II Dirac seesaw accompanied by Dirac fermionic dark matter*, *Phys. Lett. B* **821** (2021) 136605 [[1907.11557](#)].
- [642] P.-H. Gu, *From Dirac neutrino masses to baryonic and dark matter asymmetries*, *Nucl. Phys. B* **872** (2013) 38 [[1209.4579](#)].
- [643] P.-H. Gu, *Mirror symmetry: from active and sterile neutrino masses to baryonic and dark matter asymmetries*, *Nucl. Phys. B* **874** (2013) 158 [[1303.6545](#)].
- [644] P.-H. Gu, *Parity: from strong CP problem to dark matter, neutrino masses and baryon asymmetry*, [1304.7647](#).
- [645] M. Singer, J.W.F. Valle and J. Schechter, *Canonical Neutral Current Predictions From the Weak Electromagnetic Gauge Group $SU(3) \times u(1)$* , *Phys. Rev. D* **22** (1980) 738.
- [646] J.W.F. Valle and C.A. Vaquera-Araujo, *Dynamical seesaw mechanism for Dirac neutrinos*, *Phys. Lett. B* **755** (2016) 363 [[1601.05237](#)].
- [647] M. Reig, J.W.F. Valle and C.A. Vaquera-Araujo, *Realistic $SU(3)_c \otimes SU(3)_L \otimes U(1)_X$ model with a type II Dirac neutrino seesaw mechanism*, *Phys. Rev. D* **94** (2016) 033012 [[1606.08499](#)].
- [648] L.J. Hall and K. Harigaya, *Implications of Higgs Discovery for the Strong CP Problem and Unification*, *JHEP* **10** (2018) 130 [[1803.08119](#)].
- [649] D. Dunsky, L.J. Hall and K. Harigaya, *Higgs Parity, Strong CP, and Dark Matter*, *JHEP* **07** (2019) 016 [[1902.07726](#)].
- [650] N. Craig, I. Garcia Garcia, G. Koszegi and A. McCune, *P not PQ*, *JHEP* **09** (2021) 130 [[2012.13416](#)].

Bibliography

- [651] Z. Chacko, H.-S. Goh and R. Harnik, *The Twin Higgs: Natural electroweak breaking from mirror symmetry*, *Phys. Rev. Lett.* **96** (2006) 231802 [[hep-ph/0506256](#)].
- [652] Q. Bonnefoy, L. Hall, C.A. Manzari and C. Scherb, *A Colorful Mirror Solution to the Strong CP Problem*, [2303.06156](#).
- [653] A.E. Nelson, *Naturally Weak CP Violation*, *Phys. Lett. B* **136** (1984) 387.
- [654] S.M. Barr, *Solving the Strong CP Problem Without the Peccei-Quinn Symmetry*, *Phys. Rev. Lett.* **53** (1984) 329.
- [655] M.A. Diaz, M.A. Garcia-Jareno, D.A. Restrepo and J.W.F. Valle, *Neutrino mass and missing momentum Higgs boson signals*, *Phys. Rev. D* **58** (1998) 057702 [[hep-ph/9712487](#)].
- [656] J. Schechter and J.W.F. Valle, *Neutrino decay and spontaneous violation of lepton number*, *Phys. Rev. D* **25** (1982) 774.
- [657] W. Grimus, L. Lavoura and B. Radovcic, *Type II seesaw mechanism for Higgs doublets and the scale of new physics*, *Phys. Lett. B* **674** (2009) 117 [[0902.2325](#)].
- [658] K.S. Babu and R.N. Mohapatra, *Solution to the strong CP problem without an axion*, *Phys. Rev. D* **41** (1990) 1286.
- [659] J. de Vries, P. Draper and H.H. Patel, *Do Minimal Parity Solutions to the Strong CP Problem Work?*, [2109.01630](#).
- [660] R. Barbieri, T. Gregoire and L.J. Hall, *Mirror world at the large hadron collider*, [hep-ph/0509242](#).
- [661] T.H. Jung, *Spontaneous Twin Symmetry Breaking*, *Phys. Rev. D* **100** (2019) 115012 [[1902.10978](#)].
- [662] D. Dunsky, L.J. Hall and K. Harigaya, *Sterile Neutrino Dark Matter and Leptogenesis in Left-Right Higgs Parity*, *JHEP* **01** (2021) 125 [[2007.12711](#)].
- [663] S. Coleman and E. Weinberg, *Radiative corrections as the origin of spontaneous symmetry breaking*, *Phys. Rev. D* **7** (1973) 1888.
- [664] Y. Zhang, H. An, X. Ji and R.N. Mohapatra, *General CP Violation in Minimal Left-Right Symmetric Model and Constraints on the Right-Handed Scale*, *Nucl. Phys. B* **802** (2008) 247 [[0712.4218](#)].
- [665] T.D. Lee, *CP Nonconservation and Spontaneous Symmetry Breaking*, *Phys. Rept.* **9** (1974) 143.
- [666] R. Kuchimanchi, *Leptonic CP problem in left-right symmetric model*, *Phys. Rev. D* **91** (2015) 071901 [[1408.6382](#)].

- [667] A. Arhrib, R. Benbrik, M. Chabab, G. Moultaka, M.C. Peyranere, L. Rahili et al., *The Higgs Potential in the Type II Seesaw Model*, *Phys. Rev. D* **84** (2011) 095005 [[1105.1925](#)].
- [668] K. Kannike, *Vacuum Stability Conditions From Copositivity Criteria*, *Eur. Phys. J. C* **72** (2012) 2093 [[1205.3781](#)].
- [669] C. Bonilla, R.M. Fonseca and J.W.F. Valle, *Consistency of the triplet seesaw model revisited*, *Phys. Rev. D* **92** (2015) 075028 [[1508.02323](#)].
- [670] G. Moultaka and M.C. Peyranère, *Vacuum stability conditions for Higgs potentials with $SU(2)_L$ triplets*, *Phys. Rev. D* **103** (2021) 115006 [[2012.13947](#)].
- [671] C. Han, S. Huang and Z. Lei, *Vacuum stability of the type II seesaw leptogenesis from inflation*, [2208.11336](#).
- [672] A. Barroso and P.M. Ferreira, *Charge breaking bounds in the Zee model*, *Phys. Rev. D* **72** (2005) 075010 [[hep-ph/0507128](#)].
- [673] G.C. Branco and G. Senjanović, *The question of neutrino mass*, *Phys. Rev. D* **18** (1978) 1621.
- [674] D. Ross and M. Veltman, *Neutral currents and the higgs mechanism*, *Nuclear Physics B* **95** (1975) 135.
- [675] CDF collaboration, *High-precision measurement of the W boson mass with the CDF II detector*, *Science* **376** (2022) 170.
- [676] J. Heeck, *W -boson mass in the triplet seesaw model*, *Phys. Rev. D* **106** (2022) 015004 [[2204.10274](#)].
- [677] M.E. Peskin and T. Takeuchi, *New constraint on a strongly interacting higgs sector*, *Phys. Rev. Lett.* **65** (1990) 964.
- [678] M.E. Peskin and T. Takeuchi, *Estimation of oblique electroweak corrections*, *Phys. Rev. D* **46** (1992) 381.
- [679] G. Senjanovic and V. Tello, *Strong CP violation: problem or blessing?*, [2004.04036](#).
- [680] J.R. Ellis and M.K. Gaillard, *Strong and Weak CP Violation*, *Nucl. Phys. B* **150** (1979) 141.
- [681] W.-Y. Ai, J.S. Cruz, B. Garbrecht and C. Tamarit, *Consequences of the order of the limit of infinite spacetime volume and the sum over topological sectors for CP violation in the strong interactions*, *Phys. Lett. B* **822** (2021) 136616 [[2001.07152](#)].
- [682] W.-Y. Ai, J.S. Cruz, B. Garbrecht and C. Tamarit, *The limits of the strong CP problem*, *PoS DISCRETE2020-2021* (2022) 084 [[2205.15093](#)].

Bibliography

- [683] R.N. Mohapatra and G. Senjanovic, *Natural Suppression of Strong p and t Noninvariance*, *Phys. Lett. B* **79** (1978) 283.
- [684] A. Hook, *Anomalous solutions to the strong CP problem*, *Phys. Rev. Lett.* **114** (2015) 141801 [[1411.3325](#)].
- [685] M. Carena, D. Liu, J. Liu, N.R. Shah, C.E.M. Wagner and X.-P. Wang, ν solution to the strong CP problem, *Phys. Rev. D* **100** (2019) 094018 [[1904.05360](#)].
- [686] V. Baluni, CP-nonconserving effects in quantum chromodynamics, *Phys. Rev. D* **19** (1979) 2227.
- [687] R. Crewther, P. Di Vecchia, G. Veneziano and E. Witten, *Chiral estimate of the electric dipole moment of the neutron in quantum chromodynamics*, *Physics Letters B* **88** (1979) 123.
- [688] C. Baker, D. Doyle, P. Geltenbort, K. Green, M. van der Grinten et al., *An Improved experimental limit on the electric dipole moment of the neutron*, *Phys. Rev. Lett.* **97** (2006) 131801 [[hep-ex/0602020](#)].
- [689] B. Graner, Y. Chen, E.G. Lindahl and B.R. Heckel, *Reduced Limit on the Permanent Electric Dipole Moment of ^{199}Hg* , *PRL* **116** (2016) 161601 [[1601.04339](#)].
- [690] J. Kawamura, S. Okawa, Y. Omura and Y. Tang, *WIMP dark matter in the parity solution to the strong CP problem*, *JHEP* **04** (2019) 162 [[1812.07004](#)].
- [691] S.K. Lamoreaux and R. Golub, *Experimental searches for the neutron electric dipole moment*, *J. Phys. G* **36** (2009) 104002.
- [692] C.A. Baker et al., *The search for the neutron electric dipole moment at the Paul Scherrer Institute*, *Phys. Procedia* **17** (2011) 159.
- [693] nEDM collaboration, *The nEDM experiment at the SNS*, *Phys. Part. Nucl.* **45** (2014) 249.
- [694] L. Michel, *Interaction between four half spin particles and the decay of the μ meson*, *Proc. Phys. Soc. A* **63** (1950) 514.
- [695] C. Bouchiat and L. Michel, *Theory of μ -meson decay with the hypothesis of nonconservation of parity*, *Phys. Rev.* **106** (1957) 170.
- [696] Y. Kuno and Y. Okada, *Muon decay and physics beyond the standard model*, *Rev. Mod. Phys.* **73** (2001) 151 [[hep-ph/9909265](#)].
- [697] S. Mishra, K. Bachmann, R. Blair, C. Foudas, B. King, W. Lefmann et al., *Inverse muon decay, $\nu_\mu + e^- \rightarrow \mu^- + \nu_e$, at the fermilab tevatron*, *Physics Letters B* **252** (1990) 170.

[698] CHARM-II collaboration, *Precision measurement of electroweak parameters from the scattering of muon-neutrinos on electrons*, *Phys. Lett. B* **335** (1994) 246.

[699] CHARM-II collaboration, *Measurement of differential cross-sections for muon-neutrino electron scattering*, *Phys. Lett. B* **302** (1993) 351.

[700] TEXONO collaboration, *Measurement of $\bar{\nu}_e$ -Electron Scattering Cross-Section with a CsI(Tl) Scintillating Crystal Array at the Kuo-Sheng Nuclear Power Reactor*, *Phys. Rev. D* **81** (2010) 072001 [0911.1597].

[701] A.G. Beda, E.V. Demidova, A.S. Starostin, V.B. Brudanin, V.G. Egorov, D.V. Medvedev et al., *GEMMA experiment: Three years of the search for the neutrino magnetic moment*, *Phys. Part. Nucl. Lett.* **7** (2010) 406 [0906.1926].

[702] A.G. Beda, V.B. Brudanin, V.G. Egorov, D.V. Medvedev, V.S. Pogosov, M.V. Shirchenko et al., *Upper limit on the neutrino magnetic moment from three years of data from the GEMMA spectrometer*, 1005.2736.

[703] MUON G-2 collaboration, *Final Report of the Muon E821 Anomalous Magnetic Moment Measurement at BNL*, *Phys. Rev. D* **73** (2006) 072003 [hep-ex/0602035].

[704] MUON G-2 collaboration, *Measurement of the Positive Muon Anomalous Magnetic Moment to 0.46 ppm*, *Phys. Rev. Lett.* **126** (2021) 141801 [2104.03281].

[705] L. Lavoura, *General formulae for $f(1) \rightarrow f(2)$ gamma*, *Eur. Phys. J. C* **29** (2003) 191 [hep-ph/0302221].

[706] MEG collaboration, *Search for the lepton flavour violating decay $\mu^+ \rightarrow e^+ \gamma$ with the full dataset of the MEG experiment*, *Eur. Phys. J. C* **76** (2016) 434 [1605.05081].

[707] MEG II collaboration, *The design of the MEG II experiment*, *Eur. Phys. J. C* **78** (2018) 380 [1801.04688].

[708] J. Hisano and D. Nomura, *Solar and atmospheric neutrino oscillations and lepton flavor violation in supersymmetric models with the right-handed neutrinos*, *Phys. Rev. D* **59** (1999) 116005 [hep-ph/9810479].

[709] U. Bellgardt, G. Otter, R. Eichler, L. Felawka, C. Niebuhr, H. Walter et al., *Search for the decay $\mu^+ \rightarrow e^+ e^+ e^-$* , *Nuclear Physics B* **299** (1988) 1.

[710] MU3E collaboration, *The Rare and Forbidden: Testing Physics Beyond the Standard Model with Mu3e*, *SciPost Phys. Proc.* **1** (2019) 052 [1812.00741].

[711] XENON collaboration, *Search for New Physics in Electronic Recoil Data from XENONnT*, 2207.11330.

Bibliography

- [712] ALEPH collaboration, *Search for scalar leptons in $e+e-$ collisions at center-of-mass energies up to 209-GeV*, *Phys. Lett. B* **526** (2002) 206 [[hep-ex/0112011](#)].
- [713] OPAL collaboration, *Search for anomalous production of dilepton events with missing transverse momentum in $e+e-$ collisions at $s^{**}(1/2) = 183$ -Gev to 209-GeV*, *Eur. Phys. J. C* **32** (2004) 453 [[hep-ex/0309014](#)].
- [714] L3 collaboration, *Search for scalar leptons and scalar quarks at LEP*, *Phys. Lett. B* **580** (2004) 37 [[hep-ex/0310007](#)].
- [715] DELPHI collaboration, *Searches for supersymmetric particles in $e+e-$ collisions up to 208-GeV and interpretation of the results within the MSSM*, *Eur. Phys. J. C* **31** (2003) 421 [[hep-ex/0311019](#)].
- [716] ATLAS collaboration, *Search for doubly charged Higgs boson production in multi-lepton final states with the ATLAS detector using proton-proton collisions at $\sqrt{s} = 13$ TeV*, *Eur. Phys. J. C* **78** (2018) 199 [[1710.09748](#)].
- [717] Y. Du, A. Dunbrack, M.J. Ramsey-Musolf and J.-H. Yu, *Type-II Seesaw Scalar Triplet Model at a 100 TeV pp Collider: Discovery and Higgs Portal Coupling Determination*, *JHEP* **01** (2019) 101 [[1810.09450](#)].
- [718] LEP, ALEPH, DELPHI, L3, OPAL, LEP ELECTROWEAK WORKING GROUP, SLD ELECTROWEAK GROUP, SLD HEAVY FLAVOR GROUP collaboration, *A Combination of preliminary electroweak measurements and constraints on the standard model*, [hep-ex/0312023](#).
- [719] Y.B. Zel'Dovich, I.Y. Kobzarev and L.B. Okun', *Cosmological consequences of a spontaneous breakdown of a discrete symmetry*, *Soviet Journal of Experimental and Theoretical Physics* **40** (1975) 1.
- [720] G.B. Gelmini, M. Gleiser and E.W. Kolb, *Cosmology of biased discrete symmetry breaking*, *Phys. Rev. D* **39** (1989) 1558.
- [721] R.T. D'Agnolo and A. Hook, *Finding the Strong CP problem at the LHC*, *Phys. Lett. B* **762** (2016) 421 [[1507.00336](#)].
- [722] T. Yamagata, Y. Takamori and H. Utsunomiya, *Search for anomalously heavy hydrogen in deep sea water at 4000-m*, *Phys. Rev. D* **47** (1993) 1231.
- [723] P. Verkerk, G. Grynberg, B. Pichard, M. Spiro, S. Zylberajch, M.E. Goldberg et al., *Search for superheavy hydrogen in sea water*, *Phys. Rev. Lett.* **68** (1992) 1116.
- [724] T.K. Hemmick, D. Elmore, T. Gentile, P.W. Kubik, S.L. Olsen, D. Ciampa et al., *Search for low- z nuclei containing massive stable particles*, *Phys. Rev. D* **41** (1990) 2074.

- [725] E.B. Norman, S.B. Gazes and D.A. Bennett, *Searches for Supermassive X -Particles in Iron*, *Phys. Rev. Lett.* **58** (1987) 1403.
- [726] C.F. Berger, L. Covi, S. Kraml and F. Palorini, *The Number density of a charged relic*, *JCAP* **10** (2008) 005 [[0807.0211](#)].
- [727] Z. Chacko, N. Craig, P.J. Fox and R. Harnik, *Cosmology in Mirror Twin Higgs and Neutrino Masses*, *JHEP* **07** (2017) 023 [[1611.07975](#)].
- [728] P.-H. Gu and H.-J. He, *Neutrino Mass and Baryon Asymmetry from Dirac Seesaw*, *JCAP* **12** (2006) 010 [[hep-ph/0610275](#)].
- [729] G. Lazarides and Q. Shafi, *Origin of matter in the inflationary cosmology*, *Phys. Lett. B* **258** (1991) 305.
- [730] T. Asaka, H.B. Nielsen and Y. Takanishi, *Nonthermal leptogenesis from the heavier Majorana neutrinos*, *Nucl. Phys. B* **647** (2002) 252 [[hep-ph/0207023](#)].
- [731] J. Liu and G. Segre, *Reexamination of generation of baryon and lepton number asymmetries by heavy particle decay*, *Phys. Rev. D* **48** (1993) 4609 [[hep-ph/9304241](#)].
- [732] M. Flanz, E.A. Paschos and U. Sarkar, *Baryogenesis from a lepton asymmetric universe*, *Phys. Lett. B* **345** (1995) 248 [[hep-ph/9411366](#)].
- [733] M. Flanz, E.A. Paschos, U. Sarkar and J. Weiss, *Baryogenesis through mixing of heavy Majorana neutrinos*, *Phys. Lett. B* **389** (1996) 693 [[hep-ph/9607310](#)].
- [734] L. Covi, E. Roulet and F. Vissani, *CP violating decays in leptogenesis scenarios*, *Phys. Lett. B* **384** (1996) 169 [[hep-ph/9605319](#)].
- [735] A. Pilaftsis, *Resonant CP violation induced by particle mixing in transition amplitudes*, *Nucl. Phys. B* **504** (1997) 61 [[hep-ph/9702393](#)].
- [736] A. Pilaftsis, *Heavy Majorana neutrinos and baryogenesis*, *Int. J. Mod. Phys. A* **14** (1999) 1811 [[hep-ph/9812256](#)].
- [737] G.F. Giudice, M. Peloso, A. Riotto and I. Tkachev, *Production of massive fermions at preheating and leptogenesis*, *JHEP* **08** (1999) 014 [[hep-ph/9905242](#)].
- [738] N.D. Barrie, C. Han and H. Murayama, *Type II Seesaw leptogenesis*, *JHEP* **05** (2022) 160 [[2204.08202](#)].
- [739] M. Dine, L. Randall and S.D. Thomas, *Supersymmetry breaking in the early universe*, *Phys. Rev. Lett.* **75** (1995) 398 [[hep-ph/9503303](#)].
- [740] R.T. Co, L.J. Hall, K. Harigaya, K.A. Olive and S. Verner, *Axion Kinetic Misalignment and Parametric Resonance from Inflation*, *JCAP* **08** (2020) 036 [[2004.00629](#)].

Bibliography

- [741] J. Kang, M.A. Luty and S. Nasri, *The Relic abundance of long-lived heavy colored particles*, *JHEP* **09** (2008) 086 [[hep-ph/0611322](#)].
- [742] M. Drewes, Y. Georis and J. Klarić, *Mapping the Viable Parameter Space for Testable Leptogenesis*, *Phys. Rev. Lett.* **128** (2022) 051801 [[2106.16226](#)].
- [743] T. Vachaspati and A. Vilenkin, *Gravitational radiation from cosmic strings*, *Phys. Rev. D* **31** (1985) 3052.
- [744] W. Buchmüller, V. Domcke, K. Kamada and K. Schmitz, *The Gravitational Wave Spectrum from Cosmological $B - L$ Breaking*, *JCAP* **10** (2013) 003 [[1305.3392](#)].
- [745] W. Chao, W.-F. Cui, H.-K. Guo and J. Shu, *Gravitational wave imprint of new symmetry breaking*, *Chin. Phys. C* **44** (2020) 123102 [[1707.09759](#)].
- [746] N. Okada and O. Seto, *Probing the seesaw scale with gravitational waves*, *Phys. Rev. D* **98** (2018) 063532 [[1807.00336](#)].
- [747] W. Buchmuller, V. Domcke, H. Murayama and K. Schmitz, *Probing the scale of grand unification with gravitational waves*, *Phys. Lett. B* **809** (2020) 135764 [[1912.03695](#)].
- [748] T. Hasegawa, N. Okada and O. Seto, *Gravitational waves from the minimal gauged $U(1)_{B-L}$ model*, *Phys. Rev. D* **99** (2019) 095039 [[1904.03020](#)].
- [749] N. Haba and T. Yamada, *Gravitational waves from phase transition in minimal SUSY $U(1)_{B-L}$ model*, *Phys. Rev. D* **101** (2020) 075027 [[1911.01292](#)].
- [750] J.A. Dror, T. Hiramatsu, K. Kohri, H. Murayama and G. White, *Testing the Seesaw Mechanism and Leptogenesis with Gravitational Waves*, *Phys. Rev. Lett.* **124** (2020) 041804 [[1908.03227](#)].
- [751] S. Blasi, V. Brdar and K. Schmitz, *Fingerprint of low-scale leptogenesis in the primordial gravitational-wave spectrum*, *Phys. Rev. Res.* **2** (2020) 043321 [[2004.02889](#)].
- [752] D.I. Dunsky, A. Ghoshal, H. Murayama, Y. Sakakihara and G. White, *GUTs, hybrid topological defects, and gravitational waves*, *Phys. Rev. D* **106** (2022) 075030 [[2111.08750](#)].
- [753] Y. Fukuda, T. Hayakawa, K. Inoue, K. Ishihara, H. Ishino, S. Joukou et al., *Solar neutrino data covering solar cycle 22*, *Physical Review Letters* **77** (1996) 1683.
- [754] SUPER-KAMIOKANDE collaboration, *Constraints on neutrino oscillations using 1258 days of Super-Kamiokande solar neutrino data*, *Phys. Rev. Lett.* **86** (2001) 5656 [[hep-ex/0103033](#)].

- [755] SUPER-KAMIOKANDE collaboration, *Determination of solar neutrino oscillation parameters using 1496 days of Super-Kamiokande I data*, *Phys. Lett. B* **539** (2002) 179 [[hep-ex/0205075](#)].
- [756] SNO collaboration, *Direct evidence for neutrino flavor transformation from neutral current interactions in the Sudbury Neutrino Observatory*, *Phys. Rev. Lett.* **89** (2002) 011301 [[nucl-ex/0204008](#)].
- [757] SUPER-KAMIOKANDE collaboration, *A Measurement of atmospheric neutrino oscillation parameters by SUPER-KAMIOKANDE I*, *Phys. Rev. D* **71** (2005) 112005 [[hep-ex/0501064](#)].
- [758] B. Aharmim, S. Ahmed, J. Amsbaugh, J. Anaya, A. Anthony, J. Banar et al., *Measurement of the ν_e and total 8b solar neutrino fluxes with the sudbury neutrino observatory phase-iii data set*, *Physical Review C* **87** (2011) .
- [759] SUPER-KAMIOKANDE COLLABORATION collaboration, *Solar neutrino measurements in super-kamiokande-iv*, *Phys. Rev. D* **94** (2016) 052010.
- [760] BOREXINO collaboration, *Measurement of neutrino flux from the primary proton-proton fusion process in the Sun with Borexino detector*, *Phys. Part. Nucl.* **47** (2016) 995 [[1507.02432](#)].
- [761] ICECUBE collaboration, *Measurement of Atmospheric Neutrino Oscillations at 6–56 GeV with IceCube DeepCore*, *Phys. Rev. Lett.* **120** (2018) 071801 [[1707.07081](#)].
- [762] ANTARES collaboration, *Measuring the atmospheric neutrino oscillation parameters and constraining the 3+1 neutrino model with ten years of ANTARES data*, *JHEP* **06** (2019) 113 [[1812.08650](#)].
- [763] KAMLAND collaboration, *Precision Measurement of Neutrino Oscillation Parameters with KamLAND*, *Phys. Rev. Lett.* **100** (2008) 221803 [[0801.4589](#)].
- [764] T2K collaboration, *Observation of Electron Neutrino Appearance in a Muon Neutrino Beam*, *Phys. Rev. Lett.* **112** (2014) 061802 [[1311.4750](#)].
- [765] EBOSS collaboration, *Completed SDSS-IV extended Baryon Oscillation Spectroscopic Survey: Cosmological implications from two decades of spectroscopic surveys at the Apache Point Observatory*, *Phys. Rev. D* **103** (2021) 083533 [[2007.08991](#)].
- [766] L.P. Grishchuk, *Amplification of gravitational waves in an istropic universe*, *Zh. Eksp. Teor. Fiz.* **67** (1974) 825.
- [767] A.A. Starobinsky, *Spectrum of relict gravitational radiation and the early state of the universe*, *JETP Lett.* **30** (1979) 682.

Bibliography

- [768] V.A. Rubakov, M.V. Sazhin and A.V. Veryaskin, *Graviton Creation in the Inflationary Universe and the Grand Unification Scale*, *Phys. Lett. B* **115** (1982) 189.
- [769] M.C. Guzzetti, N. Bartolo, M. Liguori and S. Matarrese, *Gravitational waves from inflation*, *Riv. Nuovo Cim.* **39** (2016) 399 [[1605.01615](#)].
- [770] N. Seto and J. Yokoyama, *Probing the equation of state of the early universe with a space laser interferometer*, *J. Phys. Soc. Jap.* **72** (2003) 3082 [[gr-qc/0305096](#)].
- [771] L.A. Boyle and P.J. Steinhardt, *Probing the early universe with inflationary gravitational waves*, *Phys. Rev. D* **77** (2008) 063504 [[astro-ph/0512014](#)].
- [772] L.A. Boyle and A. Buonanno, *Relating gravitational wave constraints from primordial nucleosynthesis, pulsar timing, laser interferometers, and the CMB: Implications for the early Universe*, *Phys. Rev. D* **78** (2008) 043531 [[0708.2279](#)].
- [773] S. Kuroyanagi, T. Chiba and N. Sugiyama, *Precision calculations of the gravitational wave background spectrum from inflation*, *Phys. Rev. D* **79** (2009) 103501 [[0804.3249](#)].
- [774] K. Nakayama and J. Yokoyama, *Gravitational Wave Background and Non-Gaussianity as a Probe of the Curvaton Scenario*, *JCAP* **01** (2010) 010 [[0910.0715](#)].
- [775] S. Kuroyanagi, C. Ringeval and T. Takahashi, *Early universe tomography with CMB and gravitational waves*, *Phys. Rev. D* **87** (2013) 083502 [[1301.1778](#)].
- [776] R. Jinno, T. Moroi and K. Nakayama, *Inflationary Gravitational Waves and the Evolution of the Early Universe*, *JCAP* **01** (2014) 040 [[1307.3010](#)].
- [777] K. Saikawa and S. Shirai, *Primordial gravitational waves, precisely: The role of thermodynamics in the Standard Model*, *JCAP* **05** (2018) 035 [[1803.01038](#)].
- [778] N. Bernal, A. Ghoshal, F. Hajkarim and G. Lambiase, *Primordial Gravitational Wave Signals in Modified Cosmologies*, *JCAP* **11** (2020) 051 [[2008.04959](#)].
- [779] K. Nakayama, S. Saito, Y. Suwa and J. Yokoyama, *Space laser interferometers can determine the thermal history of the early Universe*, *Phys. Rev. D* **77** (2008) 124001 [[0802.2452](#)].
- [780] K. Nakayama, S. Saito, Y. Suwa and J. Yokoyama, *Probing reheating temperature of the universe with gravitational wave background*, *JCAP* **06** (2008) 020 [[0804.1827](#)].
- [781] S. Kuroyanagi, K. Nakayama and S. Saito, *Prospects for determination of thermal history after inflation with future gravitational wave detectors*, *Phys. Rev. D* **84** (2011) 123513 [[1110.4169](#)].

- [782] W. Buchmuller, V. Domcke, K. Kamada and K. Schmitz, *A Minimal Supersymmetric Model of Particle Physics and the Early Universe*, 1309.7788.
- [783] R. Jinno, T. Moroi and T. Takahashi, *Studying Inflation with Future Space-Based Gravitational Wave Detectors*, *JCAP* **12** (2014) 006 [1406.1666].
- [784] S. Kuroyanagi, K. Nakayama and J. Yokoyama, *Prospects of determination of reheating temperature after inflation by DECIGO*, *PTEP* **2015** (2015) 013E02 [1410.6618].
- [785] S. Schettler, T. Boeckel and J. Schaffner-Bielich, *Imprints of the QCD Phase Transition on the Spectrum of Gravitational Waves*, *Phys. Rev. D* **83** (2011) 064030 [1010.4857].
- [786] F. Hajkarim, J. Schaffner-Bielich, S. Wystub and M.M. Wygas, *Effects of the QCD Equation of State and Lepton Asymmetry on Primordial Gravitational Waves*, *Phys. Rev. D* **99** (2019) 103527 [1904.01046].
- [787] R. Jinno, T. Moroi and K. Nakayama, *Probing dark radiation with inflationary gravitational waves*, *Phys. Rev. D* **86** (2012) 123502 [1208.0184].
- [788] R.R. Caldwell, T.L. Smith and D.G.E. Walker, *Using a Primordial Gravitational Wave Background to Illuminate New Physics*, *Phys. Rev. D* **100** (2019) 043513 [1812.07577].
- [789] V.C. Rubin and W.K. Ford, Jr., *Rotation of the Andromeda Nebula from a Spectroscopic Survey of Emission Regions*, *Astrophys. J.* **159** (1970) 379.
- [790] D. Clowe, M. Bradac, A.H. Gonzalez, M. Markevitch, S.W. Randall, C. Jones et al., *A direct empirical proof of the existence of dark matter*, *Astrophys. J. Lett.* **648** (2006) L109 [[astro-ph/0608407](#)].
- [791] M.A. Luty, *Baryogenesis via leptogenesis*, *Phys. Rev. D* **45** (1992) 455.
- [792] M. Plumacher, *Baryogenesis and lepton number violation*, *Z. Phys. C* **74** (1997) 549 [[hep-ph/9604229](#)].
- [793] G. Arcadi, M. Dutra, P. Ghosh, M. Lindner, Y. Mambrini, M. Pierre et al., *The waning of the WIMP? A review of models, searches, and constraints*, *Eur. Phys. J. C* **78** (2018) 203 [1703.07364].
- [794] G.B. Gelmini and P. Gondolo, *Neutralino with the right cold dark matter abundance in (almost) any supersymmetric model*, *Phys. Rev. D* **74** (2006) 023510 [[hep-ph/0602230](#)].
- [795] A. Falkowski, J.T. Ruderman and T. Volansky, *Asymmetric Dark Matter from Leptogenesis*, *JHEP* **05** (2011) 106 [1101.4936].

Bibliography

- [796] A. Falkowski, E. Kuflik, N. Levi and T. Volansky, *Light Dark Matter from Leptogenesis*, *Phys. Rev. D* **99** (2019) 015022 [[1712.07652](#)].
- [797] K. Moffat, S. Pascoli, S.T. Petcov, H. Schulz and J. Turner, *Three-flavored nonresonant leptogenesis at intermediate scales*, *Phys. Rev. D* **98** (2018) 015036 [[1804.05066](#)].
- [798] S. Dell’Oro, S. Marcocci, M. Viel and F. Vissani, *Neutrinoless double beta decay: 2015 review*, *Adv. High Energy Phys.* **2016** (2016) 2162659 [[1601.07512](#)].
- [799] R.E. Shrock, *New Tests For, and Bounds On, Neutrino Masses and Lepton Mixing*, *Phys. Lett. B* **96** (1980) 159.
- [800] B. Kayser and R.E. Shrock, *Distinguishing Between Dirac and Majorana Neutrinos in Neutral Current Reactions*, *Phys. Lett. B* **112** (1982) 137.
- [801] J. De Vries, H.K. Dreiner, J.Y. Günther, Z.S. Wang and G. Zhou, *Long-lived Sterile Neutrinos at the LHC in Effective Field Theory*, *JHEP* **03** (2021) 148 [[2010.07305](#)].
- [802] T. Endoh, S. Kaneko, S.K. Kang, T. Morozumi and M. Tanimoto, *CP violation in neutrino oscillation and leptogenesis*, *Phys. Rev. Lett.* **89** (2002) 231601 [[hep-ph/0209020](#)].
- [803] I. Esteban, M.C. Gonzalez-Garcia, M. Maltoni, I. Martinez-Soler and T. Schwetz, *Updated fit to three neutrino mixing: exploring the accelerator-reactor complementarity*, *JHEP* **01** (2017) 087 [[1611.01514](#)].
- [804] E. Bertuzzo, P. Di Bari and L. Marzola, *The problem of the initial conditions in flavoured leptogenesis and the tauon N_2 -dominated scenario*, *Nucl. Phys. B* **849** (2011) 521 [[1007.1641](#)].
- [805] S. Ipek, A.D. Plascencia and J. Turner, *Assessing Perturbativity and Vacuum Stability in High-Scale Leptogenesis*, *JHEP* **12** (2018) 111 [[1806.00460](#)].
- [806] D. Croon, N. Fernandez, D. McKeen and G. White, *Stability, reheating and leptogenesis*, *JHEP* **06** (2019) 098 [[1903.08658](#)].
- [807] B. Barman, D. Borah, A. Dasgupta and A. Ghoshal, *Probing high scale Dirac leptogenesis via gravitational waves from domain walls*, *Phys. Rev. D* **106** (2022) 015007 [[2205.03422](#)].
- [808] A. Dasgupta, P.S.B. Dev, A. Ghoshal and A. Mazumdar, *Gravitational wave pathway to testable leptogenesis*, *Phys. Rev. D* **106** (2022) 075027 [[2206.07032](#)].
- [809] D. Borah, A. Dasgupta and I. Saha, *Leptogenesis and dark matter through relativistic bubble walls with observable gravitational waves*, *JHEP* **11** (2022) 136 [[2207.14226](#)].

- [810] A. Ghoshal, R. Samanta and G. White, *Bremsstrahlung High-frequency Gravitational Wave Signatures of High-scale Non-thermal Leptogenesis*, 2211.10433.
- [811] N. Bhaumik, A. Ghoshal and M. Lewicki, *Doubly peaked induced stochastic gravitational wave background: testing baryogenesis from primordial black holes*, *JHEP* **07** (2022) 130 [2205.06260].
- [812] N. Bhaumik, A. Ghoshal, R.K. Jain and M. Lewicki, *Distinct signatures of spinning PBH domination and evaporation: doubly peaked gravitational waves, dark relics and CMB complementarity*, 2212.00775.
- [813] M. Fujii, K. Hamaguchi and T. Yanagida, *Leptogenesis with almost degenerate majorana neutrinos*, *Phys. Rev. D* **65** (2002) 115012 [hep-ph/0202210].
- [814] PARTICLE DATA GROUP collaboration, *Review of Particle Physics*, *PTEP* **2022** (2022) 083C01.
- [815] F. Hahn-Woernle and M. Plumacher, *Effects of reheating on leptogenesis*, *Nucl. Phys. B* **806** (2009) 68 [0801.3972].
- [816] M.A.G. Garcia, Y. Mambrini, K.A. Olive and M. Peloso, *Enhancement of the Dark Matter Abundance Before Reheating: Applications to Gravitino Dark Matter*, *Phys. Rev. D* **96** (2017) 103510 [1709.01549].
- [817] M.A.G. Garcia, K. Kaneta, Y. Mambrini and K.A. Olive, *Reheating and Post-inflationary Production of Dark Matter*, *Phys. Rev. D* **101** (2020) 123507 [2004.08404].
- [818] A. Datta, R. Roshan and A. Sil, *Effects of Reheating on Charged Lepton Yukawa Equilibration and Leptogenesis*, 2206.10650.
- [819] G. Engelhard, Y. Grossman, E. Nardi and Y. Nir, *The Importance of N2 leptogenesis*, *Phys. Rev. Lett.* **99** (2007) 081802 [hep-ph/0612187].
- [820] F. Ertas, F. Kahlhoefer and C. Tasillo, *Turn up the volume: listening to phase transitions in hot dark sectors*, *JCAP* **02** (2022) 014 [2109.06208].
- [821] K. Hamaguchi, H. Murayama and T. Yanagida, *Leptogenesis from N dominated early universe*, *Phys. Rev. D* **65** (2002) 043512 [hep-ph/0109030].
- [822] E. Nardi, Y. Nir, E. Roulet and J. Racker, *The Importance of flavor in leptogenesis*, *JHEP* **01** (2006) 164 [hep-ph/0601084].
- [823] A. Abada, S. Davidson, A. Ibarra, F.X. Josse-Michaux, M. Losada and A. Riotto, *Flavour Matters in Leptogenesis*, *JHEP* **09** (2006) 010 [hep-ph/0605281].
- [824] A. Abada, S. Davidson, F.-X. Josse-Michaux, M. Losada and A. Riotto, *Flavor issues in leptogenesis*, *JCAP* **04** (2006) 004 [hep-ph/0601083].

Bibliography

- [825] T. Hugle, M. Platscher and K. Schmitz, *Low-Scale Leptogenesis in the Scotogenic Neutrino Mass Model*, *Phys. Rev. D* **98** (2018) 023020 [[1804.09660](#)].
- [826] A. Liu, Z.-L. Han, Y. Jin and F.-X. Yang, *Leptogenesis and dark matter from a low scale seesaw mechanism*, *Phys. Rev. D* **101** (2020) 095005 [[2001.04085](#)].
- [827] M. Kawasaki, T. Moroi and T. Yanagida, *Constraint on the reheating temperature from the decay of the Polonyi field*, *Phys. Lett. B* **370** (1996) 52 [[hep-ph/9509399](#)].
- [828] S. Tremaine and J.E. Gunn, *Dynamical role of light neutral leptons in cosmology*, *Phys. Rev. Lett.* **42** (1979) 407.
- [829] R. Coy, A. Gupta and T. Hambye, *Seesaw neutrino determination of the dark matter relic density*, *Phys. Rev. D* **104** (2021) 083024 [[2104.00042](#)].
- [830] A. Mazumdar, S. Qutub and K. Saikawa, *Nonthermal axion dark radiation and constraints*, *Phys. Rev. D* **94** (2016) 065030 [[1607.06958](#)].
- [831] R.H. Cyburt, B.D. Fields, K.A. Olive and T.-H. Yeh, *Big Bang Nucleosynthesis: 2015*, *Rev. Mod. Phys.* **88** (2016) 015004 [[1505.01076](#)].
- [832] CMB-HD collaboration, *Snowmass2021 CMB-HD White Paper*, [2203.05728](#).
- [833] CMB-BHARAT collaboration, “CMB-Bharat.”
- [834] S. Datta and R. Samanta, *Gravitational Waves-Tomography of Low-Scale-Leptogenesis*, [2208.09949](#).
- [835] BICEP, KECK collaboration, *Improved Constraints on Primordial Gravitational Waves using Planck, WMAP, and BICEP/Keck Observations through the 2018 Observing Season*, *Phys. Rev. Lett.* **127** (2021) 151301 [[2110.00483](#)].
- [836] A.R. Liddle and D.H. Lyth, *The Cold dark matter density perturbation*, *Phys. Rept.* **231** (1993) 1 [[astro-ph/9303019](#)].
- [837] R.H. Brandenberger, A. Nayeri, S.P. Patil and C. Vafa, *Tensor Modes from a Primordial Hagedorn Phase of String Cosmology*, *Phys. Rev. Lett.* **98** (2007) 231302 [[hep-th/0604126](#)].
- [838] M. Baldi, F. Finelli and S. Matarrese, *Inflation with violation of the null energy condition*, *Phys. Rev. D* **72** (2005) 083504 [[astro-ph/0505552](#)].
- [839] T. Kobayashi, M. Yamaguchi and J. Yokoyama, *G-inflation: Inflation driven by the Galileon field*, *Phys. Rev. Lett.* **105** (2010) 231302 [[1008.0603](#)].
- [840] G. Calcagni and S. Tsujikawa, *Observational constraints on patch inflation in noncommutative spacetime*, *Phys. Rev. D* **70** (2004) 103514 [[astro-ph/0407543](#)].

- [841] G. Calcagni, S. Kuroyanagi, J. Ohashi and S. Tsujikawa, *Strong Planck constraints on braneworld and non-commutative inflation*, *JCAP* **03** (2014) 052 [[1310.5186](#)].
- [842] J.L. Cook and L. Sorbo, *Particle production during inflation and gravitational waves detectable by ground-based interferometers*, *Phys. Rev. D* **85** (2012) 023534 [[1109.0022](#)].
- [843] S. Mukohyama, R. Namba, M. Peloso and G. Shiu, *Blue Tensor Spectrum from Particle Production during Inflation*, *JCAP* **08** (2014) 036 [[1405.0346](#)].
- [844] S. Kuroyanagi, T. Takahashi and S. Yokoyama, *Blue-tilted inflationary tensor spectrum and reheating in the light of NANOGrav results*, *JCAP* **01** (2021) 071 [[2011.03323](#)].
- [845] M.S. Turner, M.J. White and J.E. Lidsey, *Tensor perturbations in inflationary models as a probe of cosmology*, *Phys. Rev. D* **48** (1993) 4613 [[astro-ph/9306029](#)].
- [846] S. Chongchitnan and G. Efstathiou, *Prospects for direct detection of primordial gravitational waves*, *Phys. Rev. D* **73** (2006) 083511 [[astro-ph/0602594](#)].
- [847] S. Kuroyanagi, T. Takahashi and S. Yokoyama, *Blue-tilted Tensor Spectrum and Thermal History of the Universe*, *JCAP* **02** (2015) 003 [[1407.4785](#)].
- [848] T.W.B. Kibble, *Topology of Cosmic Domains and Strings*, *J. Phys. A* **9** (1976) 1387.
- [849] M. Redi and A. Tesi, *The meso-inflationary QCD axion*, [2211.06421](#).
- [850] G.W. Gibbons and S.W. Hawking, *Cosmological event horizons, thermodynamics, and particle creation*, *Phys. Rev. D* **15** (1977) 2738.
- [851] LIGO SCIENTIFIC, VIRGO collaboration, *Observation of Gravitational Waves from a Binary Black Hole Merger*, *Phys. Rev. Lett.* **116** (2016) 061102 [[1602.03837](#)].
- [852] LIGO SCIENTIFIC, VIRGO collaboration, *GW151226: Observation of Gravitational Waves from a 22-Solar-Mass Binary Black Hole Coalescence*, *Phys. Rev. Lett.* **116** (2016) 241103 [[1606.04855](#)].
- [853] LIGO SCIENTIFIC, VIRGO collaboration, *GW170104: Observation of a 50-Solar-Mass Binary Black Hole Coalescence at Redshift 0.2*, *Phys. Rev. Lett.* **118** (2017) 221101 [[1706.01812](#)].
- [854] LIGO SCIENTIFIC, VIRGO collaboration, *GW170608: Observation of a 19-solar-mass Binary Black Hole Coalescence*, *Astrophys. J. Lett.* **851** (2017) L35 [[1711.05578](#)].

Bibliography

- [855] LIGO SCIENTIFIC, VIRGO collaboration, *GW170814: A Three-Detector Observation of Gravitational Waves from a Binary Black Hole Coalescence*, *Phys. Rev. Lett.* **119** (2017) 141101 [1709.09660].
- [856] LIGO SCIENTIFIC, VIRGO collaboration, *GW170817: Observation of Gravitational Waves from a Binary Neutron Star Inspiral*, *Phys. Rev. Lett.* **119** (2017) 161101 [1710.05832].
- [857] G.M. Harry and (for the LIGO Scientific Collaboration), *Advanced ligo: the next generation of gravitational wave detectors*, *Classical and Quantum Gravity* **27** (2010) 084006.
- [858] LIGO SCIENTIFIC collaboration, *Advanced LIGO*, *Class. Quant. Grav.* **32** (2015) 074001 [1411.4547].
- [859] VIRGO collaboration, *Advanced Virgo: a second-generation interferometric gravitational wave detector*, *Class. Quant. Grav.* **32** (2015) 024001 [1408.3978].
- [860] LIGO SCIENTIFIC, VIRGO collaboration, *Open data from the first and second observing runs of Advanced LIGO and Advanced Virgo*, *SoftwareX* **13** (2021) 100658 [1912.11716].
- [861] L. Badurina, O. Buchmueller, J. Ellis, M. Lewicki, C. McCabe and V. Vaskonen, *Prospective sensitivities of atom interferometers to gravitational waves and ultralight dark matter*, *Phil. Trans. A. Math. Phys. Eng. Sci.* **380** (2021) 20210060 [2108.02468].
- [862] P.W. Graham, J.M. Hogan, M.A. Kasevich and S. Rajendran, *Resonant mode for gravitational wave detectors based on atom interferometry*, *Phys. Rev. D* **94** (2016) 104022 [1606.01860].
- [863] MAGIS collaboration, *Mid-band gravitational wave detection with precision atomic sensors*, 1711.02225.
- [864] L. Badurina et al., *AION: An Atom Interferometer Observatory and Network*, *JCAP* **05** (2020) 011 [1911.11755].
- [865] M. Punturo et al., *The Einstein Telescope: A third-generation gravitational wave observatory*, *Class. Quant. Grav.* **27** (2010) 194002.
- [866] S. Hild et al., *Sensitivity Studies for Third-Generation Gravitational Wave Observatories*, *Class. Quant. Grav.* **28** (2011) 094013 [1012.0908].
- [867] LIGO SCIENTIFIC collaboration, *Exploring the Sensitivity of Next Generation Gravitational Wave Detectors*, *Class. Quant. Grav.* **34** (2017) 044001 [1607.08697].
- [868] D. Reitze et al., *Cosmic Explorer: The U.S. Contribution to Gravitational-Wave Astronomy beyond LIGO*, *Bull. Am. Astron. Soc.* **51** (2019) 035 [1907.04833].

[869] P. Amaro-Seoane, H. Audley, S. Babak, J. Baker, E. Barausse, P. Bender et al., *Laser Interferometer Space Antenna*, *arXiv e-prints* (2017) arXiv:1702.00786 [1702.00786].

[870] J. Baker et al., *The Laser Interferometer Space Antenna: Unveiling the Millihertz Gravitational Wave Sky*, 1907.06482.

[871] J. Crowder and N.J. Cornish, *Beyond LISA: Exploring future gravitational wave missions*, *Phys. Rev. D* **72** (2005) 083005 [gr-qc/0506015].

[872] V. Corbin and N.J. Cornish, *Detecting the cosmic gravitational wave background with the big bang observer*, *Class. Quant. Grav.* **23** (2006) 2435 [gr-qc/0512039].

[873] G.M. Harry, P. Fritschel, D.A. Shaddock, W. Folkner and E.S. Phinney, *Laser interferometry for the big bang observer*, *Classical and Quantum Gravity* **23** (2006) 4887.

[874] N. Seto, S. Kawamura and T. Nakamura, *Possibility of direct measurement of the acceleration of the universe using 0.1-Hz band laser interferometer gravitational wave antenna in space*, *Phys. Rev. Lett.* **87** (2001) 221103 [astro-ph/0108011].

[875] H. Kudoh, A. Taruya, T. Hiramatsu and Y. Himemoto, *Detecting a gravitational-wave background with next-generation space interferometers*, *Phys. Rev. D* **73** (2006) 064006 [gr-qc/0511145].

[876] S. Kawamura, T. Nakamura, M. Ando, N. Seto, K. Tsubono, K. Numata et al., *The Japanese space gravitational wave antenna—decigo*, *Classical and Quantum Gravity* **23** (2006) S125.

[877] K. Yagi and N. Seto, *Detector configuration of DECIGO/BBO and identification of cosmological neutron-star binaries*, *Phys. Rev. D* **83** (2011) 044011 [1101.3940].

[878] S. Kawamura et al., *Current status of space gravitational wave antenna DECIGO and B-DECIGO*, *PTEP* **2021** (2021) 05A105 [2006.13545].

[879] AEDGE collaboration, *AEDGE: Atomic Experiment for Dark Matter and Gravity Exploration in Space*, *EPJ Quant. Technol.* **7** (2020) 6 [1908.00802].

[880] A. Sesana et al., *Unveiling the gravitational universe at μ -Hz frequencies*, *Exper. Astron.* **51** (2021) 1333 [1908.11391].

[881] J. Garcia-Bellido, H. Murayama and G. White, *Exploring the early Universe with Gaia and Theia*, *JCAP* **12** (2021) 023 [2104.04778].

[882] C.L. Carilli and S. Rawlings, *Science with the Square Kilometer Array: Motivation, key science projects, standards and assumptions*, *New Astron. Rev.* **48** (2004) 979 [astro-ph/0409274].

Bibliography

- [883] G. Janssen et al., *Gravitational wave astronomy with the SKA*, *PoS AASKA14* (2015) 037 [1501.00127].
- [884] A. Weltman et al., *Fundamental physics with the Square Kilometre Array*, *Publ. Astron. Soc. Austral.* **37** (2020) e002 [1810.02680].
- [885] M. Kramer and D.J. Champion, *The european pulsar timing array and the large european array for pulsars*, *Classical and Quantum Gravity* **30** (2013) 224009.
- [886] L. Lentati et al., *European Pulsar Timing Array Limits On An Isotropic Stochastic Gravitational-Wave Background*, *Mon. Not. Roy. Astron. Soc.* **453** (2015) 2576 [1504.03692].
- [887] S. Babak et al., *European Pulsar Timing Array Limits on Continuous Gravitational Waves from Individual Supermassive Black Hole Binaries*, *Mon. Not. Roy. Astron. Soc.* **455** (2016) 1665 [1509.02165].
- [888] M.A. McLaughlin, *The North American Nanohertz Observatory for Gravitational Waves*, *Class. Quant. Grav.* **30** (2013) 224008 [1310.0758].
- [889] NANOGrav collaboration, *The NANOGrav 11-year Data Set: Pulsar-timing Constraints On The Stochastic Gravitational-wave Background*, *Astrophys. J.* **859** (2018) 47 [1801.02617].
- [890] K. Aggarwal et al., *The NANOGrav 11-Year Data Set: Limits on Gravitational Waves from Individual Supermassive Black Hole Binaries*, *Astrophys. J.* **880** (2019) 2 [1812.11585].
- [891] A. Brazier et al., *The NANOGrav Program for Gravitational Waves and Fundamental Physics*, 1908.05356.
- [892] NANOGrav collaboration, *The NANOGrav 12.5 yr Data Set: Search for an Isotropic Stochastic Gravitational-wave Background*, *Astrophys. J. Lett.* **905** (2020) L34 [2009.04496].
- [893] BICEP2, KECK ARRAY collaboration, *BICEP2 / Keck Array x: Constraints on Primordial Gravitational Waves using Planck, WMAP, and New BICEP2/Keck Observations through the 2015 Season*, *Phys. Rev. Lett.* **121** (2018) 221301 [1810.05216].
- [894] T.J. Clarke, E.J. Copeland and A. Moss, *Constraints on primordial gravitational waves from the Cosmic Microwave Background*, *JCAP* **10** (2020) 002 [2004.11396].
- [895] M. Hazumi et al., *LiteBIRD: A Satellite for the Studies of B-Mode Polarization and Inflation from Cosmic Background Radiation Detection*, *J. Low Temp. Phys.* **194** (2019) 443.

[896] A. Kogut, D. Fixsen, D. Chuss, J. Dotson, E. Dwek, M. Halpern et al., *The primordial inflation explorer (pixie): a nulling polarimeter for cosmic microwave background observations*, *Journal of Cosmology and Astroparticle Physics* **2011** (2011) 025.

[897] A. Kogut, M.H. Abitbol, J. Chluba, J. Delabrouille, D. Fixsen, J.C. Hill et al., *CMB Spectral Distortions: Status and Prospects*, [1907.13195](#).

[898] J. Chluba et al., *Spectral Distortions of the CMB as a Probe of Inflation, Recombination, Structure Formation and Particle Physics: Astro2020 Science White Paper*, *Bull. Am. Astron. Soc.* **51** (2019) 184 [[1903.04218](#)].

[899] E. Thrane and J.D. Romano, *Sensitivity curves for searches for gravitational-wave backgrounds*, *Phys. Rev. D* **88** (2013) 124032 [[1310.5300](#)].

[900] C. Caprini et al., *Science with the space-based interferometer eLISA. II: Gravitational waves from cosmological phase transitions*, *JCAP* **04** (2016) 001 [[1512.06239](#)].

[901] M. Maggiore, *Gravitational wave experiments and early universe cosmology*, *Phys. Rept.* **331** (2000) 283 [[gr-qc/9909001](#)].

[902] S. Weinberg, *Damping of tensor modes in cosmology*, *Phys. Rev. D* **69** (2004) 023503 [[astro-ph/0306304](#)].

[903] Y. Watanabe and E. Komatsu, *Improved Calculation of the Primordial Gravitational Wave Spectrum in the Standard Model*, *Phys. Rev. D* **73** (2006) 123515 [[astro-ph/0604176](#)].

[904] B.A. Stefanek and W.W. Repko, *Analytic description of the damping of gravitational waves by free streaming neutrinos*, *Phys. Rev. D* **88** (2013) 083536 [[1207.7285](#)].

[905] J.B. Dent, L.M. Krauss, S. Sabharwal and T. Vachaspati, *Damping of Primordial Gravitational Waves from Generalized Sources*, *Phys. Rev. D* **88** (2013) 084008 [[1307.7571](#)].

[906] A. Hook, G. Marques-Tavares and D. Racco, *Causal gravitational waves as a probe of free streaming particles and the expansion of the Universe*, *JHEP* **02** (2021) 117 [[2010.03568](#)].

[907] T. Asaka and H. Okui, *Neutrino masses and gravitational wave background*, *Phys. Lett. B* **814** (2021) 136074 [[2012.13527](#)].

[908] J.A. Casas, V. Di Clemente, A. Ibarra and M. Quiros, *Massive neutrinos and the Higgs mass window*, *Phys. Rev. D* **62** (2000) 053005 [[hep-ph/9904295](#)].

Bibliography

- [909] J. Elias-Miro, J.R. Espinosa, G.F. Giudice, G. Isidori, A. Riotto and A. Strumia, *Higgs mass implications on the stability of the electroweak vacuum*, *Phys. Lett. B* **709** (2012) 222 [[1112.3022](#)].
- [910] F. Vissani, *Do experiments suggest a hierarchy problem?*, *Phys. Rev. D* **57** (1998) 7027 [[hep-ph/9709409](#)].
- [911] J.D. Clarke, R. Foot and R.R. Volkas, *Electroweak naturalness in the three-flavor type I seesaw model and implications for leptogenesis*, *Phys. Rev. D* **91** (2015) 073009 [[1502.01352](#)].
- [912] I. Brivio and M. Trott, *Radiatively Generating the Higgs Potential and Electroweak Scale via the Seesaw Mechanism*, *Phys. Rev. Lett.* **119** (2017) 141801 [[1703.10924](#)].
- [913] I. Brivio and M. Trott, *Examining the neutrino option*, *JHEP* **02** (2019) 107 [[1809.03450](#)].
- [914] S. Dimopoulos and L. Susskind, *On the Baryon Number of the Universe*, *Phys. Rev. D* **18** (1978) 4500.
- [915] A.A. Starobinsky and J. Yokoyama, *Equilibrium state of a selfinteracting scalar field in the De Sitter background*, *Phys. Rev. D* **50** (1994) 6357 [[astro-ph/9407016](#)].
- [916] T. Gherghetta, C.F. Kolda and S.P. Martin, *Flat directions in the scalar potential of the supersymmetric standard model*, *Nucl. Phys.* **B468** (1996) 37 [[hep-ph/9510370](#)].
- [917] I. Affleck and M. Dine, *A New Mechanism for Baryogenesis*, *Nucl. Phys.* **B249** (1985) 361.
- [918] A.G. Cohen and D.B. Kaplan, *Thermodynamic Generation of the Baryon Asymmetry*, *Phys. Lett. B* **199** (1987) 251.
- [919] A. Kusenko, K. Schmitz and T.T. Yanagida, *Leptogenesis via Axion Oscillations after Inflation*, *Phys. Rev. Lett.* **115** (2015) 011302 [[1412.2043](#)].
- [920] A. De Simone and T. Kobayashi, *Cosmological Aspects of Spontaneous Baryogenesis*, *JCAP* **08** (2016) 052 [[1605.00670](#)].
- [921] V. Domcke, Y. Ema, K. Mukaida and M. Yamada, *Spontaneous Baryogenesis from Axions with Generic Couplings*, *JHEP* **08** (2020) 096 [[2006.03148](#)].
- [922] R.T. Co and K. Harigaya, *Axiogenesis*, *Phys. Rev. Lett.* **124** (2020) 111602 [[1910.02080](#)].
- [923] R.D. Peccei and H.R. Quinn, *CP Conservation in the Presence of Instantons*, *Phys. Rev. Lett.* **38** (1977) 1440.

- [924] S. Weinberg, *A New Light Boson?*, *Phys. Rev. Lett.* **40** (1978) 223.
- [925] J.E. Kim, *Weak Interaction Singlet and Strong CP Invariance*, *Phys. Rev. Lett.* **43** (1979) 103.
- [926] M.A. Shifman, A.I. Vainshtein and V.I. Zakharov, *Can Confinement Ensure Natural CP Invariance of Strong Interactions?*, *Nucl. Phys.* **B166** (1980) 493.
- [927] R.T. Co, L.J. Hall and K. Harigaya, *Axion Kinetic Misalignment Mechanism*, *Phys. Rev. Lett.* **124** (2020) 251802 [[1910.14152](#)].
- [928] B. Barman, N. Bernal, N. Ramberg and L. Visinelli, *QCD Axion Kinetic Misalignment without Prejudice*, *Universe* **8** (2022) 634 [[2111.03677](#)].
- [929] J. Preskill, M.B. Wise and F. Wilczek, *Cosmology of the Invisible Axion*, *Phys. Lett.* **B120** (1983) 127.
- [930] K. Harigaya and I.R. Wang, *Axiogenesis from $SU(2)_R$ phase transition*, *JHEP* **10** (2021) 022 [[2107.09679](#)].
- [931] R.T. Co, V. Domcke and K. Harigaya, *Baryogenesis from Decaying Magnetic Helicity in Axiogenesis*, [2211.12517](#).
- [932] J.E. Kim, H.P. Nilles and M. Peloso, *Completing natural inflation*, *JCAP* **01** (2005) 005 [[hep-ph/0409138](#)].
- [933] R.T. Co, L.J. Hall and K. Harigaya, *Predictions for Axion Couplings from ALP Cogenesis*, *JHEP* **01** (2021) 172 [[2006.04809](#)].
- [934] R.T. Co, T. Gherghetta and K. Harigaya, *Axiogenesis with a heavy QCD axion*, *JHEP* **10** (2022) 121 [[2206.00678](#)].
- [935] V. Domcke, K. Harigaya and K. Mukaida, *Charge transfer between rotating complex scalar fields*, *JHEP* **08** (2022) 234 [[2205.00942](#)].
- [936] R.T. Co, D. Dunsky, N. Fernandez, A. Ghalsasi, L.J. Hall, K. Harigaya et al., *Gravitational wave and CMB probes of axion kination*, *JHEP* **09** (2022) 116 [[2108.09299](#)].
- [937] R.T. Co, K. Harigaya and A. Pierce, *Gravitational waves and dark photon dark matter from axion rotations*, *JHEP* **12** (2021) 099 [[2104.02077](#)].
- [938] Y. Gouttenoire, G. Servant and P. Simakachorn, *Revealing the Primordial Irreducible Inflationary Gravitational-Wave Background with a Spinning Peccei-Quinn Axion*, [2108.10328](#).
- [939] Y. Gouttenoire, G. Servant and P. Simakachorn, *Kination cosmology from scalar fields and gravitational-wave signatures*, [2111.01150](#).

Bibliography

- [940] E. Madge, W. Ratzinger, D. Schmitt and P. Schwaller, *Audible axions with a booster: Stochastic gravitational waves from rotating ALPs*, *SciPost Phys.* **12** (2022) 171 [[2111.12730](#)].
- [941] K. Harigaya, K. Inomata and T. Terada, *Axion Poltergeist*, [2305.14242](#).
- [942] R.T. Co, N. Fernandez, A. Ghalsasi, L.J. Hall and K. Harigaya, *Lepto-Axiogenesis*, *JHEP* **03** (2021) 017 [[2006.05687](#)].
- [943] J. Kawamura and S. Raby, *Lepto-axiogenesis in minimal SUSY KSVZ model*, *JHEP* **04** (2022) 116 [[2109.08605](#)].
- [944] P. Barnes, R.T. Co, K. Harigaya and A. Pierce, *Lepto-axiogenesis and the scale of supersymmetry*, [2208.07878](#).
- [945] R.T. Co, K. Harigaya, Z. Johnson and A. Pierce, *R-parity violation axiogenesis*, *JHEP* **11** (2021) 210 [[2110.05487](#)].
- [946] H.K. Dreiner, *An Introduction to explicit R-parity violation*, [hep-ph/9707435](#).
- [947] G.B. Gelmini and M. Roncadelli, *Left-Handed Neutrino Mass Scale and Spontaneously Broken Lepton Number*, *Phys. Lett. B* **99** (1981) 411.
- [948] Y. Chikashige, R.N. Mohapatra and R.D. Peccei, *Are There Real Goldstone Bosons Associated with Broken Lepton Number?*, *Phys. Lett. B* **98** (1981) 265.
- [949] S. Chakraborty, T.H. Jung and T. Okui, *Composite neutrinos and the QCD axion: Baryogenesis, dark matter, small Dirac neutrino masses, and vanishing neutron electric dipole moment*, *Phys. Rev. D* **105** (2022) 015024 [[2108.04293](#)].
- [950] M. Ibe and K. Kaneta, *Spontaneous thermal Leptogenesis via Majoron oscillation*, *Phys. Rev. D* **92** (2015) 035019 [[1504.04125](#)].
- [951] K. Harigaya, M. Ibe, M. Kawasaki and T.T. Yanagida, *Dynamics of Peccei-Quinn Breaking Field after Inflation and Axion Isocurvature Perturbations*, *JCAP* **11** (2015) 003 [[1507.00119](#)].
- [952] R.T. Co, L.J. Hall and K. Harigaya, *QCD Axion Dark Matter with a Small Decay Constant*, *Phys. Rev. Lett.* **120** (2018) 211602 [[1711.10486](#)].
- [953] D. Borah, S. Jyoti Das and N. Okada, *Affleck-Dine cogenesis of baryon and dark matter*, *JHEP* **05** (2023) 004 [[2212.04516](#)].
- [954] C.-Y. Yao and G.-J. Ding, *Systematic analysis of Dirac neutrino masses from a dimension five operator*, *Phys. Rev. D* **97** (2018) 095042 [[1802.05231](#)].
- [955] J.R. Ellis, M.K. Gaillard and D.V. Nanopoulos, *A Phenomenological Profile of the Higgs Boson*, *Nucl. Phys. B* **106** (1976) 292.

- [956] M.A. Shifman, A.I. Vainshtein, M.B. Voloshin and V.I. Zakharov, *Low-Energy Theorems for Higgs Boson Couplings to Photons*, Sov. J. Nucl. Phys. **30** (1979) 711.
- [957] N. Ishizuka and M. Yoshimura, *Axion and Dilaton Emissivity From Nascent Neutron Stars*, Prog. Theor. Phys. **84** (1990) 233.
- [958] J. Heeck and H.H. Patel, *Majoron at two loops*, Phys. Rev. D **100** (2019) 095015 [1909.02029].
- [959] P. Sikivie, *Of Axions, Domain Walls and the Early Universe*, Phys. Rev. Lett. **48** (1982) 1156.
- [960] M. Reig, J.W.F. Valle and M. Yamada, *Light majoron cold dark matter from topological defects and the formation of boson stars*, JCAP **09** (2019) 029 [1905.01287].
- [961] S.M. Barr and D. Seckel, *Planck scale corrections to axion models*, Phys. Rev. **D46** (1992) 539.
- [962] I.Z. Rothstein, K.S. Babu and D. Seckel, *Planck scale symmetry breaking and majoron physics*, Nucl. Phys. B **403** (1993) 725 [hep-ph/9301213].
- [963] P. Agrawal and K. Howe, *A Flavorful Factoring of the Strong CP Problem*, JHEP **12** (2018) 035 [1712.05803].
- [964] P. Agrawal and K. Howe, *Factoring the Strong CP Problem*, JHEP **12** (2018) 029 [1710.04213].
- [965] M. Kachelriess, R. Tomas and J.W.F. Valle, *Supernova bounds on Majoron emitting decays of light neutrinos*, Phys. Rev. D **62** (2000) 023004 [hep-ph/0001039].
- [966] Y. Farzan, *Bounds on the coupling of the Majoron to light neutrinos from supernova cooling*, Phys. Rev. D **67** (2003) 073015 [hep-ph/0211375].
- [967] L. Heurtier and Y. Zhang, *Supernova Constraints on Massive (Pseudo)Scalar Coupling to Neutrinos*, JCAP **02** (2017) 042 [1609.05882].
- [968] T.S. Bunch and P.C.W. Davies, *Quantum Field Theory in de Sitter Space: Renormalization by Point Splitting*, Proc. Roy. Soc. Lond. A **360** (1978) 117.
- [969] S.W. Hawking and I.G. Moss, *Supercooled Phase Transitions in the Very Early Universe*, Phys. Lett. B **110** (1982) 35.
- [970] A. Vilenkin, *Creation of Universes from Nothing*, Phys. Lett. B **117** (1982) 25.
- [971] A. Vilenkin and L.H. Ford, *Gravitational Effects upon Cosmological Phase Transitions*, Phys. Rev. D **26** (1982) 1231.

Bibliography

- [972] A.D. Linde, *Scalar Field Fluctuations in Expanding Universe and the New Inflationary Universe Scenario*, *Phys. Lett. B* **116** (1982) 335.
- [973] A.A. Starobinsky, *Dynamics of Phase Transition in the New Inflationary Universe Scenario and Generation of Perturbations*, *Phys. Lett. B* **117** (1982) 175.
- [974] A. Vilenkin, *Quantum Fluctuations in the New Inflationary Universe*, *Nucl. Phys. B* **226** (1983) 527.
- [975] A.D. Linde, *The New Mechanism of Baryogenesis and the Inflationary Universe*, *Phys. Lett. B* **160** (1985) 243.
- [976] K. Enqvist, K.W. Ng and K.A. Olive, *Scalar Field Fluctuations in the Early Universe*, *Nucl. Phys. B* **303** (1988) 713.
- [977] T. Opferkuch, P. Schwaller and B.A. Stefanek, *Ricci Reheating*, *JCAP* **07** (2019) 016 [[1905.06823](#)].
- [978] M. Kawasaki and T. Takesako, *Hubble Induced Mass in Radiation Dominated Universe*, *Phys. Lett. B* **711** (2012) 173 [[1112.5823](#)].
- [979] M. Kawasaki and T. Takesako, *Remarks on Hubble Induced Mass from Fermion Kinetic Term*, *Phys. Lett. B* **718** (2012) 522 [[1208.1323](#)].
- [980] M. Kawasaki, F. Takahashi and T. Takesako, *Hubble-induced mass from MSSM plasma*, *JCAP* **04** (2013) 008 [[1211.4921](#)].
- [981] K. Enqvist and M.S. Sloth, *Adiabatic CMB perturbations in pre - big bang string cosmology*, *Nucl. Phys. B* **626** (2002) 395 [[hep-ph/0109214](#)].
- [982] D.H. Lyth and D. Wands, *Generating the curvature perturbation without an inflaton*, *Phys. Lett. B* **524** (2002) 5 [[hep-ph/0110002](#)].
- [983] T. Moroi and T. Takahashi, *Effects of cosmological moduli fields on cosmic microwave background*, *Phys. Lett. B* **522** (2001) 215 [[hep-ph/0110096](#)].
- [984] A. Kusenko, L. Pearce and L. Yang, *Postinflationary Higgs relaxation and the origin of matter-antimatter asymmetry*, *Phys. Rev. Lett.* **114** (2015) 061302 [[1410.0722](#)].
- [985] L. Yang, L. Pearce and A. Kusenko, *Leptogenesis via Higgs Condensate Relaxation*, *Phys. Rev. D* **92** (2015) 043506 [[1505.07912](#)].
- [986] M. Kawasaki, L. Pearce, L. Yang and A. Kusenko, *Relaxation leptogenesis, isocurvature perturbations, and the cosmic infrared background*, *Phys. Rev. D* **95** (2017) 103006 [[1701.02175](#)].
- [987] J. Kearney, N. Orlofsky and A. Pierce, *High-Scale Axions without Isocurvature from Inflationary Dynamics*, *Phys. Rev. D* **93** (2016) 095026 [[1601.03049](#)].

- [988] Y. Bao, J. Fan and L. Li, *Opening up window of post-inflationary QCD axion*, 2209.09908.
- [989] M. Beltran, J. Garcia-Bellido, J. Lesgourges and M. Viel, *Squeezing the window on isocurvature modes with the lyman-alpha forest*, *Phys. Rev. D* **72** (2005) 103515 [[astro-ph/0509209](#)].
- [990] F. Graziani and K.A. Olive, *Chaotic Inflation in Models With Flat Directions*, *Phys. Lett. B* **216** (1989) 31.
- [991] M.P. Hertzberg, M. Tegmark and F. Wilczek, *Axion Cosmology and the Energy Scale of Inflation*, *Phys. Rev. D* **78** (2008) 083507 [[0807.1726](#)].
- [992] A. Anisimov and M. Dine, *Some issues in flat direction baryogenesis*, *Nucl. Phys. B* **619** (2001) 729 [[hep-ph/0008058](#)].
- [993] M. Fujii, K. Hamaguchi and T. Yanagida, *Reheating temperature independence of cosmological baryon asymmetry in Affleck-Dine leptogenesis*, *Phys. Rev. D* **63** (2001) 123513 [[hep-ph/0102187](#)].
- [994] R. Allahverdi and A. Mazumdar, *Affleck-Dine condensate, late thermalization and the gravitino problem*, *Phys. Rev. D* **78** (2008) 043511 [[0802.4430](#)].
- [995] M. Laine and M.E. Shaposhnikov, *Thermodynamics of nontopological solitons*, *Nucl. Phys. B* **532** (1998) 376 [[hep-ph/9804237](#)].
- [996] K. Mukaida and K. Nakayama, *Dynamics of oscillating scalar field in thermal environment*, *JCAP* **01** (2013) 017 [[1208.3399](#)].
- [997] K. Mukaida and K. Nakayama, *Dissipative Effects on Reheating after Inflation*, *JCAP* **03** (2013) 002 [[1212.4985](#)].
- [998] J. Turner and Y.-L. Zhou, *Leptogenesis via Varying Weinberg Operator: the Closed-Time-Path Approach*, *JHEP* **01** (2020) 022 [[1808.00470](#)].
- [999] P. Kozów and M. Olechowski, *Early universe dynamics of PQ field with very small self-coupling and its implications for axion dark matter*, 2212.03518.
- [1000] A.G. Cohen, D.B. Kaplan and A.E. Nelson, *Progress in electroweak baryogenesis*, *Ann. Rev. Nucl. Part. Sci.* **43** (1993) 27 [[hep-ph/9302210](#)].
- [1001] A. Dolgov, K. Freese, R. Rangarajan and M. Srednicki, *Baryogenesis during reheating in natural inflation and comments on spontaneous baryogenesis*, *Phys. Rev. D* **56** (1997) 6155 [[hep-ph/9610405](#)].
- [1002] A.D. Dolgov, *Baryogenesis, 30 years after*, in *25th ITEP Winter School of Physics*, 7, 1997, DOI [[hep-ph/9707419](#)].
- [1003] E.V. Arbuzova, A.D. Dolgov and V.A. Novikov, *General properties and kinetics of spontaneous baryogenesis*, *Phys. Rev. D* **94** (2016) 123501 [[1607.01247](#)].

Bibliography

- [1004] A. Dasgupta, R.K. Jain and R. Rangarajan, *Effective chemical potential in spontaneous baryogenesis*, *Phys. Rev. D* **98** (2018) 083527 [[1808.04027](#)].
- [1005] T. Bossingham, N.E. Mavromatos and S. Sarkar, *Leptogenesis from Heavy Right-Handed Neutrinos in CPT Violating Backgrounds*, *Eur. Phys. J. C* **78** (2018) 113 [[1712.03312](#)].
- [1006] M. Berbig, *S.M.A.S.H.E.D.: Standard Model Axion Seesaw Higgs inflation Extended for Dirac neutrinos*, *JCAP* **11** (2022) 042 [[2207.08142](#)].
- [1007] S. Betts et al., *Development of a Relic Neutrino Detection Experiment at PTOLEMY: Princeton Tritium Observatory for Light, Early-Universe, Massive-Neutrino Yield*, in *Community Summer Study 2013: Snowmass on the Mississippi (CSS2013) Minneapolis, MN, USA, July 29-August 6, 2013*, 2013 [[1307.4738](#)].
- [1008] PTOLEMY collaboration, *PTOLEMY: A Proposal for Thermal Relic Detection of Massive Neutrinos and Directional Detection of MeV Dark Matter*, [1808.01892](#).
- [1009] D. McKeen, *Cosmic neutrino background search experiments as decaying dark matter detectors*, *Phys. Rev. D* **100** (2019) 015028 [[1812.08178](#)].
- [1010] Z. Chacko, P. Du and M. Geller, *Detecting a Secondary Cosmic Neutrino Background from Majoron Decays in Neutrino Capture Experiments*, *Phys. Rev. D* **100** (2019) 015050 [[1812.11154](#)].
- [1011] T.W.B. Kibble, G. Lazarides and Q. Shafi, *Walls Bounded by Strings*, *Phys. Rev. D* **26** (1982) 435.
- [1012] T.W.B. Kibble, *Some Implications of a Cosmological Phase Transition*, *Phys. Rept.* **67** (1980) 183.
- [1013] S. Chang, C. Hagmann and P. Sikivie, *Studies of the motion and decay of axion walls bounded by strings*, *Phys. Rev. D* **59** (1999) 023505 [[hep-ph/9807374](#)].
- [1014] C. Hagmann, S. Chang and P. Sikivie, *Axions from string decay*, *Nucl. Phys. B Proc. Suppl.* **72** (1999) 81 [[hep-ph/9807428](#)].
- [1015] C. Hagmann, S. Chang and P. Sikivie, *Axion radiation from strings*, *Phys. Rev. D* **63** (2001) 125018 [[hep-ph/0012361](#)].
- [1016] C.J.A.P. Martins and E.P.S. Shellard, *Extending the velocity dependent one scale string evolution model*, *Phys. Rev. D* **65** (2002) 043514 [[hep-ph/0003298](#)].
- [1017] M. Yamaguchi and J. Yokoyama, *Quantitative evolution of global strings from the Lagrangian view point*, *Phys. Rev. D* **67** (2003) 103514 [[hep-ph/0210343](#)].

- [1018] J.N. Moore, E.P.S. Shellard and C.J.A.P. Martins, *On the evolution of Abelian-Higgs string networks*, *Phys. Rev. D* **65** (2002) 023503 [[hep-ph/0107171](#)].
- [1019] T. Hiramatsu, M. Kawasaki, T. Sekiguchi, M. Yamaguchi and J. Yokoyama, *Improved estimation of radiated axions from cosmological axionic strings*, *Phys. Rev. D* **83** (2011) 123531 [[1012.5502](#)].
- [1020] T. Hiramatsu, M. Kawasaki, K. Saikawa and T. Sekiguchi, *Axion cosmology with long-lived domain walls*, *JCAP* **01** (2013) 001 [[1207.3166](#)].
- [1021] V.B. Klaer and G.D. Moore, *The dark-matter axion mass*, *JCAP* **11** (2017) 049 [[1708.07521](#)].
- [1022] M. Kawasaki, T. Sekiguchi, M. Yamaguchi and J. Yokoyama, *Long-term dynamics of cosmological axion strings*, *PTEP* **2018** (2018) 091E01 [[1806.05566](#)].
- [1023] A. Vaquero, J. Redondo and J. Stadler, *Early seeds of axion miniclusters*, *JCAP* **04** (2019) 012 [[1809.09241](#)].
- [1024] V.B. Klaer and G.D. Moore, *Global cosmic string networks as a function of tension*, *JCAP* **06** (2020) 021 [[1912.08058](#)].
- [1025] M. Gorgetto, E. Hardy and G. Villadoro, *More axions from strings*, *SciPost Phys.* **10** (2021) 050 [[2007.04990](#)].
- [1026] C.A.J. O'Hare, G. Pierobon, J. Redondo and Y.Y.Y. Wong, *Simulations of axionlike particles in the postinflationary scenario*, *Phys. Rev. D* **105** (2022) 055025 [[2112.05117](#)].
- [1027] M. Dine, N. Fernandez, A. Ghalsasi and H.H. Patel, *Comments on axions, domain walls, and cosmic strings*, *JCAP* **11** (2021) 041 [[2012.13065](#)].
- [1028] M. Kawasaki, K. Saikawa and T. Sekiguchi, *Axion dark matter from topological defects*, *Phys. Rev. D* **91** (2015) 065014 [[1412.0789](#)].
- [1029] M.S. Turner and F. Wilczek, *Inflationary axion cosmology*, *Phys. Rev. Lett.* **66** (1991) 5.
- [1030] M. Dine and A. Anisimov, *Is there a Peccei-Quinn phase transition?*, *JCAP* **07** (2005) 009 [[hep-ph/0405256](#)].
- [1031] I.I. Tkachev, *Phase transitions at preheating*, *Phys. Lett. B* **376** (1996) 35 [[hep-th/9510146](#)].
- [1032] L. Kofman, A.D. Linde and A.A. Starobinsky, *Nonthermal phase transitions after inflation*, *Phys. Rev. Lett.* **76** (1996) 1011 [[hep-th/9510119](#)].
- [1033] S. Kasuya, M. Kawasaki and T. Yanagida, *Cosmological axion problem in chaotic inflationary universe*, *Phys. Lett. B* **409** (1997) 94 [[hep-ph/9608405](#)].

Bibliography

- [1034] S. Kasuya and M. Kawasaki, *Can topological defects be formed during preheating?*, *Phys. Rev. D* **56** (1997) 7597 [[hep-ph/9703354](#)].
- [1035] S. Kasuya and M. Kawasaki, *Topological defects formation after inflation on lattice simulation*, *Phys. Rev. D* **58** (1998) 083516 [[hep-ph/9804429](#)].
- [1036] I. Tkachev, S. Khlebnikov, L. Kofman and A.D. Linde, *Cosmic strings from preheating*, *Phys. Lett. B* **440** (1998) 262 [[hep-ph/9805209](#)].
- [1037] S. Kasuya and M. Kawasaki, *Comments on cosmic string formation during preheating on lattice simulations*, *Phys. Rev. D* **61** (2000) 083510 [[hep-ph/9903324](#)].
- [1038] A. Vilenkin, *Cosmic Strings and Domain Walls*, *Phys. Rept.* **121** (1985) 263.
- [1039] R.L. Davis, *Cosmic Axions from Cosmic Strings*, *Phys. Lett. B* **180** (1986) 225.
- [1040] C. Eröncel, R. Sato, G. Servant and P. Sørensen, *ALP dark matter from kinetic fragmentation: opening up the parameter window*, *JCAP* **10** (2022) 053 [[2206.14259](#)].
- [1041] L. Kofman, A.D. Linde and A.A. Starobinsky, *Reheating after inflation*, *Phys. Rev. Lett.* **73** (1994) 3195 [[hep-th/9405187](#)].
- [1042] J. Jaeckel, V.M. Mehta and L.T. Witkowski, *Monodromy Dark Matter*, *JCAP* **01** (2017) 036 [[1605.01367](#)].
- [1043] J. Berges, A. Chatrchyan and J. Jaeckel, *Foamy Dark Matter from Monodromies*, *JCAP* **08** (2019) 020 [[1903.03116](#)].
- [1044] N. Fonseca, E. Morgante, R. Sato and G. Servant, *Axion fragmentation*, *JHEP* **04** (2020) 010 [[1911.08472](#)].
- [1045] L. Lopez-Honorez, O. Mena, S. Palomares-Ruiz and P. Villanueva-Domingo, *Warm dark matter and the ionization history of the Universe*, *Phys. Rev. D* **96** (2017) 103539 [[1703.02302](#)].
- [1046] M. Kawasaki, T.T. Yanagida and K. Yoshino, *Domain wall and isocurvature perturbation problems in axion models*, *JCAP* **11** (2013) 030 [[1305.5338](#)].
- [1047] R. Laureijs, J. Amiaux, S. Arduini, J.L. Auguères, J. Brinchmann, R. Cole et al., *Euclid Definition Study Report*, *arXiv e-prints* (2011) arXiv:1110.3193 [[1110.3193](#)].
- [1048] A.D. Linde, *Generation of Isothermal Density Perturbations in the Inflationary Universe*, *Phys. Lett. B* **158** (1985) 375.
- [1049] D.H. Lyth, *A Limit on the Inflationary Energy Density From Axion Isocurvature Fluctuations*, *Phys. Lett. B* **236** (1990) 408.

- [1050] M. Kawasaki, N. Sugiyama and T. Yanagida, *Isocurvature and adiabatic fluctuations of axion in chaotic inflation models and large scale structure*, *Phys. Rev. D* **54** (1996) 2442 [[hep-ph/9512368](#)].
- [1051] J.E. Kim, *A Common Scale for the Invisible Axion, Local SUSY GUTs and Sakino Decay*, *Phys. Lett. B* **136** (1984) 378.
- [1052] P. Moxhay and K. Yamamoto, *Peccei-Quinn Symmetry Breaking by Radiative Corrections in Supergravity*, *Phys. Lett. B* **151** (1985) 363.
- [1053] N. Arkani-Hamed, G.F. Giudice, M.A. Luty and R. Rattazzi, *Supersymmetry breaking loops from analytic continuation into superspace*, *Phys. Rev. D* **58** (1998) 115005 [[hep-ph/9803290](#)].
- [1054] P. Adshead, G. Holder and P. Ralegankar, *BBN constraints on dark radiation isocurvature*, *JCAP* **09** (2020) 016 [[2006.01165](#)].
- [1055] R.J. Cooke, M. Pettini and C.C. Steidel, *One Percent Determination of the Primordial Deuterium Abundance*, *Astrophys. J.* **855** (2018) 102 [[1710.11129](#)].
- [1056] S. Ghosh, S. Kumar and Y. Tsai, *Free-streaming and coupled dark radiation isocurvature perturbations: constraints and application to the Hubble tension*, *JCAP* **05** (2022) 014 [[2107.09076](#)].
- [1057] M. Kawasaki, K. Miyamoto, K. Nakayama and T. Sekiguchi, *Isocurvature perturbations in extra radiation*, *JCAP* **02** (2012) 022 [[1107.4962](#)].
- [1058] A. Dolgov and K. Freese, *Calculation of particle production by Nambu Goldstone bosons with application to inflation reheating and baryogenesis*, *Phys. Rev. D* **51** (1995) 2693 [[hep-ph/9410346](#)].
- [1059] A. Papageorgiou, P. Quilez and K. Schmitz, *Axion dark matter from frictional misalignment*, *JHEP* **01** (2023) 169 [[2206.01129](#)].
- [1060] K. Choi, S.H. Im, H.J. Kim and H. Seong, *Axion dark matter with thermal friction*, *JHEP* **02** (2023) 180 [[2206.01462](#)].
- [1061] E. Goudzovski et al., *New physics searches at kaon and hyperon factories*, *Rept. Prog. Phys.* **86** (2023) 016201 [[2201.07805](#)].
- [1062] E. Fernandez-Martinez, M. Pierre, E. Pinsard and S. Rosauro-Alcaraz, *Inverse Seesaw, dark matter and the Hubble tension*, *Eur. Phys. J. C* **81** (2021) 954 [[2106.05298](#)].
- [1063] NA62 collaboration, *Measurement of the very rare $K^+ \rightarrow \pi^+ \nu \bar{\nu}$ decay*, *JHEP* **06** (2021) 093 [[2103.15389](#)].
- [1064] NA62 collaboration, *Search for π^0 decays to invisible particles*, *JHEP* **02** (2021) 201 [[2010.07644](#)].

Bibliography

- [1065] NA62 collaboration, *Search for a feebly interacting particle X in the decay $K^+ \rightarrow \pi^+ X$* , *JHEP* **03** (2021) 058 [2011.11329].
- [1066] D. Gorbunov, I. Krasnov and S. Suvorov, *Constraints on light scalars from PS191 results*, *Phys. Lett. B* **820** (2021) 136524 [2105.11102].
- [1067] D. Egana-Ugrinovic, S. Homiller and P. Meade, *Light Scalars and the Koto Anomaly*, *Phys. Rev. Lett.* **124** (2020) 191801 [1911.10203].
- [1068] CHARM collaboration, *Search for Axion Like Particle Production in 400-GeV Proton - Copper Interactions*, *Phys. Lett. B* **157** (1985) 458.
- [1069] LHCb collaboration, *Search for hidden-sector bosons in $B^0 \rightarrow K^{*0} \mu^+ \mu^-$ decays*, *Phys. Rev. Lett.* **115** (2015) 161802 [1508.04094].
- [1070] LHCb collaboration, *Search for long-lived scalar particles in $B^+ \rightarrow K^+ \chi(\mu^+ \mu^-)$ decays*, *Phys. Rev. D* **95** (2017) 071101 [1612.07818].
- [1071] L3 collaboration, *Search for neutral Higgs boson production through the process $e+ e- \rightarrow Z^* H0$* , *Phys. Lett. B* **385** (1996) 454.
- [1072] M.W. Winkler, *Decay and detection of a light scalar boson mixing with the Higgs boson*, *Phys. Rev. D* **99** (2019) 015018 [1809.01876].
- [1073] P.S.B. Dev, R.N. Mohapatra and Y. Zhang, *Revisiting supernova constraints on a light CP-even scalar*, *JCAP* **08** (2020) 003 [2005.00490].
- [1074] A. Fradette and M. Pospelov, *BBN for the LHC: constraints on lifetimes of the Higgs portal scalars*, *Phys. Rev. D* **96** (2017) 075033 [1706.01920].
- [1075] D.I. Dunsky, L.J. Hall and K. Harigaya, *Dark Radiation Constraints on Heavy QCD Axions*, 2205.11540.